Natural Resources Canada   Ressources naturelles Canada

GEOLOGICAL SURVEY OF CANADA
OPEN FILE 7306

Geological and geochemical data from the Canadian Arctic Islands. Part XVI: permafrost thickness determination from petroleum exploration wells

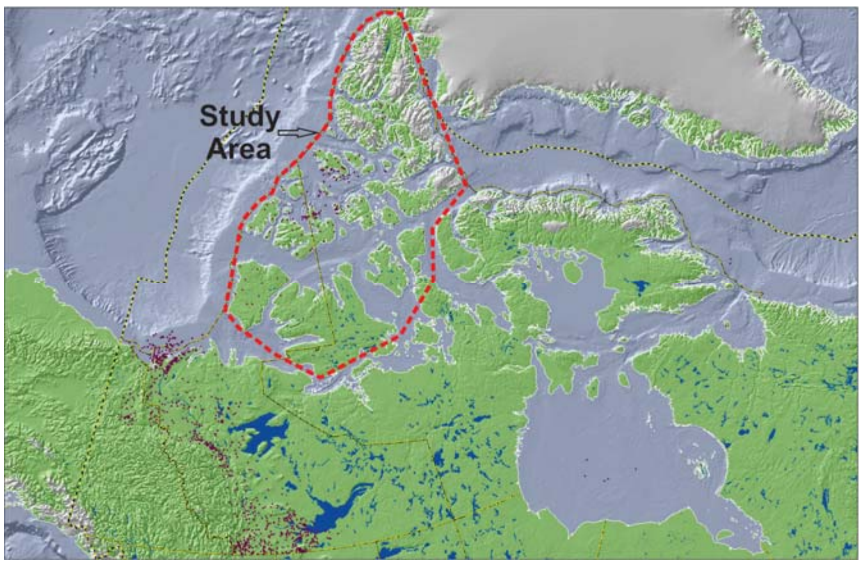

K. Hu, T.A. Brent, and K. Dewing

2018

Canada

GEOLOGICAL SURVEY OF CANADA
OPEN FILE 7306

Geological and geochemical data from the Canadian Arctic Islands. Part XVI: permafrost thickness determination from petroleum exploration wells

K. Hu, T.A. Brent, and K. Dewing

2018

Permanent link: https://doi.org/10.4095/311129

This publication is available for free download through GEOSCAN (http://geoscan.nrcan.gc.ca/).

Recommended citation
Hu, K., Brent, T.A., and Dewing, K., 2018. Geological and geochemical data from the Canadian Arctic Islands. Part XVI: permafrost thickness determination from petroleum exploration wells; Geological Survey of Canada, Open File 7306, 1 .zip file. https://doi.org/10.4095/311129

Publications in this series have not been edited; they are released as submitted by the author.

TABLE OF CONTENTS

SUMMARY

Permafrost occurrence is widespread in northern Canada and occurs continuously beneath the islands of the Canadian Arctic Archipelago (Fig. 1). This study was conducted to infer depths to the base of ice-bearing permafrost (IBPF) at petroleum exploration wells located on these islands, and compile this alongside the directly measured depth to the 0° Celsius level, or true base of permafrost (PF). The depths to the 0° Celsius isotherm were previously determined from 32 wells (one offshore and 31 onshore) by repeated shallow temperature surveys (Judge *et al*, 1979a, 1979b, 1981 and 1987). In this study area (Fig. 2), a determination was made for the base of IBPF for 140 onshore wells. Numerous data sets were consulted including suites of geophysical well logs, and well seismic surveys in conjunction with lithological analysis, and other data. Results at each well are provided graphically as composite borehole depth plots with wireline logs, velocity surveys, shallow temperature data, drilling rate and lithology interpretations, to illustrate geophysical responses, and to provide multi-parameter evidence for integrated interpretations of the IBPF/PF zone. IBPF/PF determinations are quality-assessed in terms of their reliability using a practical scale based on the type of methods used and the quality of data available.

The depths to the base of permafrost (0° Celsius) derived from temperature surveys were used to corroborate the interpretations of correlative well log records and well seismic surveys, which were better able to discern ice in the pore spaces of sedimentary rocks and thus base of IBPF, rather than the zero degree Celsius temperature level.

For most of the wells, the base of the interpreted fully frozen ice-bearing permafrost ($IBPF_F$) may be constrained by a notable change in electrical and acoustic properties, borehole size, drilling rate and well seismic velocity. For 106 wells, a transition zone below the base of $IBPF_F$ (between 9.5 m to 170 m in thickness) is interpreted to represent partially frozen ice-bearing permafrost ($IBPF_P$), in which ice and unfrozen water may coexist. The base of permafrost (PF), or the 0°C isotherm, as extrapolated from return-to- equilibrium calculations of repeat temperature surveys, ranges in depth from 143 m to 726 m below ground level (GL) in 31 onshore wells, and 40 m below sea floor (SF) in the only offshore well with a temperature survey. Depth to the base of $IBPF_F$ and $IBPF_P$ defined by other

geophysical methods varies from 37 m to 843 m below GL and 184 m to 779 m below GL respectively across the study area. For 93 of 143 wells total (> 65%), defined $IBPF_F$/PF bases occur in Mesozoic strata, distributed in sandstones, siltstones and shales, except one well in conglomerate. For 62 wells, $IBPF_F$/PF bases are located in Cretaceous strata. $IBPF_F$/PF bases are encountered in Paleozoic sandstone, siltstone, and carbonates in 48 wells. Among the 106 wells with an interpreted ice transition zone, from fully frozen to unfrozen with depth, $IBPF_P$ base in 103 wells is predominantly confined to shale, siltstone, and sandstone. Both $IBPF_F$ and $IBPF_P$ bases occur within highly porous sandstone of the Miocene-Pliocene Beaufort Formation in one well on Meighen Island, and one well on the northwest edge of Ellef Ringnes Island.

INTRODUCTION

Permafrost is defined on the basis of temperature and it occurs where ground (soil or rock) temperatures have remained at or below 0°C for at least two consecutive years (Permafrost Subcommittee, 1988; van Everdingen, ed., 1998). The base of permafrost (PF) is defined by the lower position of the 0ºC isotherm and temperatures are perennially greater than 0ºC beneath this boundary. Ice-bearing permafrost (IBPF) refers to soil or rock that contains or is interpreted to contain ice (Permafrost Subcommittee, 1988; Collett *et al*., 1988). Within permafrost, the ground may be variably frozen or unfrozen, depending on its moisture content and due to various factors that affect the freezing process such as salinity, and matrix mineral composition, grain size and texture (e.g., Anderson and Morgenstern, 1973; Hivon and Sego, 1995).

Permafrost, in various forms and extents, underlies almost half of Canada. Permafrost distribution has been conventionally represented in terms of broad latitudinal zones in which permafrost is spatially continuous, widespread (discontinuous), scattered (sporadic), or localized (Fig. 1, modified from Heginbottom *et al*., 1995). Continuous permafrost zones have a minimum of 90% coverage; extensive discontinuous permafrost zones have 50-89% coverage; sporadic discontinuous permafrost zones have 10-49% coverage; whereas "isolated patches" refers to areas having less than 10% permafrost coverage (Fig. 1). The continuous permafrost zone covers the northernmost regions of Canada, including the

Arctic Archipelago and extending south to cover the southwestern shore of Hudson Bay. The second zone is the extensive discontinuous permafrost zone which forms a thin band following the southern border of the continuous zone. The third zone is the sporadic permafrost zone, a thick band south of the extensive discontinuous zone, reaching from the Pacific to the Atlantic coast and extending south of James Bay. And, lastly, the mountain permafrost zone is found in the Coast Mountains of British Columbia, in the Rocky Mountains, in Newfoundland, and on the Gaspé Peninsula in Quebec (Fig. 1).

Over the last 40 years, various borehole geophysical methods have been applied in permafrost detection in the Mackenzie Delta/Beaufort Sea region, the Mackenzie valley and Yukon Territory, and Canadian Arctic Islands (Walker and Stuart, 1976; Hnatiuk and Randall, 1977; MacAulay *et al*., 1979; Hatlelid and MacDonald, 1982; D & S Group, 1983; Hardy Associates (1978) Ltd., 1984; Thurber Consultants Ltd., 1986, 1988; Palacky and Stephens, 1992; Stevens *et al*., 2008). Smith and Burgess (2002) compiled a digital database of permafrost thickness for northern Canada using published and unpublished data that were collected mainly between 1960 and the mid-1980s. Jessop *et al*. (2005) prepared a digital compilation of Canadian geothermal data generated over a 40 year period that includes downhole temperature cable data gathered for permafrost studies.

It should be noted that nearly all of Canada's offshore areas are considered permafrost free (Fig.1). The exception is the Beaufort Sea shallow water shelf, where extensive, thick, relict permafrost exists (see red area in Figure 1). Mackenzie - Beaufort regional borehole permafrost studies (e.g., D & S Group, 1983; Hu *et al*., 2013), presented interpretations of permafrost thickness and included details of detection techniques and methodologies, and quality assessment methods. However, Smith and Burgess (2002) reported that the occurrence of ice-bearing permafrost (IBPF) were identified in 13 offshore wells (up to >700 m in depth) located in the inter-island marine areas of the Canadian Arctic Islands. Most of the 13 listed IBPF picks appeared in different datum from those of their cited publications, including seven offshore wells from Hardy Associates (1978) Ltd. (1984), and six offshore wells from Thurber Consultants Ltd. (1986, 1988). But none of the IBPF picks in the 13 offshore wells from previous studies is supported by our integrated review of available geophysical data and lithology interpretations. Additionally, the Quaternary glacial history associated with the evolution of these marine channels (Dyke, 2004) suggest it unlikely submarine permafrost, if previously present, would be present today, given the post glacial emergence of that region.

In the Canadian Arctic Islands, 192 exploration wells were drilled between 1961 and 1987 (Fig. 2). From the mid-1960s to early 1990s, the Geological Survey of Canada added downhole geothermal surveys to a select number of exploration wells to investigate permafrost of the Canadian Arctic Archipelago north of 75°N (Judge, 1973; Taylor *et al.*, 1982). These data often yielded a direct temperature measurement to the zero degree isotherm, thus defining the thickness of permafrost at points in the region. Borehole data were used to estimate permafrost thickness over a similar region (Hardy Associates (1978) Ltd., 1984). That study examined paper copies of wireline logs and did not comprehensively look at all factors such as well seismic velocity and drilling rate, for example. Seismic data in this region has also been used to provide permafrost thickness estimates (Brent and Harrison, 1998). 2-D seismic reflectors, their amplitude expression, and reliable frozen/unfrozen formation interval velocities, were used to calculate the base of ice-bearing permafrost. This work confirmed examples of seismically-defined IBPF features correlated directly to the base of IBPF as picked on petrophysical log suites. It provides a methodology, away from well control, to determine and map the base of ice-bearing permafrost.

No previous permafrost study in the Canadian Arctic Islands produced comprehensive borehole data montages to support and illustrate the evidence for determining the base of permafrost (PF) or ice-bearing permafrost (IBPF). In this study, the integrated, multi-parameter approach used is adapted mainly from Hu *et al.* (2013), which corroborated downhole temperature surveys, with well seismic surveys, wireline logs, drilling rate, and other relevant information (e.g., lithology, and well testing) to interpret PF/IBPF. This study: 1) presents all downhole data consulted, including temperature survey data, wireline logs, drilling rate, and well seismic velocity data; 2) displays the lithology interpretation primarily from new log analysis for this study; and 3) provides picks for the depth to base of true permafrost (PF) and ice-bearing permafrost (IBPF) with supporting evidence and reliability assessment. Unless otherwise indicated, the datum used for downhole depths in this report is Kelly Bushing “KB”, other depth datums are specified when used, such as Ground Level “GL” or Sea Floor “SF”.

TECHNIQUES FOR PERMAFROST DETECTION

The base of permafrost is defined by temperature, specifically at the 0°C isotherm, which ideally is delineated on the basis of precise temperature surveys in boreholes. However, detailed temperature logging of wells is very limited in the study area. Conventional well logs, including wireline logs and drilling rate, are common for petroleum exploration wells, and abundant well seismic velocity data are available which can be used to detect and map frozen section ($IBPF_F$) or partially frozen section (ice and water may coexist, $IBPF_P$) within the permafrost zone. The base of ice-bearing permafrost (IBPF) is often a well-defined physical boundary that can be seen on wireline logs, drilling rate and seismic survey because an ice-saturated porous medium has a much higher formation resistivity and acoustic velocity, lower drilling speed and higher seismic velocity than a water-saturated porous interval. In general, the electrical resistivity of frozen sediment are affected to a greater extent than are seismic velocities (Hnatiuk and Randall, 1977). This physical permafrost ice/water boundary will occur at a negative temperature, and at depths shallower than the 0°C isotherm because the freezing point of interstitial water is depressed as a function of the amount of dissolved salts.

Temperature surveys

Downhole temperature surveys are the most direct indicator of the presence of permafrost and the most accurate method for permafrost thickness determination. However, the circulation of drilling fluid within the wellbore over the weeks to months required to drill a well causes a substantial thermal disturbance around the borehole wall. The largest disturbance is at shallow depth in the permafrost zone which can lead to extensive thawing around the borehole. By the end of drilling, the permafrost zone may be highly disturbed and far from thermal equilibrium. In order to monitor the gradual recovery to thermal equilibrium, a series of temperatures are recorded at different times at similar fixed depth points within a well using a multisensor thermistor cable or a portable single thermistor probe. After a period of time (months to several years), temperatures in the borehole approach equilibrium with the undisturbed formation temperatures, so that true temperatures can be estimated by logarithmic extrapolation method (Lachenbruch and Brewer, 1959; Tayler and Judge, 1974).

In the Canadian Arctic Islands, such temperature survey data were available for 32 wells, including 31 onshore wells and a single offshore well, (Cape Allison C-47, Table 1). The raw temperature data are mostly included in the Canadian geothermal data compilation of Jessop *et al*. (2005) which comprises the direct temperature measurements in a time series of repeated readings made after the initial thermal disturbance of drilling. Equilibrium temperature data used in this study, which were estimated from the above raw data, are from the Canadian Geothermal Data Collection (Taylor and Judge, 1974, 1975, 1976, 1977; Judge *et al*., 1979a, 1979b, 1981; Taylor *et al*., 1982, 1985).

Table 1 lists the 32 wells with temperature survey results, reported from various datums of kelly bushing (KB), ground level (GL), or sea floor (SF; Taylor *et al*., 1982). Column 5 and 6 in Table 1 list the depth to the base of permafrost (0°C) interpreted from logarithmically extrapolated temperature profile series. The estimated base of frozen layer ($IBPF_F$) and the thickness of a transition zone, between the frozen base and the true base of permafrost, is given in column 7 and in column 8 for the Bent Horn N-72 well on Cameron Island, respectively. Column 9 lists the distance to the nearest waterbody (or distance offshore from coast) may have an influence on the permafrost for each well. Column 10, 11 and 12 lists rig release date, the date of the most recent temperature log run, and the period between the latest log run and drilling stop, respectively. Column 13 lists the interpretation quality ranking determined in this study for the interpreted base of permafrost, which will be discussed below. Figure 2 is a map that shows all well locations and the distribution of repeated shallow temperature and well seismic surveys throughout the eastern Arctic Archipelago.

Quality assessment of permafrost (PF) from temperature surveys

As the only direct indicator and the most accurate method for permafrost thickness determination, temperature surveys have the highest quality rank, so that any temperature log-based records are considered of “A” quality, which is the most reliable.

The quality of the base of permafrost interpretations from temperature survey data depends on the depth of the measure interval, the number of temperature surveys and the period over which they were acquired. To account for this in quality grading, there are four groups of temperature survey data with corresponding quality rankings; “Aa” (excellent), “Ab” (good), “Ac” (fair), and “Ad” (poor). The quality letter grades are "Aa" (best) to "Ad" (worst). Figure 3 illustrates examples of the four quality rankings of temperature interpretations compiled in this study. These quality ranks are described below:

Aa – excellent

Multiple temperature logs were acquired with sufficient intervening time, with the borehole was almost certainly returned to equilibrium, that extend below the permafrost zone and the depth to the base of permafrost is determined using an equilibrium-corrected temperature curve (Fig. 3a).

Ab – good, from one of the below cases

(1) Multiple temperature logs are available but the total logged depth may vary between runs, equilibrium calculations may not have been found or determined, or equilibrium calculations may have larger uncertainty than for “Aa” quality data because they are based on fewer logging runs. Therefore, in some cases, the permafrost base is interpolated from the most recent log when no equilibrium estimates are available (Fig. 3b);

(2) Shallow temperature logs over a relatively long time interval that did not completely penetrate the full permafrost zone, but approached the inferred base of permafrost (e.g., <100 m above PF), and depth to the base of permafrost is estimated by extrapolating equilibrium temperature trend to the 0°C level (Fig. 3c).

Ac – fair, from one of the below cases

(1) Temperature logs with shallow depth of penetration from single logging run were acquired over relatively long of a time interval (e.g., elapsed time $\geq$ 5 months), depth to base of permafrost is extrapolated (Fig. 3d where the elapsed time is greater than 21 months).

(2) Multiple temperature logs recorded over very short of a time interval after drilling did not completely penetrate the permafrost zone, depth to base of permafrost is estimated by extrapolating equilibrium temperature trends to PF (e.g., Fig. 3e where calculated equilibrium log has not been found).

Ad – **poor,** from one of the below cases

(1) It is not possible to estimate the base of permafrost reliably due to incomplete and/or poor quality data. Recorded temperature logs are too shallow (e.g., >400 m above PF) for reliable PF extrapolation (Fig. 3f);

(2) Single temperature log was recorded over a relatively short time interval when borehole was far from equilibrium, making permafrost estimation unreliable (e.g., the elapsed time is only one day in Fig. 3g).

In Figure 3, the "Aa" quality temperature example is the Gemini E-10 well on Ellesmere Island. It extends below the base of permafrost and the later temperature measurements show a close approach to calculated equilibrium (Fig. 3a). The "Ab" quality example is the Cornwall O-30 well, Cornwall Island, which penetrated through the permafrost zone for most of the log runs but no equilibrium temperature calculation has been found or made (Fig. 3b). For the Mokka A-02 well on Axel Heiberg Island, the "Ab" quality multiple temperature logs, which did not penetrate the full permafrost zone but approached the inferred base of permafrost, are used to calculate an equilibrium temperature extrapolation (Fig. 3c). The "Ac" quality example is the Dome Bay P-36 well on Ellef Ringnes Island, PF was extrapolated from a single temperature log that was run over greater than 21 months of elapsed time and penetrated close to the inferred base of permafrost (Fig.3d). Another "Ac" quality example is the Fosheim N-27 well, Ellesmere Island, where PF was estimated based on multiple temperature measurements made within one week after rig released but the calculated equilibrium log has not been found for this study (Fig. 3e). The "Ad" quality example is the Devon E-45 well, Devon Island (Fig. 3f). The temperature logs penetrated only top part of permafrost zone (<150 m) and terminated over 450 m above the inferred base of permafrost estimated by Judge *et al*. (e.g., 1981). Another "Ad" quality example is the Garnier O-21 well, Somerset Island (Fig. 3g). A single temperature log was made just one day after drilling stopped. The penetrated permafrost thickness is probably unreliable because borehole may be highly disturbed and far from thermal equilibrium due to a very short elapsed time.

Among the 32 wells with temperature survey data (Table 1), permafrost interpretations from repeated temperature surveys are classified as "Aa" (excellent) for 19 wells, "Ab" (good) for 5 wells, "Ac" (fair) for 6 wells, and "Ad" (poor) for 2 wells.

Cape Allison C-47

The single offshore well with a temperature survey is Cape Allison C-47 (Table 1), located in 244 m of water between Ellef Ringnes and King Christian islands (Fig. 2). Downhole temperature measurements were made from May to November in 1985, after the well rig was released on March 29 of 1985 (Taylor *et al*., 1985; Taylor and Judge, 1986; Judge *et al.*, 1987). Data retrieval and analysis of the thermal regime, and PF interpretation near the sea bed in C-47 well (40 m SF) were presented in previous studies (Taylor *et al.,* 1989; Taylor *et al.,* 2008). Figure 4 illustrates selected temperature-depth profiles and equilibrium temperature calculations for the Cape Allison C-47 well, no more detailed discussions are provided in this study, except the previous comments in the introduction, which state submarine permafrost ice is unlikely to exist in this offshore area.

Well seismic surveys

Well seismic velocity survey data includes both check shot, and crystal cable surveys. The latter has a higher vertical velocity resolution and is specifically designed with closer spacing of receivers (15.24 m), than conventional check shot surveys. They are run to relatively shallow depths ideally to provide interval velocities through the base of permafrost. In the Canadian Arctic Islands, one or both types of these velocity surveys are available for 136 wells located in both offshore and onshore localities (Fig. 2; Table 2). Both crystal cable and check shot velocity survey methods can be used to define the relationship between time and depth, which can then be converted to velocity as a function of depth (Hu *et al*., 2013).

The ice-bearing permafrost zone, is characterized by a relatively higher seismic velocity compared to unfrozen rock, primarily as a function of the amount of ice in the pore space. If near surface velocity data has enough detail, a relative shift from high to low velocity may be evident and define at best, and often aid at least, in positioning the level of the base of IBPF, as long as lithological changes are not dramatic, such as introducing volcanics or carbonates for example. Interval well seismic velocities (V_{INT}) within a permafrost zone vary depending on factors such as lithology, porosity, water content and salinity, and temperature. Seismic velocities for frozen shales range between 1800 and 3100 m/s, frozen sands range between 3200 and 4000 m/s, and frozen gravels from 3600 to 4700 m/s (Hnatiuk and Randall, 1977). In this study the results usually show seismic velocity in excess of 3000 m/s within frozen sand and gravel, which decreases to a velocity in the order of 2500 m/s below its base. Commonly the IBPF zone within frozen shaly sandstone, siltstone and shale is characterized by interval velocity values in excess of 2500 m/s which decrease to <2500 m/s below the base of IBPF. Figure 5 shows seismic velocity profiles (including crystal cable and check shot survey data) from two wells on Melville Island. In the North Sabine H-49 well, the point of 290 m depth marks the point at which interval velocities change from >3000 m/s in the unconsolidated sandstone of the Eureka Sound, to <2500 m/s in the Kanguk siltstone, and is considered to mark the base of IBPF (Fig. 5a). However, a range for the base of ice-bearing permafrost is interpreted from well seismic surveys for the Drake Point K-79 well, where four steps of interval velocities are observed (Fig. 5b). The interval velocities show a sharp decrease at 152 m depth from >3000 m/s to <3000 m/s in the upper Hassel sandstone. The depth of 183 m marks the interval velocity change from >2600 m/s to around 2500 m/s against the siltstone and shale of the Hassel through Christopher formations. The interval velocity shows a shift from > 2500 to <2100 m/s at 213 m. The depth of 243 m can be marked as the transition base where the interval velocities decrease from >2100 m/s to <2000 m/s in the upper Christopher shale. Therefore, IBPF is interpreted that includes $IBPF_F$ base at 152 m, $IBPF_P$ base at 243 m and a transition zone between $IBPF_F$ and $IBPF_P$, which are marked by a solid orange line, a dashed orange line and a pink coloured area, respectively (Fig. 5b).

This technique is limited because the seismic velocity shift at the base of IBPF is not necessarily exclusively caused by ice replacing water in the pore space. Factors such as significant lithology changes affecting rock matrix velocity, or porosity, and degree of compaction are complicating factors. It is also limited by the vertical resolution and quality of the velocity data. However, velocity measurements from well seismic surveys are not affected by invasive borehole conditions (unlike wireline tools) because the acoustic wave travel paths are outside the immediate borehole where thawing can occur. In some cases, well logging was initiated below the permafrost zone and seismic velocity data are all that is available to constrain IBPF interpretations. In summary, velocity surveys may establish a reasonable depth or depth range to base of IBPF on their own, and confirm interpretations of IBPF from well logs.

Geophysical well logging

Well logging is performed in boreholes drilled for oil and gas exploration, groundwater, mineral and geothermal exploration, as well as part of environmental and geotechnical studies. A well log is a detailed geological or geophysical record acquired downhole. Some types of geophysical well logs can be done during any phase of a well's history: drilling, completing, producing, or abandoning. Geophysical well logs can be used to identify IBPF because they provide information on specific physical properties of sedimentary rocks (e.g., electrical, acoustic, and drilling rate) that can change substantially when ice replaces water in the pore spaces of the rocks.

Wireline logs

Wireline logging is performed by lowering a 'logging tool' into a borehole on the end of a wireline cable to measure depth while recording petrophysical properties using a variety of sensors. There are many types of wireline logs, and they can be categorized either by their function or by the technology that they use. Conventional logging tools developed over the past several decades measure the natural gamma ray, electrical, acoustic, stimulated radioactive responses, electromagnetic, pressure and other properties of the rocks and their contained fluids.

Conventional wireline logs for the shallow interval (≤1000 m) are available in 192 wells in the Canadian Arctic Islands. The basic log data include spontaneous potential (SP), gamma ray (GR), caliper (general caliper - CAL, sonic caliper - CALS, density caliper - CAX/CALD, deep resistivity (deep induction - ILD, deep laterolog - LLD, long normal 64"- LN, with radius of 18'8" - LAT), medium resistivity (medium induction log - ILM, shallow laterolog - LLS, short normal 16"- SN), shallow resistivity (spherically focused log - SFL, micro spherically focused log - MSFL, or laterolog-8 - LL8), sonic transit-time (DT), bulk density (RHOB), and neutron porosity (neutron porosity calibrated with sandstone - NPss or neutron porosity calibrated with limestone - NPls) or neutron log (NEUT).

Resistivity logs

Resistivity logging data (deep, medium and shallow) are the most useful and reliable logs for detecting base of IBPF because porous formations normally exhibit much higher resistivity when they are frozen compared to when they are unfrozen (Hnatiuk and Randall, 1977). With the greatest depth of investigation, resistivity log readings increase dramatically in the presence of ice in porous rocks, and values increase exponentially in fine-grained rocks until most of the pore water is frozen (Durham and Marr, 1998; King, *et al.*; 1988).

Dual Induction Laterolog (DIL-SFL or DIL-LL8) can be used effectively to determine the base of IBPF if the thermally-invaded zone around the borehole is less than the investigative depth of the logging tool (Hnatiuk and Randall, 1977). The Dual Laterolog (DLL) is the best indicator of IBPF in enlarged, deeply invaded boreholes with highly resistive formations and salty drilling muds, and this tool was used to log the permafrost zone for many Arctic Archipelago boreholes.

In the Canadian Arctic Islands, near surface geological formations contain primarily sandstone, siltstone and shale, as well as small amount of conglomerate, carbonates, gravel, and igneous and metamorphic rocks. In coarse-grained rocks (such as sandstone and gravel), resistivity increases rapidly where the interstitial water changes phase into ice when the temperature is below 0^0C. The resistivity response observed in fine-grained siltstone and shale, is markedly more gradual and does not necessarily increase sharply at any single level. Resistivity readings may change markedly as a response to resistive non-clastic lithology such as that of dominantly carbonate and igneous rocks, making permafrost detection by using resistivity measurements problematic in those rock types.

However, a partially frozen transition zone may exist beneath the base of the fully frozen zone (Johansen *et al*., 2003), indicated by a more gradual decrease in resistivity with increasing depth. Pressure, grain size and the presence of mineral salts affect the freezing point and can lead to variations in the unfrozen water content (Hnatiuk and Randall, 1977).

Dielectric constant log

The dielectric constant logging tool measures the dielectric constant of the formation by the propagating electromagnetic energy of very high frequencies, 25-1100 MHz (megahertz) along the borehole wall. This approach was designed to distinguish oil from water in reservoir by the large contrast between the dielectric constant of water (80) and oil (2~4). Dielectric constant also changes significantly between frozen and unfrozen material, having values of 3~4 for ice, around 6 for frozen sediment, around 25 for unfrozen sediment and 80 for fresh water (Moorman *et al.,* 2003). Similarly, a distinct jump in the log value occurs when formation thaws (Durham and Marr, 1999). However, the dielectric constant log has a very shallow depth of investigation which may not be deep enough to penetrate the thawed zone that occurs in permafrost from drilling operations. This technique has not been used in this study because no dielectric constant log was run in the shallow interval of any wells in the Canadian Arctic Islands, so its effectiveness for detecting permafrost has not been established.

Borehole compensated sonic

The Borehole Compensated Sonic tool measures the compressional wave interval transit time (DT) in the rocks next to the well bore and was utilized widely in the exploration of the Canadian Arctic Islands. DT values not only depend on porosity, but also the lithology and the composition of the pore medium for the formation under investigation. If the pores contain ice instead of water, the measured transit time decreases significantly, especially in high porosity materials. However, the sonic travel times in the permafrost zone can be obscured when the IBPF has thawed around the borehole during drilling. Therefore, the sonic log is best used to provide supplementary information and confirmation of IBPF determinations based on resistivity logs which are less susceptible to drilling-related borehole effects.

Caliper logs

Caliper tool measures the diameter of the borehole, using either 2 or 4 mechanical arms. It can detect regions where the borehole walls are compromised and the well logs may be less reliable. One or two caliper logs (CALS, CAX/CALD, CAL) are available for most of the wells in the study area. In the permafrost zone, IBPF inhibits the formation of a stable filter cake and thawing-induced caving of the formation can lead to overgauged holes that are identified easily on caliper logs. Overgauged holes can sometimes indicate permafrost but their absence does not mean that there is no permafrost because caving is unlikely to occur in a competent formation with permafrost.

Other wireline logs

Other wireline logs can be used in conjunction with direct indicators of the physical properties of frozen sediment, such as resistivity, caliper and sonic transit time (or velocity), to further constrain interpretations of IBPF. Some of these logs are sensitive to degraded borehole conditions related to drilling-induced thawing of the IBPF zone.

Density (RHOB) and neutron (NPss, NPls, NEUT) logs: The freezing of formation pore fluids has little effect on density measurements but the overgauged boreholes that can occur in thawed IBPF zones can lead to anomalously low bulk density and high porosity values because the density tool requires close contact with the formation and is very sensitive to borehole conditions. Neutron porosity values tend to be high in permafrost zones because of their high hydrogen content but overgauged boreholes also lead to high neutron porosity values.

Gamma ray (GR): GR is a good lithology indicator that is mainly used to distinguish between clay (higher GR values) and sand or other non-shale rock (low GR values). Within the permafrost zone, the degree of freezing can depend on lithology and grain size and therefore GR is used with other logs to detect IBPF in porous sandstone intervals.

Spontaneous potential (SP): The SP log normally responds to changes in temperature or water salinity. In some cases, a SP drift has been observed to coincide with the established base of permafrost. Generally, SP is not a very reliable indicator of permafrost.

Mud logs

Mud logs are well logs prepared by describing rock cuttings brought to the surface by mud circulating in the borehole. It typically tracks drilling rate, i.e., rate of penetration (ROP), lithology, and gas hydrocarbon, as well as other drilling parameters (e.g., deviation surveys, weight on bit, etc.).

Drilling rate (rate of penetration, ROP)

ROP log is recorded at the wellsite as the well is being drilled. ROP log units are normally measured in minutes per foot and minutes or hours per meter, it is also expressed in feet per minute (meters per hour). ROP depends on many factors, which mainly include formation properties, mud rheology, weight on bit, bit rotation speed, type of bit, wellbore inclination and bit hydraulics. However, once a drilling routine is established with the rig steadily making hole, many of the mud, bit, and rig-floor variables become nearly constant or change systematically. Under these conditions, formation properties (rock type, porosity, compaction, and strength) primarily influence changes in ROP. Because ROP depends on formation hardness, it can be used to estimate the base of ice-bearing permafrost, and to confirm picks based on other techniques. For some wells in the study area, wireline logging was initiated near the base of, or below, the zone of IBPF, making it difficult to obtain reliable log-based interpretations of depth to the base of IBPF. For these cases, the drilling rates were used to help estimate this boundary.

A slowed drilling rate can indicate ice in pore space rather than water, but could also be a change to harder lithology. A higher drilling speed does not necessarily mean that there is no permafrost because thawing may have occurred in overgauged boreholes while drilling in porous and permeable sandstones, especially in unconsolidated sandstones with permafrost. These types of pitfalls were considered during ROP interpretations.

Gas logs and other information

Gas log entails gathering qualitative and semi-quantitative data from hydrocarbon gas detectors that record the level of natural gas brought up in the mud, mainly including total gas (TG), connection gas (CON), and heavier hydrocarbons (C_2 - ethane), C_3 - propane, C_4 - butane) which help to determine the type of oil or gas the formation contains. Gas log can be used to confirm gas hydrate interpretation.

Sometimes lithology and other information from mud log, well testing information from well history reports, and log analysis results were used to help confirm, or estimate the base of IBPF ($IBPF_F$ or/and $IBPF_P$).

As an example, Figure 6 shows responses from geophysical well logs and well seismic velocity to a geophysically interpreted permafrost zone that includes both a base of fully frozen $IBPF_F$ (174 m) and a base of partially frozen $IBPF_P$ (243 m) in the Drake Point K-79 well located on Melville Island. It is observed that resistivity logs (deep-ILD and shallow-SFL) respond with higher values in the interpreted IBPF zone. The sonic transit time curve (DT) shows very low values for most of the sandstone and siltstone zones, and caving is indicated in the sandstone and siltstone of the frozen zone by the density caliper log (CAX) and the difference between caliper (CAX) and bit size (BS) (see the yellow colored area in track 1 of Fig. 6). A sharp change in drilling rate (ROP, the light blue curve in track 1) confirms the picks based on wireline logs. Interval well seismic velocity (V_{INT}) gives a possible range of the base of fully frozen zone ($IBPF_F$, in the green coloured area in track 5). Figure 6 also shows a comparison of geophysical well logs and well seismic surveys for the upper 1000 m of the well. All available geophysical data included in this study used for IBPF determination and relevant interpretation of base of IBPF are listed in Figure 6.

Figure 7 illustrates a typical example in which borehole compensate sonic is successfully used to detect the base of IBPF for the Bar Harbour E-76 well on Banks Island, demonstrating that where permafrost occurs in sandstone with good porosity, the sonic log is a better method than resistivity logs.

Figure 8 shows that drilling rate (ROP, the blue curve in track 1) helps estimate the base of IBPF where wireline log signatures are ambiguous and well seismic velocity response are subtle in the permafrost zone for the Sabine Bay A-07 well located on Melville Island.

Figure 9 illustrates the possible base of $IBPF_F$ as estimated only from drilling rate (ROP, the blue curve in track 1) for the Hoodoo N-52 well on Ellef Ringnes Island while neither wireline logs nor well seismic survey was run for the shallow interval of the well.

The information shown in Figure 10 is from the well King Christian N-06 located on King Christian Island. The well includes conventional wireline logs (except the shallowest interval, <168 m), drilling rate (ROP), gas log (total gas), well testing, and limited check shot velocity data. For some shallow intervals, resistivity logs exhibit relatively higher values (the purple coloured areas in track 3), and sonic transit time values are a little bit lower (the purple coloured areas in track 4), in addition, abundant gas trips show in the total gas log (the orange curve in track 5). On the basis of a combination of well logs in conjunction with the gas log, and lithology interpretation, possible gas hydrate zones are identified throughout the Awingak Formation to Sandy Point Formation (in the blue coloured areas between track 3 and 4 in Figure 10), indicating that $IBPF_F$ may be in the shallowest zone (<168m), which is confirmed by drilling rate (ROP, the blue curve in track 1), and the base of partially frozen zone ($IBPF_P$) may be at 281 m in Deer Bay shale, characterized by a little bit higher resistivity, lower sonic transit time (Fig. 10). Log analysis indicates a free gas reservoir in Heiberg Formation (the red coloured area between track 3 and 4 in Figure 10), which is supported by well test result.

INTERPRETATION OF PERMAFROST THICKNESS

Lithology interpretation from well logs

In the Canadian Arctic Islands, the near-surface lithologies consist of sandstone, siltstone, shale, conglomerate and gravel for most of the well boreholes, but also include in some wells, carbonates (limestone and dolomite), evaporite (anhydrite and gypsum), igneous and metamorphic rocks, and coal beds. Sandstone and shale produce distinct geophysical and petrophysical characteristics in frozen and unfrozen states (Hnatiuk and Randall, 1977). However, it is difficult using the same methodologies to detect permafrost within carbonate, evaporite and igneous intervals. The identification of formation lithology is therefore fundamental to the accuracy and ability to detect permafrost.

Accurate lithology determination were performed by an integrated method of well log responses, related to core and sample descriptions, and by using commercial log-analysis software of PRIZM (LMKR GeoGraphix®). Lithology determinations were derived from interpretation of routine wireline logs such as gamma ray, density, photoelectric index, neutron, sonic, and resistivity. The identified lithologies mainly include sandstone, shale, limestone, calcareous sandstone, dolomite, anhydrite, gypsum, halite, chert, mica, pyrite, siderite, igneous rocks, carbonaceous rocks, and coal. Lithologies identified and logged in this study, and the symbols used to represent these are listed in Figure 5.

The gamma ray log is the main wireline tool used for distinguishing between shale and non-shale. Accordingly, the shale content in the study wells were derived from the gamma ray and neutron logs, with minimum shale-content values selected from the two log calculations. The gamma ray log produced the minimum values in most well sections, indicating that shale content (and not variations in sandstone mineralogy) controlled most of the gamma ray log responses.

The bulk density, sonic, and neutron logs and photoelectric index (PE) are used to differentiate other lithologies. The bulk density log is the most useful wireline tool for coal identification. Coal is characterized by low density values (as low as 1750 kg/m^3 or less) and high apparent porosity as reflected in the neutron log (most coals >52%; anthracite coal ~ 38%). In addition, the sonic transit time in coal beds is generally greater than 340 μs/m (>300 μs/m for deep coal units). Thick coal beds have high deep-resistivity values, but thin coal beds may have no obvious resistivity response. Evaporite rocks, such as anhydrite, gypsum, and halite, can be easily identified from a combination of density, neutron and sonic logs. Concentrations of heavy minerals (density>2900 kg/m^3), such as pyrite and siderite, can be identified from the photoelectric index (PE if available), density, sonic and other logs. Combining core and sample descriptions, mica, chert in sands, and other heavy minerals in granites can also be identified from various well logs, including spectral gamma ray, density, PE, and neutron. For example, halite has very low density (2040 kg/m^3), anhydrite has high density (2980 kg/m^3), and pyrite has very high density (4990 kg/m^3) and low sonic transit times (129 μs/m). PE is used to identify limestone and halite which have higher PE values (limestone 5.1 B/E; halite 4.7 B/E) than sandstone, dolomite, or anhydrite.

Integrated PF/IBPF interpretation using composite plots

As described above, accurate temperature survey data can provide the best estimate of the base of permafrost, which are only available in 32 wells in the Canadian Arctic Islands. Geophysical well logs were the main tool used to detect the base of ice-bearing permafrost because most of wells in the study area have well logs. Individual well log types, have unique responses to ice-bearing permafrost, but because frozen rock is a complex medium the relative accuracy can be improved by a multiproxy approach. Wireline logs are available in the shallow interval (≤1000 m) in 192 drilled exploration wells in the Canadian Arctic Islands. There are 136 wells with well seismic survey data (Table 2, Fig. 2), and 89 wells with drilling rate records (Table 3). This section presents the determination of the true base (0°C) isotherm that defines the lower extent of permafrost from temperature surveys, and base of ice-bearing permafrost from integrating of conventional wireline logs, drilling rate and well seismic velocity data.

A composite plot, consisting of temperature survey (if available), other various geophysical data (wireline logs, drilling rate, and well seismic surveys), and lithology interpretations from log analyses, are used to display the detailed interpretations of PF and IBPF. Ideally in any individual composite well plot, up to six tracks of wireline logs, drilling rate, well seismic and temperature survey data are plotted against depth from a kelly bushing (m KB) datum, to 1000 m, as shown in the Gemini E-10 well, Ellesmere Island (Fig. 11). The first 4 tracks are mainly well logs and can include sonic caliper curve (CALS, track 1), drilling rate (ROP, track 1), and bit size (BS, track 1); gamma ray curve (GR, track 2); DIL-LL8 resistivity logs (track 3), deep induction (ILD), medium (ILM) and shallow (LL8); track 4 contains borehole compensated sonic transit time (DT), bulk density (RHOB) and neutron porosity (NPss – neutron porosity calibrated with sandstone). Track 5 plots well seismic survey data (WSS); and track 6 shows the temperature surveys that mainly consists of the earliest and latest measurements and equilibrium calculations (if available). Track 7 illustrates the basic lithology interpretation for the shallow well interval. A stratigraphic column is included on the right side of track 8 to provide geological context. Most formations and their chronostratigraphic divisions that permafrost penetrated are listed in Figure 12, more complete stratigraphic context is described in previous publications (e.g., Beauchamp *et al.,* 2001; Dewing and Embry, 2007; Dewing *et al*., 2008; Embry, 1991, 2011; Hadlari *et al*., 2014).

According to interpreted lithology for the shallow interval (≤1000 m) of the Gemini E-10 well (Fig. 11), sandstone is the dominant lithology for Eureka Sound Formation; Kanguk Formation contains shale, sandstone and siltstone; Hassel Formation mainly consists of sandstone and siltstone; siltstone and shale are predominant in Christopher Formation. The temperature survey log identifies the base of permafrost (PF) at 508 m which is located in the base of siltstone of the upper Christopher Formation (track 6 and 7 in Fig. 11). Resistivity logs show a sharp change from high (>50 ohmm for the most sandy and silty zones) to low values (≤25 ohmm) with increasing depth at 461 m. Drilling time (min/ft) also exhibits a change from generally long to short at 461 m. A big step of V_{INT} in the well seismic velocity profile is observed (at 426 m depth) from high value (>3000 m/s) above 426 m (except shale interval) to low (<2500 m/s) below the depth, indicating an apparent change in lithology and a possible IBPF base range (green shaded range in Fig. 11). As a result, resistivity logs indicate the base of fully frozen zone ($IBPF_F$) is at 461 m, supported by drilling rate and well seismic velocity data (marked as a solid orange line in Fig. 11). Additionally, the defined $IBPF_F$ base is coincident with the casing shoe depth.

A transition zone from 461 m to 513 m, consisting of predominantly siltstone and shale, is observed in the Gemini E-10 well (Fig. 11), and exhibits a relatively low sonic transit time and slight higher resistivity (ILD, ILM, LL8), but variable seismic interval velocities. In this report the transition zone is labelled as partially frozen ice-bearing permafrost zone ($IBPF_P$), the base of which is also identified using well logs and seismic velocity survey data. The base of $IBPF_P$ (depth at 513 m) is marked by a dashed orange line in Figure 11. In this case, the base of permafrost (PF) determined by temperature surveys is at 508 m, between the base of fully frozen ice-bearing permafrost ($IBPF_F$) and the base of partially frozen ice-bearing permafrost ($IBPF_P$) from other geophysical methods, including wireline logs, drilling rate and well seismic velocity data.

Figure 13, Storkerson Bay A-15 well on Banks Island, is another example illustrating IBPF determination from geophysical well logs and PF interpretation from a temperature survey. Deep resistivity log (ILD) shows an obvious decrease from ≥100 to ≤ 20 ohmm at 501 m, marking a base of fully frozen zone within Eureka Sound Formation sandstone. A transition zone and the base of partially frozen base ($IBPF_P$) at 559 m within Eureka Sound Formation conglomerate are also defined by resistivity logs. The single temperature log did not fully penetrate the PF zone and was extrapolated to greater depth to provide an estimate of the base of permafrost at 505 m (Taylor and Judge, 1974; Taylor *et al.*, 1982).

IBPF determined from well logs and well seismic surveys

Geophysical well logs and well seismic velocity surveys are available for most of the petroleum exploration wells. Figure 6 shows an example of ice-bearing permafrost determination using geophysical well logs and well seismic velocity survey data for the Drake Point K-79 well which is located on Melville Island. As discussed above, the $IBPF_F$ zone is mainly characterized by extremely high resistivities, low sonic transit time and drilling speed, high neutron porosity, and an unstable oversized borehole. A sharp change occurs at 174 m on these logs, interpreting as the base of $IBPF_F$ (Fig. 6). An estimate, the possible range of IBPF base given by well seismic velocity data (Fig. 5b and Fig. 6), provides independent support for the fully frozen zone ($IBPF_F$) interpretation. A transition zone consisting of predominantly shale is observed from 174 m to 243 m. Beneath the $IBPF_F$ interval, there is a shift to higher sonic transit time, lower resistivity, stable and smaller borehole conditions, and higher drilling speed, but variable lower seismic interval velocity values within the interpreted $IBPF_P$ zone (Figs. 6 and 5b).

As another example, bases of $IBPF_F$ and $IBPF_P$ occurred within unconsolidated sandstones are identified from well logs and well seismic surveys for the West Pollux E-59 well on Ellef Ringnes Island (Fig. 14). The fully frozen zone (base of $IBPF_F$ at 386 m) is characterized by higher resistivity values (LN curve, track 3), lower sonic transit time values (DT, track 4), and higher interval seismic velocity values (V_{INT}, track 5 in Fig. 14). Whereas the base of $IBPF_P$ (at 511 m) is identified by an abrupt decrease in the caliper log and an obvious decrease on resistivity log. However, ROP shows higher drilling speed in the unconsolidated sandstones with ice-bearing permafrost zone in Eureka Sound Formation, indicating that thawing occurred and led to an unstable overgauged borehole identified by caliper log (yellow coloured area in track 1) while drilling was conducted.

IBPF determined from well logs

Where wells lack seismic and temperature surveys the base of IBPF is defined based on the various available well logs. Figure 15 shows an example for the Kitson River C-71 well, Melville Island, where a complete conventional log set is available, including caliper log, gamma ray log, spontaneous potential, resistivity logs, sonic transit time, bulk density and neutron logs. The base of fully frozen $IBPF_F$ (at 295 m) is characterized by a distinct decline and then pronounced flattening of the resistivity logs, coincident with the abrupt decrease in the caliper log, and notable change in neutron porosity and SP log. Sonic transit time, resistivity and caliper logs indicate that the base of partially frozen $IBPF_P$ zone is at 379 m within Bjorne Formation sandstone.

As an example, Figure 16 shows that an ice-bearing permafrost zone is interpreted from wireline logs, drilling rate and lithology interpretation in the Weatherall O-10 well located on Melville Island. Obviously resistivity logs (ILD, ILM, LL8) respond with notable high values to non-shale intervals above 230 m to lower values at greater depth, and the sonic transit time curve (DT) with depth shows an abrupt change from low to high values at 230 m, where a dashed black line is marked. However, lithology interpretation and drilling rate indicate that the base of $IBPF_F$ is at 214 m within Sabine Bay sandstone rather than at 230 m within Belcher Channel limestone, which is confirmed by wireline logs (with very high resistivity values and very low sonic transit time above 214 m), and is coincident with the casing shoe depth. A base of $IBPF_P$ (345 m) is also interpreted (Fig. 16).

PF/IBPF interpretation for the wells lack wireline logs in permafrost zone

In cases where wireline logs are not available in the shallow interval, accurate temperature survey data can provide the best estimate of the base of permafrost. Figure 17 shows the base of 0^0C permafrost at 148 m in the Hecla I-69 well, Melville Island, determined using calculated equilibrium temperatures from a series of temperature measurements. ROP log shows a decrease at 101 m of depth from a longer drilling time to shorter, indicating a possible fully frozen zone ($IBPF_F$, the purple coloured area in track 1 in Figure 17).

In other sites where only well seismic surveys and drilling rate are available, $IBPF_F$ can be estimated. In the North Sabine H-49 well on Melville Island, a notable sandstone zone with very high interval seismic velocities (from crystal cable) is observed. A sharp change occurs at 290 m on the interval velocity curve, where ROP log also shows a decrease of drilling time (minute per foot). As an estimation, the depth of 290 m is interpreted as the base of $IBPF_F$ (Fig. 18).

QUALITY ASSESSMENT FOR IBPF DETERMINATION

As described above, determinations of the base of permafrost (PF) based on shallow temperature direct measurements have the highest reliability. Temperature log-based records lead true equilibrium temperatures are considered of “A” quality. Furthermore, PF interpretations from temperature surveys are classified as “Aa” (excellent), “Ab” (good), “Ac” (fair) and “Ad” (poor). Identifications of ice-bearing permafrost IBPF based on other geophysical information are less reliable than estimates from temperature surveys, and they are considered less “B” in terms of quality.

Quality assessment for geophysical determination of IBPF

Geophysical information for IBPF determinations mainly includes geophysical well logs (wireline logs and drilling rate) and well seismic surveys. The geophysical methods have different investigation depths, vertical resolutions, and sensitivities to the boundary and transition from unfrozen to frozen zone. Wireline logs have the highest vertical resolution. This study shows that resistivity logs are the best indicator to IBPF followed by caliper and sonic logs, and then drilling rate and relatively lower vertical resolution seismic velocity surveys. However, interval velocity data from crystal cable survey has higher vertical resolution than check shot due to a smaller sample interval (15.24 m), therefore, combining with quality drilling rate, it may assist in IBPF interpretation when overgauged borehole occurs that reduces log responses to IBPF or well logs are absent for some wells.

IBPF interpretations based on geophysical well logs and well seismic surveys are classified as "Ba" (high reliability), "Bb" (medium reliability), and "Bc" (low reliability):

Ba – high reliability, from one of two cases

(1) Resistivity logs show a sharp change from high values to low values at the base of fully frozen (IBPF$_F$) or/and partially frozen (IBPF$_P$) probably individually or it is supported by other well logs and other methods (e.g., IBPF$_F$ identification in Fig. 6 and Fig. 15);

(2) Sonic log shows a remarkable change at the base of fully frozen (IBPF$_F$) or/and partially frozen (IBPF$_P$), and it is supported by resistivity and other logs (e.g., IBPF$_P$ detection in Figs. 7 and 15, and determination of base of IBPF$_F$ in Fig. 19).

Bb – medium reliability, from one of the cases

(1) A remarkable change is not observed on single resistivity log or/and sonic log at the base of IBPF$_F$ or/and IBPF$_P$, but the base can be estimated from a combination of well logs and well seismic surveys (e.g., IBPF$_P$ identifications in Fig. 11).

(2) The base of IBPF is defined by multiple geophysical parameters because the result from resistivity logs differs with respect to other wireline logs or/and the seismic velocity survey or/and drilling rate (e.g., base of IBPF$_F$ is defined by resistivity logs in Fig. 20; the defined base of IBPF$_F$ is mainly based on ROP and WSS rather than wireline logs in Fig. 21);

(3) The base of IBPF$_F$ or/and IBPF$_P$ cannot be determined by wireline logs because more than one obvious change from high values to low values in resistivity log are observed, other information such as ROP and gas log assist in IBPF base identification (e.g., IBPF$_F$ identification in Fig. 22);

(4) Wireline logs (resistivity or/and sonic or/and caliper) shows vague response to the base of IBPF, but well seismic and/or drilling rate exhibits notable change (Fig. 8);

(5) Both quality interval seismic velocity (V_{INT}) from crystal cable survey and drilling rate (ROP) give consistent estimation of the base of IBPF where lack wireline logs in the ice-bearing permafrost zone (e.g., $IBPF_F$ determination in Fig. 18).

Bc – low reliability, from one of the cases

(1) Well logs and well seismic survey show vague response to the base of IBPF, which is estimated but uncertain (Fig. 23);

(2) Limited check shot velocity data and ROP are used to estimate the base of IBPF because no wireline logs data are available in permafrost zone (Fig. 24);

(3) Only well seismic survey data is used to estimate the base of IBPF because no wireline log data or quality ROP data are available in permafrost zone (Fig. 25);

(4) Approximation for the base of IBPF is estimated only from drilling rate because no wireline logs or well seismic survey data are available (Fig. 9).

For interval with permafrost zone in the study area, the resistivity may take a wide range of values, therefore, it is usually presented on a logarithmic scale from, for example, 0.2 to 2000 ohmm. However, for some wells, a linear-scaled resistivity log is better to illustrate the response to ice-bearing permafrost. As an example, Figure 26 displays deep resistivity (LLD/ILD) readings on both logarithmic scale (the dashed light blue curve in track 3) and linear scale (the solid dark blue curve in track 3) throughout the same interval of ice-bearing permafrost zone in the Beverley Inlet G-13 well on Melville Island. Obviously, the linear-scaled deep resistivity log improved its visualization of the response to the base of $IBPF_F$, providing a better $IBPF_F$ interpretation (with quality "Ba"; marked by the solid orange line in Fig. 26) than that from log-scaled LLD (with quality "Bb"; marked by the dashed black line in Fig. 26).

Comparison of thermally defined PF and IBPF from other geophysical methods

Table 4 and Figure 27 show a comparison of the depth to base of permafrost (PF) derived from temperature surveys and the base of IBPF determined from other geophysical methods (wireline logs, well seismic surveys and drilling rate). In Figure 27, the qualities of PF data are differed by symbols: dot represents quality "Aa" data, square is for quality

“Ab” data, circle stands for quality “Ac” data, and triangle is for quality “Ad” data. The qualities of IBPF data are distinguished by colors: blue is for quality “Ba” data, green is for quality “Bb” data, and pink denotes quality “Bc” data. There is a relationship between the temperature-defined PF with “Aa”, “Ab” and “Ac” quality (“Ad” quality data – circled points are excluded) and the $IBPF_F$ with “Ba”, “Bb”, and “Bc” quality determined from other geophysical methods (Fig. 27a). A better relation exists between the base of PF defined by temperature surveys (“Ad” quality data – circled point is excluded) and the base of $IBPF_P$ from other geophysical methods (Fig. 27b).

The results in Fig. 27a show that the depth to the 0°C isotherm falls below the depth of ice at the base of $IBPF_F$ estimated from other geophysical methods with the exception of one point with poor quality PF. Disregarding 2 points with “Ad” quality PF, the difference between base of $IBPF_F$ and base of PF ranges from 2.2 m (the Winter Harbour No.1 well on Melville Island, Fig. 1-19 in Appendix 1), and up to 154 m (the Drake Point D-68 well on Melville Island, Fig. 1-22 in Appendix 1). It appears that the difference between the two bases ($IBPF_F$ and PF) slightly decreases with increasing depth (Fig. 27a). As an exception, the $IBPF_F$ base is below PF base by 88 m in the Devon E-45 well on Devon Island, for which the PF is from poor quality of temperature surveys (the circled triangle point on the right side of Fig. 27a). Excepting one point from the Devon E-45 well, estimated base of partially frozen zone ($IBPF_P$) is much closer to PF base (Fig. 27b) than $IBPF_F$ base (Fig. 27a), but slightly below the base of permafrost (PF) in most of the wells.

In Fig. 27c which illustrates geophysical-defined $IBPF_F$ bases and temperature records, the data points can be categorized three zones by lithology (I- shale, II - siltstone, and III – sandstone) because only one point is from other lithology - dolomite. Zone I, which contains 11 points, illustrates that within shale formations, the base of $IBPF_F$ occurs at temperatures between -6.72~-4.18°C, and the base depth of $IBPF_F$ mainly ranges from 102~238 m (one dolomitic and silty tight shale is exceptional, Fig. 27c). Zone II represents records of $IBPF_F$ base located in fine siltstone with a depth range from 251~479 m, for which temperature logs indicate between -3.89 and -3.08°C, which contains only 4 points. In Zone III with 9 points, the base of $IBPF_F$ occurs within sandstones at depths from 359~682 m, and corresponds to temperature logs of between -2.3~-0.08°C (Fig. 27c). It is evident that the freezing point ranges from -0.08°C in sandstone to -6.72°C in shale, and notable freezing point depression occurs in fine-grained siltstone and shale (Fig. 27c). This is because depression of the freezing point of pore water which is a function of pressure, chemical and formation particle effects (Smith and Burgess, 2002; Collett *et al*., 1988; Hardy, 1984; D&S Petrophysical, 1983) is related to multiple issues such as free water content mainly depends on formation porosity, permeability and water saturation; formation water salinity; lithology; and grain type, size and texture. In coarse-grained sandstones with high effective porosity, high permeability and free water content, the freezing point mainly varies due to pore water salinity, and ranges from -2°C to 0 in the study area (Fig. 27c), providing a similar result in the Beaufort-Mackenzie Basin (Hu, *et al*. 2013). However, fine-grained shales exhibit high surface areas and contain a large amount of clay bound water and a small amount of effective porosity and free water content, in which the freezing point of water is depressed by up to 7 degrees Celsius. Siltstones have more effective porosity than shales and are more affected by freezing than shales. Therefore, it takes a much lower temperature to freeze shale and siltstone completely than it does to freeze highly porous sandstone.

On the other hand, defined base of partially frozen ($IBPF_P$) from geophysical methods are predominantly located in shale, siltstone and sandstone, with a temperature range from -2.07~2.12°C (Fig. 27d). The depth of $IBPF_P$ base located at shale ranges from 202~452 m (the black dashed lines in Zone I of Fig. 27d). For all the non-shale points downward deeper base of the $IBPF_P$, their temperature values are in a narrow range, -0.17~2.43°C, including one point with mixed shale and siltstone, fewer data points located at fine-grained siltstone (Zone II), one point in dolomitic and silty tight shale, one point with conglomerate, and two points are in sandstone - Zone III (Fig. 27d). About 87% of the 23 records of ($IBPF_P$) have a temperature range -0.17~2.12°C (between the orange dashed lines in Fig. 27d).

PF/IBPF interpretation

The base of permafrost (PF) is determined using repeat temperature surveys (if available) for a given well. Interpreted depths to base of IBPF are determined using other geophysical relevant data, which may include wireline logs (resistivities, caliper, sonic transit time, neutron porosity, spontaneous potential, and bulk density), drilling rate (ROP), well seismic surveys (WSS), and other supplementary information (such as sample and core descriptions, gas log, well testing) from well history reports, in addition to log analysis results in this study (such as interpreted lithology, possible hydrate information and potential hydrocarbon zones).

The depths to base of true permafrost (PF) are compiled for 32 wells, with 19 wells of "Aa" quality, 4 wells of "Ab" quality, 6 wells of "Ac" quality, and 2 wells of "Ad" quality. Base of ice-bearing permafrost (IBPF) is interpreted for 140 wells in the study area. Over 81% of the IBPF$_F$ determinations are of "Ba" (49 wells, 35%) or "Bb" (65 wells, >46%) quality, whereas 26 wells (<19%) have "Bc" quality. Partially frozen zone (IBPF$_P$) occurs in 106 wells, in which 13 wells have "Ba" quality, 75 wells have "Bb" quality, and 18 well have "Bc" quality.

Figure 28 shows the distributions of base of PF (if available), base of fully frozen (IBPF$_F$) and partially frozen (IBPF$_P$) for 143 wells across the Canadian Arctic Islands. Depth to the base of PF, IBPF$_F$ and IBPF$_P$ ranges from 143 m to 726 m below GL in 31 onshore wells (except 40 m below SF in one offshore well), 37 m to 843 m below GL in 140 onshore wells, and 184 m to 779 m below GL in 106 onshore wells, respectively. 93 wells (>65%) of the defined IBPF$_F$ and PF bases occur in Mesozoic strata, distributing in sandstones, siltstones and shales except one well in conglomerate. 62 wells of IBPF$_F$ and PF bases are located in Cretaceous strata. Base of IBPF$_F$ and PF is encountered in Paleozoic sandstone, siltstone and shale in 41 wells, and in carbonates in 7 wells located in Victoria, Prince Wales, Somerset, Cornwallis, Bathurst and Melville islands. Among the 106 wells with partially frozen zones, 67 wells (63%) of defined IBPF$_P$ bases occur in Mesozoic strata, and 41 wells of IBPF$_P$ bases are located in Cretaceous strata. IBPF$_P$ base is encountered in Paleozoic succession in 37 wells. Both IBPF$_F$ and IBPF$_P$ bases also occur within highly porous sandstone of the Miocene-Pliocene Beaufort Formation in the Crocker I-53 well located on Meighen Island and the Isachsen J-37 well on Ellef Ringnes Island.

Table 5 provides full details of the determination of the depth to the base of permafrost (PF, if available) and IBPF from geophysical methods for this study, which includes four parts: 1) basic well information, such as UWI, well short name, ground elevation, kelly bushing, well location with latitude and longitude, island the well located; 2) PF interpretation result from temperature surveys, mainly including base of PF, quality rank, formation age and lithology PF located in, 3) ice-bearing permafrost (IBPF) thickness interpretation result from geophysical methods (well logs and well seismic surveys), including fully frozen zone and partially frozen zone, and the quality rank of the base determination, the formation age and lithology at the base of $IBPF_F$ and $IBPF_P$, the thickness of transition zone, as well as the figure number in Appendix which illustrates a composite plot and detailed PF/IBPF interpretation; and 4) IBPF results from previous studies, mainly including IBPF result from Panarctic Oils seen in Canadian National Energy Board (NEB) well history files, and Hardy & Associates Ltd. in 1984. However, the IBPF determinations for 7 offshore and 3 onshore wells from Hardy and Associates (1984) are not included in Table 5 for comparison because none of the IBPF picks is evidenced by an integrate analysis of various geophysical data and lithological interpretations.

Appendix 1 includes wells with temperature logs which show the base of permafrost (PF) identified by the 0°C isotherm for 32 wells, ordered from "Aa" quality to "Ad" quality, from Fig. 1-1 for well Bent Horn F-72/A on Cameron Island to Fig. 1-32 for the Garnier O-21well on Somerset Island. Other information contained in a composite plot are also shown, indicating IBPF interpretation for comparison. Appendix 2 illustrates IBPF defined from geophysical methods for 49 wells in which all fully frozen ($IBPF_F$) picks are "Ba" quality, ordered by well names, from Fig. 2-1 for the Andreasen L-32 well on Prince Patrick Island, to Fig. 2-47 for the Young Inlet D-21 well on Bathurst Island. Appendix 3 illustrates geophysical-defined IBPF for 65 wells in which all fully frozen ($IBPF_F$) picks are "Bb" quality, ordered by well names, from Fig. 3-1 for the Allison River N-12 well on Bathurst Island to Fig. 3-64 for the Zeus F-11 well on Melville Island. Appendix 4 illustrates geophysical-defined IBPF for 26 wells in which all fully frozen ($IBPF_F$) picks are "Bc" quality, ordered by well names, from Fig. 4-1 for the Blue Fiord E-46 well on Ellesmere Island to Fig. 4-26 for the Young Bay F-62 well on Prince of Wales Island.

CONCLUSIONS

The depths to the base of permafrost (PF) and/or ice-bearing permafrost (IBPF) are presented for 143 exploration wells (142 onshore and 1 offshore) in the Canadian Arctic Islands. The base of thermally defined PF and data quality are compiled for 32 wells, which varies from 143 m to 726 m below GL in 31 onshore wells, and 40 m below SF in one offshore well, and distributes in shale, siltstone, sandstone and carbonates. Based on other geophysical methods (geophysical well logs and well seismic surveys), the fully frozen zone ($IBPF_F$) in 140 onshore wells and partially frozen zone ($IBPF_P$) in 106 onshore wells are detected, and their quality assessments are analyzed across the study area.

Notable changes in electrical and acoustic properties, borehole size, and drilling rate can mark the base of the interpreted fully frozen zone ($IBPF_F$) and/or partially frozen zone ($IBPF_P$), and available well seismic surveys show good agreement with the IBPF determination from well logs for most of the wells. Depth to the base of $IBPF_F$ ranges from 37 m to 843 m below GL and occurs in sandstones, siltstones, shales and conglomerate in Mesozoic succession in 90 wells, and in Paleozoic sandstones, siltstones and carbonates in 48 wells. Whereas the depth to the base of $IBPF_P$ varies from 184 m to 779 m below GL, and it is confined to Mesozoic siltstones, shales, sandstone and conglomerate in 67 wells, and Paleozoic siltstone, sandstone, shales and carbonates in 37 wells. Defined $IBPF_F$ and $IBPF_P$ bases also occur in highly porous sandstone of the Miocene-Pliocene Beaufort Formation in 2 wells. The thickness of the defined transition zone, in which ice and unfrozen water may coexist, varies from 9.5 to 170 m in the 106 wells.

A correlation between the base of true permafrost (PF) thermally defined at 0°C, and the base of ice-bearing permafrost (IBPF) derived using geophysical methods demonstrates that borehole geophysical methods can predict ice-bearing permafrost distribution, including fully frozen zone ($IBPF_F$) and partially frozen zone ($IBPF_P$), especially for the wells that lack temperature surveys.

ACKNOWLEDGEMENTS

The authors would like to thank Drs. Rod Smith and Zhuoheng Chen for their comprehensive reviews of this report and giving valuable comments and suggestions that have greatly improved the report. We are especially thankful to Drs. Alan Taylor and Alan Judge for their detailed discussions about temperature surveys on the Cape Allison C-47 and Fosheim F-27 wells. Thanks also to Dr. Ashton Embry for providing advice on stratigraphy. This study is supported by Western Arctic project of the GEM program.

REFERENCES

Anderson, D.M. and Morgenstern, N.R., 1973. Physics, chemistry and mechanics of frozen ground: A review. Proceedings, Second International Conference on Permafrost, Yakutsk, U.S.S.R., July 1973, North American Contribution, U.S. National Academy of Sciences, Washington, D.C., p. 257-288.

Beauchamp, B., Harrison, J.C., Utting, J., Brent, T.A., and Pinard, S., 2001. Carboniferous and Permian subsurface stratigraphy, Prince Patrick Island, Norwest Territories, Canadian Arctic. GSC Bulletin 565.

Brent, T.A. and Harrison J.C., 1998. Characterization and mapping of the permafrost zone on land based seismic reflection data, Canadian Arctic Islands. Permafrost: Seventh International Conference, Yellowknife, Canada, proceedings and abstracts; Lewkowicz, A G (ed.); Allard, M (ed.). Collection Nordicana No. 57, 2000, p. 83-88; 1 CD-ROM (GSC Cont. # 1997171).

Collett, T. S., K. J. Bird, K. A. Kvenvolden, and L. B. Magoon, 1988. Geologic interrelations relative to gas hydrates within the North Slope of Alaska. U.S. Geological Survey, Open File Rep., 88-389, 150 pp.

D & S Group, 1983. Study of Well Logs in the Mackenzie Delta-Beaufort Sea Area to Outline Permafrost Thickness and/or Gas Hydrate Occurrence. Earth Physics Branch Open file No.83-10.

Dewing, K; Embry, A F., 2007. Geological and geochemical data from the Canadian Arctic Islands. Part I: Stratigraphic tops from Arctic Islands' oil and gas exploration boreholes. Geological Survey of Canada, Open File 5442, 1 CD-ROM, https://doi.org/10.4095/223386

Dewing, K., Mayr, U., Harrison, J.C., and de Freitas, T., 2008. Upper Neoproterozoic to Lower Devonian stratigraphy of northeast Ellesmere Island, *in* Mayr, U., ed., Geology of Northeast Ellesmere Island Adjacent to Kane Basin and Kennedy Channel, Nunavut. Geological Survey of Canada Bulletin 592, p. 31–108.

Durham, G.N. and Marr, W.A., editors, 1999. Field instrumentation for soil and rock. American Society for Testing and Materials. STP; 1358. ISBN 0-8031-2604-2 P. 273~279.

Dyke, A S., 2004. An outline of North American deglaciation with emphasis on central and northern Canada *in* Developments in Quaternary Sciences, Quaternary Glaciations-Extent and Chronology: Part II: North America, (J. Ehlers and P.L. Gibbard, Eds.) Vol. 2, Part B, Pages 373-424.

Embry, A.F., 2011. Petroleum prospectively of the Triassic-Jurassic succession of Sverdrup Basin, Canadian Arctic Archipelago, Chapter 36, in Spencer, A.M., Embry, A.F., Gautier, D.L., Stoupakova, A.V. & Sϕrensen, K.(eds), 2011. Arctic Petroleum Geology. Geological Society, London, Memoirs, 35, p. 545-558.

Embry, A.F., 1991. Geology of the Innuitian Orogen and Arctic platform of Canada and Greenland, chapter 10: Middle-Upper Devonian clastic wedge of the Arctic Islands.

Geology of North America, Vol. E. p.263-279.

Hadlari, T., Davis, W.J., and Dewing, K., 2014. A pericratonic model for the Pearya terrane as an extension of the Franklinian margin of Laurentia, Canadian Arctic. Geological Society of America Bulletin. https://doi.org/10.1130/B30843.1

Hardy Associates (1978) Ltd., 1984. Study of well logs in the Arctic Islands to outline permafrost thickness and/or gas hydrate occurrence. Earth Physics Branch Open files Report 84-8. Energy Mines and Resources Canada.

Hatlelid, W.G. and MacDonald, J.R., 1982. Permafrost determination by seismic velocity analyses. Journal of the Canadian Society of Exploration Geophysicists, Vol. 18, No.1, p. 14-22.

Heginbottom, J.A., Dubreuil, M.A. and Harker, P.A., 1995. Canada - Permafrost, *In*: National Atlas of Canada, 5th Edition, National Atlas Information Service, Natural Resources Canada, MCR 4177.

Hivon, E.G. and Sego, D.C., 1995. Strength of frozen saline soils. Canadian Geotechnical Journal, Vol. 32, p. 336–354.

Hnatiuk, J. and Randall, A.G., 1977. Determination of permafrost thickness in wells in northern Canada. Canadian Journal of Earth Sciences, Vol. 14, p. 375-383.

Hu, K., Issler, D.R., Chen, Z., and Brent, T.A., 2013. Permafrost investigation by well logs, and seismic velocity and repeated shallow temperature surveys, Beaufort-Mackenzie Basin. Geological Survey of Canada, Open File 6956, 33 p. https://doi.org/10.4095/293120

Jessop, A. M., Allen, V. S., Bentkowski, W, Burgess, M., Drury, M., Judge, A. S., Lewis, T., Majorowicz, J., Mareschal, J. C., Taylor, A. E., 2005. The Canadian geothermal data compilation. Geological Survey of Canada, Open File 4887, 1 CD-ROM, https://doi.org/10.4095/220364

Johansen, T.A., Digranes, P., Schaack, M.V., and Lonne, I., 2003. Seismic mapping and modeling of near-surface sediments in polar areas. Geophysics, Vol. 68, No.2 (March-April 2003); p.566-573.

Judge, A.S., 1973. The Prediction of Permafrost Thickness. Canadian Geotechnical Journal, Vol. 10, p. 1-11.

Judge, A.S., Pelletier, B.R. and Norquay, I., 1987. Permafrost base and distribution of gas hydrates. *In*: Marine Science Atlas of the Beaufort Sea: Geology and Geophysics / B.R. Pelletier (ed.). Geological Survey of Canada, Miscellaneous Report 40, p. 39. https://doi.org/10.4095/126969

Judge, A.S., Taylor, A. E. and Burgess, M., 1979a. Canadian Geothermal Data Collection - Northern Wells 1977-78. Earth Physics Branch, Geothermal Series No. 11.

Judge, A.S., Taylor, A.E. and Rutledge, L., 1979b. Canadian Geothermal Data Collection- Northern Wells 1977-78. Earth Physics Branch, Open File 79-13.

Judge, A.S., Taylor, A.E., Burgess, M. and Allen, V.S., 1981. Canadian Geothermal Data Collection - Northern Wells 1978-80. Earth Physics Branch, Geothermal Series

No.12.

Judge, A.S., Taylor, A.E., Duguid, A., Allen, V.S., Hill, M., Woodroffe, D., Harrington, J., Beaudais, D., and Uhrich, I., 1987. Automatic data acquisition system installed in offshore Canadian Arctic well: Monitoring precise temperatures by acoustic telemetry. Marine technology society and IEEE ocean engineering society, Halifax, N.S. Vol. 1, pp.156-160 (1987).

King, M.S., Zimmerman, R.W., Corwin, R.F., 1988. Seismic and electrical properties of unconsolidated permafrost. Geophysical Prospecting 36, 349–364.

Lachenbruch, A.H. and Brewer, M.C., 1959. Dissipation of the temperature effect in drilling a well in arctic Alaska. U.S. Geological Survey Bulletin 1083-C, p.73-109.

MacAulay, H.A., Judge, A.S., Hunter, J.A., Burgess, M., Gagné, R.M., Allen, V.S. and Burns, R.A., 1979. A study of sub-seabottom permafrost in the Beaufort Sea-Mackenzie Delta by hydraulic drilling methods, Spring 1978. Geological Survey of Canada, Open File 624 and Earth Physics Branch, Open File 79-11, 46 p., https://doi.org/10.4095/8358

Moorman, B.J., Robinson, S.D., Burgess, M.M., 2003. Imaging periglacial conditions with ground-penetrating radar. Permafrost and Periglacial Processes 14, 319–329.

Palacky, G.J. and Stephens, L.E., 1992. Detection of subbottom ice-bonded permafrost on the Canadian Beaufort Shelf by ground electromagnetic measurements. Geophysics, Vol. 57, No. 11, p. 1419-1427.

Permafrost Subcommittee, 1988. Glossary of Permafrost and Related Ground-Ice Terms. National Research Council of Canada. Technical Memorandum No. 142, 156 p.

Smith, S.L. and Burgess, M.M., 2002. A digital database of permafrost thickness in Canada. Geological Survey of Canada, Open File 4173, 38 pages; 1 diskette, https://doi.org/10.4095/213043

Stevens, C.W., Moorman, B.J. and Solomon, S.M., 2008. Detection of Frozen and Unfrozen Interfaces with Ground Penetrating Radar in the Nearshore Zone of the Mackenzie Delta, Canada. *In*: Ninth International Conference on Permafrost, v. 2. D.L. Kane and K.M. Hinkel (eds.). Institute of Northern Engineering, University of Alaska Fairbanks, p. 1711-1716.

Taylor, A.E. and Judge, A.S., 1974. Canadian Geothermal Data Collection - Northern Wells 1955 to February 1974. Earth Physics Branch, Geothermal Series no. 1.

Taylor, A.E. and Judge, A.S., 1975. Canadian Geothermal Data Collection - Northern Wells 1974. Earth Physics Branch, Geothermal Series no. 3.

Taylor, A.E. and Judge, A.S., 1976. Canadian Geothermal Data Collection - Northern Wells 1975. Earth Physics Branch, Geothermal Series no. 6.

Taylor, A.E. and Judge, A.S., 1977. Canadian Geothermal Data Collection - Northern Wells 1976-77. Earth Physics Branch, Geothermal Series no. 10.

Taylor, A.E., Burgess, M.M., Judge, A.S. and Allen, V.S., 1982. Canadian Geothermal Data Collection – Northern Wells 1981. Earth Physics Branch, Geothermal Series no.13, 153 p., https://doi.org/10.4095/8274

Taylor, A.E., Allen V., and Judge A., 1985. Installation of a multithermistor cable and data acquisition system at Panarctic *et al.* Cape Allison C-47 offshore well, Arctic Islands. Earth Physics Branch, Gravity, Geothermics and Geodynamics, internal report 85-19.

Taylor, A.E., and Judge A., 1986. Monitoring temperatures in an offshore Arctic well: A brief note. The Northern Engineer, Vol. 17, No.2.

Taylor, A.E., Judge A., and Allen V., 1989. The automatic well temperature measuring system installed at Cape Allison C-47, offshore well, Arctic Islands of Canada. Part 2 – data retrieval and analysis of the thermal regime. The Journal of Canadian Petroleum Technology, March-April 1989, Vol. 28, No.2.

Taylor, A.E., and Wang, K., 2008. Geothermal inversion of Canadian Arctic ground temperature and effect of permafrost aggradation at emergent shorelines. Geochem. Geophys. Geosyst., 9, Q07019, https://doi.org/ 10.1029/2008GC002064.

Thurber Consultants Ltd., 1988. Update of well log studies Mackenzie Delta/Beaufort Sea area, Arctic Islands and offshore East Coast, Vol. 1: Arctic Canada; Prepared for supply and services Canada on behalf of Geological Survey of Canada, Energy Mine and Resources Canada, SSC File: 692SZ.23233-7-0925.

Thurber Consultants Ltd., 1986. Study of well logs in the Mackenzie Delta/Beaufort Sea area, Arctic Islands to outline permafrost thickness and/or gas hydrate occurrence: An update of wells; Prepared for DSS on behalf of Earth Physics Branch, Energy Mine and Resources Canada, DSS File: 15SQ.23235-5-1145.

van Everdingen, R., editor, 1998 revised May 2005. Multi-language glossary of permafrost and related ground-ice terms. Boulder, Colorado, National Snow and Ice Data Center.

Walker, J.H.D. and Stuart, A.J., 1976. Permafrost investigations by crystal cable surveys, Mackenzie Delta, NWT. Journal of the Canadian Society of Exploration Geophysicists, v. 12, no. 1, p. 38-55.

LIST OF TABLES

LIST OF FIGURES

responses are subtle in the permafrost zone for the Sabine Bay A-07 well on Melville Island in the Canadian Arctic Islands.

9. Base of $IBPF_F$ is estimated only from drilling rate for the Hoodoo N-52 well on Ellef Ringnes Island in the Canadian Arctic Islands.

10. Estimation of IBPF from wireline logs, drilling rate, gas log and other well information for the King Christian N-06 well located on King Christian Island in the Canadian Arctic Islands.

11. Determinations of base of PF from temperature surveys, and IBPF ($IBPF_F$ and $IBPF_P$) from geophysical well logs and well seismic surveys for the Gemini E-10 well on Ellesmere Island in the Canadian Arctic Islands.

12 Stratigraphic chart of Canadian Arctic Islands.

13. Estimations of base of PF from temperature surveys, and IBPF using geophysical well logs for the Storkerson Bay A-15 well on Banks Island in the Canadian Arctic Islands.

14. Example showing that bases of $IBPF_F$ and $IBPF_P$ are identified from geophysical well logs and well seismic surveys for the West Pollux E-59 well on Ellef Ringnes Island in the Canadian Arctic Islands. In the unconsolidated sandstone interval with permafrost zone, ROP responded with a high speed of drilling rate since thawing occurred and led to an unstable overgauged borehole.

15. Determinations of base of $IBPF_F$ and $IBPF_P$ using geophysical well logs for the Kitson River C-71 well on Melville Island in the Canadian Arctic Islands.

16. Example showing that lithology interpretation and drilling rate assist in determination of the base of IBPF from wireline logs for the Weatherall O-10 well on Melville Island in the Canadian Arctic Islands.

17. Example showing that accurate temperature survey data provide the best estimate (with quality "Aa") of the base of permafrost (PF), a possible base of $IBPF_F$ with quality "Bc" is estimated from ROP log for the Hecla I-69 well that lacks wireline logs in the permafrost zone, on Melville Island in the Canadian Arctic Islands.

18. Example showing determination of the base of $IBPF_F$ from crystal cable surveys and drilling rate (ROP) for the North Sabine H-49 well on Melville Island in the Canadian Arctic Islands.

19. Example showing a remarkable response to base of $IBPF_F$ on sonic log and is supported by other well logs for the Wallis A-73 well on King Christian Island in the Canadian Arctic Islands.

20. Example showing $IBPF_F$ and $IBPF_P$ interpretation with quality "Bb" for the Halcyon O-16 well on Ellesmere Island in the Canadian Arctic Islands. Defined base of $IBPF_F$ by resistivity logs (the solid orange and dashed black lines) differs with respect to sonic log (the dashed purple line), ROP (the dashed light blue line) and well seismic surveys (the green coloured area).

21. Example showing $IBPF_F$ interpretation with quality "Bb" for the Dome Bay P-36 well on Ellef Ringnes Island in the Canadian Arctic Islands. Defined base of $IBPF_F$ (the solid orange line) is based on ROP (the dashed black line) and WSS (the green

coloured area) rather than wireline logs (RT and DT, the dashed purple line) that were badly affected by borehole rugosity and washouts as indicated by caliper log and the difference between caliper and borehole size (in the yellow coloured area) in track 1.

22. $IBPF_F$ interpretation with quality "Bb" is based on multiple information, including wireline logs, mud logs (ROP in track 1 and gas log in track 5), well seismic velocity, and possible gas hydrate interpretation for the Hearne F-85 well on Melville Island in the Canadian Arctic Islands.

23. Example showing uncertain base of $IBPF_F$ with "Bc" quality is estimated using geophysical methods for the Blue Fiord E-46 well on Ellesmere Island in the Canadian Arctic Islands.

24. Base of $IBPF_F$ with Bc" quality is estimated from drilling rate and well seismic surveys for the Collingwood K-33 well on Melville Island in the Canadian Arctic Islands.

25. Example showing bases of $IBPF_F$ and $IBPF_P$ with "Bc" quality are estimated only from well seismic surveys for the Vesey A-27 well on Vesey Hamilton Island in the Canadian Arctic Islands.

26. Example shows deep resistivity (LLD) readings on both logarithmic and linear scales throughout the same interval of ice-bearing permafrost zone, indicating that linear-scaled LLD display (the solid dark blue curve in track 3) improves visualization of the response to the base of $IBPF_F$ and gives a better $IBPF_F$ interpretation (with quality "Ba"; the solid orange line) than log-scaled LLD (the dashed light blue curve in track 3) for the Beverley Inlet G-13 well on Melville Island in the Canadian Arctic Islands.

27. Comparison of 0^0C permafrost base (PF) from "Aa", "Ab", "Ac" and "Ad" quality temperature surveys and base of IBPF (with "Ba", "Bb" and "Bc" quality) from other geophysical methods in the Canadian Arctic Islands.

28. Base map indicating base of permafrost (PF), base of fully frozen zone ($IBPF_F$) and partially frozen ($IBPF_P$) for the petroleum exploration wells in the Canadian Arctic Islands.

APPENDICES

Appendix 1 (Figs. 1-1 to 1-32)

Appendix 2 (Figs. 2-1 to 2-47)

Appendix 3 (Figs. 3-1 to 3-64)

Appendix 4 (Figs. 4-1 to 4-26)

Table 1. Base of permafrost (0°C isotherm) from temperature surveys in the Canadian Arctic Islands

Basic well information				Base of permafrost (0°C isotherm)		Frozen Base	Trans. Zone	Distance to waterbody	Rig release	The date of latest log run	Period between latest log run and drilling stop	Quality	Comments
UWI	Well name	LAT	LONG	PF (m KB)	PF (m GL/SF)	IBPF (m GL)	PF-IBPF (m)	(km)	yyyy-mm-dd	yyyy-mm-dd	(Month)		
302F727630103300	BENT HORN F-72A	76.358333	-103.972498	666.7	660			2	1975-12-19	1980-05-16	>52	Aa	
300N727630103300	BENT HORN N-72	76.364943	-103.971666	733.7	726	680±15	46	2	1974-04-05	1979-05-27	>60	Aa	
300I207800114300	BROCK I-20	77.995242	-114.567451	428.9	422			5	1972-06-28	1977-05-18	>58	Aa	
300C477750100000	CAPE ALLISON C-47*	77.768056	-100.288889	295	40			-8**	1985-05-08	1985-11-23	>6	Ab	quality is uncertain
300O307730094300	CORNWALL O-30	77.497294	-94.650227	374.8	365			2	1979-10-15	1980-05-15	7	Ab	EQ log is not available
300L417450094300	CORNWALLIS RESOLUTE BAY L-41	74.678557	-94.744606	603.9	600			1.3	1963-12-15	1973-04-27	>112	Ac	
300E457510091300	DEVON E-45	75.073275	-91.805993	607.6	600			1.6	1972-03-05	1980-05-14	>98	Ad	too shallow
300P367830103000	DOME BAY P-36	78.43236	-103.266278	665.3	660			7	1972-07-18	1974-05-20	>21	Ac	single log and shallow
300B447630108000	DRAKE B-44	76.386581	-108.269747	192.9	188			0.2	1972-10-22	1981-08-21	106	Aa	
300E787630108000	DRAKE E-78	76.456138	-108.492506	175.5	171			0.1	1974-05-27	1981-08-21	>80	Aa	
300D687630108300	DRAKE POINT D-68	76.452131	-108.930756	270.8	264			12	1974-03-25	1974-08-05	<5	Ab	
300C807440113000	DUNDAS C-80	74.651182	-113.385732	584	577			>10	1973-01-19	1980-05-12	>87	Aa	
300N277940084300	FOSHEIM N-27	79.616056	-84.721399	306.7	300			>10	1971-12-25	1971-12-30	<1	Ac	EQ log is not available
300O217350090300	GARNIER O-21	73.68189	-90.612519	502.7	500			2	1971-07-09	1971-07-10	<1	Ad	single log
300E108000084000	GEMINI E-10	79.990451	-84.068848	507.7	501			>10	1973-03-15	1980-05-15	>84	Aa	
300I697620110000	HECLA I-69	76.31091	-110.389927	147.6	143			0.02	1973-04-11	1980-05-12	>84	Aa	
300H377810099300	HOODOO DOME H-37	78.108509	-99.763517	307.8	303			>10	1970-08-17	1976-05-14	>68	Aa	
300C317650116300	JAMESON BAY C-31	76.670708	-116.732396	487.8	483			12	1971-05-16	1974-05-17	>36	Aa	
300B067820102300	KRISTOFFER BAY B-06	78.251404	-102.543447	450.2	445			0.3	1972-03-17	1980-05-16	98	Aa	
300P467750097300	LINCKENS ISLAND P-46	77.763967	-97.759126	259.1	253			0.01	1973-05-12	1978-05-26	>60	Aa	
300O257850102300	LOUISE O-25	78.750227	-102.701906	265.2	260			>10	1973-02-04	1976-05-14	>39	Aa	further temperature logs may exist after listed latest log run
300K717630108300	MARRYATT K-71	76.344512	-108.976076	365	354			***	1983-07-17	***	***	Ab	
300A027940087000	MOKKA A-02	79.520995	-87.020395	508.2	500			3	1973-04-15	1980-05-15	85	Ab	
300O158050083000	NEIL O-15	80.746871	-83.113109	555.7	549			4.5	1974-05-07	1980-05-15	>72	Aa	
300A727730105000	PAT BAY A-72	77.351287	-105.451241	306.7	300			2	1975-05-06	1980-05-12	>60	Ac	too shallow
300D497540118300	PEDDER POINT D-49	75.636463	-118.807528	345.6	341			7	1974-11-10	1977-05-18	>30	Aa	
300D737630108000	S. DRAKE D-73	76.369133	-108.493686	292.9	288			6	1975-05-10	1981-08-21	>75	Aa	
300A157300124300	STORKERSON BAY A-15	72.900438	-124.561129	505.2	500			1.6	1971-12-10	1972-05-10	5	Ac	single log
300O237750102001	SUTHERLAND O-23	77.715741	-102.147476	327.5	318			1	1973-06-13	1980-05-16	>83	Aa	
300P387810103000	THOR P-38	78.132013	-103.256952	343.2	338			0.1	1972-05-10	1980-05-16	>96	Aa	
300E607800111000	WILKINS E-60	77.989503	-111.36545	275.9	271			9	1971-01-20	1971-05-09	<4	Ac	single log
300A097450110300	WINTER HARBOUR NO.1(A-09)	74.802348	-110.512537	539.5	535			1	1962-04-07	1972-05-09	>120	Aa	

* The only offshore well

** distance offshore from coast

*** detailed data is not available

Table 2. Wells with well seismic surveys in the Canadian Arctic Islands

UWI	SHORT_NAME	GL (m)	KB (m)	LAT	LONG	Check shot	Crystal cable & check shot
300H407820096000	AMUND CENTRAL DOME H-40	62.9	68.1	78.32544	-96.265627	✓	
300L327720118000	ANDREASEN L-32	41.5	46	77.194434	-118.240659	✓	
300C737540111300	APOLLO C-73	261.2	268.5	75.534024	-111.985214		✓
300D587740100000	BALAENA D-58	-236.6	4.9	77.620973	-100.376067	✓	
300E767420123300	BAR HARBOUR E-76	48.5	52.7	74.258001	-123.900617	✓	
300J347540098300	BATHURST CALEDONIAN R. J-34	140.2	144.8	75.559409	-98.717693	✓	
300A577630103300	BENT HORN A-57	61.8	68.6	76.43439	-103.823609	✓	
300F727630103300	BENT HORN F-72	43.3	50	76.358333	-103.972498	✓	
300N727630103300	BENT HORN N-72	62.8	62.8	76.364943	-103.971666		✓
300G137510108000	BEVERLEY INLET G-13	172.2	179.8	75.039594	-108.091685	✓	
300E467720086000	BLUE FIORD E-46	278.9	285.6	77.258352	-86.301968		✓
300C507750114000	BROCK C-50	7.3	13.1	77.817484	-114.293215	✓	
300O687710091000	BUCKINGHAM O-68	-79.3	11.2	77.13428	-91.399035	✓	
300C477750100000	CAPE ALLISON C-47	-243.9	11.7	77.769048	-100.292037	✓	
300L507750100000	CAPE ALLISON L-50	0.8	7.8	77.826247	-100.303306		✓
300M217640103300	CAPE FLEETWOOD M-21	49.4	57	76.51406	-103.678614		✓
302K157750099000	CAPE MACMILLAN 2K-15	-118.4	11.1	77.744646	-99.102345	✓	
300F247740109000	CAPE MAMEN F-24	-365	12.7	77.555514	-109.168096	✓	
300A807730110000	CAPE NOREM A-80	9.2	14	77.487812	-110.454008		✓
300C687410120300	CASTEL BAY C-68	150.6	155.1	74.120267	-120.836139	✓	
300B647630109300	CHADS CREEK B-64	72.8	79.9	76.386362	-109.908161	✓	
300G077740099300	CHAR G-07	-276	7	77.60895	-99.521535	✓	
300G077630103000	CHARLES POINT G-07	27.7	35.4	76.441572	-103.019097	✓	
300B667730106000	CISCO B-66	-282.8	9.8	77.417849	-106.395525	✓	
300C427730106000	CISCO C-42	-324	7.5	77.354423	-106.287347	✓	
300K587730106000	CISCO K-58	-283.5	10.4	77.46082	-106.354684	✓	
300M227730106000	CISCO M-22	-163	11.6	77.367619	-106.188754	✓	
300K337640108300	COLLINGWOOD K-33	49.4	53.9	76.546527	-108.726529	✓	
300K407510094300	CORNWALLIS CENTRAL DOME K-40	187.5	192.8	75.161988	-94.721132	✓	
300I538010098300	CROCKER I-53	12.2	21.9	80.046496	-98.923729		✓
300C447630114000	DEPOT ISLAND C-44	30.2	37.2	76.388083	-114.29857		✓
300L247930085300	DEPOT POINT L-24	602	609.6	79.395438	-85.739053	✓	
300B737650105300	DESBARATS B-73	-146.9	4.9	76.704408	-105.956235	✓	
300E457510091300	DEVON E-45	243.8	247.5	75.073275	-91.805993	✓	
300P367830103000	DOME BAY P-36	153.6	158.9	78.43236	-103.266278	✓	
300B447630108000	DRAKE B-44	3.9	8.8	76.386581	-108.269747		✓
300E787630108000	DRAKE E-78	3.7	8.2	76.456138	-108.492506	✓	
300F167630108302	DRAKE F-16	53.3	54.3	76.421746	-108.596207	✓	
300D687630108300	DRAKE POINT D-68	37.4	44.2	76.452131	-108.930756		✓
300K797630108300	DRAKE POINT K-79	87.8	92.4	76.477409	-108.982433	✓	
300E497830100000	DUMBBELLS E-49	107	113.4	78.474386	-100.406149	✓	
300C807440113000	DUNDAS C-80	240.2	247.2	74.651182	-113.385732		✓
300L497610121300	DYER BAY L-49	31.7	36.3	76.143779	-121.813667	✓	
300M057830095000	E. AMUND M-05	77.4	86	78.414279	-95.074666	✓	
300C327630110000	E. HECLA C-32	10.7	15.5	76.353357	-110.231858		✓
300F627630110001	E. HECLA F-62	1.2	1.2	76.355161	-110.413073		✓

UWI	SHORT_NAME	GL (m)	KB (m)	LAT	LONG	Check shot	Crystal cable & check shot
300I557630107300	EAST DRAKE I-55	-141.7	4.6	76.411835	-107.817232	✓	
300L067630107300	EAST DRAKE L-06	-337.6	10	76.427143	-107.55515	✓	
300P247600118000	EGLINTON P-24	71	75.6	75.898711	-118.130584		✓
300M667730086000	EIDS M-66	227.7	234.1	77.43364	-86.434992		✓
300E797600109000	ELDRIDGE BAY E-79	21.6	29.3	75.973236	-109.496232		✓
300M407810101300	ELVE M-40	4.9	10.1	78.167452	-101.831695		✓
300E108000084000	GEMINI E-10	125.9	132.6	79.990451	-84.068848		✓
300C527730090300	GRAHAM C-52	21.3	25.9	77.354792	-90.85721	✓	
300I347630113000	GRASSY I-34	-219.7	4.9	76.396119	-113.192255	✓	
300A267730099300	GRENADIER A-26	-161.4	11.6	77.419337	-99.638535	✓	
300O168020084000	HALCYON O-16	125.9	132.6	80.265795	-84.110512		✓
300F547710110000	HAZEN F-54	-234.8	9.8	77.055364	-110.356427	✓	
300F857450110300	HEARNE F-85	81.2	85.8	74.738399	-110.934985	✓	
300J607620110000	HECLA J-60	0.7	5.2	76.327937	-110.332672	✓	
300J127850100300	HELICOPTER J-12	79.2	85.6	78.693581	-100.616058	✓	
300H377810099300	HOODOO DOME H-37	156.4	161.2	78.108509	-99.763517	✓	
300J207610104000	HOTSPUR J-20	206.8	211.9	76.161055	-104.080242	✓	
300H497700118300	INTREPID INLET H-49	65.2	70	76.974734	-118.754359	✓	
300J377920105000	ISACHSEN J-37	2.7	9.1	79.278684	-105.279444		✓
302G167810101000	JACKSON 2G-16	-67.1	6.1	78.090479	-101.117002	✓	
300C317650116300	JAMESON BAY C-31	58.3	63.1	76.670708	-116.732396	✓	
300O517620104000	KEY POINT O-51	15.5	22.3	76.182581	-104.336217	✓	✓
300N067750101000	KING CHRISTIAN N-06	28.7	35.5	77.765976	-101.041776	✓	
300B067820102300	KRISTOFFER BAY B-06	15.2	20.4	78.251404	-102.543447	✓	
300D167330120000	KUSRHAAK D-16	132.1	138.8	73.418306	-120.091138	✓	
300P467750097300	LINCKENS ISLAND P-46	0.3	6.4	77.763967	-97.759126		✓
300O257850102300	LOUISE O-25	89	94.2	78.750227	-102.701906	✓	
300I727740103300	MACLEAN I-72	-303	11.8	77.528418	-103.941841	✓	
300K717630108300	MARRYATT K-71	80.5	91	76.344512	-108.976076	✓	
300H027930085000	MAY POINT H-02	7.6	14.3	79.357632	-85.012645		✓
300D237830104300	MOCKLIN POINT D-23	31.1	37.8	78.370056	-104.750512		✓
300A027940087000	MOKKA A-02	253.3	261.5	79.520995	-87.020395	✓	
300L717720091000	N. BUCKINGHAM L-71	-80	11.6	77.179145	-91.491347	✓	
300N827450113000	N. DUNDAS N-82	221	228	74.697211	-113.430545	✓	
300H497650108300	N. SABINE H-49	53.4	60.4	76.804984	-108.755452		✓
300P407630107000	N.E. DRAKE P-40	-362.4	4.9	76.499592	-107.200348	✓	
300M257630111000	N.W. HECLA M-25	-276.2	4.7	76.415855	-111.18948		✓
300D767310123000	NANUK D-76	94.5	99.7	73.087408	-123.398886	✓	
300D417830104000	NOICE D-41	107.8	117.7	78.335496	-104.407071	✓	
300G447830104000	NOICE G-44	92.5	97.9	78.391	-104.364169		✓
300I447230122300	ORKSUT I-44	129.5	136.6	72.396202	-122.705361	✓	
300J727340115300	PARKER RIVER J-72	184	191.6	73.528945	-115.876135		✓
300A727730105000	PAT BAY A-72	17.1	23.8	77.351287	-105.451241		✓
300D497540118300	PEDDER POINT D-49	101.2	105.8	75.636463	-118.807528		✓
300G607910104300	POLLUX G-60	53.3	59.7	79.157542	-104.959299		✓
300G127550105300	RICHARDSON POINT G-12	138.7	148.4	75.68849	-105.582719	✓	
300K077640104000	ROBERT HARBOUR K-07	11.6	18.3	76.609723	-104.038982		✓
300J437650109300	ROCHE POINT O-43	-154.5	6.7	76.713275	-109.775171	✓	

UWI	SHORT_NAME	GL (m)	KB (m)	LAT	LONG	Check shot	Crystal cable & check shot
300C428000084000	ROMULUS C-42	153.3	160	79.85231	-84.377744	✓	
300D737630108000	S. DRAKE D-73	33.2	38.1	76.369133	-108.493686	✓	✓
300C587620111000	S.W. HECLA C-58	-305.4	4.9	76.285378	-111.350485	✓	
300A077530110000	SABINE BAY A-07	140.5	147.5	75.435705	-110.016113		✓
300L467630115000	SANDY POINT L-46	32.6	35.8	76.428047	-115.306874	✓	
300F687720116300	SATELLITE F-68	20.7	25.3	77.291547	-116.922699	✓	
300K087810104300	SCULPIN K-08	-550.6	11.9	78.129069	-104.562534	✓	
300F147620108300	SHERARD BAY F-14	43	50	76.222844	-108.599871		✓
300F347620108300	SHERARD BAY F-34	62	72.5	76.223427	-108.729777	✓	
300O547620108000	SHERARD O-54	17.4	21	76.230376	-108.339202	✓	
300P377820089300	SHERWOOD P-37	488.6	496.8	78.280647	-89.757286	✓	
300K287920103300	SIRIUS K-28	14	20.7	79.293867	-103.72988		✓
300B807750104300	SKATE B-80	-348	6.7	77.821412	-104.957421	✓	
300C597750104300	SKATE C-59	-360	10.3	77.805107	-104.860087	✓	
300M117720105000	SKYBATTLE BAY M-11	2.6	19	77.182973	-105.114346	✓	
300G197620103000	SOPHIE PT. G-19	18	24.7	76.307263	-103.083688	✓	
300J117630101300	STOKES RANGE J-11	334.5	341.4	76.343668	-101.585841	✓	
300O237750102001	SUTHERLAND O-23	20.7	30.2	77.715741	-102.147476		✓
300P387810103000	THOR P-38	4.9	10.1	78.132013	-103.256952	✓	
300H077340123000	UMINMAK H-07	107	112.2	73.608545	-123.011471	✓	
300A277700109000	VESEY A-27	7.8	15	76.935407	-109.137719		✓
300F367250117000	VICTORIA ISLAND F-36	147.5	155.8	72.755532	-117.189452	✓	
300A027630104000	W. BENT HORN A-02	18.3	25.9	76.352359	-104.016418	✓	
300C447630104000	W. BENT HORN C-44	12.8	20.1	76.386687	-104.287818		✓
300E437630104000	W. BENT HORN E-43	19.2	26.5	76.371854	-104.314068		✓
300G027630104000	W. BENT HORN G-02	9.4	19.4	76.356776	-104.022253	✓	
300I017630104000	W. BENT HORN I-01	37.5	44.2	76.34336	-104.01161		✓
302I017630104000	W. BENT HORN I-01A	37.5	44.2	76.34336	-104.01161	✓	
300M127630104000	W. BENT HORN M-12	9.8	17.4	76.365802	-104.117461		✓
300N497730097000	W. CORNWALL N-49	-149	11.7	77.482286	-97.293648	✓	
300C057630110300	W. HECLA C-05	2.4	7	76.403246	-110.534343	✓	
300N527630110300	W. HECLA N-52	-128.3	5.2	76.36552	-110.850487		✓
300P627630110300	W. HECLA P-62	-138.2	4.9	76.364909	-110.878823	✓	
300E597910105000	W. POLLUX E-59	6.4	12.8	79.141039	-105.491454		✓
300A737800102000	WALLIS A-73	5.4	12.2	77.871357	-102.449139	✓	
300K627800102000	WALLIS K-62	19.5	27.7	77.863191	-102.424327		✓
302H637720106300	WHITEFISH 2H-63	-275.8	9.8	77.207555	-106.892552	✓	
300A267720106300	WHITEFISH A-26	-361	10.2	77.253418	-106.639315	✓	
300H637720106300	WHITEFISH H-63	-273	6.7	77.205722	-106.882718	✓	
300J517640117000	WILKIE POINT J-51	135.3	140.5	76.509307	-117.333151	✓	
300E607800111000	WILKINS E-60	64	68.9	77.989503	-111.36545	✓	
300F627250096300	YOUNG BAY F-62	21.3	25.9	72.69041	-96.826586	✓	✓

Table 3. Wells with scanned drilling rate log (ROP) in the Canadian Arctic Islands

UWI	SHORT_NAME	GL (m)	KB (m)	LAT	LONG	ROP LOG
300N127520098300	ALLISON RIVER N-12	223.1	229.3	75.198671	-98.596177	✓
300H407820096000	AMUND CENTRAL DOME H-40	62.9	68.1	78.32544	-96.265627	✓
300L327720118000	ANDREASEN L-32	41.5	46	77.194434	-118.240659	✓
300C737540111300	APOLLO C-73	261.2	268.5	75.534024	-111.985214	✓
300E767420123300	BAR HARBOUR E-76	48.5	52.7	74.258001	-123.900617	✓
300J347540098300	BATHURST CALEDONIAN R. J-34	140.2	144.8	75.559409	-98.717693	✓
300A577630103300	BENT HORN A-57	61.8	68.6	76.43439	-103.823609	✓
300F727630103300	BENT HORN F-72	43.3	50	76.358333	-103.972498	✓
300G137510108000	BEVERLEY INLET G-13	172.2	179.8	75.039594	-108.091685	✓
300E467720086000	BLUE FIORD E-46	278.9	285.6	77.258352	-86.301968	✓
300C507750114000	BROCK C-50	7.3	13.1	77.817484	-114.293215	✓
300I207800114300	BROCK I-20	16.2	23.1	77.995242	-114.567451	✓
300A807730110000	CAPE NOREM A-80	9.2	14	77.487812	-110.454008	✓
300C687410120300	CASTEL BAY C-68	150.6	155.1	74.120267	-120.836139	✓
300G077630103000	CHARLES POINT G-07	27.7	35.4	76.441572	-103.019097	✓
300K337640108300	COLLINGWOOD K-33	49.4	53.9	76.546527	-108.726529	✓
300K407510094300	CORNWALLIS CENTRAL DOME K-40	187.5	192.8	75.161988	-94.721132	✓
300C447630114000	DEPOT ISLAND C-44	30.2	37.2	76.388083	-114.29857	✓
300L247930085300	DEPOT PT. L-24	602	609.6	79.395438	-85.739053	✓
300P367830103000	DOME BAY P-36	153.6	158.9	78.43236	-103.266278	✓
300B447630108000	DRAKE B-44	3.9	8.8	76.386581	-108.269747	✓
300E787630108000	DRAKE E-78	3.7	8.2	76.456138	-108.492506	✓
300F167630108302	DRAKE F-16	53.3	54.3	76.421746	-108.596207	✓
300D687630108300	DRAKE POINT D-68	37.4	44.2	76.452131	-108.930756	✓
300K797630108300	DRAKE POINT K-79	87.8	92.4	76.477409	-108.982433	✓
300L677630108300	DRAKE POINT L-67	56.5	60.9	76.444352	-108.925281	✓
300E497830100000	DUMBBELLS E-49	107	113.4	78.474386	-100.406149	✓
300C807440113000	DUNDAS C-80	240.2	247.2	74.651182	-113.385732	✓
300L497610121300	DYER BAY L-49	31.7	36.3	76.143779	-121.813667	✓
300C327630110000	E. HECLA C-32	10.7	15.5	76.353357	-110.231858	✓
300F627630110001	E. HECLA F-62	1.2	1.2	76.355161	-110.413073	✓
300P247600118000	EGLINTON P-24	71	75.6	75.898711	-118.130584	✓
300M667730086000	EIDS M-66	227.7	234.1	77.43364	-86.434992	✓
300E797600109000	ELDRIDGE BAY E-79	21.6	29.3	75.973236	-109.496232	✓
300M407810101300	ELVE M-40	4.9	10.1	78.167452	-101.831695	✓
300K337650113300	EMERALD K-33	4.3	12.2	76.712696	-113.725296	✓
300N277940084300	FOSHEIM N-27	561.6	568.3	79.616056	-84.721399	✓
300O217350090300	GARNIER O-21	368.5	371.2	73.68189	-90.612519	✓
300E108000084000	GEMINI E-10	125.9	132.6	79.990451	-84.068848	✓
300O168020084000	HALCYON O-16	125.9	132.6	80.265795	-84.110512	✓
300F857450110300	HEARNE F-85	81.2	85.8	74.738399	-110.934985	✓
300I697620110000	HECLA I-69	1.5	6.1	76.31091	-110.389927	✓
300J127850100300	HELICOPTER J-12	79.2	85.6	78.693581	-100.616058	✓
300E057810099300	HOODOO E-05	115.2	125	78.07225	-99.566237	✓
300N527820099300	HOODOO N-52	40.5	50.5	78.200796	-99.975777	✓
300H497700118300	INTREPID INLET H-49	65.2	70	76.974734	-118.754359	✓
300J377920105000	ISACHSEN J-37	2.7	9.1	79.278684	-105.279444	✓

UWI	SHORT_NAME	GL (m)	KB (m)	LAT	LONG	ROP LOG
300O517620104000	KEY POINT O-51	15.5	22.3	76.182581	-104.336217	✓
300D187750101000	KING CHRISTIAN D-18	30.5	35.7	77.786839	-101.115314	✓
300N067750101000	KING CHRISTIAN N-06	28.7	35.5	77.765976	-101.041776	✓
300D167330120000	KUSRHAAK D-16	132.1	138.8	73.418306	-120.091138	✓
300P467750097300	LINCKENS ISLAND P-46	0.3	6.4	77.763967	-97.759126	✓
300O257850102300	LOUISE O-25	89	94.2	78.750227	-102.701906	✓
300H027930085000	MAY POINT H-02	7.6	14.3	79.357632	-85.012645	✓
300D237830104300	MOCKLIN POINT D-23	31.1	37.8	78.370056	-104.750512	✓
300D877340117000	MUSKOX D-87	247	253	73.602812	-117.452628	✓
300H497650108300	N. SABINE H-49	53.4	60.4	76.804984	-108.755452	✓
300D767310123000	NANUK D-76	94.5	99.7	73.087408	-123.398886	✓
300D417830104000	NOICE D-41	107.8	117.7	78.335496	-104.407071	✓
300G447830104000	NOICE G-44	92.5	97.9	78.391	-104.364169	✓
300I447230122300	ORKSUT I-44	129.5	136.6	72.396202	-122.705361	✓
300A727730105000	PAT BAY A-72	17.1	23.8	77.351287	-105.451241	✓
300G607910104300	POLLUX G-60	53.3	59.7	79.157542	-104.959299	✓
300E827400098300	RUSSELL E-82	114	120.4	73.858891	-98.947646	✓
300D737630108000	S. DRAKE D-73	33.2	38.1	76.369133	-108.493686	✓
300A077530110000	SABINE BAY A-07	140.5	147.5	75.435705	-110.016113	✓
300F687720116300	SATELLITE F-68	20.7	25.3	77.291547	-116.922699	✓
300F347620108300	SHERARD BAY F-34	62	72.5	76.223427	-108.729777	✓
300O547620108000	SHERARD O-54	17.4	21	76.230376	-108.339202	✓
300K287920103300	SIRIUS K-28	14	20.7	79.293867	-103.72988	✓
300C157720105000	SKYBATTLE BAY C-15	24.1	30.5	77.237645	-105.10119	✓
300M117720105000	SKYBATTLE BAY M-11	2.6	19	77.182973	-105.114346	✓
300J117630101300	STOKES RANGE J-11	334.5	341.4	76.343668	-101.585841	✓
300H077340123000	UMINMAK H-07	107	112.2	73.608545	-123.011471	✓
300F367250117000	VICTORIA ISLAND F-36	147.5	155.8	72.755532	-117.189452	✓
300I447830097300	W. AMUND I-44	12.8	16.2	78.395609	-97.839564	✓
300A027630104000	W. BENT HORN A-02	18.3	25.9	76.352359	-104.016418	✓
300C447630104000	W. BENT HORN C-44	12.8	20.1	76.386687	-104.287818	✓
300I017630104000	W. BENT HORN I-01	37.5	44.2	76.34336	-104.01161	✓
300M127630104000	W. BENT HORN M-12	9.8	17.4	76.365802	-104.117461	✓
300C057630110300	W. HECLA C-05	2.4	7	76.403246	-110.534343	✓
300E597910105000	W. POLLUX E-59	6.4	12.8	79.141039	-105.491454	✓
300O107550108300	WEATHERALL O-10	153	157.7	75.831856	-108.532654	✓
300J517640117000	WILKIE POINT J-51	135.3	140.5	76.509307	-117.333151	✓
300E607800111000	WILKINS E-60	64	68.9	77.989503	-111.36545	✓
300F627250096300	YOUNG BAY F-62	21.3	25.9	72.69041	-96.826586	✓
300F117600113300	ZEUS F-11	196	200.6	75.840305	-113.609452	✓

Table 4. Comparison of thermally defined permafrost (PF) and ice-bearing permafrost (IBPF) from geophysical methods in the Canadian Arctic Islands

* LITH (lithology): SS-sandstone, SLT-siltstone, SH-shale, DOL-dolomite, CONG-conglomerate, LS- limestone, (CAL)SS-calcareous sandstone

UWI	Well name	PF from temperature surveys				IBPF from other geophysical methods (well logs and well seismic surveys)										Comments
		PF at 0^0C				Fully frozen zone					Partially frozen zone					
		Base of PF		Quality	LITH located *	base of $IBPF_F$		Quality	Tempe-rature (^0C)	LITH located *	base of $IBPF_P$		Quality	Tempe-rature (^0C)	LITH located *	
		(m KB)	(m GL/SF)			(m KB)	(m GL)				(m KB)	(m GL)				
302F727630103300	BENT HORN F-72A	666.7	660	Aa	SLT	587	580.3	Ba	-2.3	SS	700	693.3	Bc	0.93	SS	
300N727630103300	BENT HORN N-72	734	726	Aa	SLT	682	674	Bb	-1.03	SS	726	718	Bc	-0.17	SS	
300I207800114300	BROCK I-20	428.9	422	Aa	SS	401	394.1	Bb	-1.41	SS	458	451.1	Bb	1.16	SH-SLT	
300C477750100000	CAPE ALLISON C-47	295.6	40	Ab	SS											IBPF may not exist
300O307730094300	CORNWALL O-30	374.8	365	Ab	(CAL)SS	359	349.2	Bb	-0.23	(CAL)SS	378	368.2	Bb	0.36	(CAL)SS	EQ log is not available
300L417450094300	CORNWALLIS RESOLUTE BAY L-41	603.9	600	Ac	DOL	516.7	512.8	Bc	-2.4	DOL						
300E457510091300	DEVON E-45	604	600	Ad	LS	692.3	688.3	Bb	2.36	SS-LS	779	775	Bb	4.7	LS	PF is unreliable
300P367830103000	DOME BAY P-36	665.3	660	Ac	SH	525	519.7	Bb	-6.57	SH	692	686.7	Bc	1.29	SH	
300B447630108000	DRAKE B-44	192.9	188	Aa	SH	130	125.1	Bb	-5.93	SH	202	197.1	Bc	0.85	SH	
300E787630108000	DRAKE E-78	175.5	171	Aa	SH											IBPF is unknown
300D687630108300	DRAKE POINT D-68	270.8	264	Ab	SH	117	110.2	Bc	-4.77	SH	248	241.2	Bc	-2.07	SH	
300C807440113000	DUNDAS C-80	584	577	Aa	SLT	479	472	Ba	-3.61	SLT-SS	633	626	Bb	2.06	SLT	
300N277940084300	FOSHEIM N-27	306.7	300	Ac	SLT	249	242.3	Bc		SH-SLT	294	287.3	Bc		SLT-SH	EQ log is not available
300O217350090300	GARNIER O-21	502.7	500	Ad	DOL	271	268.3	Bb	-0.53	LS						PF is unreliable
300E108000084000	GEMINI E-10	507.7	501	Aa	SLT-SH	461	454.3	Ba	-1.26	SLT-SS	513.4	506.7	Bb	0.24	SLT-SH	
300I697620110000	HECLA I-69	147.6	143	Aa	SH	102	97.4	Bc	-5.02	SH						
300H377810099300	HOODOO DOME H-37	307.8	303	Aa	SH	219.8	215	Bb	-4.53	SH	286	281.2	Bc	-1.28	SH	
300C317650116300	JAMESON BAY C-31	487.8	483	Aa	SS	418	413.2	Ba	-1.64	SS	491	486.2	Bc	0.07	SLT	
300B067820102300	KRISTOFFER BAY B-06	450.2	445	Aa	SH	374.4	369.2	Bb	-3.8	SLT	452	446.8	Bb	0.15	SH	
300P467750097300	LINCKENS ISLAND P-46	259.1	253	Aa	SH	178	171.9	Bb	-4.18	SH	310	303.9	Bb	1.65	SH	
300O257850102300	LOUISE O-25	265.2	260	Aa	SH	182	176.8	Bc	-4.46	SH	272	266.8	Bb	0.84	SH	
300K717630108300	MARRYATT K-71	365	354	Ab	SH-SLT											IBPF is unknown
300A027940087000	MOKKA A-02	508.2	500	Ab	SLT	470	461.8	Bb	-1.49	SLT	520	511.8	Bb	0.43	SLT	
300O158050083000	NEIL O-15	555.7	549	Aa	SS	493	486.3	Ba	-1.44	SS	572	565.3	Bb	0.25	SLT	
300A727730105000	PAT BAY A-72	306.7	300	Ac	SH	236.3	229.6	Bb	-6.57	SH	327	320.3	Bb	1.85	SH	
300D497540118300	PEDDER POINT D-49	345.6	341	Aa	SH	283	278.4	Ba	-3.08	SLT	349	344.4	Bb	0.04	SH	
300D737630108000	S. DRAKE D-73	292.9	288	Aa	SH	224	219.1	Bc	-5.08	SH						
300A157300124300	STORKERSON BAY A-15	505.2	500	Ac	SS	500	494.8	Ba	-0.24	SS	559	553.8	Ba	2.43	CONG	
300O237750102001	SUTHERLAND O-23	327.5	318	Aa	SH-SLT	251	241.5	Bb	-3.89	SLT	363	353.5	Bb	2.12	SH	
300P387810103000	THOR P-38	343.2	338	Aa	SH	238	232.8	Bb	-6.72	SH	344	338.8	Bb	0.17	SH	
300E607800111000	WILKINS E-60	275.9	271	Ac	SH	196.2	191.3	Bc	-5.39	SH	286	281.1	Bc	0.83	SH	
300A097450110300	WINTER HARBOUR NO.1 (A-09)	539.5	535	Aa	SLT	537.3	532.8	Bb	-0.08	SS-SLT	560	555.5	Bb	0.7	SLT	

Table 5. Base of permafrost (PF) from temperature surveys and base of ice-bearing permafrost (IBPF) from other geophysical methods for 143 exploration wells, Canadian Arctic Islands

* The only well (Bent Horn N-72) where frozen zone was identified (688±15 m KB) by temperature surveys

** The only offshore well (Cape Allison C-47) where base PF was determined using temperature surveys

***Fm (formation) age: T-Tertiary; K-Cretaceous; J-Jurassic; TR-Triassic; P-Permian; C-Carboniferous; D-Devonian; S-Silurian; O-Ordovician

****LITH, lithology: SS-sandstone, (CAL)SS- calcareous sandstone, (CH)SS-cherty sandstone, SLT-siltstone, SH-shale, LS-limestone, DOL-dolomite, CONG-conglomerate

Basic well information							PF from temperature surveys					Base of ice-bearing permafrost (IBPF) from other geophysical methods (well logs and well seismic surveys)												IBPF from previous studies			COMMENTS
UWI	Short Name	GL	KB	LAT	LONG	Island located	Depth to 0^0C Isotherm					Fully frozen zone					Partially frozen zone					Transition zone thickness	Figure No. in Appendix	Panarctic Oils	Hardy (1984)		
							Base PF		Quality	Fm age located ***	LITH located ****	Base $IBPF_F$		Quality	Fm age located ***	LITH located ****	Base $IBPF_P$		Quality	Fm age located ***	LITH located ****				BASE $IBPF_F$	BASE $IBPF_P$	
		(m)	(m)				(m KB)	(m GL/SF)				(m KB)	(m GL)				(m KB)	(m GL)				(m)		(m KB)	(m KB)	(m KB)	
300N127520098300	ALLISON RIVER N-12	223.1	229.3	75.198671	-98.596177	Bathurst						393.7	387.5	Bb	D	SS	455	448.8	Bb	S	SLT	61.3	3-1	411	396	454	
300H407820096000	AMUND CENTRAL DOME H-40	62.9	68.1	78.32544	-96.265627	Amund Ringnes						214	208.8	Bb	J	SLT-SH							3-2		285		
300M057830095000	E. AMUND M-05	77.4	86	78.414279	-95.074666	Amund Ringnes						267.2	258.6	Bb	K-J	SLT-SH	352	343.4	Bb	K-J	SH	84.8	3-3		357	364	
300I447830097300	W. AMUND I-44	12.8	16.2	78.395609	-97.839564	Amund Ringnes						260.1	256.7	Bb	K-J	SH	371.9	368.5	Bb	J	SH	111.8	3-4		256	320	
300L327720118000	ANDREASEN L-32	41.5	46	77.194434	-118.24066	Prince Patrick						356	351.5	Ba	J	SS-SLT							2-1		302	396	
300C737540111300	APOLLO C-73	261.2	268.5	75.534024	-111.98521	Melville						220	212.7	Ba	D	SLT	355.3	348	Bb	D	SLT	135.3	2-2	344	549	671	
300E767420123300	BAR HARBOUR E-76	48.5	52.7	74.258001	-123.90062	Banks						316	311.8	Bb	K	SS	362	357.8	Ba	K	SS	46	3-5	247	283	363	
300J347540098300	BATHURST CALEDONIAN R. J-34	140.2	144.8	75.559409	-98.717693	Bathurst						847.1	842.5	Bb	S	LS-SLT							3-6	415	808	846	
300A577630103300	BENT HORN A-57	61.8	68.6	76.43439	-103.82361	Cameron						540	533.2	Ba	D	SS	672.6	665.8	Bc	D	SS	132.6	2-3	326	540	660	
300F727630103300	BENT HORN F-72	43.3	50	76.358333	-103.9725	Cameron						587	580.3	Ba	D	SS	700	693.3	Bc	D	SS	113	1-1; 2-4	512			Combine data from wells Bent Horn F-72 and F-72A
302F727630103301	BENT HORN F-72A	43.3	50	76.358333	-103.9725	Cameron	667	660.3	Aa	D	SLT	587	580.3	Ba	D	SS	700	693.3	Bc	D	SS	113	1-1; 2-4		587	701	Combine data from wells Bent Horn F-72 and F-72A
300N727630103300	BENT HORN N-72*	62.8	70.5	76.364943	-103.97167	Cameron	734	726.3	Aa	D	SLT	682	674.3	Bb	D	SS	726	718.3	Bb	D	SS	44	1-2; 3-7		680±15	732	Frozen zone (688±15) from temperature surveys
300N727630103301	BENT HORN N-72A	62.8	70.5	76.364943	-103.97167	Cameron						682	674.3	Bb	D	SS	726	718.3	Bb	D	SS	44	1-2; 3-7				Combine data from wells Bent Horn N-72 and N-72A
300A027630104000	W. BENT HORN A-02	18.3	25.9	76.352359	-104.01642	Cameron						197.4	189.8	Bb	P	SLT	257.3	249.7	Bc	P	SLT-SH	59.9	3-8	268	224	320	
300C447630104000	W. BENT HORN C-44	12.8	20.1	76.386687	-104.28782	Cameron						418.5	411.2	Ba	D	SS	493.2	485.9	Bc	D	SLT	74.7	2-5	427	419	500	
300E437630104000	W. BENT HORN E-43	19.2	26.5	76.371854	-104.31407	Cameron						214	206.7	Ba	P	SS	290	282.7	Bc	P	SLT	76	2-6	299	262	299	
300G027630104000	W. BENT HORN G-02	9.4	19.4	76.356776	-104.02225	Cameron						222	212	Bb	P	SLT	316.1	306.1	Bc	P	SLT	94.1	3-9		300	465	
300I017630104000	W. BENT HORN I-01	37.5	44.2	76.34336	-104.01161	Cameron						274.1	267.4	Ba	P	SH	346.9	340.2	Bb	P	SH	72.8	2-7	396	<610		Combine data from wells W.Bent Horn I-01 & I-01A
302I017630104000	W. BENT HORN I-01A	37.5	44.2	76.34336	-104.01161	Cameron						274.1	267.4	Ba	P	SH	346.9	340.2	Bb	P	SH	72.8	2-7	396	<610		Combine data from wells W.Bent Horn I-01 & I-01A
300M127630104000	W. BENT HORN M-12	9.8	17.4	76.365802	-104.11746	Cameron						346.6	339	Bb	P	SS	426	418.4	Bb	P	SS	79.4	3-10	408	695		
300G137510108000	BEVERLEY INLET G-13	172.2	179.8	75.039594	-108.09169	Melville						216	208.4	Ba	D	SH	294	286.4	Bb	D	SS	78	2-8		308	357	
300E467720086000	BLUE FIORD E-46	278.9	285.6	77.258352	-86.301968	Ellesmere						399	392.3	Bc	D	SH							4-1		430	527	
300C507750114000	BROCK C-50	7.3	13.1	77.817484	-114.29322	Brock						290	284.2	Ba	TR	(CAL)SS	421.5	415.7	Ba	TR	(CAL)SS	131.5	2-9	366	293		
300I207800114300	BROCK I-20	16.2	23.1	77.995242	-114.56745	Brock	429	422.1	Aa	TR	SS	401	394.1	Bb	TR	SS	458	451.1	Bb	TR	SH-SLT	57	1-3; 3-11	427	460	572	
300C477750100000	CAPE ALLISON C-47**	-243.9	11.7	77.769048	-100.29204	Offshore well**	295.6	40	Ab	K	SS												1-20				IBPF may not exist
300L507750100000	CAPE ALLISON L-50	0.8	7.8	77.826247	-100.30331	Ellef Ringnes						158.3	151.3	Bc	K	SS	214.9	207.9	Bb	K	SS	56.6	4-2	207	567		
300M217640103300	CAPE FLEETWOOD M-21	49.4	57	76.51406	-103.67861	Cameron						551	543.4	Ba	D	SS	593	585.4	Ba	D	SS	42	2-10	590	466	614	
300A807730110000	CAPE NOREM A-80	9.2	14	77.487812	-110.45401	Mackenzie King						163.8	159	Bb	K	SS	266	261.2	Bb	K	SLT	102.2	3-12	241	177	259	
300C687410120300	CASTEL BAY C-68	150.6	155.1	74.120267	-120.83614	Banks						458	453.5	Ba	K	SS	568	563.5	Ba	K	SLT	110	2-11	475	514	555	
300B647630109300	CHADS CREEK B-64	72.8	79.9	76.386362	-109.90816	Melville						153.0	145.9	Bc	K	SH							4-3		<421		
300G077630103000	CHARLES POINT G-07	27.7	35.4	76.441572	-103.0191	Cameron						452.0	444.3	Bc	D	SLT							4-4		457	597	
300K337640108300	COLLINGWOOD K-33	49.4	53.9	76.546527	-108.72653	Melville						326.3	321.8	Bc	K	SH							4-5	223	<610		
300O307730094300	CORNWALL O-30	20	29.8	77.497294	-94.650227	Cornwall	374.8	365	Ab	TR	(CAL)SS	359	349.2	Bb	TR	SS	378	368.2	Bb	TR	(CAL)SS	19	1-21; 3-13		555	673	
300K407510094300	CORNWALLIS CENTRAL DOME K-4(	187.5	192.8	75.161988	-94.721132	Cornwallis						743	737.7	Bb	O	LS							3-14		860	1021	
300L417450094300	CORNWALLIS RESOLUTE BAY L-41	61	64.9	74.678557	-94.744606	Cornwallis	604	600.1	Ac	S	DOL	516.7	512.8	Bc	S	DOL							1-26; 4-6		518		
300I538010098300	CROCKER I-53	12.2	21.9	80.046496	-98.923729	Meighen						454.0	444.3	Ba	T	SS	495.6	485.9	Ba	T	SS	41.6	2-12		494		
300C447630114000	DEPOT ISLAND C-44	30.2	37.2	76.388083	-114.29857	Melville						399.0	392	Ba	J	SS	539	532	Bb	J	SH	140	2-13	512	506	613	
300L247930085300	DEPOT POINT L-24	602	609.6	79.395438	-85.739053	Axel Heiberg						372.0	364.4	Bb	TR	(CAL)SS							3-15		372		
300E457510091300	DEVON E-45	243.8	247.5	75.073275	-91.805993	Devon	604	600	Ad	S	LS	692.3	688.6	Bb	S	SS-LS	779	775.3	Bb	S	LS	86.7	1-31; 3-16	914	780	875	
300P367830103000	DOME BAY P-36	153.6	158.9	78.43236	-103.26628	Ellef Ringnes	665	660	Ac	K-J	SH	525.0	519.7	Bb	K-J	SH	692	686.7	Bc	K-J	SH	167	1-25; 3-17		661	756	
300P587830103000	DOME BAY STRAT P-58	79.9	83.2	78.464078	-103.42113	Ellef Ringnes						270	266.7	Bb	K-J	SS	333	329.7	Bb	K-J	SLT	63	3-18				
300B447630108000	DRAKE B-44	3.9	8.8	76.386581	-108.26975	Melville	193	188.1	Aa	K	SH	130	125.1	Bb	K	SH	202	197.1	Bc	K	SH	72	1-4; 3-19	201	131	224	
300E787630108000	DRAKE E-78	3.7	8.2	76.456138	-108.49251	Melville	176	171.5	Aa	K	SH	IBPF is unknown											1-5	200	530	552	
300F167630108302	DRAKE F-16	53.3	54.3	76.421746	-108.59621	Melville						493.7	492.7	Bc	K	SS							4-7		411	491	

UWI	Short Name	GL (m)	KB (m)	LAT	LONG	Island located	PF from temperature surveys: Depth to 0^0C Isotherm: Base PF (m KB)	Base PF (m GL/SF)	Quality	Fm age located ***	LITH located ****	Base of ice-bearing permafrost (IBPF) from other geophysical methods (well logs and well seismic surveys): Fully frozen zone: Base $IBPF_F$ (m KB)	Base $IBPF_F$ (m GL)	Quality	Fm age located ***	LITH located ****	Partially frozen zone: Base $IBPF_P$ (m KB)	Base $IBPF_P$ (m GL)	Quality	Fm age located ***	LITH located ****	Transition zone thickness (m)	Figure No. in Appendix	IBPF from previous studies: Panarctic Oils (m KB)	Hardy (1984): BASE $IBPF_F$ (m KB)	Hardy (1984): BASE $IBPF_P$ (m KB)	COMMENTS
300D737630108000	S. DRAKE D-73	33.2	38.1	76.369133	-108.49369	Melville	293	288.1	Aa	K	SH	224	219.1	Bc	K	SH							1-6; 4-8	219	432		
300D687630108300	DRAKE POINT D-68	37.4	44.2	76.452131	-108.93076	Melville	271	264.2	Ab	K	SH	117	110.2	Bc	K	SH	248	241.2	Bc	K	SH	131	1-22; 4-9	165	<420		
300K797630108300	DRAKE POINT K-79	87.8	92.4	76.477409	-108.98243	Melville						174	169.4	Ba	K	SLT-SH	243	238.4	Bb	K	SH	69	2-14	219	174	299	
300L677630108300	DRAKE POINT L-67	56.5	60.9	76.444352	-108.92528	Melville						237	232.4	Bb	K	SLT	286	281.6	Bb	K	SH	49.2	3-20		238	277	
300E497830100000	DUMBBELLS E-49	107	113.4	78.474386	-100.40615	Ellef Ringnes						452	445.6	Bb	K	SS	551.4	545	Bb	K	SLT	99.4	3-21	555	366	457	
300C807440113000	DUNDAS C-80	240.2	247.2	74.651182	-113.38573	Melville	584	577	Aa	D	SLT	479	472	Ba	D	SS	633	626	Bb	D	SLT	154	1-7; 2-15	550	479	543	
300N827450113000	N. DUNDAS N-82	221	228	74.697211	-113.43055	Melville						485.6	478.6	Ba	D	SS	560	553	Ba	D	SS	74.4	2-16	610	342	420	
300L497610121300	DYER BAY L-49	31.7	36.3	76.143779	-121.81367	Prince Patrick						722.6	718	Bb	D	SLT	783.3	778.7	Bb	D	SLT	60.7	3-22		652	783	
300P247600118000	EGLINTON P-24	71	75.6	75.898711	-118.13058	Eglinton						415.0	410.4	Ba	K	SLT-SS	505	500.4	Bb	K	SS	90	2-17	530	317	415	
300M667730086000	EIDS M-66	227.7	234.1	77.43364	-86.434992	Ellesmere						184.0	177.6	Bb	S	SLT-SH							3-23		338	393	
300E797600109000	ELDRIDGE BAY E-79	21.6	29.3	75.973236	-109.49623	Melville						531.0	523.3	Bb	P	(CH)SS	630.6	622.9	Bb	P	(CAL)SS	99.6	3-24	578	509	631	
300M407810101300	ELVE M-40	4.9	10.1	78.167452	-101.8317	Ellef Ringnes						202.7	197.5	Bb	K	SS	294.5	289.3	Bc	K	SLT-SH	91.8	3-25	189	204	296	
300K337650113300	EMERALD K-33	4.3	12.2	76.712696	-113.7253	Emerald						652.3	644.4	Bb	K	SLT	701	693.1	Bb	K	SH	48.7	3-26		701	802	
300N277940084300	FOSHEIM N-27	561.6	568.3	79.616056	-84.721399	Ellesmere	307	300	Ac	TR	SLT	248.6	241.9	Bc	TR	SH-SLT	294	287.3	Bc	TR	SLT-SH	45.4	1-27; 4-10	251	252	296	
300O217350090300	GARNIER O-21	368.5	371.2	73.68189	-90.612519	Somerset	503	500.3	Ad	S	DOL	271	268.3	Bb	S	LS							1-32; 3-27	500	274	311	
300E108000084000	GEMINI E-10	125.9	132.6	79.990451	-84.068848	Ellesmere	508	501.3	Aa	K	SH	461	454.3	Ba	K	SLT-SS	513.4	506.7	Bb	K	SH-SLT	52.4	1-8; 2-18	475	411	539	
300C527730090300	GRAHAM C-52	21.3	25.9	77.354792	-90.85721	Graham						309.0	304.4	Ba	K	SS	410.6	406	Bb	K	SS	101.6	2-19		308	475	
300O168020084000	HALCYON O-16	125.9	132.6	80.265795	-84.110512	Ellesmere						383.0	376.3	Bb	K	SLT	497.5	490.8	Bb	K	SH	114.5	3-28		384	530	
300F857450110300	HEARNE F-85	81.2	85.8	74.738399	-110.93499	Melville						324.0	319.4	Bb	D	SS	356	351.4	Bb	D	SS	32	3-29	875	310	340	
300C327630110000	E. HECLA C-32	10.7	15.5	76.353357	-110.23186	Melville						161.0	156.2	Bb	K	SLT-SH							3-30	177	486	529	
300F627630110001	E. HECLA F-62	1.2	6	76.355161	-110.41307	Melville						102.0	97.2	Bc	K	SH							4-11	107	411	457	
300I697620110000	HECLA I-69	1.5	6.1	76.31091	-110.38993	Melville	148	143.4	Aa	K	SH	102	97.4	Bc	K	SH							1-9; 4-12	130	347	381	
300J127850100300	HELICOPTER J-12	79.2	85.6	78.693581	-100.61606	Ellef Ringnes						424.5	418.1	Bb	K	SLT	550	543.6	Bb	K	SLT	125.5	3-31		436	550	
300E057810099300	HOODOO E-05	115.2	125	78.07225	-99.566237	Ellef Ringnes						47	37.2	Bc	K	SH							4-13		<239		
300H377810099300	HOODOO DOME H-37	156.4	161.2	78.108509	-99.763517	Ellef Ringnes	308	303.2	Aa	K	SH	219.8	215	Bb	K	SH	286	281.2	Bb	K	SH	66.2	1-10; 3-32		198	259	
300L417820099300	HOODOO L-41	73.2	79.6	78.177933	-99.906514	Ellef Ringnes						234.1	227.7	Bb	K	SS	294	287.6	Bb	K	SS	59.9	3-33		241	296	
300N527820099300	HOODOO N-52	40.5	50.5	78.200796	-99.975777	Ellef Ringnes						324	314	Bc	K	SS							4-14		390	450	
300J207610104000	HOTSPUR J-20	206.8	211.9	76.161055	-104.08024	Vanier						634	628.9	Bc	D	SS							4-15		530	573	Estimated IBPF is minimum in this study
300M647230121300	IKKARIKTOK M-64	120.9	127.7	72.396935	-121.85252	Banks						305.0	298.2	Ba	K	SLT	400.2	393.4	Bb	K	SH	95.2	2-20		305	360	
300H497700118300	INTREPID INLET H-49	65.2	70	76.974734	-118.75436	Prince Patrick						320.0	315.2	Bc	J	SLT							4-16		628	692	
300J377920105000	ISACHSEN J-37	2.7	9.1	79.278684	-105.27944	Ellef Ringnes						464.0	457.6	Ba	T	SS	555.4	549	Ba	T	SS	91.4	2-21	565	556	591	
300C317650116300	JAMESON BAY C-31	58.3	63.1	76.670708	-116.7324	Prince Patrick	488	483.2	Aa	J	SS	418	413.2	Ba	J	SS	491	486.2	Bc	J	SLT-SS	73	1-11; 2-22	500	396	466	
300O517620104000	KEY POINT O-51	15.5	22.3	76.182581	-104.33622	Vanier						608.0	601.2	Bb	D	SS-SLT	778.3	771.5	Bb	D	SS	170.3	3-34	771	779	831	
302D187750101000	KING CHRISTIAN 2D-18	27	31.1	77.786839	-101.11531	King Christian						380.0	375.9	Bc	J	SS-SLT							4-17		728		
300N067750101000	KING CHRISTIAN N-06	28.7	35.5	77.765976	-101.04178	King Christian						142.0	135.2	Bc	J	SLT-SH	281.4	274.6	Bb	J	SH	139.4	4-18		229	366	
300B537540108000	KING POINT WEST B-53	228.9	236.8	75.534901	-108.34288	Melville						252.3	244.4	Ba	D	SLT	330.6	322.7	Bb	D	SLT	78.3	2-23	335	296	335	
300C717620112300	KITSON RIVER C-71	70.1	76.3	76.170855	-112.98484	Melville						294.6	288.4	Ba	TR	SS	379	372.8	Ba	TR	SS	84.4	2-24		296	360	
300B067820102300	KRISTOFFER BAY B-06	15.2	20.4	78.251404	-102.54345	Ellef Ringnes	450	444.8	Aa	K	SH	374.4	369.2	Bb	K	SLT-SH	452	446.8	Bb	K	SH	77.6	1-12; 3-35	405	326	376	
300E277820102000	KRISTOFFER STRAT E-27	0.3	3.8	78.274812	-102.25077	Ellef Ringnes						325.0	321.5	Bb	K	SLT	420	416.5	Bb	K	SS-SLT	95	3-36				
300I477820102000	KRISTOFFER STRAT I-47	13.4	16.8	78.276454	-102.33899	Ellef Ringnes						223.0	219.6	Bb	K	SS	278.7	275.3	Bb	K	SS	55.7	3-37				
300D167330120000	KUSRHAAK D-16	132.1	138.8	73.418306	-120.09114	Banks						625.0	618.3	Ba	D	SS	634.5	627.8	Bb	D	SLT	9.5	2-25		434	503	
300P467750097300	LINCKENS ISLAND P-46	0.3	6.4	77.763967	-97.759126	Linckens	259	252.9	Aa	K-J	SH	178	171.9	Bb	K-J	SH	310	303.9	Bb	K-J	SH	132	1-13; 3-38		131	280	
300O257850102300	LOUISE O-25	89	94.2	78.750227	-102.70191	Ellef Ringnes	265.2	260	Aa	K-J	SH	182	176.8	Bc	K-J	SH	272	266.8	Bb	K-J	SH	90	1-14; 4-19		<221	271	
300D027630115300	MARIE BAY D-02	21	24.7	76.351013	-115.56161	Melville						393	389.3	Ba	TR	SLT-SS							2-26		393		
300K717630108300	MARRYATT K-71	80.5	91	76.344512	-108.97608	Melville	365	354.5	Ab	K	SH-SLT	IBPF is unknown											1-23	426	550	850	
300H027930085000	MAY POINT H-02	7.6	14.3	79.357632	-85.012645	Axel Heiberg						237.0	230.3	Bb	K	SLT-SH	311	304.3	Bb	K	SH	74	3-39		610	655	
300J538000094300	MID FIORD J-53	342.6	350.5	79.87793	-94.953703	Axel Heiberg						293.0	285.1	Bb	K	SLT							3-40	191	332	375	
300D237830104300	MOCKLIN POINT D-23	31.1	37.8	78.370056	-104.75051	Ellef Ringnes						358.7	352	Bb	K-J	SLT-SH	452.6	445.9	Bb	K-J	SLT-SH	93.9	3-41		524	605	
300A027940087000	MOKKA A-02	253.3	261.5	79.520995	-87.020395	Axel Heiberg	508	500	Ab	TR	SLT	469.8	461.6	Bb	TR	SLT	520	511.8	Bb	TR	SLT	50.2	1-24; 3-42	475	460	503	
300D877340117000	MUSKOX D-87	247	253	73.602812	-117.45263	Banks						499.3	493.3	Bb	D	SS	570	564	Bb	D	SS	70.7	3-43		765	825	

Basic well information							PF from temperature surveys					Base of ice-bearing permafrost (IBPF) from other geophysical methods (well logs and well seismic surveys)												IBPF from previous studies			COMMENTS
UWI	Short Name	GL	KB	LAT	LONG	Island located	Depth to 0°C Isotherm					Fully frozen zone					Partially frozen zone					Transition zone thickness	Figure No. in Appendix	Panarctic Oils	Hardy (1984)		
							Base PF		Quality	Fm age located ***	LITH located ****	Base $IBPF_F$		Quality	Fm age located ***	LITH located ****	Base $IBPF_P$		Quality	Fm age located ***	LITH located ****				BASE $IBPF_F$	BASE $IBPF_P$	
		(m)	(m)				(m KB)	(m GL/SF)				(m KB)	(m GL)				(m KB)	(m GL)				(m)		(m KB)	(m KB)	(m KB)	
300D767310123000	NANUK D-76	94.5	99.7	73.087408	-123.39889	Banks						247.3	242.1	Bc	K	SS-CONG							4-20		603		
300O158050083000	NEIL O-15	496.2	502.9	80.746871	-83.113109	Ellesmere	556	549.3	Aa	J	SS	493	486.3	Ba	J	SS	571.6	564.9	Bb	J	SLT	78.6	1-15; 2-27		373	495	
300D417830104000	NOICE D-41	107.8	117.7	78.335496	-104.40707	Ellef Ringnes						316.5	306.6	Ba	K	SLT	423	413.1	Bb	K	SH	106.5	2-28	423	320	365	
300G447830104000	NOICE G-44	92.5	97.9	78.391	-104.36417	Ellef Ringnes						297.1	291.7	Bb	K-J	SLT	375.4	370	Bb	K-J	SLT-SH	78.3	3-44	381	628	768	
300H417830104000	NOICE STRAT H-41	115.8	119.2	78.339664	-104.35012	Ellef Ringnes						324.0	320.6	Bb	K	SS-SLT							3-45				
300B247830104300	NOICE W. STRAT B-24	47.9	51.2	78.385307	-104.69123	Ellef Ringnes						306.0	302.7	Ba	K	SS-SLT							2-29				
300N337830104300	NOICE W. STRAT N-33	2.4	6.1	78.3815	-104.812596	Ellef Ringnes						160.0	156.3	Ba	K	SLT	188	184.3	Bb	K	SLT	28	2-30				
300I447230122300	ORKSUT I-44	129.5	136.6	72.396202	-122.70536	Banks						616.0	608.9	Ba	K	SS	675.4	668.3	Ba	K	SS	59.4	2-31		616	680	
300J727340115300	PARKER RIVER J-72	184	191.6	73.528945	-115.87614	Banks						484.0	476.4	Bb	D	SLT	522.8	515.2	Bc	D	SH	38.8	3-46		523	607	
300A727730105000	PAT BAY A-72	17.1	23.8	77.351287	-105.45124	Lougheed	307	300	Ac	K	SH	236.3	229.6	Bb	K	SH	327.2	320.5	Bb	K	SH	90.9	1-28; 3-47		475	567	
300D497540118300	PEDDER POINT D-49	101.2	105.8	75.636463	-118.80753	Eglinton	345.6	341	Aa	K	SH	283	278.4	Ba	K	SLT	349	344.4	Bb	K	SH	66	1-16; 2-32	446			
300G607910104300	POLLUX G-60	53.3	59.7	79.157542	-104.9593	Ellef Ringnes						502.3	495.9	Ba	K	SS							2-33	518	509	564	
300E597910105000	W. POLLUX E-59	6.4	12.8	79.141039	-105.49145	Ellef Ringnes						386.0	379.6	Ba	K	SS	510.8	504.4	Bb	K	SS	124.8	2-34	427	361	408	
300K327530105300	REA POINT STRAT K-32	12.2	15.5	75.360078	-105.72905	Melville						250.0	246.7	Bb	D	SLT							3-48				
300G127550105300	RICHARDSON POINT G-12	138.7	148.4	75.68849	-105.58272	Melville						748	738.3	Ba	D	SS	768.4	758.7	Ba	D	SS	20.4	2-35	750	747	768	
300K077640104000	ROBERT HARBOUR K-07	11.6	18.3	76.609723	-104.03898	Cameron						707.0	700.3	Ba	TR	SS	734	727.3	Ba	TR	SLT	27	2-36	735	622	707	
300C428000084000	ROMULUS C-42	153.3	160	79.85231	-84.377744	Ellesmere						261.0	254.3	Ba	K	SLT	300	293.3	Ba	K	SLT-SH	39	2-37	335	262	407	
300E827400098300	RUSSELL E-82	114	120.4	73.858891	-98.947646	Prince of Wales						304.8	298.4	Bb	D	LS-SLT	349.7	343.3	Bb	D	LS-SLT	44.9	3-49		305	349	
300H497650108300	N. SABINE H-49	53.4	60.4	76.804984	-108.75545	Melville						290.0	283	Bb	K	SLT	434	427	Bb	K	SH	144	3-50	290	436	511	
300A077530110000	SABINE BAY A-07	140.5	147.5	75.435705	-110.01611	Melville						404.6	397.6	Bb	D	SLT	500	493	Bb	D	SLT	95.4	3-51		<366		
300L467630115000	SANDY POINT L-46	32.6	35.8	76.428047	-115.30687	Melville						491.0	487.8	Bb	J	SS	570	566.8	Bb	J	SH	79	3-52		491	546	
300F687720116300	SATELLITE F-68	20.7	25.3	77.291547	-116.9227	Prince Patrick						208.8	204.2	Ba	J	SLT	270.4	265.8	Bc	J	SH	61.6	2-38		210	271	
300F147620108300	SHERARD BAY F-14	43	50	76.222844	-108.59987	Melville						184	177	Bb	K	SH	276.6	269.6	Bb	K	SH	92.6	3-53	235	183	259	
300F347620108300	SHERARD BAY F-34	62	72.5	76.223427	-108.72978	Melville						397.3	386.8	Bc	K	SH							4-21		<368		
300O547620108000	SHERARD O-54	17.4	21	76.230376	-108.3392	Melville						192.4	188.8	Ba	K	SLT	230.7	227.1	Bb	K	SH-SLT	38.3	2-39	232	248	349	
300P377820089300	SHERWOOD P-37	488.6	496.8	78.280647	-89.757286	Axel Heiberg						245.0	236.8	Ba	J	SS	291.6	283.4	Bb	J	SLT-SH	46.6	2-40	299	247	299	
300K287920103300	SIRIUS K-28	14	20.7	79.293867	-103.72988	Ellef Ringnes						319.8	313.1	Bb	K	SLT	461.3	454.6	Bb	K	SLT-SH	141.5	3-54	442	338	460	
300C157720105000	SKYBATTLE BAY C-15	24.1	30.5	77.237645	-105.10119	Lougheed						246.0	239.6	Bb	K	SS	334	327.6	Bb	K	SH-SLT	88	3-55	335	244	335	
300M117720105000	SKYBATTLE BAY M-11	2.6	19	77.182973	-105.11435	Lougheed						492.4	476	Bc	K	SH							4-22		755	815	
300G197620103000	SOPHIE PT. G-19	18	24.7	76.307263	-103.08369	Vanier						597.0	590.3	Ba	D	SS-SLT	670	663.3	Bb	D	SLT	73	2-41	646	597	674	
300J117630101300	STOKES RANGE J-11	334.5	341.4	76.343668	-101.58584	Bathurst						515.0	508.1	Ba	D	SS	619.7	612.8	Bb	D	SLT	104.7	2-42		521	692	
300A157300124300	STORKERSON BAY A-15	14.3	19.5	72.900438	-124.56113	Banks	505	500	Ac	K	SS	500.0	494.8	Ba	K	SS	559.3	554.1	Ba	K	CONG	59.3	1-29; 2-43	558	529	561	
300O237750102001	SUTHERLAND O-23	20.7	30.2	77.715741	-102.14748	King Christian	328	318.5	Aa	J	SH-SLT	251	241.5	Bb	J	SLT	362.5	353	Bb	J	SH	111.5	1-17; 3-56	415	253	290	
300J348000083300	TALEMEN J-34	268.2	275.1	79.895643	-83.780682	Ellesmere						717	710.1	Ba	K	SLT	761	754.1	Bb	K	SH	44	2-44	899	716	762	
300P387810103000	THOR P-38	4.9	10.1	78.132013	-103.25695	Thor	343.2	338	Aa	K-J	SH	238	232.8	Bb	K	SH	343.7	338.5	Bb	K-J	SH	105.7	1-18; 3-57		253	344	
300M487250120300	TIRITCHIK M-48	106.7	111.3	72.797996	-120.74946	Banks						749.6	745	Bb	K	SH							3-58		764	829	
300F637600106000	TOWSON POINT F-63	276.1	279.8	75.872216	-106.41214	Melville						646.0	642.3	Bb	D	DOL							3-59		646		
300H077340123000	UMINMAK H-07	107	112.2	73.608545	-123.01147	Banks						464.9	459.7	Bb	K	SLT	537.8	532.6	Bb	K	SH	72.9	3-60				
300A277700109000	VESEY A-27	7.8	15	76.935407	-109.13772	Vesey Hamilton						137.4	130.2	Bc	K	SS	195	187.8	Bc	K	SH	57.6	4-23		690	785	IBPF<375 m from wireline logs
300F367250117000	VICTORIA ISLAND F-36	147.5	155.8	72.755532	-117.18945	Victoria						226.0	217.7	Bc	D	DOL	311	302.7	Bc	D	DOL	85	4-24		235	290	
300A737800102000	WALLIS A-73	5.4	12.2	77.871357	-102.44914	King Christian						396.6	389.8	Ba	K	SLT	430.2	423.4	Bb	K	SS	33.6	2-45		375	440	
300K627800102000	WALLIS K-62	19.5	27.7	77.863191	-102.42433	King Christian						393.2	385	Bb	K	SS	490	481.8	Bb	K	SS	96.8	3-61	443	393	491	
300O107550108300	WEATHERALL O-10	153	157.7	75.831856	-108.53265	Melville						213.5	208.8	Ba	P	SS	345.4	340.7	Bb	P	SS	131.9	2-46	207	235	352	Identified lithology assists in IBPF determination
300J517640117000	WILKIE POINT J-51	135.3	140.5	76.509307	-117.33315	Prince Patrick						219.6	214.4	Bb	J	SH	250	244.8	Bb	J	SH	30.4	3-62	280	305	344	
300E607800111000	WILKINS E-60	64	68.9	77.989503	-111.36545	Mackenzie King	276	271	Ac	J	SH	196.2	191.3	Bc	J	SH	286	281.1	Bc	J	SH	89.8	1-30; 4-25	395	<366	451	
300A097450110300	WINTER HARBOUR NO.1(A-09)	22.9	27.4	74.802348	-110.51254	Melville	540	535.5	Aa	D	SLT	537.3	532.8	Bb	D	SLT	560	555.5	Bb	D	SLT	22.7	1-19; 3-63		384		
300F627250096300	YOUNG BAY F-62	21.3	25.9	72.69041	-96.826586	Prince of Wales						216.6	212	Bc	S	SS							4-26	253	253	277	
300D217630098300	YOUNG INLET D-21	213.4	219.7	76.336943	-98.67608	Bathurst						561.2	554.9	Ba	S	SS-SLT	598.4	592.1	Bb	S	SLT	37.2	2-47		399	495	
300F117600113300	ZEUS F-11	196	200.6	75.840305	-113.60945	Melville						444.6	440	Bb	D	SH-SLT	525	520.4	Bb	D	SLT-SH	80.4	3-64	268	445	524	

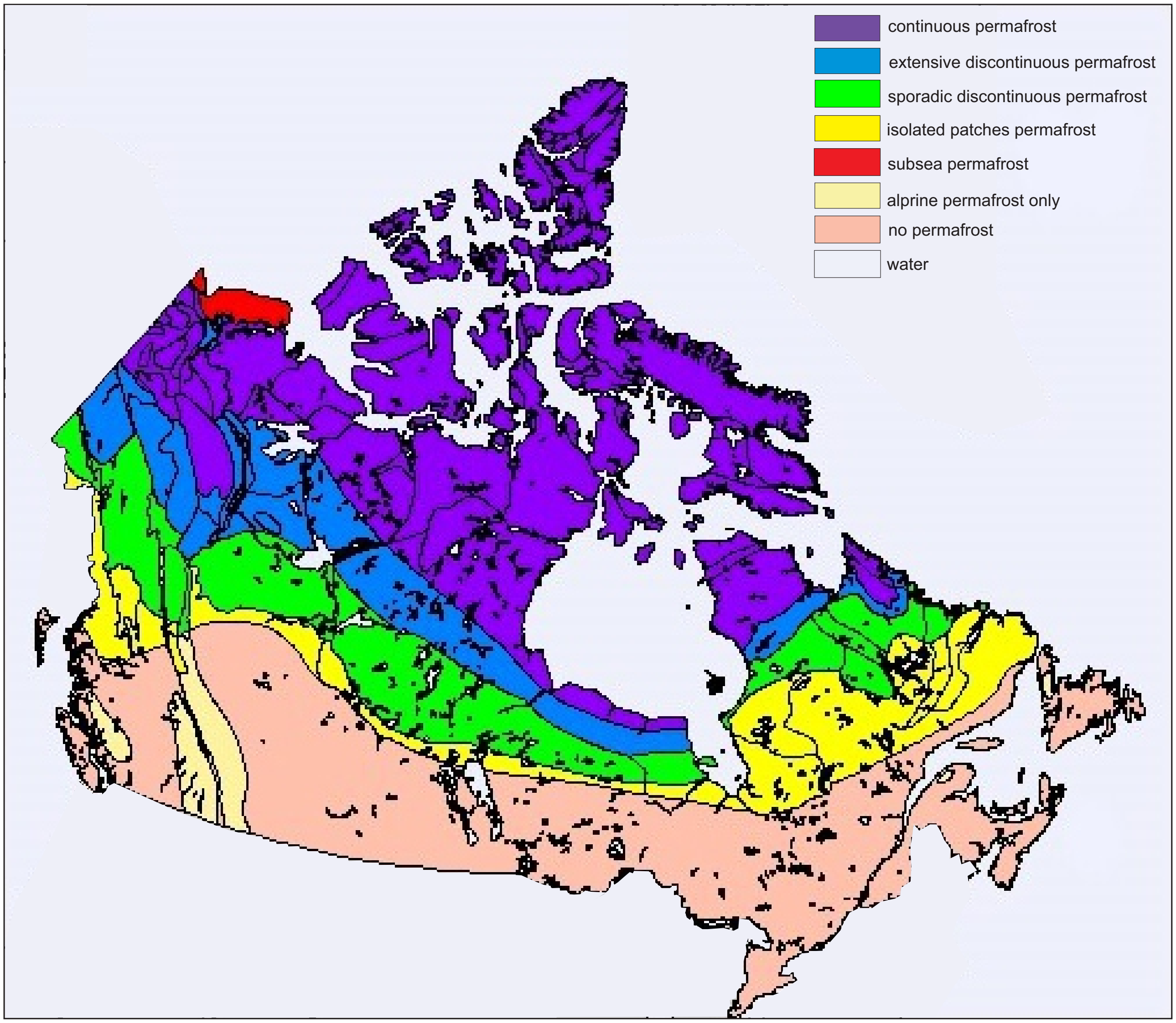

Figure 1. Permafrost distribution in Canada (modified from Heginbottom et al., 1995)

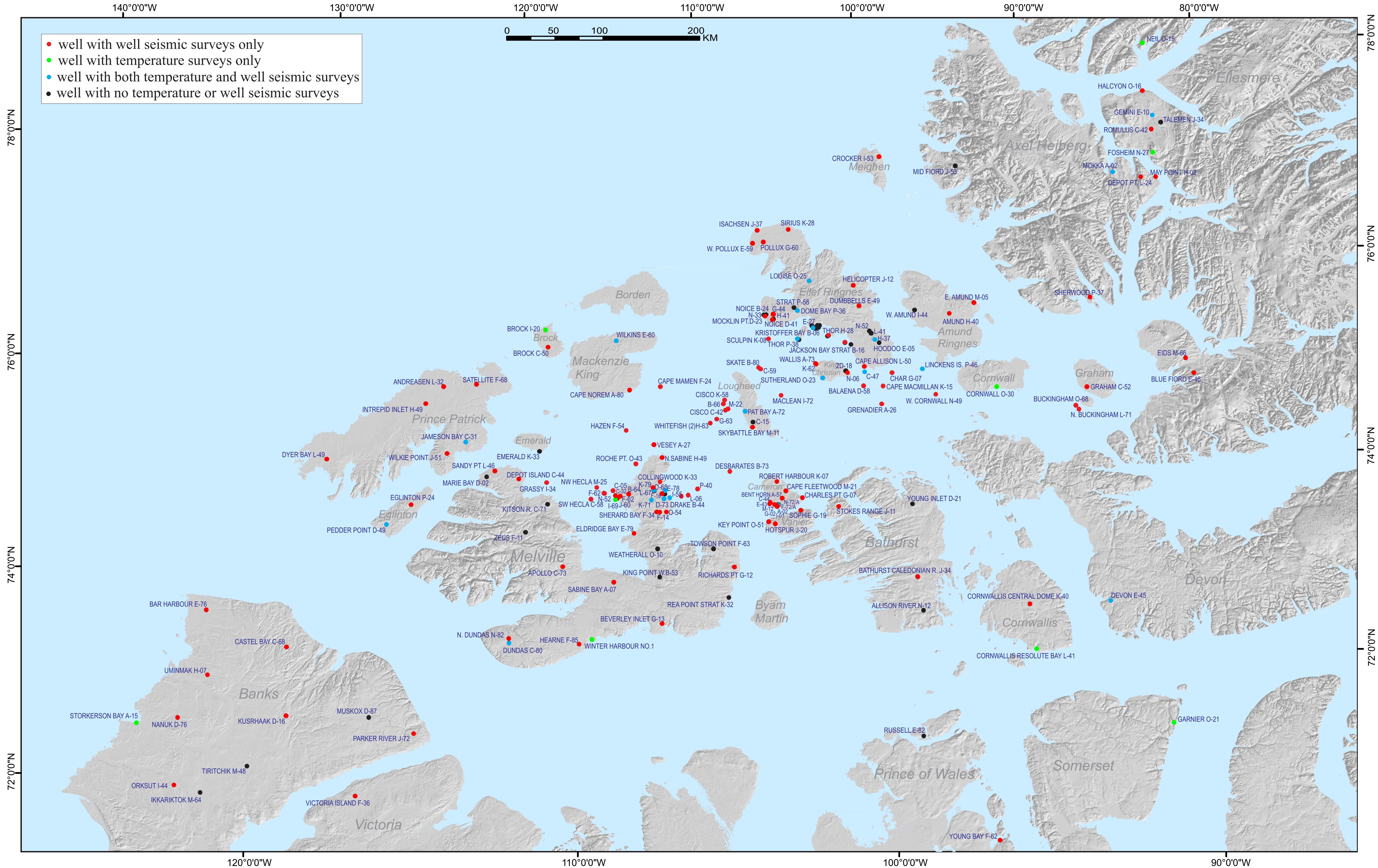

Figure 2. The location of 192 petroleum exploration wells drilled between 1961 and 1987 in the Canadian Arctic Islands, 113 of which only contain well seismic surveys, 23 wells have both well seismic and temperature surveys, 9 wells contain temperature survey data only.

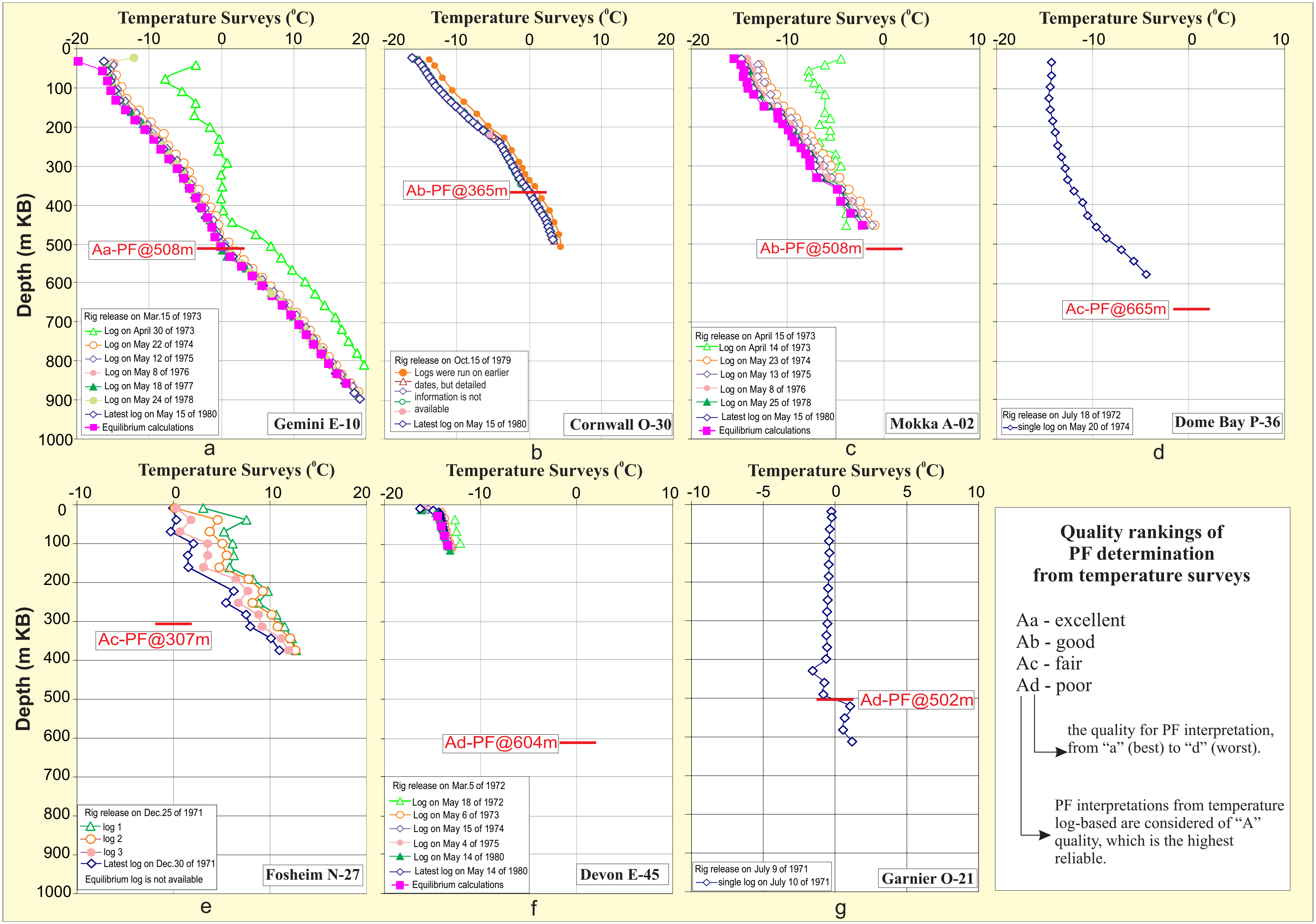

Figure 3. Temperature logs (original temperature measurements and calculated equilibrium temperatures), and the base of permafrost determinations with different quality rankings for seven representative wells in the Canadian Arctic Islands.

a - "**Aa**" quality data for the Gemini E-10 well on Ellesmere Island; b - "**Ab**" quality data for the Cornwall O-30 well on Cornwall Island; c - "**Ab**" quality data for the Mokka A-02 well on Axel Heiberg Island; d - "**Ac**" quality data for the Dome Bay P-36 well on Ellef Ringnes Island; e - "**Ac**" quality data for the Fosheim N-27 well on Ellesmere Island; f - "**Ad**" quality data the Devon E-45 well on Devon Island; g - "**Ad**" quality data for the Garnier O-21 well on Somerset Island.

300C477750100000/CAPE ALLISON C-47

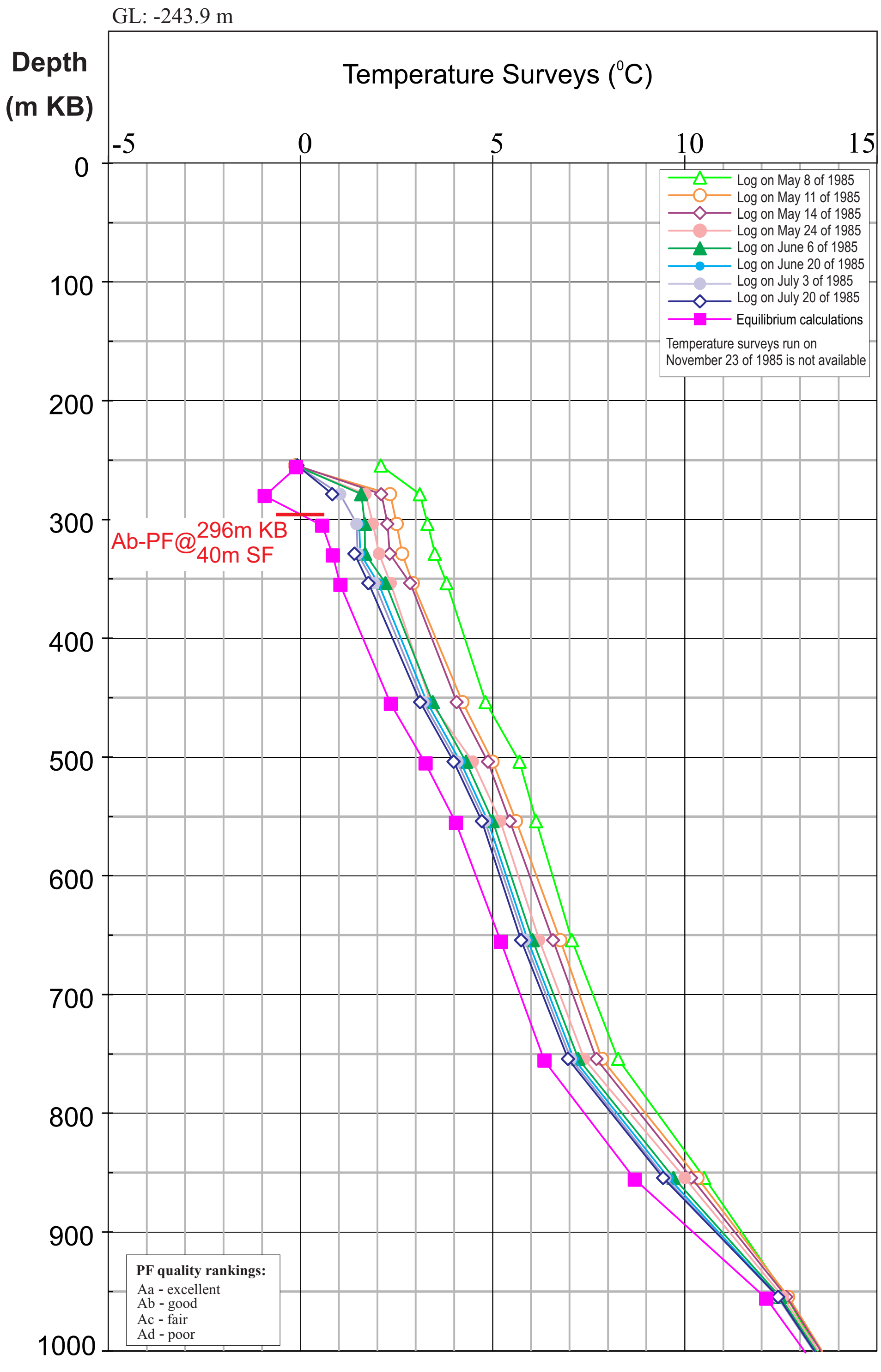

Figure 4. Selected temperature-depth profiles and equilibrium temperature calculations are illustrated for the shallow (<750 m SF) interval of the offshore well Cape Allison C-47, located in 244 m of water between Ellef Ringnes and King Christian islands, in the Canadian Arctic Islands.

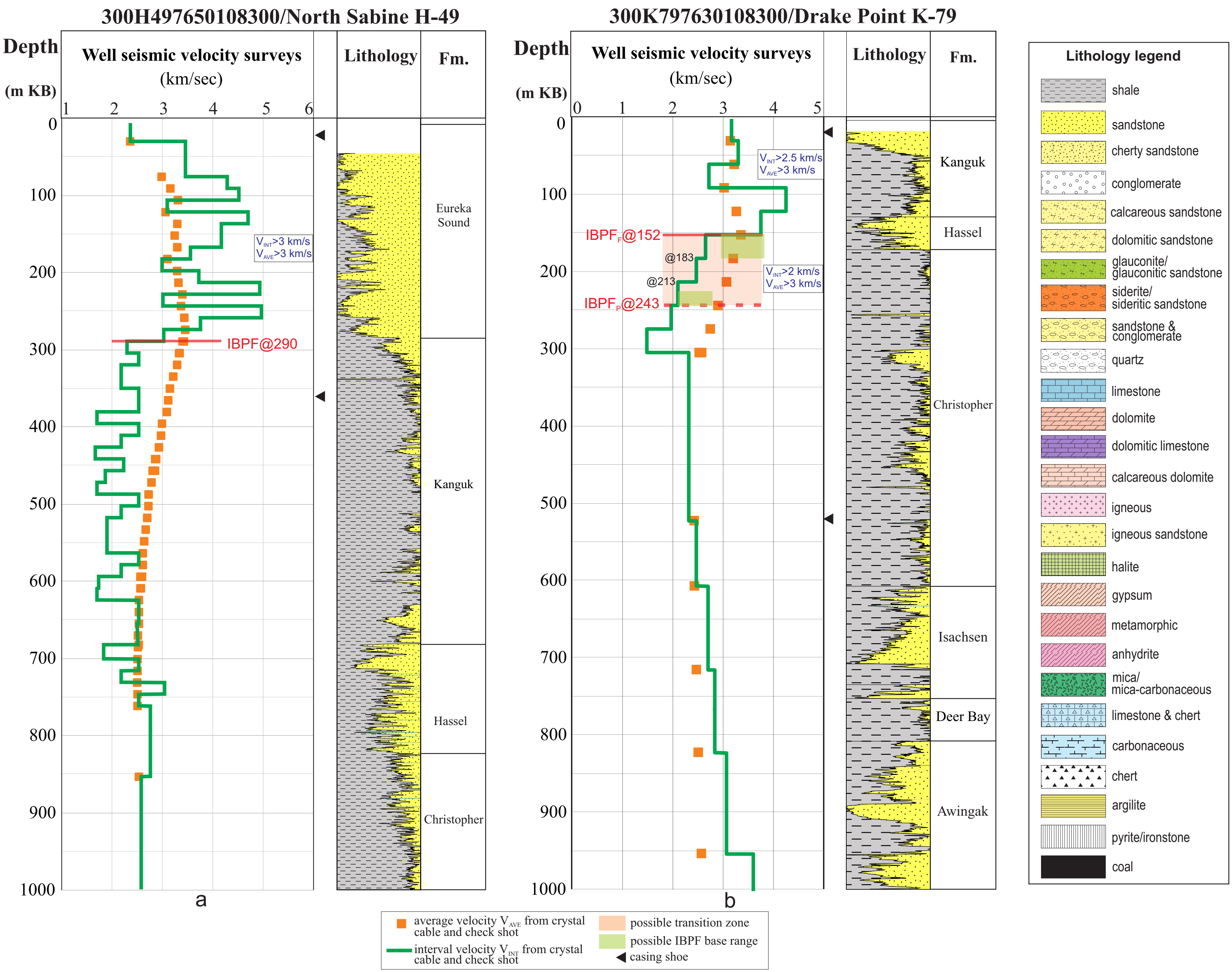

Figure 5. Well seismic velocity surveys and their relationship to the base of ice-bearing permafrost for wells North Sabine H-49 (a) and Drake Point K-79 (b) on Melville Island in the Canadian Arctic Islands.

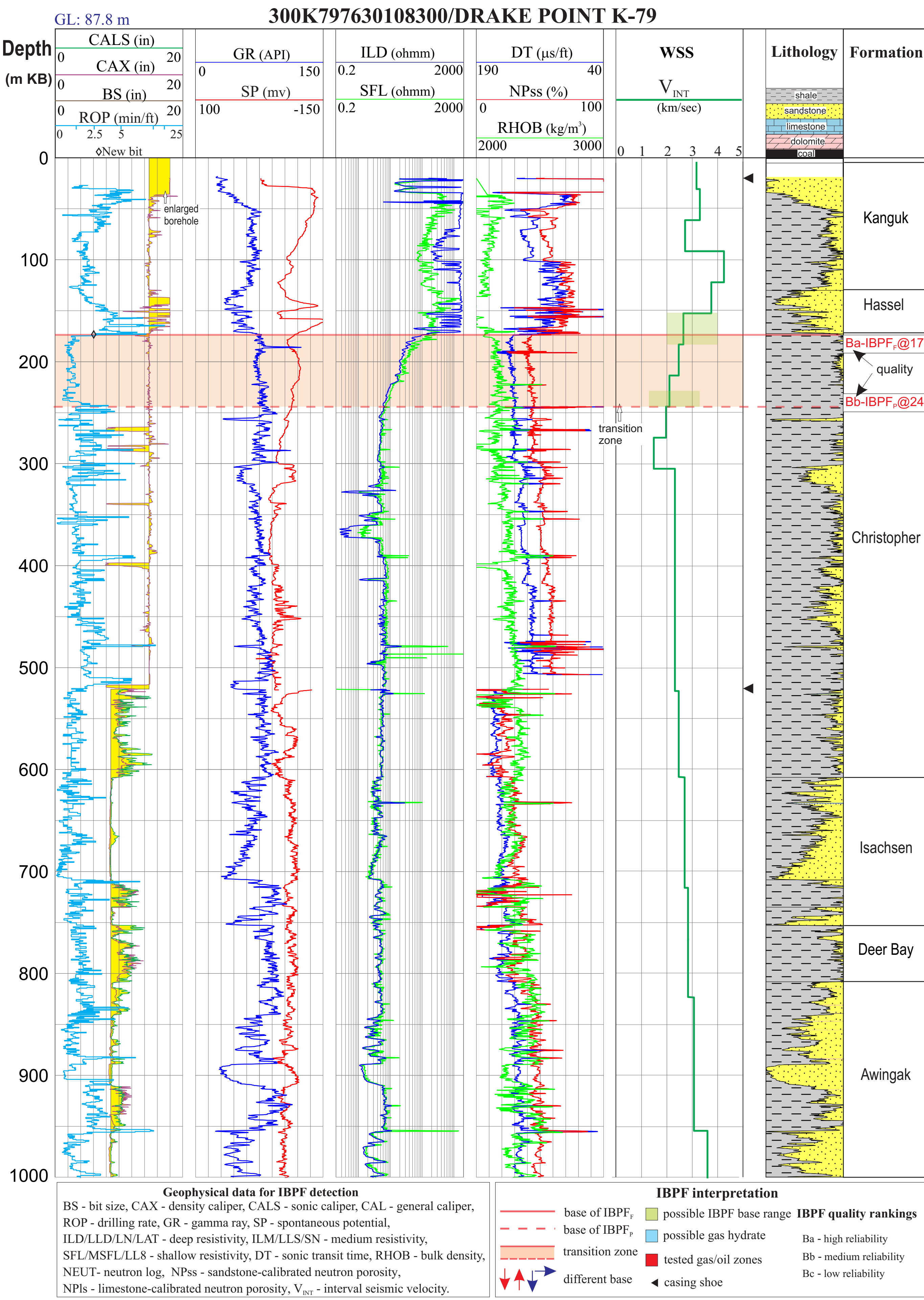

Figure 6. Example showing responses to permafrost zone that includes both a fully frozen ($IBPF_F$) and a partially frozen ($IBPF_P$) from geophysical well logs and well seismic velocity in the Drake Point K-79 well located on Melville Island in the Canadian Arctic Islands.

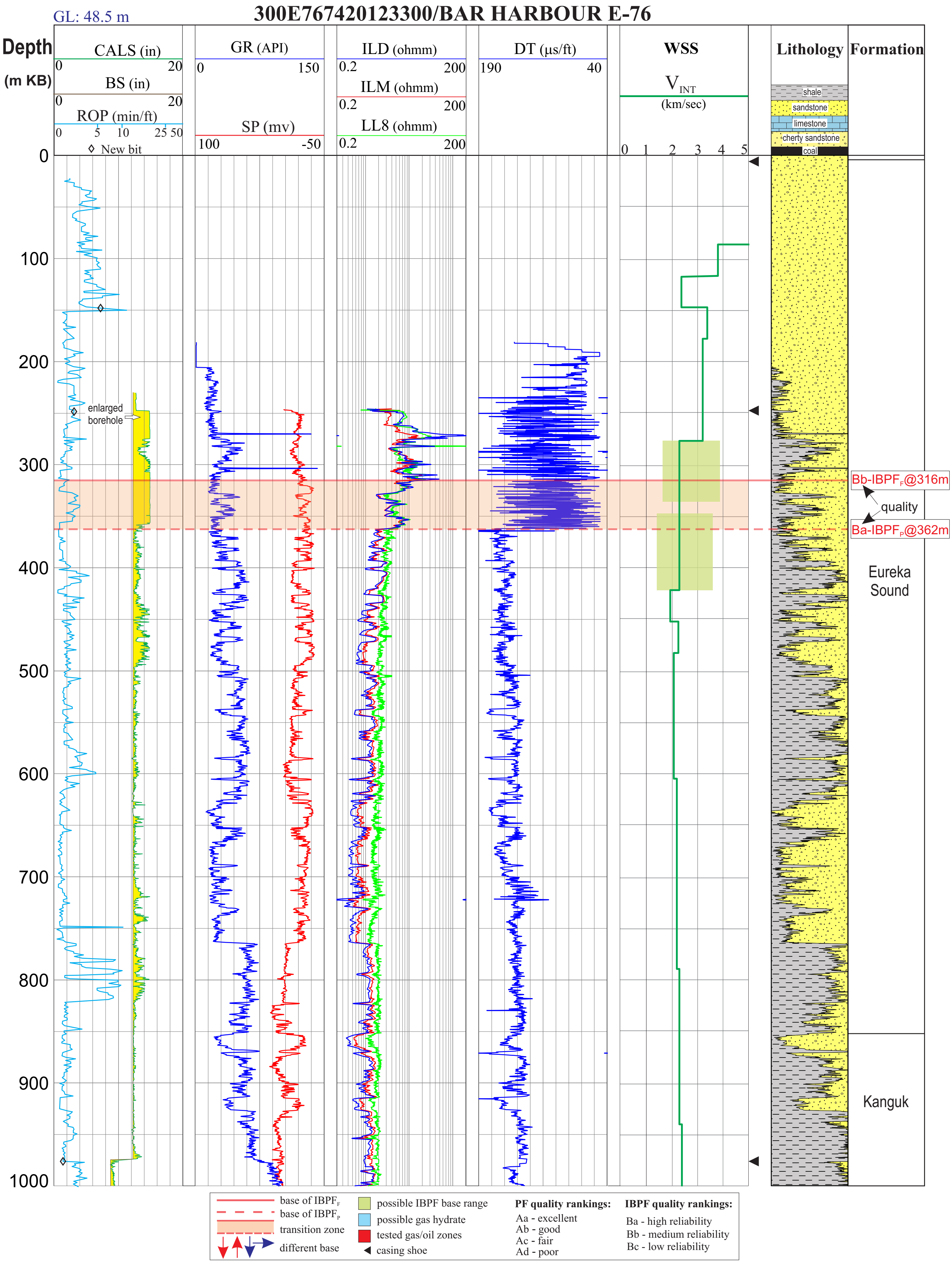

Figure 7. Example showing borehole compensate sonic log is successfully used to determine the bases of $IBPF_F$ and $IBPF_P$ for the Bar Harbour E-76 well on Banks Island in the Canadian Arctic Islands.

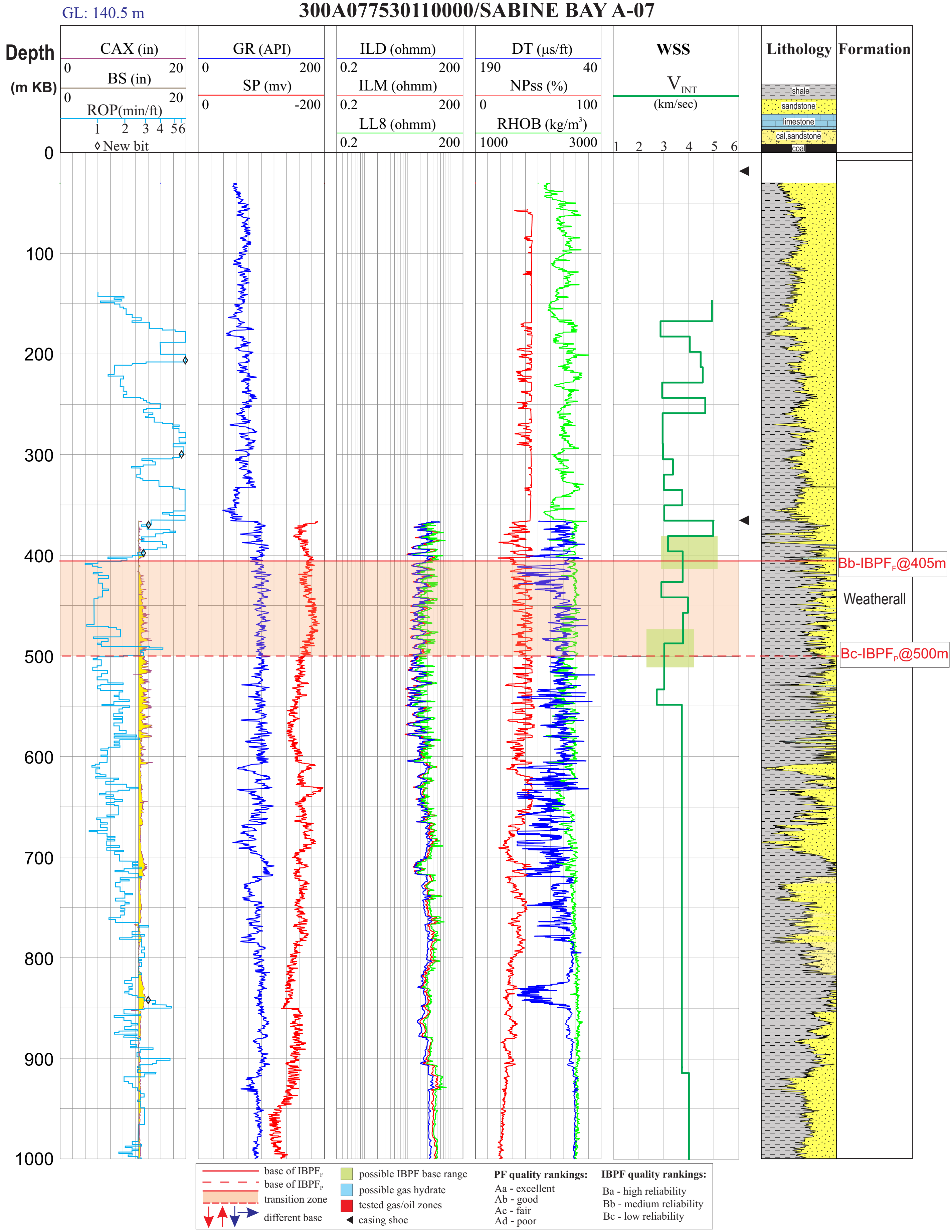

Figure 8. Example showing that drilling rate (ROP) helps estimate the bases of $IBPF_F$ and $IBPF_P$ where wireline log signatures are ambiguous and the well seismic velocity responses are subtle in the permafrost zone for the Sabine Bay A-07 well on Melville Island in the Canadian Arctic Islands.

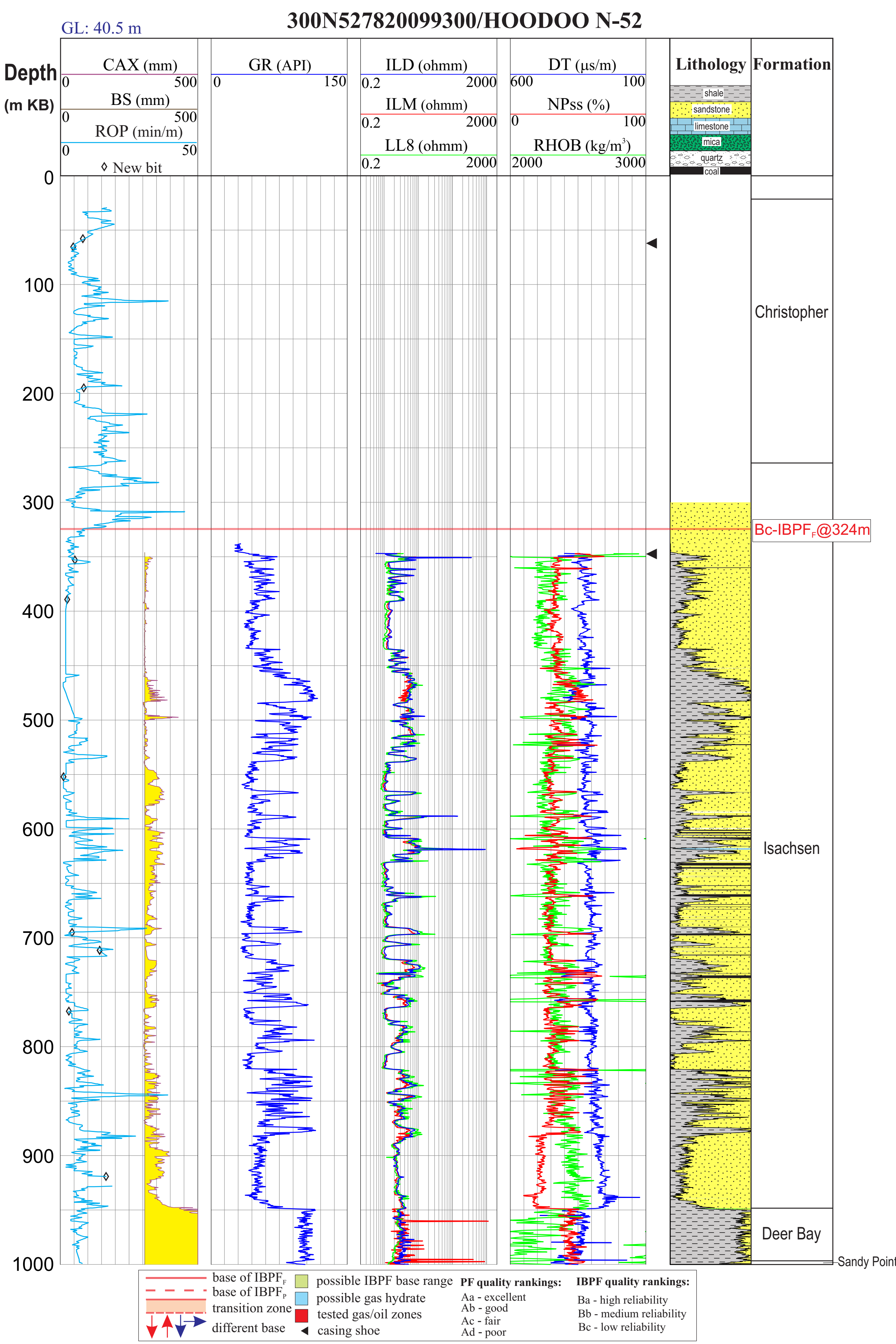

Figure 9. Base of $IBPF_F$ is estimated only from well drilling rate for the Hoodoo N-52 well on Ellef Ringnes Island in the Canadian Arctic Islands.

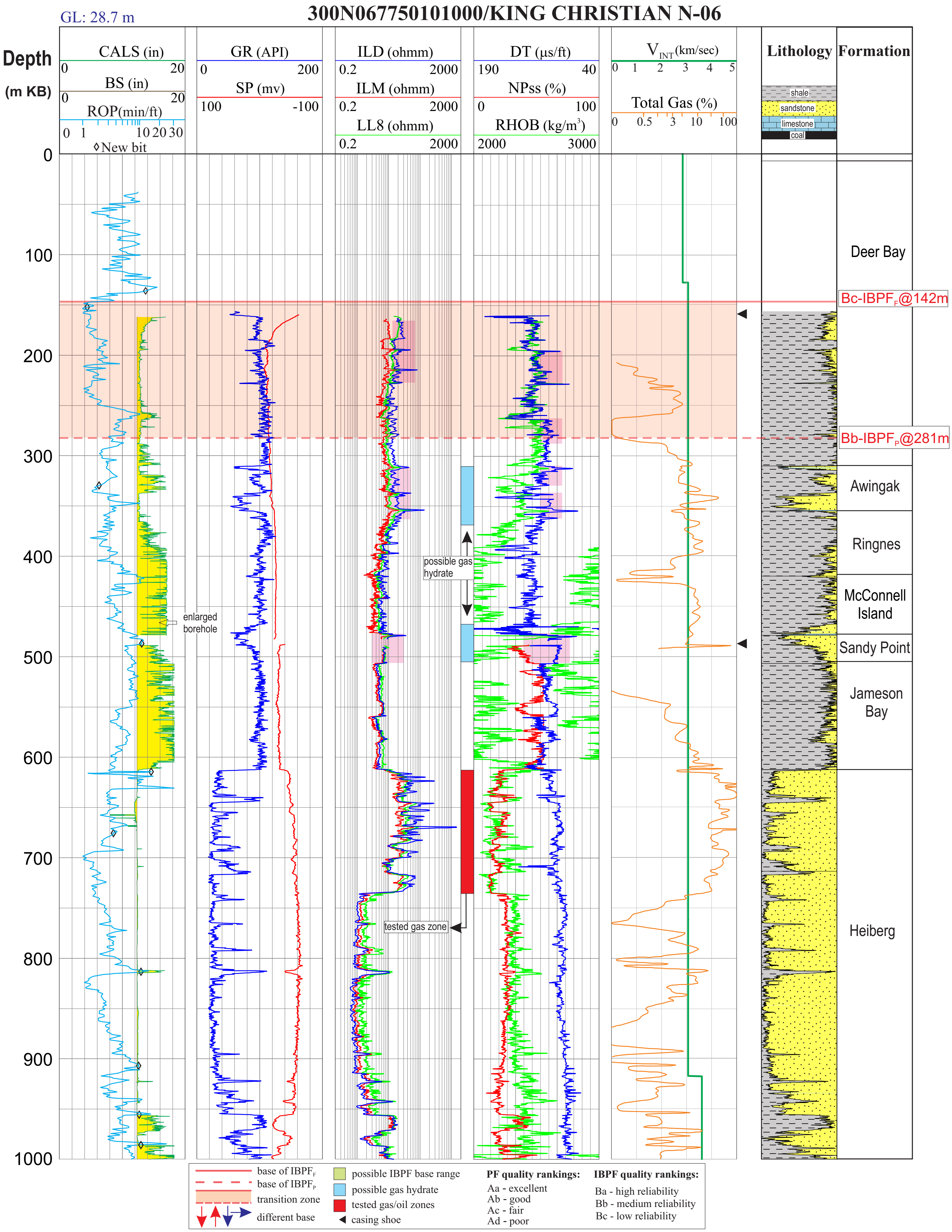

Figure 10. Estimation of IBPF from wireline logs, drilling rate, gas log and other well information for the King Christian N-06 well located on King Christian Island in the Canadian Arctic Islands.

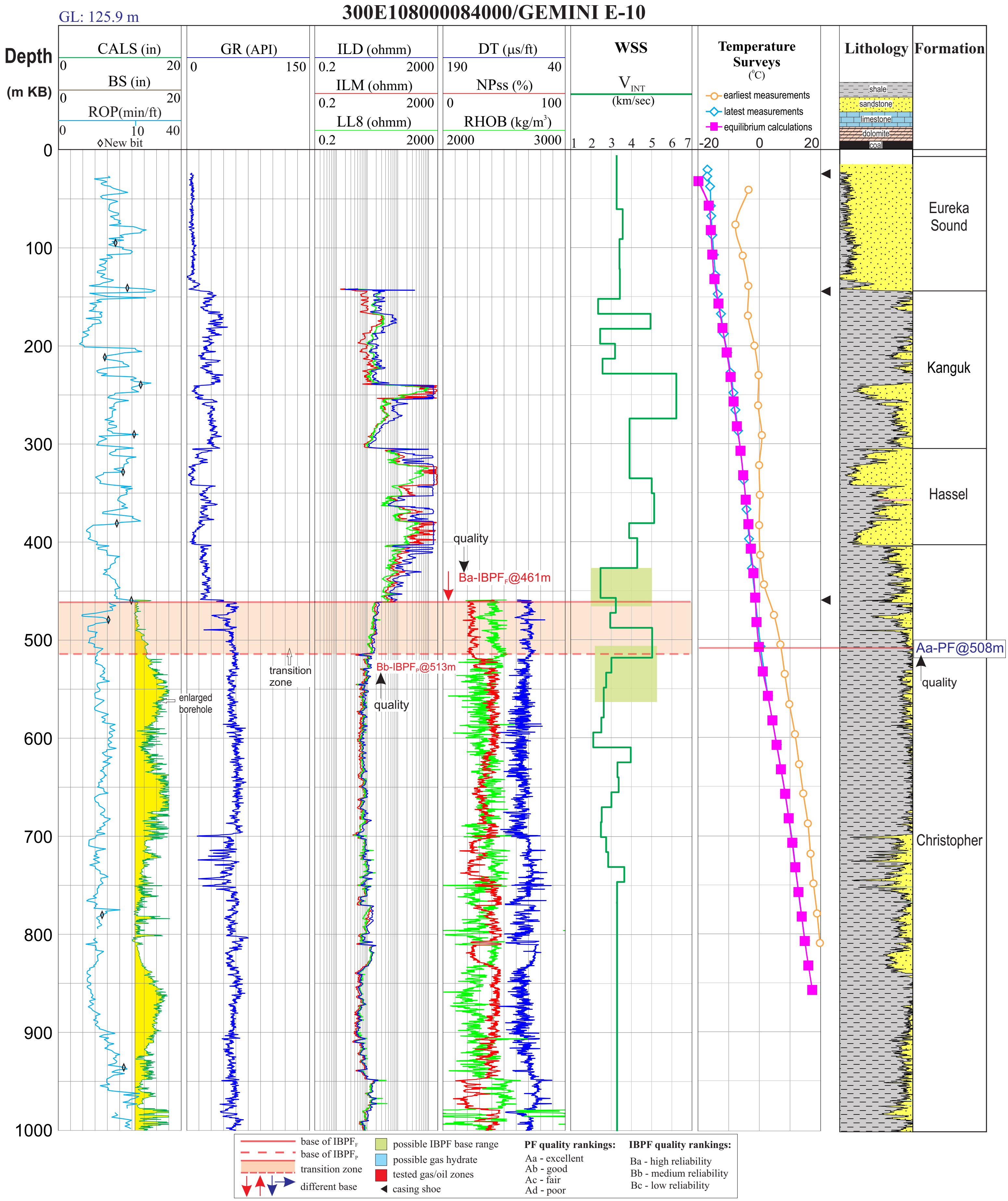

Figure 11. Determinations of base of PF from temperature surveys, and IBPF ($IBPF_F$ and $IBPF_P$) from geophysical well logs and well seismic surveys for the Gemini E-10 well on Ellesmere Island in the Canadian Arctic Islands.

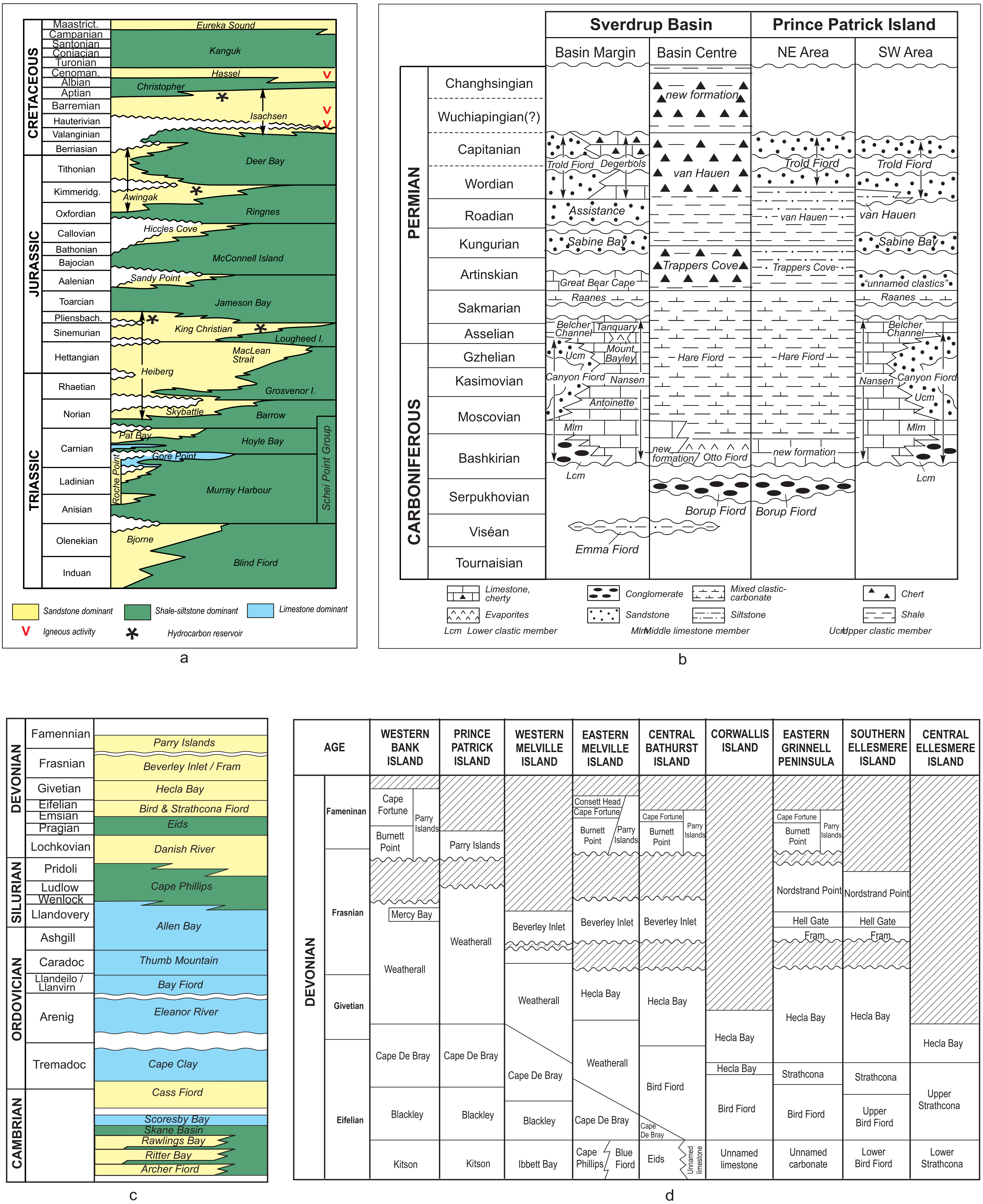

Figure 12. Stratigraphic chart of Canadian Arctic Islands.
a - Triassic-Cretaceous stratigraphy, Canadian Arctic Islands, modified from Embry (2011);
b - Schematic representation of Permian-Carboniferous formations in the Sverdrup Basin and Prince Patrick Island, modified from Beauchamp et al.(2001);
c- Stratigraphy of the Franklinian shelf, modified from Hadlari et al. (2014);
d - Correlation chart for Middle-Upper Devonian formations, Canadian Arctic Islands, modified from Embry (1991).

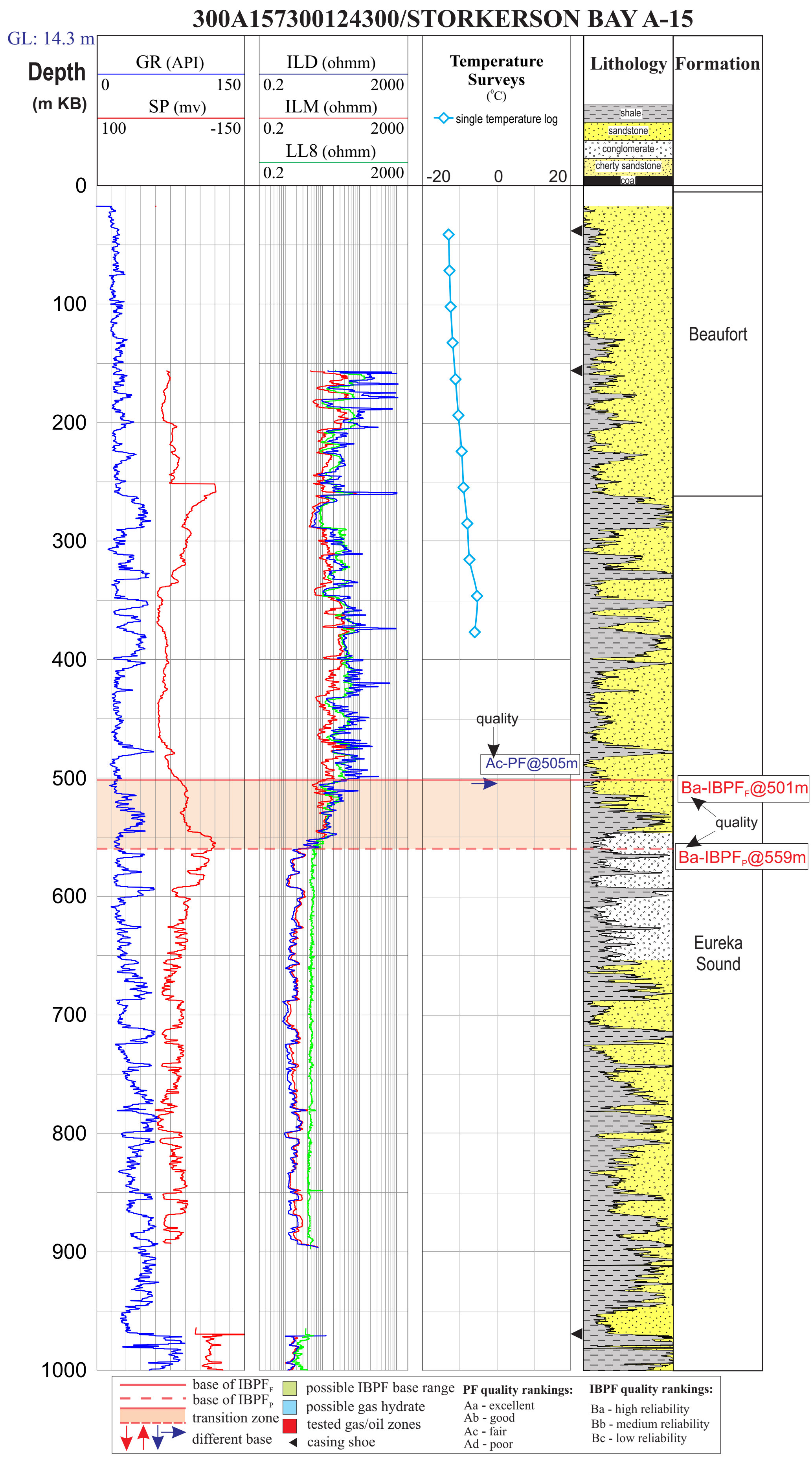

Figure 13. Estimations of base of PF from temperature surveys, and IBPF from geophysical well logs for the Storkerson Bay A-15 well on Banks Island in the Canadian Arctic Islands.

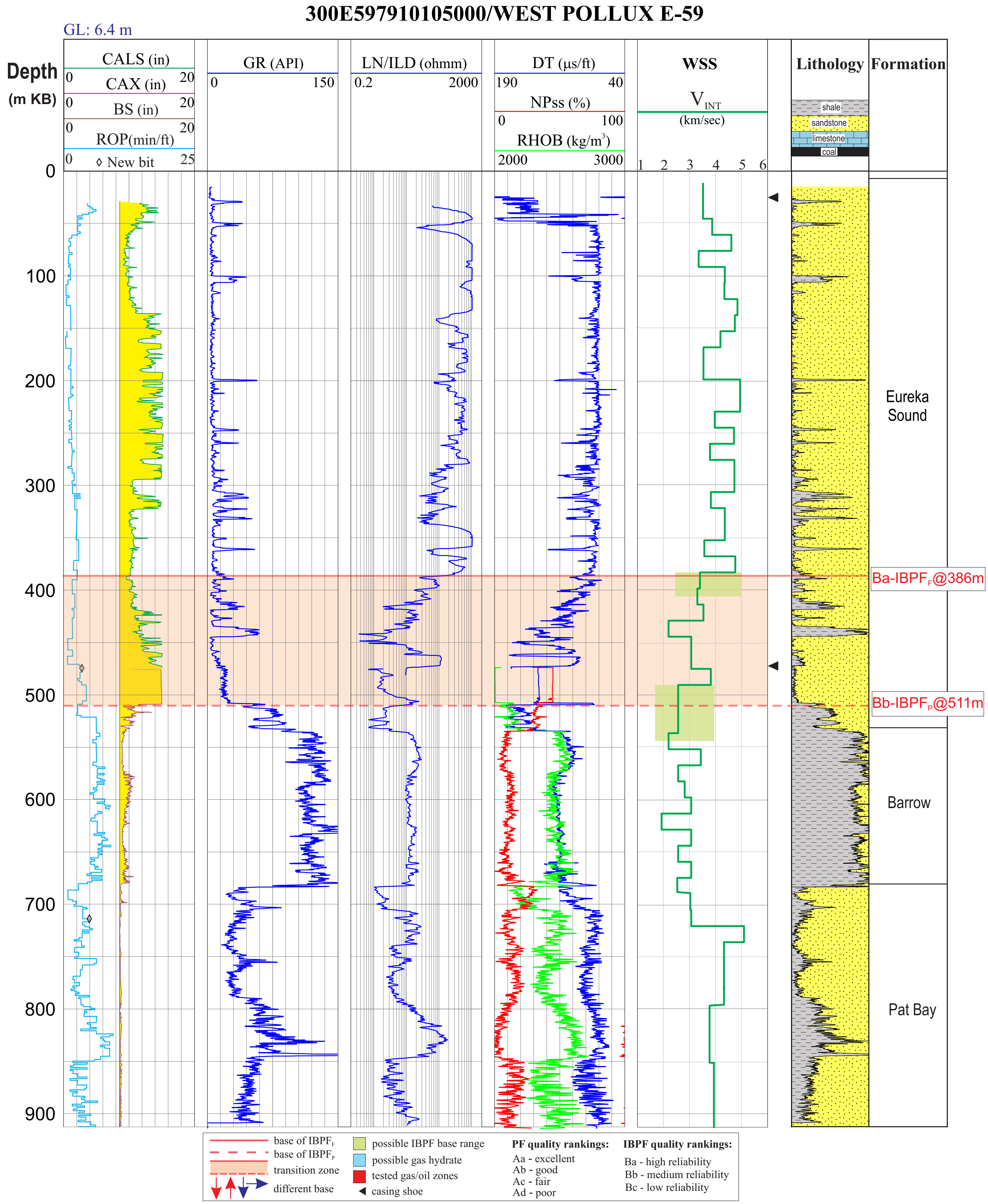

Figure 14. Example showing that bases of $IBPF_F$ and $IBPF_P$ are identified from geophysical well logs and well seismic surveys for the West Pollux E-59 well on Ellef Ringnes Island in the Canadian Arctic Islands. In the unconsolidated sandstone interval with permafrost zone, ROP responded with a high speed of drilling rate since thawing occurred and led to an unstable overgauged borehole.

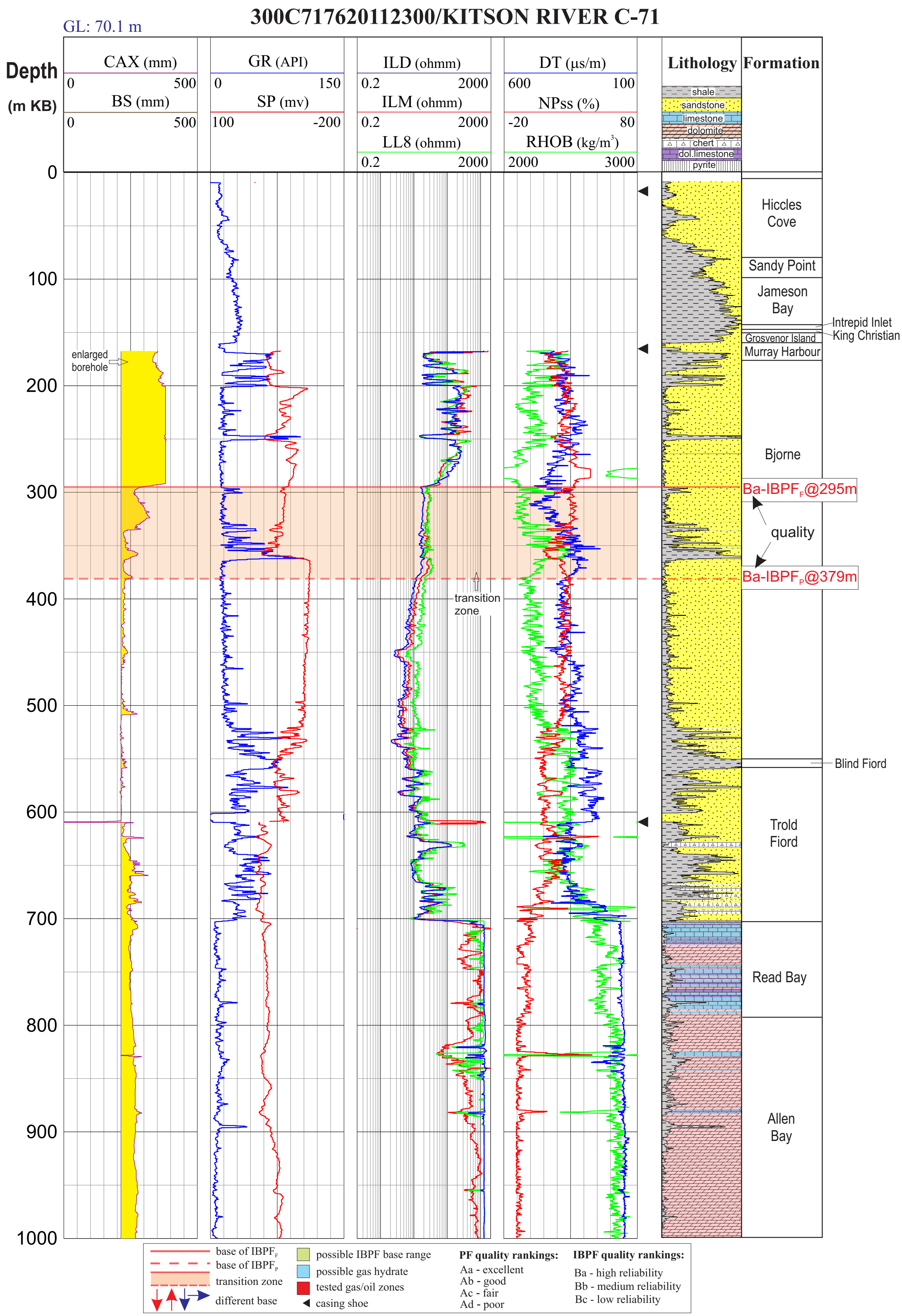

Figure 15. Determinations of base of $IBPF_F$ and $IBPF_P$ using geophysical well logs for the Kitson River C-71 well on Melville Island in the Canadian Arctic Islands.

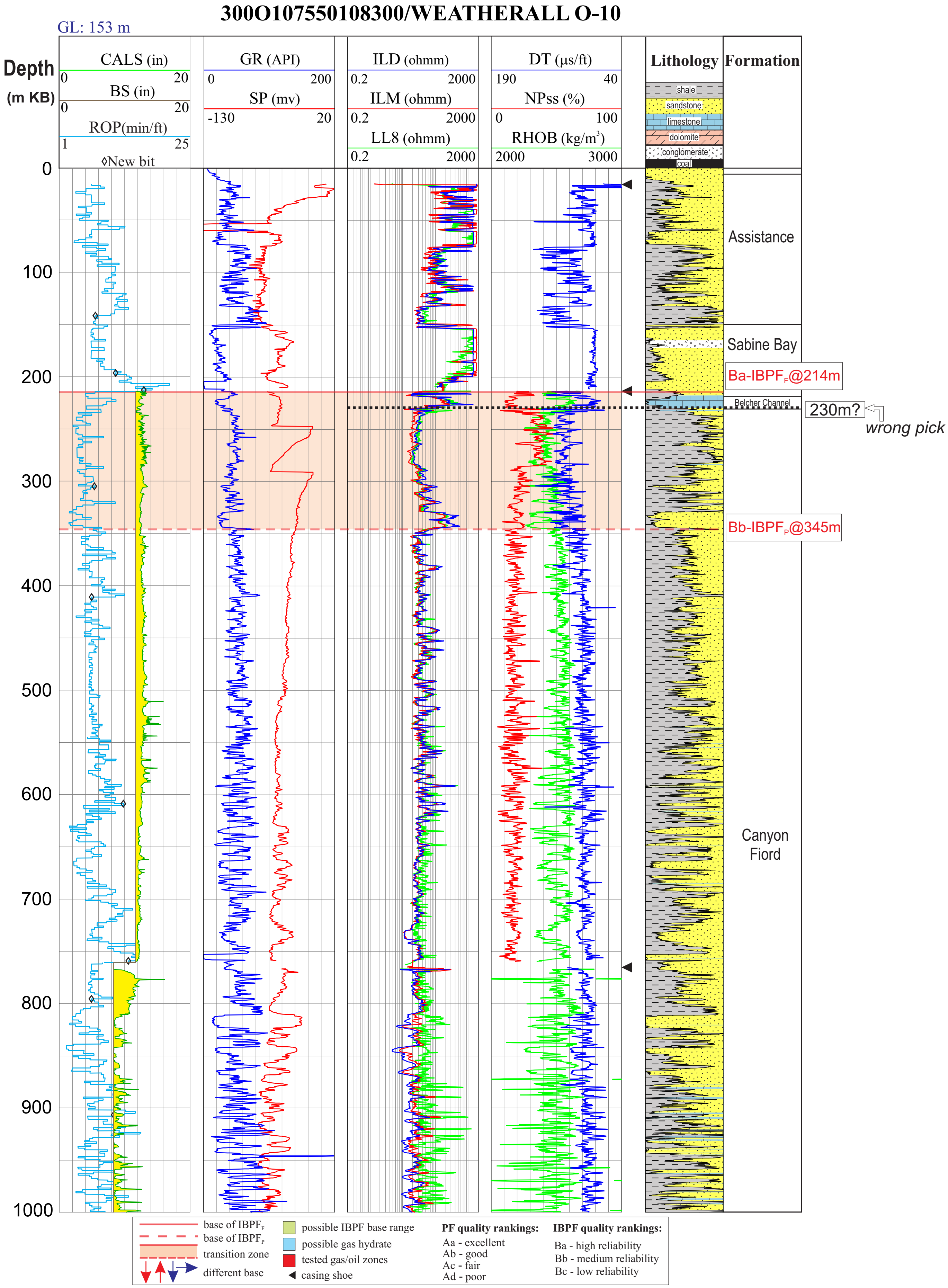

Figure 16. Example showing that lithology interpretation and drilling rate assistance in determination of the base of IBPF from wireline logs for the Weatherall O-10 well on Melville Island in the Canadian Arctic Islands.

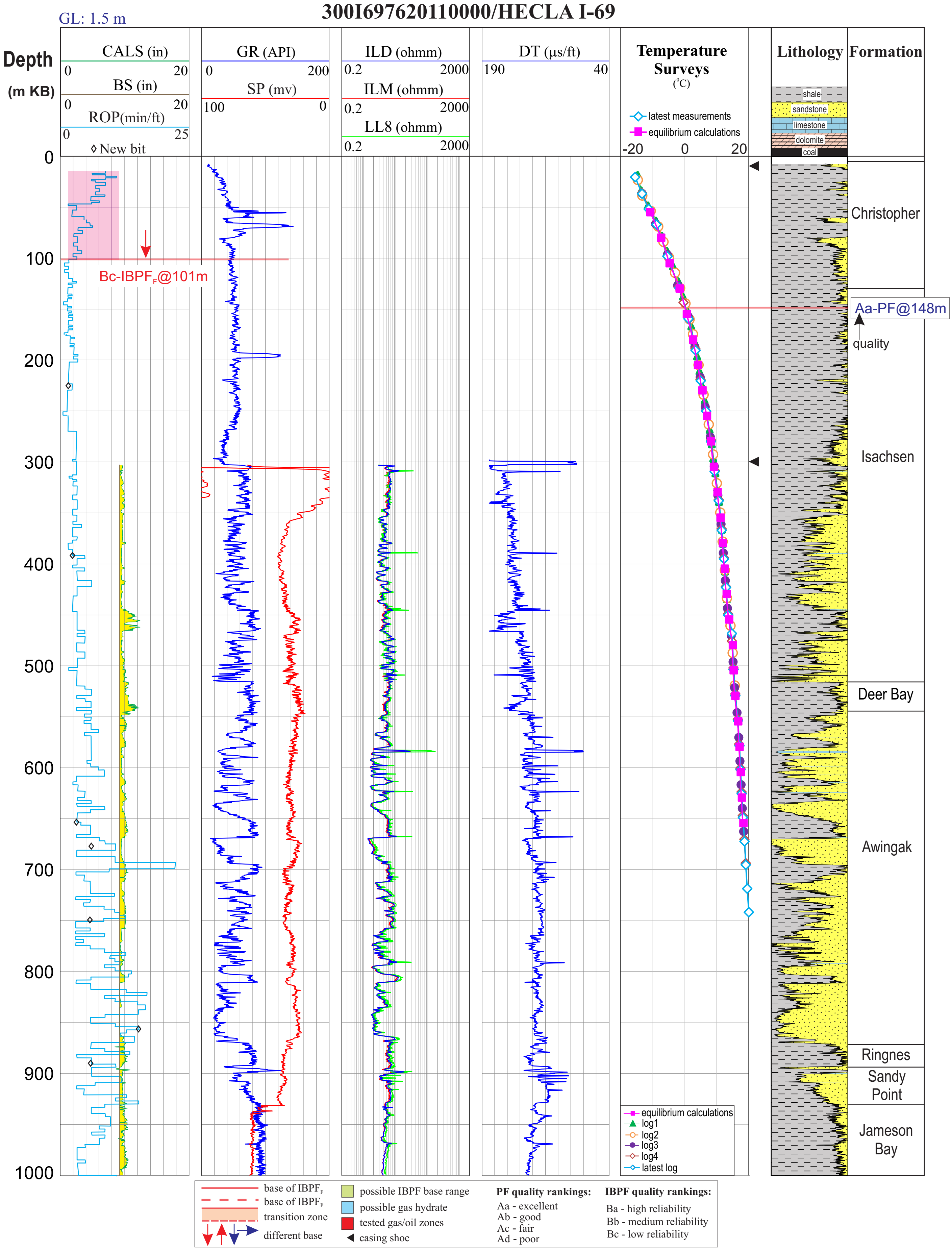

Figure 17. Example showing that accurate temperature survey data provide the best estimate (with quality "Aa") of the base of permafrost (PF), a possible base of IBPF$_F$ with quality "Bc" is estimated from ROP log for the Hecla I-69 well that lacks wireline logs in the permafrost zone, on Melville Island in the Canadian Arctic Islands.

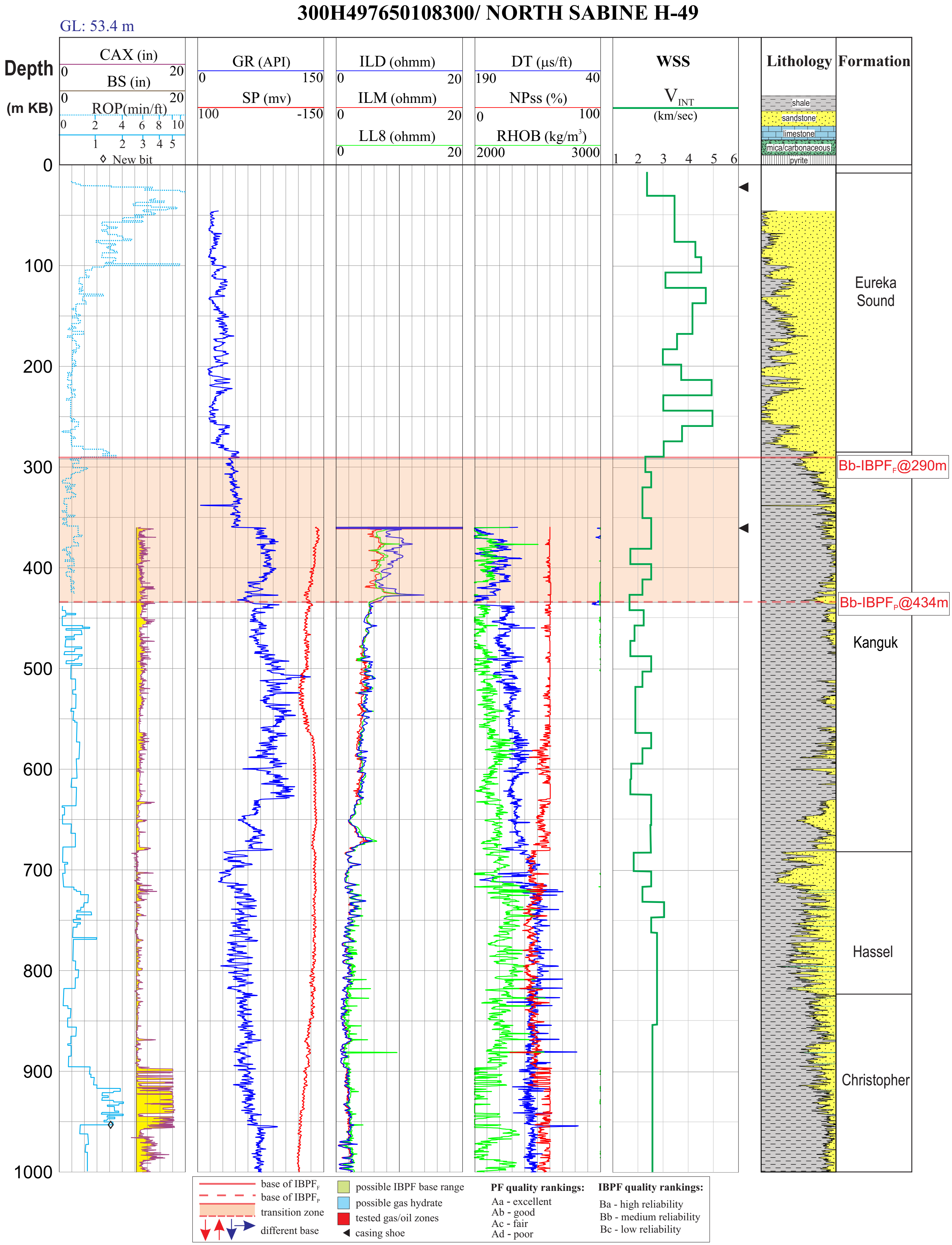

Figure 18. Example showing determination of the base of $IBPF_F$ from crystal cable surveys and drilling rate (ROP) for the North Sabine H-49 well on Melville Island in the Canadian Arctic Islands.

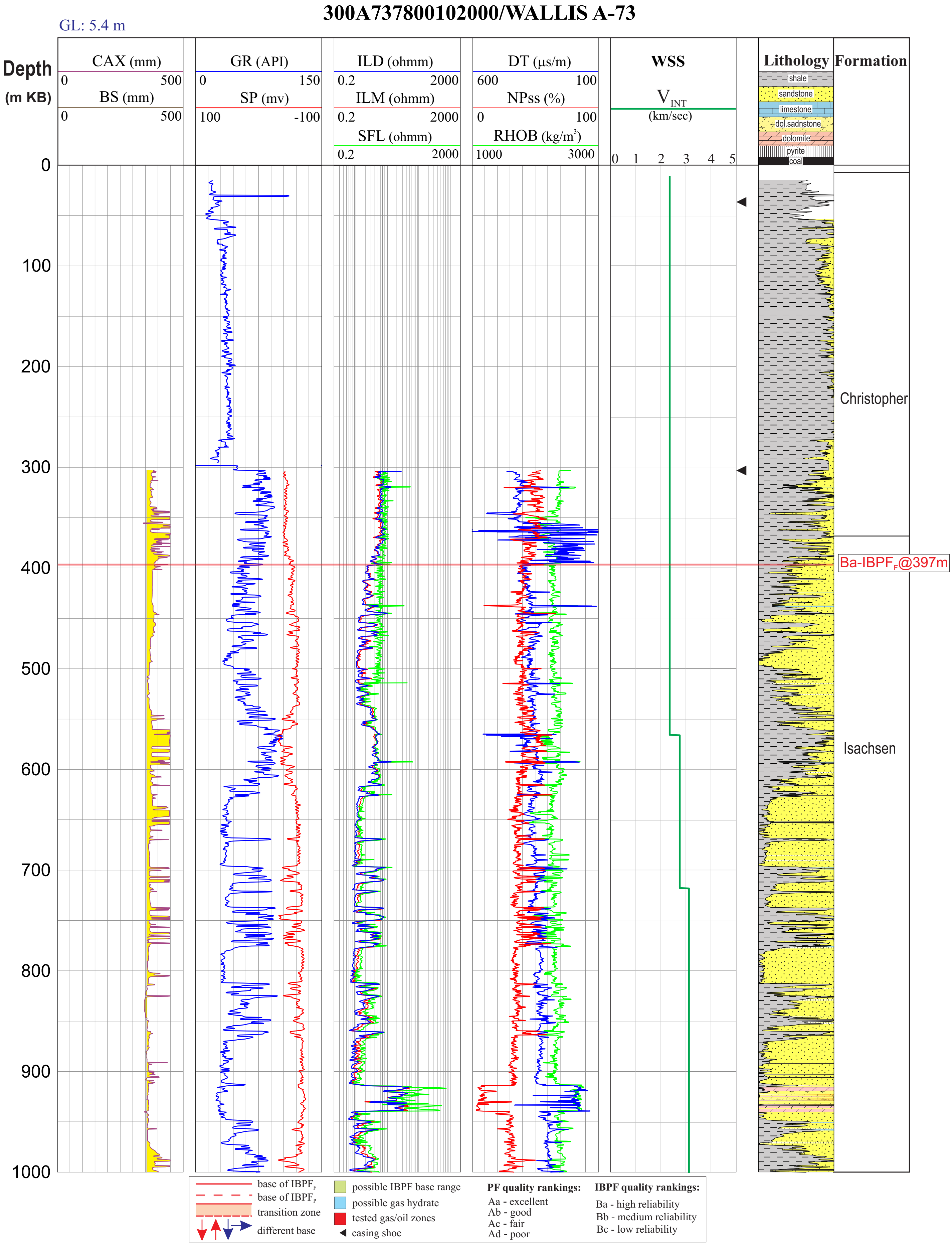

Figure 19. Example showing a remarkable response to base of $IBPF_F$ on sonic log and is supported by other wireline logs for the Wallis A-73 well on King Christian Island in the Canadian Arctic Islands.

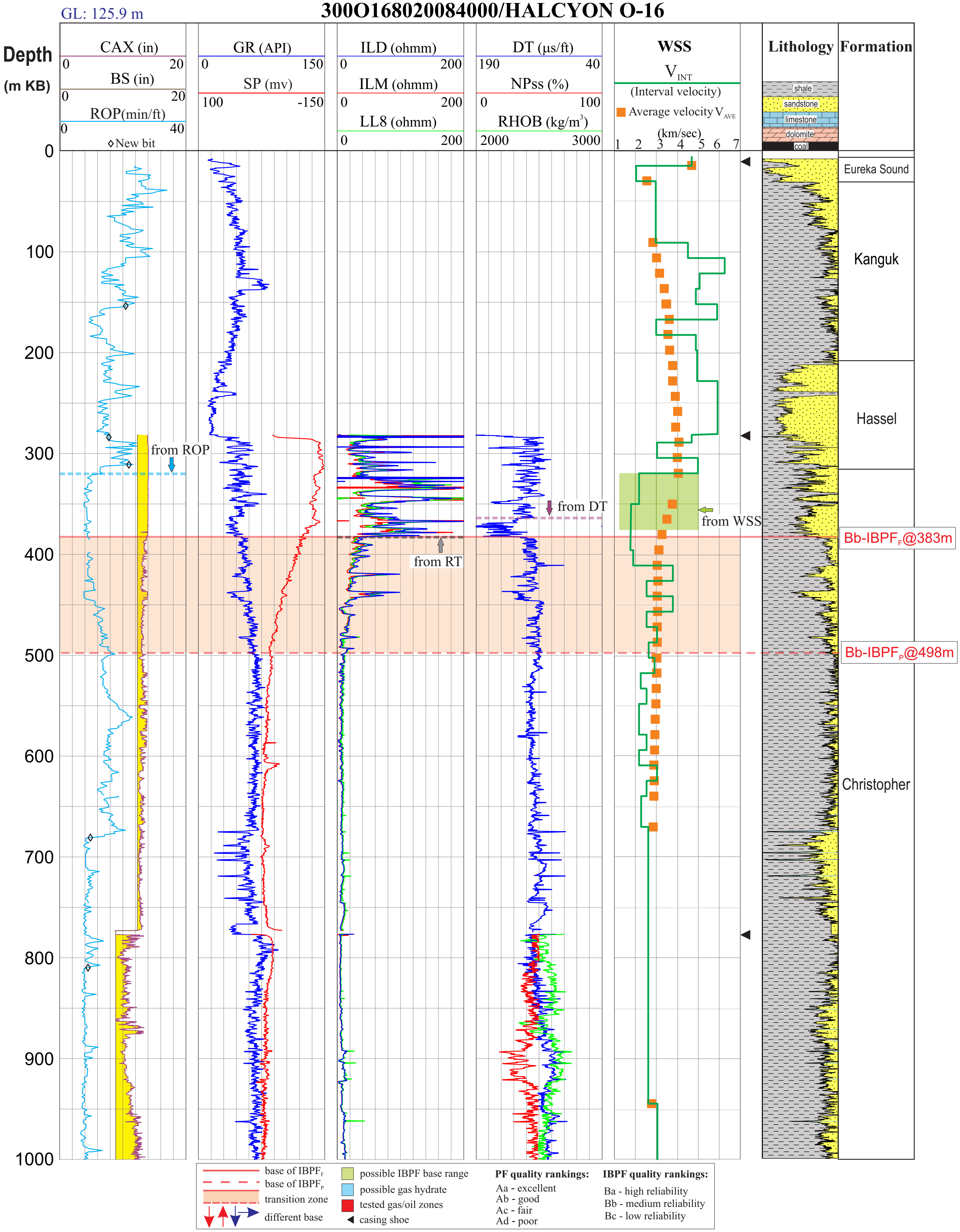

Figure 20. Example showing $IBPF_F$ and $IBPF_P$ interpretation with quality "Bb" for the Halcyon O-16 well on Ellesmere Island in the Canadian Arctic Islands. Defined base of $IBPF_F$ by resistivity logs (the solid orange and dashed black lines) differs with respect to sonic log (the dashed purple line), ROP (the dashed light blue line), and well seismic surveys (the green coloured area).

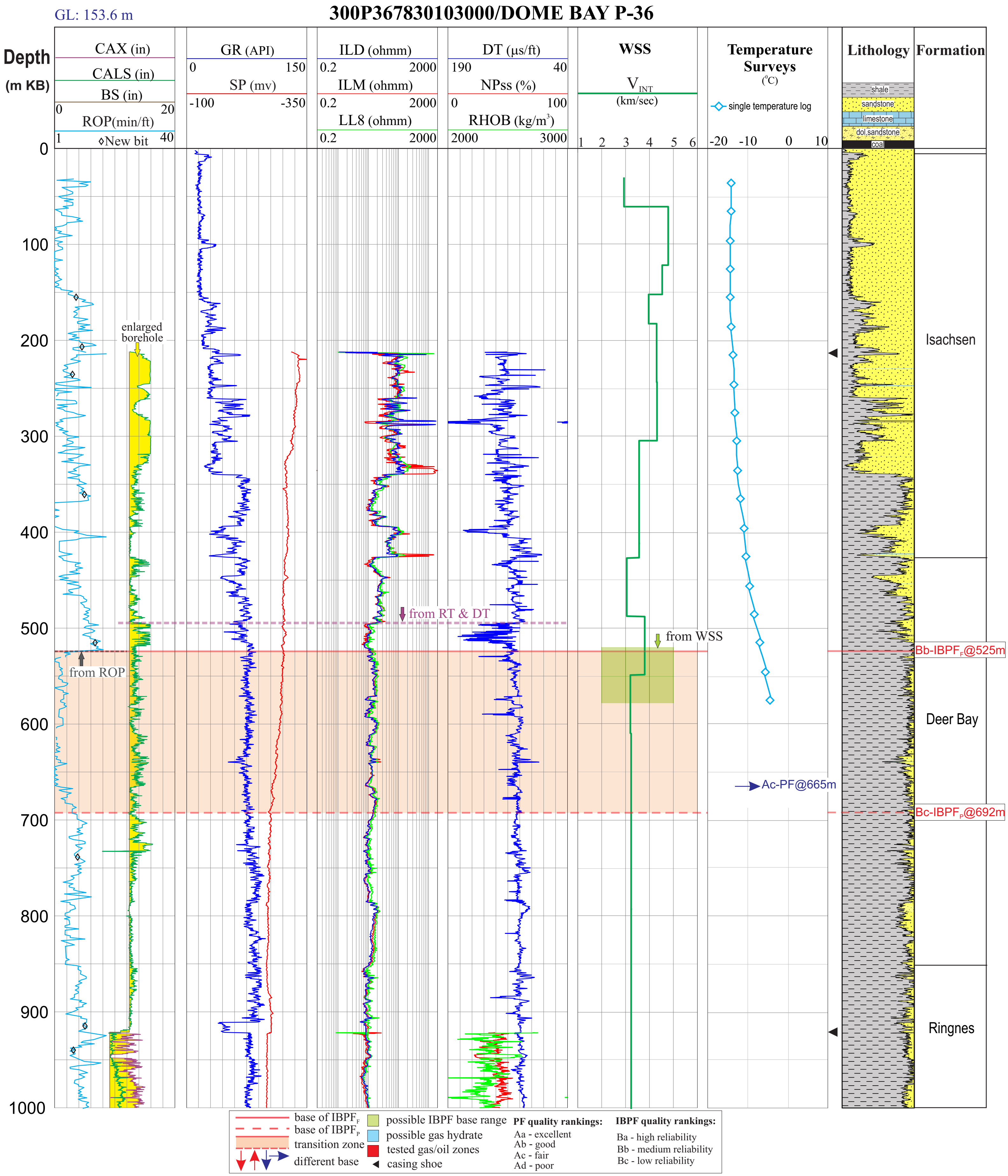

Figure 21. Example showing IBPF interpretation for the Dome Bay P-36 well on Ellef Ringnes Island in the Canadian Arctic Islands. Defined base of $IBPF_F$ (the solid orange line) with quality "Bb" is based on ROP (the dashed black line) and WSS (the green coloured area) rather than wireline logs (RT and DT, the dashed purple line) that were badly affected by borehole rugosity and washouts as indicated by caliper log and the difference between caliper and borehole size (in the yellow coloured area) in track 1.

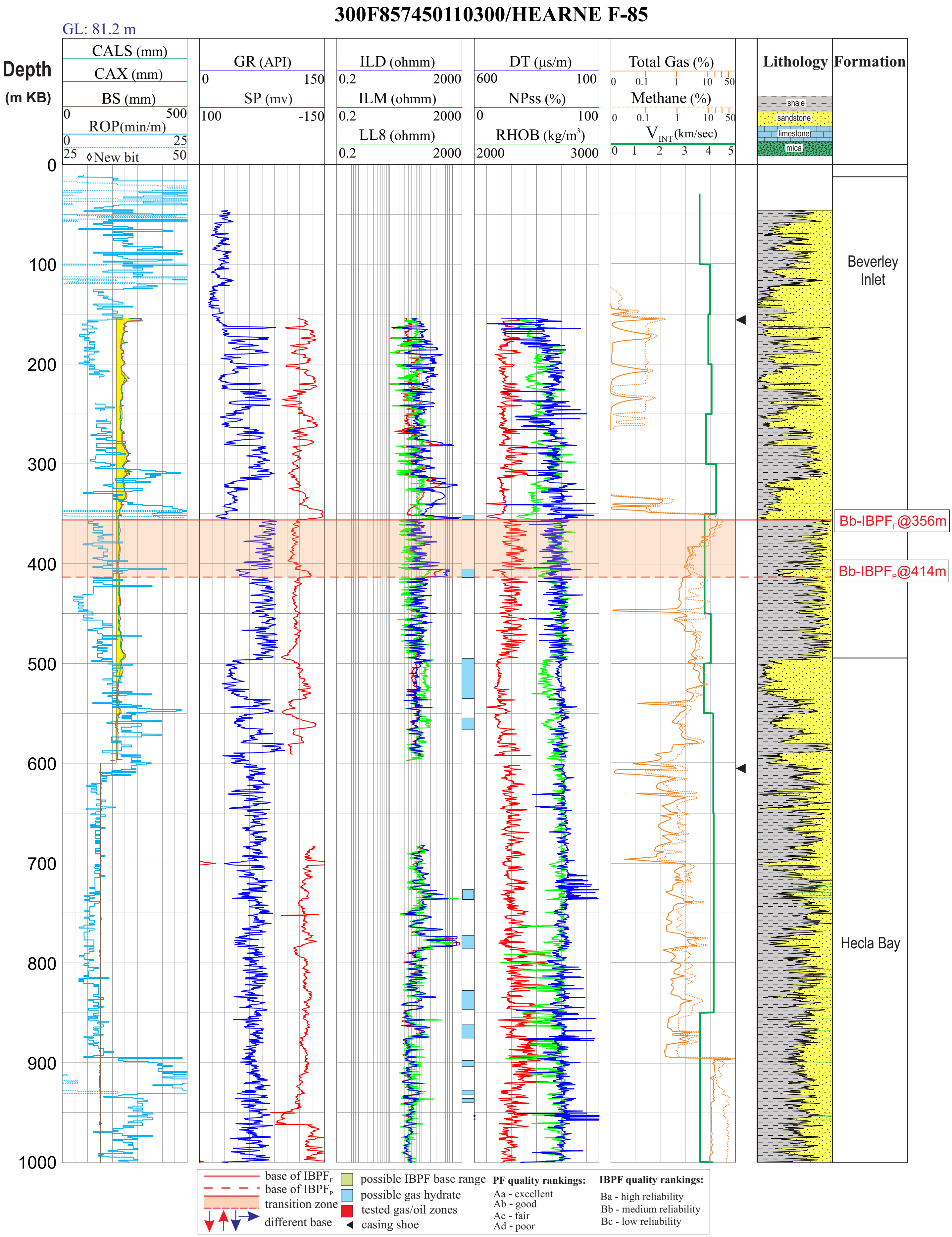

Figure 22. IBPF$_F$ interpretation with quality "Bb" is based on multiple information, including wireline logs, mud logs (ROP in track 1 and gas log in track 5), well seismic velocity, and possible gas hydrate interpretation for the Hearne F-85 well on Melville Island in the Canadian Arctic Islands.

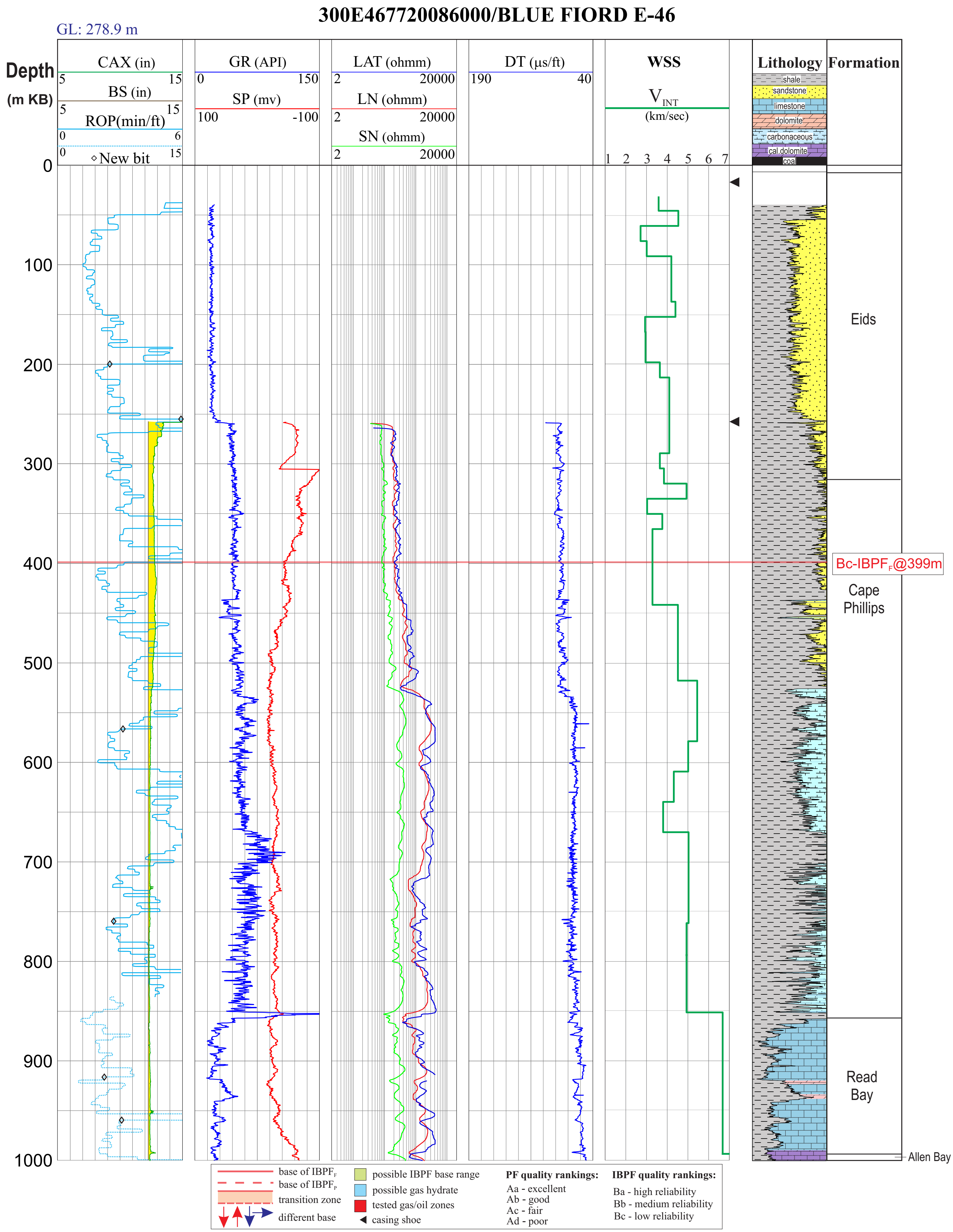

Figure 23. Example showing that base of $IBPF_F$ (with low reliability - "Bc") is estimated from well logs and well seismic surveys for the Blue Fiord E-46 well on Ellesmere Island in the Canadian Arctic Islands.

300K337640108300/COLLINGWOOD K-33

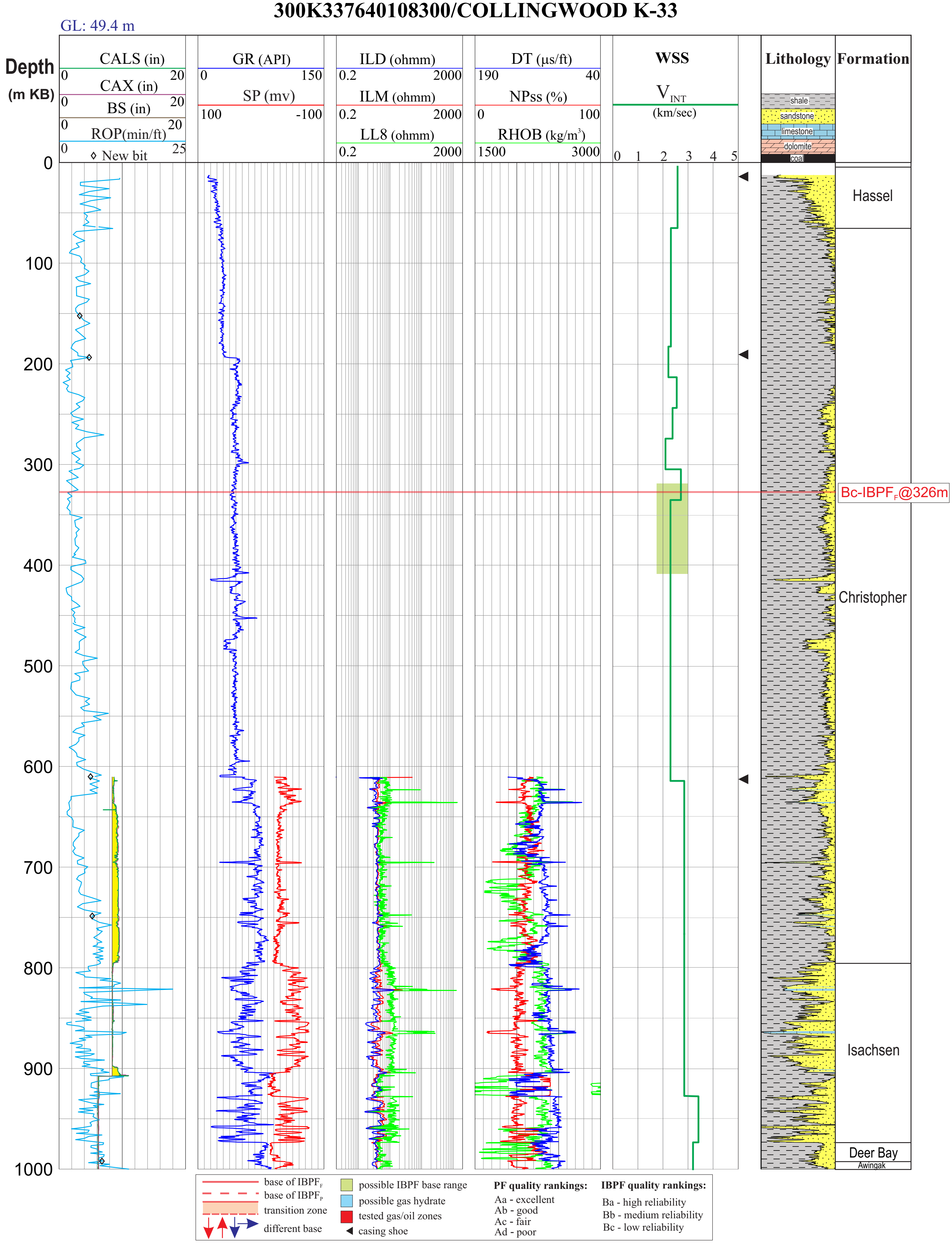

Figure 24. Base of $IBPF_F$ with "Bc" quality is estimated from well seismic surveys and drilling rate for the Collingwood K-33 well on Melville Island in the Canadian Arctic Islands.

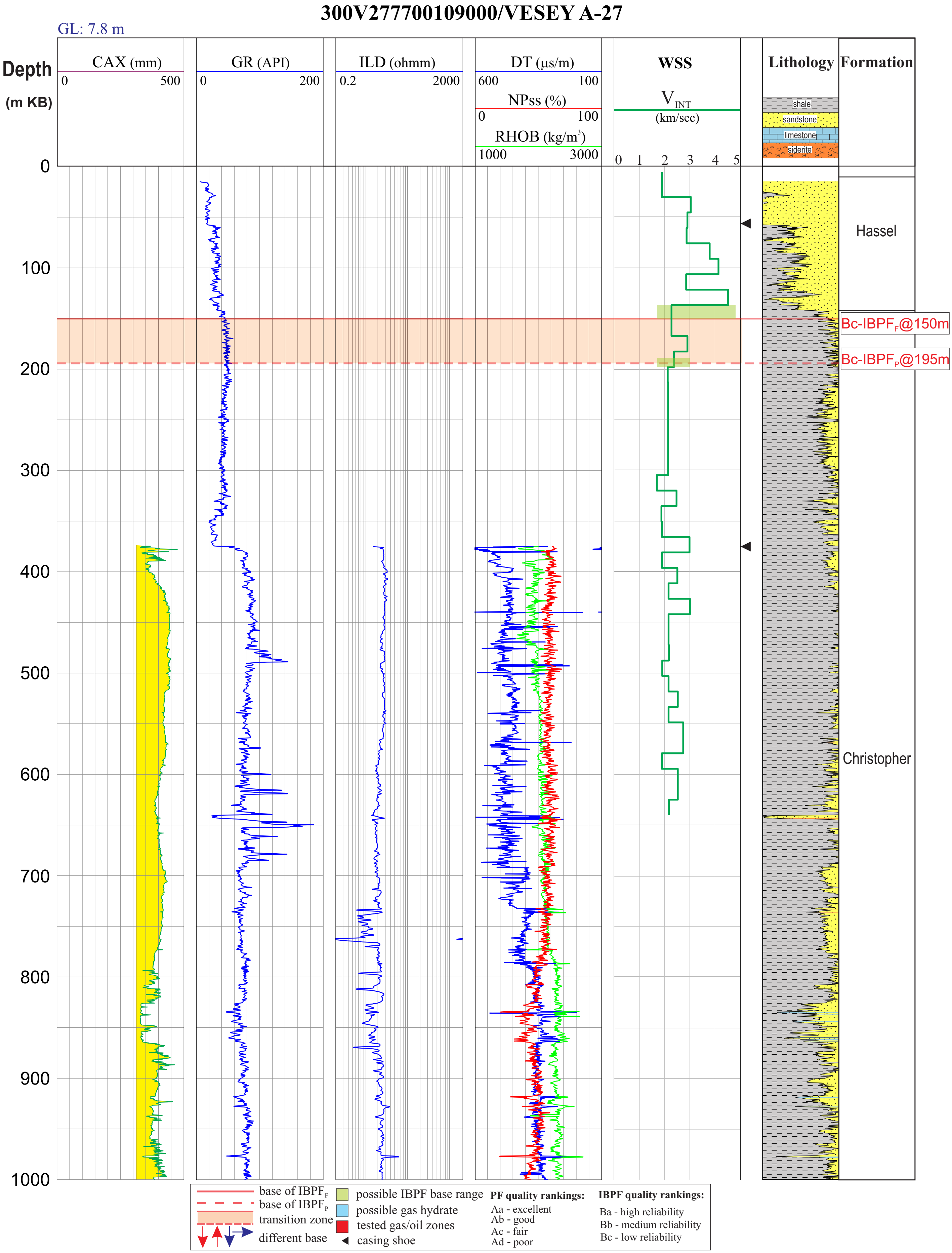

Figure 25. Example showing bases of $IBPF_F$ and $IBPF_P$ with "Bc" quality are estimated only from well seismic surveys for the Vesey A-27 well on Vesey Hamilton Island in the Canadian Arctic Islands.

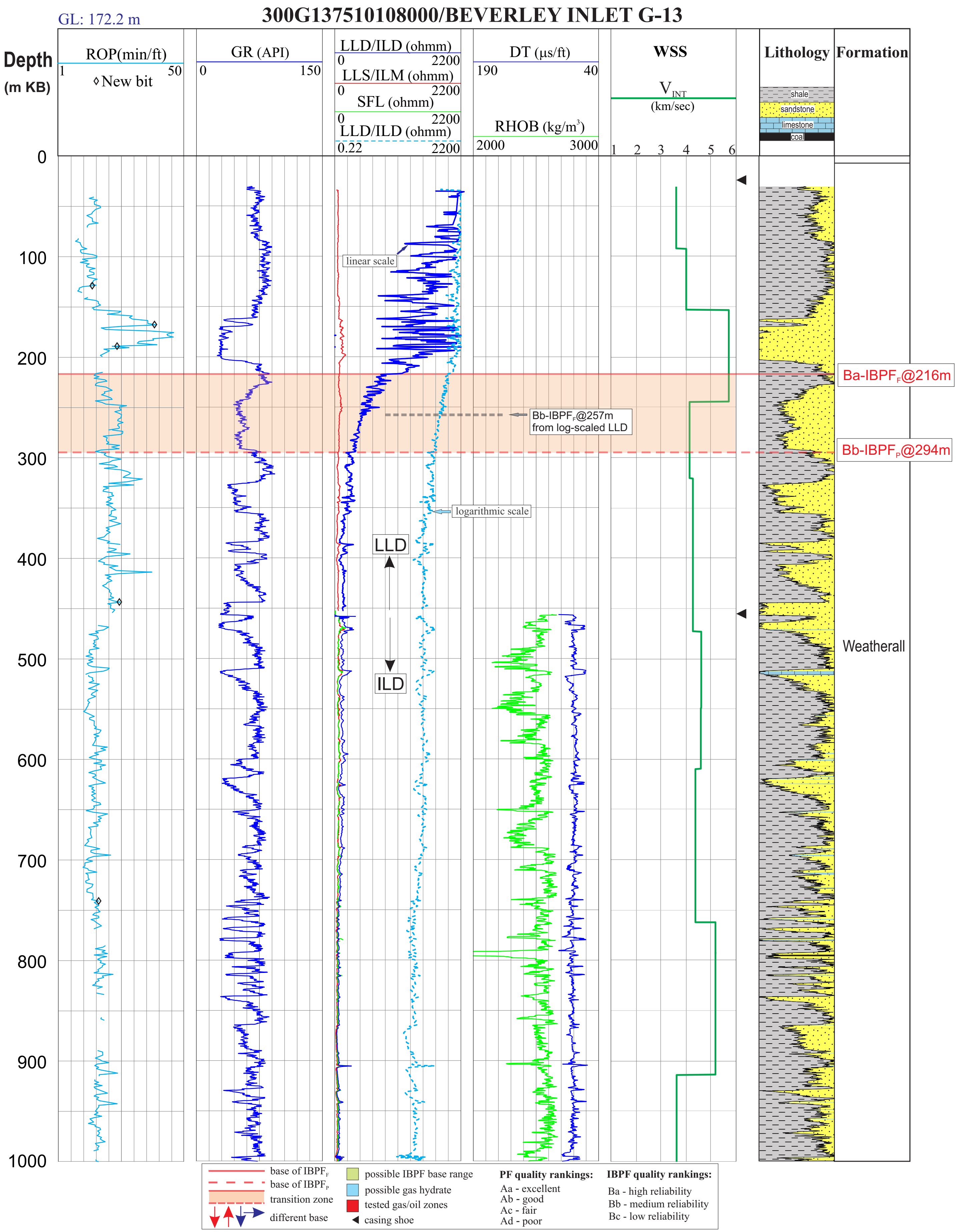

Figure 26. Example shows deep resistivity (LLD) readings on both logarithmic and linear scales throughout the same interval of ice-bearing permafrost zone, indicating that linear-scaled LLD display (the solid dark blue curve in track 3) improves visualization of the response to the base of $IBPF_F$ and gives a better $IBPF_F$ interpretation (with quality "Ba"; marked by the solid orange line) than log-scaled LLD (the dashed light blue curve in track 3) for the Beverley Inlet G-13 well on Melville Island in the Canadian Arctic Islands.

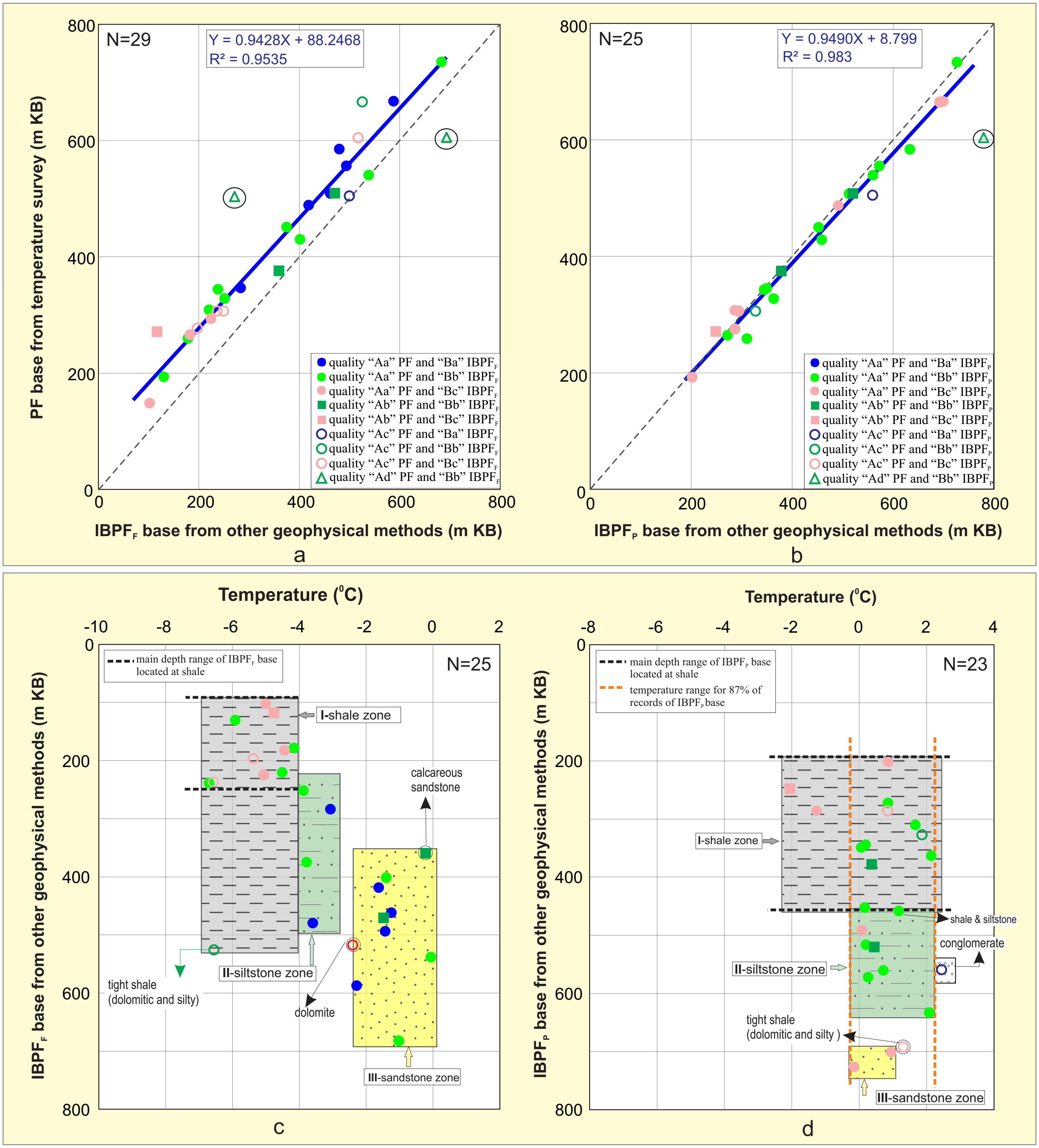

Figure 27. Comparison of 0°C permafrost (PF) base from "Aa", "Ab", "Ac", and "Ad" quality temperature surveys and base of IBPF (with "Ba", "Bb" and "Bc" quality) from other geophysical methods in the Canadian Arctic Islands. N: number of wells with both temperature surveys and other geophysical data.
a - PF base from temperature surveys versus base of fully frozen ($IBPF_F$) from other geophysical methods;
b - PF base from temperature surveys versus base of partially frozen ($IBPF_P$) from other geophysical methods;
c - Temperature distribution (quality "Ad" points are excluded) at the depth of $IBPF_F$ base from other geophysical methods; d - Temperature distribution (quality "Ad" point is excluded) at the the depth of $IBPF_P$ base from other geophysical methods.

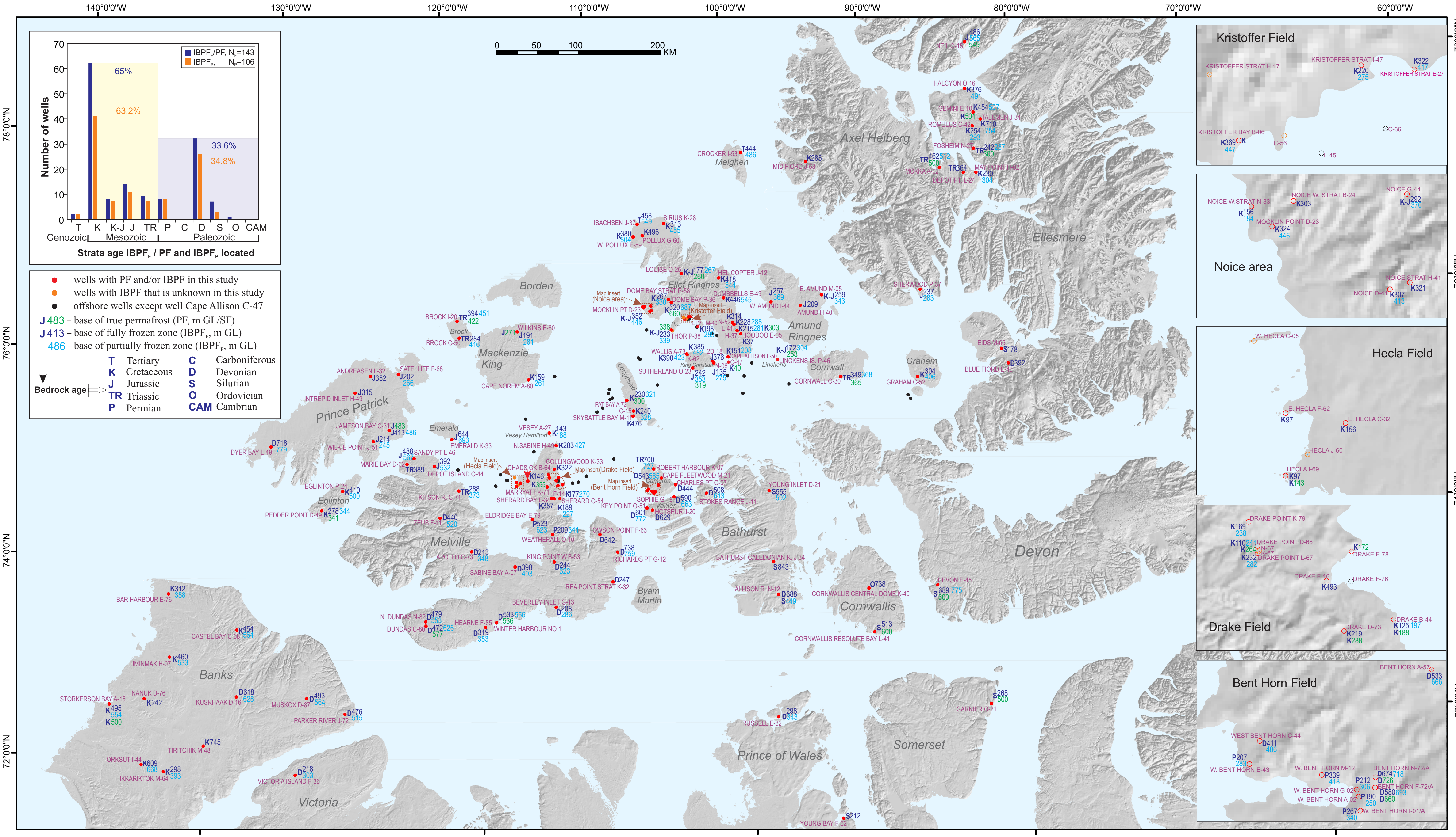

Figure 28. Base map indicating base of permafrost (PF), base of fully frozen zone (IBPF$_F$) and partially frozen zone (IBPF$_P$) for the petroleum exploration wells in the Canadian Arctic Islands.

***Note**: this figure is optimised for 17x11 inch printing.*

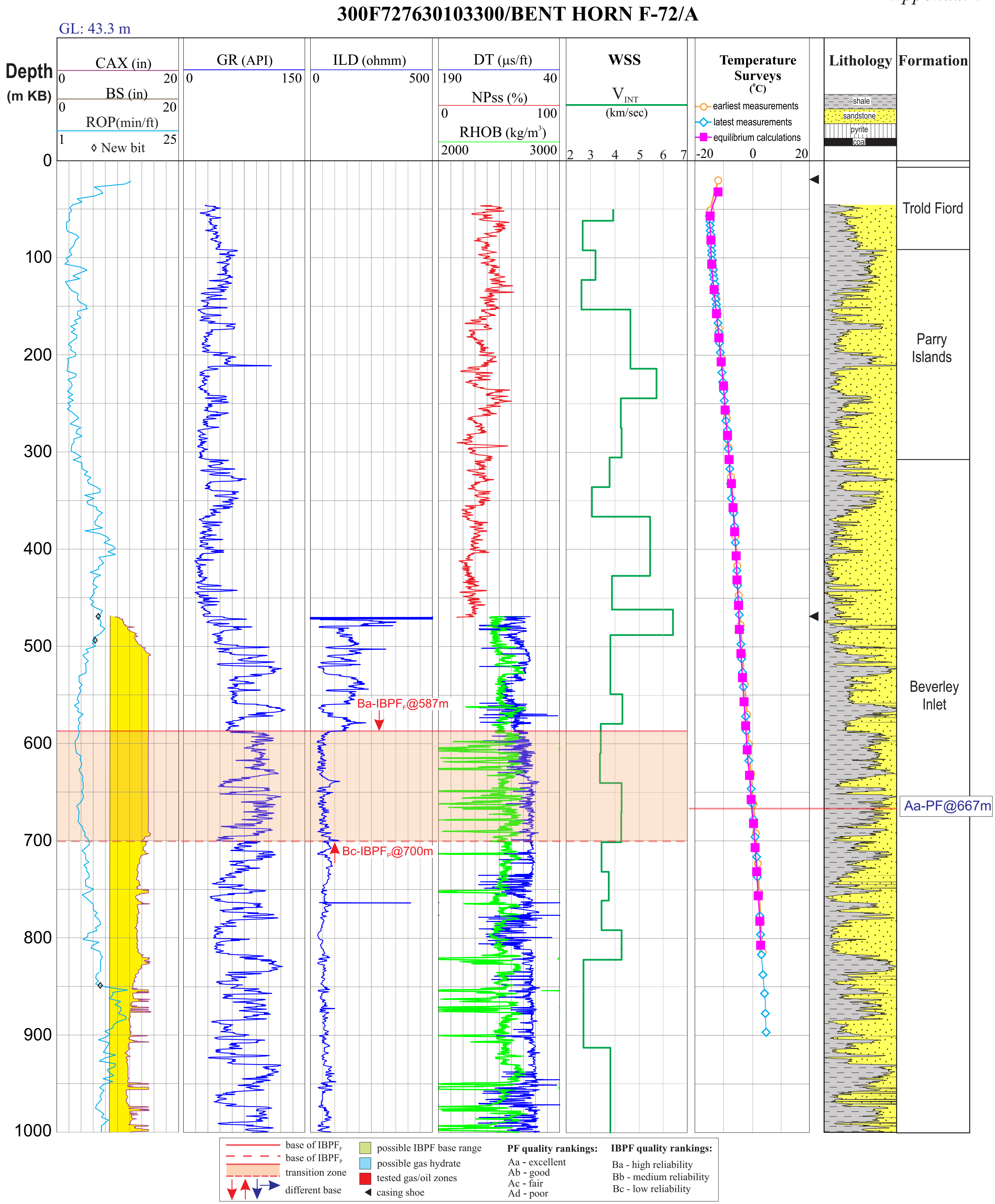

Figure 1-1. Base of PF is determined from temperature surveys with "Aa" quality for the Bent Horn F-72 and F-72A wells. IBPF interpretation based on other geophysical methods is shown for comparison.

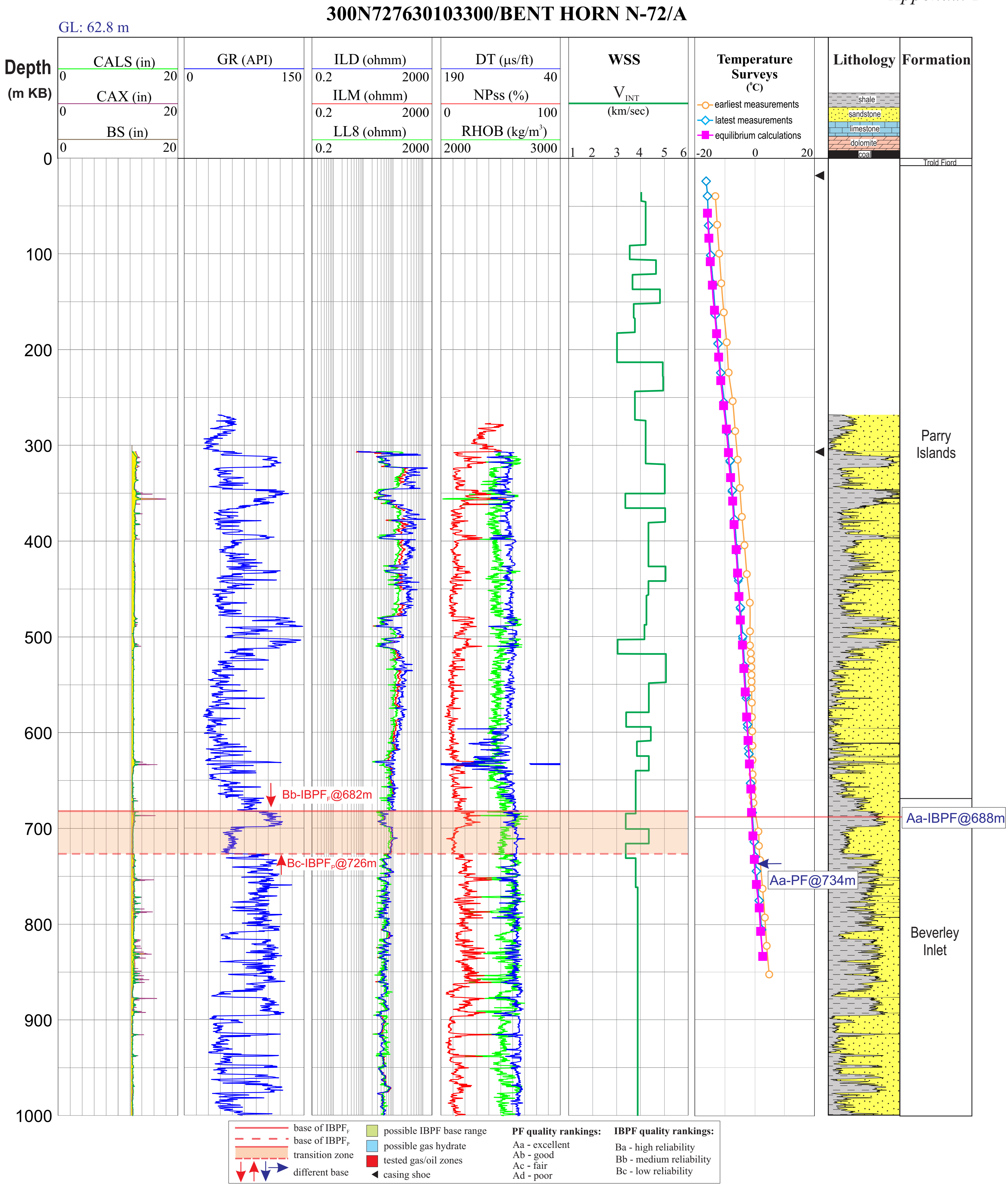

Figure 1-2. Base of PF is determined from temperature surveys with "Aa" quality for the Bent Horn N-72 and N-72A wells on Cameron Island in the Canadian Arctic Islands. IBPF interpretation based on other geophysical methods is shown for comparison.

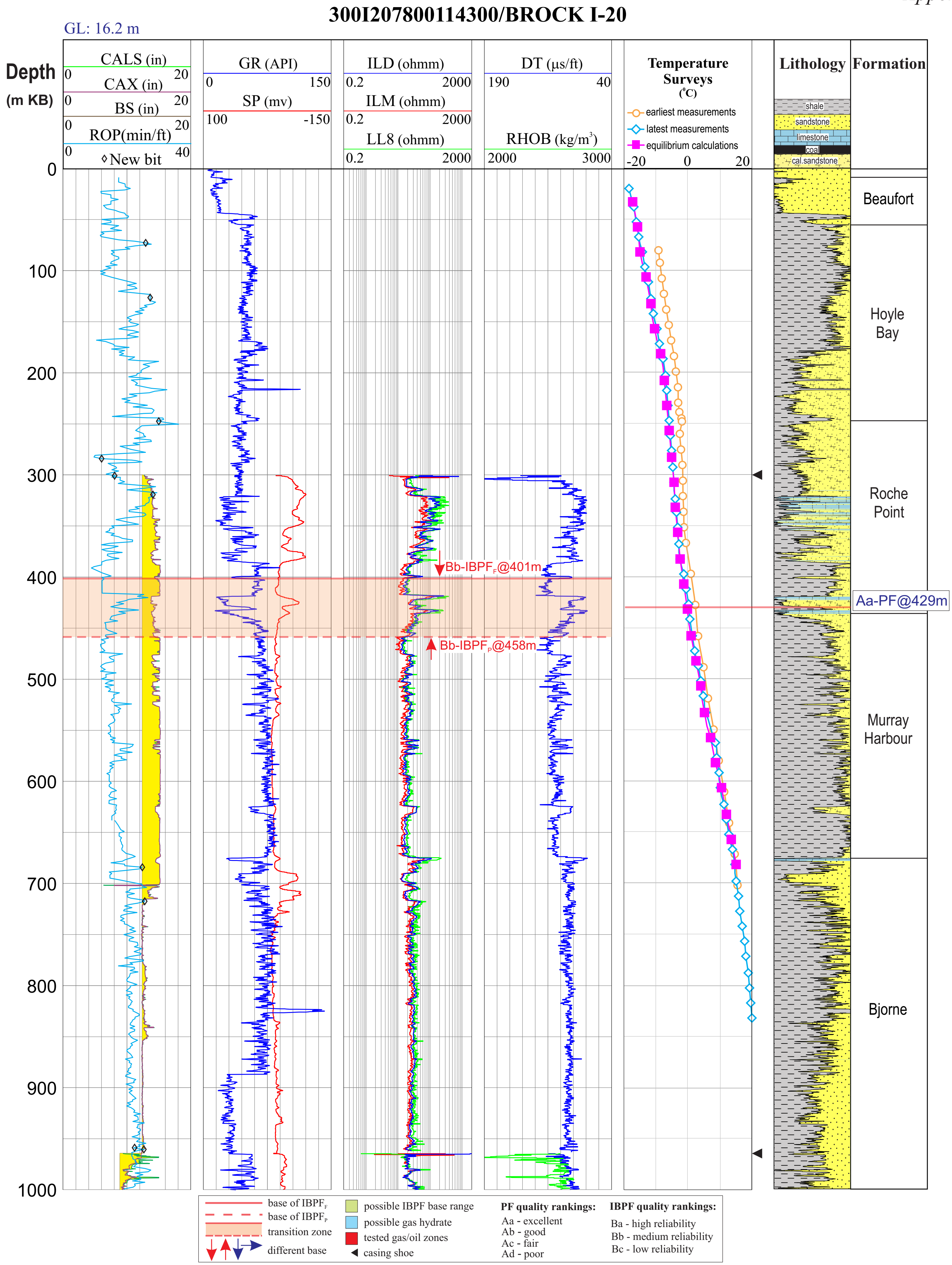

Figure 1-3. Base of PF is determined from temperature surveys with "Aa" quality for the Brock I-20 well on Brock Island in the Canadian Arctic Islands. IBPF interpretation based on other geophysical methods is shown for comparison.

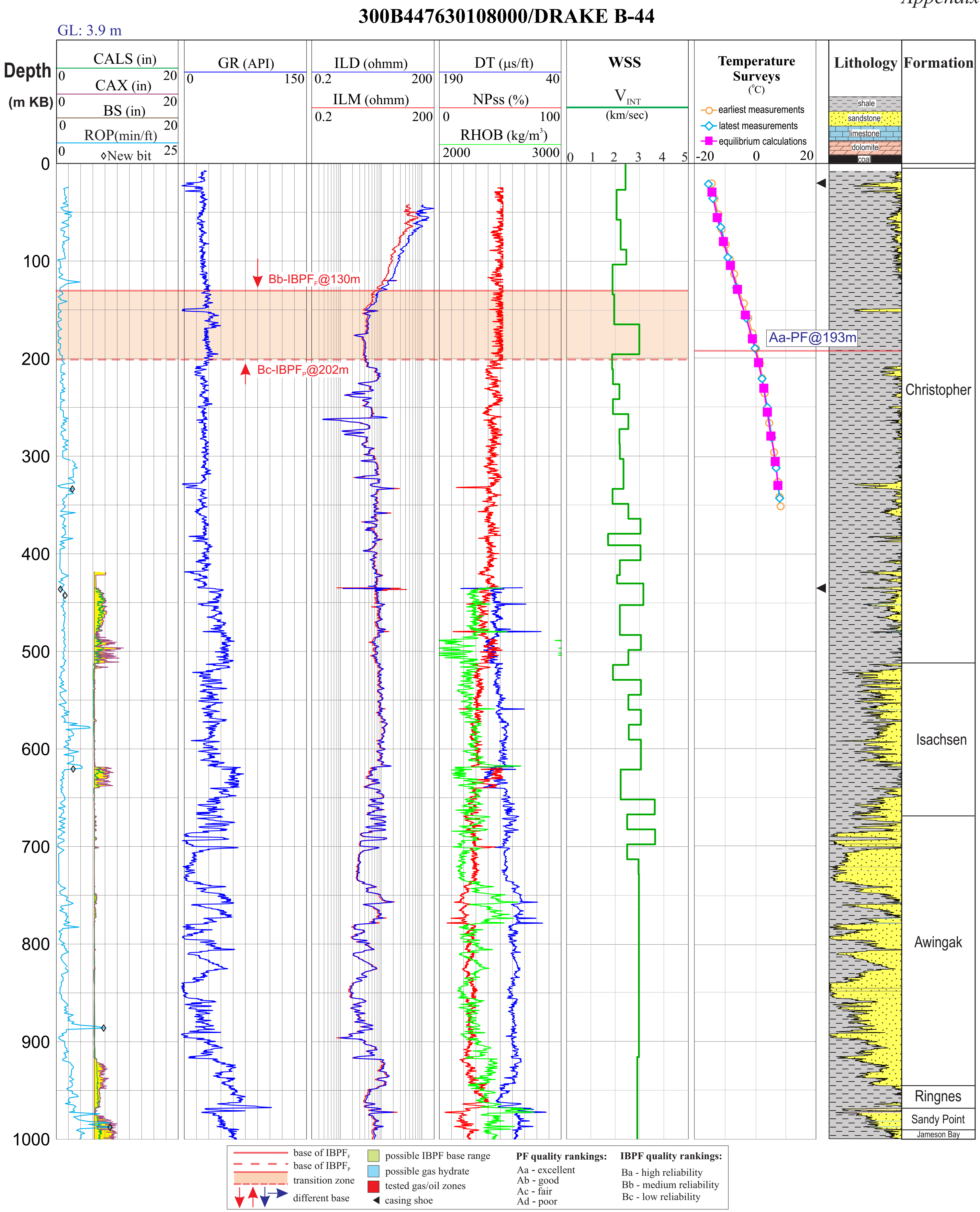

Figure 1-4. Base of PF is determined from temperature surveys with "Aa" quality for the Drake B-44 well on Melville Island in the Canadian Arctic Islands. IBPF interpretation based on other geophysical methods is shown for comparison.

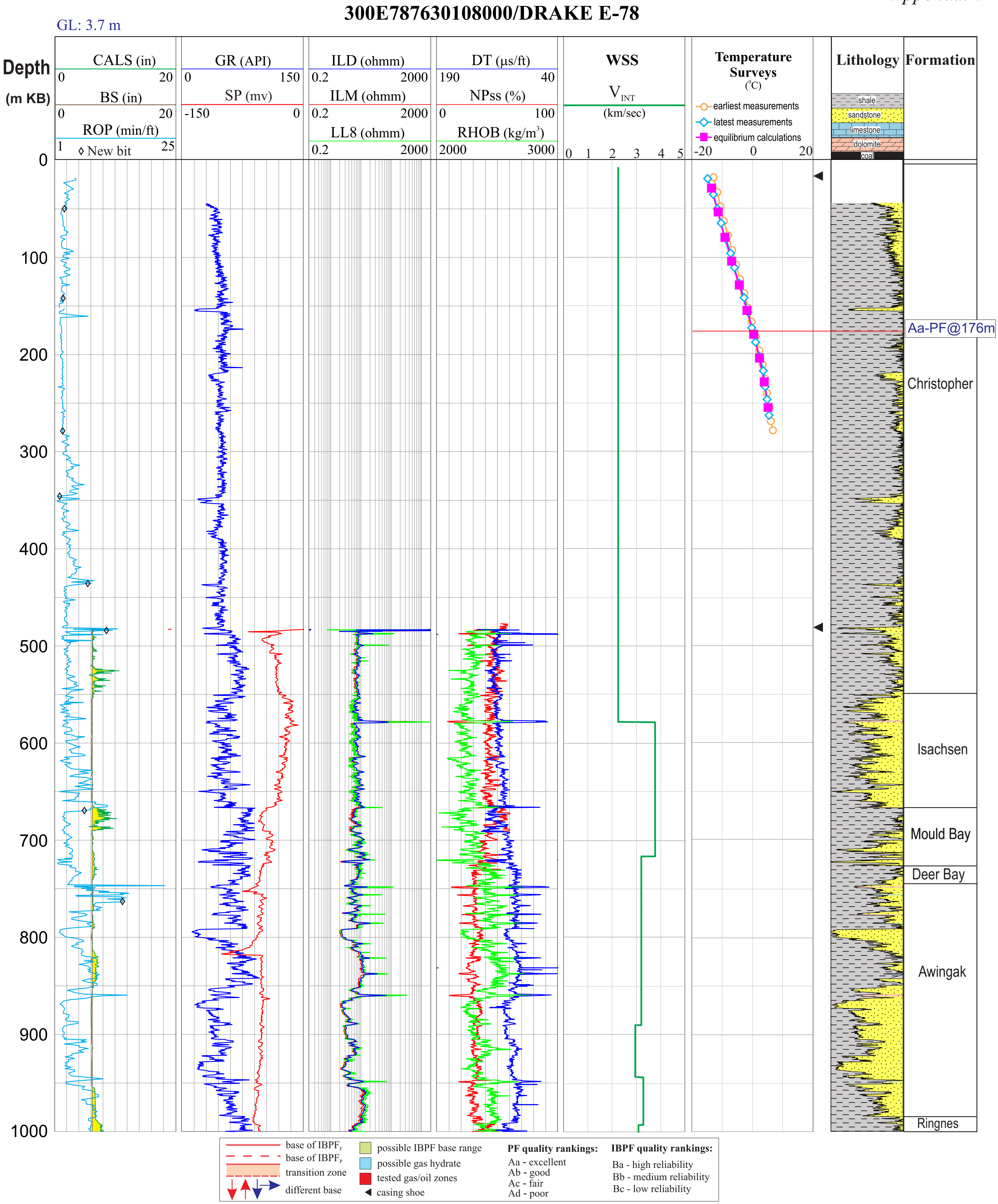

Figure 1-5. Base of PF is determined from temperature surveys with "Aa" quality for the Drake E-78 well on Melville Island in the Canadian Arctic Islands.

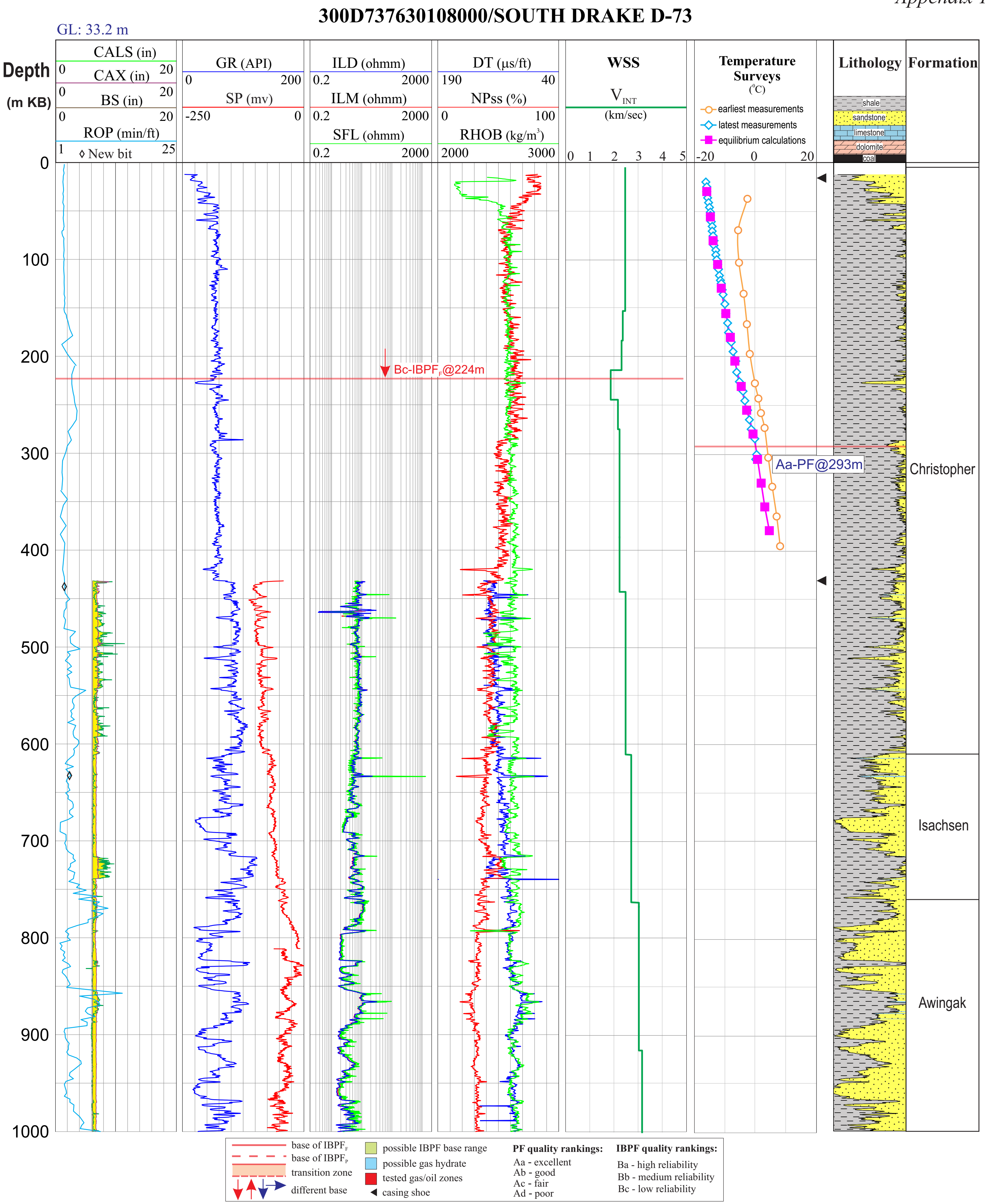

Figure 1-6. Base of PF is determined from temperature surveys with "Aa" quality for the South Drake D-73 well on Melville Island in the Canadian Arctic Islands. IBPF interpretation based on other geophysical methods is shown for comparison.

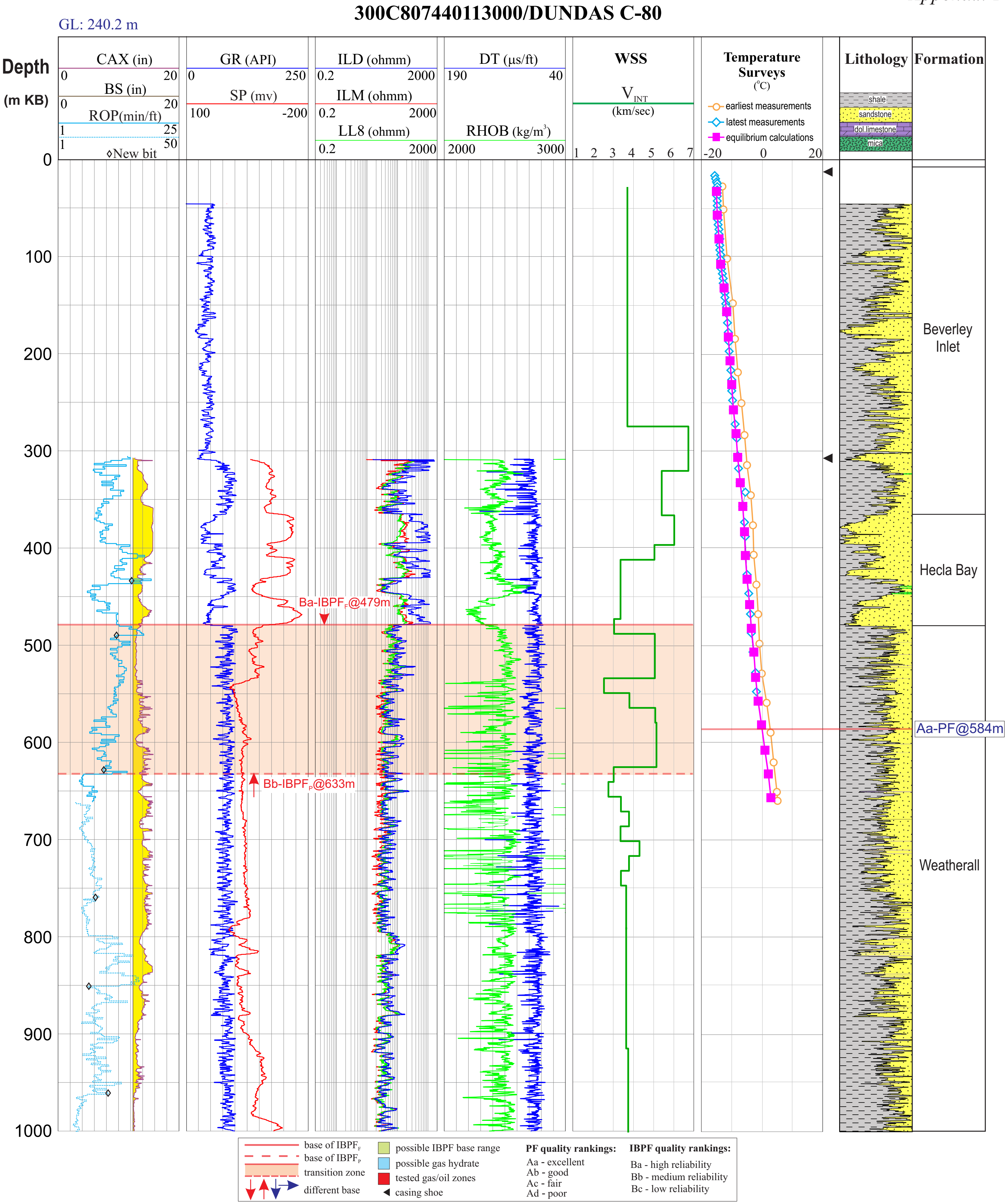

Figure 1-7. Base of PF is determined from temperature surveys with "Aa" quality for the Dundas C-80 well on Melville Island in the Canadian Arctic Islands. IBPF interpretation based on other geophysical methods is shown for comparison.

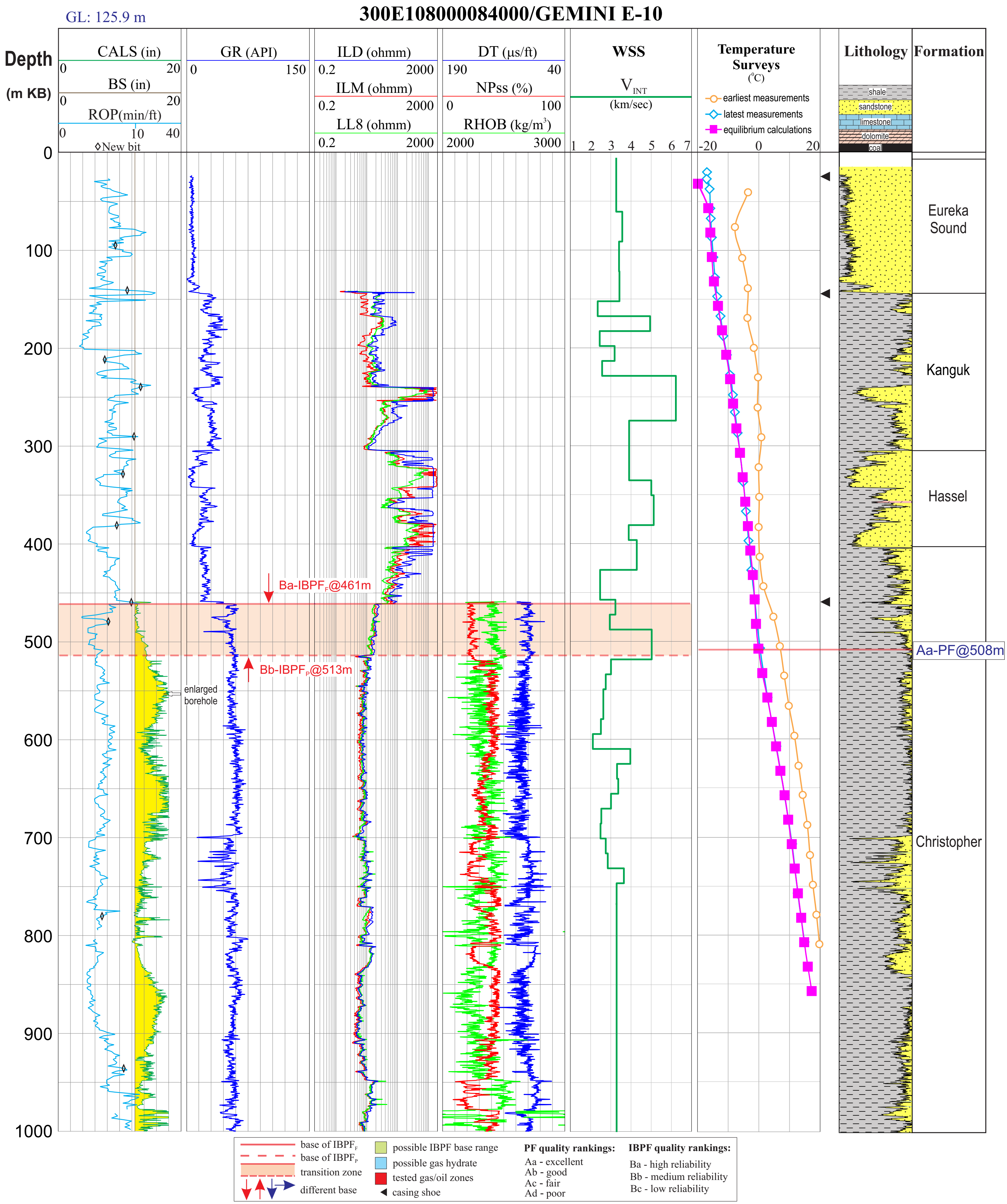

Figure 1-8. Base of PF is determined from temperature surveys with "Aa" quality for the Gemini E-10 well on Ellesmere Island in the Canadian Arctic Islands. IBPF interpretation based on other geophysical methods is shown for comparison.

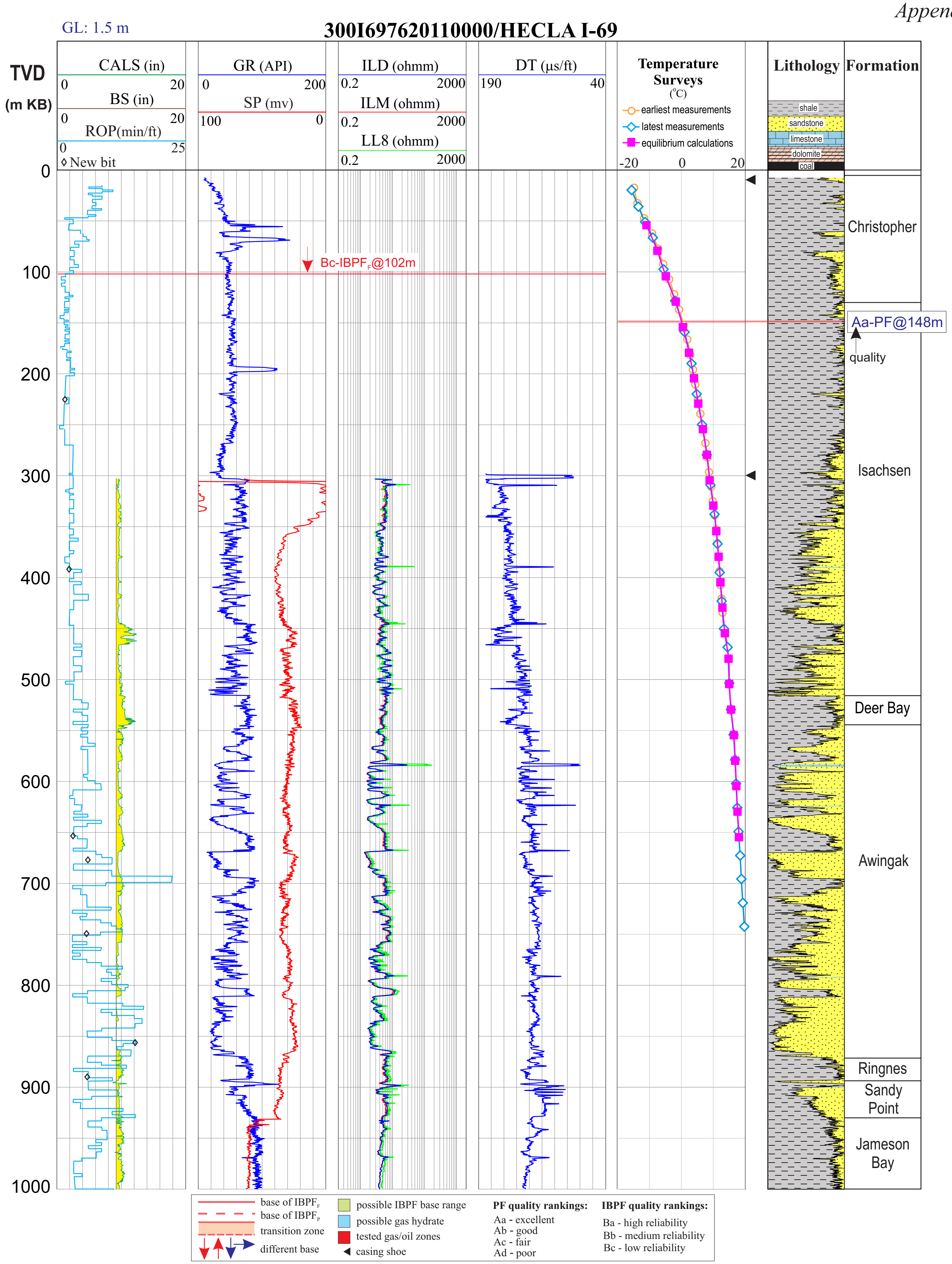

Figure 1-9. Base of PF is determined from temperature surveys with "Aa" quality for the Hecla I-69 well on Melville Island in the Canadian Arctic Islands. IBPF interpretation based on other geophysical methods is shown for comparison.

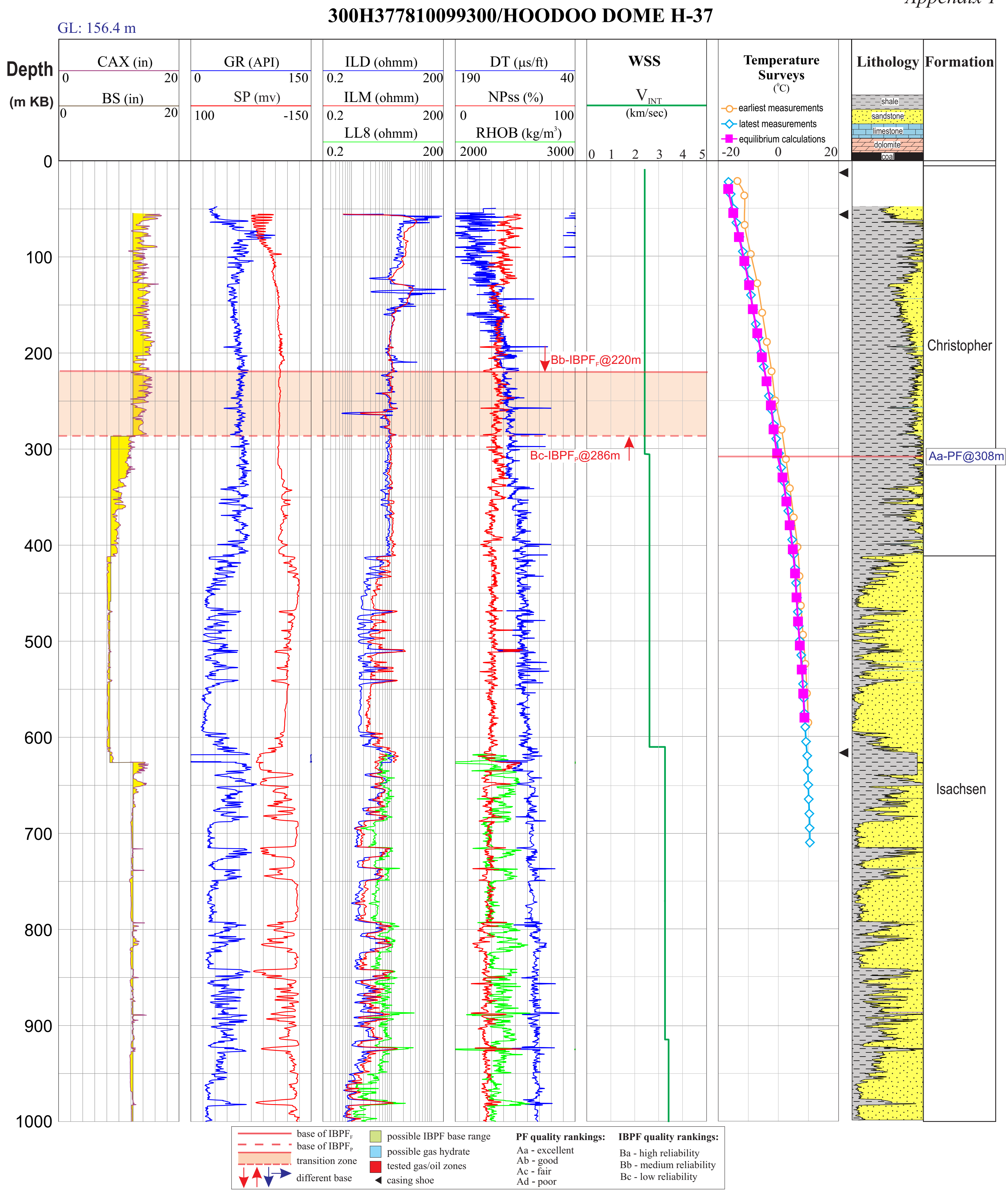

Figure 1-10. Base of PF is determined from temperature surveys with "Aa" quality for the Hoodoo Dome H-37 well on Ellef Ringnes Island in the Canadian Arctic Islands. IBPF interpretation based on other geophysical methods is shown for comparison.

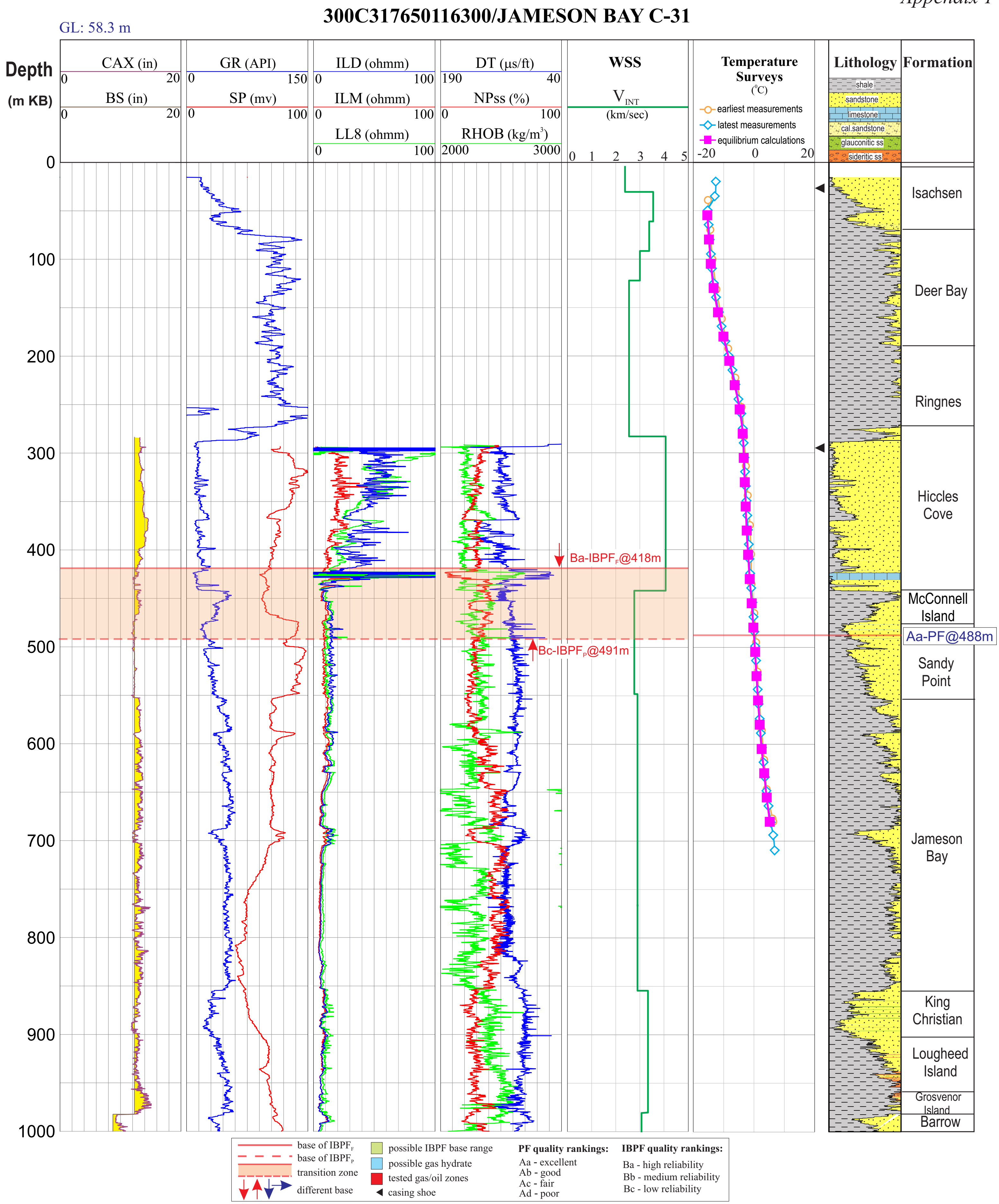

Figure 1-11. Base of PF is determined from temperature surveys with "Aa" quality for the Jameson Bay C-31 well on Prince Patrick Island in the Canadian Arctic Islands. IBPF interpretation based on other geophysical methods is shown for comparison.

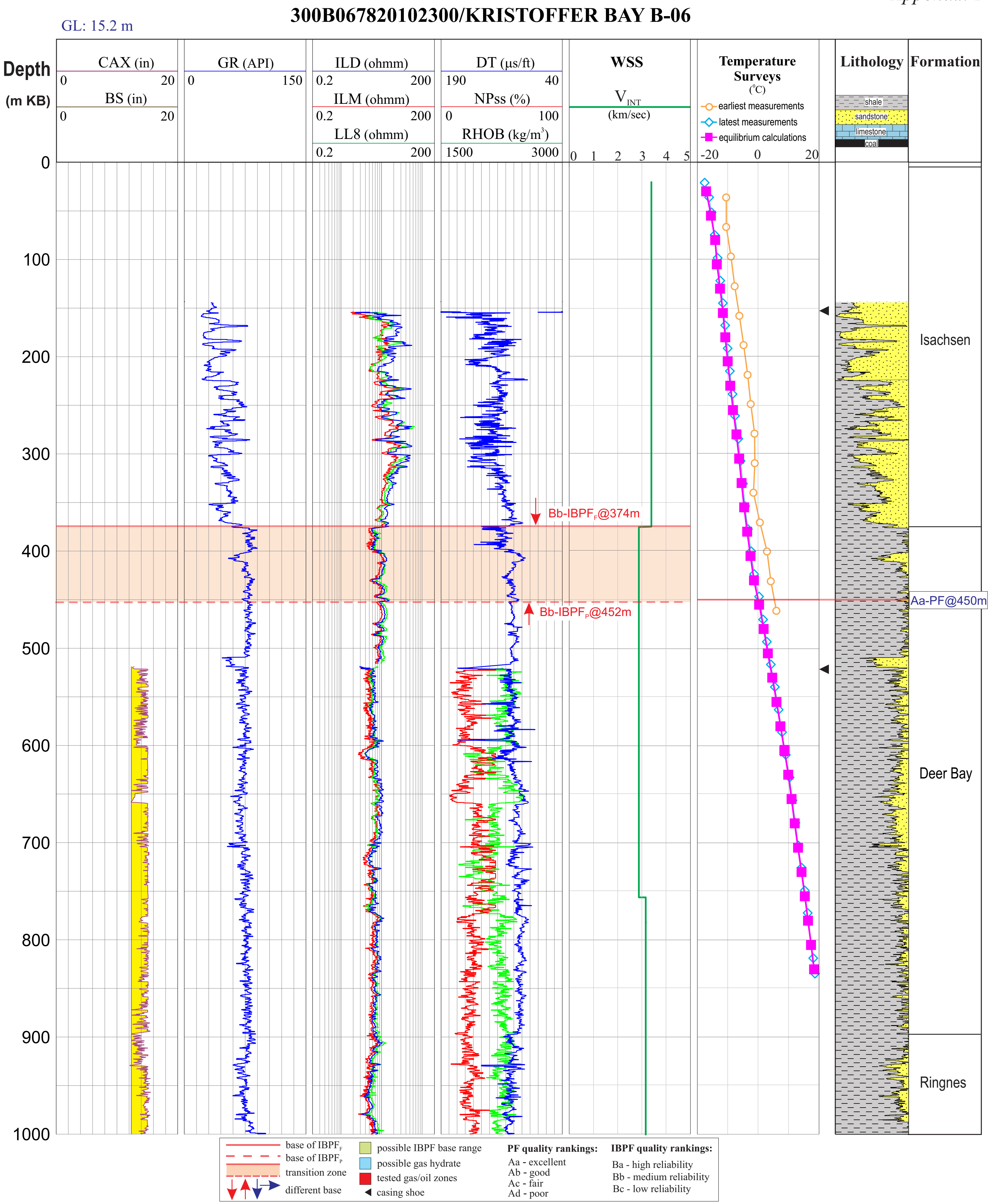

Figure 1-12. Base of PF is determined from temperature surveys with "Aa" quality for the Kristoffer Bay B-06 well on King Christian Island in the Canadian Arctic Islands. IBPF interpretation based on other geophysical methods is shown for comparison.

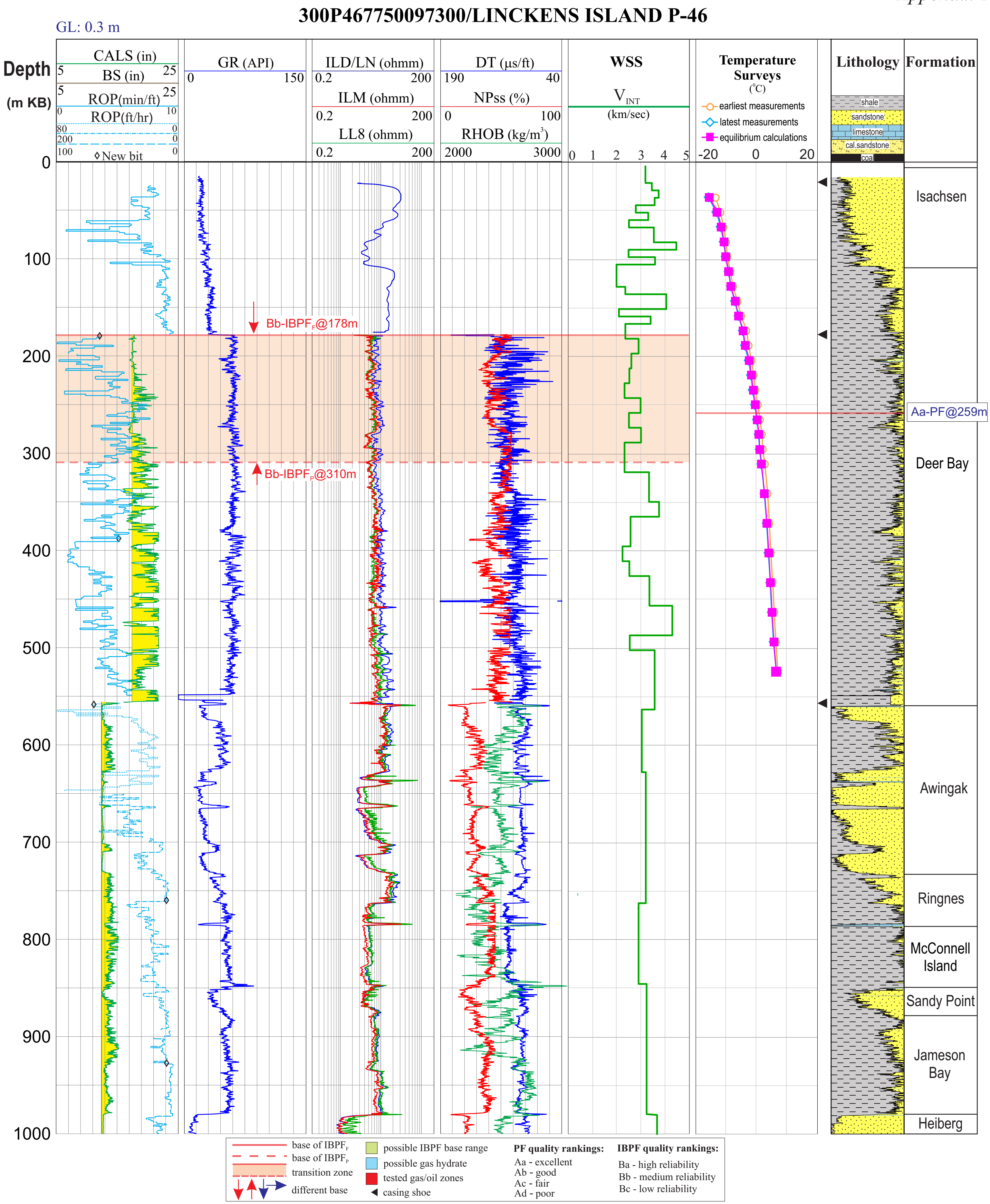

Figure 1-13. Base of PF is determined from temperature surveys with "Aa" quality for the Linckens Island P-46 well on Linckens Island in the Canadian Arctic Islands. IBPF interpretation based on other geophysical methods is shown for comparison.

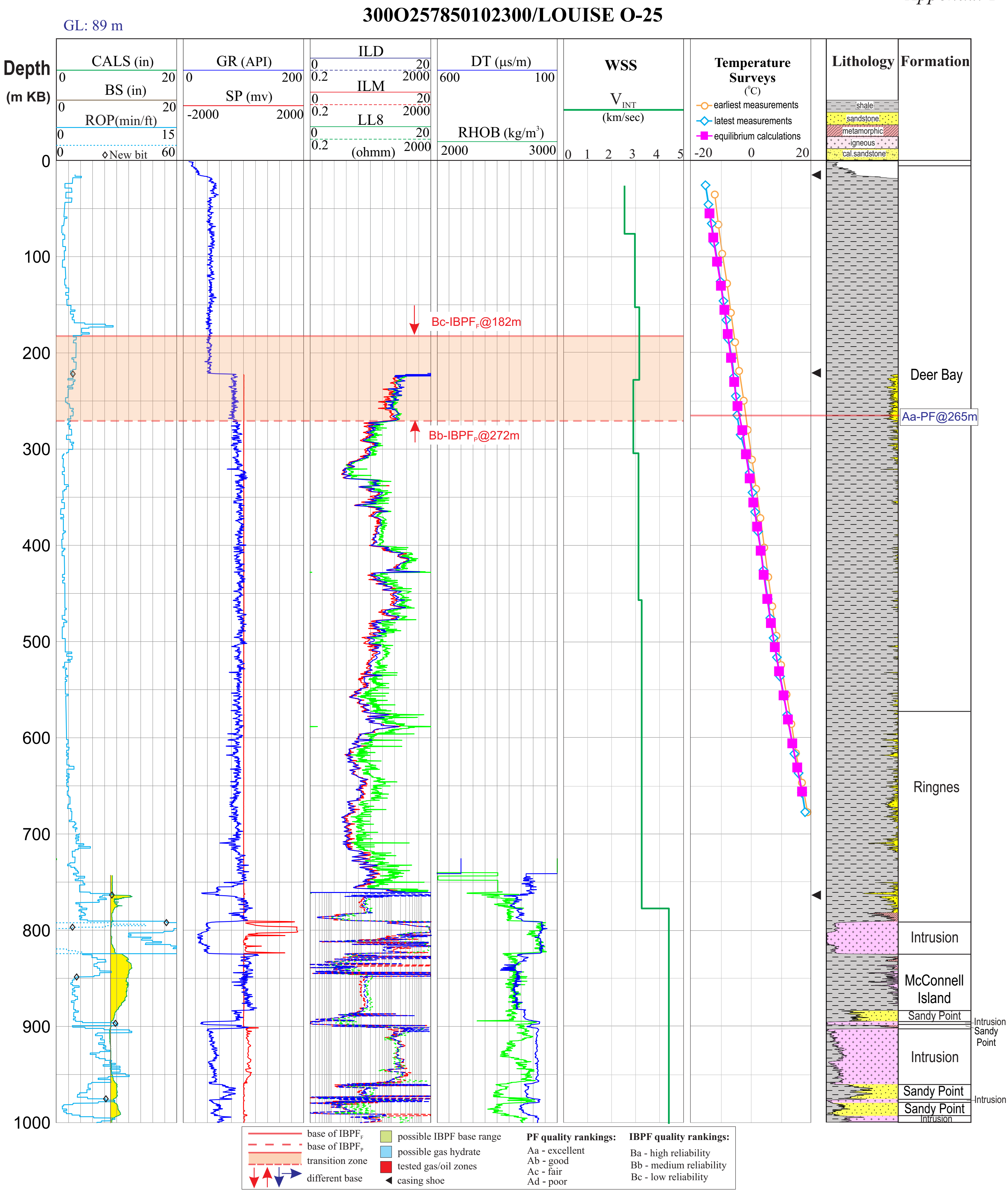

Figure 1-14. Base of PF is determined from temperature surveys with "Aa" quality for the Louise O-25 well on Ellef Ringnes Island in the Canadian Arctic Islands. IBPF interpretation based on other geophysical methods is shown for comparison.

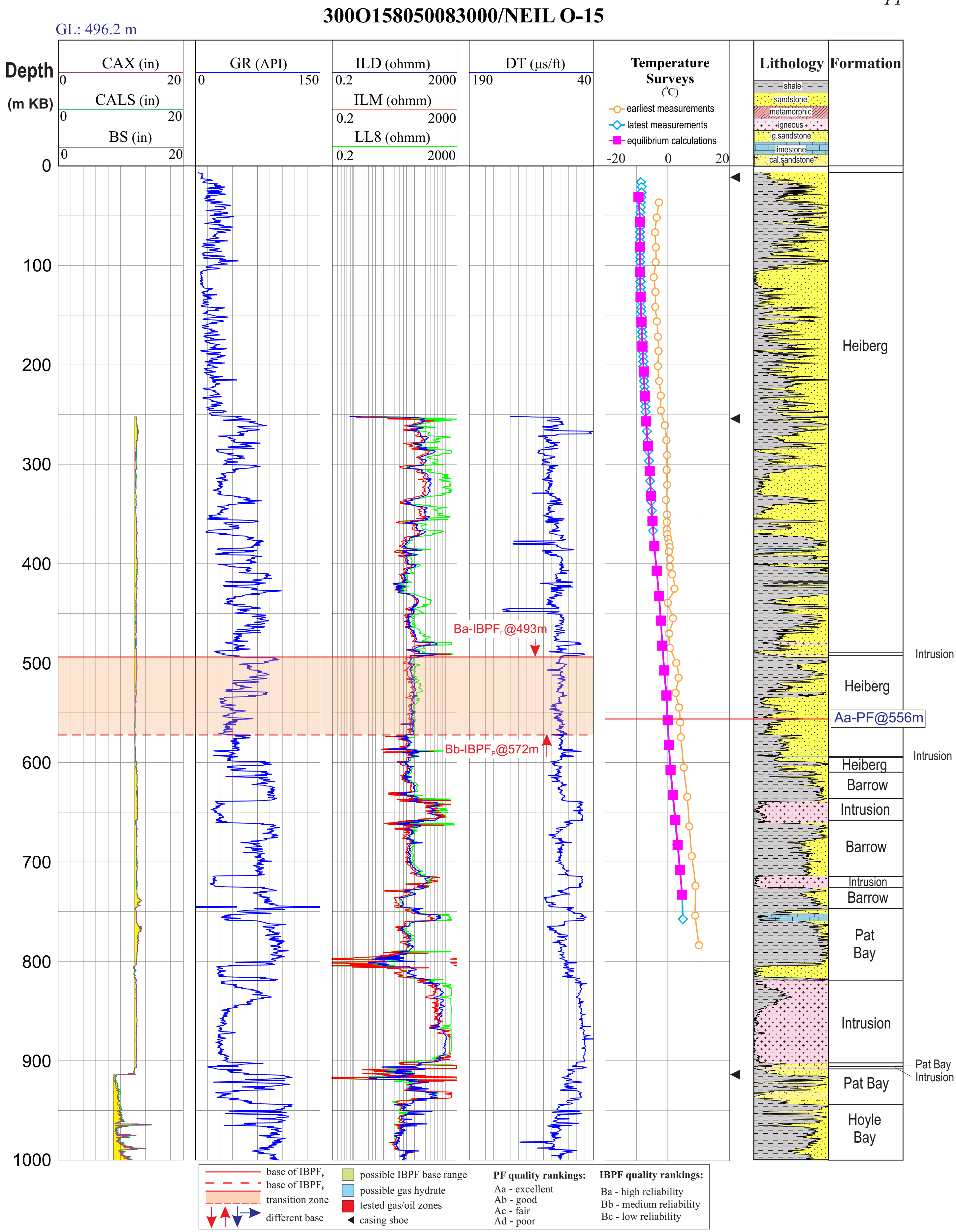

Figure 1-15. Base of PF is determined from temperature surveys with "Aa" quality for the Neil O-15 well on Ellesmere Island in the Canadian Arctic Islands. IBPF interpretation based on other geophysical methods is shown for comparison.

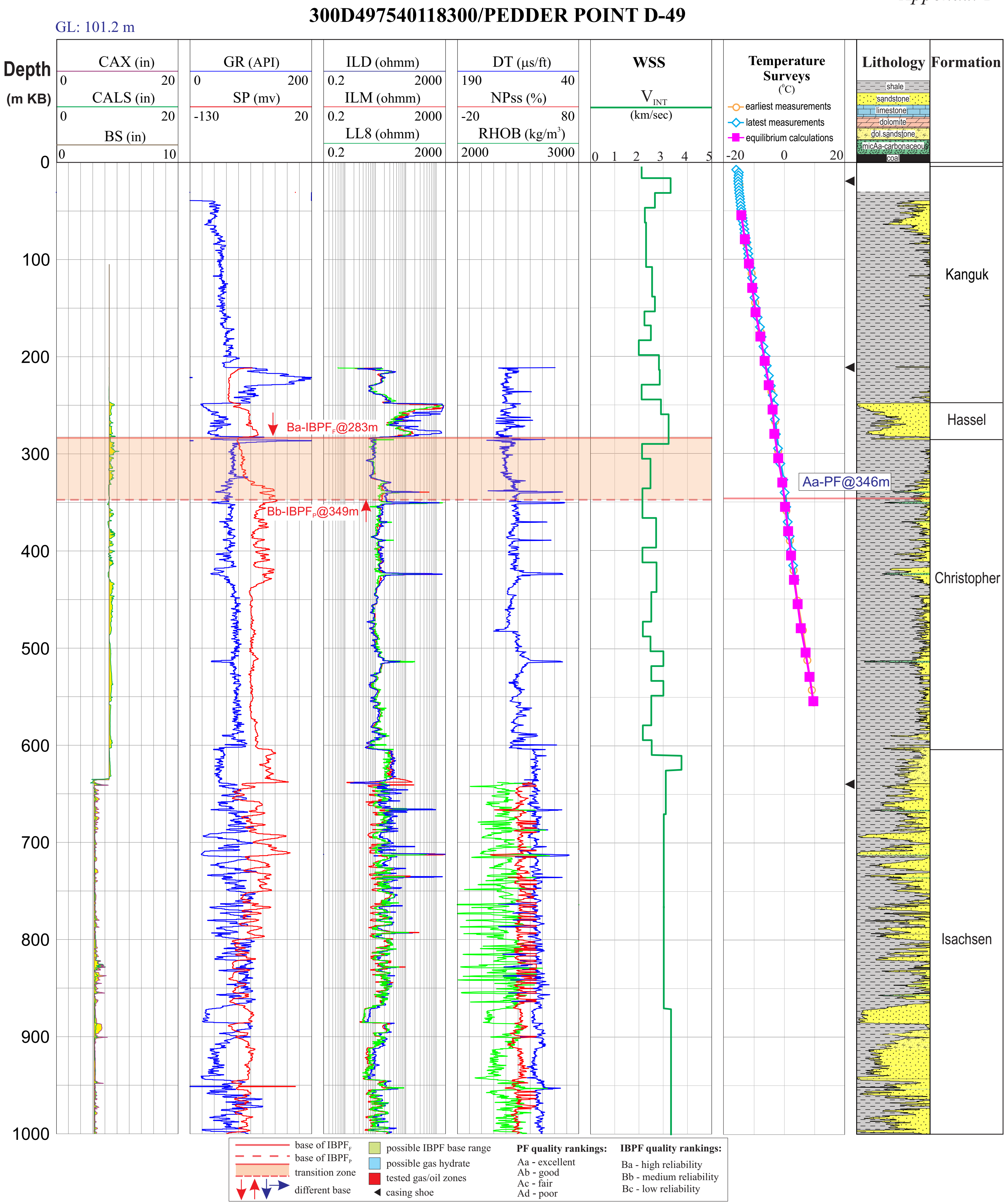

Figure 1-16. Base of PF is determined from temperature surveys with "Aa" quality for the Pedder Point D-49 well on Eglinton Island in the Canadian Arctic Islands. IBPF interpretation based on other geophysical methods is shown for comparison.

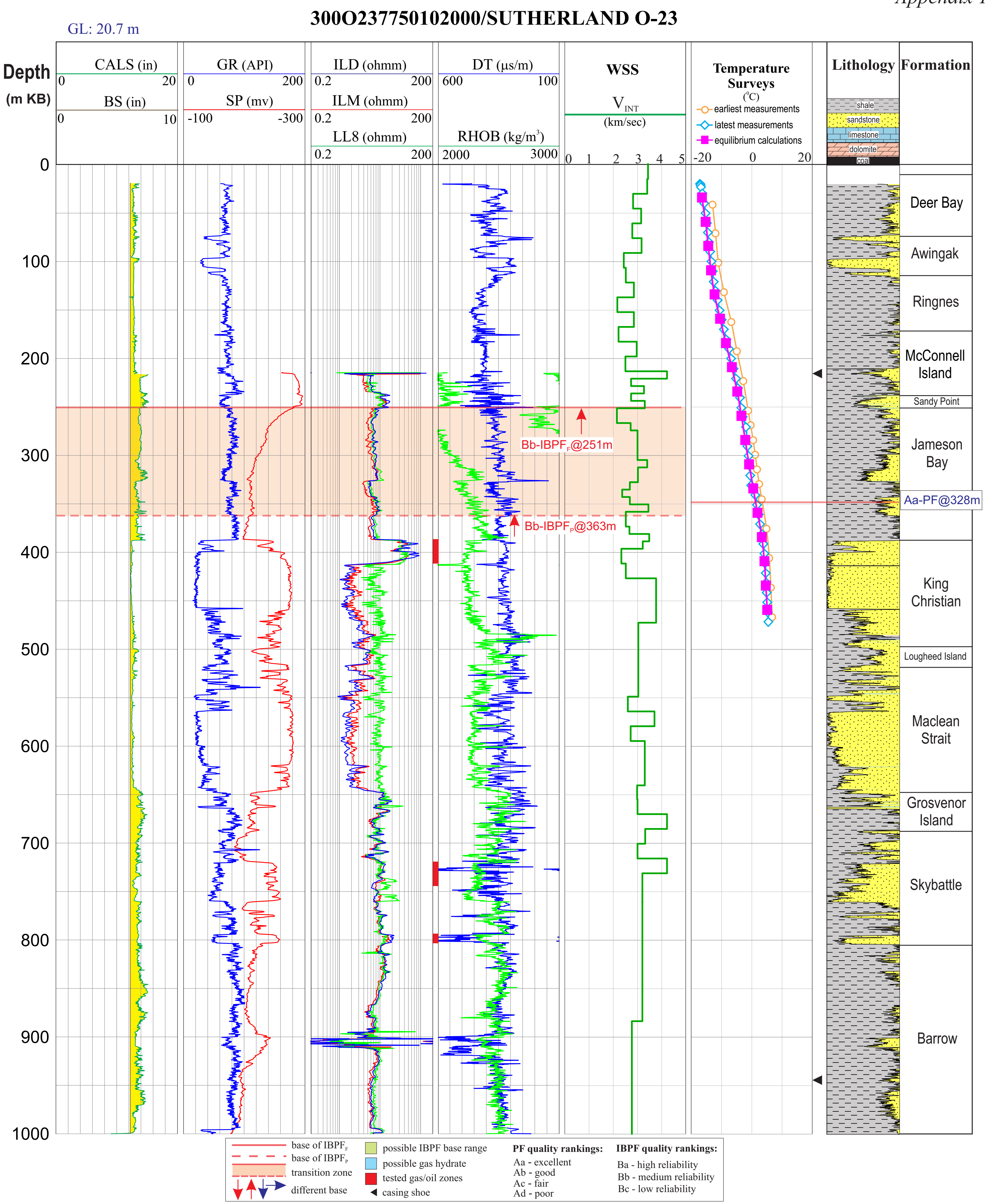

Figure 1-17. Base of PF is determined from temperature surveys with "Aa" quality for the Sutherland O-23 well on King Christian Island in the Canadian Arctic Islands. IBPF interpretation based on other geophysical methods is shown for comparison.

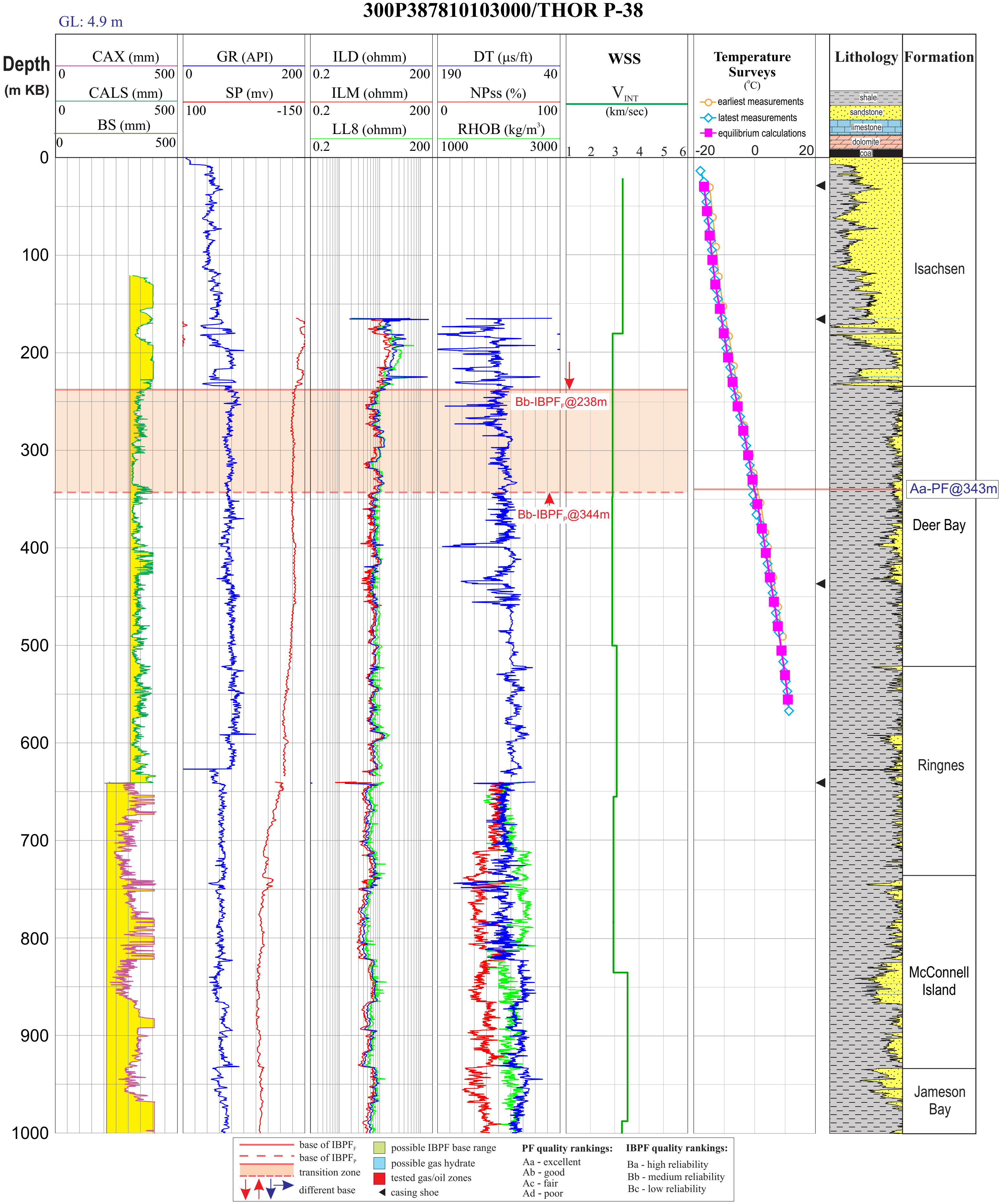

Figure 1-18. Base of PF is determined from temperature surveys with "Aa" quality for the Thor P-38 well on Thor Island in the Canadian Arctic Islands. IBPF interpretation based on other geophysical methods is shown for comparison.

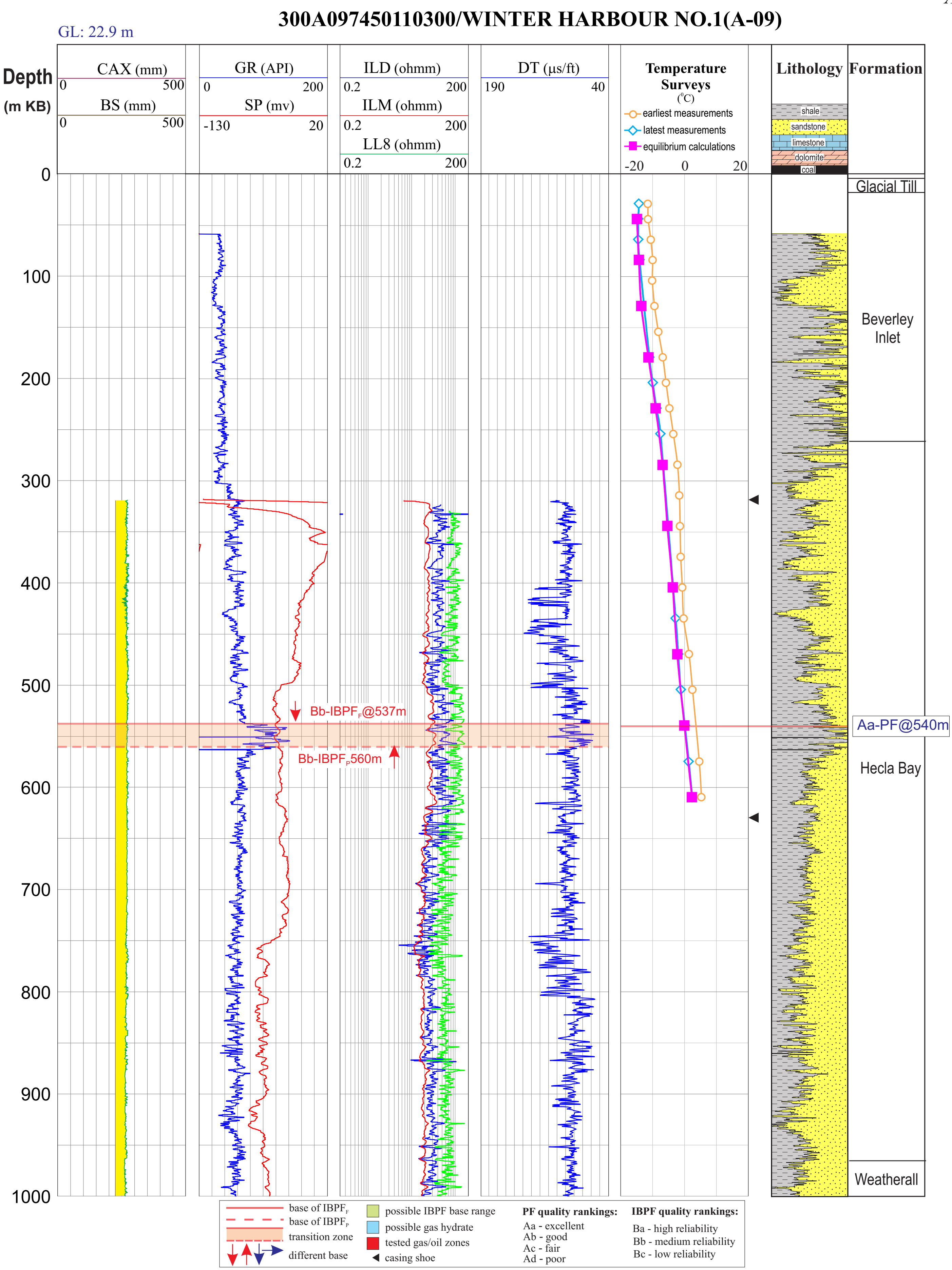

Figure 1-19. Base of PF is determined from temperature surveys with "Aa" quality for the Winter Harbour No.1 (A-09) well on Melville Island in the Canadian Arctic Islands. IBPF interpretation based on other geophysical methods is shown for comparison.

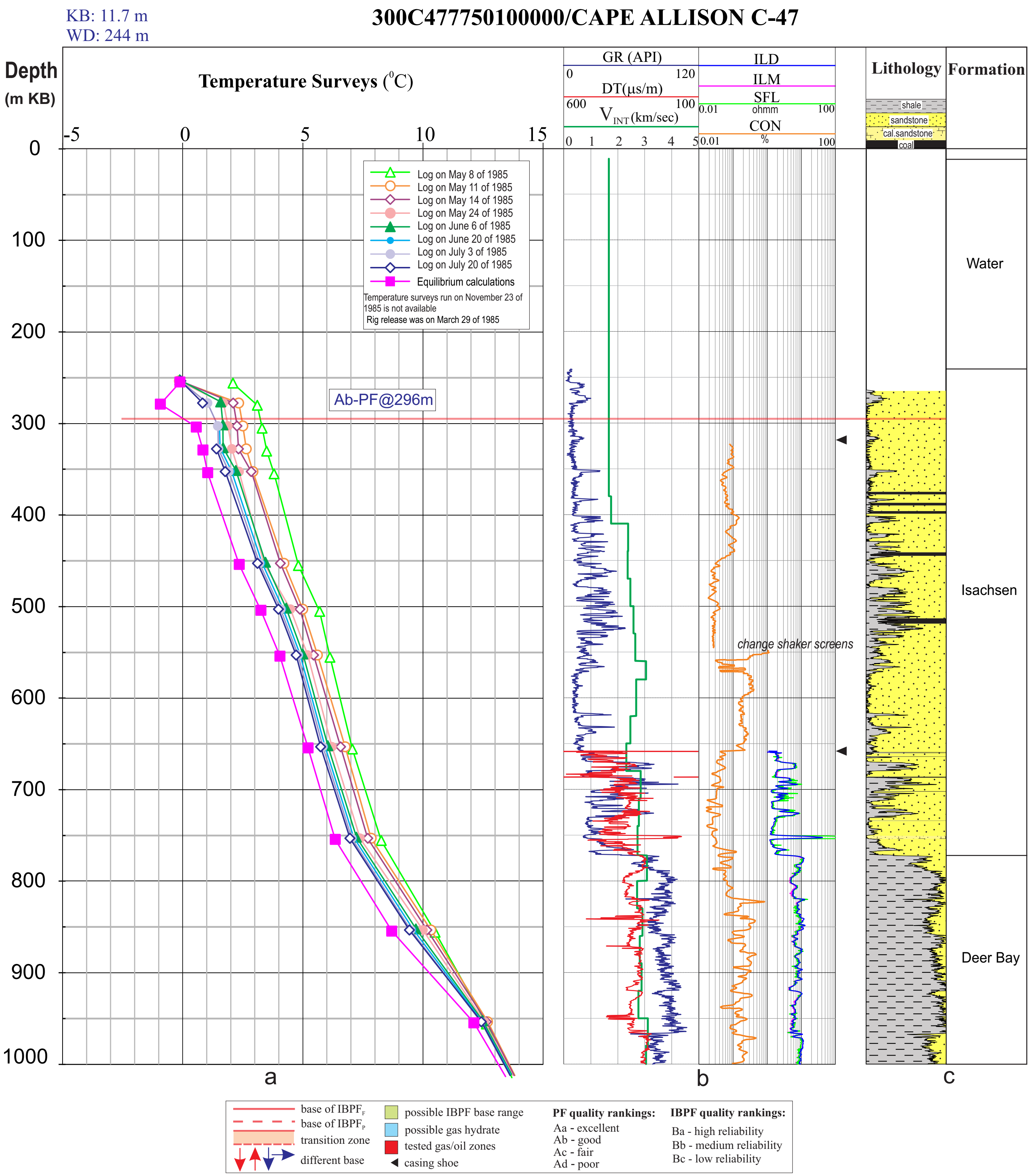

Figure 1-20. Base of PF is determined from temperature surveys with "Ab" quality for the Cape Allison C-47 well located in 244 m of water between Ellef Ringnes and King Christian islands in the Canadian Arctic Islands.
a -Temperature-depth profiles and equilibrium formation temperature calculations;
b - interval velocity (V_{INT}), sonic transit time (DT) and gamma ray log (GR); resistivity logs (ILD, ILM, SFL) and mud log (connection gas - CON);
c - lithological interpretation from well log analysis and formation tops for the shallow (<750 m SF) interval of the well.

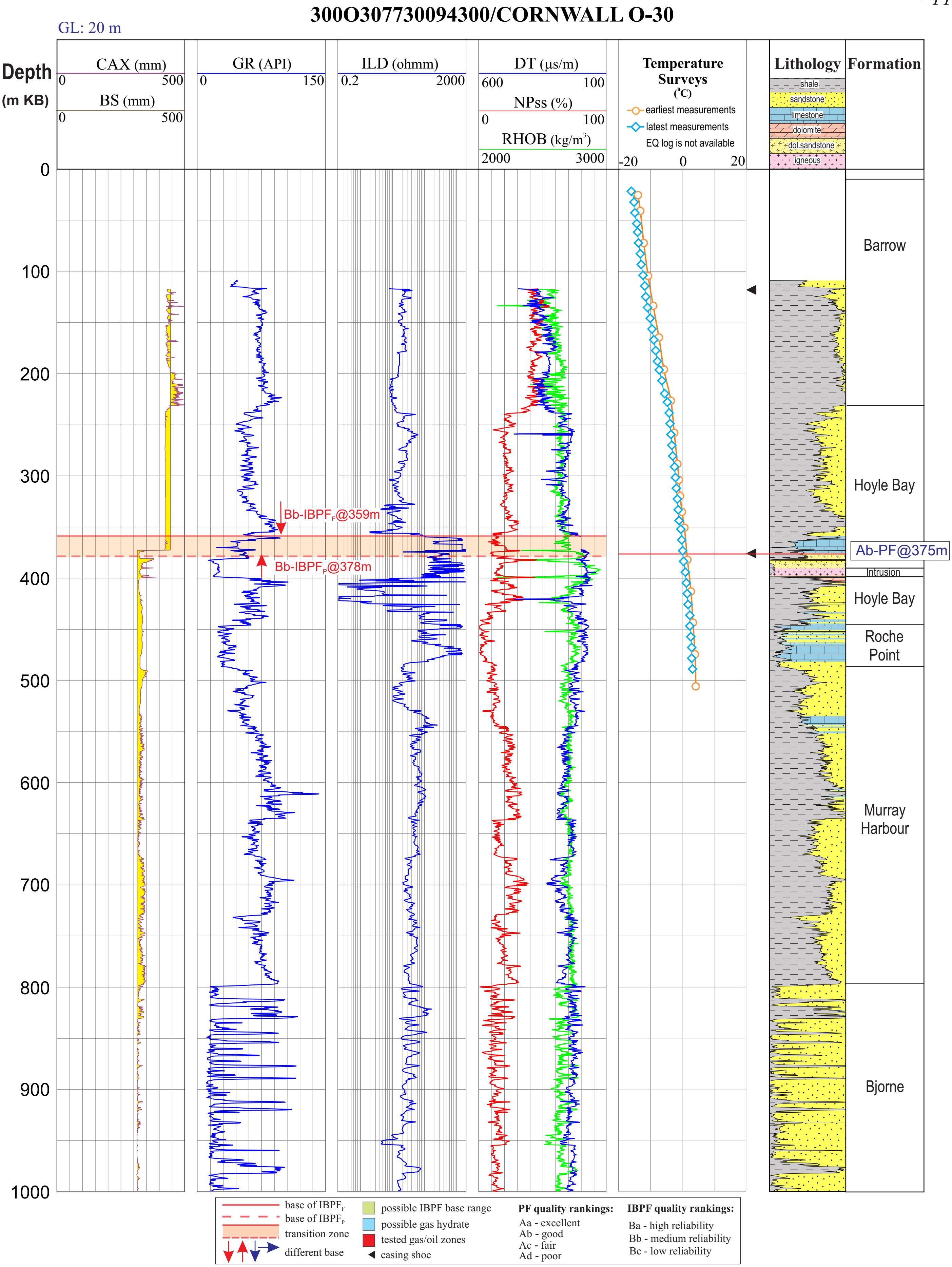

Figure 1-21. Base of PF is determined from temperature surveys with "Ab" quality for the Cornwall O-30 well on Cornwall Island in the Canadian Arctic Islands. IBPF interpretation based on other geophysical methods is shown for comparison.

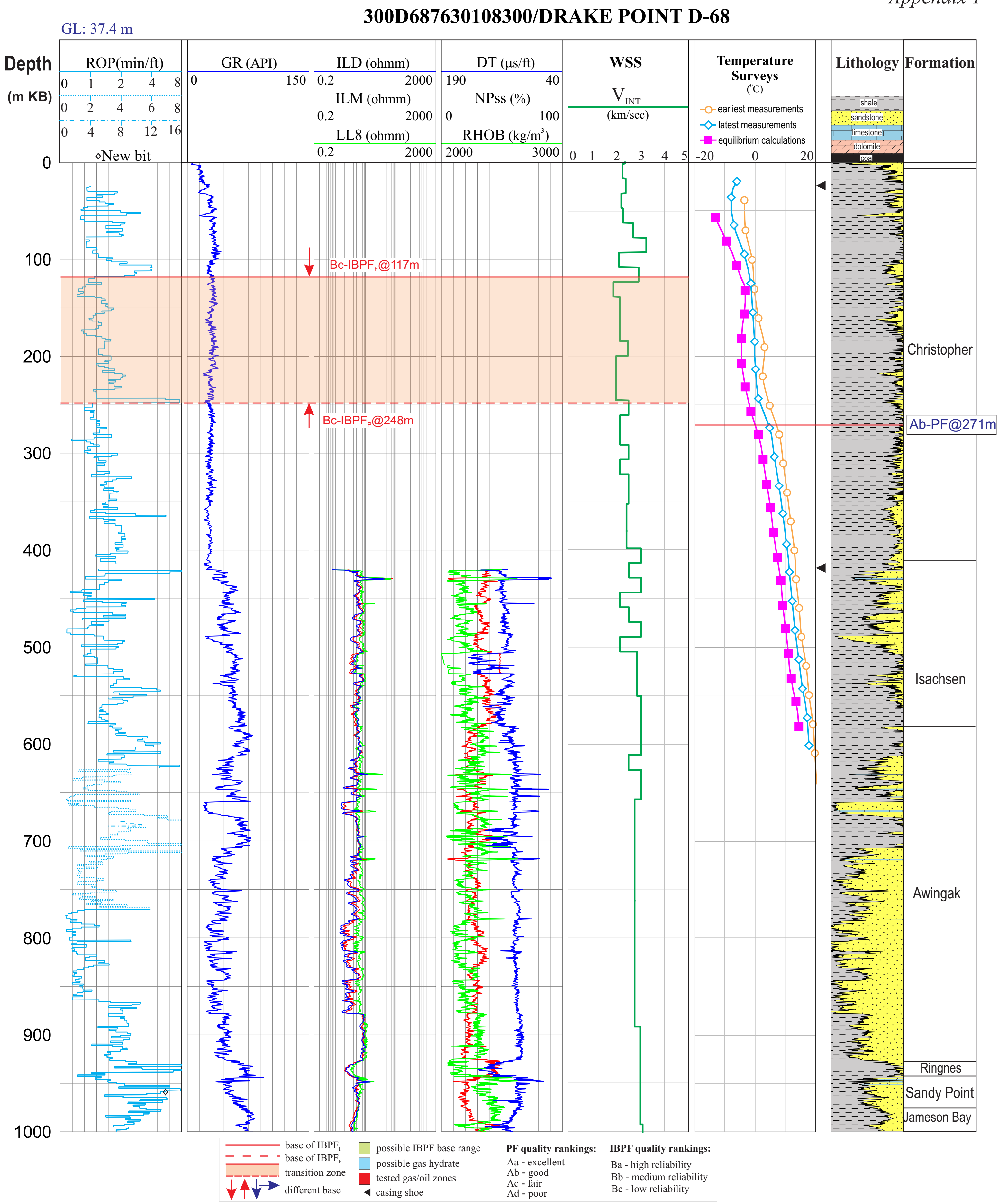

Figure 1-22. Base of PF is determined using temperature surveys with "Ab" quality for the Drake Point D-68 well on Melville Island in the Canadian Arctic Islands. IBPF interpretation based on other geophysical methods is shown for comparison.

300K717630108300/MARRYATT K-71

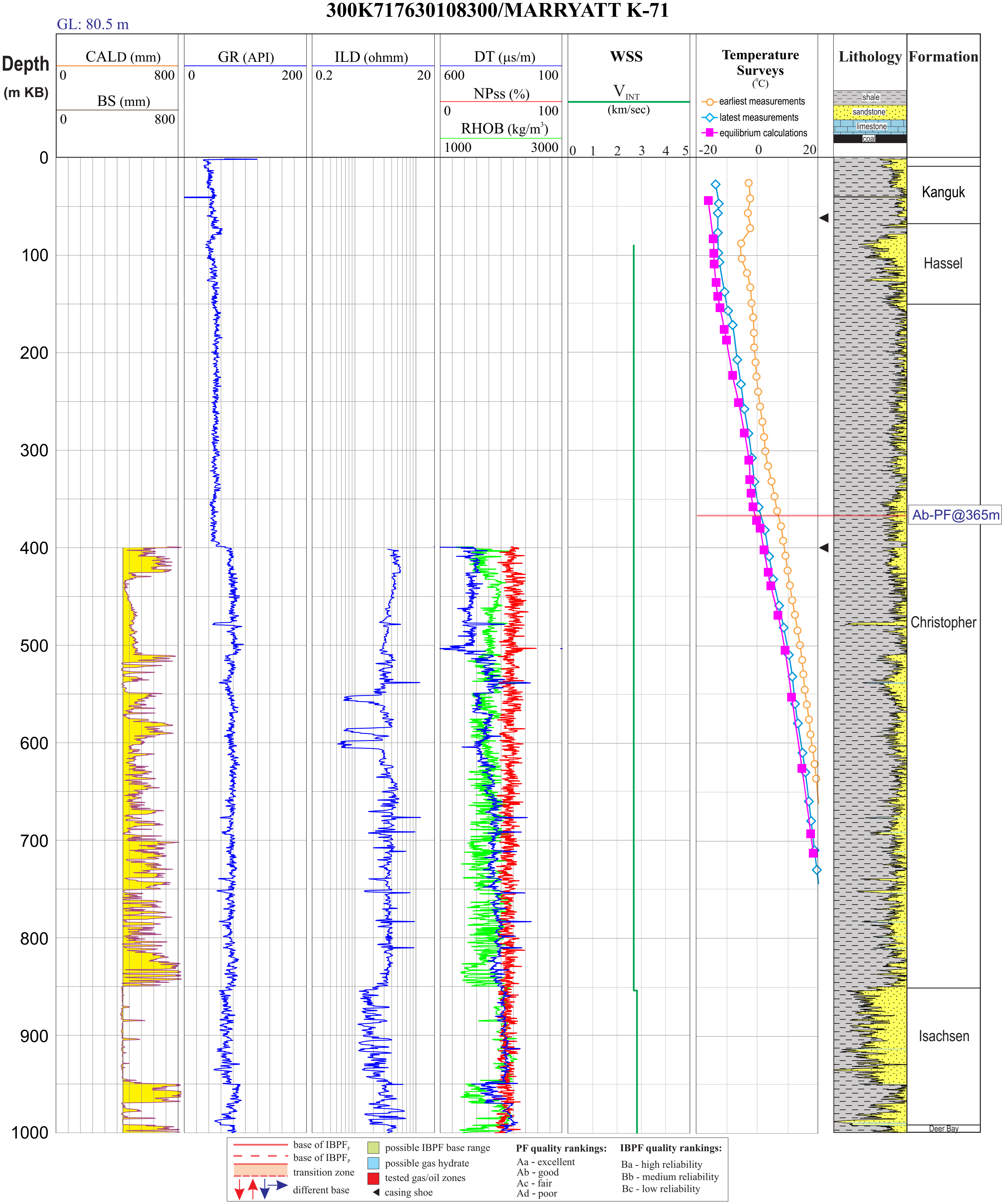

Figure 1-23. Base of PF is determined from temperature surveys with "Ab" quality for the Marryatt K-71 well on Melville Island in the Canadian Arctic Islands.

GL: 253.3 m

300A027940087000/MOKKA A-02

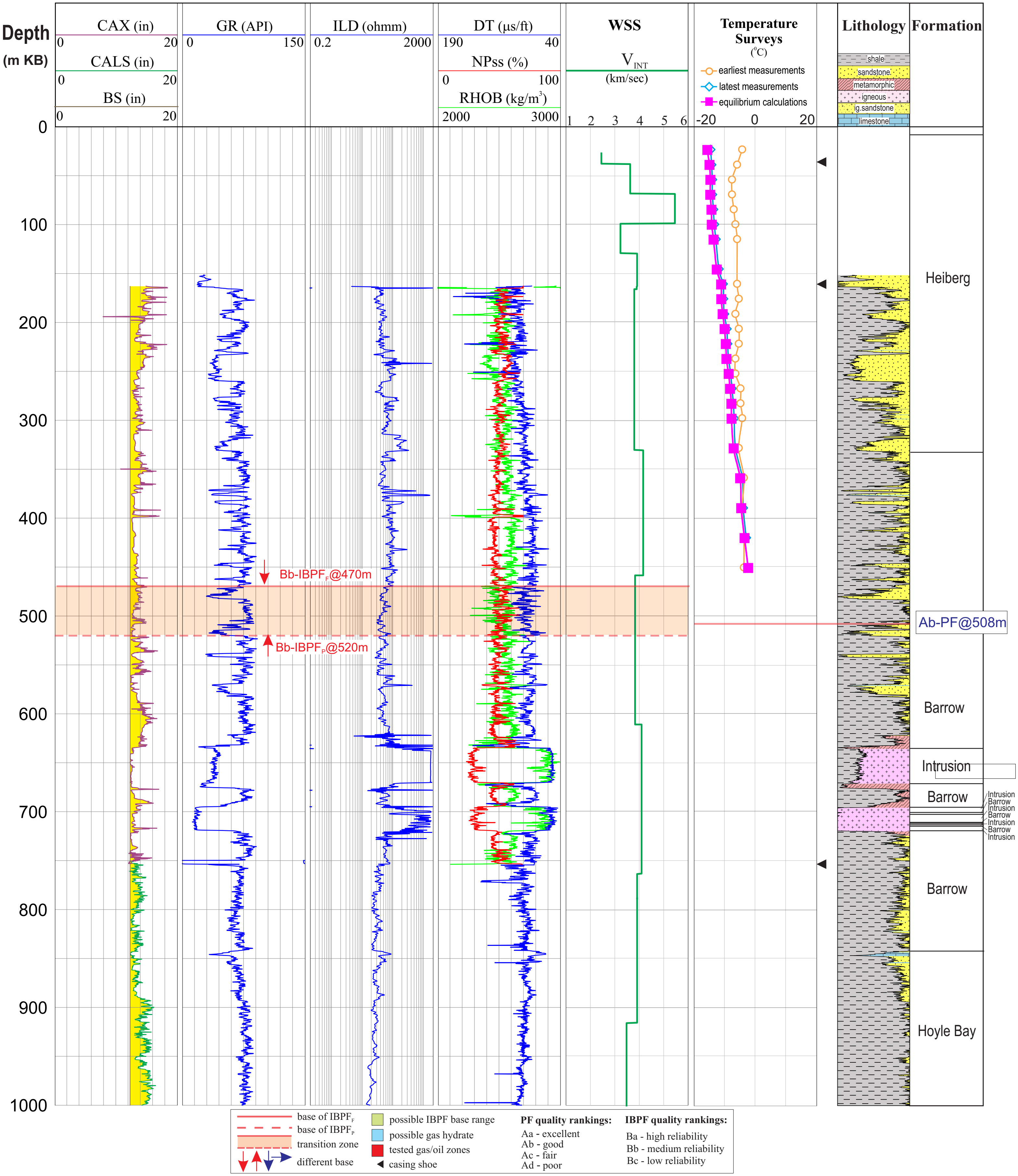

Figure 1-24. Base of PF is determined from temperature surveys with "Ab" quality for the Mokka A-02 well on Axel Heiberg Island in the Canadian Arctic Islands. IBPF interpretation based on other geophysical methods is shown for comparison.

300P367830103000/DOME BAY P-36

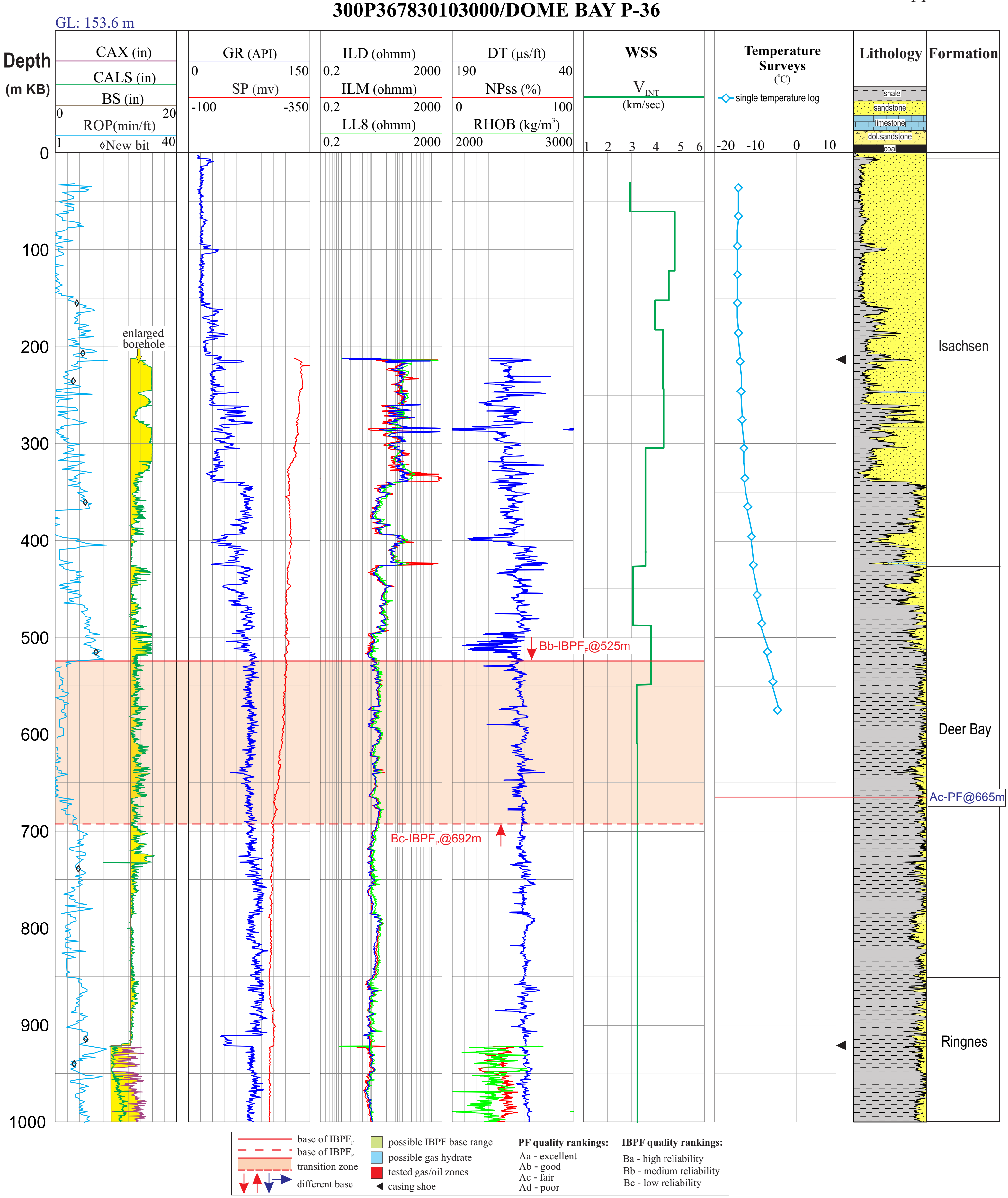

Figure 1-25. Base of PF is estimated from temperature surveys with "Ac" quality for the Dome Bay P-36 well on Ellef Ringnes Island in the Canadian Arctic Islands. IBPF interpretation based on other geophysical methods is shown for comparison.

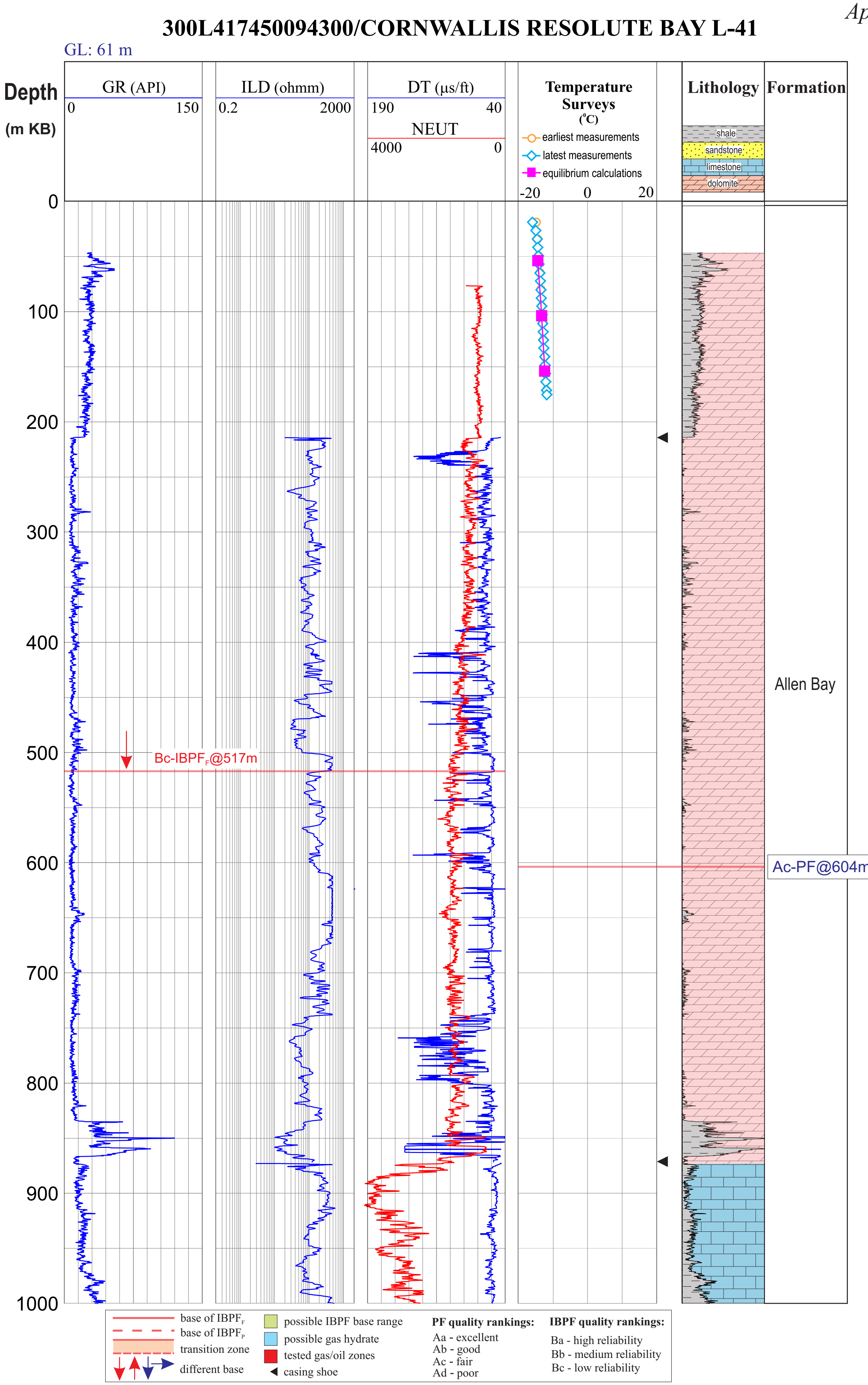

Figure 1-26. Base of PF is estimated from temperature surveys with "Ac" quality for the Cornwallis Resolute Bay L-41 well on Cornwallis Island in the Canadian Arctic Islands. IBPF interpretation based on other geophysical methods is shown for comparison.

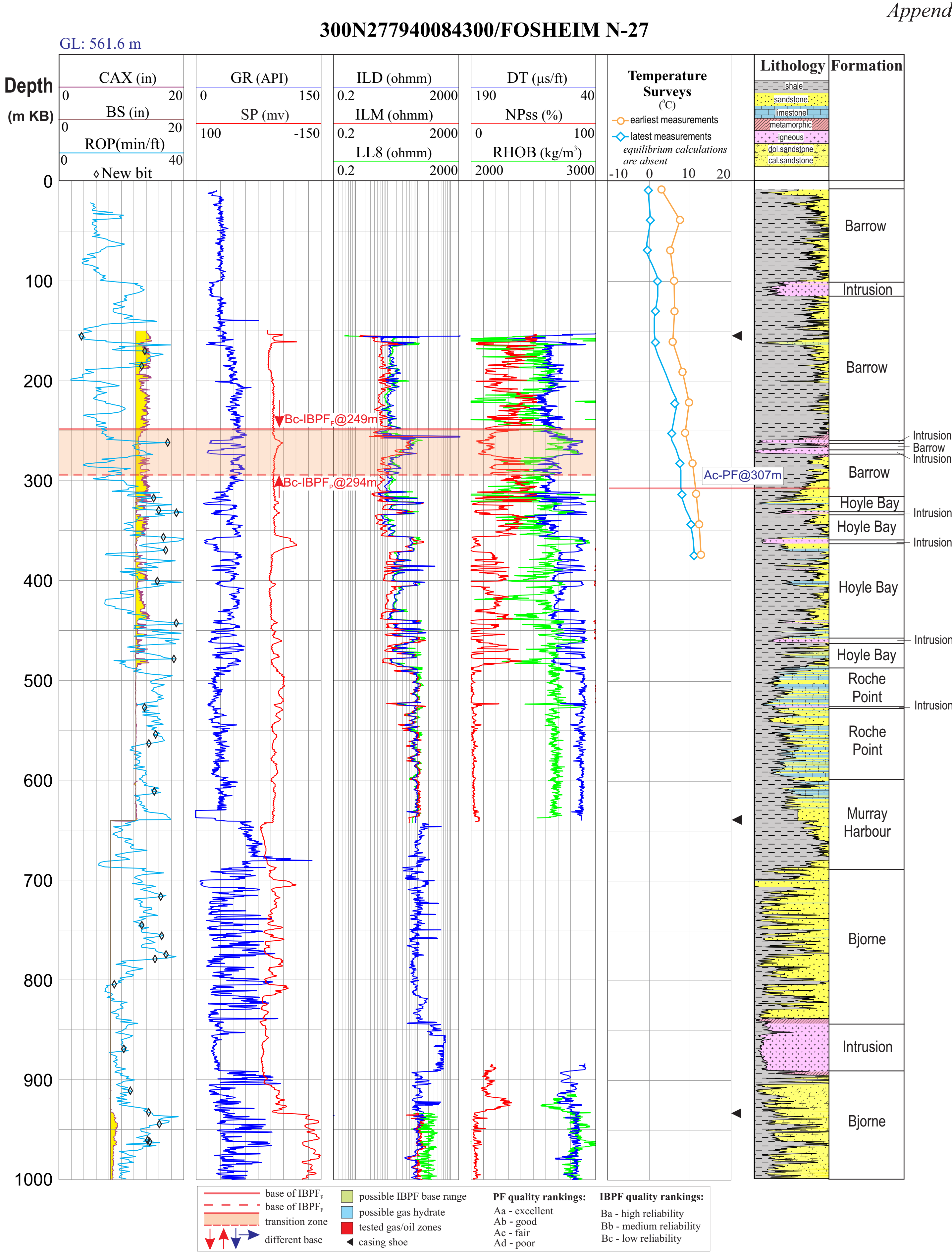

Figure 1-27. Base of PF is estimated from temperature surveys with "Ac" quality for the Fosheim N-27 well on Ellesmere Island in the Canadian Arctic Islands. IBPF interpretation based on other geophysical methods is shown for comparison.

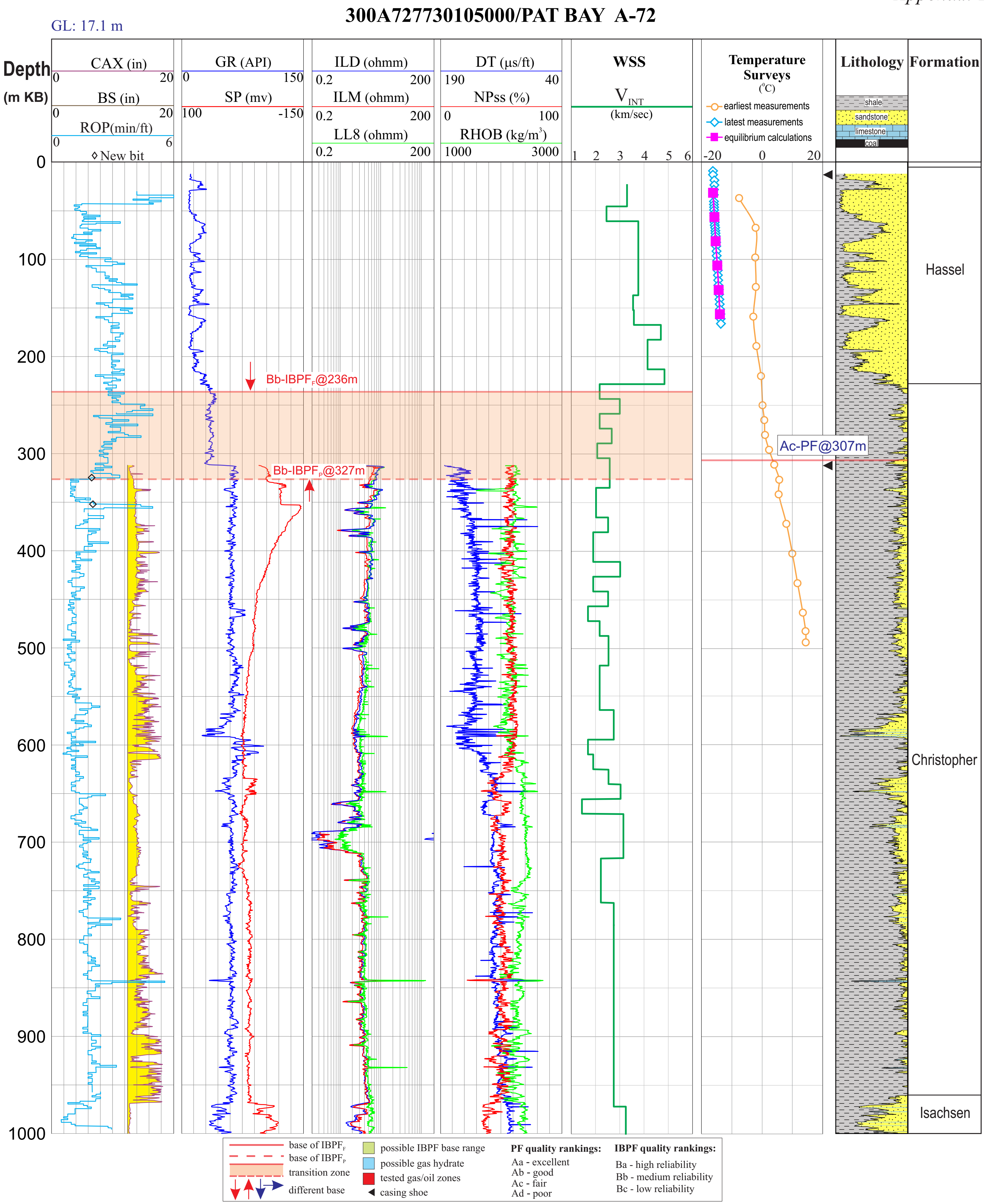

Figure 1-28. Base of PF is estimated from temperature surveys with "Ac" quality for the Pat Bay A-72 well on Lougheed Island in the Canadian Arctic Islands. IBPF interpretation based on other geophysical methods is shown for comparison.

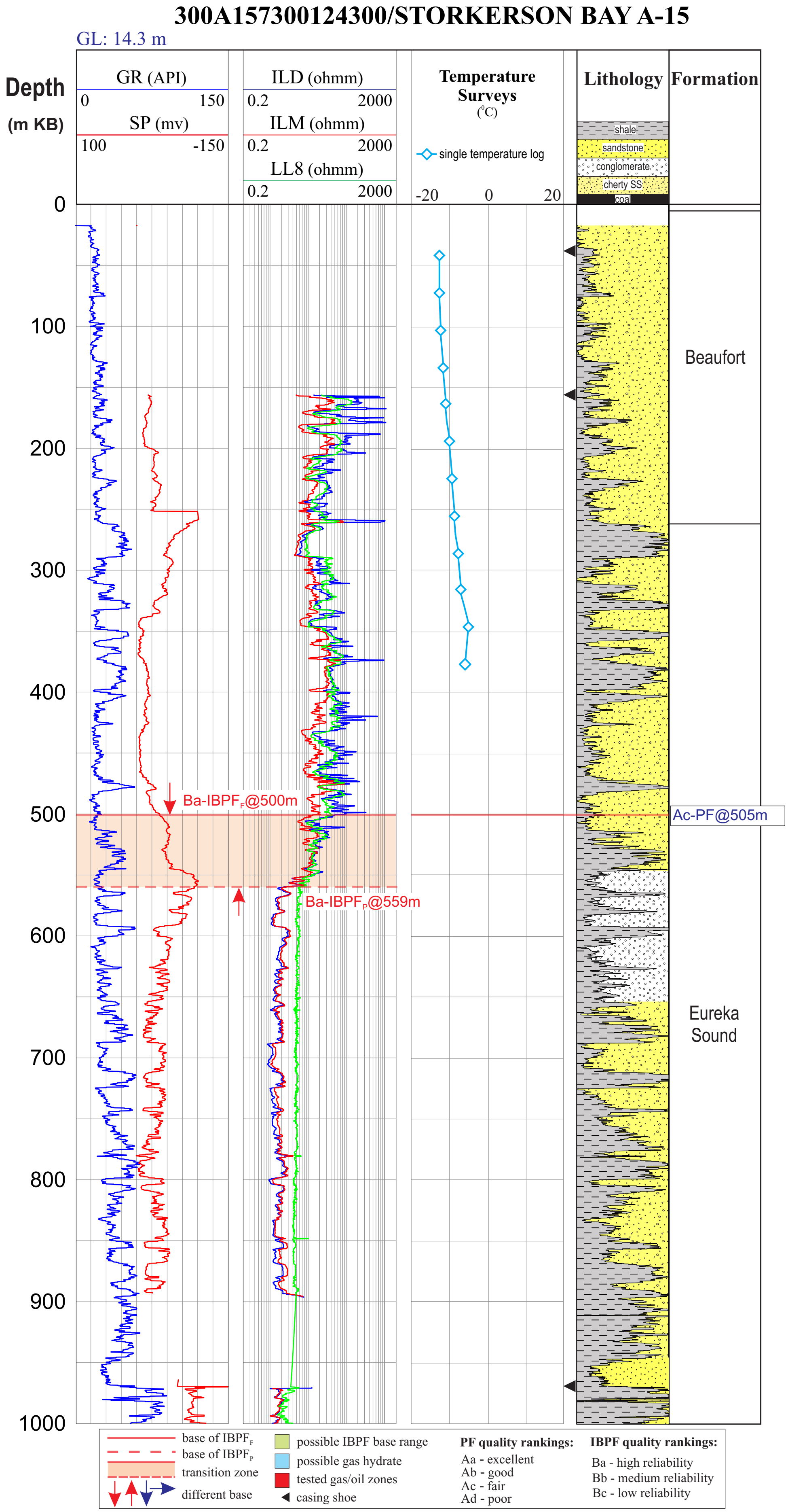

Figure 1-29. Base of PF is estimated from temperature surveys with "Ac" quality for the Storkerson Bay A-15 well on Banks Island in the Canadian Arctic Islands. IBPF interpretation based on other geophysical methods is shown for comparison.

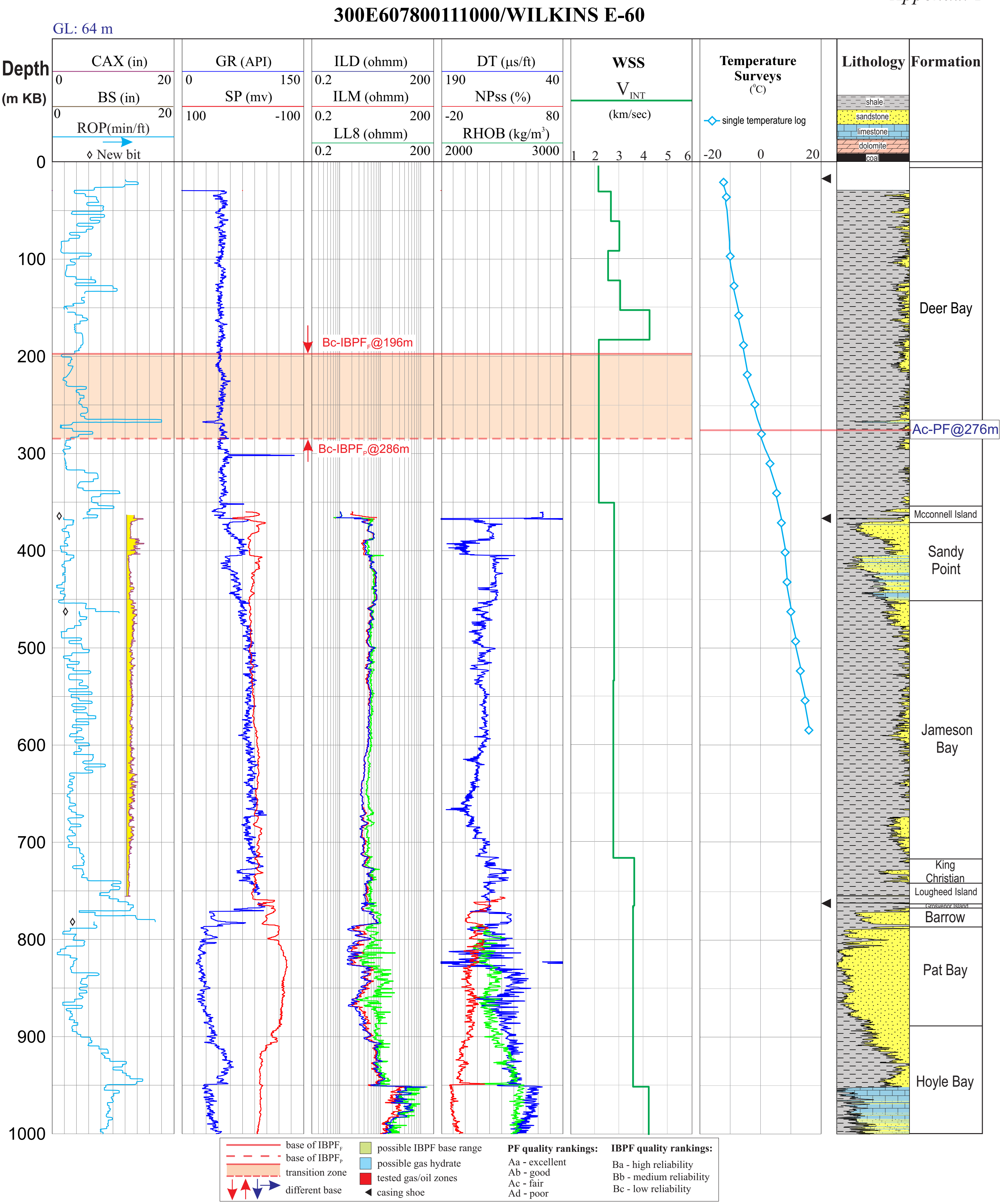

Figure 1-30. Base of PF is estimated from temperature surveys with "Ac" quality for the Wilkins E-60 well on Mackenzie King Island in the Canadian Arctic Islands. IBPF interpretation based on other geophysical methods is shown for comparison.

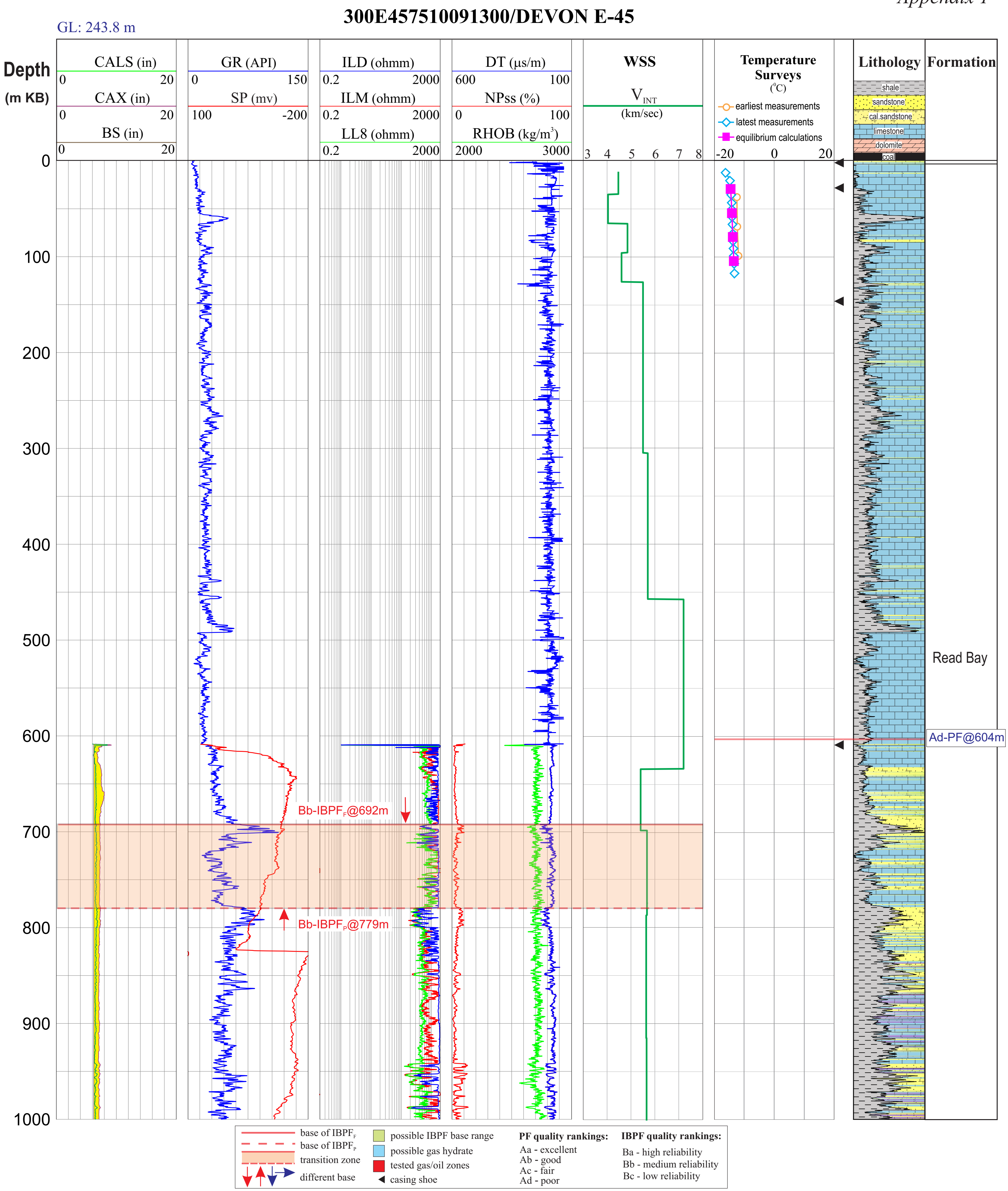

Figure 1-31. Base of PF is estimated from temperature surveys with "Ad" quality for the Devon E-45 well on Devon Island in the Canadian Arctic Islands. IBPF interpretation based on other geophysical methods is shown for comparison.

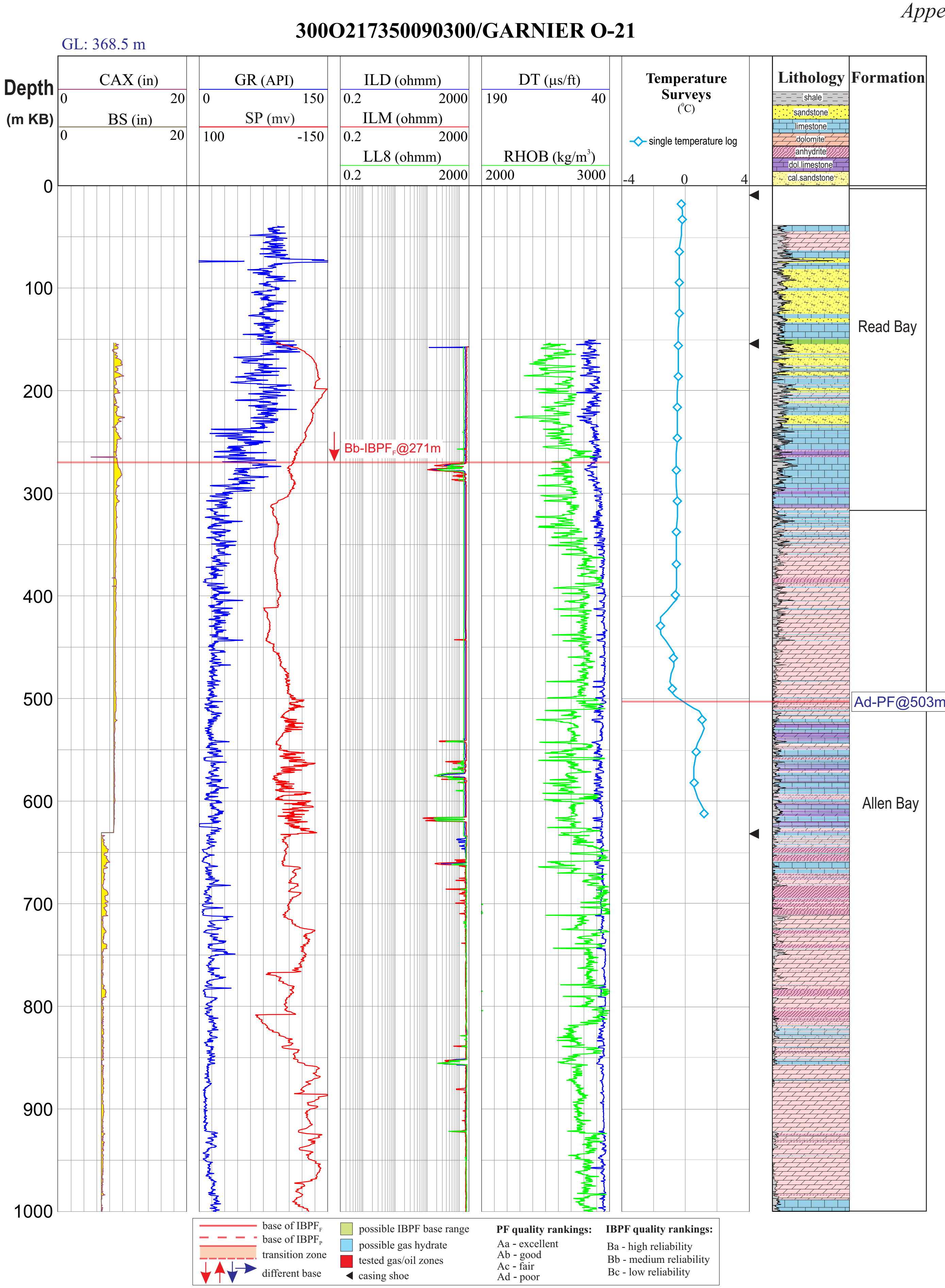

Figure 1-32. Base of PF is estimated from temperature surveys with "Ad" quality for the Garnier O-21 well on Somerset Island in the Canadian Arctic Islands. IBPF interpretation based on other geophysical methods is shown for comparison.

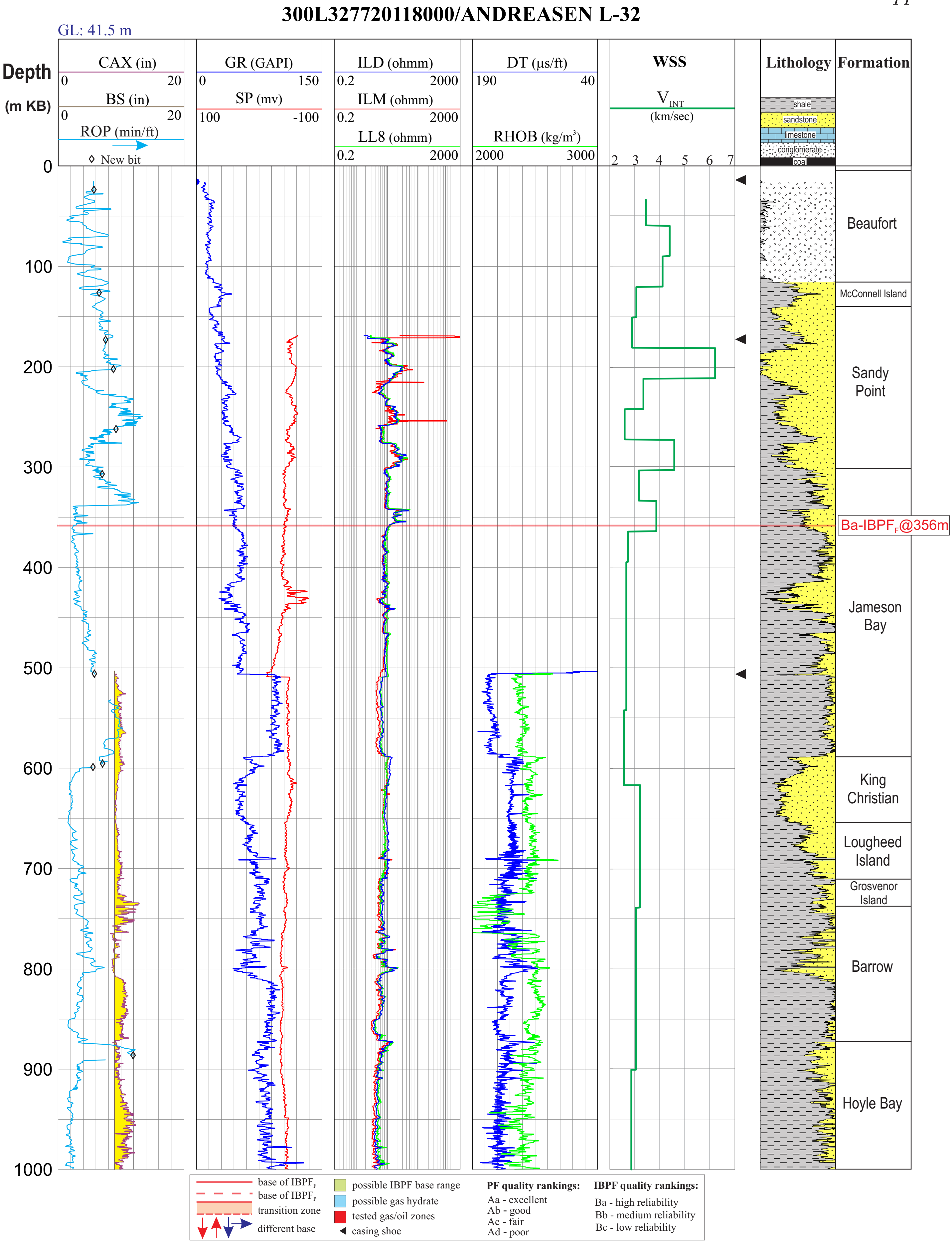

Figure 2-1. Determination of base of $IBPF_F$ with "Ba" quality using well logs and well seismic surveys for the Andreasen L-32 well on Prince Patrick Island in the Canadian Arctic Islands.

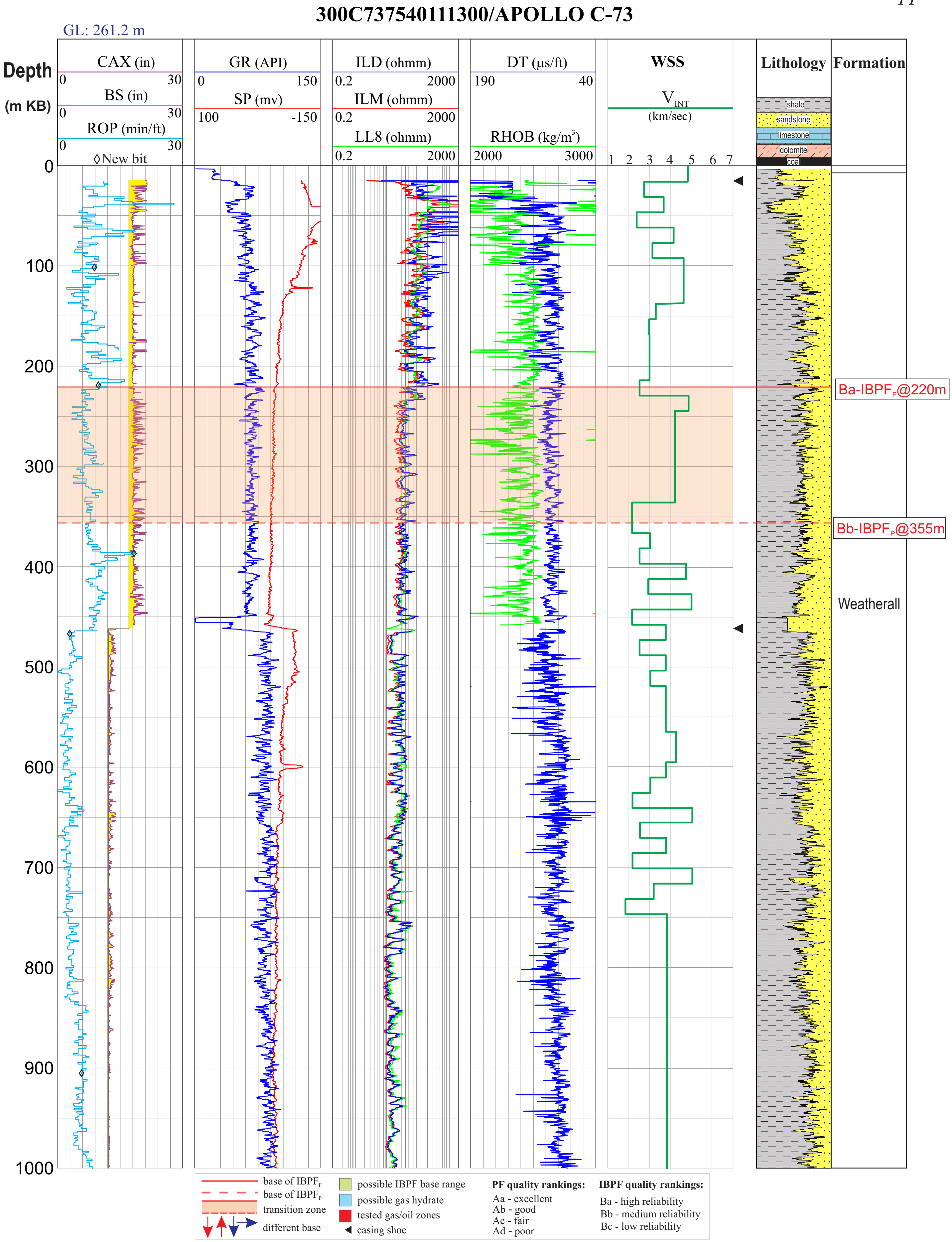

Figure 2-2. Determinations of base of $IBPF_F$ with "Ba" quality and $IBPF_P$ with "Bb" quality using well logs and well seismic surveys for the Apollo C-73 well on Melville Island in the Canadian Arctic Islands.

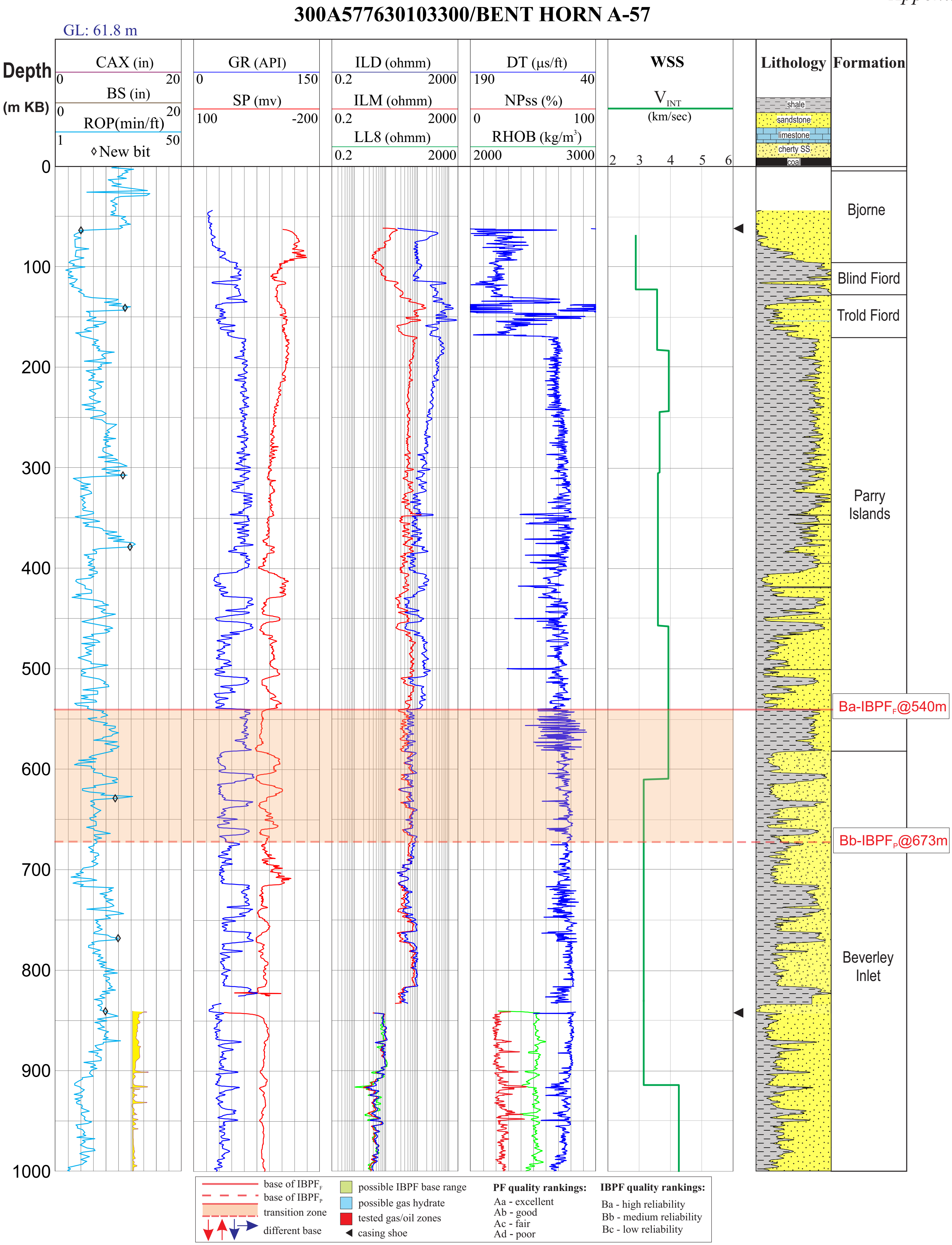

Figure 2-3. Determinations of base of IBPF$_F$ with "Ba" quality and IBPF$_P$ with "Bb" quality using well logs and well seismic surveys for the Bent Horn A-57 well on Cameron Island in the Canadian Arctic Islands.

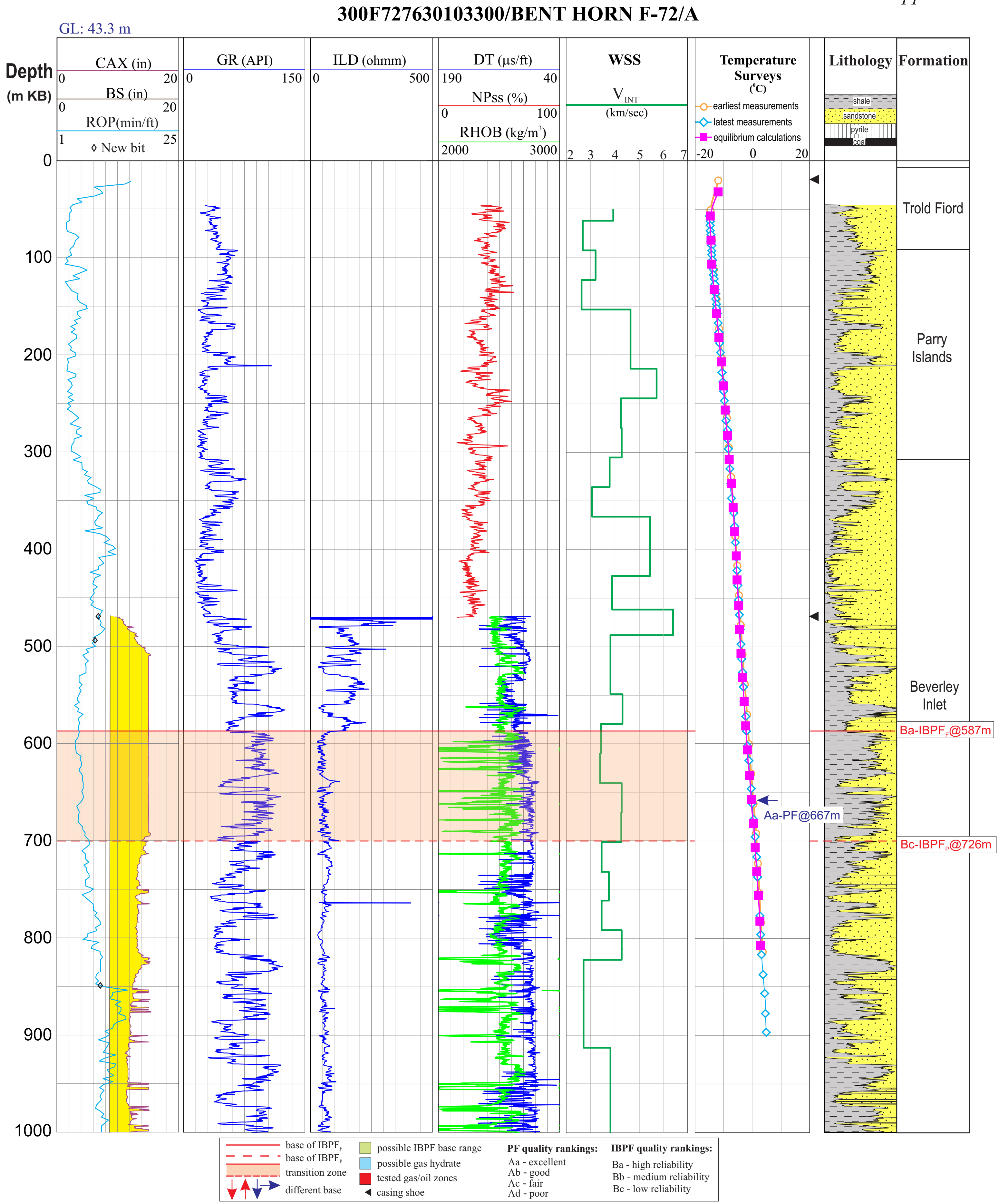

Figure 2-4. Determinations of bases of $IBPF_F$ with "Ba" quality and $IBPF_P$ with "Bc" quality using well logs and well seismic survey, and base of PF from temperature surveys for the Bent Horn F-72 and F-72A wells on Cameron Island in the Canadian Arctic Islands.

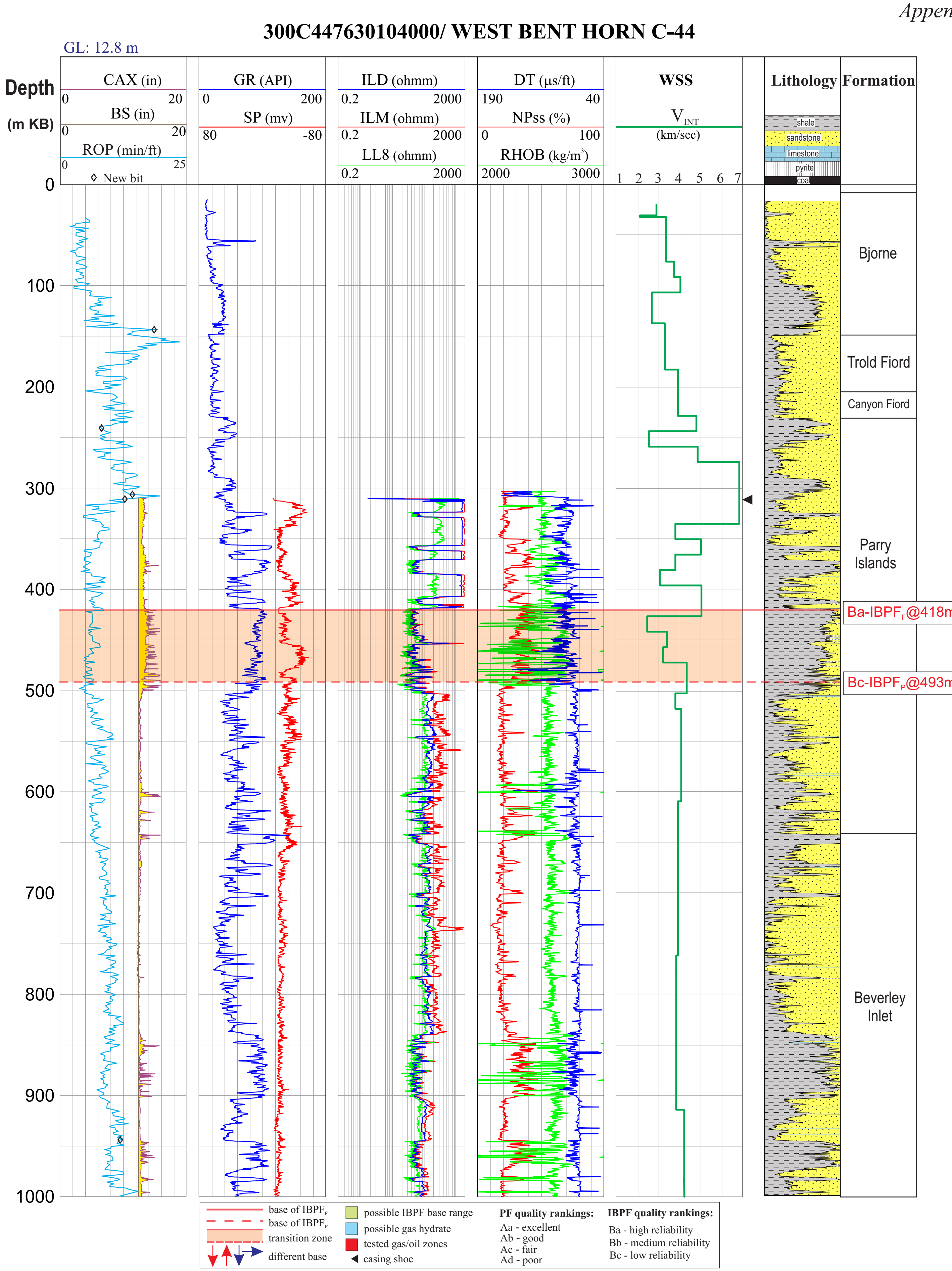

Figure 2-5. Determinations of base of $IBPF_F$ with "Ba" quality and $IBPF_P$ with "Bc" quality using well logs and well seismic surveys for the West Bent Horn C-44 well on Cameron Island in the Canadian Arctic Islands.

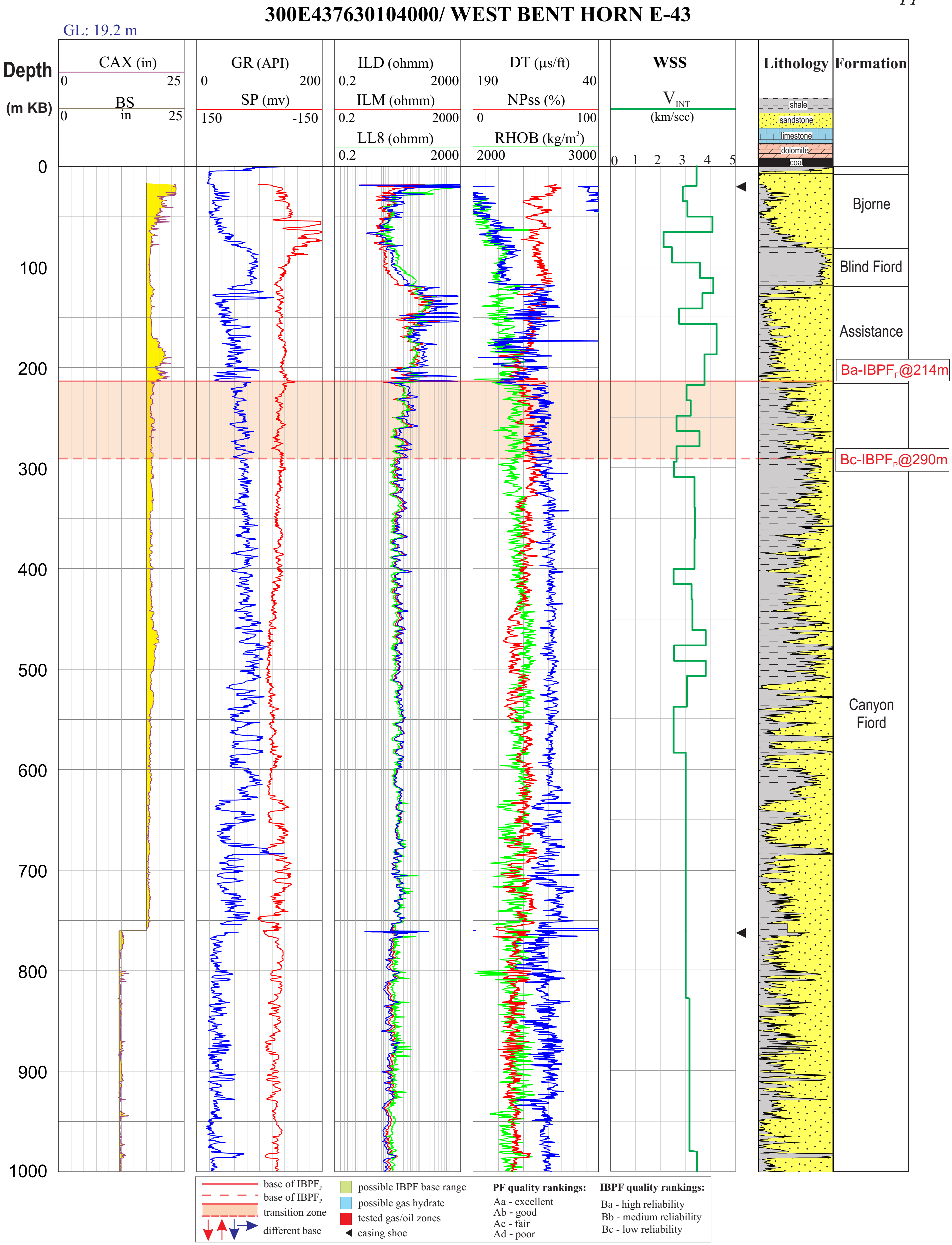

Figure 2-6. Determinations of base of $IBPF_F$ with “Ba” quality and $IBPF_P$ with “Bc” quality using well logs and well seismic surveys for the West Bent Horn E-43 well on Cameron Island in the Canadian Arctic Islands.

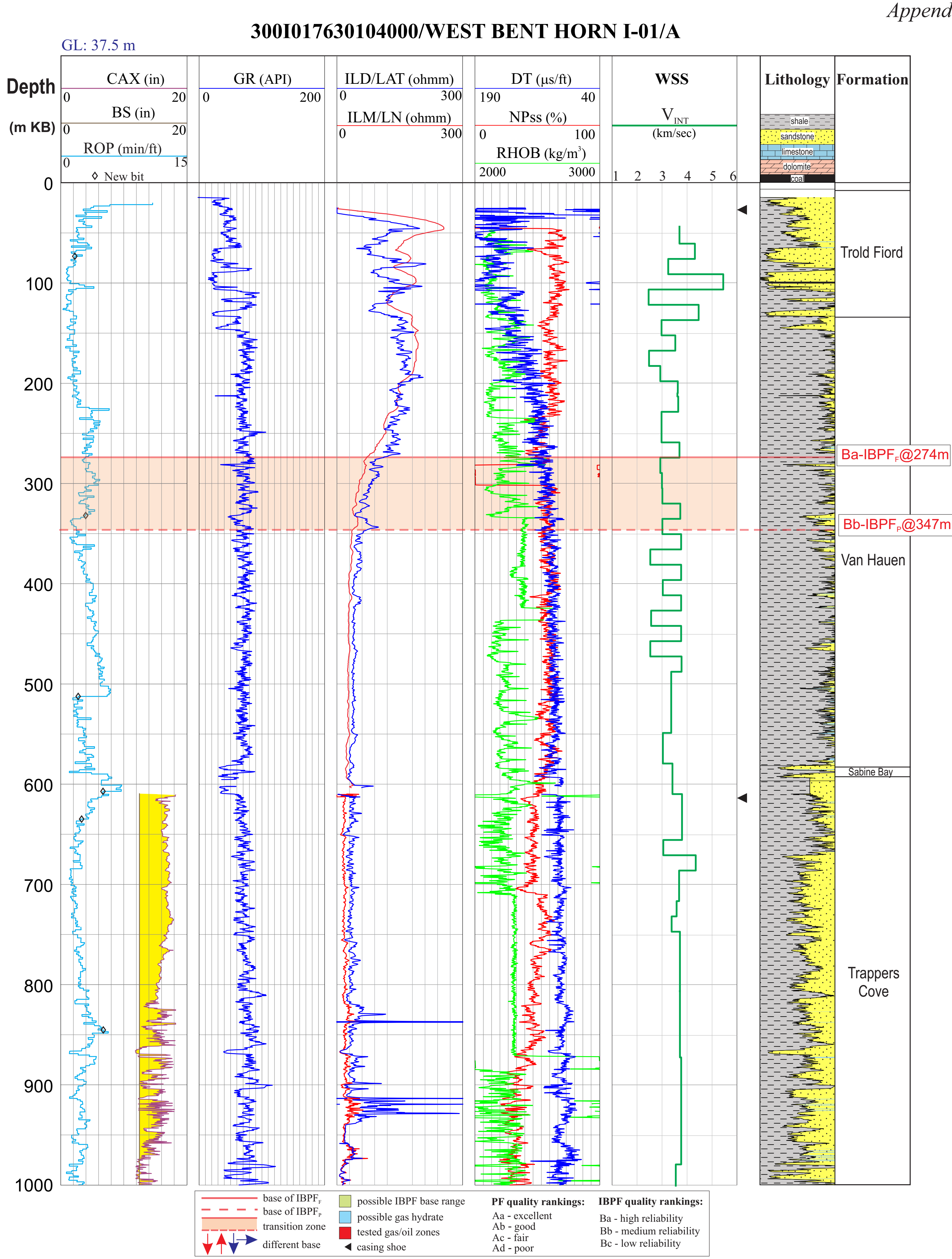

Figure 2-7. Determinations of base of $IBPF_F$ with "Ba" quality and $IBPF_P$ with "Bb" quality using well logs and well seismic surveys for the West Bent Horn I-01/A wells on Cameron Island in the Canadian Arctic Islands.

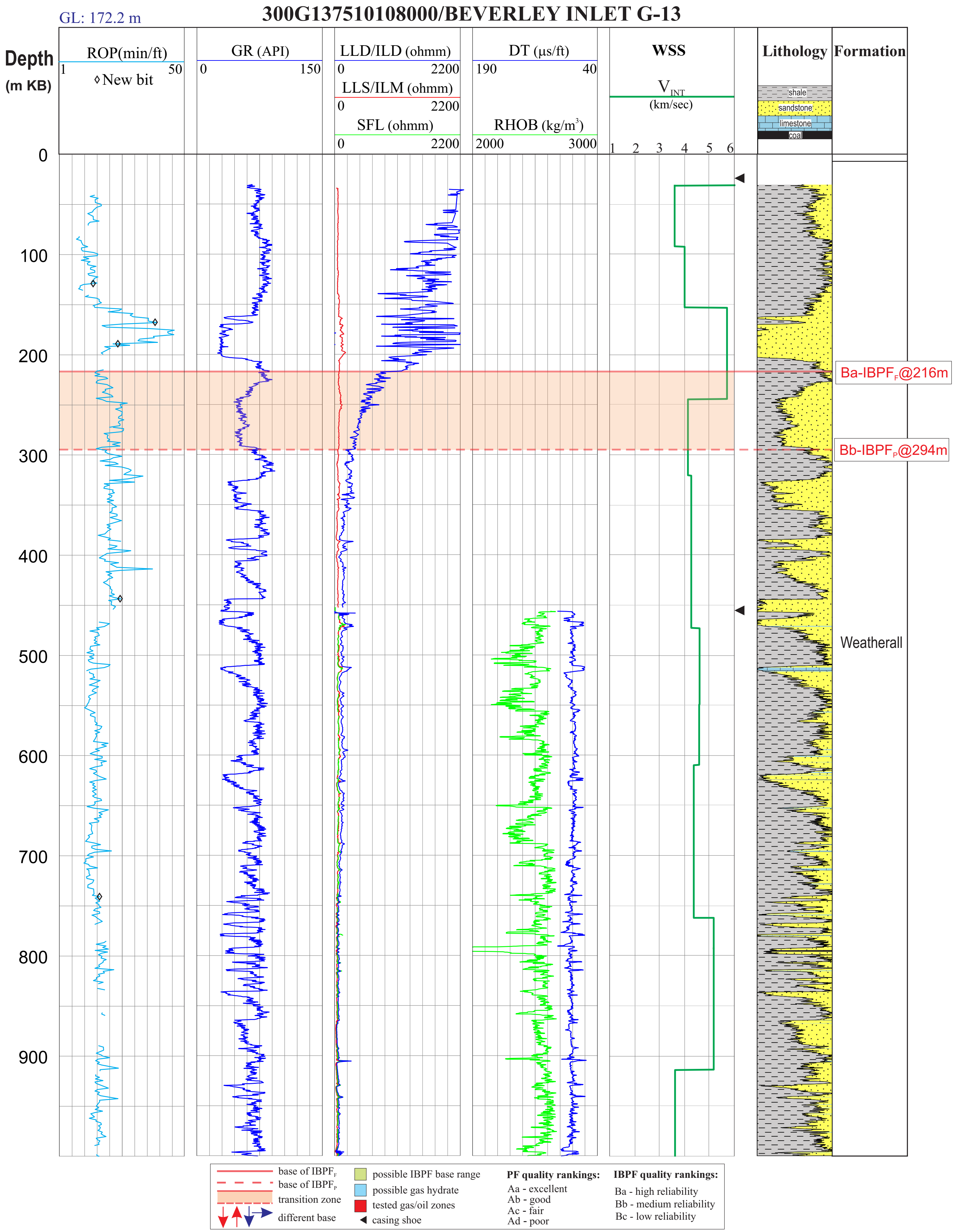

Figure 2-8. Determinations of base of $IBPF_F$ with "Ba" quality and $IBPF_P$ with "Bb" quality using well logs and well seismic surveys for the Beverley Inlet G-13 well on Melville Island in the Canadian Arctic Islands.

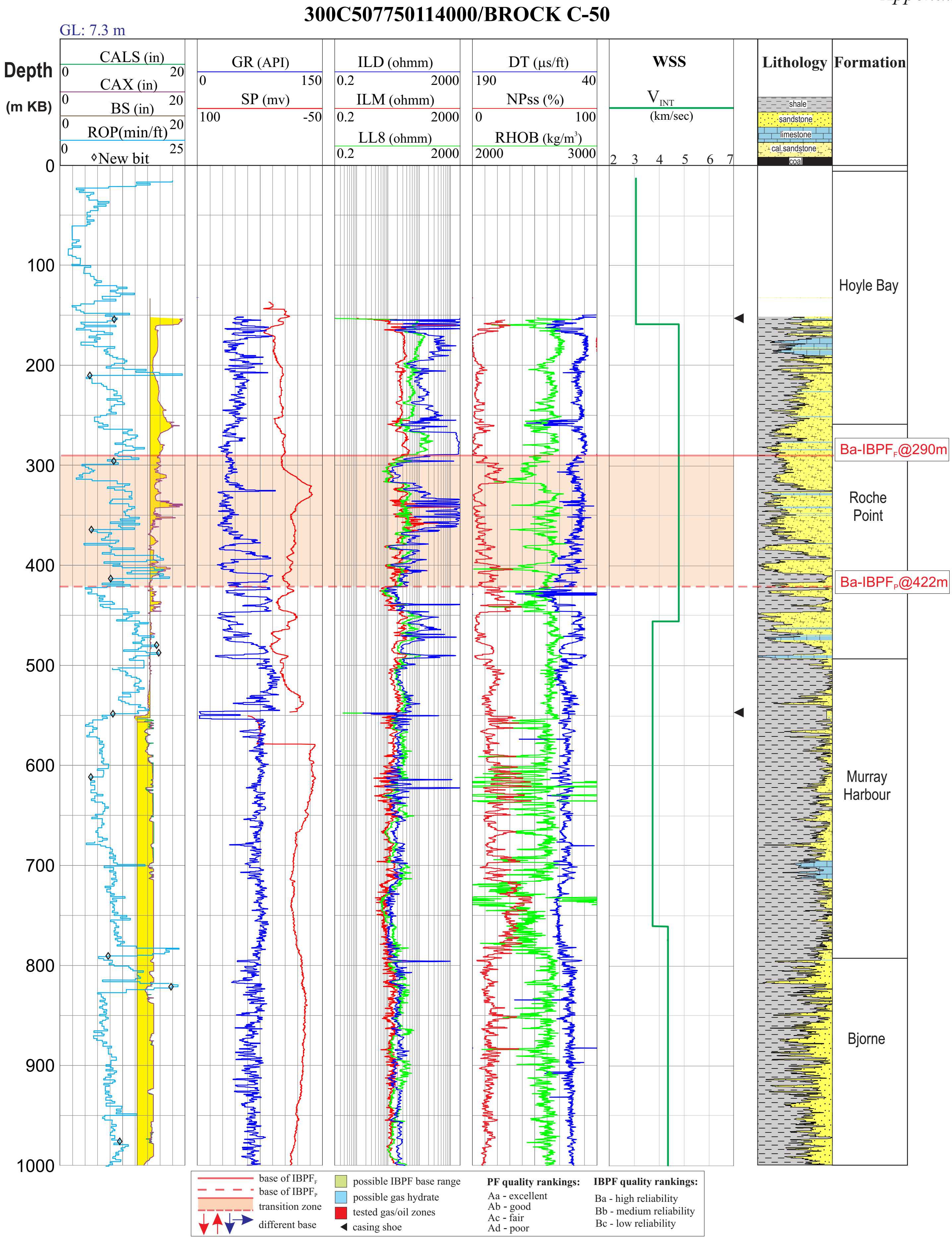

Figure 2-9. Determinations of base of $IBPF_F$ with "Ba" quality and $IBPF_P$ with "Ba" quality using well logs and well seismic surveys for the Brock C-50 well on Brock Island in the Canadian Arctic Islands.

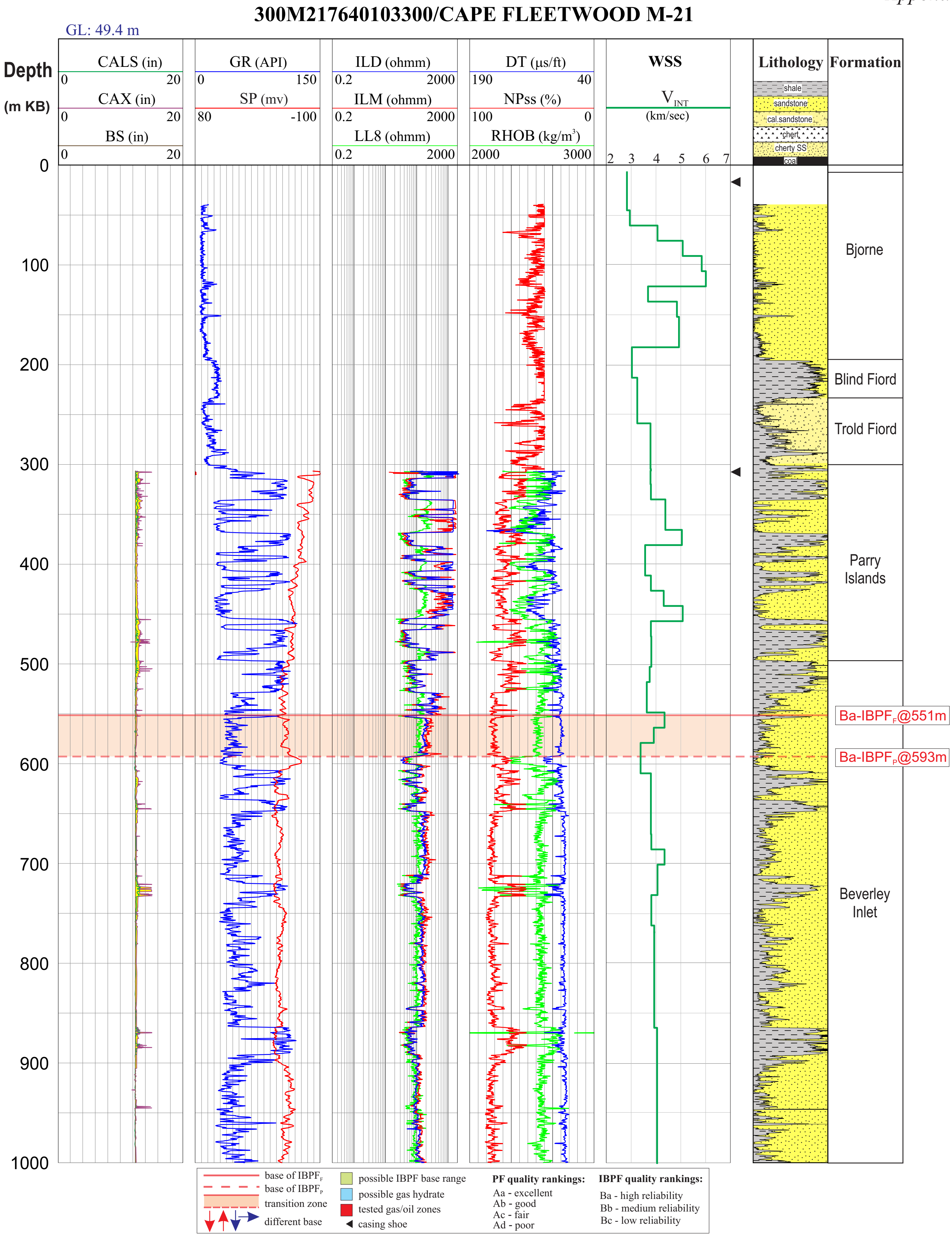

Figure 2-10. Determinations of base of $IBPF_F$ with "Ba" quality and $IBPF_P$ with "Ba" quality using well logs and well seismic surveys for the Cape Fleetwood M-21 well on Cameron Island in the Canadian Arctic Islands.

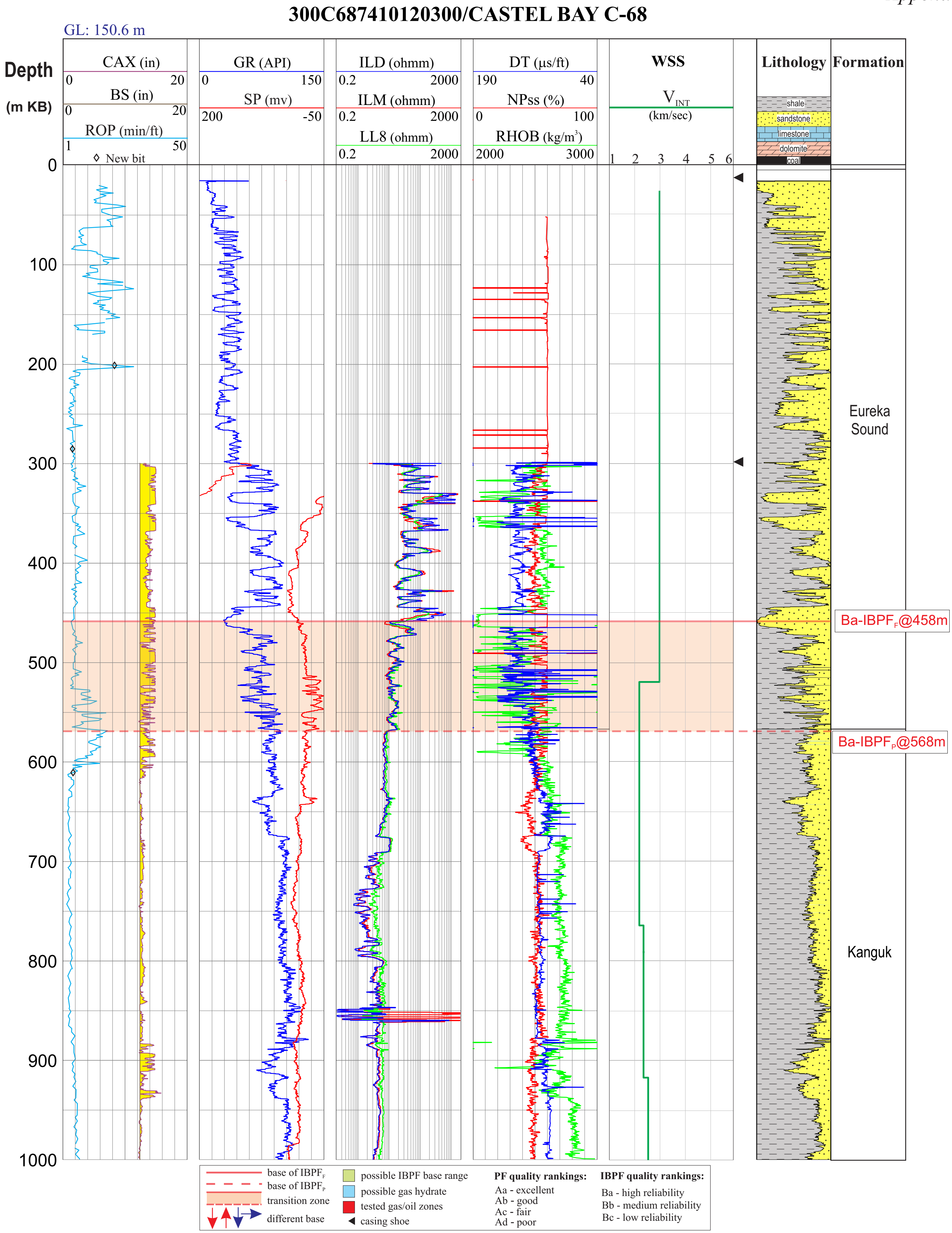

Figure 2-11. Determinations of base of $IBPF_F$ with “Ba” quality and $IBPF_P$ with “Ba” quality using well logs and well seismic surveys for the Castel Bay C-68 well on Banks Island in the Canadian Arctic Islands.

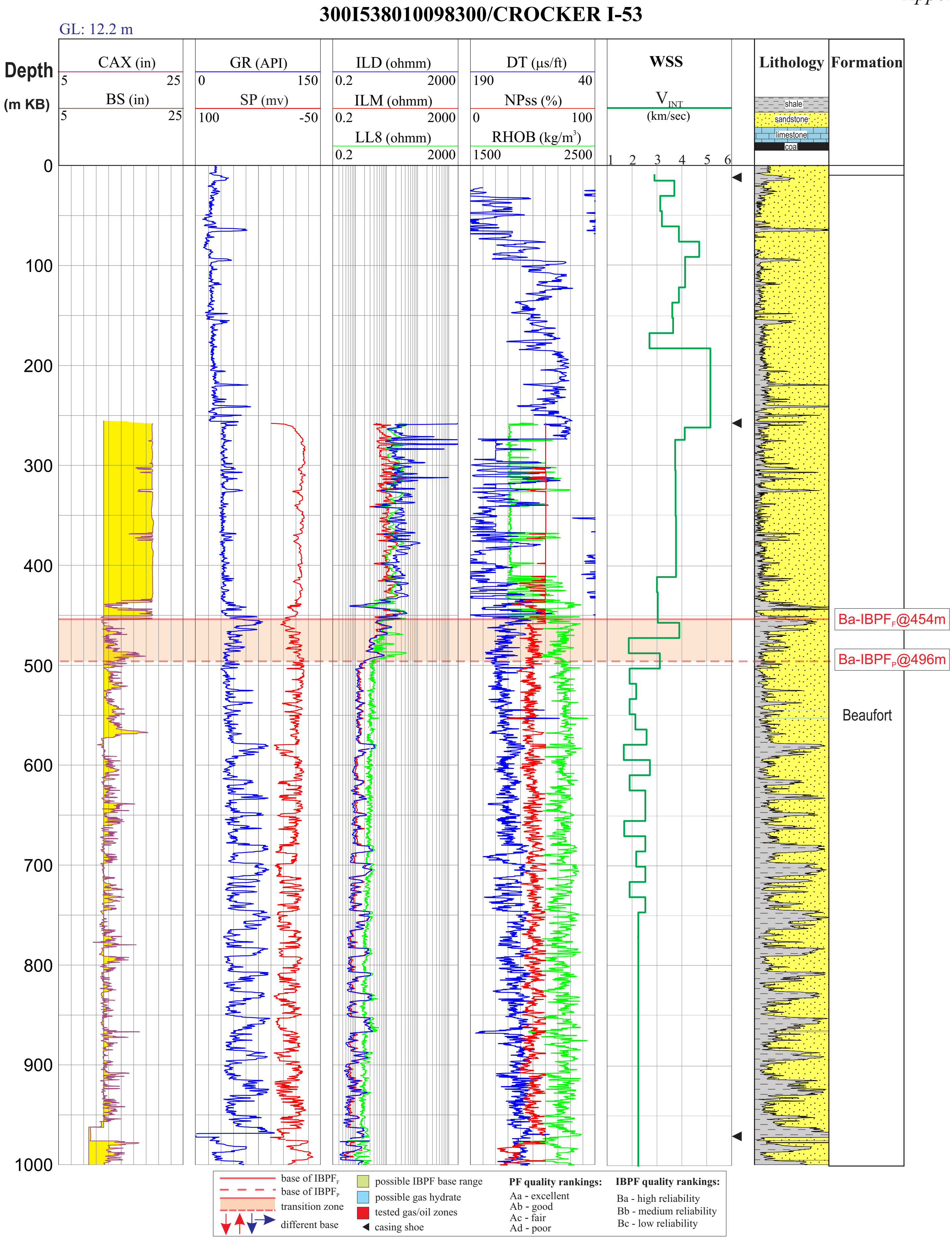

Figure 2-12. Determinations of base of $IBPF_F$ with "Ba" quality and $IBPF_P$ with "Ba" quality using well logs and well seismic surveys for the Crocker I-53 well on Meighen Island in the Canadian Arctic Islands.

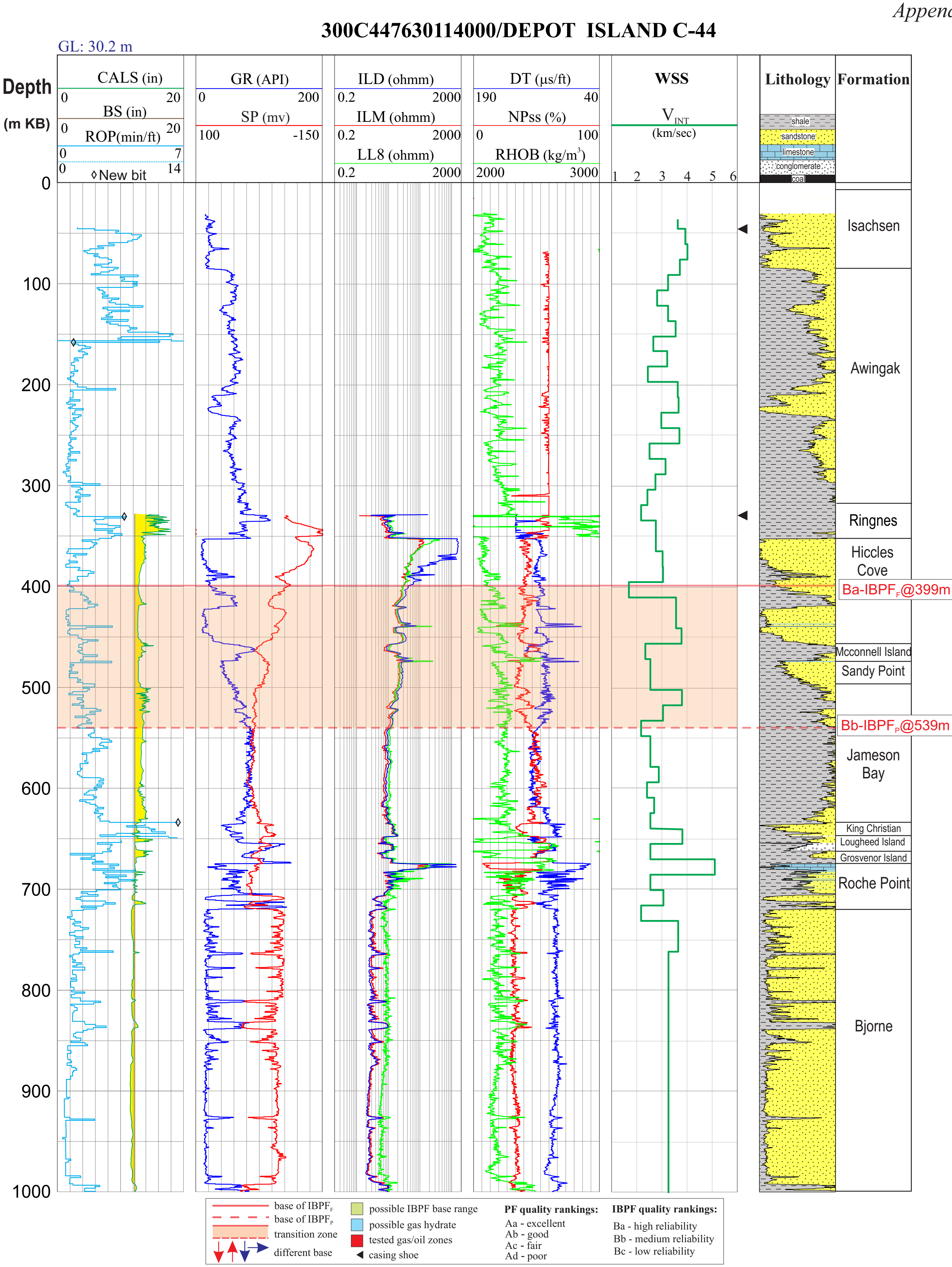

Figure 2-13. Determinations of base of $IBPF_F$ with "Ba" quality and $IBPF_P$ with "Bb" quality using well logs and well seismic surveys for the Depot Island C-44 well on Melville Island in the Canadian Arctic Islands.

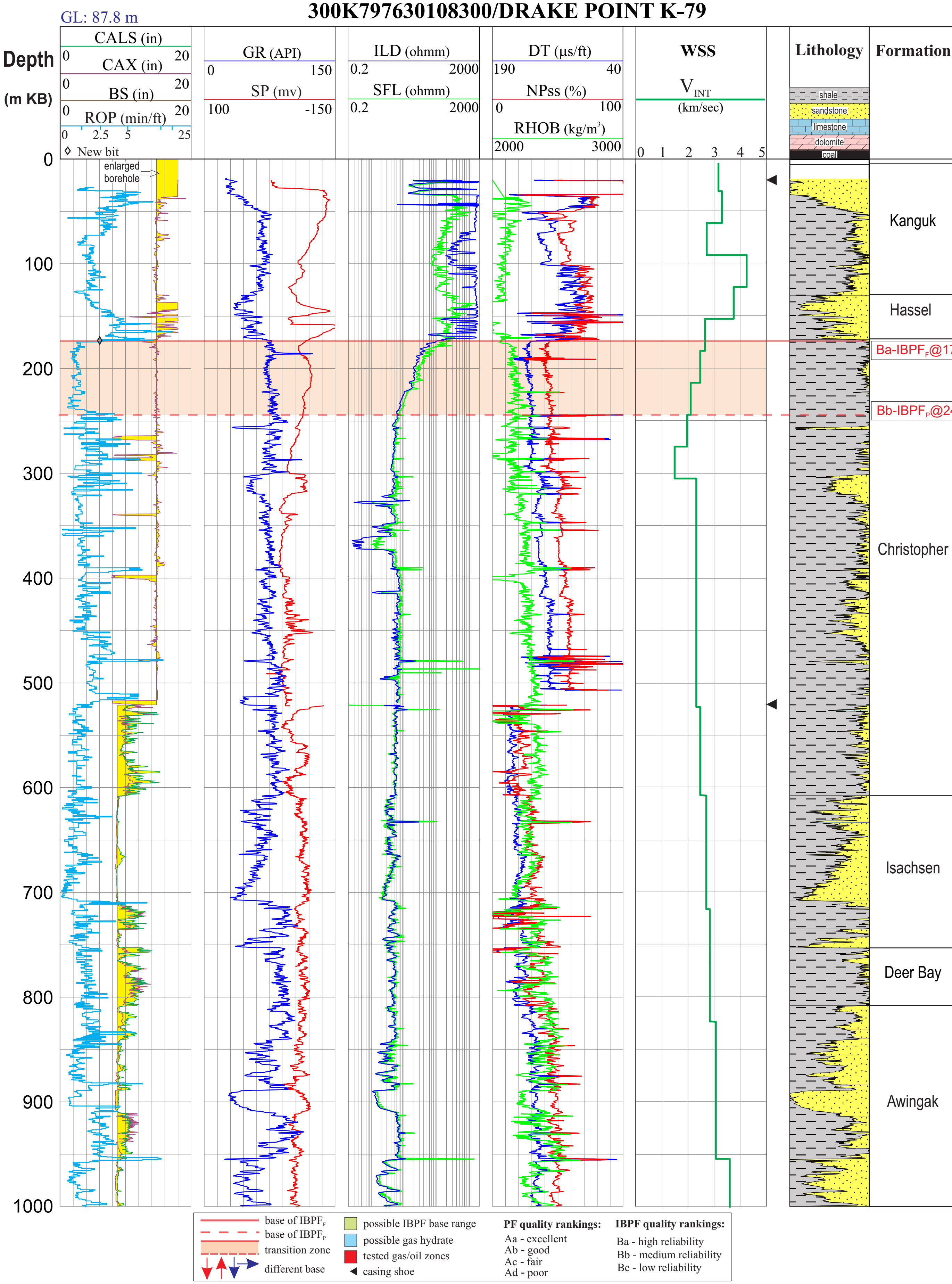

Figure 2-14. Determinations of base of $IBPF_F$ with "Ba" quality and $IBPF_P$ with "Bb" quality using well logs and well seismic surveys for the Drake Point K-79 well on Melville Island in the Canadian Arctic Islands.

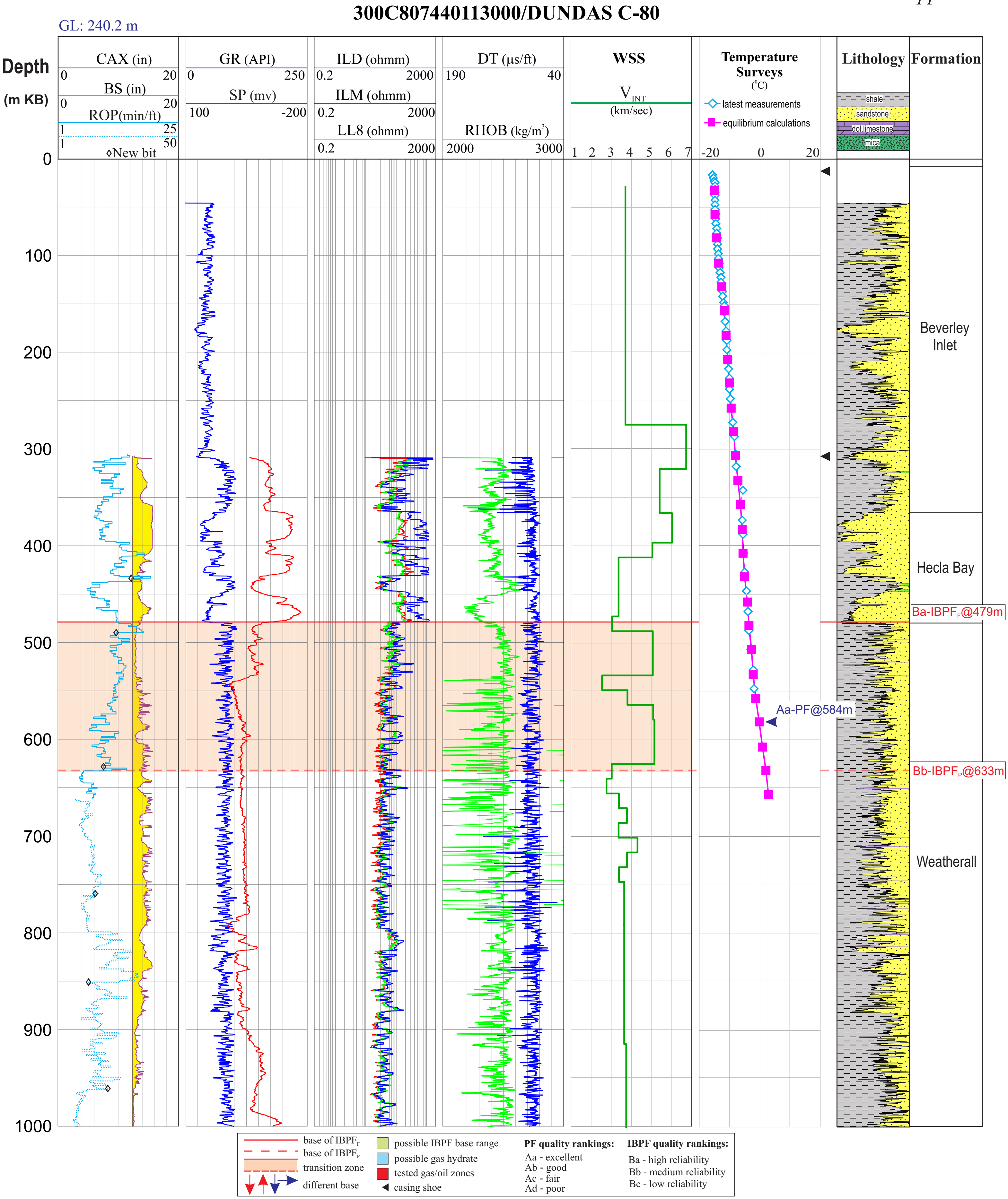

Figure 2-15. Determinations of base of $IBPF_F$ with "Ba" quality and $IBPF_P$ with "Bb" quality using well logs and well seismic survey, and base of PF from temperature survey for the Dundas C-80 well on Melville Island in the Canadian Arctic Islands.

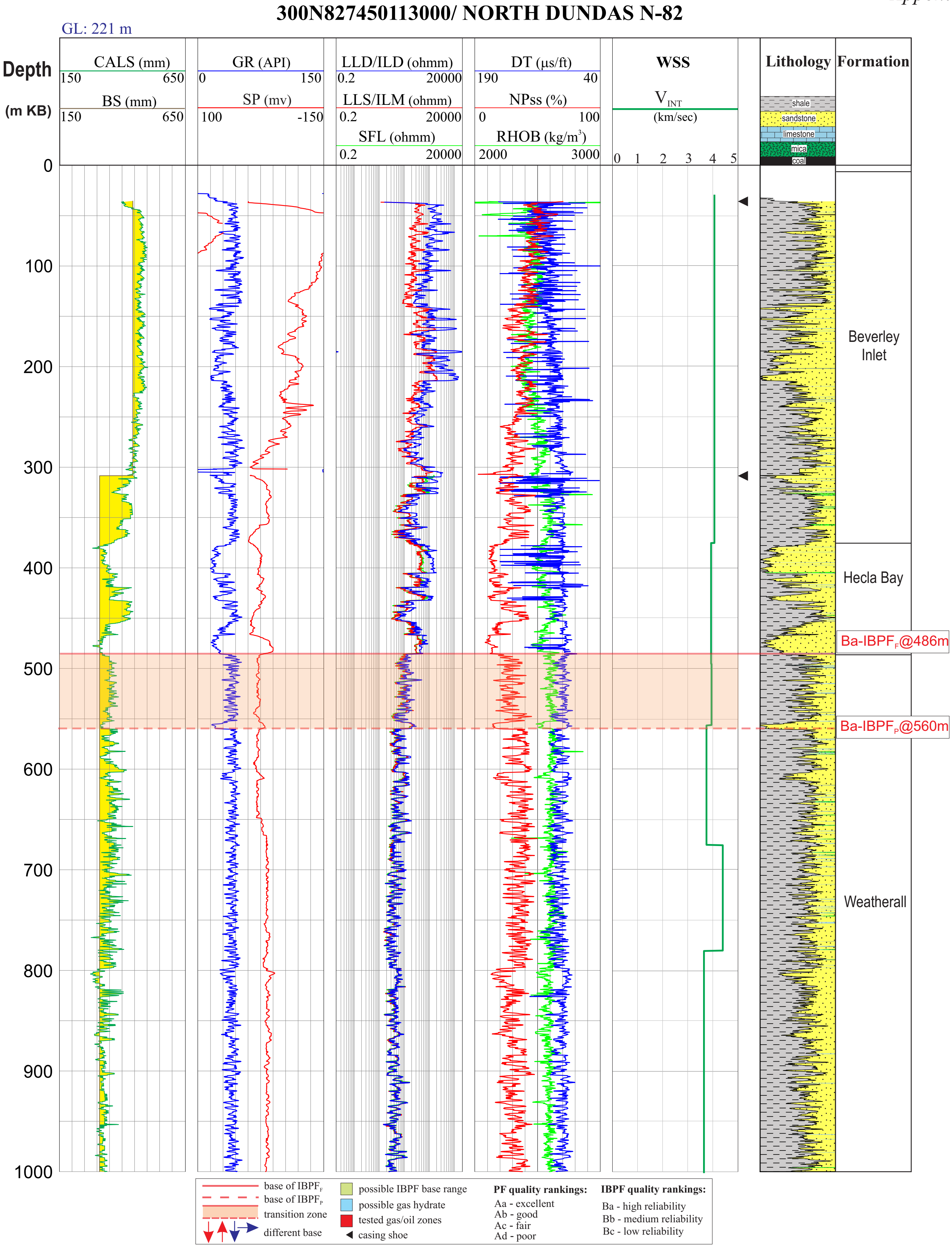

Figure 2-16. Determinations of base of $IBPF_F$ with "Ba" quality and $IBPF_P$ with "Ba" quality using well logs and well seismic surveys for the North Dundas N-82 well on Melville Island in the Canadian Arctic Islands.

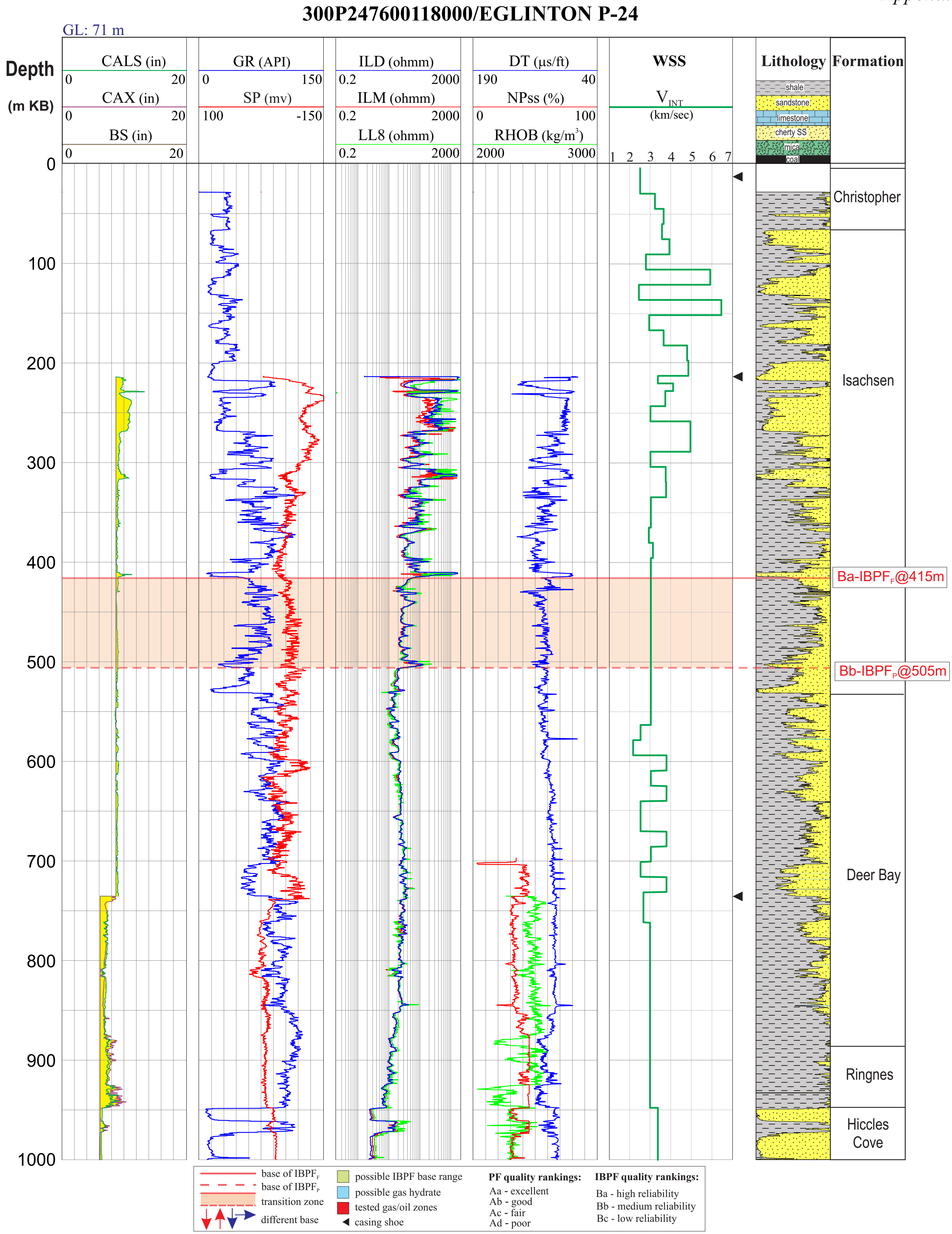

Figure 2-17. Determinations of base of $IBPF_F$ with "Ba" quality and $IBPF_P$ with "Bb" quality using well logs and well seismic surveys for the Eglinton P-24 well on Eglinton Island in the Canadian Arctic Islands.

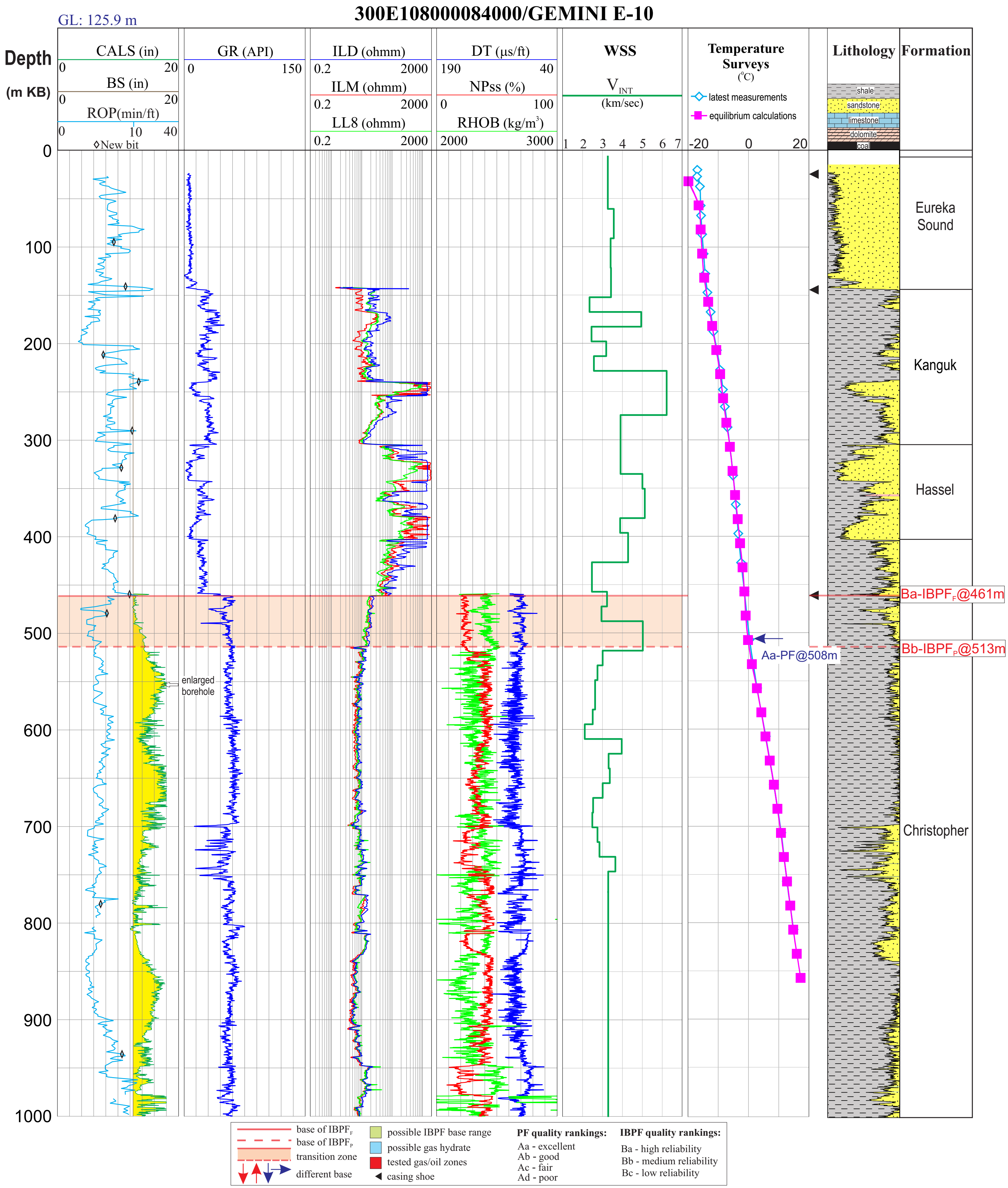

Figure 2-18. Determinations of base of $IBPF_F$ with "Ba" quality and $IBPF_P$ with "Bb" quality using well logs and well seismic survey, and base of PF from temperature surveys for the Gemini E-10 well on Ellesmere Island in the Canadian Arctic Islands.

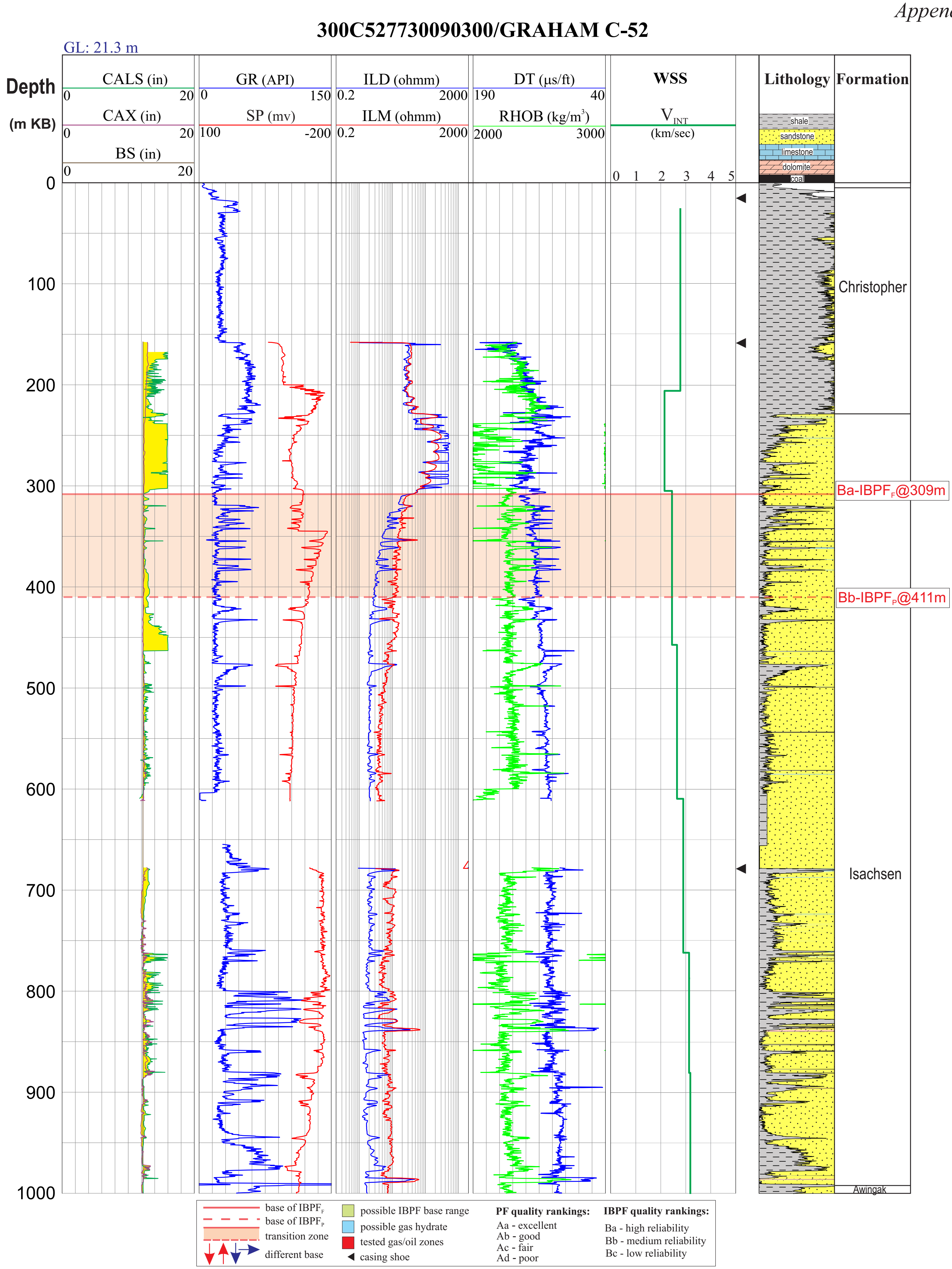

Figure 2-19. Determinations of base of $IBPF_F$ with "Ba" quality and $IBPF_P$ with "Bb" quality using well logs and well seismic surveys for the Graham C-52 well on Graham Island in the Canadian Arctic Islands.

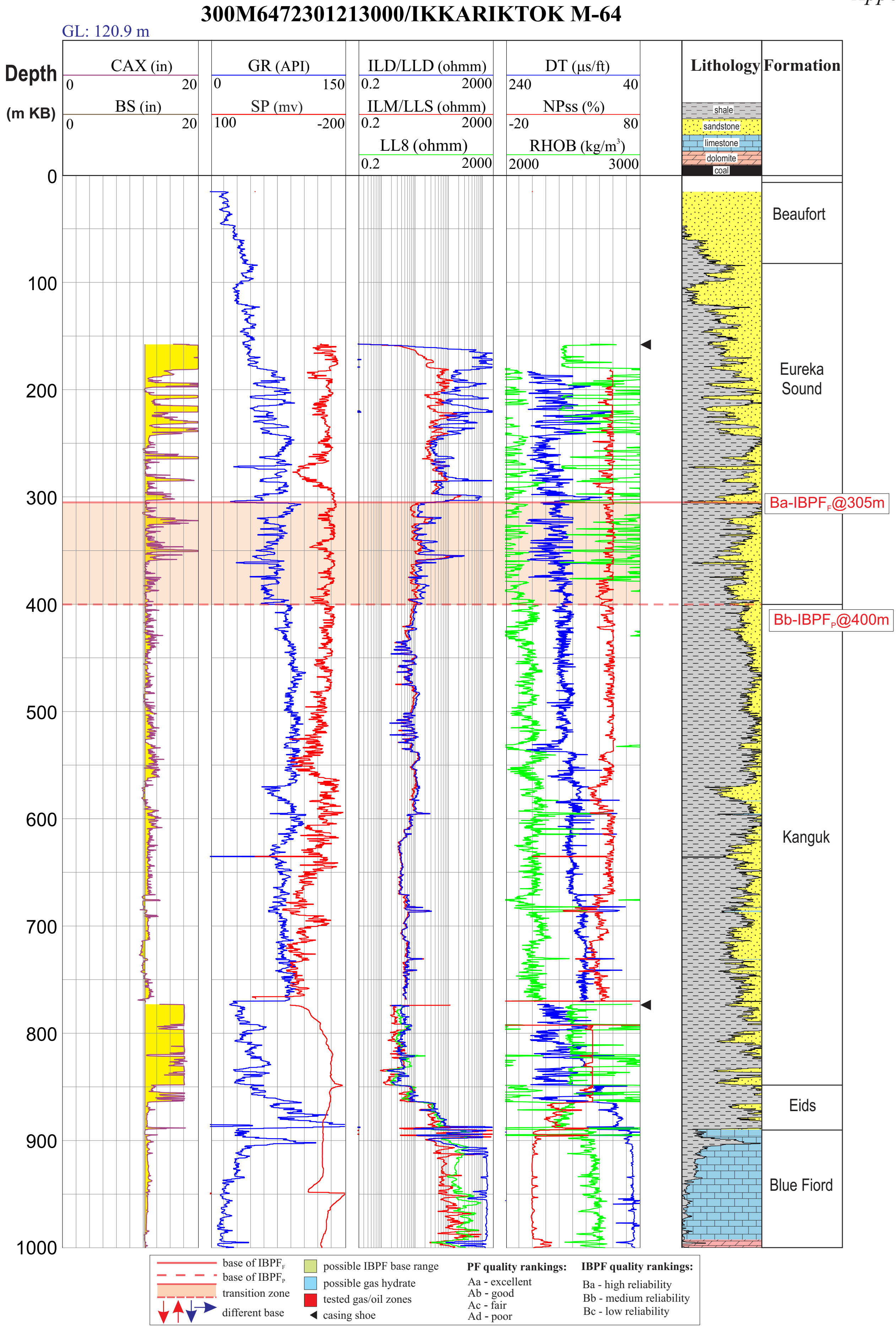

Figure 2-20. Determinations of $IBPF_F$ with "Ba" quality and $IBPF_P$ with "Bb" quality using well logs for the Ikkariktok M-64 well on Banks Island in the Canadian Arctic Islands.

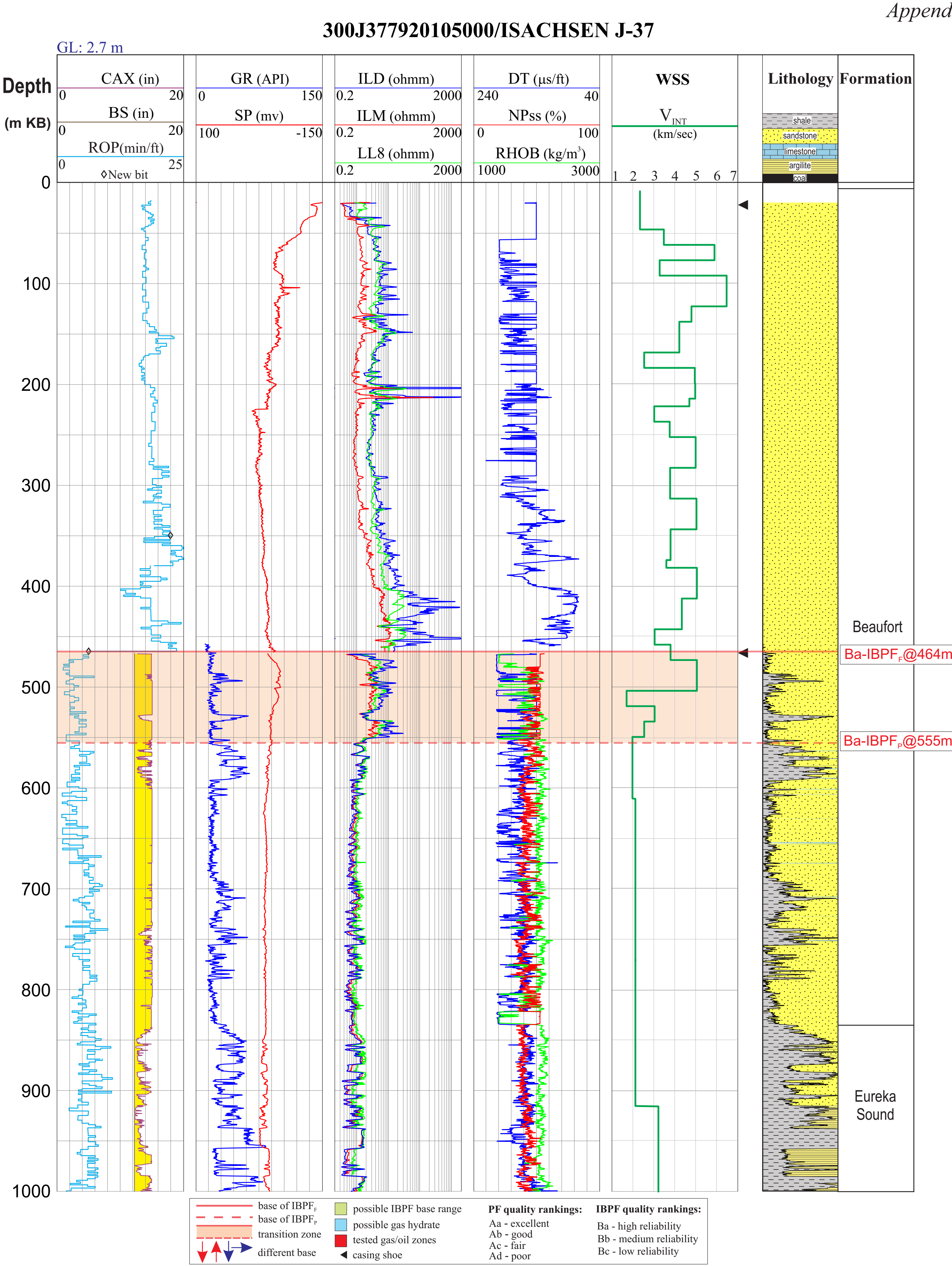

Figure 2-21. Determinations of base of $IBPF_F$ with "Ba" quality and $IBPF_P$ with "Ba" quality using well logs and well seismic surveys for the Isachsen J-37 well on Ellef Ringnes Island in the Canadian Arctic Islands.

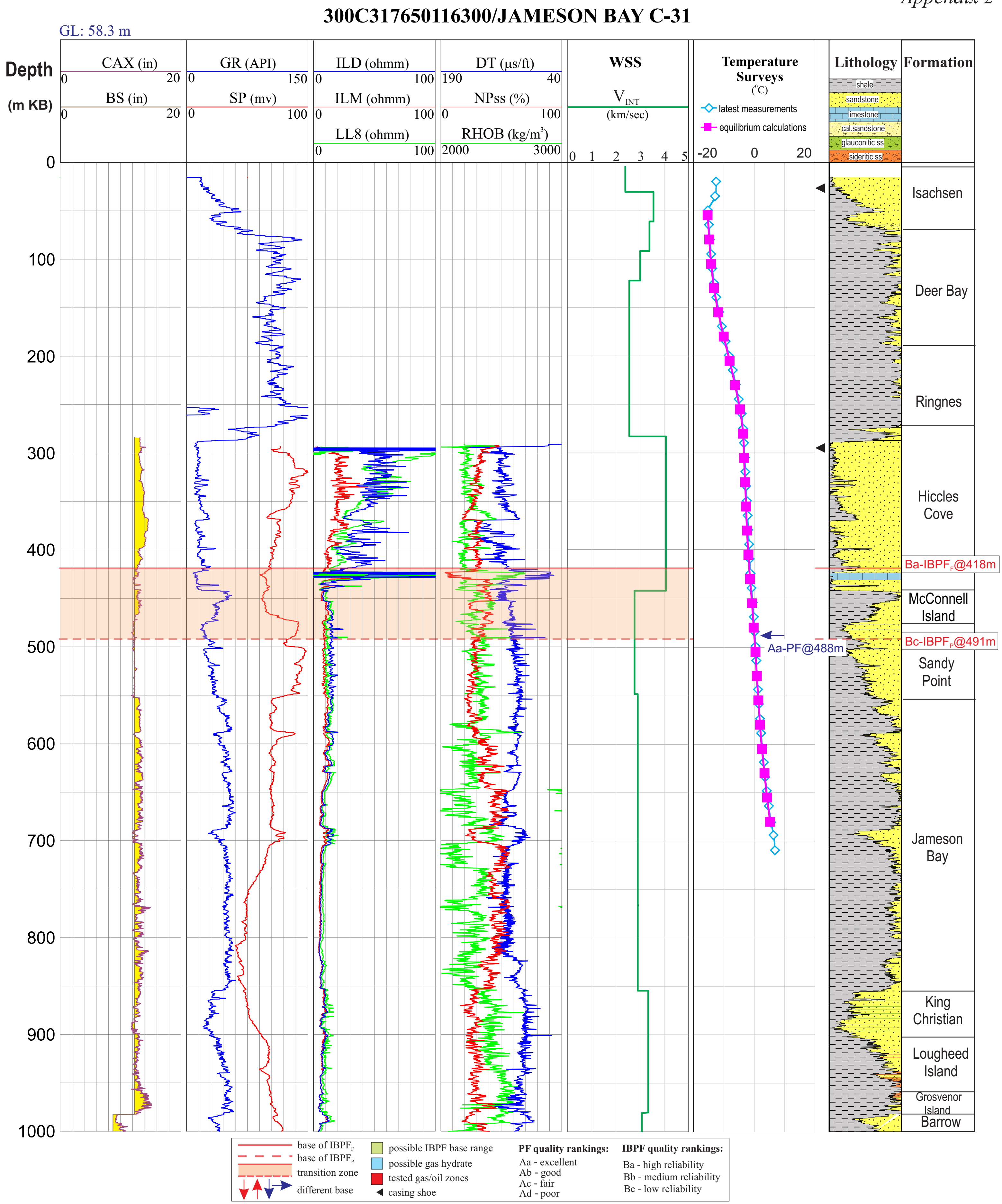

Figure 2-22. Determinations of base of $IBPF_F$ with "Ba" quality and $IBPF_P$ with "Bc" quality using well logs and well seismic surveys, and base of PF from temperature surveys for the Jameson Bay C-31 well on Prince Patrick Island in the Canadian Arctic Islands.

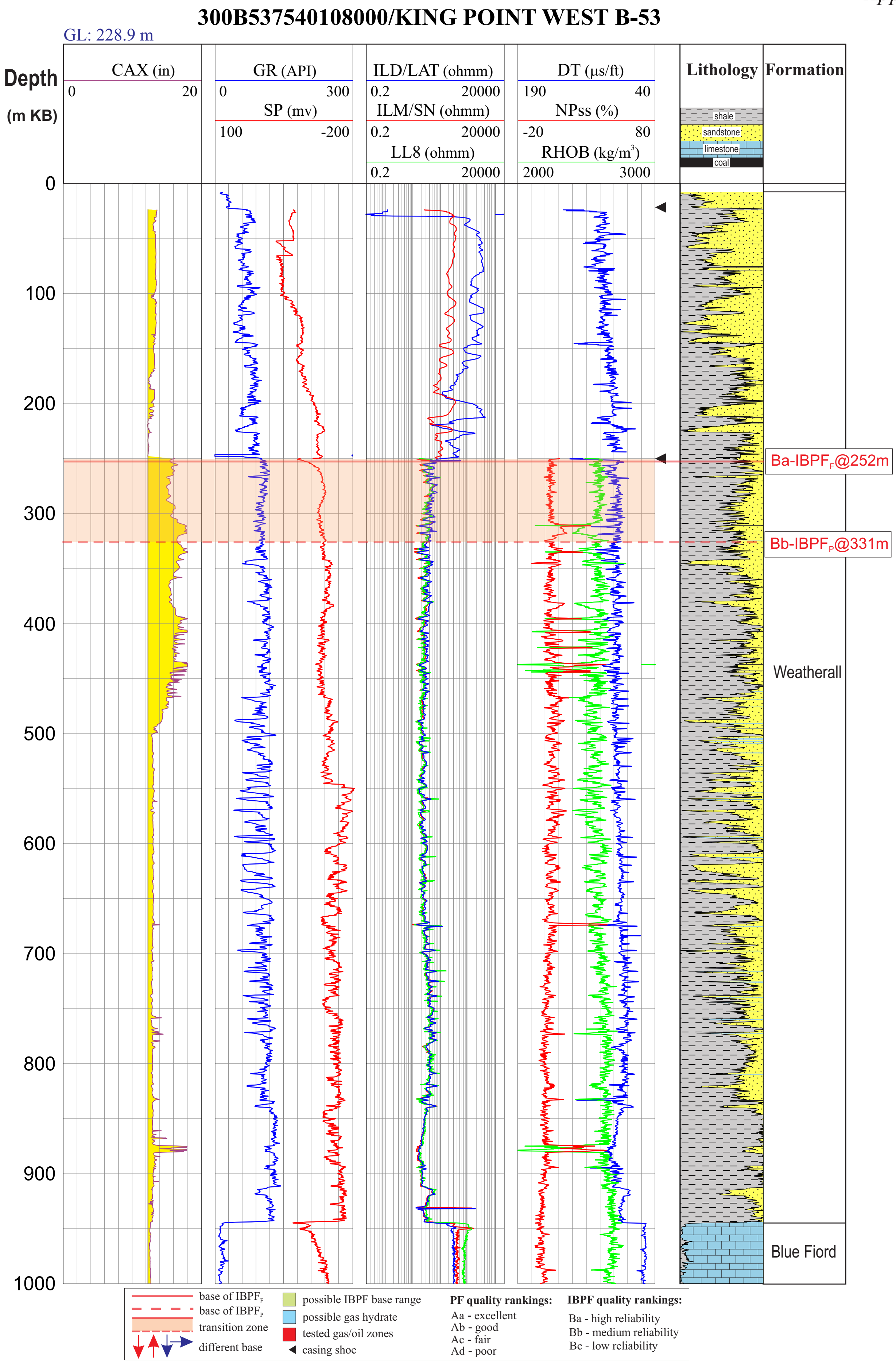

Figure 2-23. Determinations of base of $IBPF_F$ with "Ba" quality and $IBPF_P$ with "Bb" quality using well logs for the King Point West B-53 well on Melville Island in the Canadian Arctic Islands.

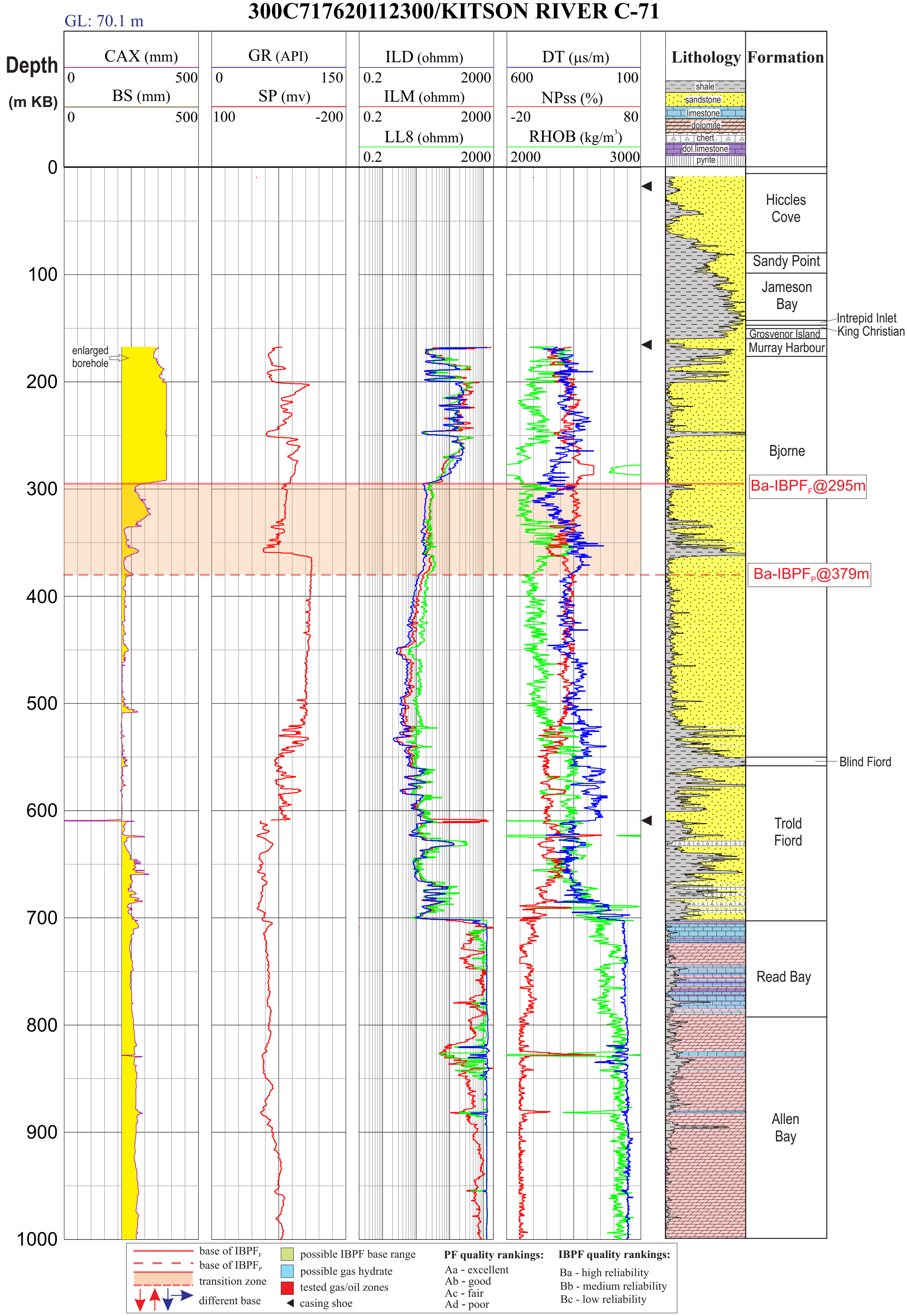

Figure 2-24. Determinations of base of $IBPF_F$ with "Ba" quality and $IBPF_P$ with "Ba" quality using well logs for the Kitson River C-71 well on Melville Island in the Canadian Arctic Islands.

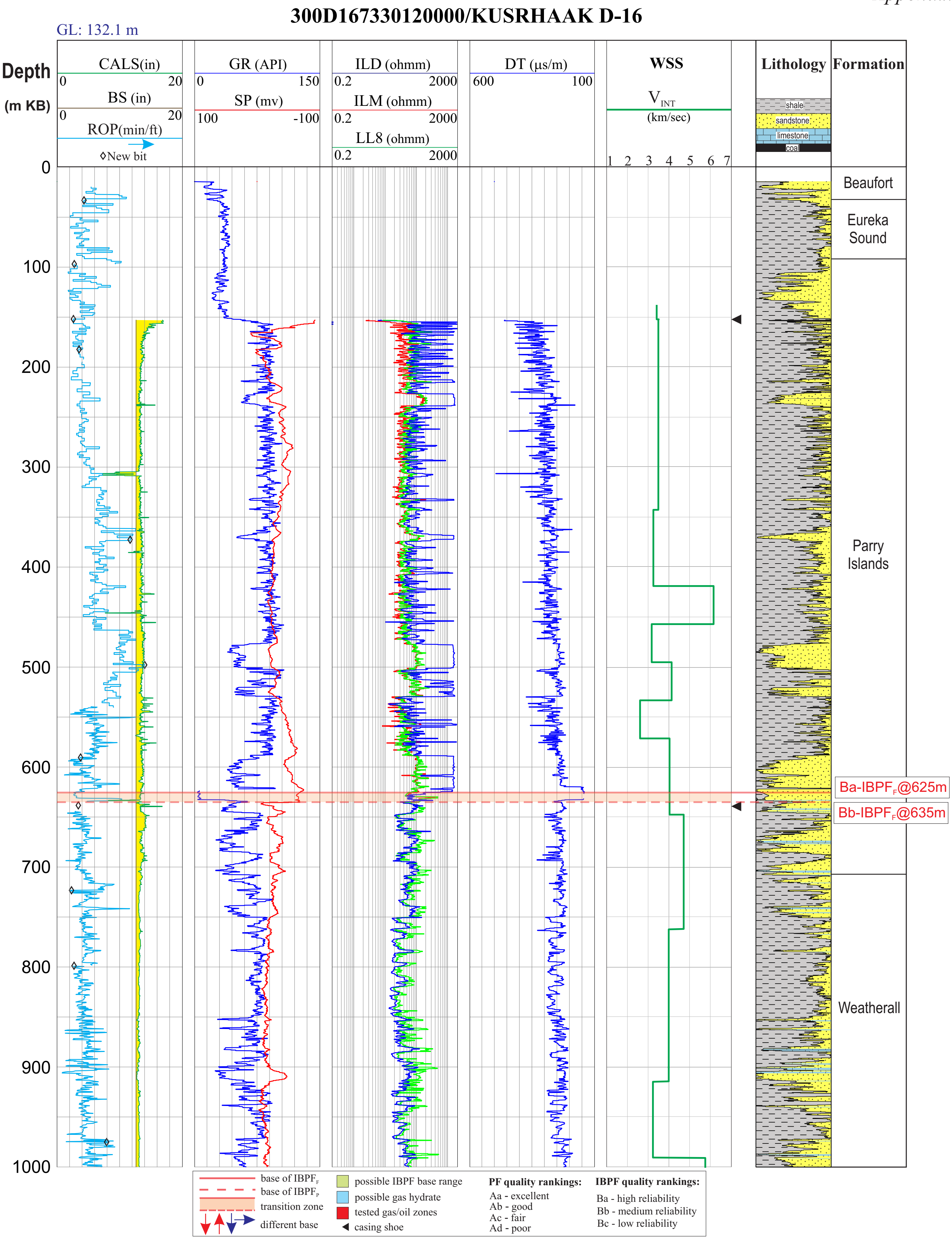

Figure 2-25. Determinations of base of $IBPF_F$ with "Ba" quality and $IBPF_P$ with "Bb" quality using well logs and well seismic surveys for the Kusrhaak D-16 well on Banks Island in the Canadian Arctic Islands.

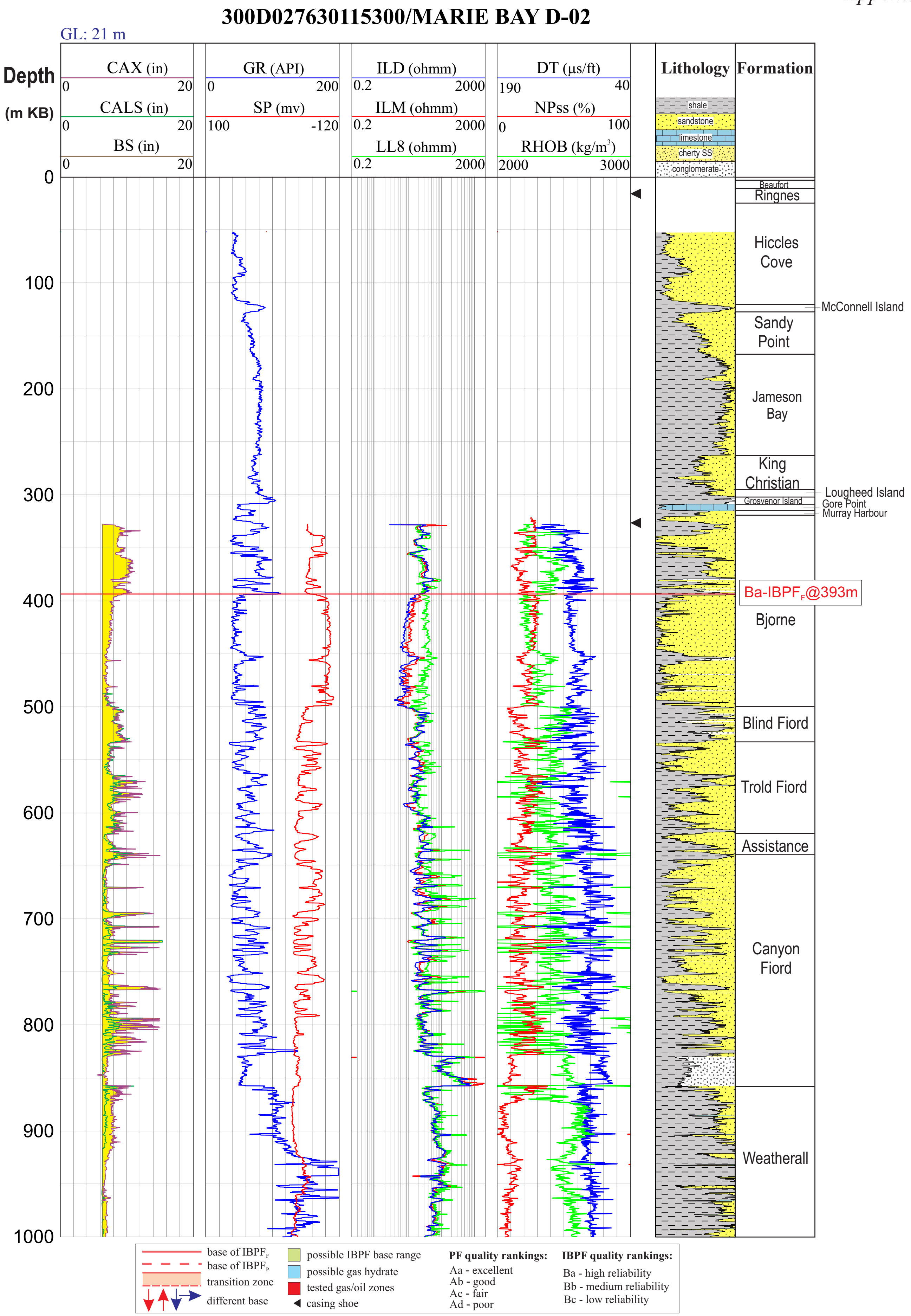

Figure 2-26. Determination of base of $IBPF_F$ with “Ba” quality using well logs for the Marie Bay D-02 well on Melville Island in the Canadian Arctic Islands.

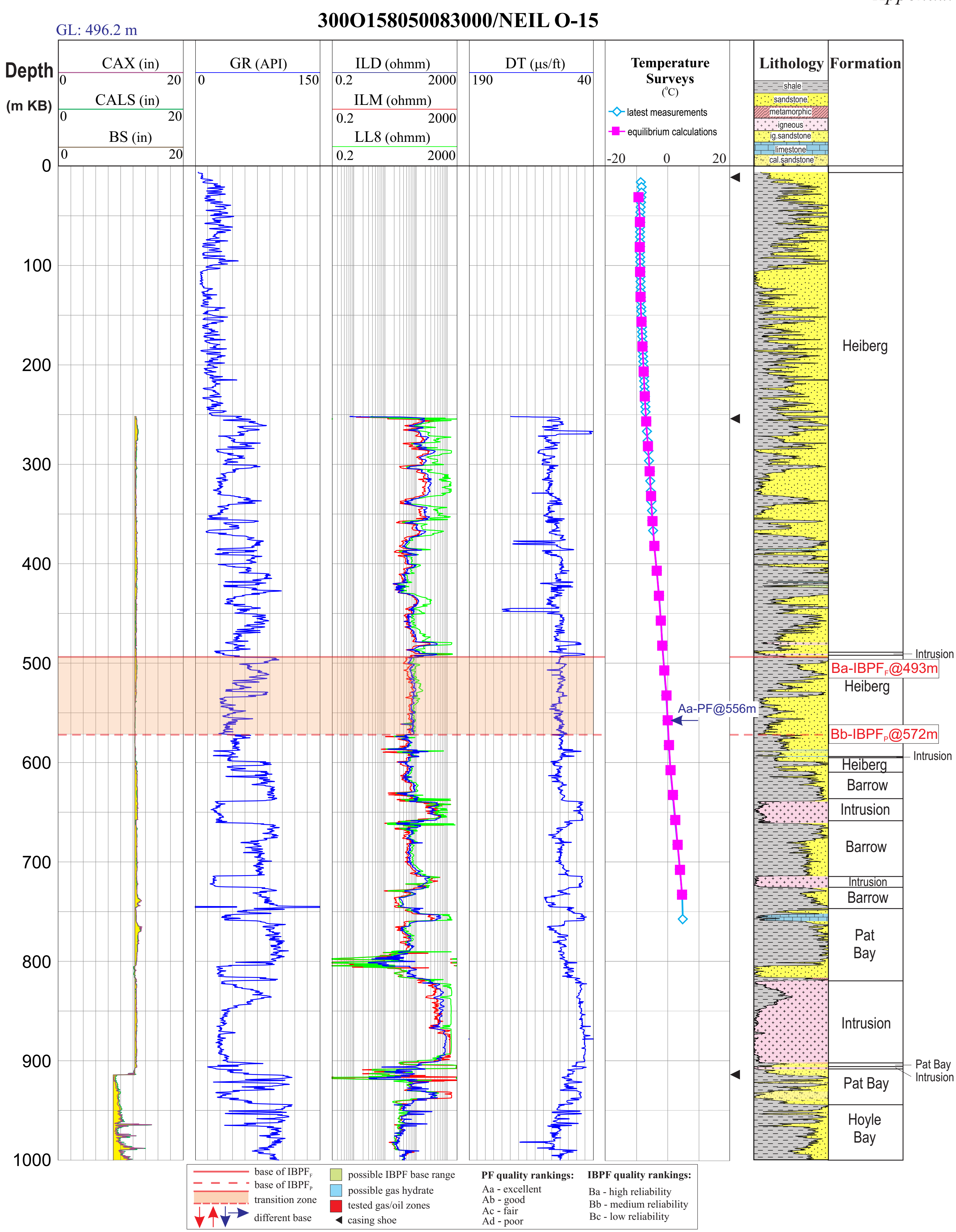

Figure 2-27. Determinations of base of $IBPF_F$ with "Ba" quality and $IBPF_P$ with "Bb" quality using well logs, and base of PF from temperature surveys for the Neil O-15 well on Ellesmere Island in the Canadian Arctic Islands.

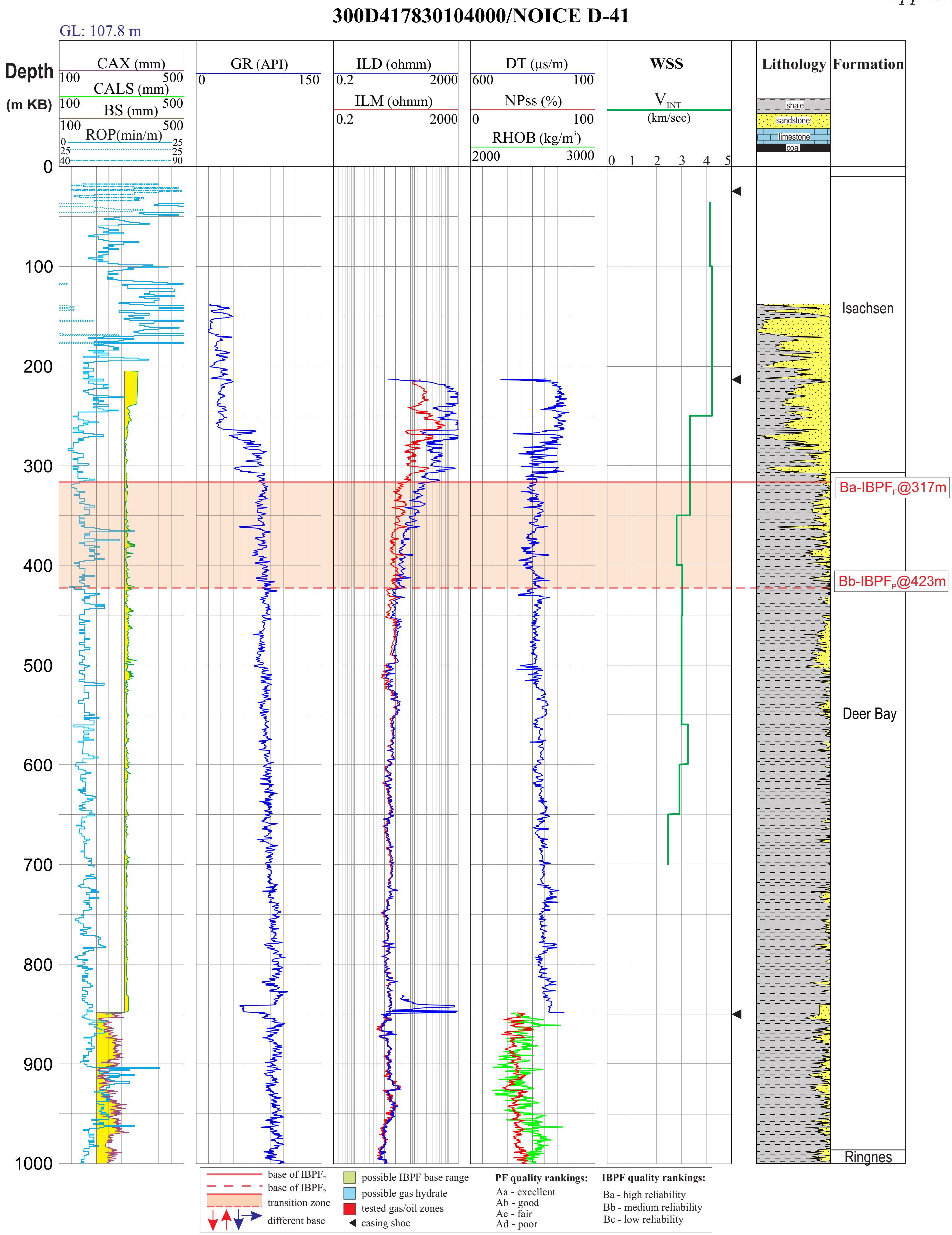

Figure 2-28. Determinations of base of $IBPF_F$ with "Ba" quality and $IBPF_P$ with "Bb" quality using well logs and well seismic surveys for the Noice D-41 well on Ellef Ringnes Island in the Canadian Arctic Islands.

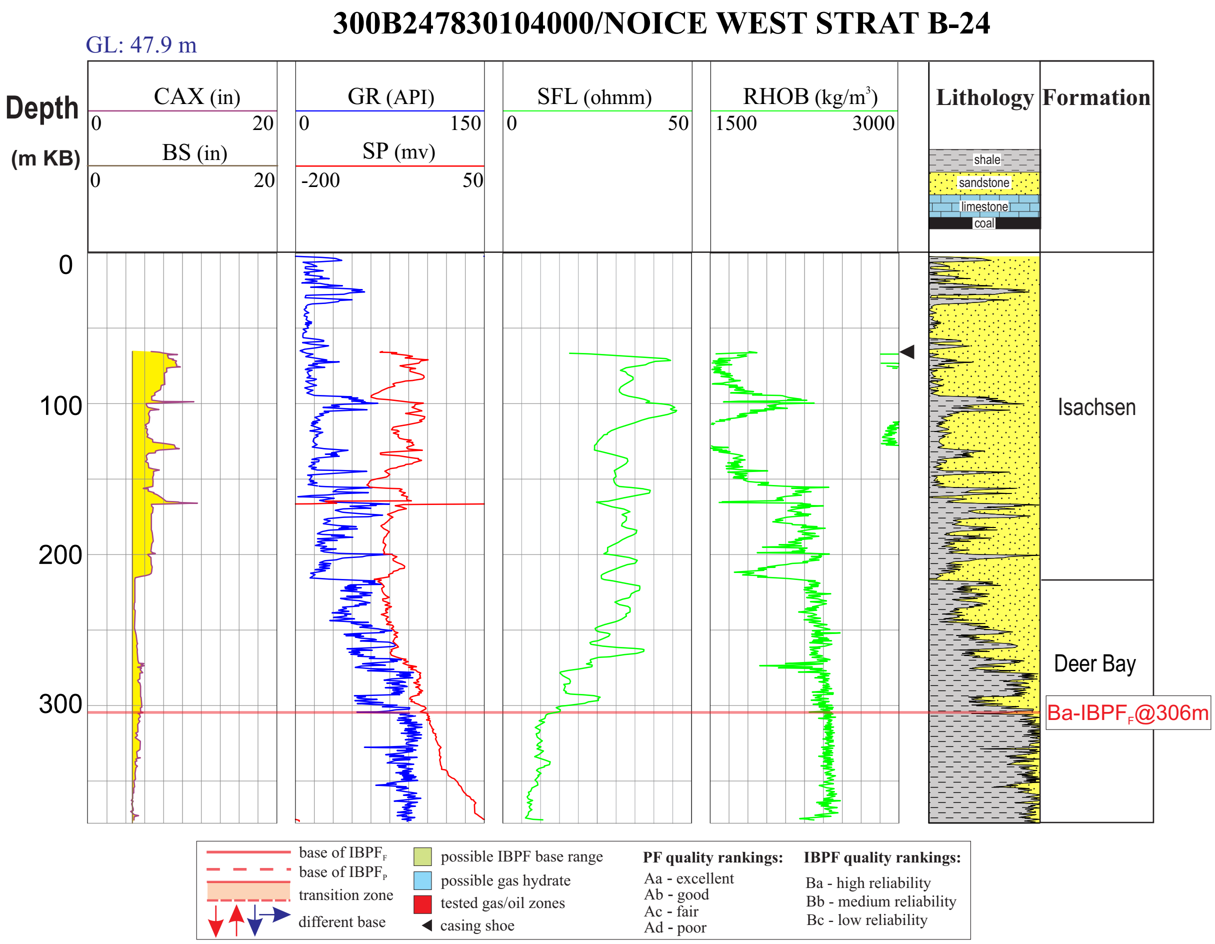

Figure 2-29. Determination of base of $IBPF_F$ with "Ba" quality from well logs for the Noice West Strat B-24 well on Ellef Ringnes Island in the Canadian Arctic Islands.

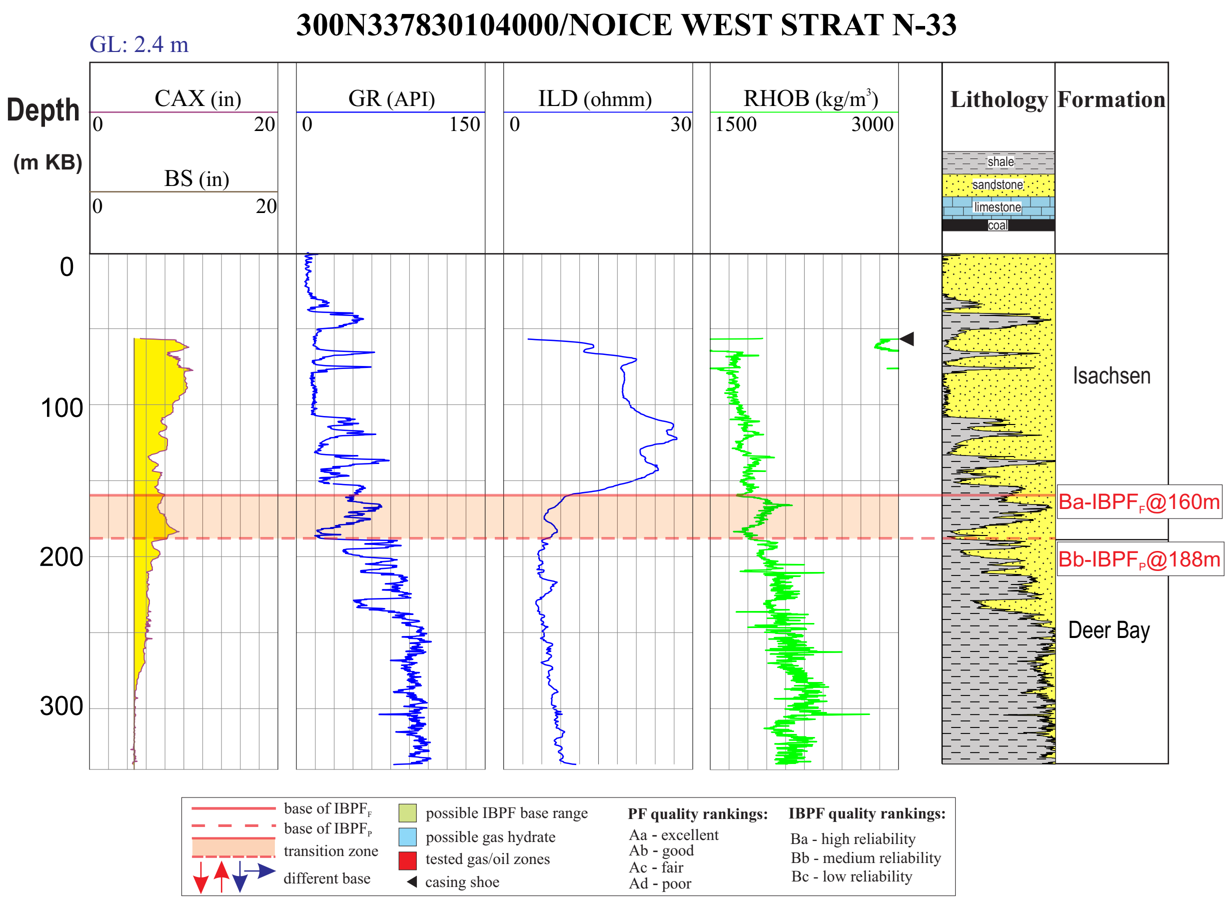

Figure 2-30. Determinations of base of $IBPF_F$ with “Ba” quality and $IBPF_P$ with “Bb” quality from well logs for the Noice West Strat N-33 well on Ellef Ringnes Island in the Canadian Arctic Islands.

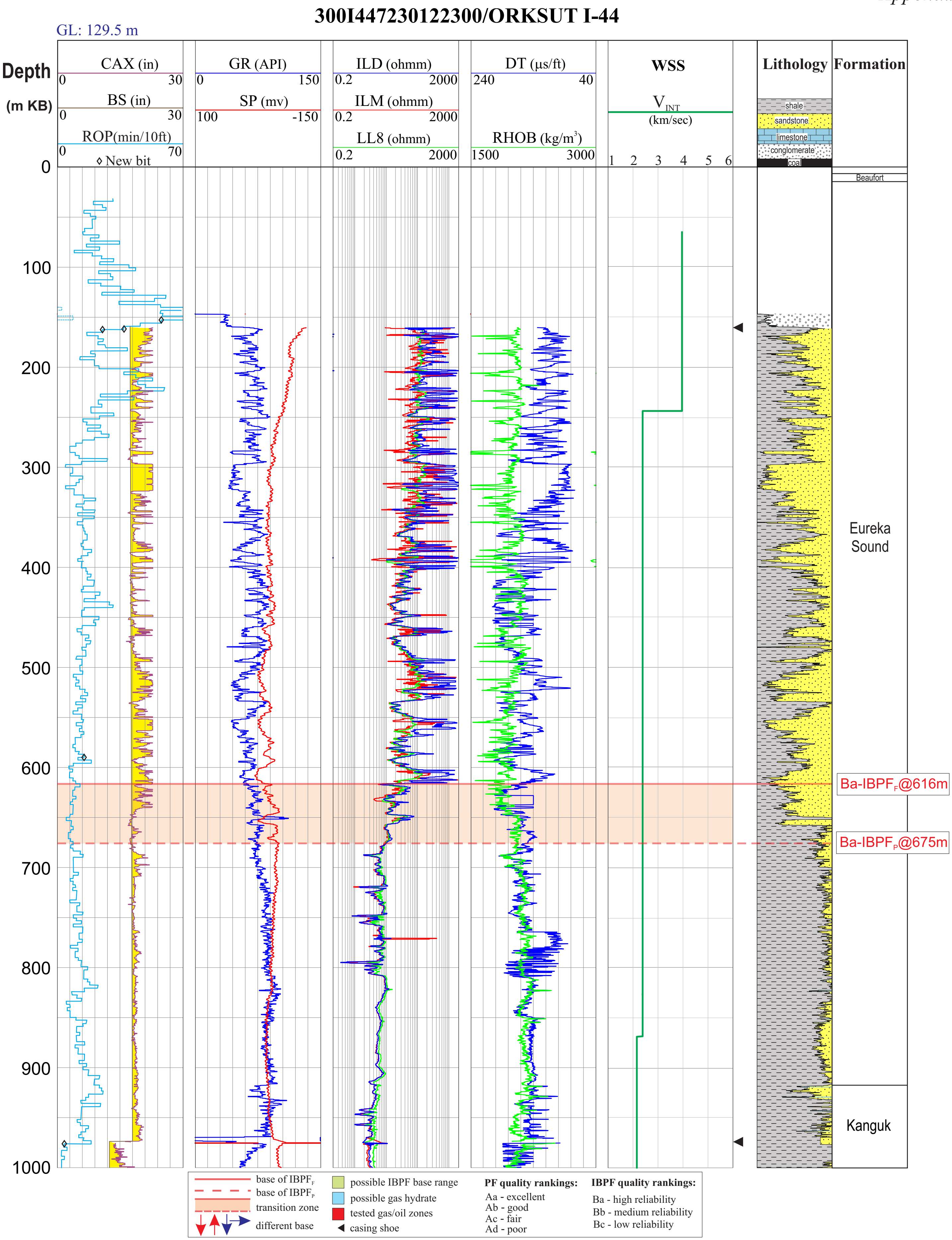

Figure 2-31. Determinations of base of $IBPF_F$ with “Ba” quality and $IBPF_P$ with “Ba” quality using well logs and well seismic surveys for the Orksut I-44 well on Banks Island in the Canadian Arctic Islands.

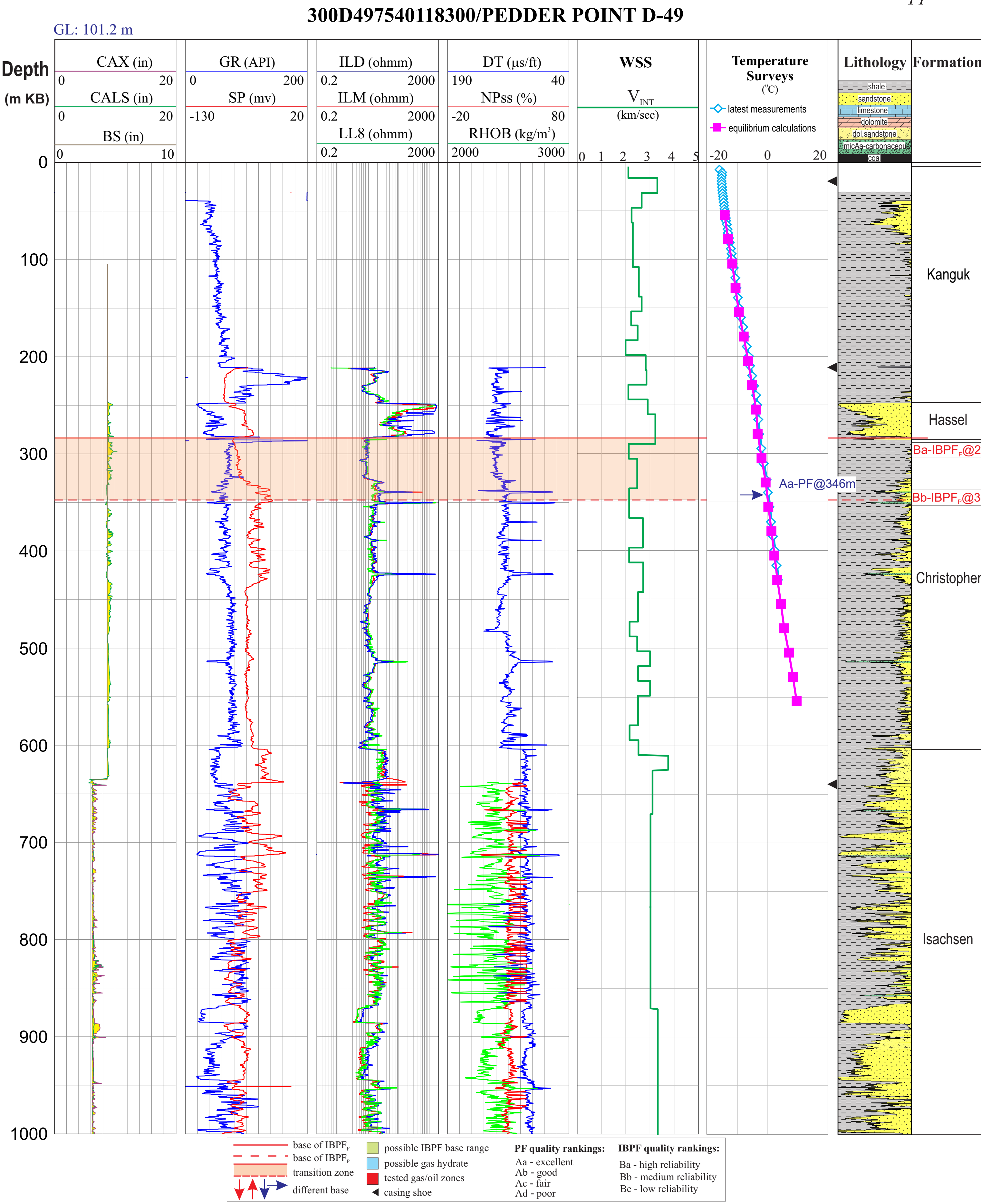

Figure 2-32. Determinations of base of $IBPF_F$ with "Ba" quality and $IBPF_P$ with "Bb" quality using well logs and well seismic surveys, and base of PF from temperature surveys for the Pedder Point D-49 well on Eglinton Island in the Canadian Arctic Islands.

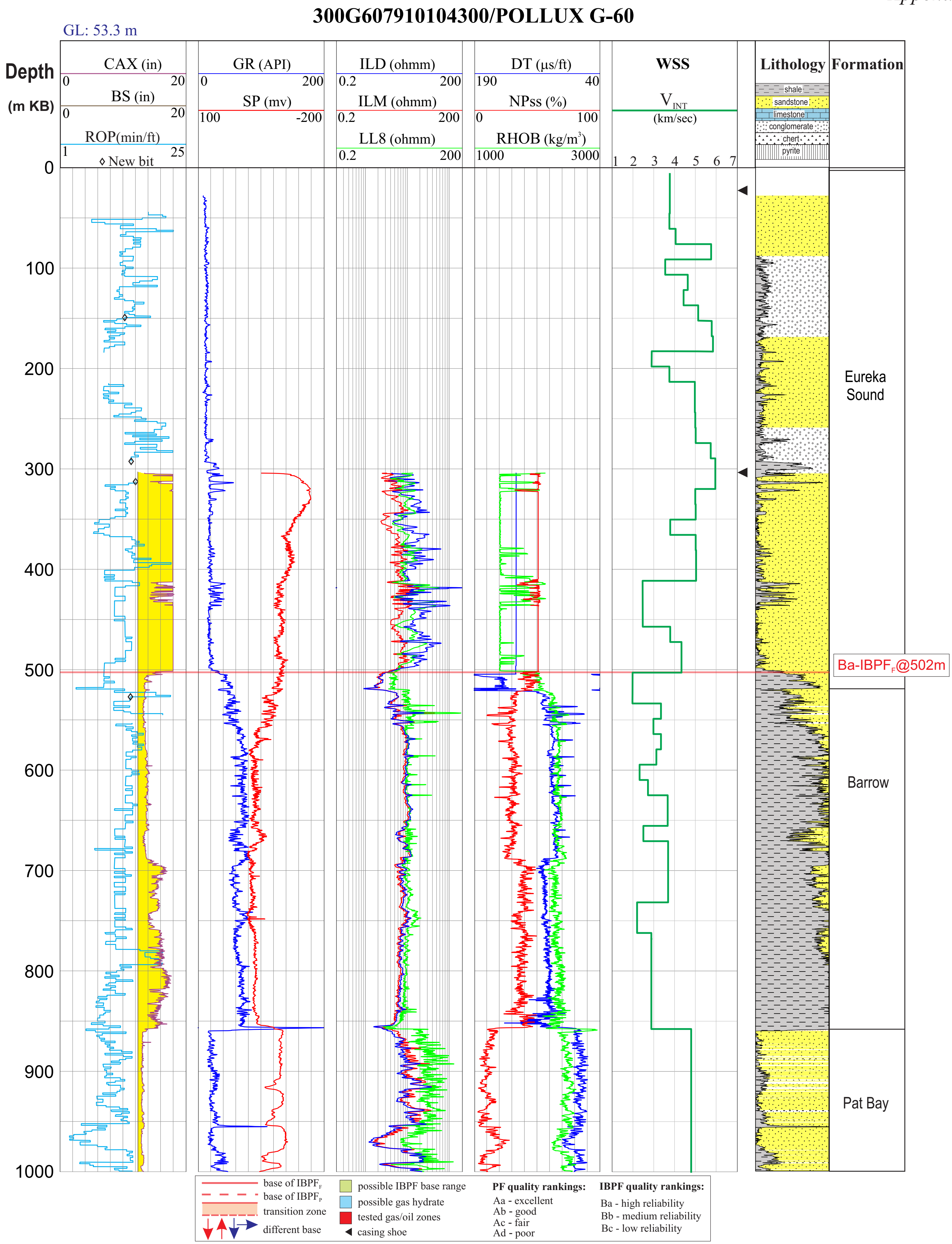

Figure 2-33. Determination of base of IBPF$_F$ with “Ba” quality using well logs and well seismic surveys for the Pollux G-60 well on Ellef Ringnes Island the Canadian Arctic Islands.

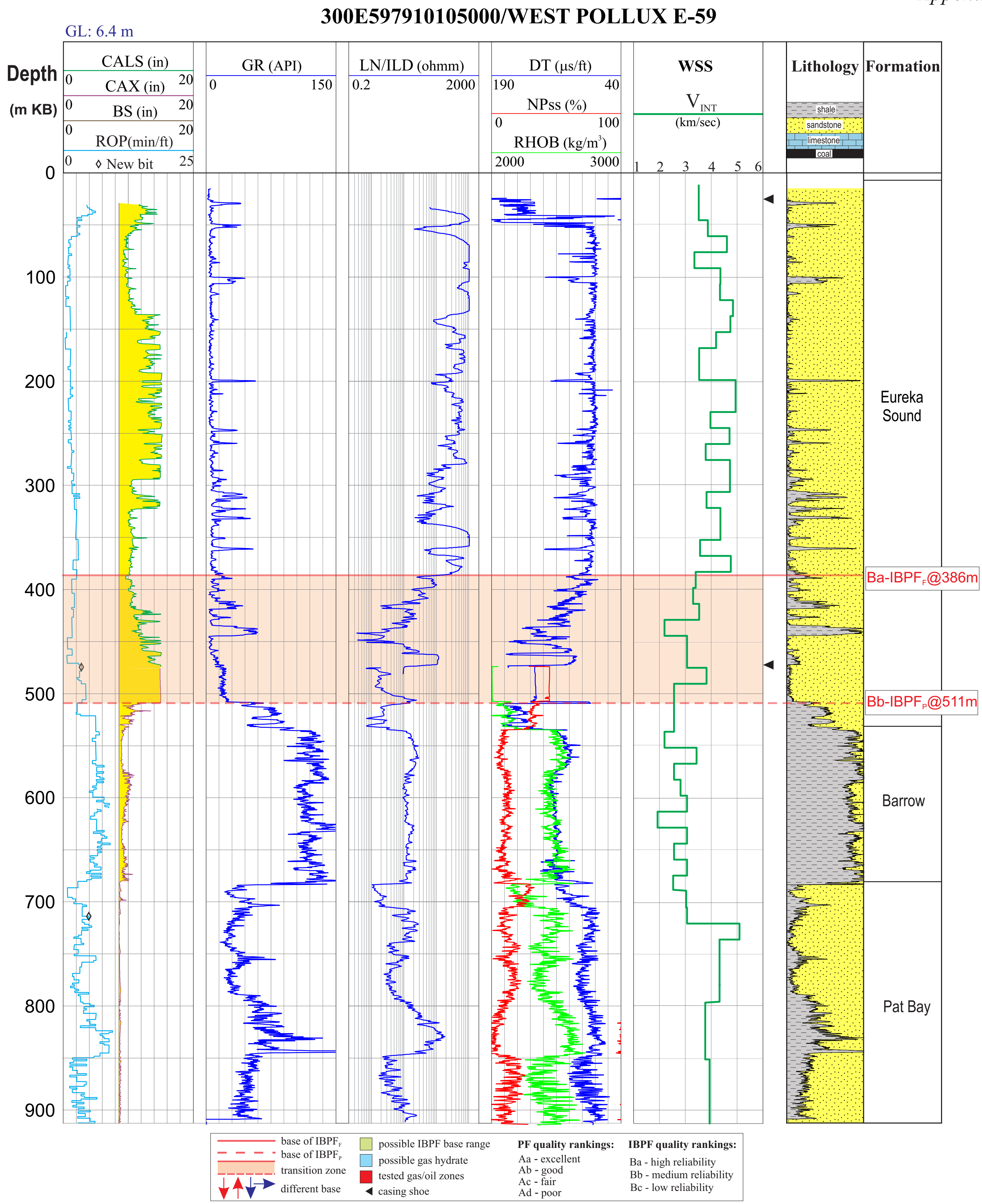

Figure 2-34. Determinations of base of $IBPF_F$ with "Ba" quality and $IBPF_P$ with "Bb" quality using well logs and well seismic surveys for the West Pollux E-59 well on Ellef Ringnes Island in the Canadian Arctic Islands.

300G127550105300/RICHARDSON POINT G-12

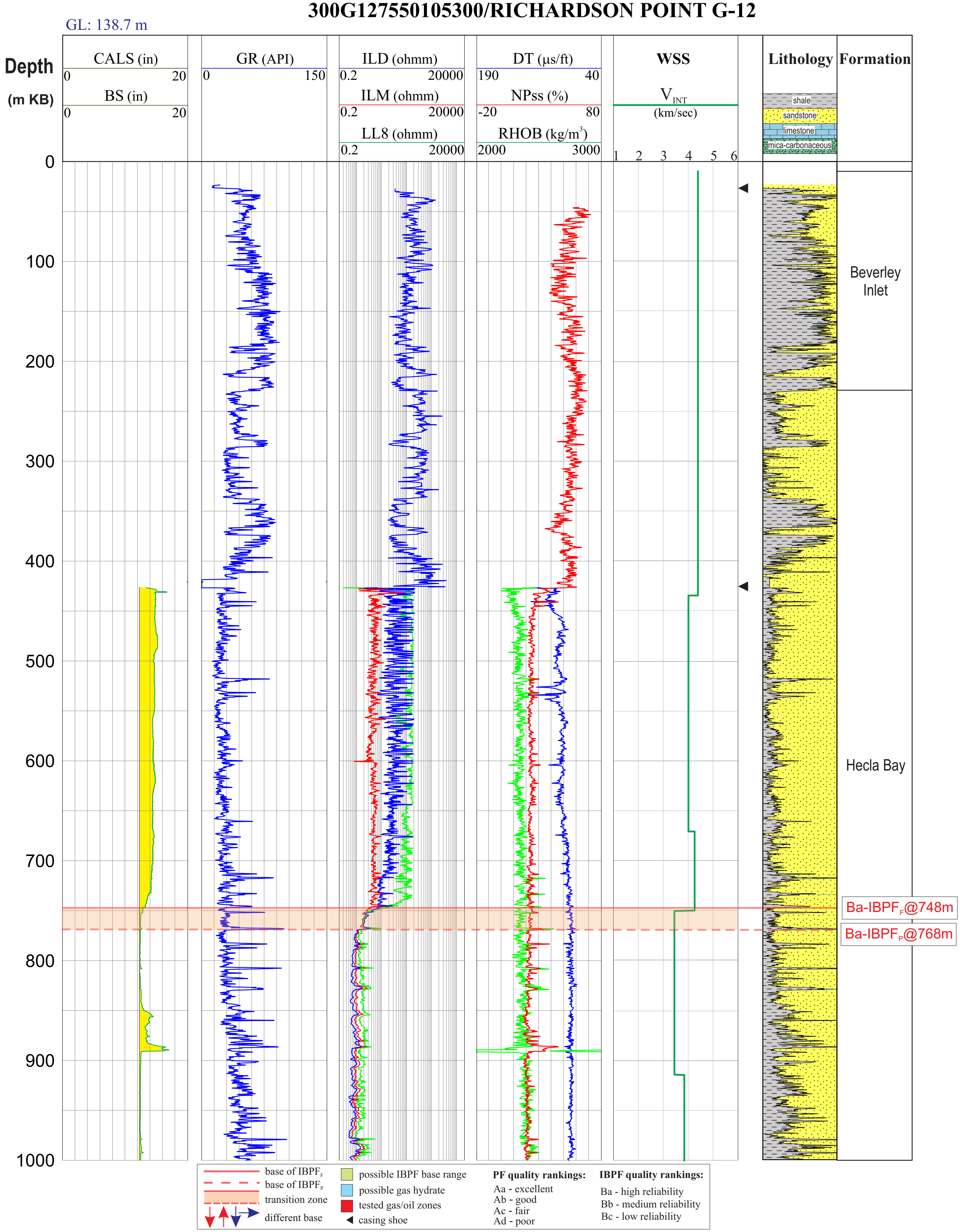

Figure 2-35. Determinations of base of $IBPF_F$ with "Ba" quality and $IBPF_P$ with "Ba" quality using well logs and well seismic surveys for the Richardson Point G-12 well on Melville Island in the Canadian Arctic Islands.

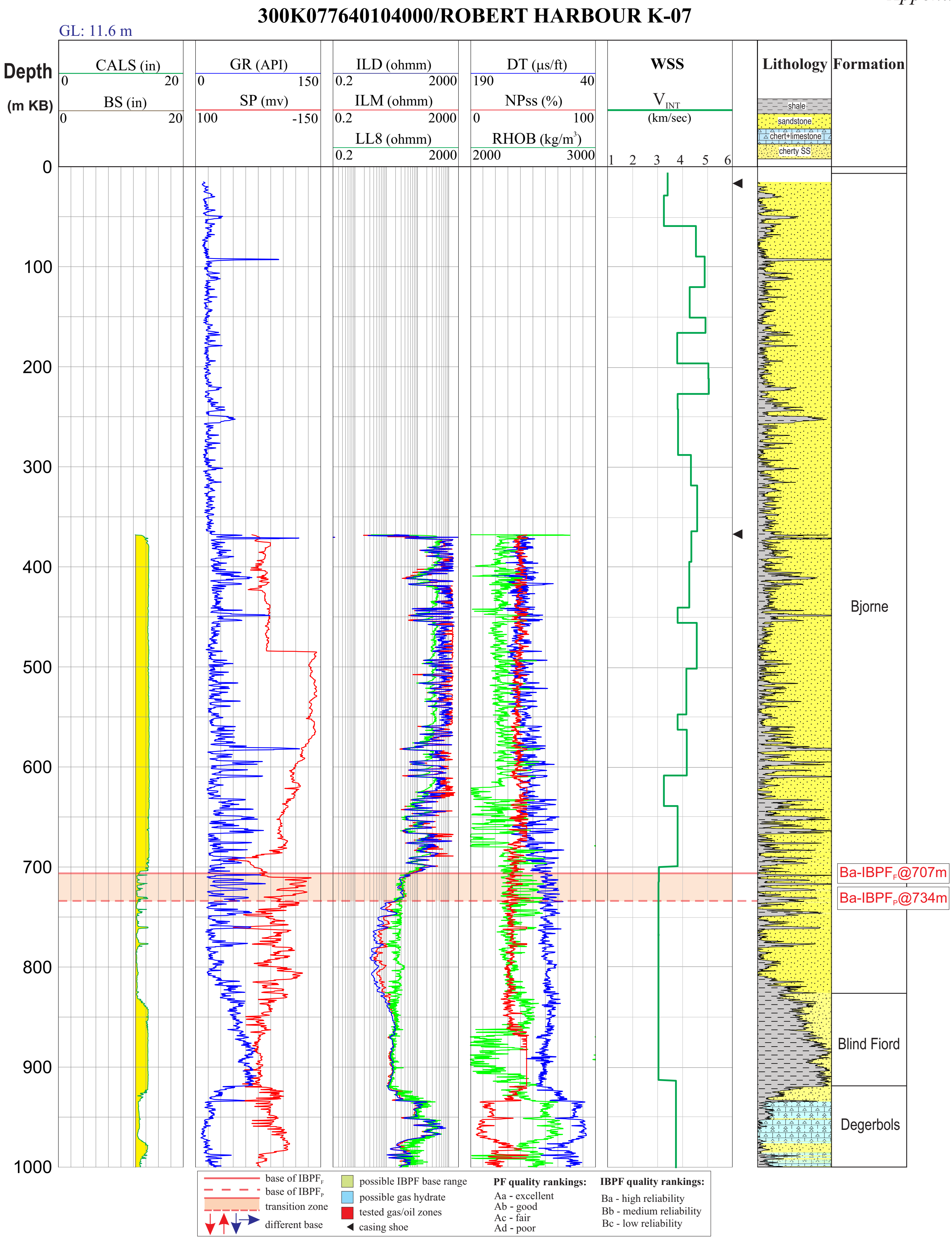

Figure 2-36. Determinations of base of $IBPF_F$ with "Ba" quality and $IBPF_P$ with "Ba" quality using well logs and well seismic surveys for the Robert Harbour K-07 well on Cameron Island in the Canadian Arctic Islands.

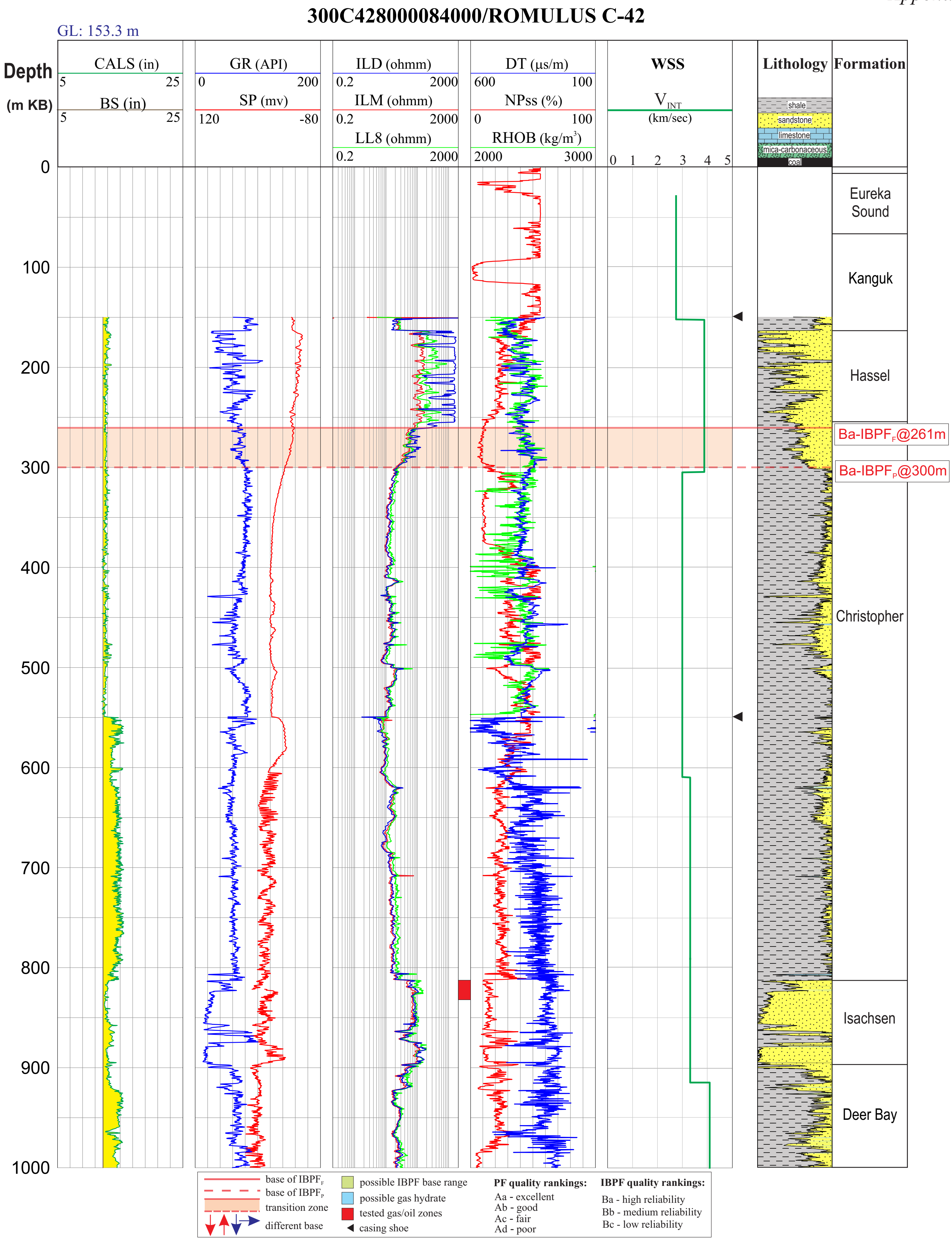

Figure 2-37. Determinations of base of $IBPF_F$ with "Ba" quality and $IBPF_P$ with "Ba" quality using well logs and well seismic surveys for the Romulus C-42 well on Ellesmere Island in the Canadian Arctic Islands.

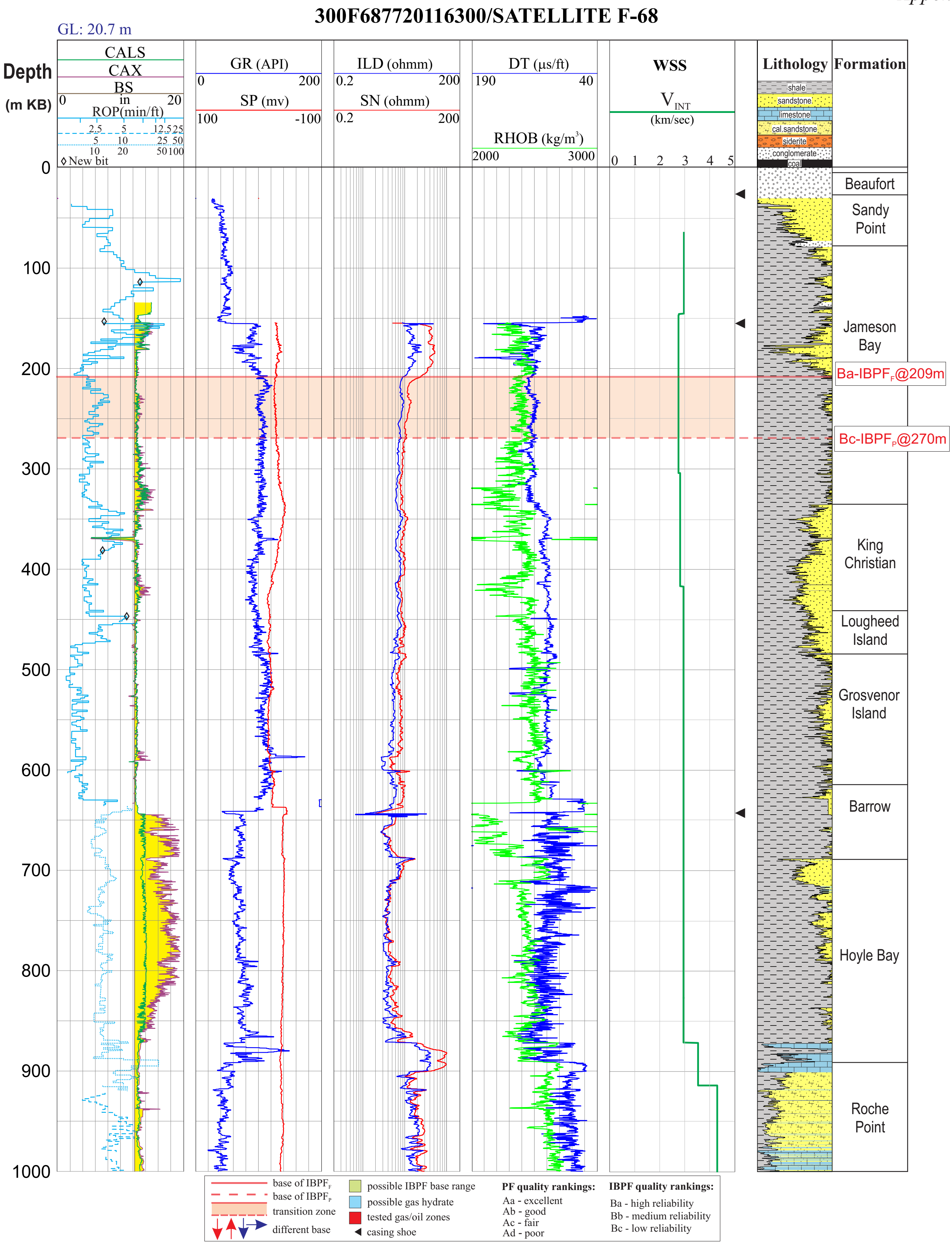

Figure 2-38. Determinations of base of $IBPF_F$ with "Ba" quality and $IBPF_P$ with "Bc" quality using well logs and well seismic surveys for the Satellite F-68 well on Prince Patrick Island in the Canadian Arctic Islands.

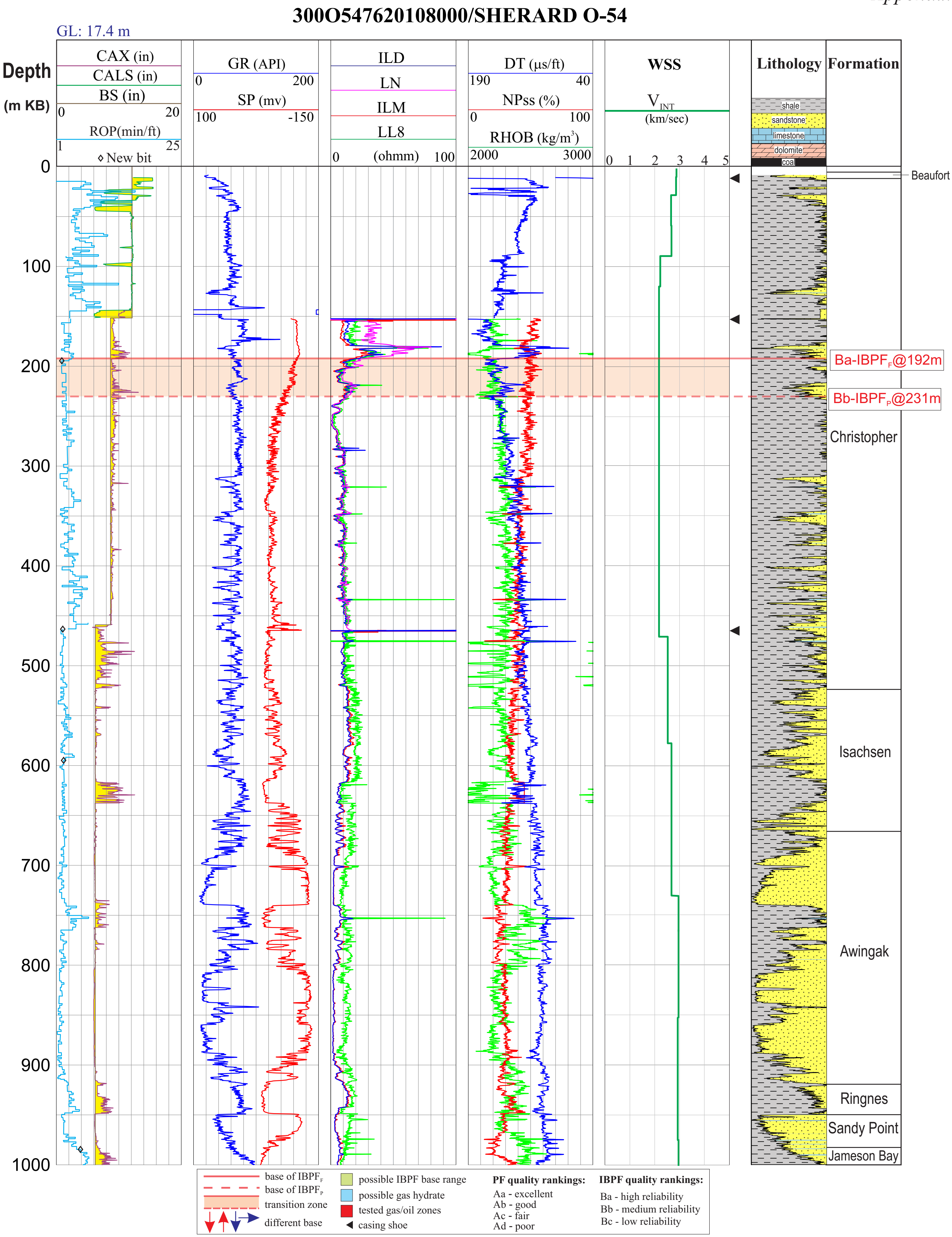

Figure 2-39. Determinations of base of $IBPF_F$ with "Ba" quality and $IBPF_P$ with "Bb" quality using well logs and well seismic surveys for the Sherard O-54 well on Melville Island in the Canadian Arctic Islands.

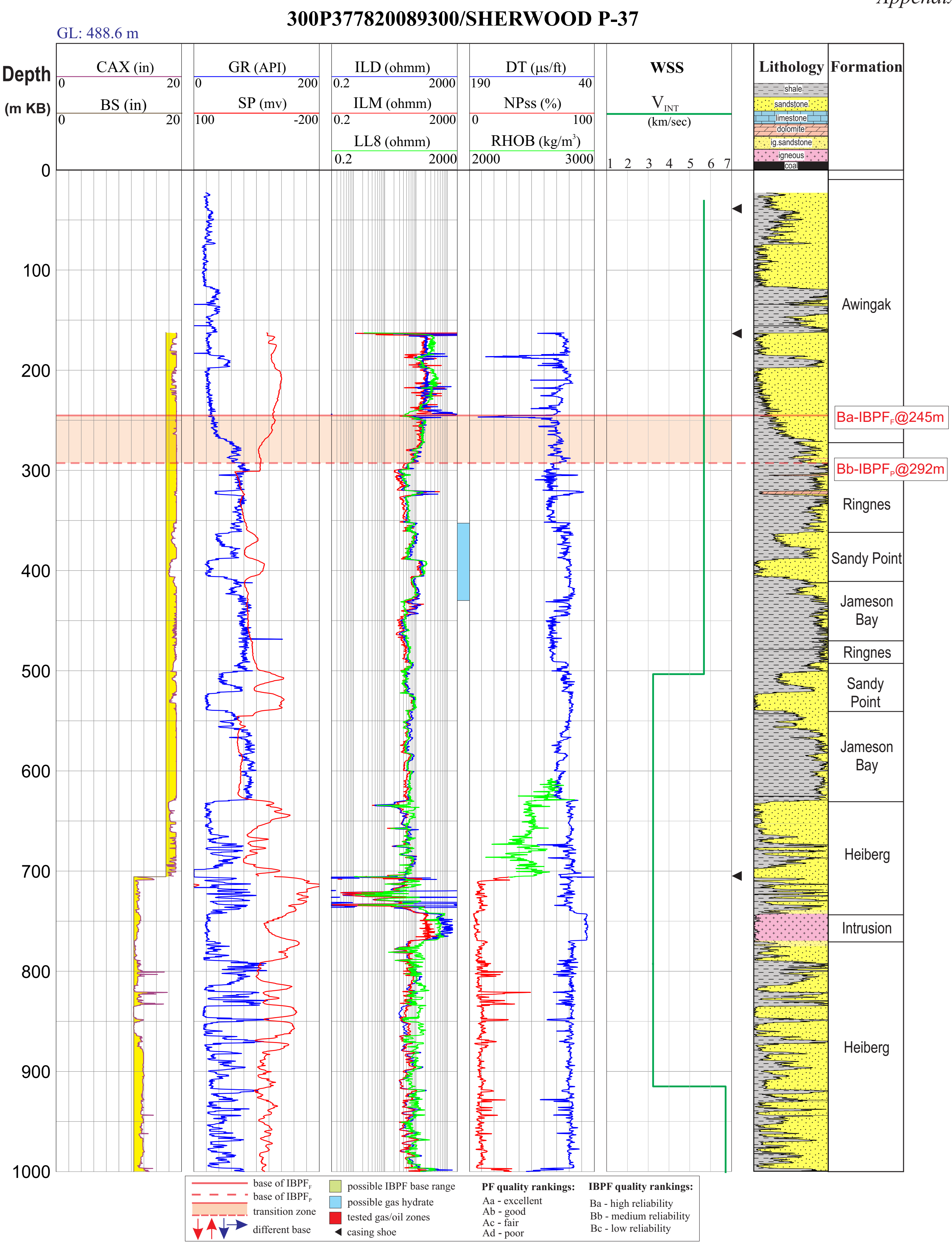

Figure 2-40. Determinations of base of $IBPF_F$ with "Ba" quality and $IBPF_P$ with "Bb" quality using well logs and well seismic surveys for the Sherwood P-37 well on Axel Heiberg Island in the Canadian Arctic Islands.

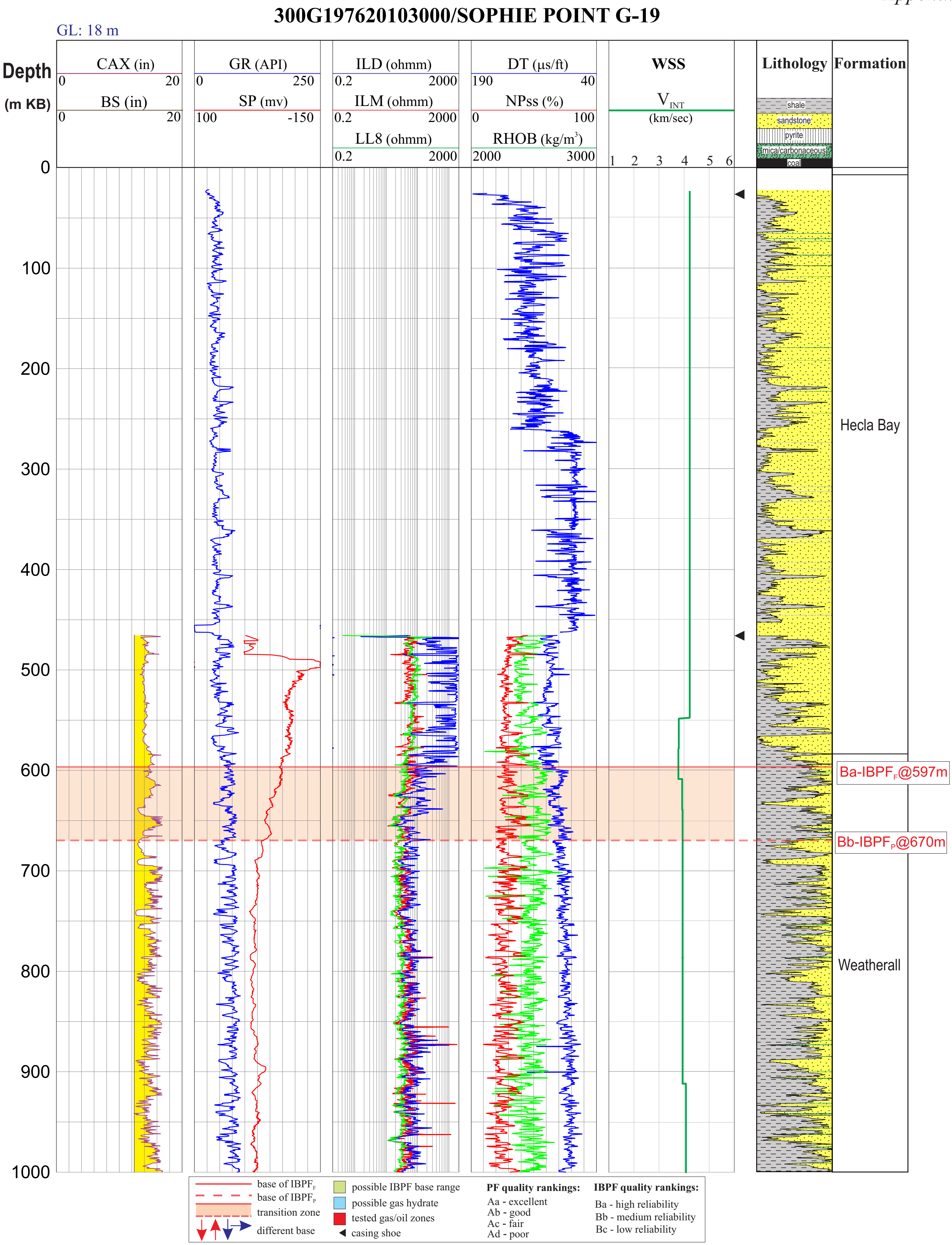

Figure 2-41. Determinations of base of $IBPF_F$ with "Ba" quality and $IBPF_P$ with "Bb" quality using well logs and well seismic surveys for the Sophie Point G-19 well on Vanier Island in the Canadian Arctic Islands.

300J117630101300/STOKES RANGE J-11

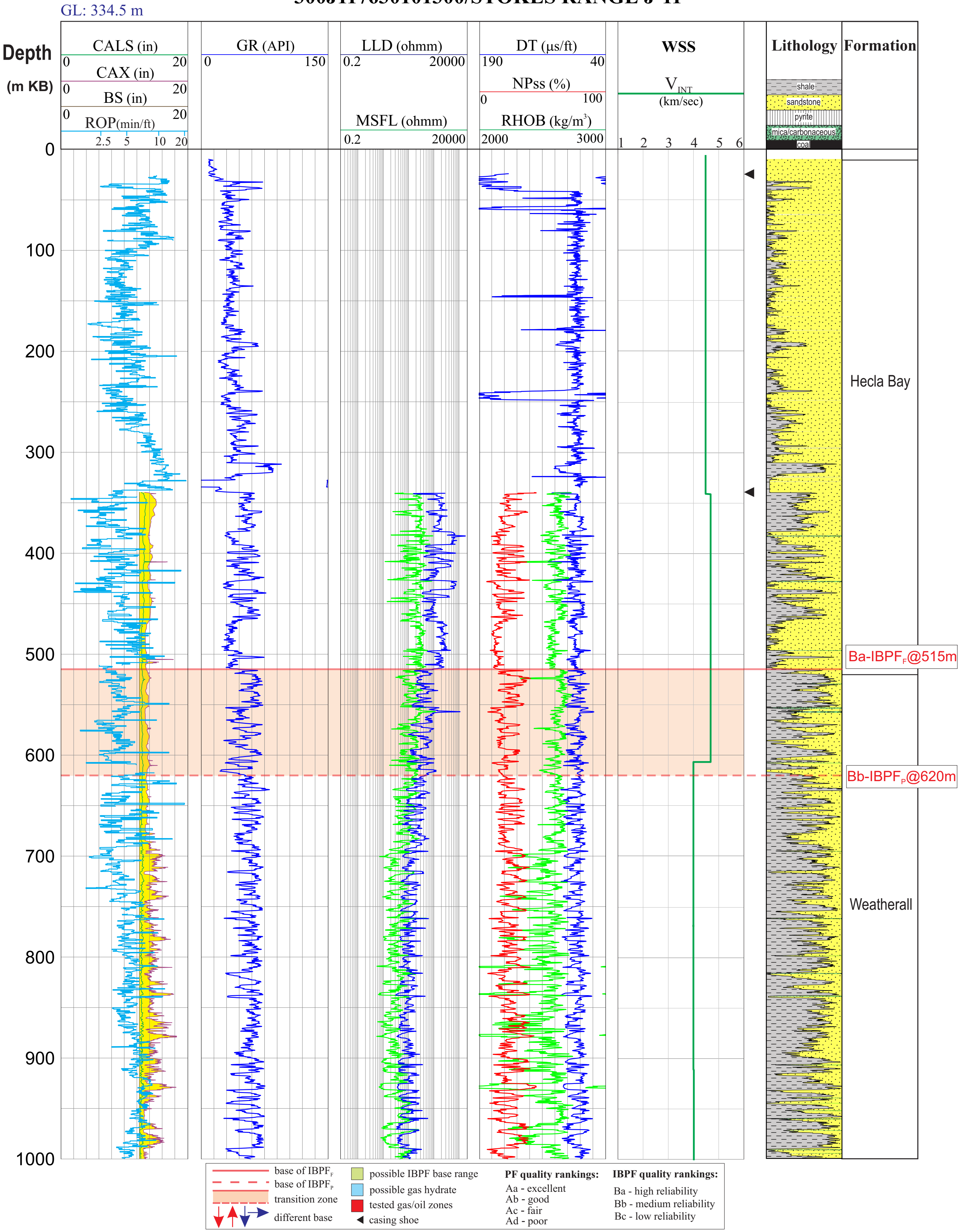

Figure 2-42. Determinations of base of $IBPF_F$ with "Ba" quality and $IBPF_P$ with "Bb" quality using well logs and well seismic surveys for the Stokees Range J-11 well on Bathurst Island in the Canadian Arctic Islands.

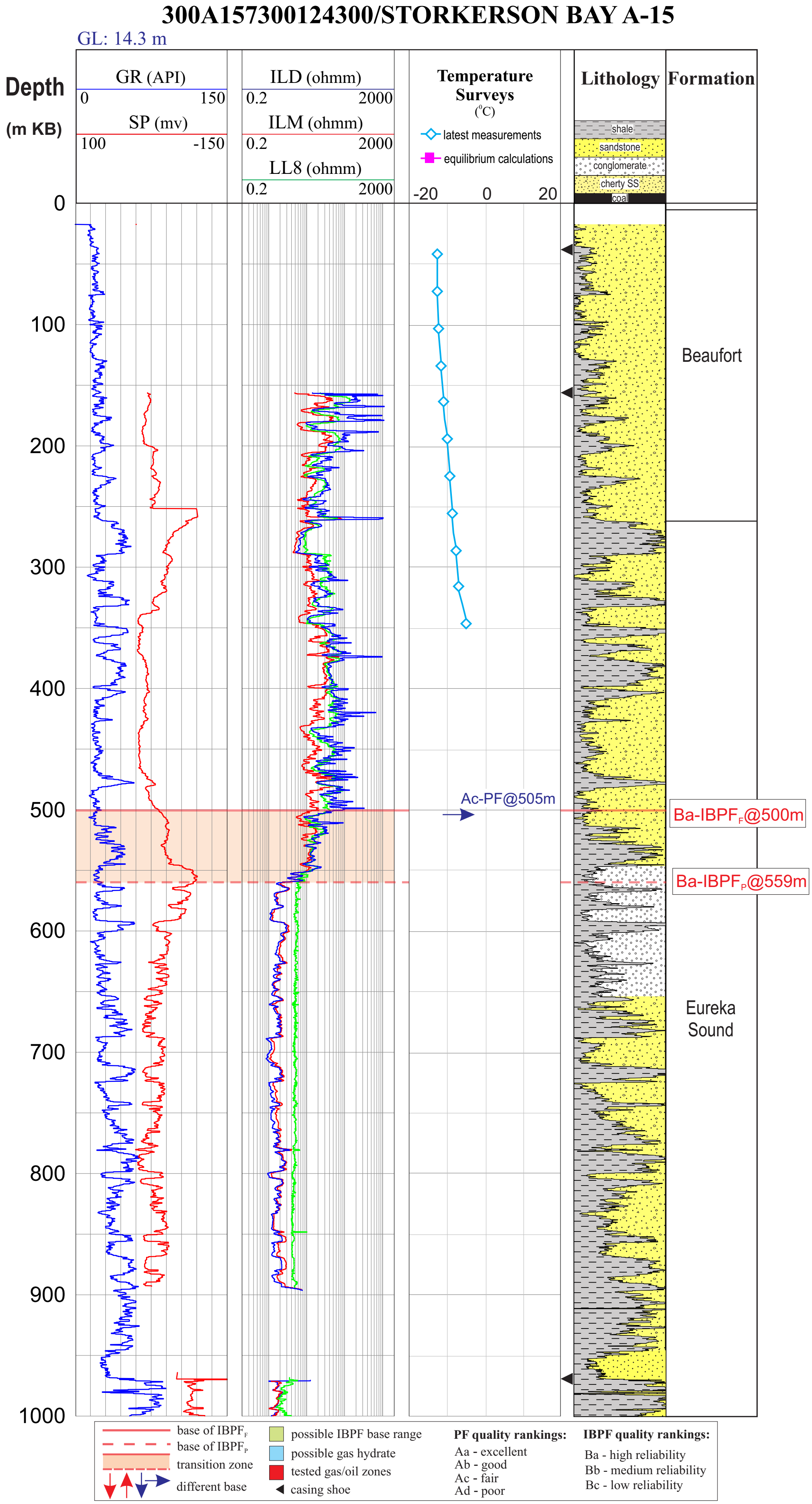

Figure 2-43. Determinations of base of $IBPF_F$ with "Ba" quality and $IBPF_P$ with "Ba" quality from well logs, and base of PF from temperature surveys for the Storkerson Bay A-15 well on Banks Island in the Canadian Arctic Islands.

300J348000083300/TALEMEN J-34

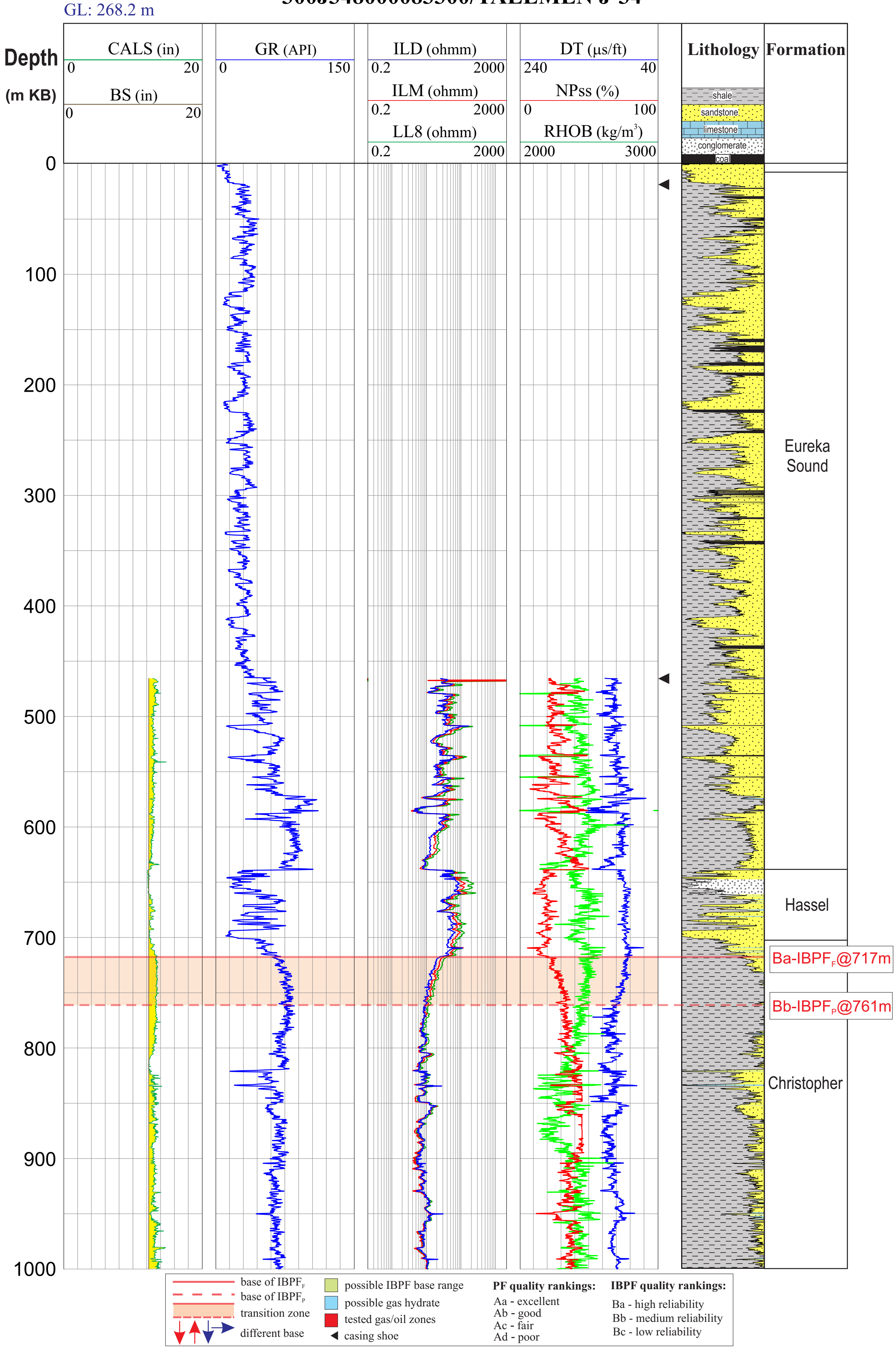

Figure 2-44. Determinations of base of $IBPF_F$ with “Ba” quality and $IBPF_P$ with “Bb” quality using l well logs for the Talemen J-34 well on Ellesmere Island in the Canadian Arctic Islands.

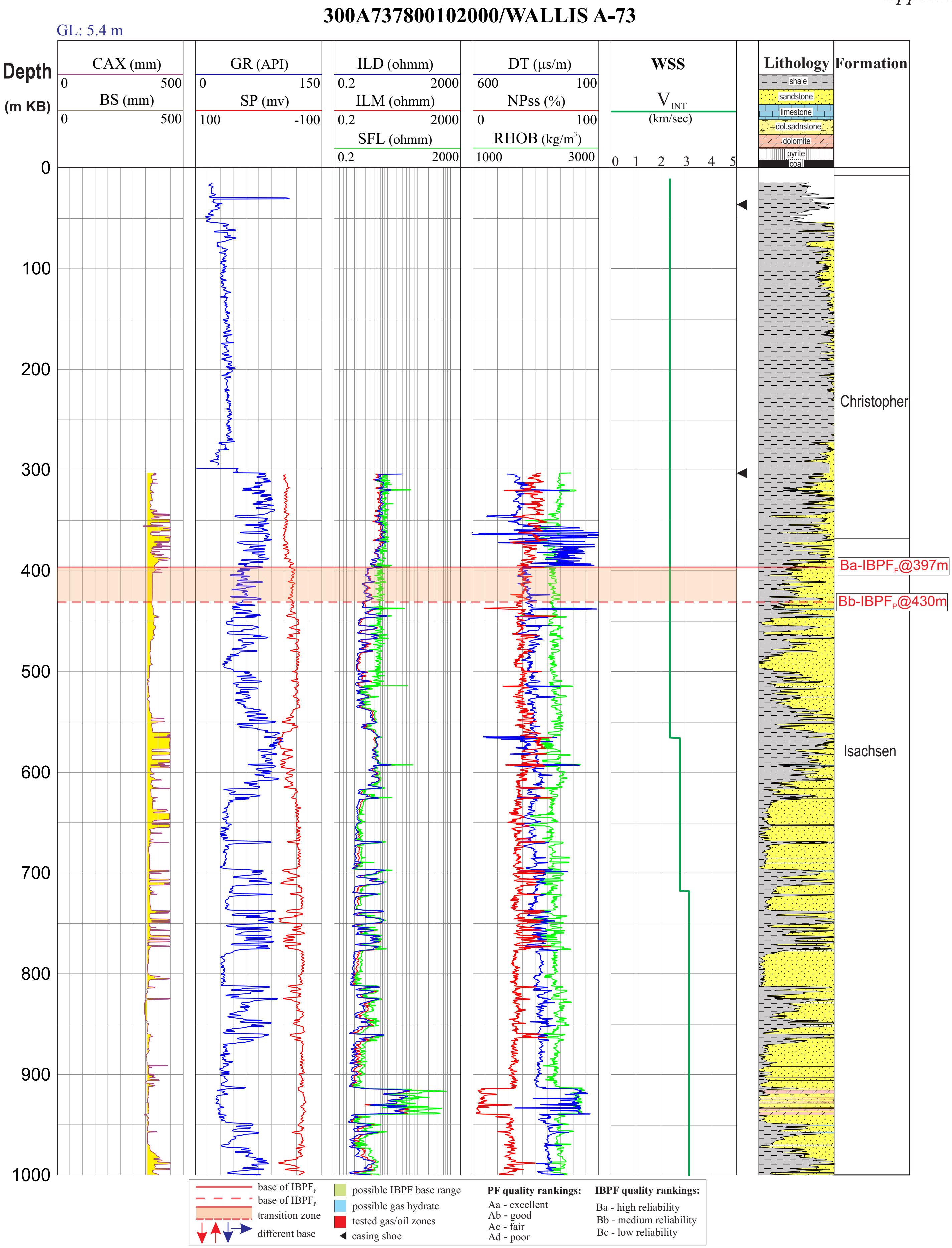

Figure 2-45. Determinations of base of $IBPF_F$ with “Ba” quality and $IBPF_P$ with “Bb” quality using well logs and well seismic surveys for the Wallis A-73 well on King Christian Island in the Canadian Arctic Islands.

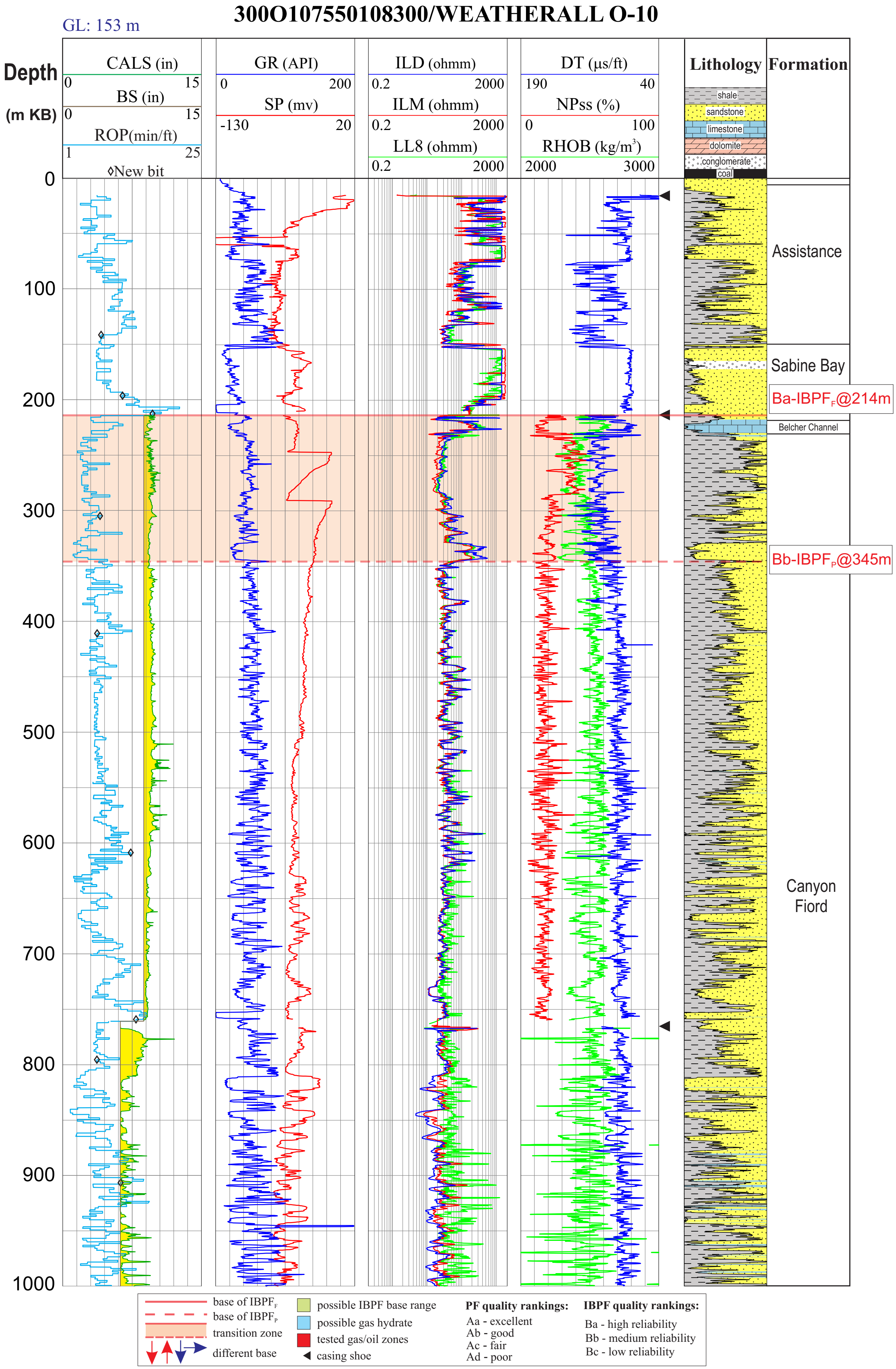

Figure 2-46. Determinations of base of $IBPF_F$ with "Ba" quality and $IBPF_P$ with "Bb" quality using well logs for the Weatherall O-10 well on Melville Island in the Canadian Arctic Islands.

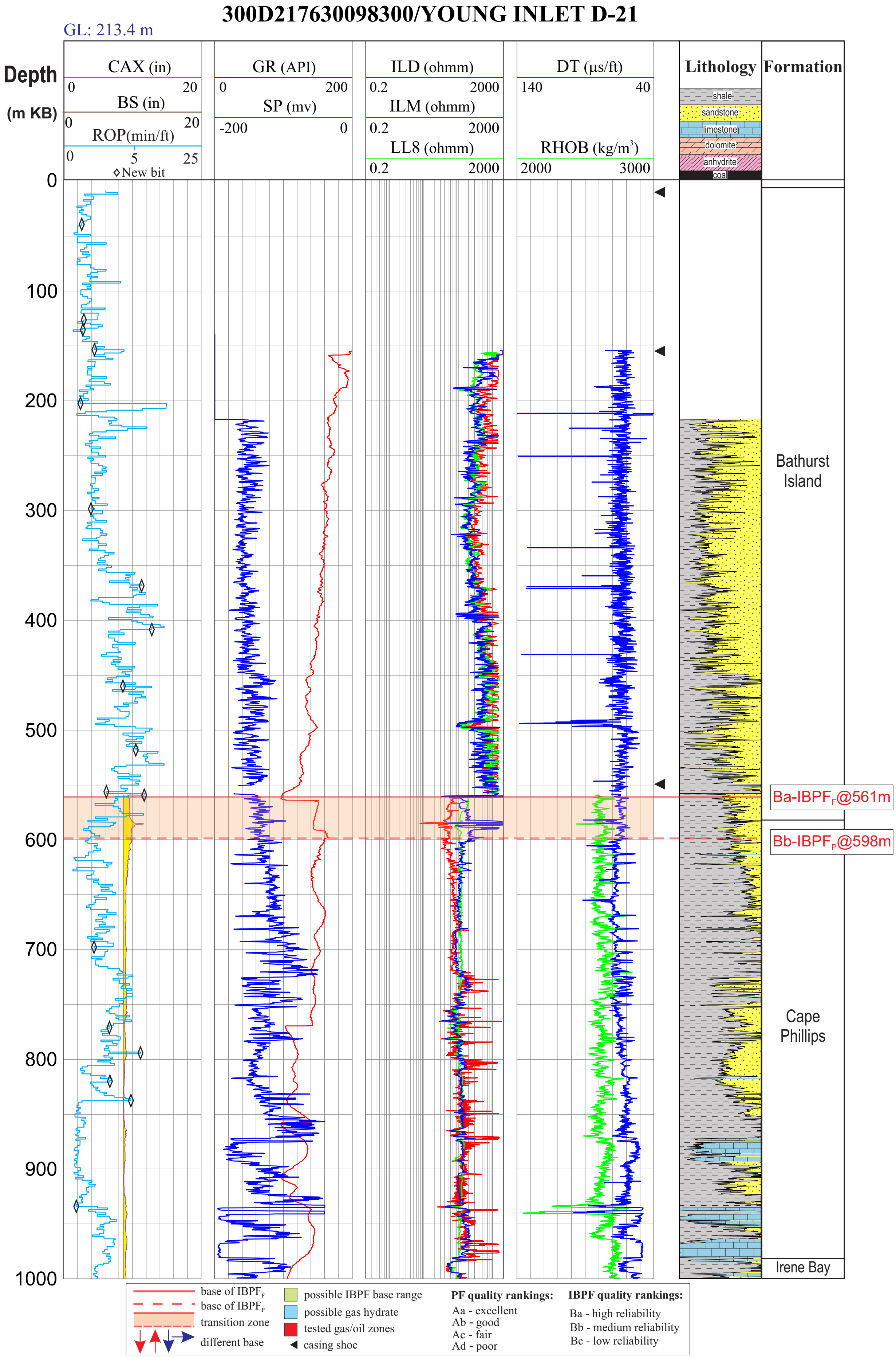

Figure 2-47. Determinations of base of $IBPF_F$ with "Ba" quality and $IBPF_P$ with "Bb" quality using well logs for the Young Inlet D-21 well on Bathurst Island in the Canadian Arctic Islands.

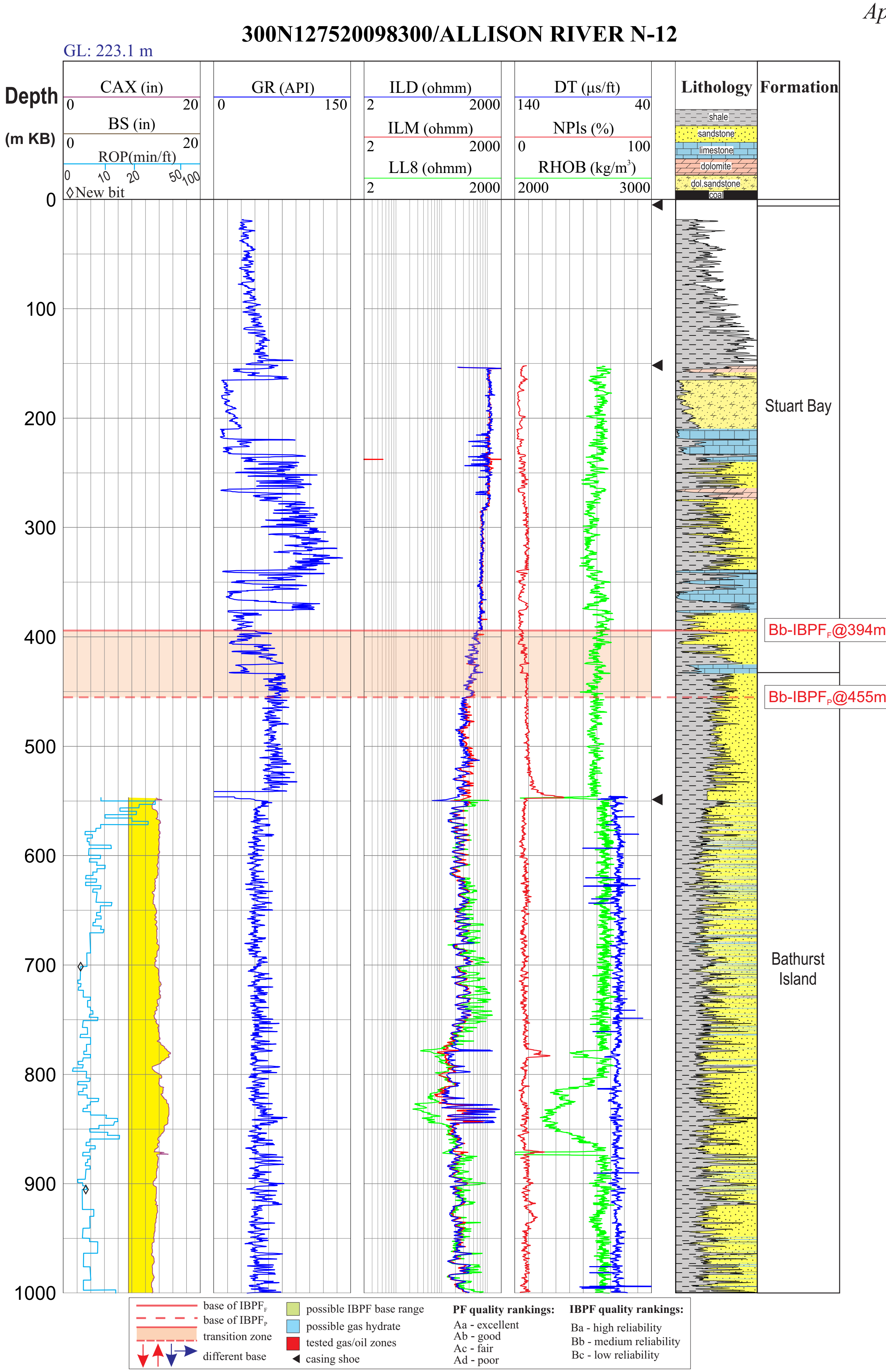

Figure 3-1. Determinations of base of $IBPF_F$ with "Bb" quality and $IBPF_P$ with "Bb" quality using well logs for the Allison River N-12 well on Bathurst Island in the Canadian Arctic Islands.

300H407820096000/AMUND CENTRAL DOME H-40

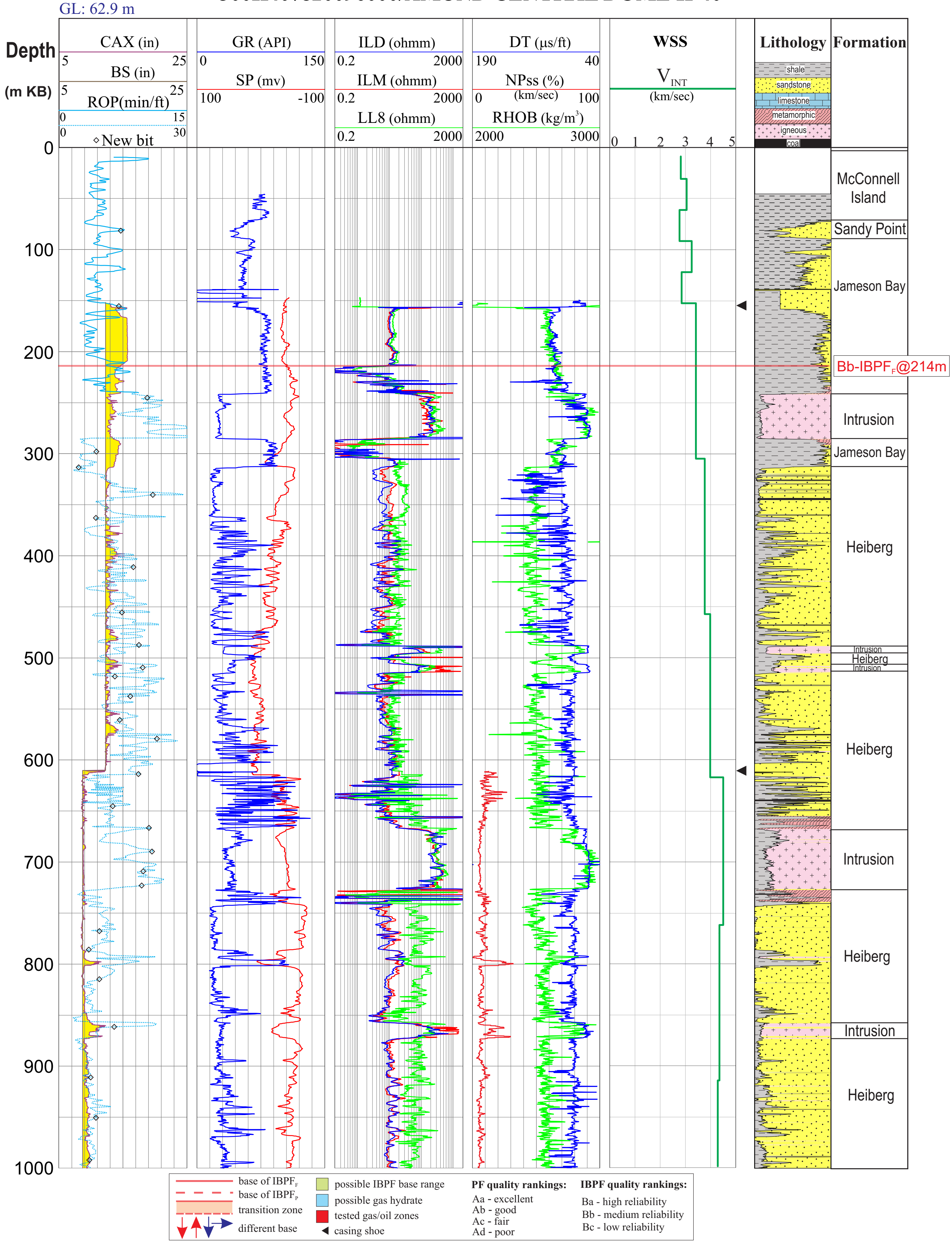

Figure 3-2. Determination of base of $IBPF_F$ with “Bb” quality using well logs and well seismic surveys for the Amund Central Dome H-40 well on Amund Ringnes Island in the Canadian Arctic Islands.

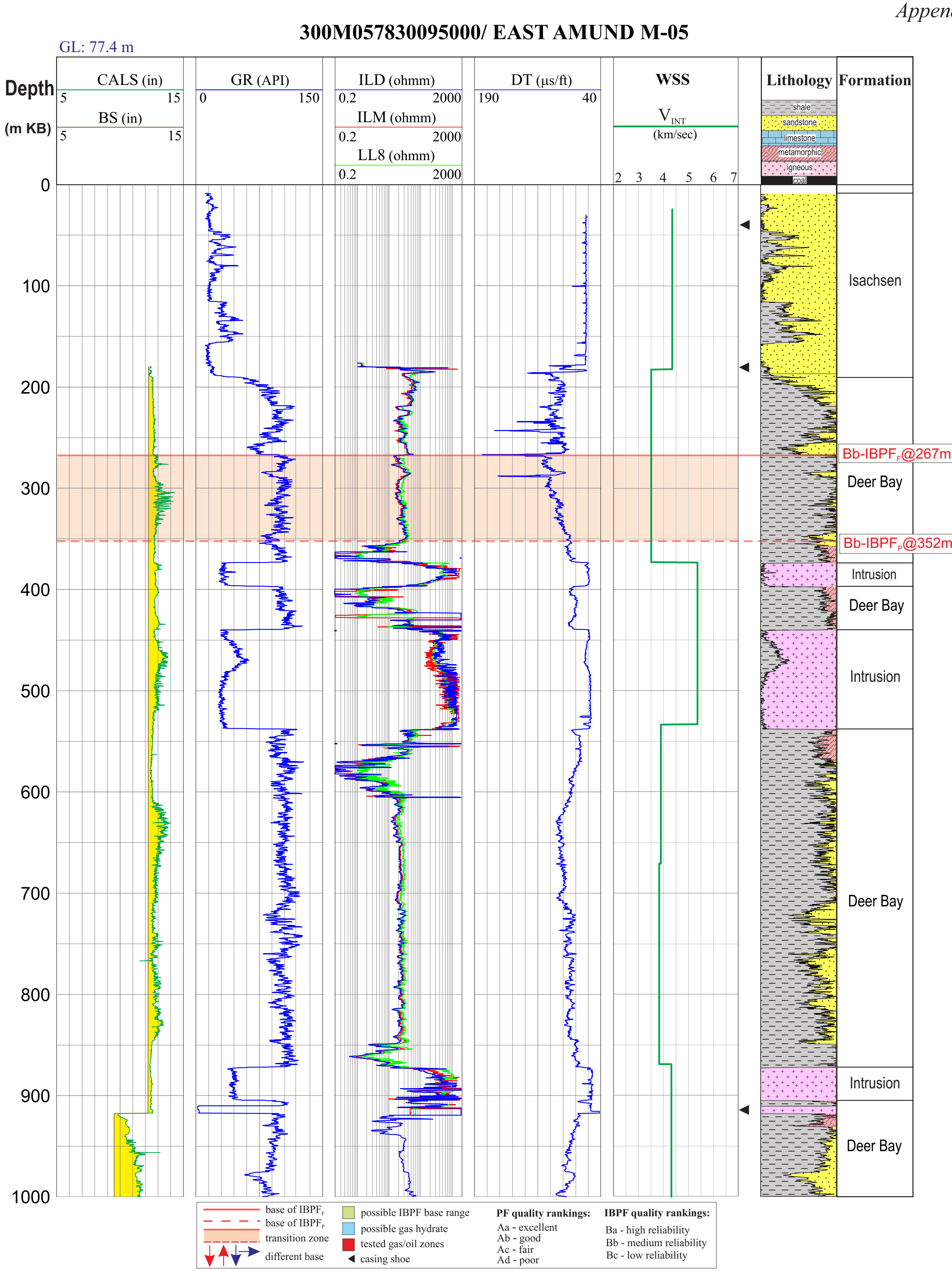

Figure 3-3. Determinations of base of $IBPF_F$ with “Bb” quality and $IBPF_P$ with “Bb” quality using well logs and well seismic surveys for the East Amund M-05 well on Amund Ringnes Island in the Canadian Arctic Islands.

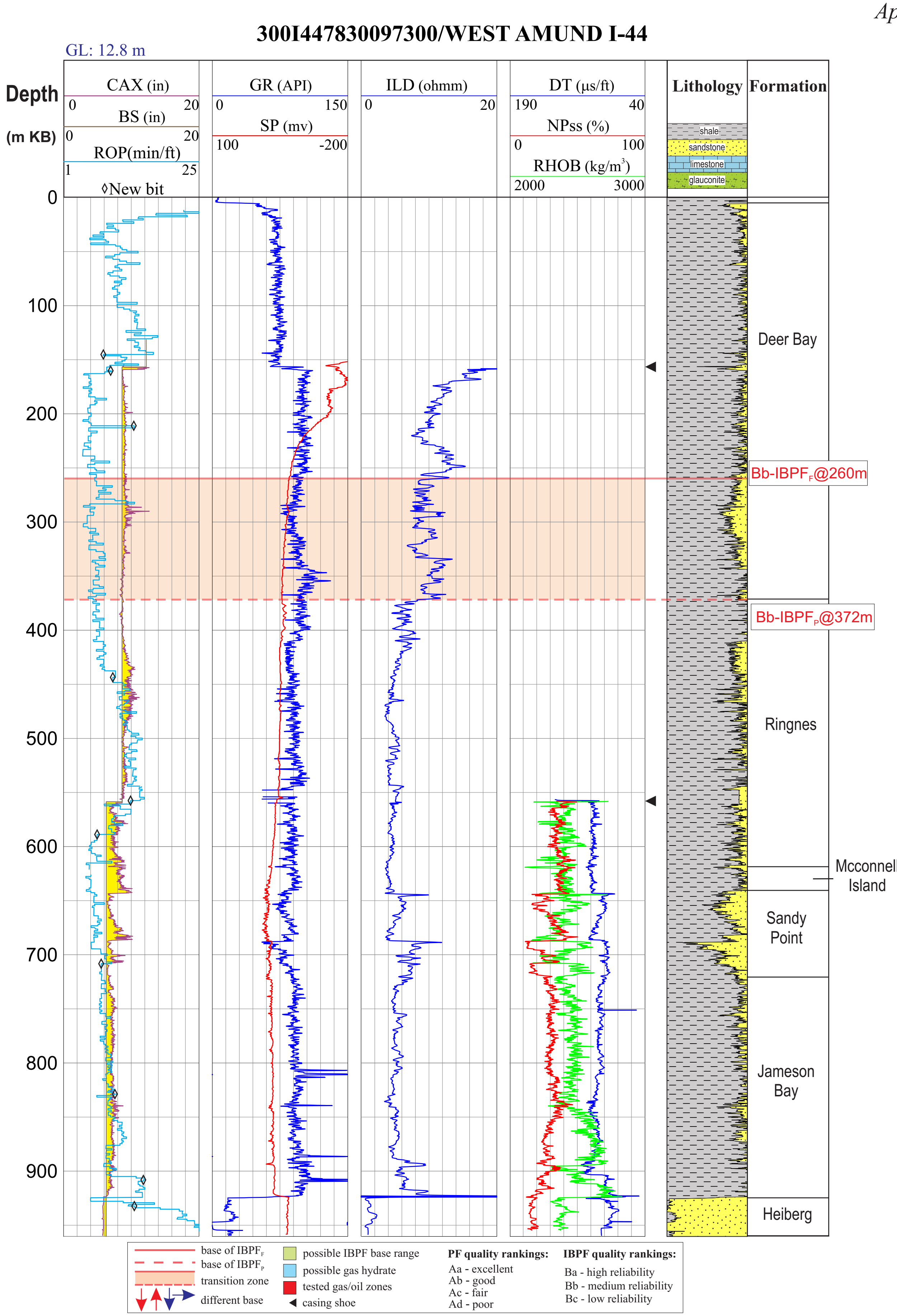

Figure 3-4. Determinations of base of $IBPF_F$ with “Bb” quality and $IBPF_P$ with “Bb” quality from well logs for the West Amund I-44 well on Amund Ringnes Island in the Canadian Arctic Islands.

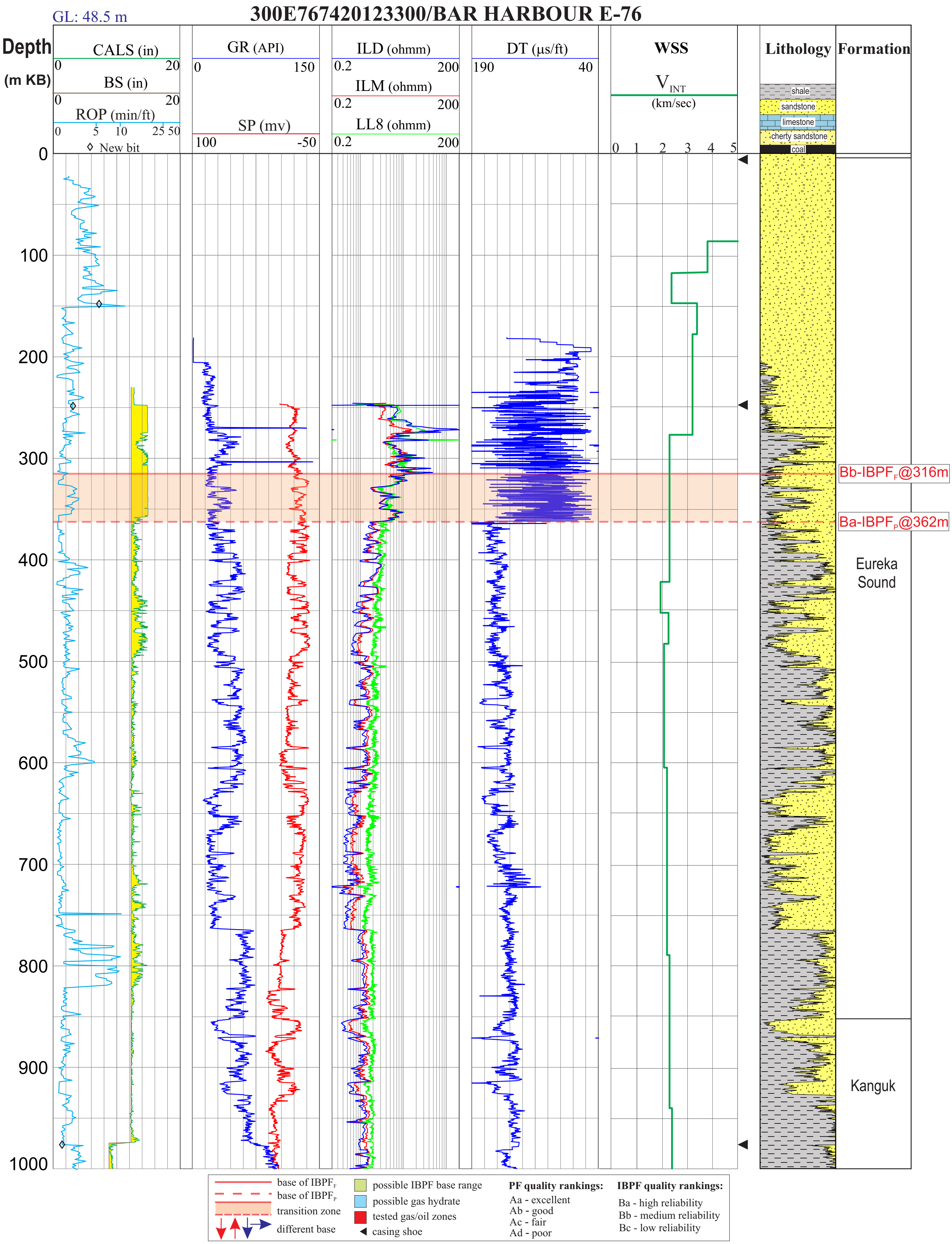

Figure 3-5. Determinations of base of $IBPF_F$ with "Bb" quality and $IBPF_P$ with "Ba" quality using well logs and well seismic surveys for the Bar Harbour E-76 well on Banks Island in the Canadian Arctic Islands.

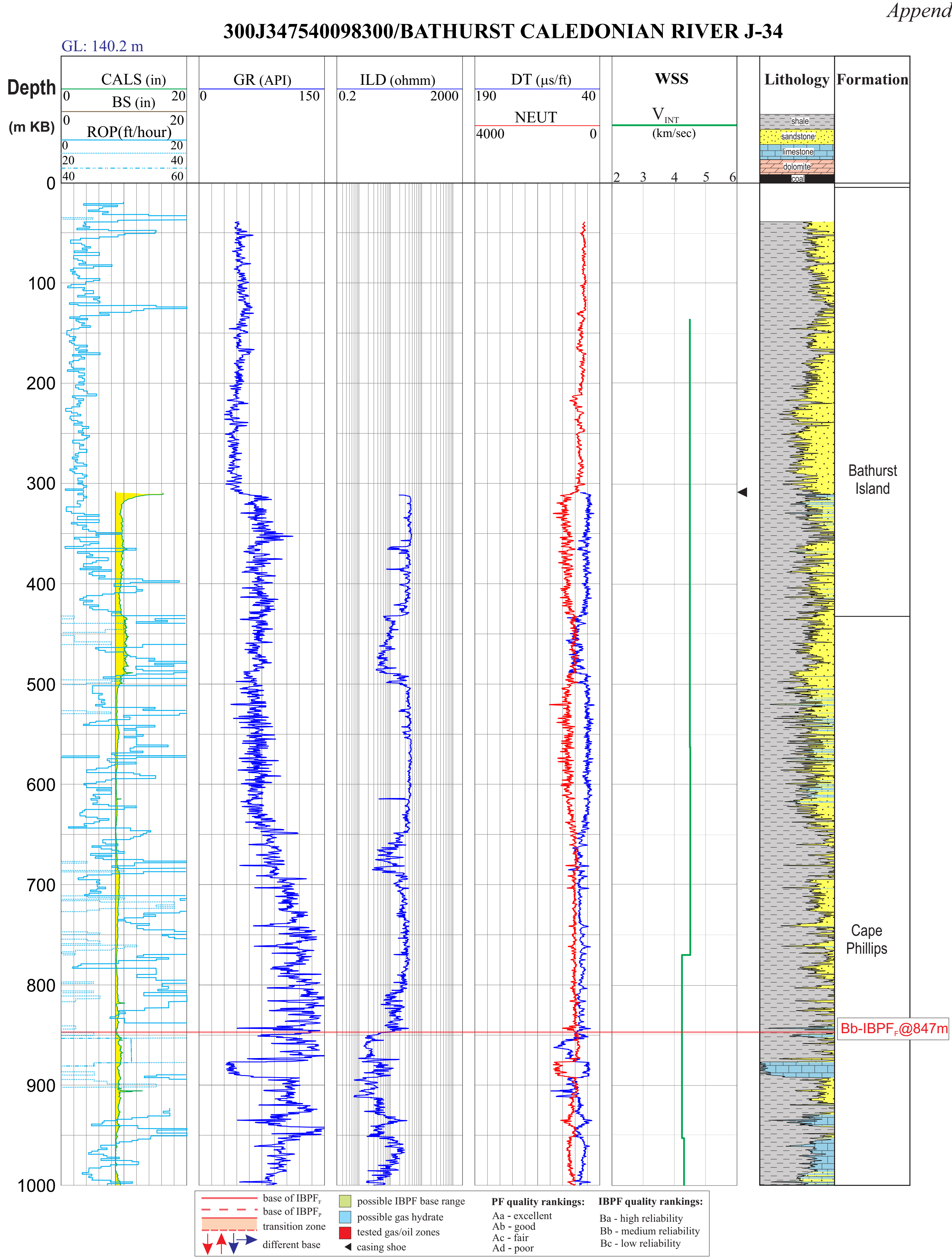

Figure 3-6. Determination of base of $IBPF_F$ with “Bb” quality using well logs and well seismic surveys for the Bathurst Caledonian River J-34 well on Bathurst Island in the Canadian Arctic Islands.

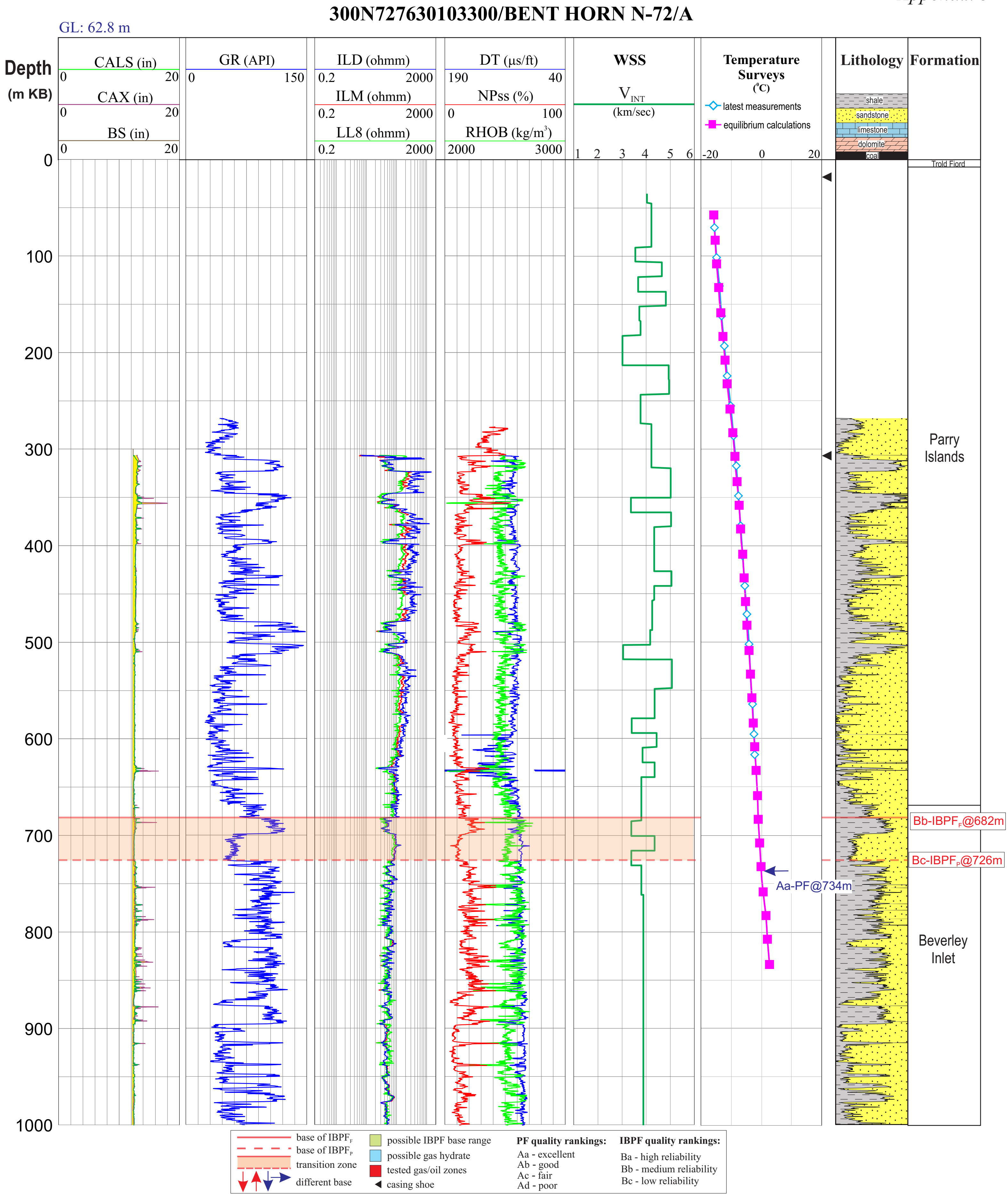

Figure 3-7. Determinations of base of $IBPF_F$ with "Bb" quality and $IBPF_P$ with "Bc" quality using well logs and well seismic surveys, and base of PF from temperature surveys for the Bent Horn N-72 and N-72A wells on Cameron Island in the Canadian Arctic Islands.

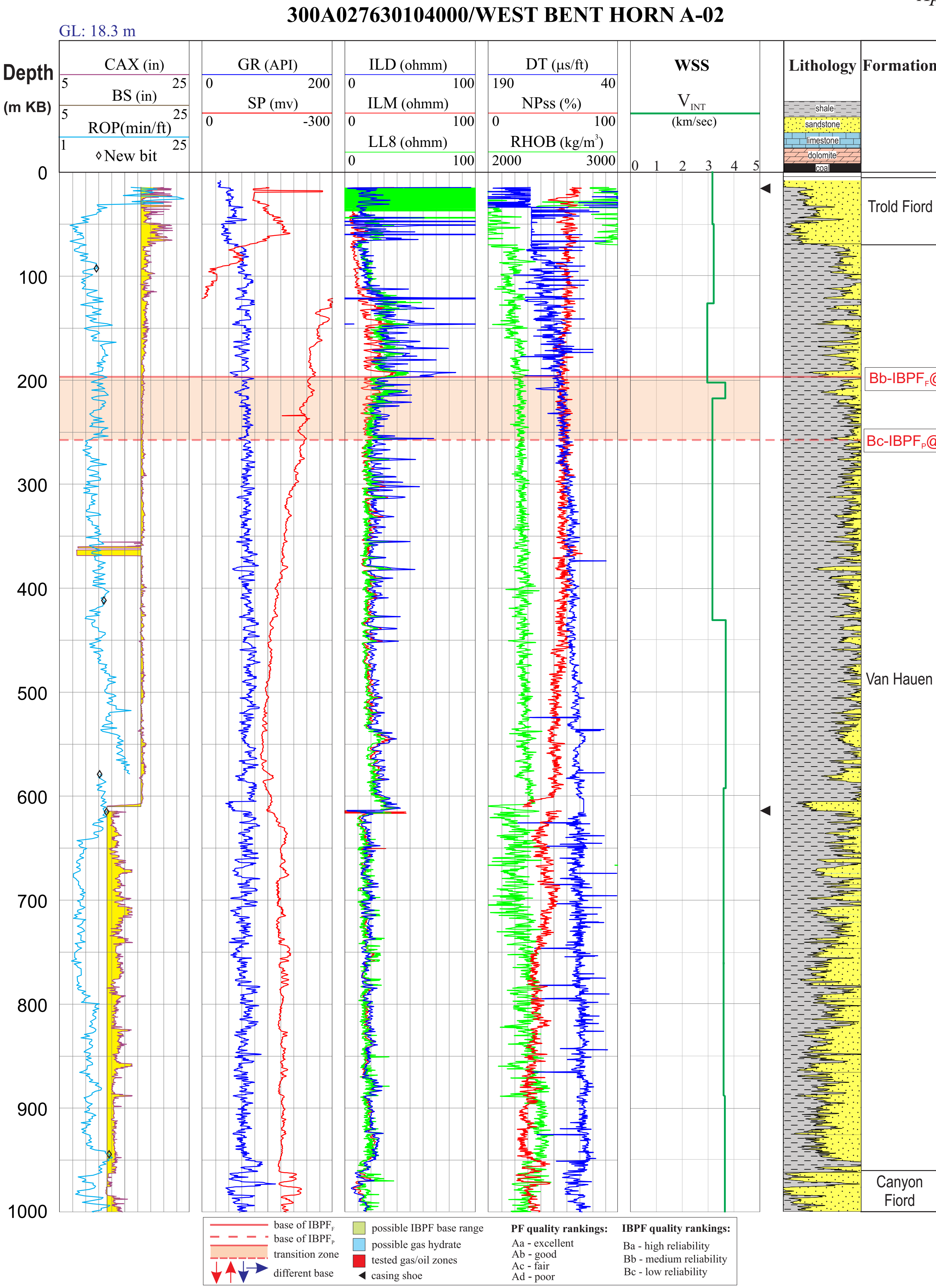

Figure 3-8. Estimations of base of $IBPF_F$ with "Bb" quality and $IBPF_P$ with "Bc" quality using well logs and well seismic surveys for the West Bent Horn A-02 well on Cameron Island in the Canadian Arctic Islands.

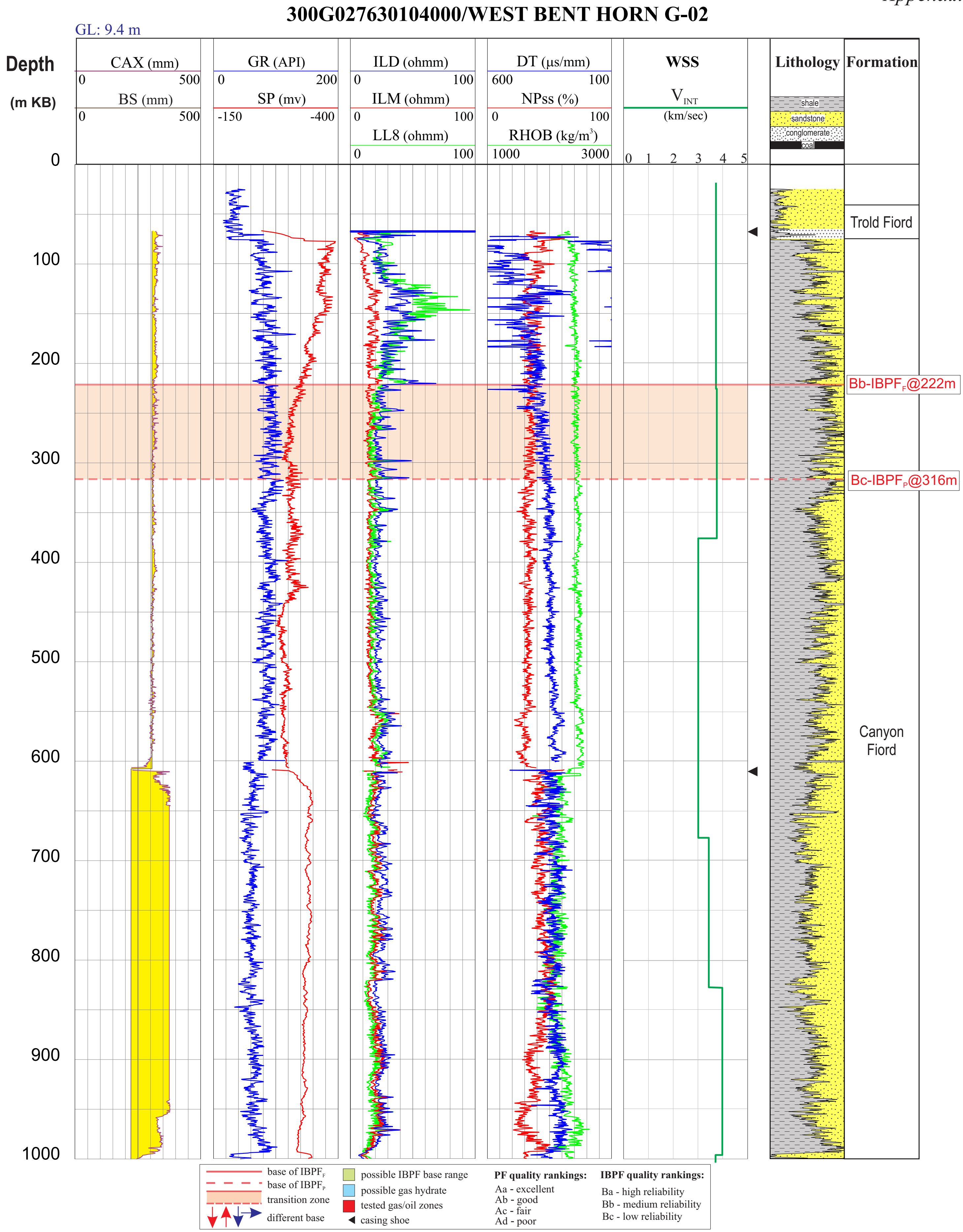

Figure 3-9. Estimations of base of $IBPF_F$ with "Bb" quality and $IBPF_P$ with "Bc" quality using well logs and well seismic surveys for the West Bent Horn G-02 well on Cameron Island in the Canadian Arctic Islands.

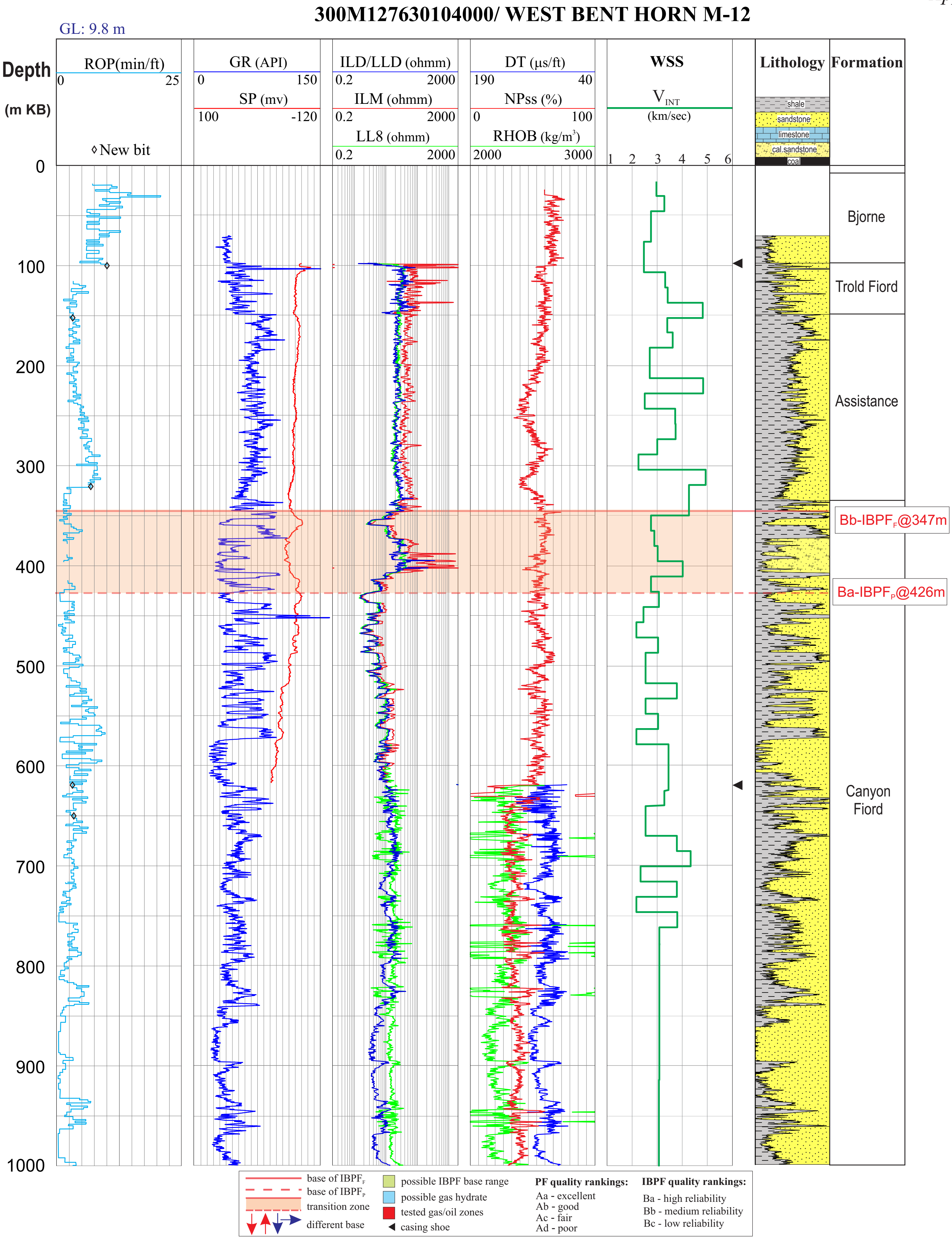

Figure 3-10. Determinations of base of $IBPF_F$ with "Bb" quality and $IBPF_P$ with "Bb" quality using well logs and well seismic surveys for the West Bent Horn M-12 well on Cameron Island in the Canadian Arctic Islands.

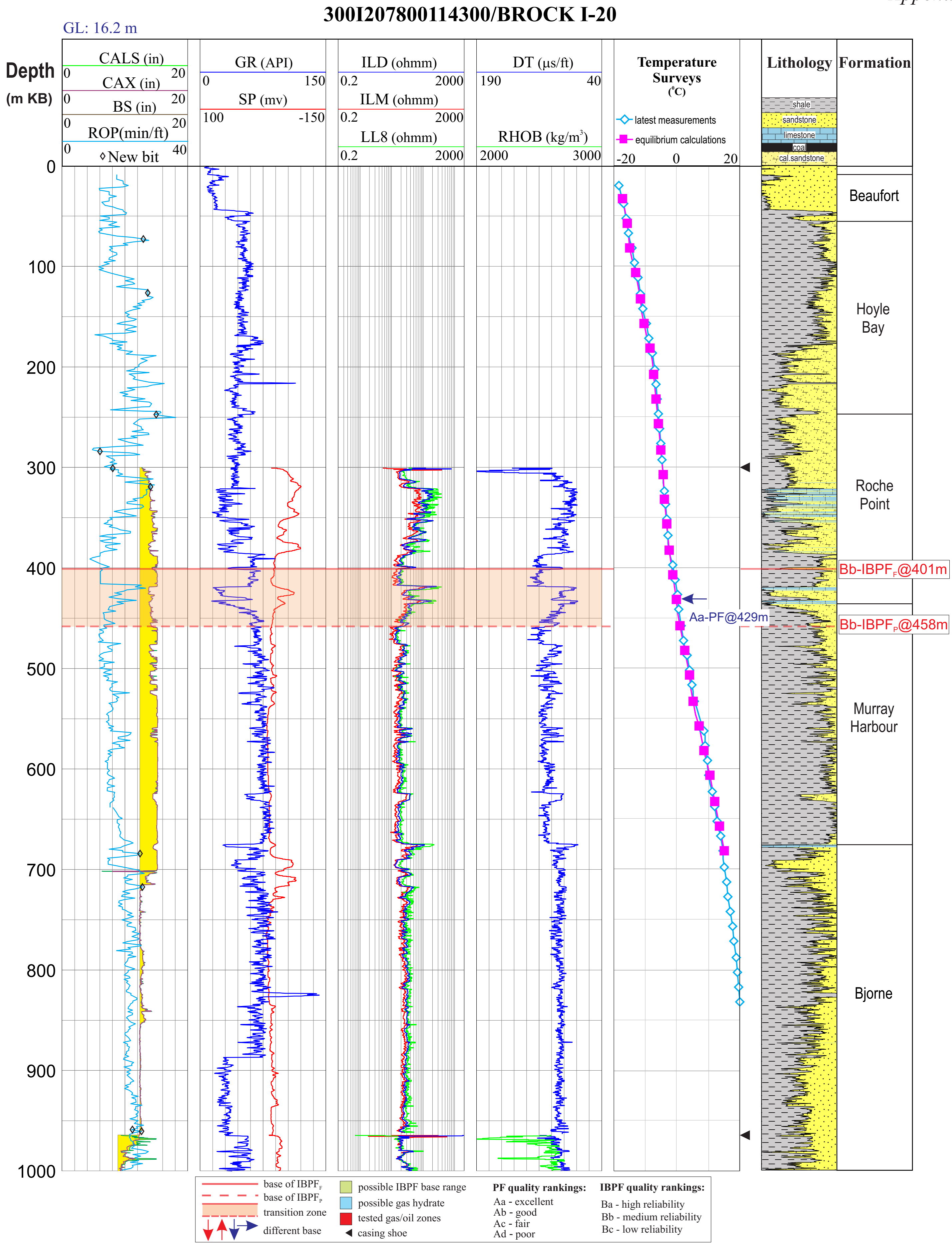

Figure 3-11. Determinations of base of $IBPF_F$ with "Bb" quality and $IBPF_P$ with "Bb" quality using well logs, and determination of base of PF from temperature surveys for the Brock I-20 well on Brock Island in the Canadian Arctic Islands.

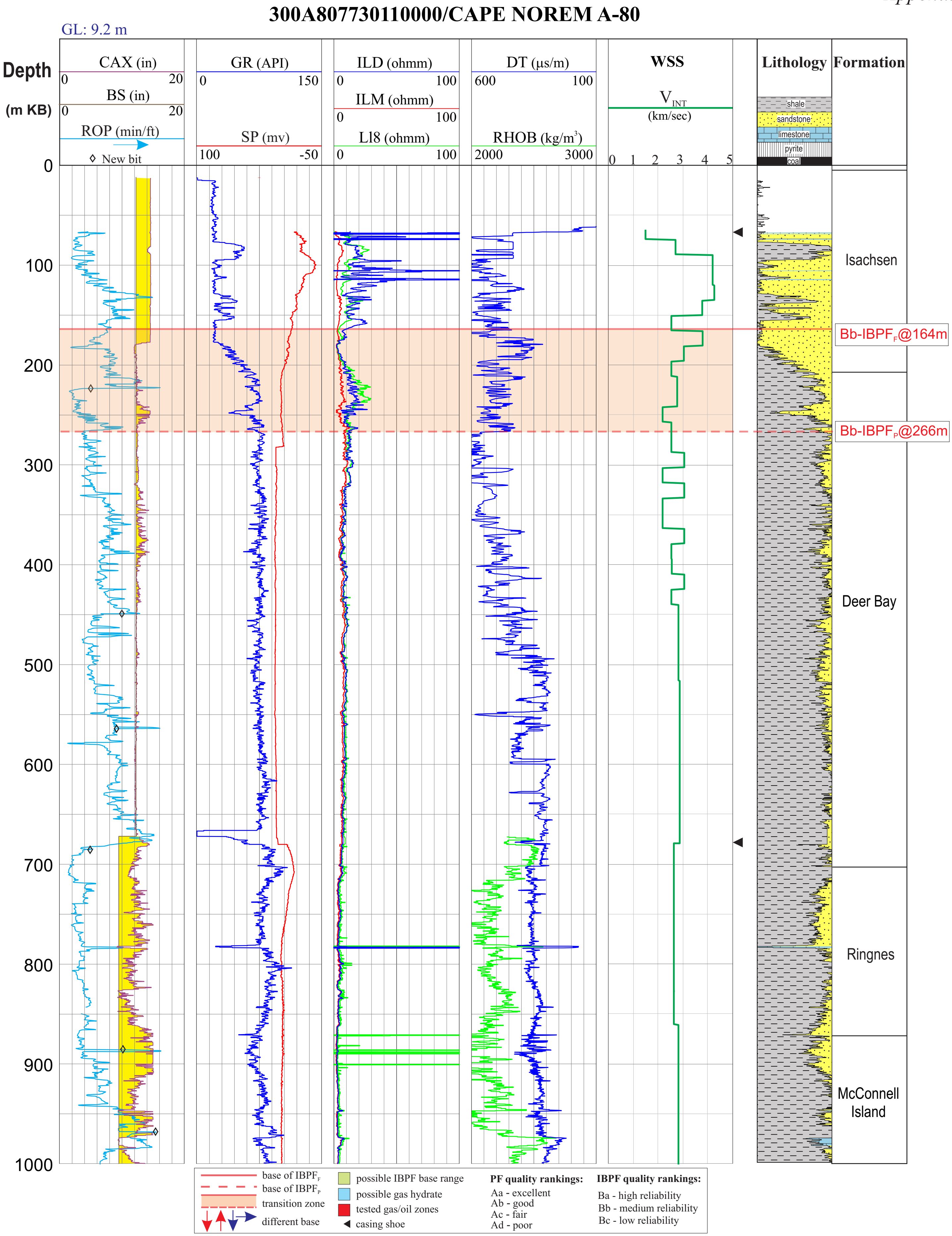

Figure 3-12. Determinations of base of $IBPF_F$ with "Bb" quality and $IBPF_P$ with "Bb" quality using well logs and well seismic surveys for the Cape Norem A-80 well on Mackenzie King Island in the Canadian Arctic Islands.

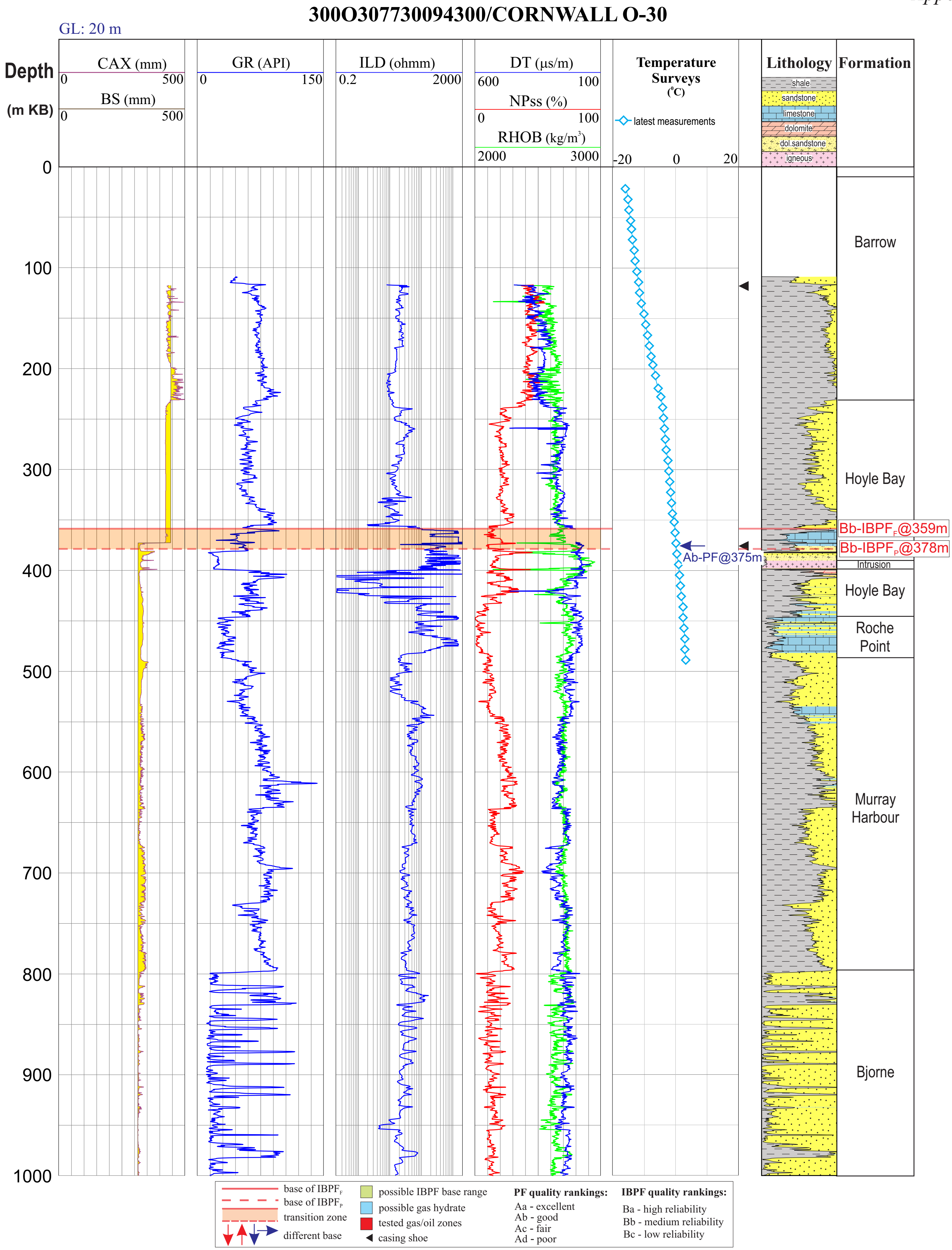

Figure 3-13. Determinations of base of $IBPF_F$ with “Bb” quality and $IBPF_P$ with “Bb” quality using well logs, and base of PF from temperature surveys for the Cornwall O-30 well on Cornwall Island in the Canadian Arctic Islands.

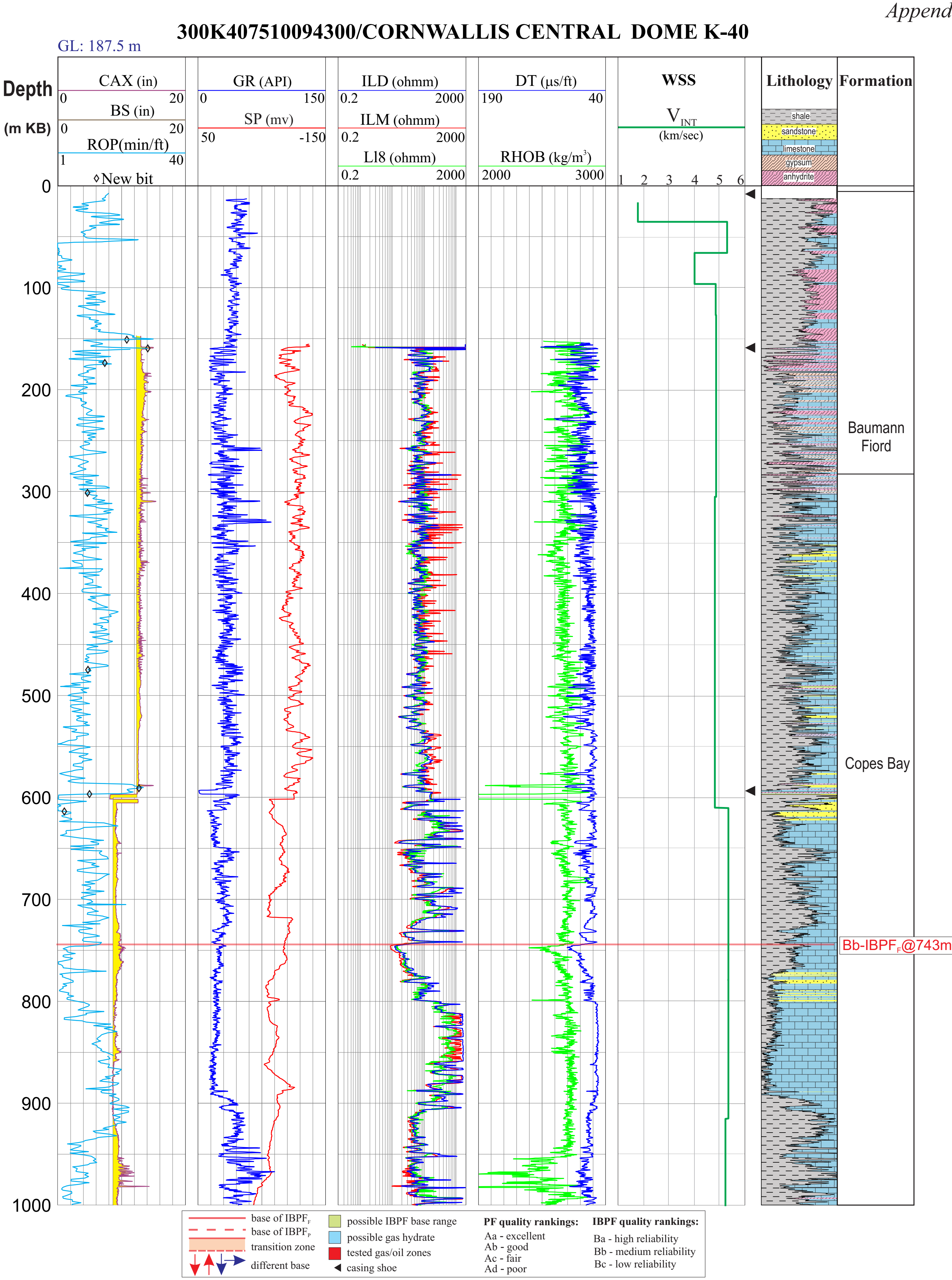

Figure 3-14. Determination of base of $IBPF_F$ with "Bb" quality using well logs and well seismic surveys for the Cornwallis Central Dome K-40 well on Cornwallis Island in the Canadian Arctic Islands.

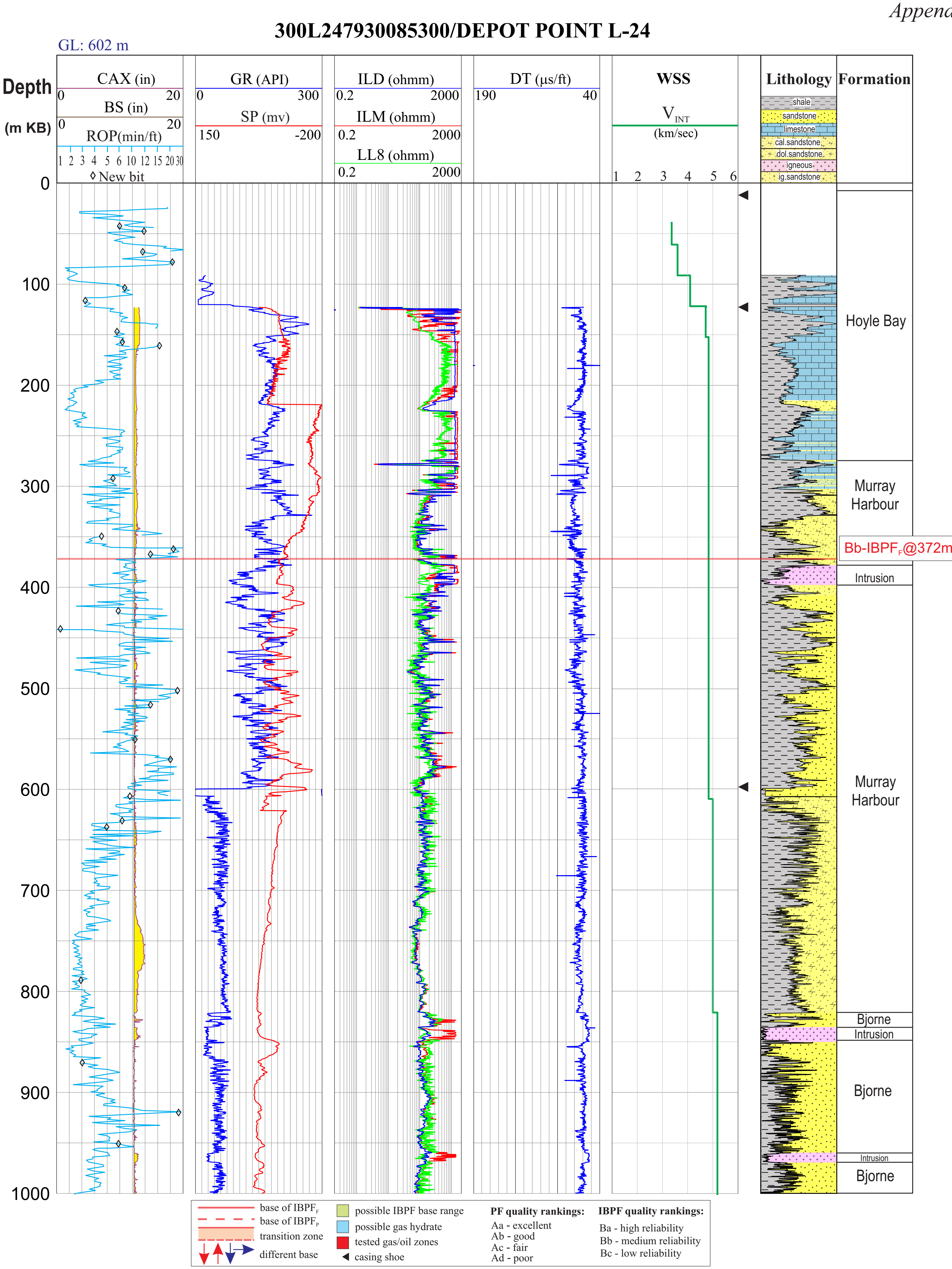

Figure 3-15. Estimation of base of $IBPF_F$ with "Bb" quality using well logs and well seismic surveys for the Depot Point L-24 well on Axel Heiberg Island in the Canadian Arctic Islands.

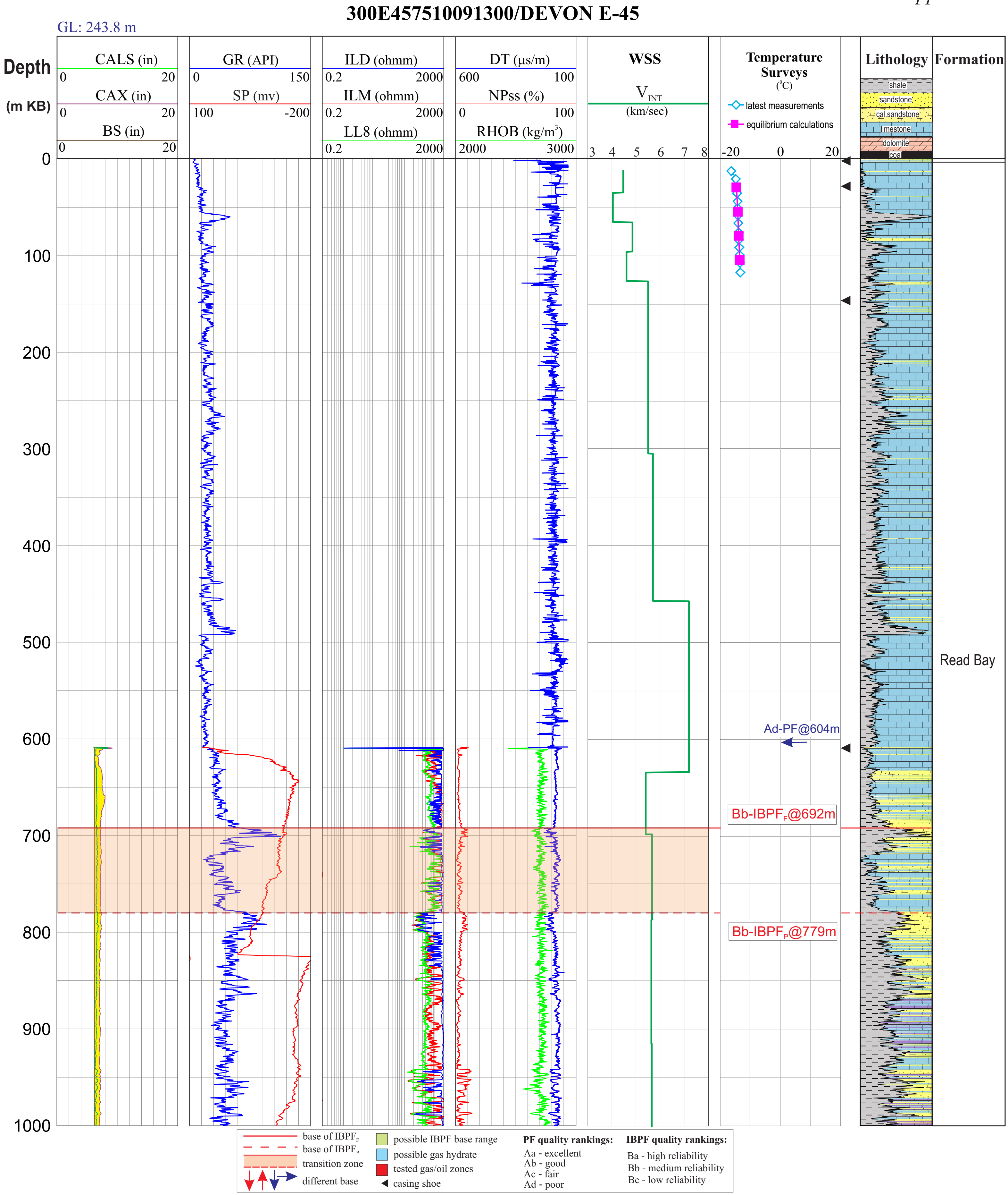

Figure 3-16. Determinations of base of $IBPF_F$ with "Bb" quality and $IBPF_P$ with "Bb" quality using well logs and well seismic surveys, and esitimation of base of PF from temperature surveys for the Devon E-45 well on Devon Island in the Canadian Arctic Islands.

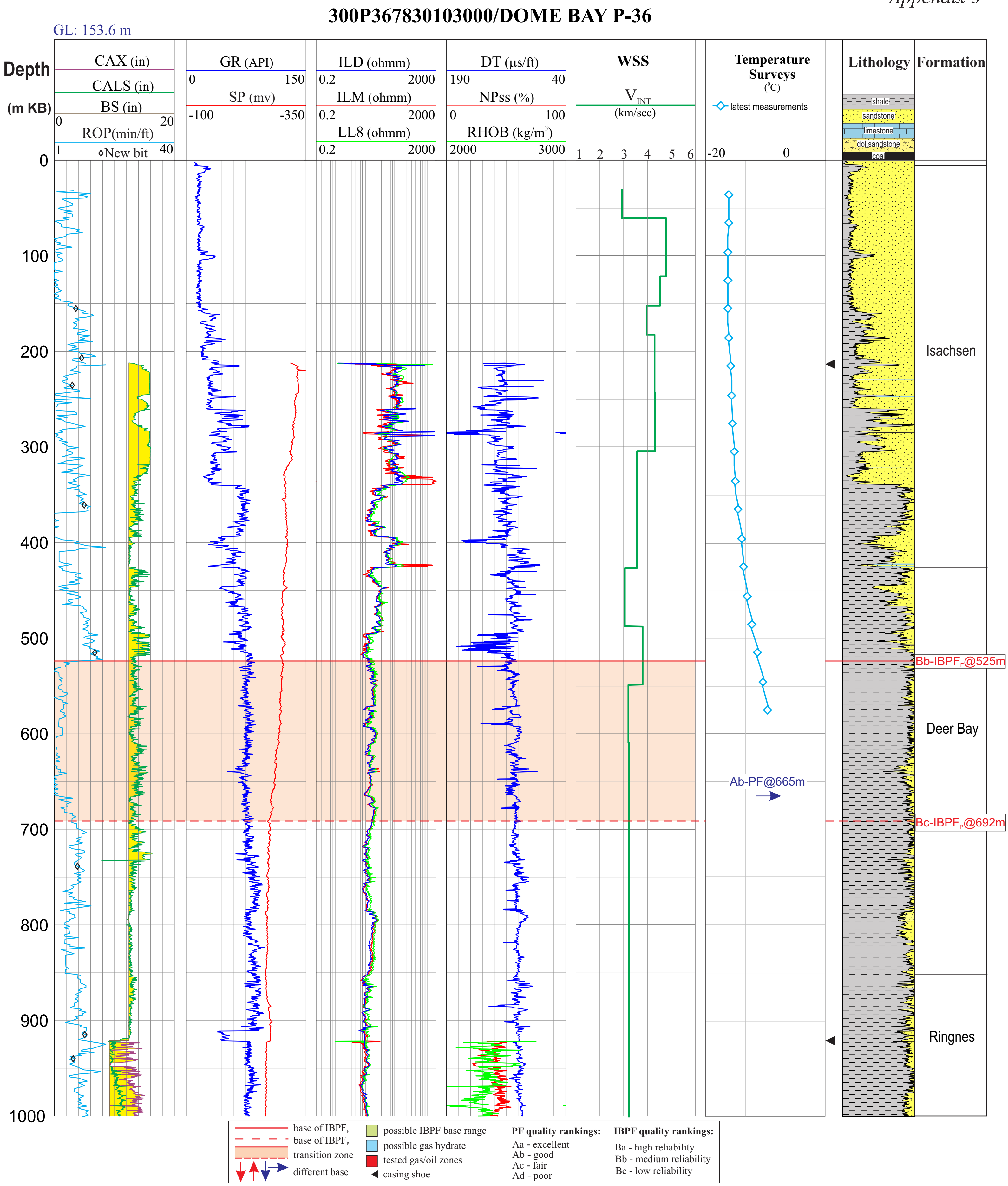

Figure 3-17. Determinations of base of $IBPF_F$ with "Bb" quality and $IBPF_P$ with "Bc" quality using well logs and well seismic surveys, and base of PF from temperature surveys for the Dome Bay P-36 well on Ellef Ringnes Island in the Canadian Arctic Islands.

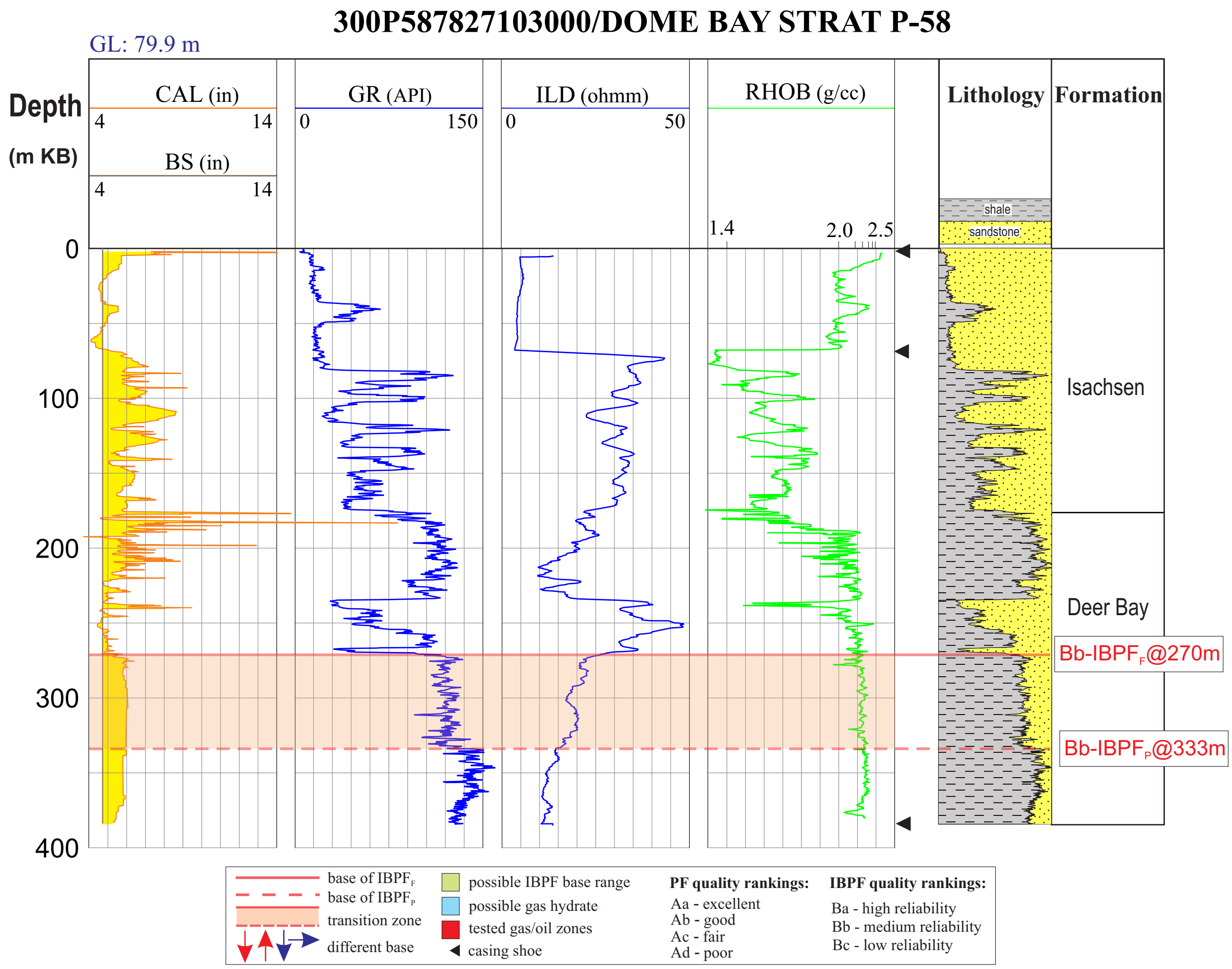

Figure 3-18. Determinations of base of $IBPF_F$ with “Bb” quality and $IBPF_P$ with “Bb” quality from well logs for the Dome Bay Strat P-58 well on Ellef Ringnes Island in the Canadian Arctic Islands.

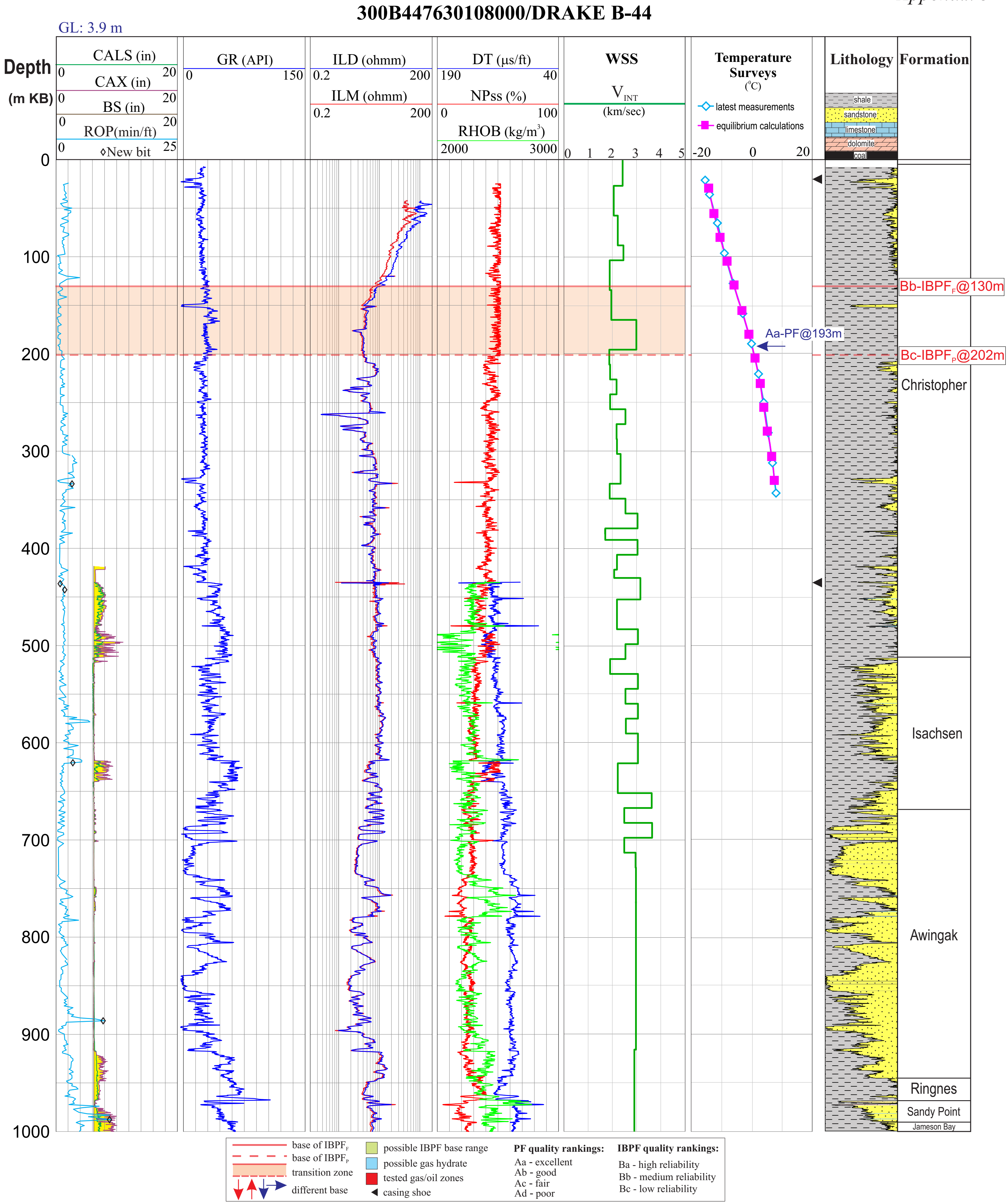

Figure 3-19. Determinations of base of IBPF$_F$ with "Bb" quality and IBPF$_P$ with "Bc" quality using well logs and well seismic surveys, and base of PF from temperature surveys for the Drake B-44 well on Melville Island in the Canadian Arctic Islands.

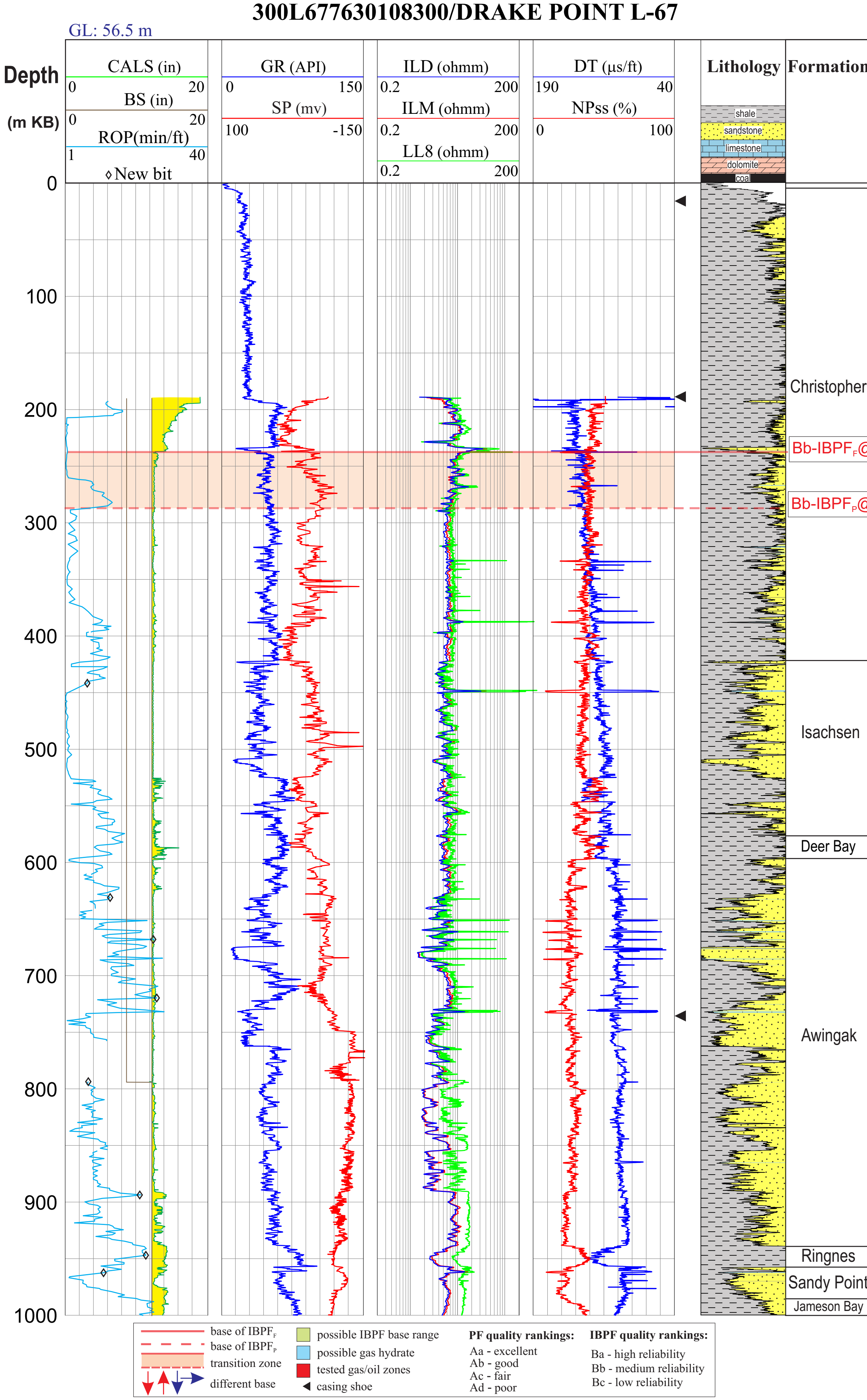

Figure 3-20. Determinations of base of IBPF$_F$ with “Bb” quality and IBPF$_P$ with “Bb” quality using well logs for the Drake Point L-67 well on Melville Island in the Canadian Arctic Islands.

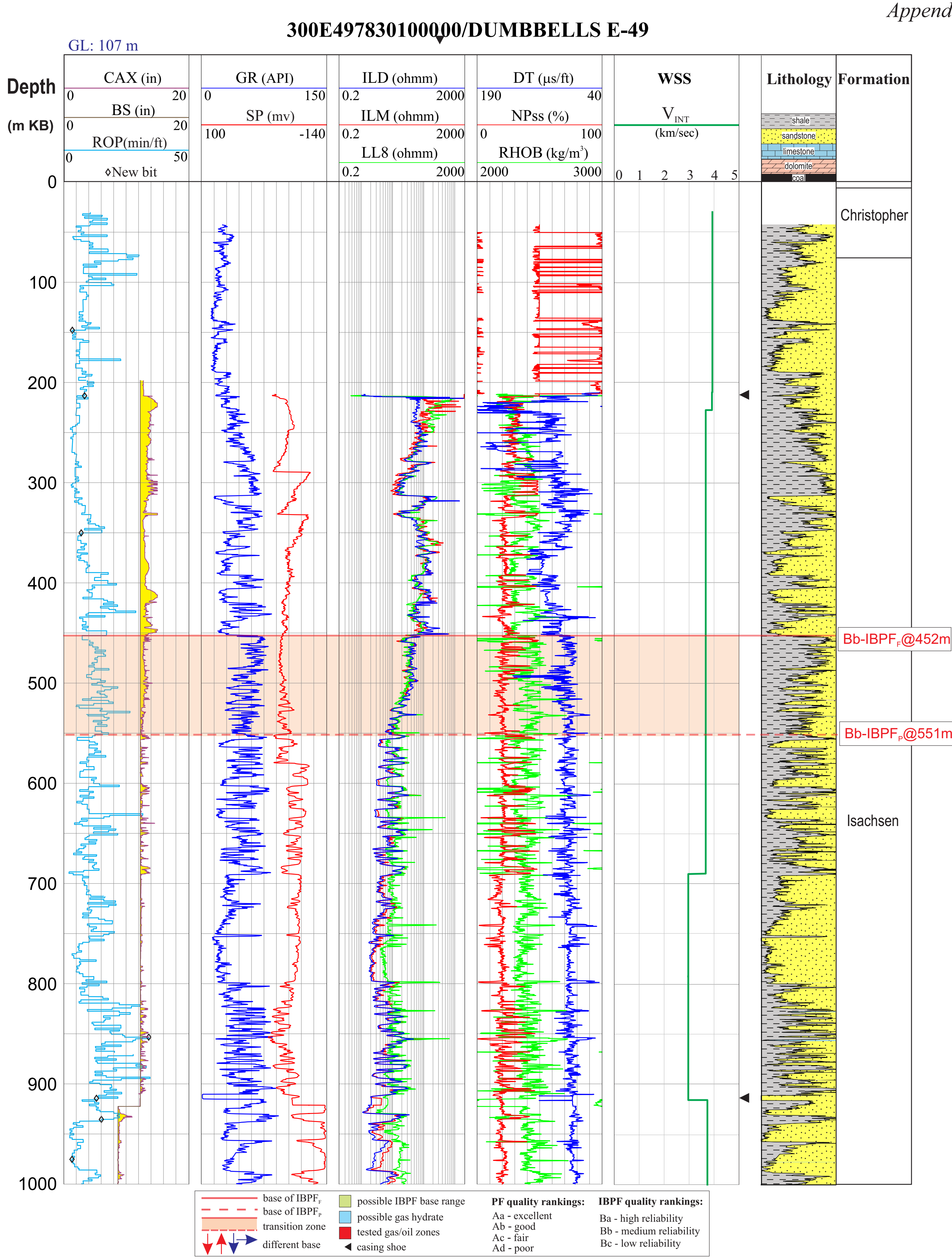

Figure 3-21. Determinations of base of $IBPF_F$ with "Bb" quality and $IBPF_P$ with "Bb" quality using well logs and well seismic surveys for the Dumbbells E-49 well on Ellef Ringnes Island in the Canadian Arctic Islands.

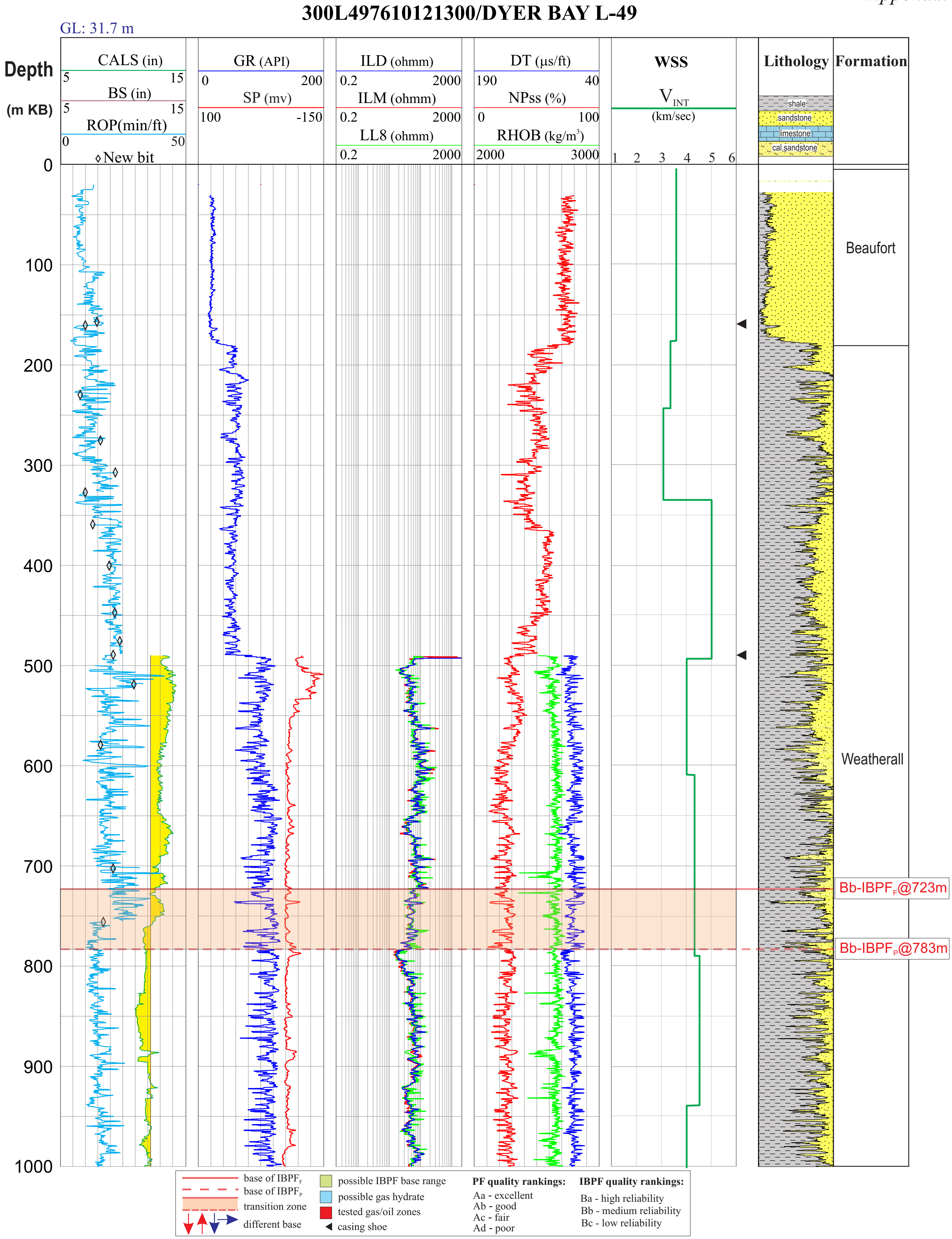

Figure 3-22. Determinations of base of $IBPF_F$ with "Bb" quality and $IBPF_P$ with "Bb" quality using well logs and well seismic surveys for the Dyer Bay L-49 well on Prince Patrick Island in the Canadian Arctic Islands.

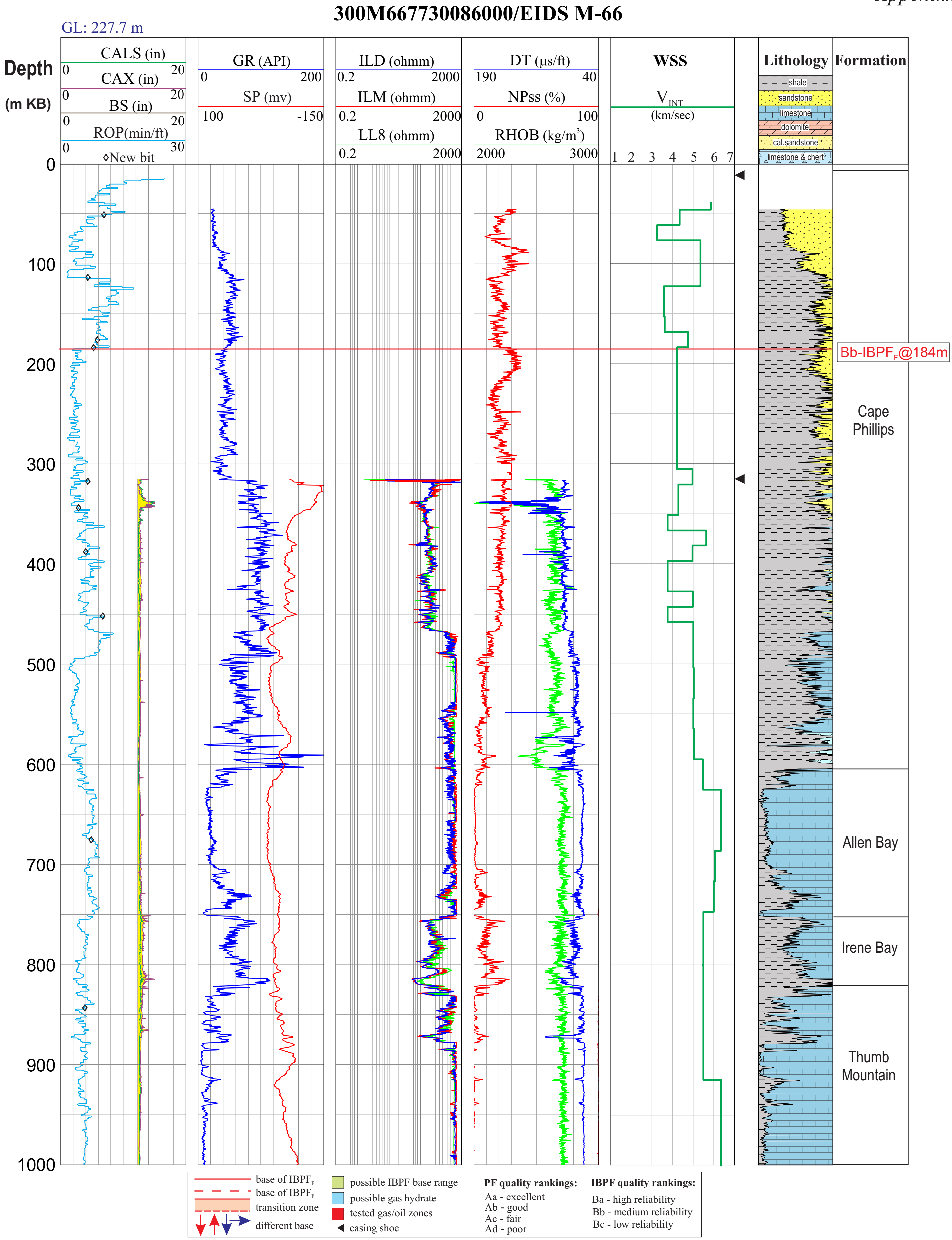

Figure 3-23. Estimation of base of $IBPF_F$ with "Bb" quality mainly using drilling rate and well seismic surveys for the Eids M-66 well on Ellesmere Island in the Canadian Arctic Islands.

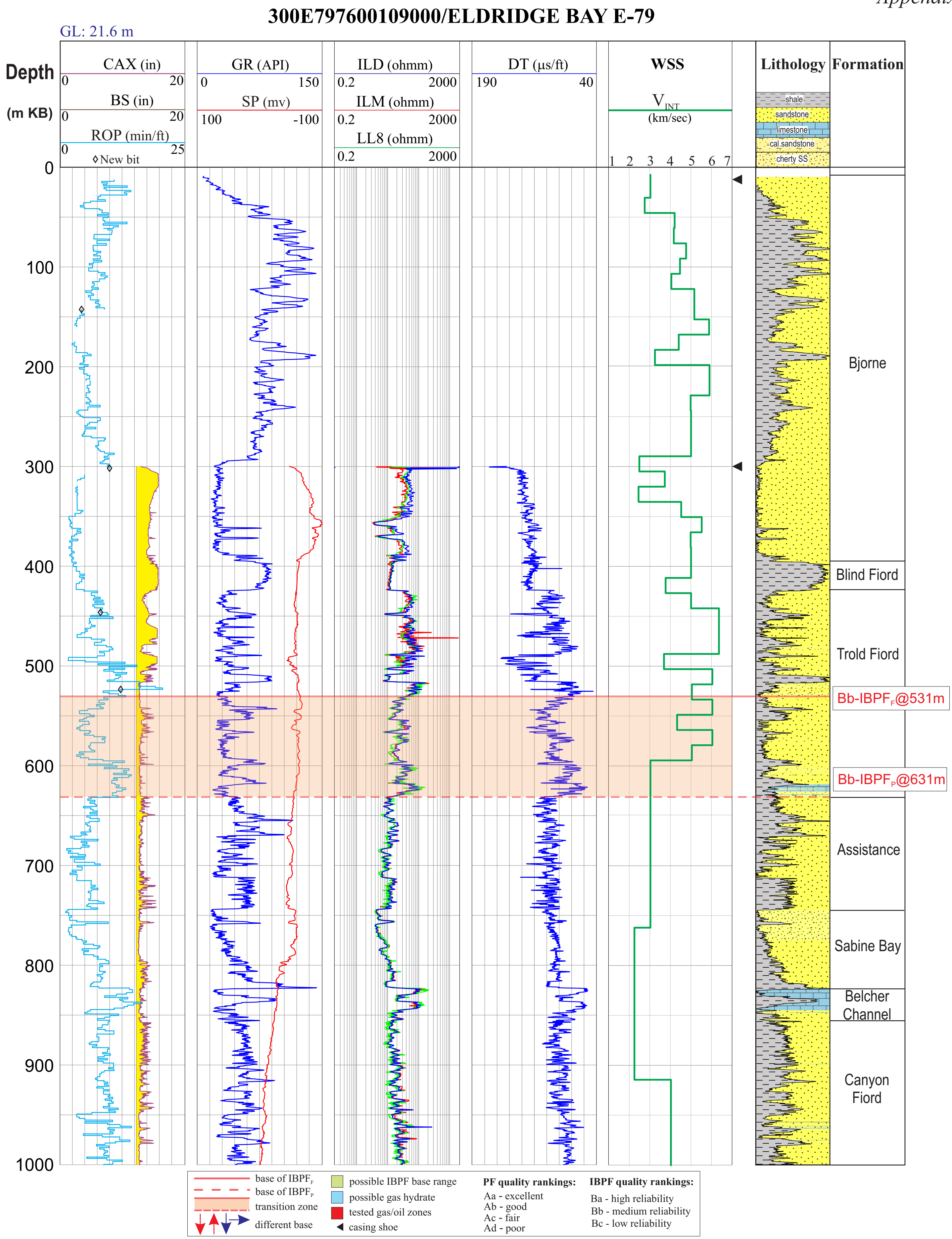

Figure 3-24. Estimations of base of $IBPF_F$ with "Bb" quality and $IBPF_P$ with "Bb" quality using well logs and well seismic surveys for the Eldridge Bay E-79 well on Melville Island in the Canadian Arctic Islands.

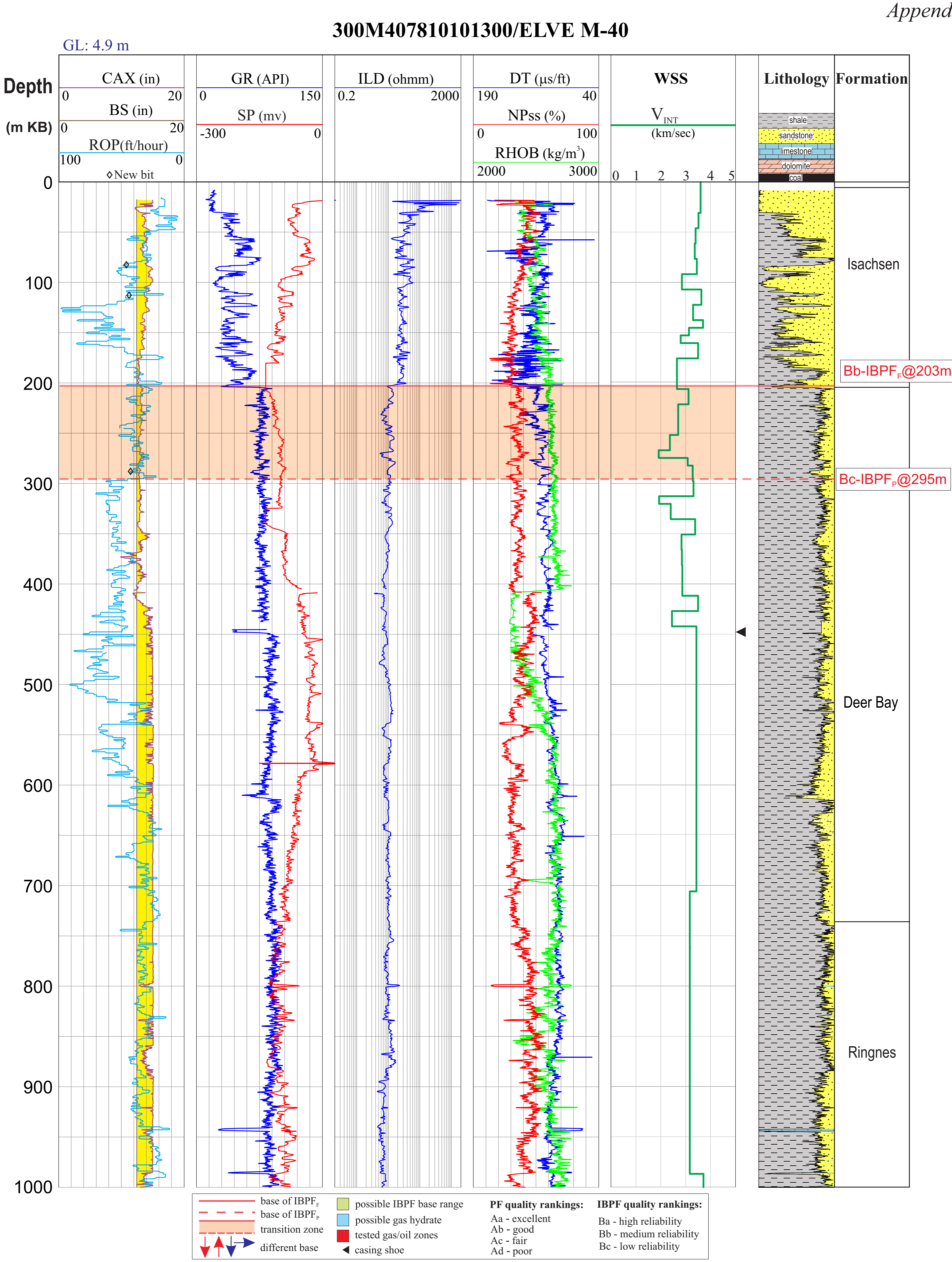

Figure 3-25. Determinations of base of $IBPF_F$ with "Bb" quality and $IBPF_P$ with "Bc" quality using well logs and well seismic surveys for the Elve M-40 well on Ellef Ringnes Island in the Canadian Arctic Islands.

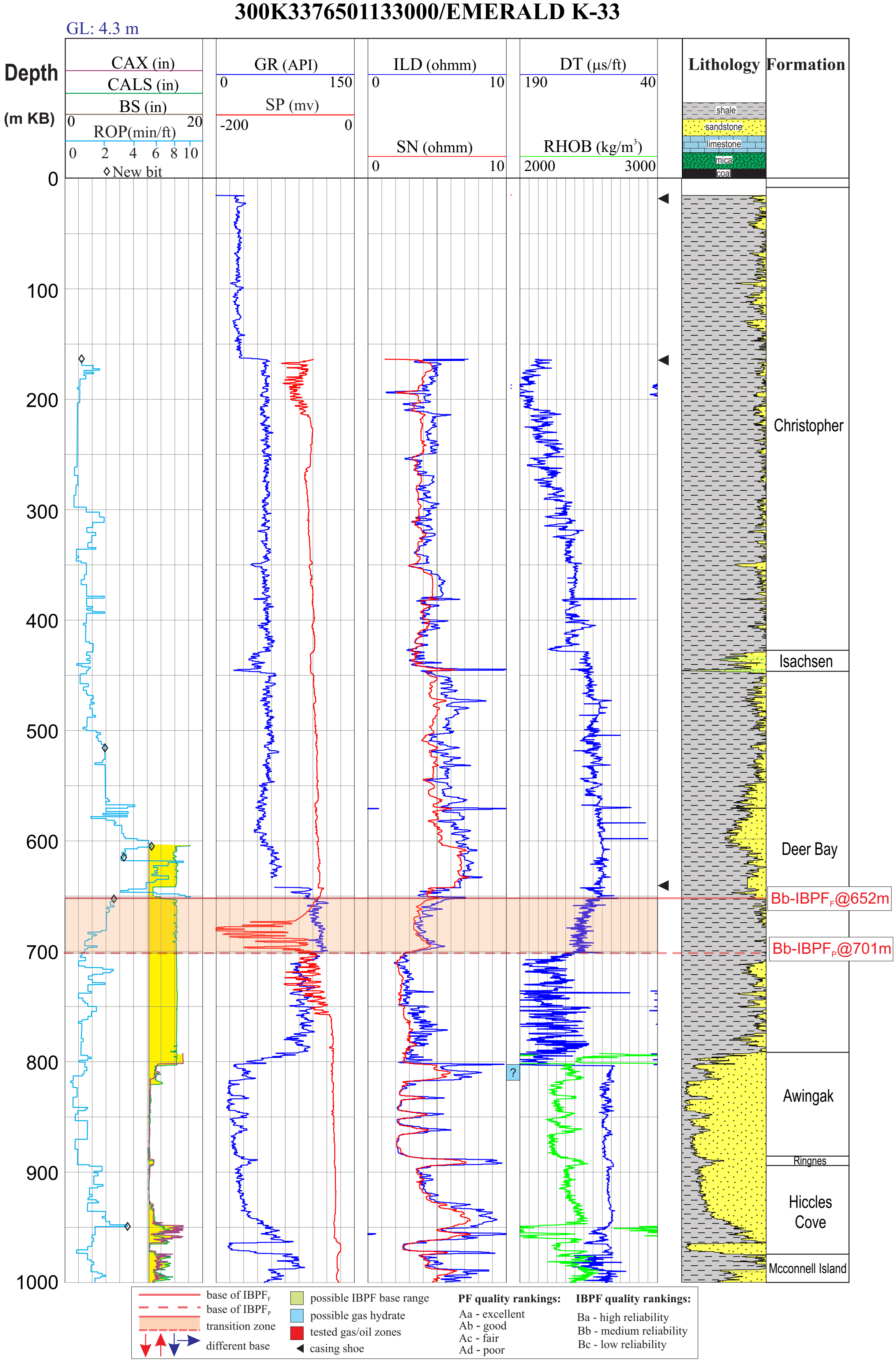

Figure 3-26. Determinations of base of $IBPF_F$ with "Bb" quality and $IBPF_P$ with "Bb" quality from well logs for the Emerald K-33 well on Melville Island in the Canadian Arctic Islands.

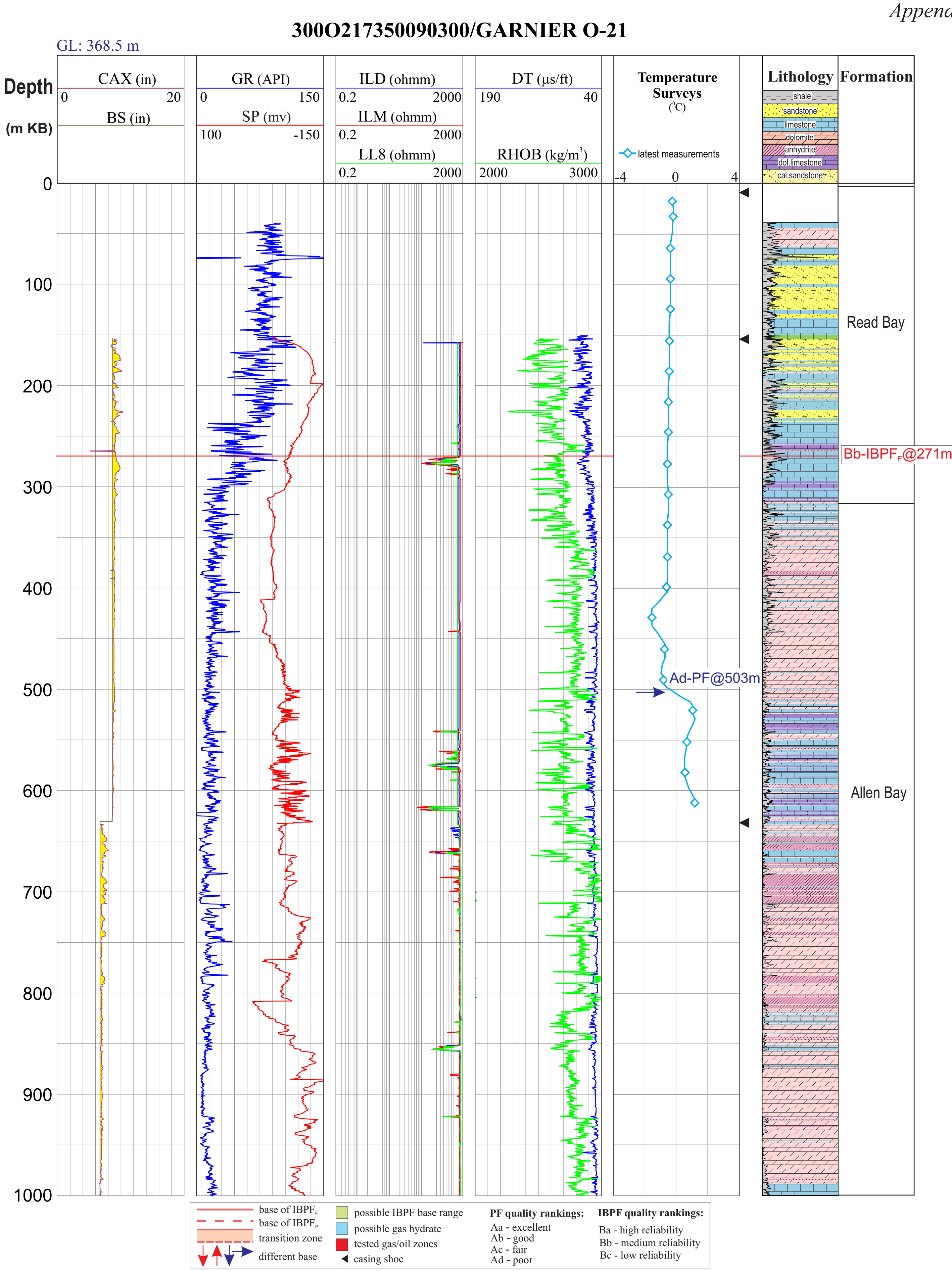

Figure 3-27. Determination of base of $IBPF_F$ with "Bb" quality from well logs and thermally defined PF with "Ad" quality for the Garnier O-21 well on Somerset Island in the Canadian Arctic Islands.

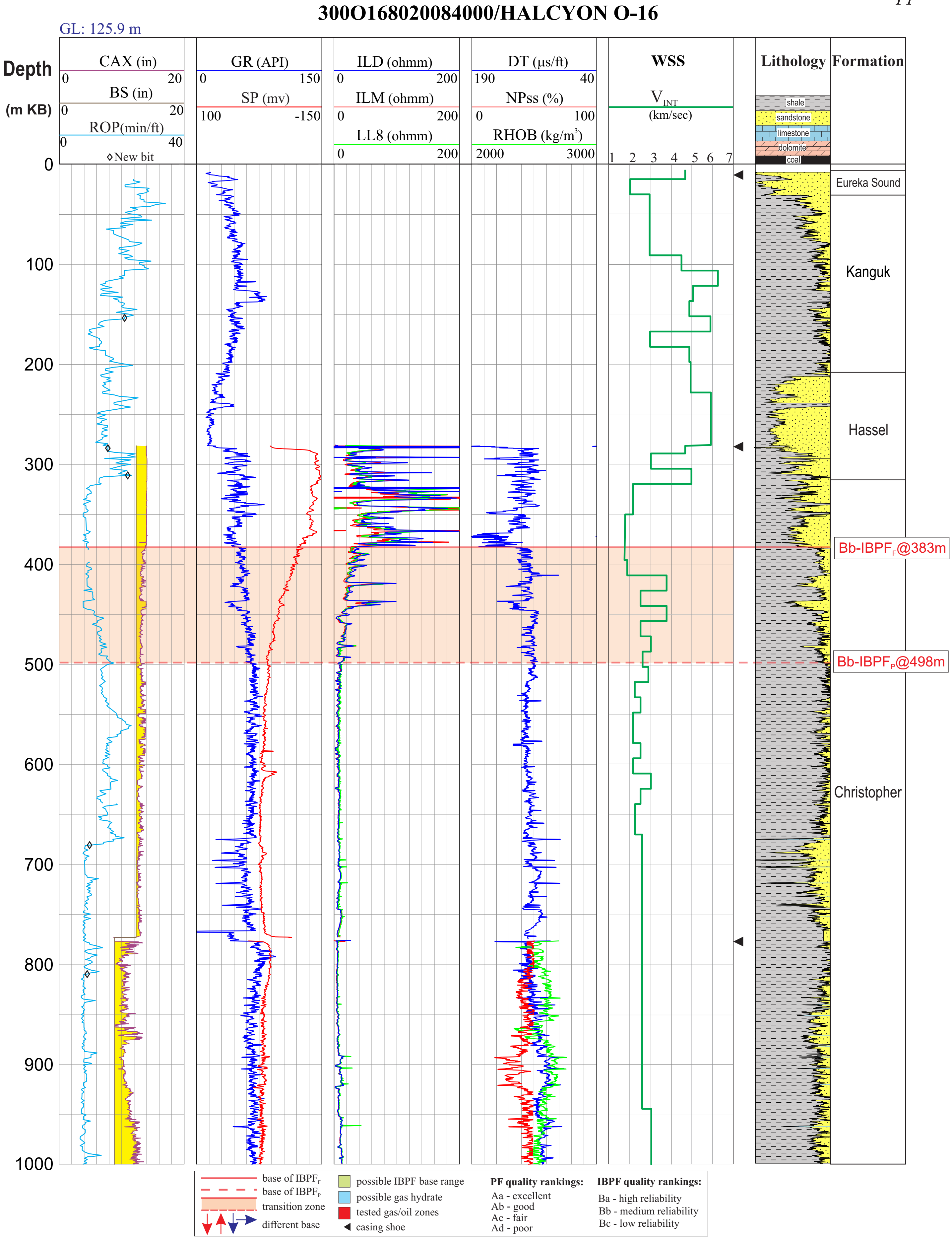

Figure 3-28. Determinations of base of $IBPF_F$ with "Bb" quality and $IBPF_P$ with "Bb" quality using well logs and well seismic surveys for the Halcyon O-16 well on Ellesmere Island in the Canadian Arctic Islands.

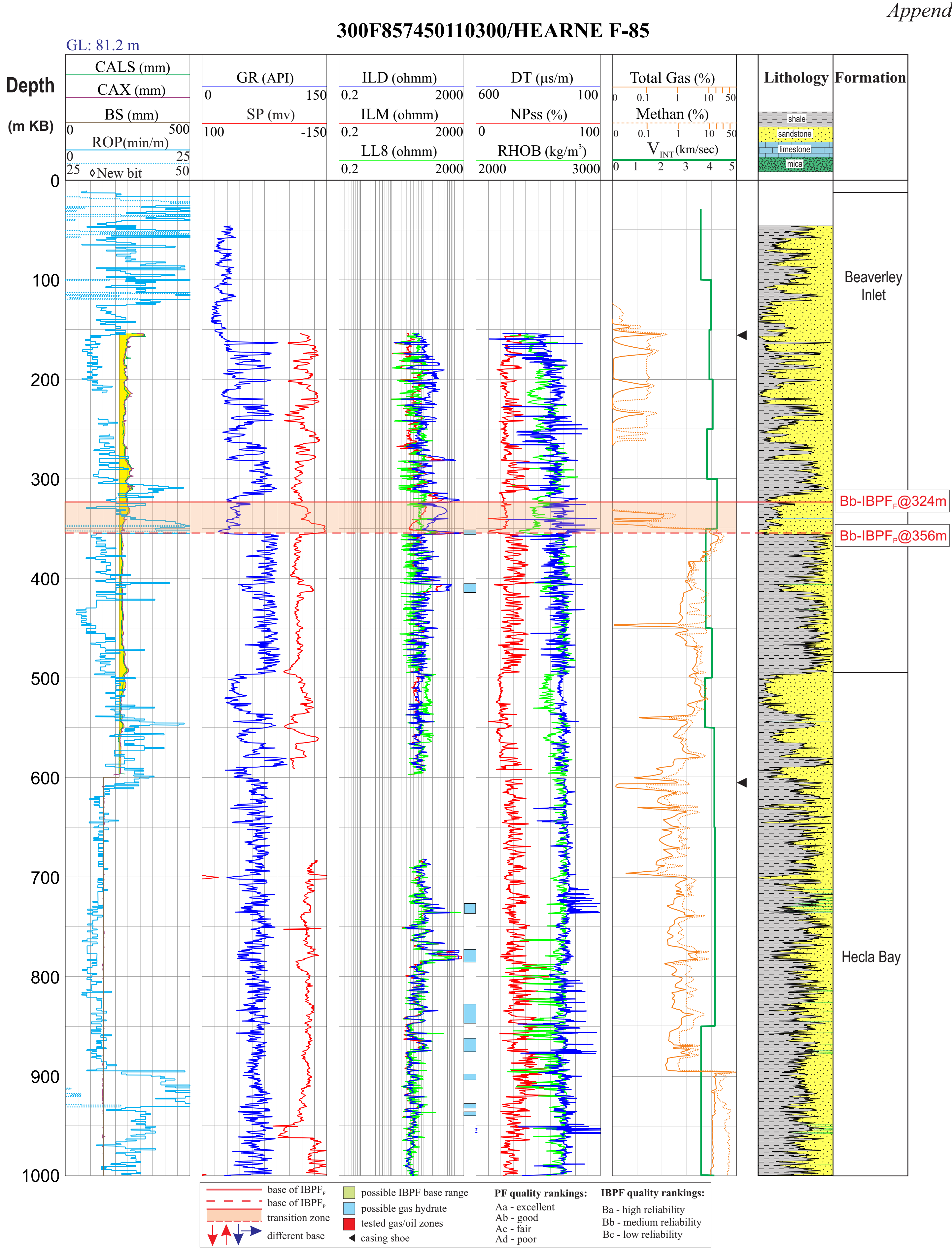

Figure 3-29. Determinations of base of $IBPF_F$ with "Bb" quality and $IBPF_P$ with "Bb" quality using well logs, well seismic surveys and other information for the Hearne F-85 well on Melville Island in the Canadian Arctic Islands.

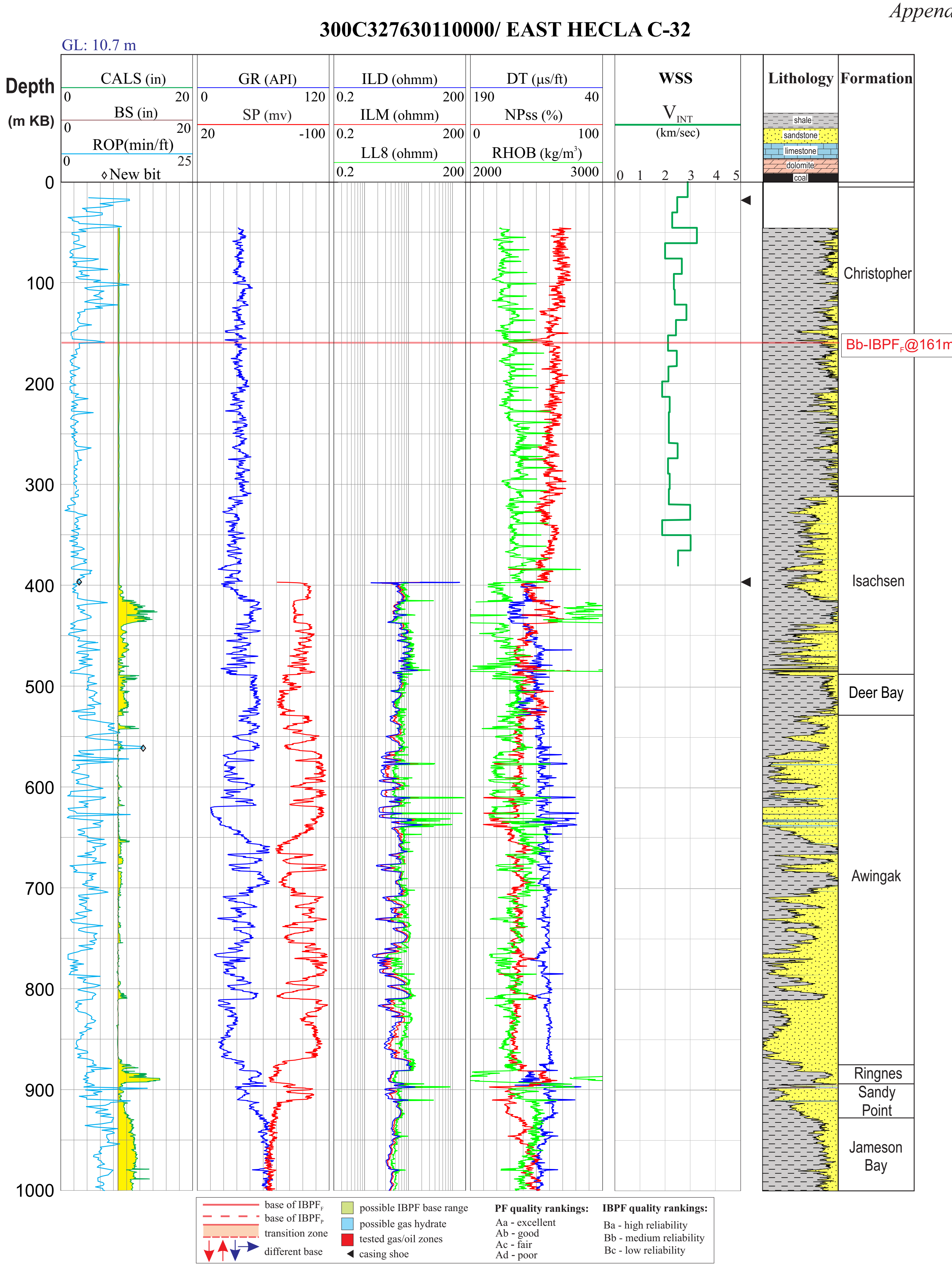

Figure 3-30. Estimation of base of $IBPF_F$ with "Bb" quality using drilling rate and well seismic surveys for the East Hecla C-32 well on Melville Island in the Canadian Arctic Islands.

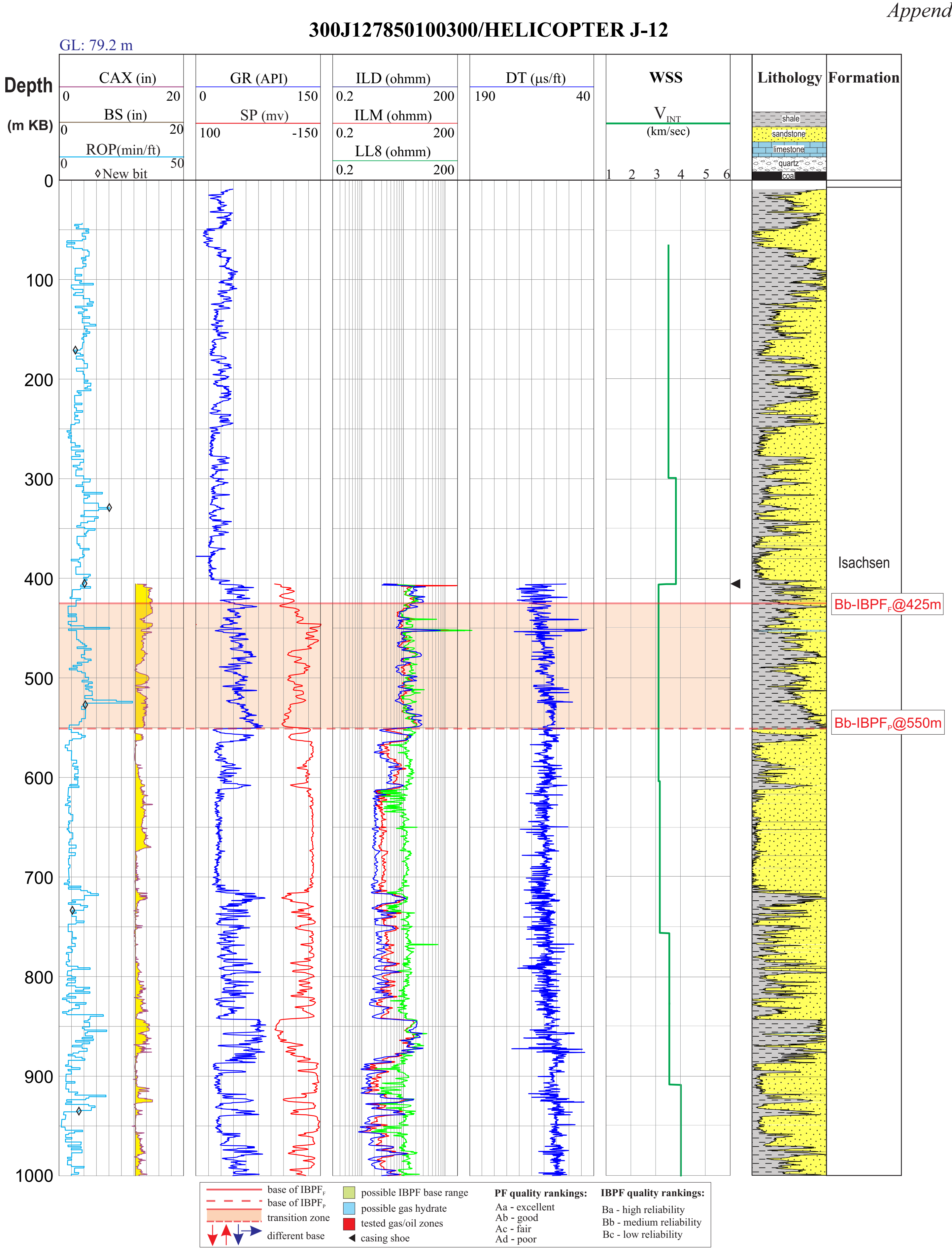

Figure 3-31. Determinations of base of $IBPF_F$ with "Bb" quality and $IBPF_P$ with "Bb" quality using well logs and welll seismic surveys for the Helicopter J-12 well on Ellef Ringnes Island in the Canadian Arctic Islands.

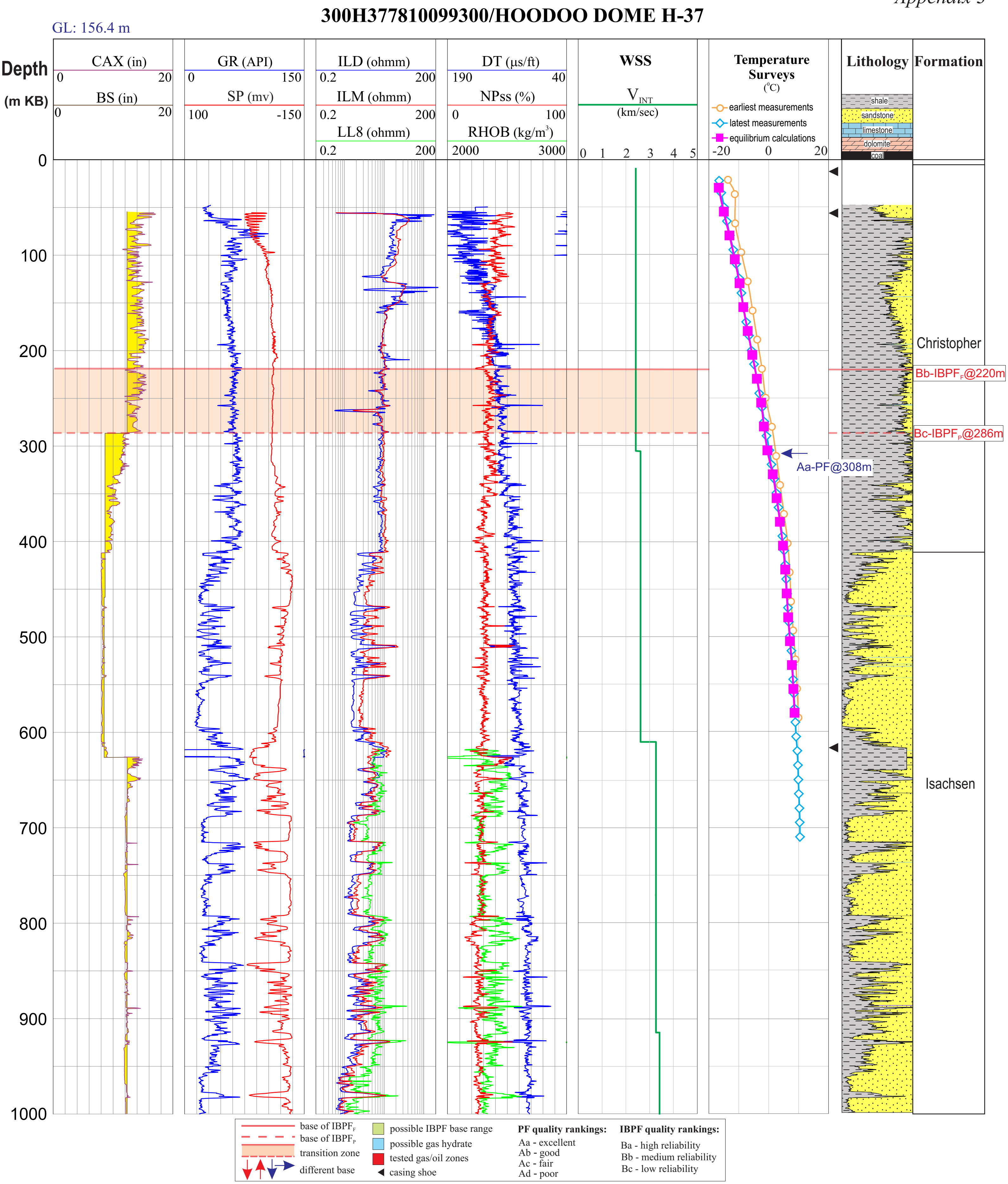

Figure 3-32. Determinations of base of $IBPF_F$ with "Bb" quality and $IBPF_P$ with "Bc" quality using well logs and welll seismic surveys, and base of PF from temperature surveys for the Hoodoo Dome H-37 well on Ellef Ringnes Island in the Canadian Arctic Islands.

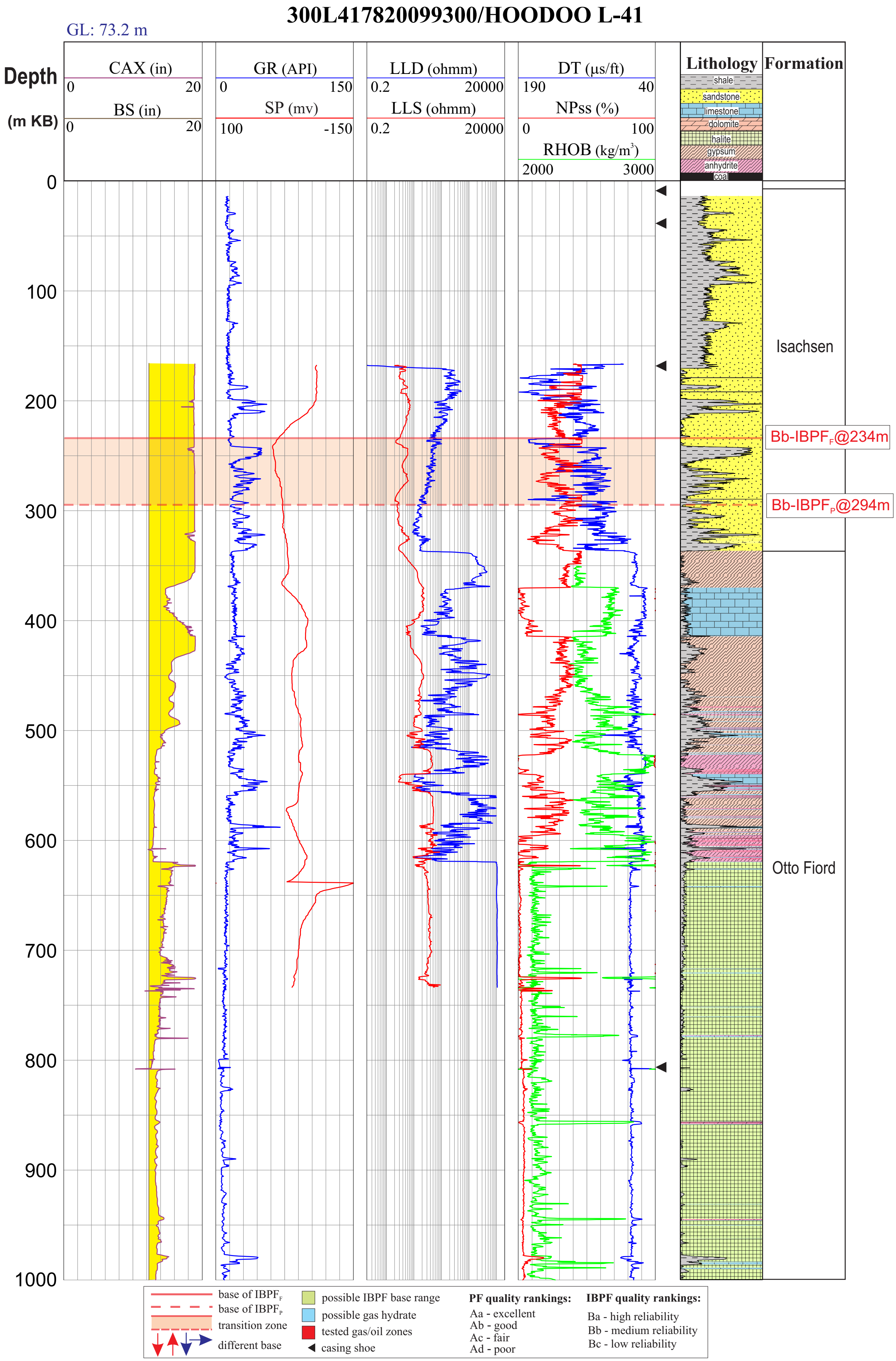

Figure 3-33. Determinations of base of $IBPF_F$ with “Bb” quality and $IBPF_P$ with “Bb” quality from well logs for the Hoodoo L-41 well on Ellef Ringnes Island in the Canadian Arctic Islands.

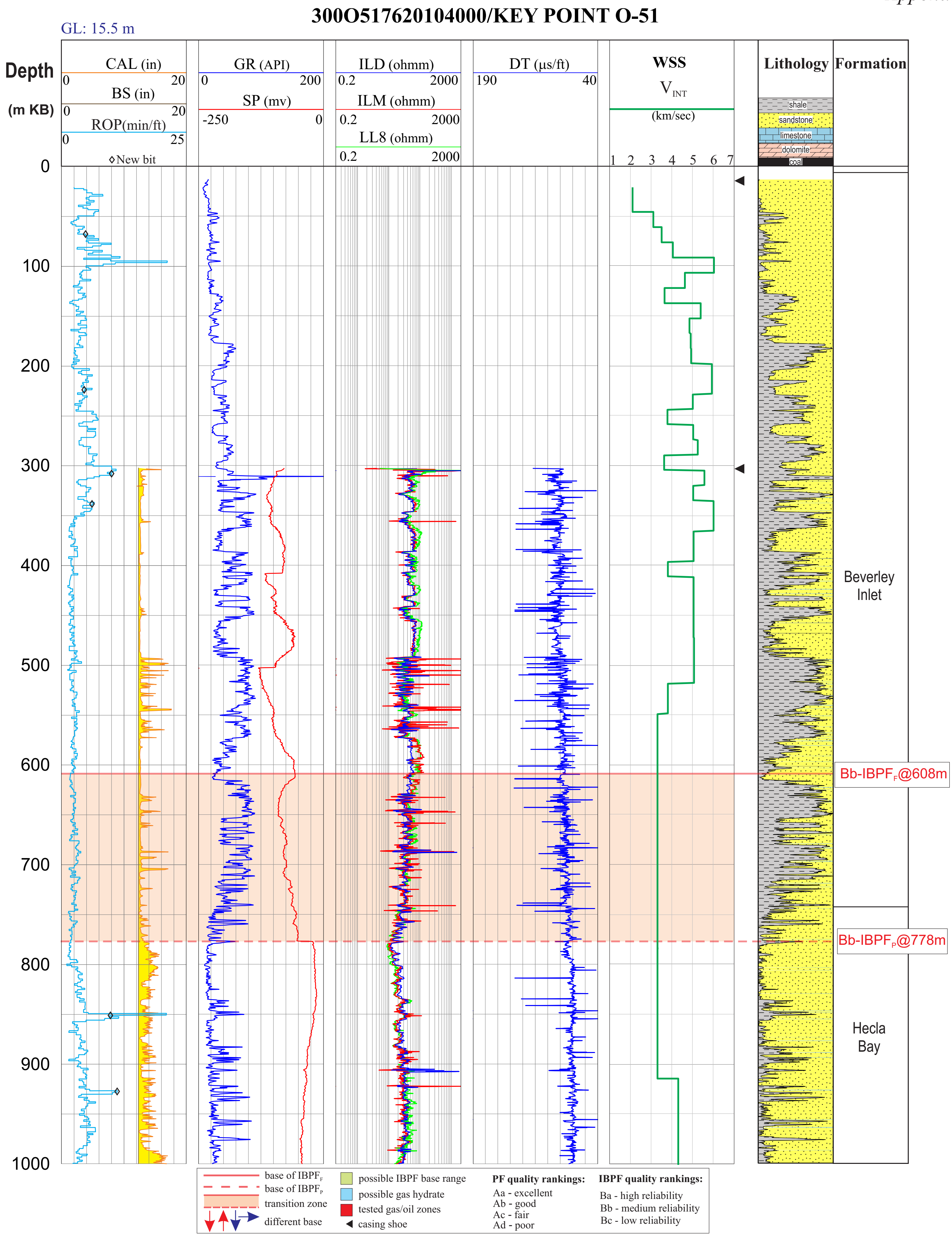

Figure 3-34. Determinations of base of $IBPF_F$ with "Bb" quality and $IBPF_P$ with "Bb" quality using well logs and welll seismic surveys for the Key Point O-51 well on Vanier Island in the Canadian Arctic Islands.

300B067820102300/KRISTOFFER BAY B-06

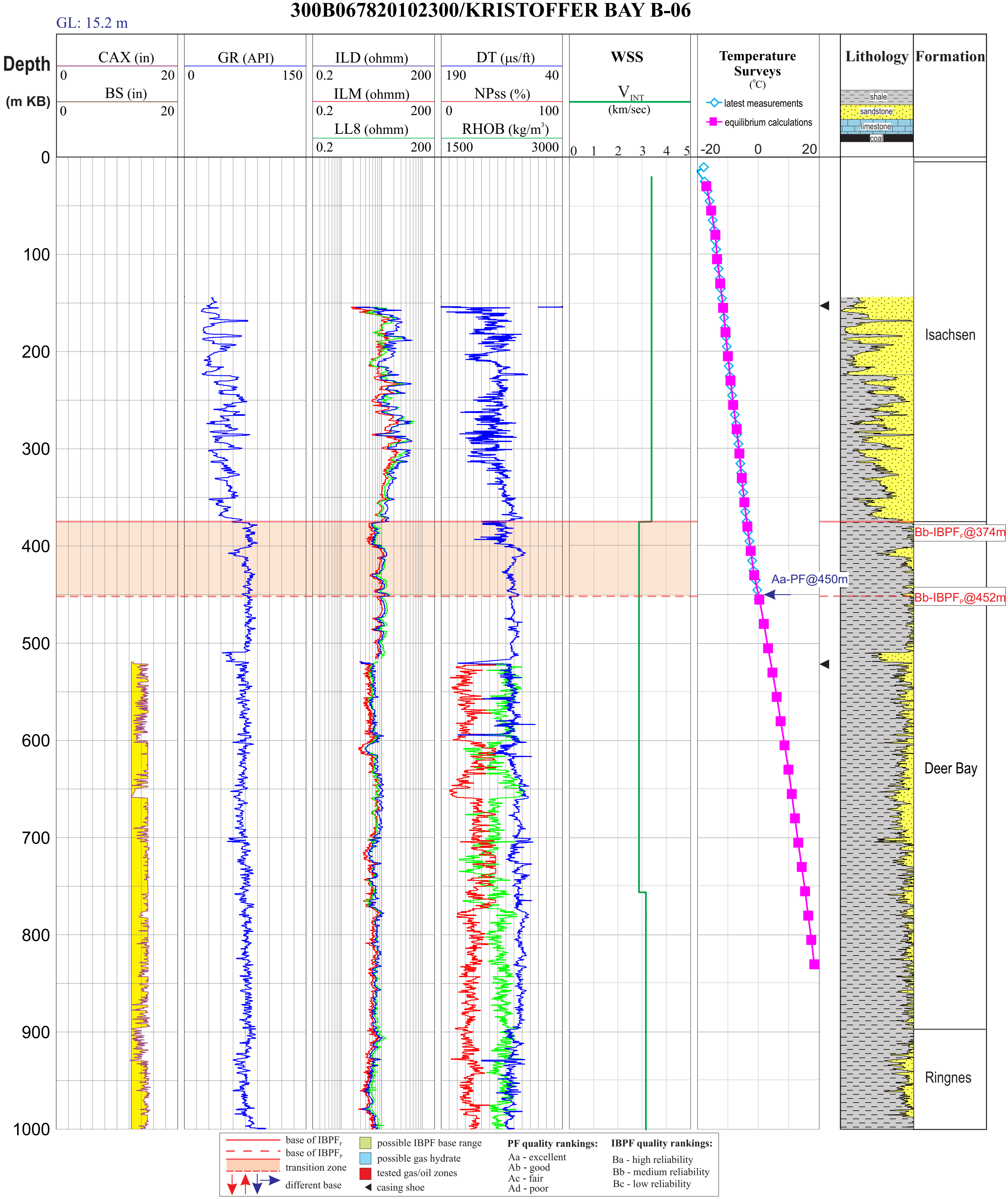

Figure 3-35. Determinations of base of $IBPF_F$ with "Bb" quality and $IBPF_P$ with "Bb" quality using well logs and welll seismic surveys, and base of PF from temperature surveys for the Kristoffer Bay B-06 well on Ellef Ringnes Island in the Canadian Arctic Islands.

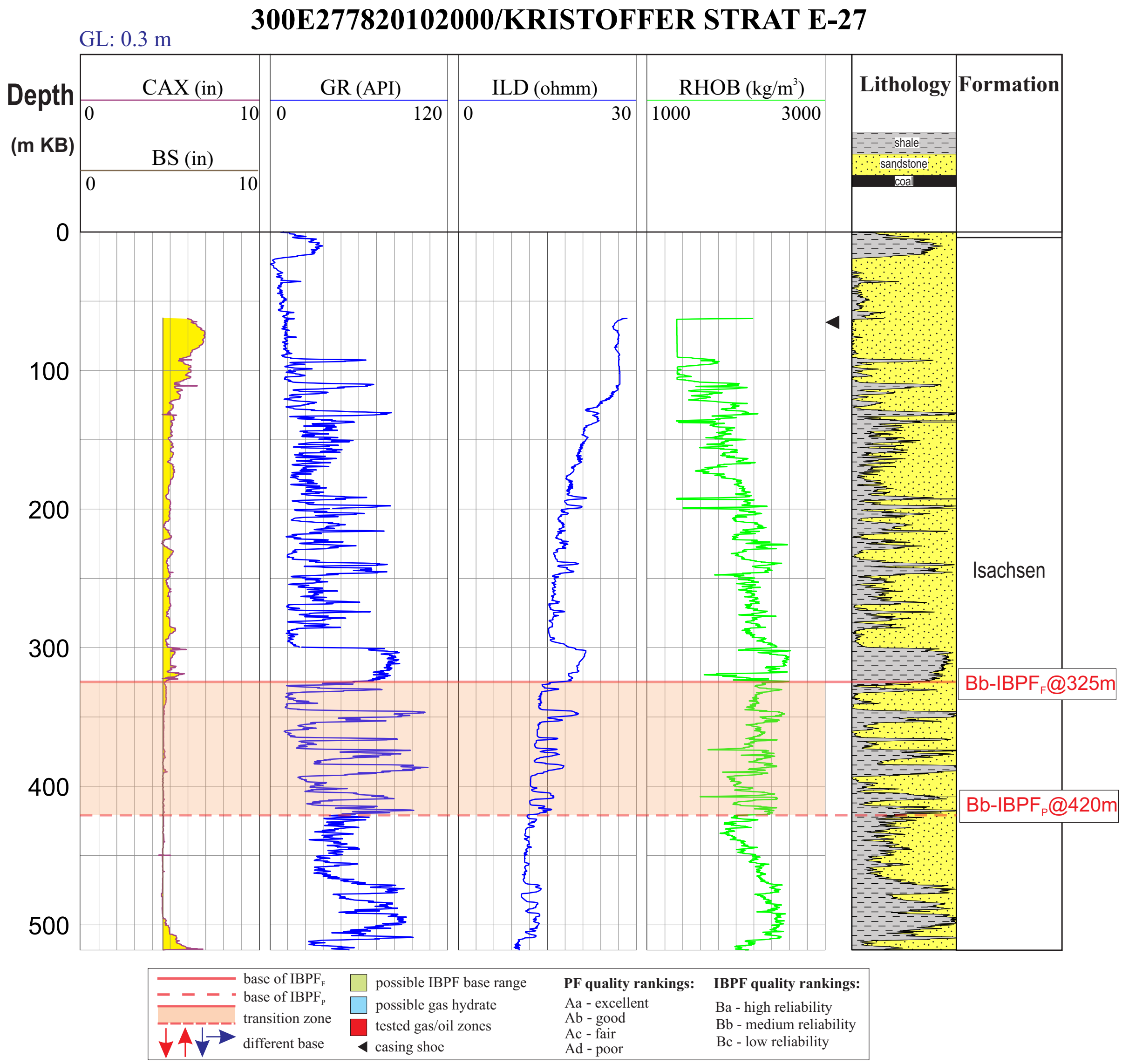

Figure 3-36. Determinations of base of $IBPF_F$ with “Bb” quality and $IBPF_P$ with “Bb” quality from well logs for the Kristoffer Strat E-27 well on Ellef Ringnes Island in the Canadian Arctic Islands.

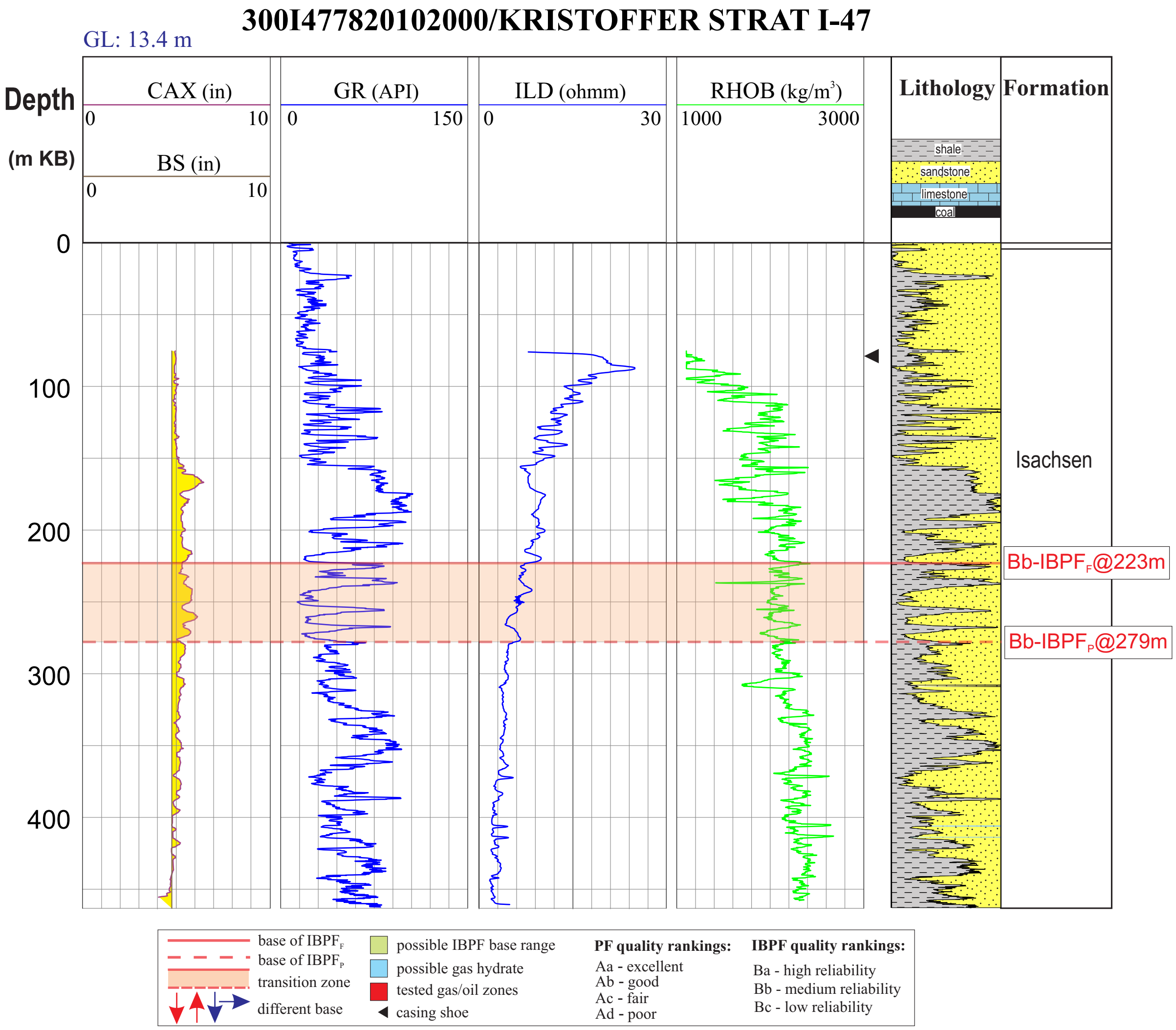

Figure 3-37. Determinations of base of $IBPF_F$ with "Bb" quality and $IBPF_P$ with "Bb" quality from well logs for the Kristoffer Strat I-47 well on Ellef Ringnes Island in the Canadian Arctic Islands.

300P467750097300/LINCKENS ISLAND P-46

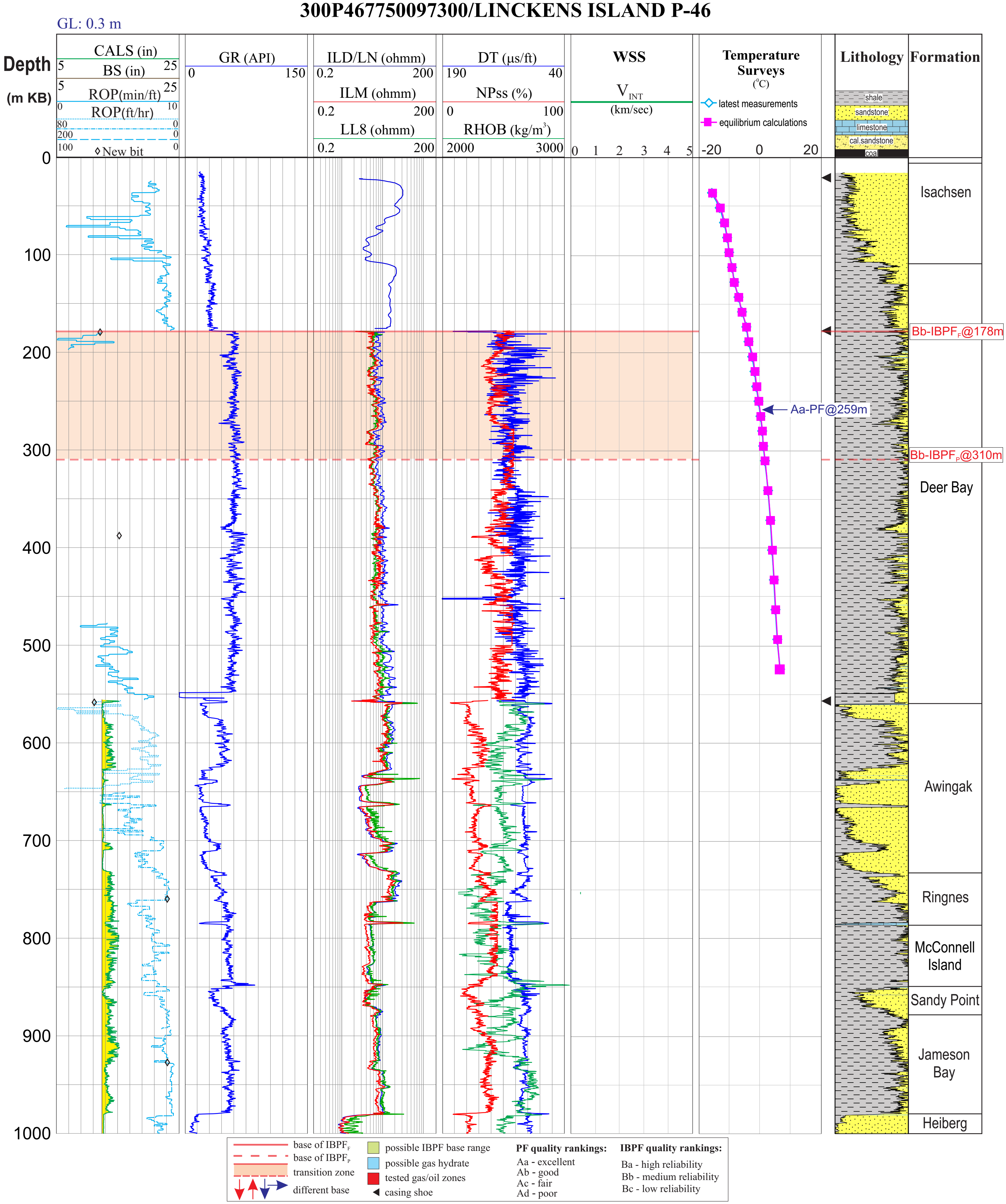

Figure 3-38. Determinations of base of $IBPF_F$ with "Bb" quality and $IBPF_P$ with "Bb" quality using well logs and welll seismic surveys, and base of PF from temperature surveys for the Linckens Island P-46 well on Linckens Island in the Canadian Arctic Islands.

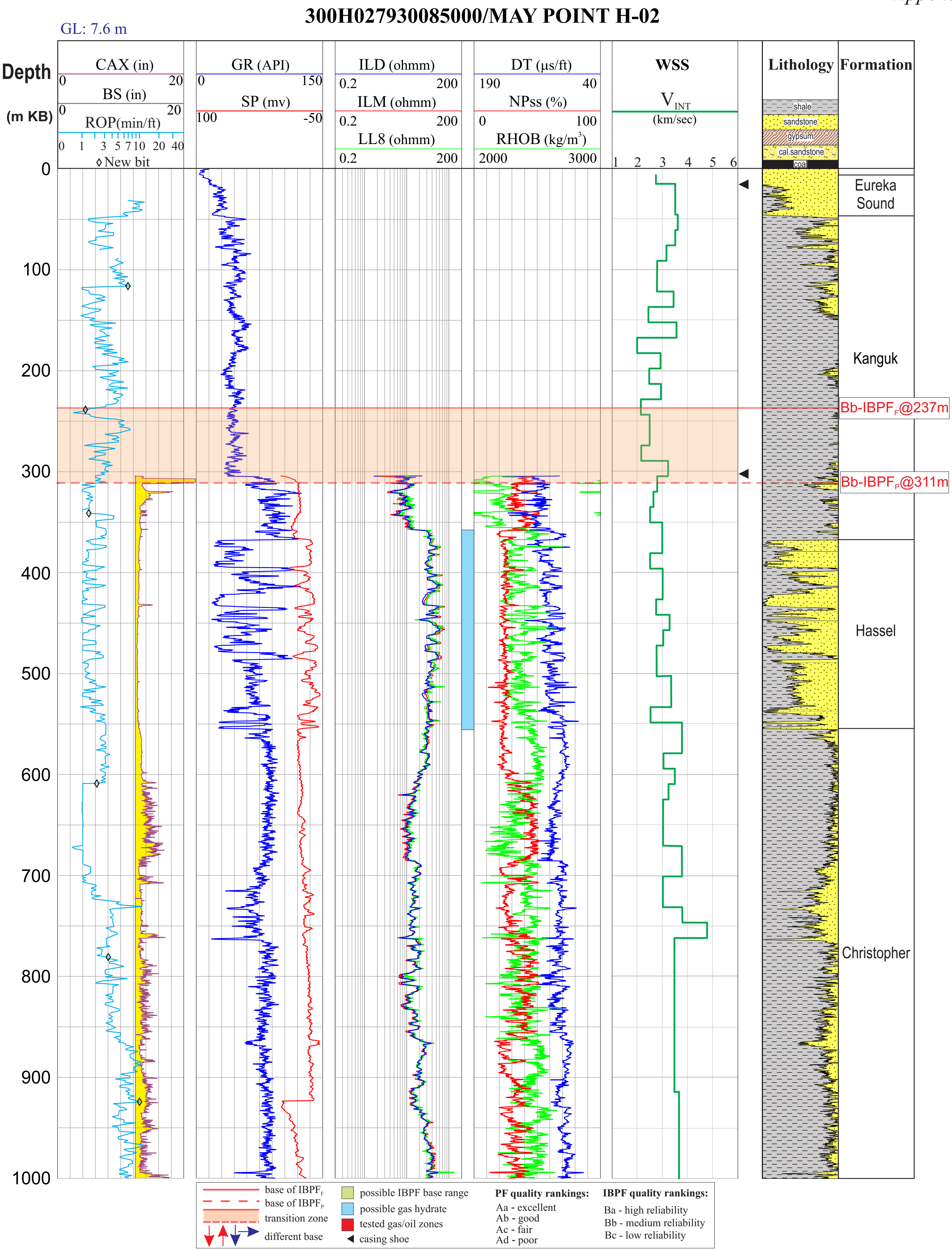

Figure 3-39. Determinations of base of $IBPF_F$ with "Bb quality and $IBPF_P$ with "Bb" quality using well seismic surveys and well logs in the May Point H-02 well on Axel Heiberg Island in the Canadian Arctic Islands.

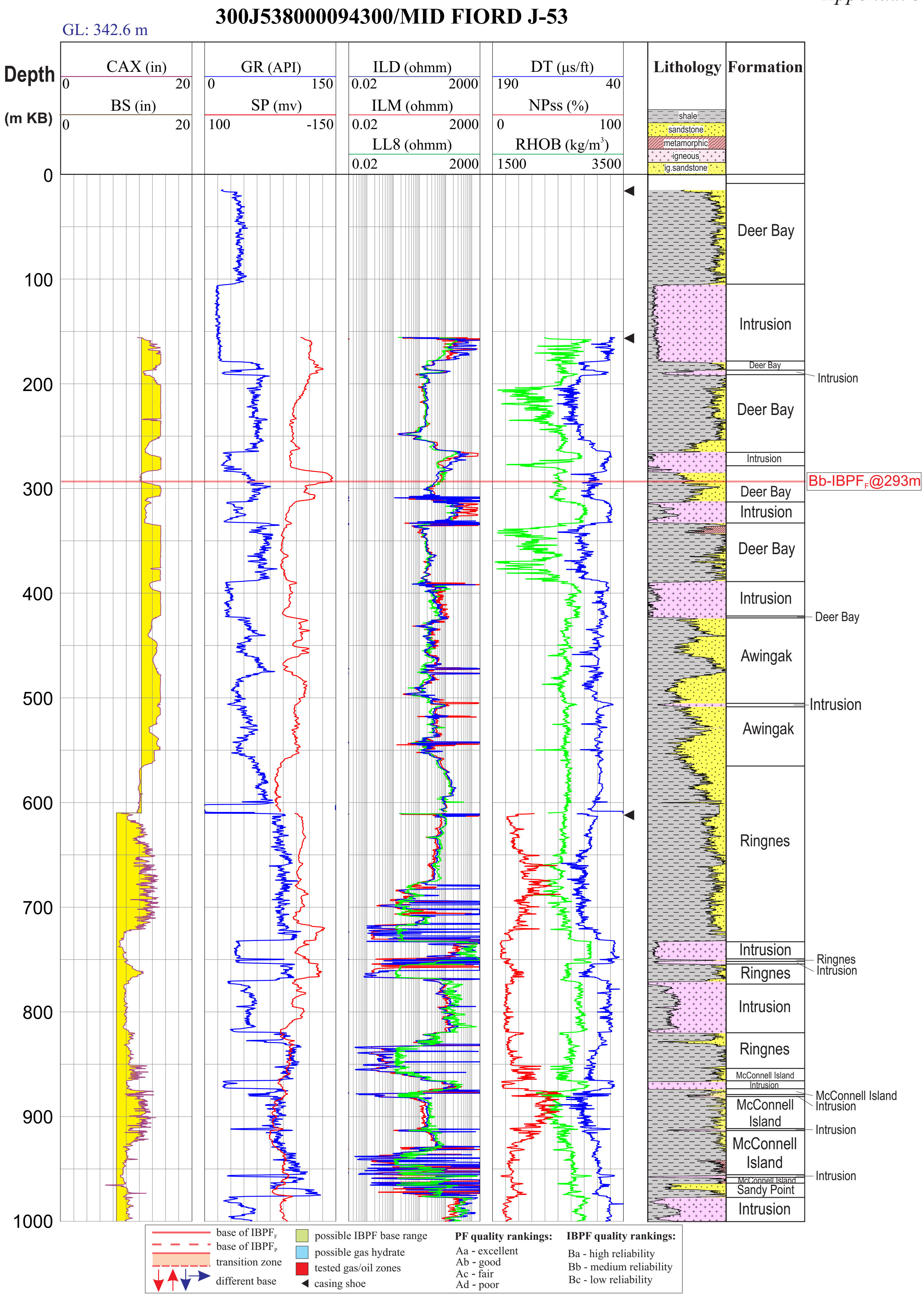

Figure 3-40. Determination of base of $IBPF_F$ with "Bb" quality from well logs for the Mid Fiord J-53 well on Axel Heiberg Island in the Canadian Arctic Islands.

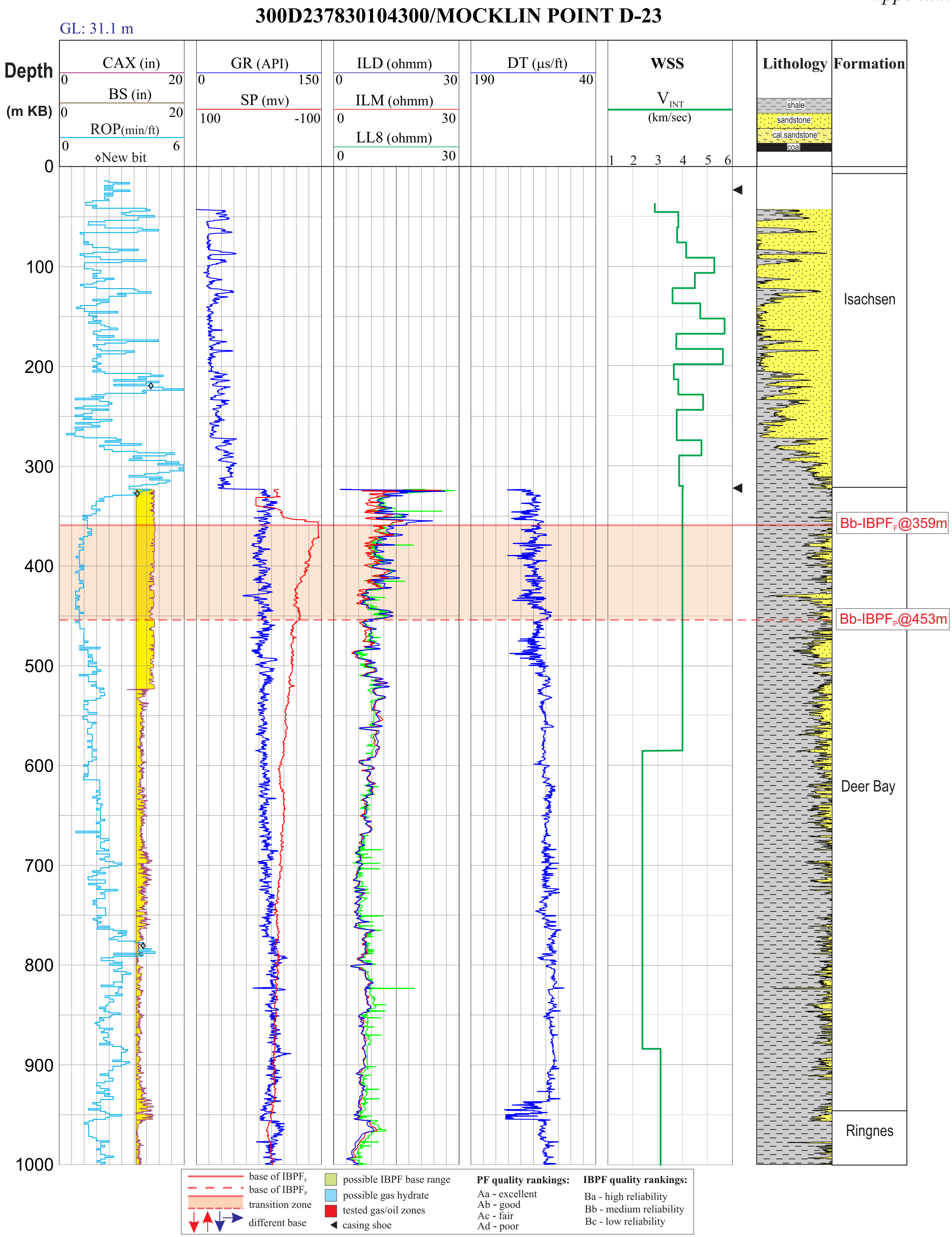

Figure 3-41. Determinations of base of $IBPF_F$ with "Bb" quality and $IBPF_P$ with "Bb" quality using well logs and welll seismic surveys for the Mocklin Point D-23 well on Ellef Ringnes Island in the Canadian Arctic Islands.

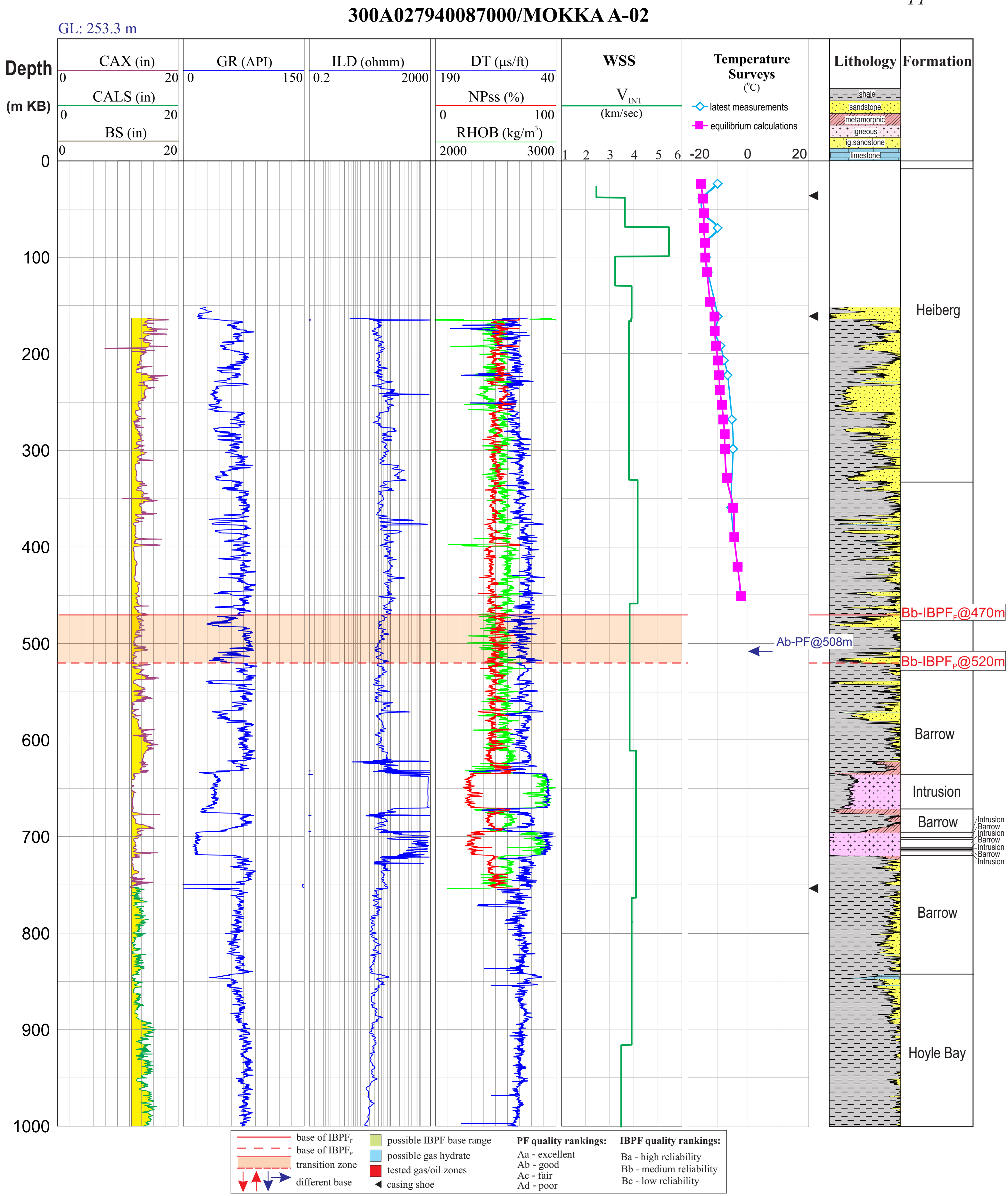

Figure 3-42. Determinations of base of $IBPF_F$ with "Bb" quality and $IBPF_P$ with "Bb" quality using well logs and welll seismic surveys, and base of PF from temperature surveys for the Mokka A-02 well on Axel Heiberg Island in the Canadian Arctic Islands.

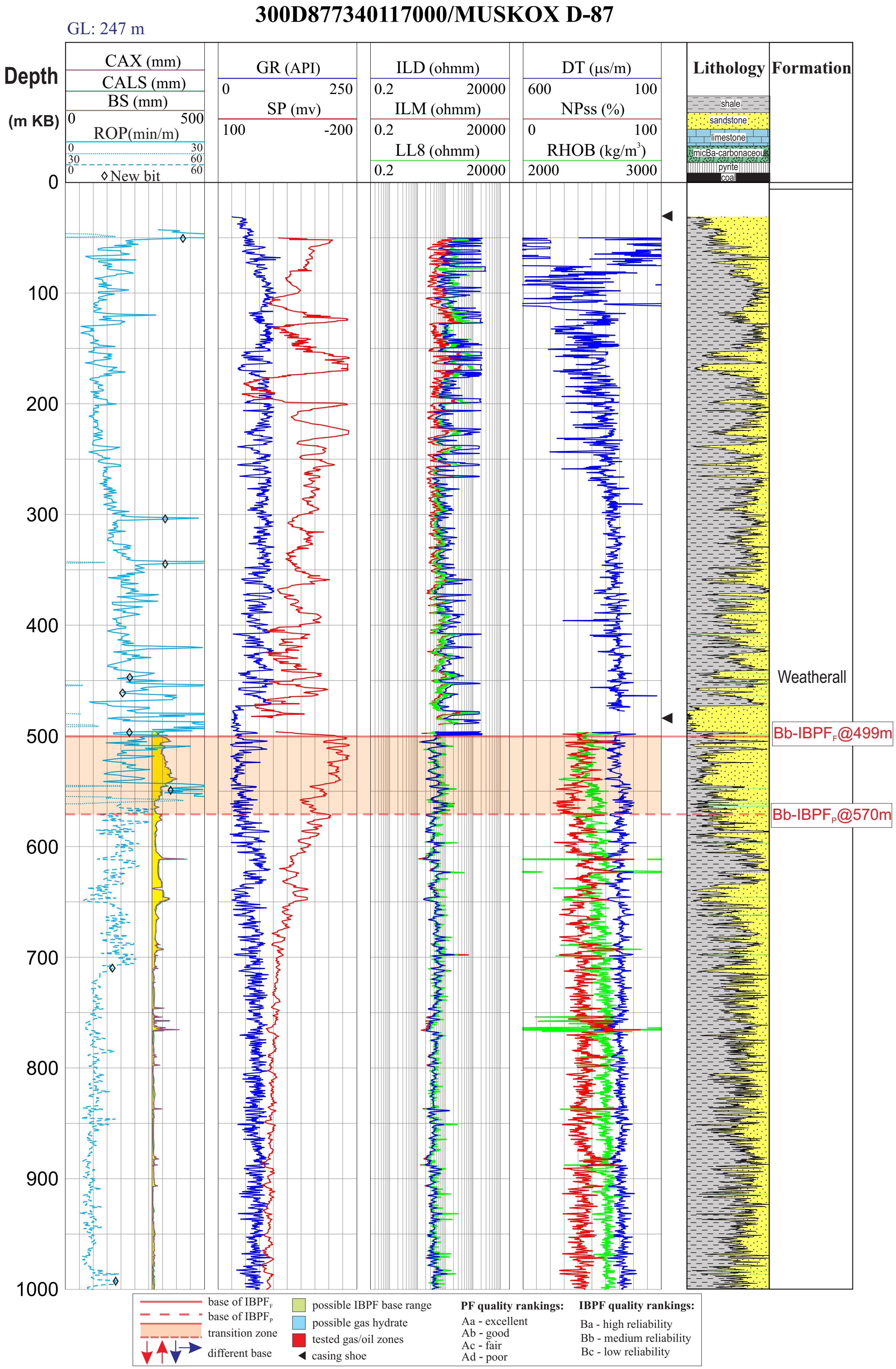

Figure 3-43. Determinations of base of $IBPF_F$ with "Bb" quality and $IBPF_P$ with "Bb" quality from well logs for the Muskox D-87 well on Banks Island in the Canadian Arctic Islands.

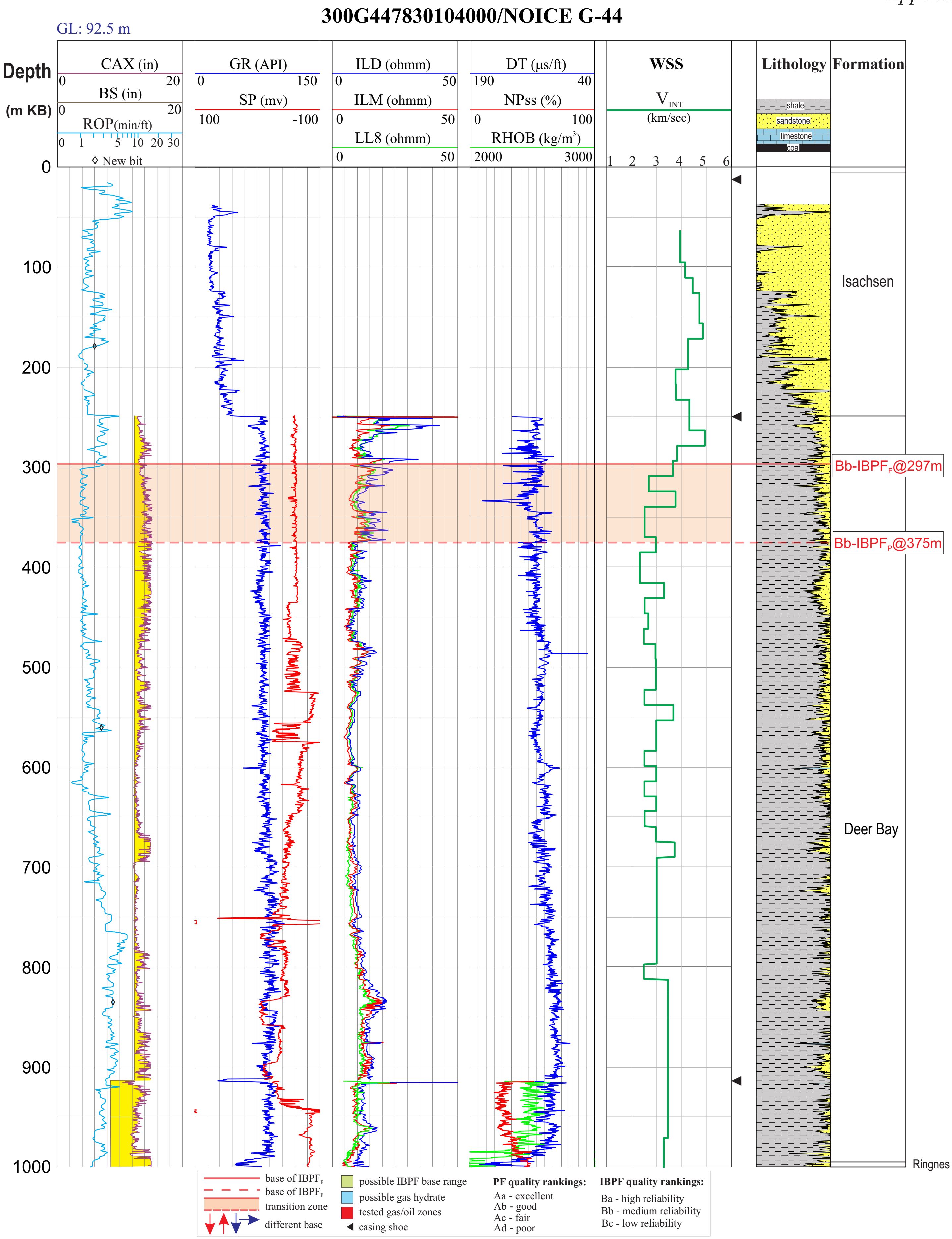

Figure 3-44. Determinations of base of $IBPF_F$ with “Bb” quality and $IBPF_P$ with “Bb” quality using well logs and welll seismic surveys for the Noice G-44 well on Ellef Ringnes Island in the Canadian Arctic Islands.

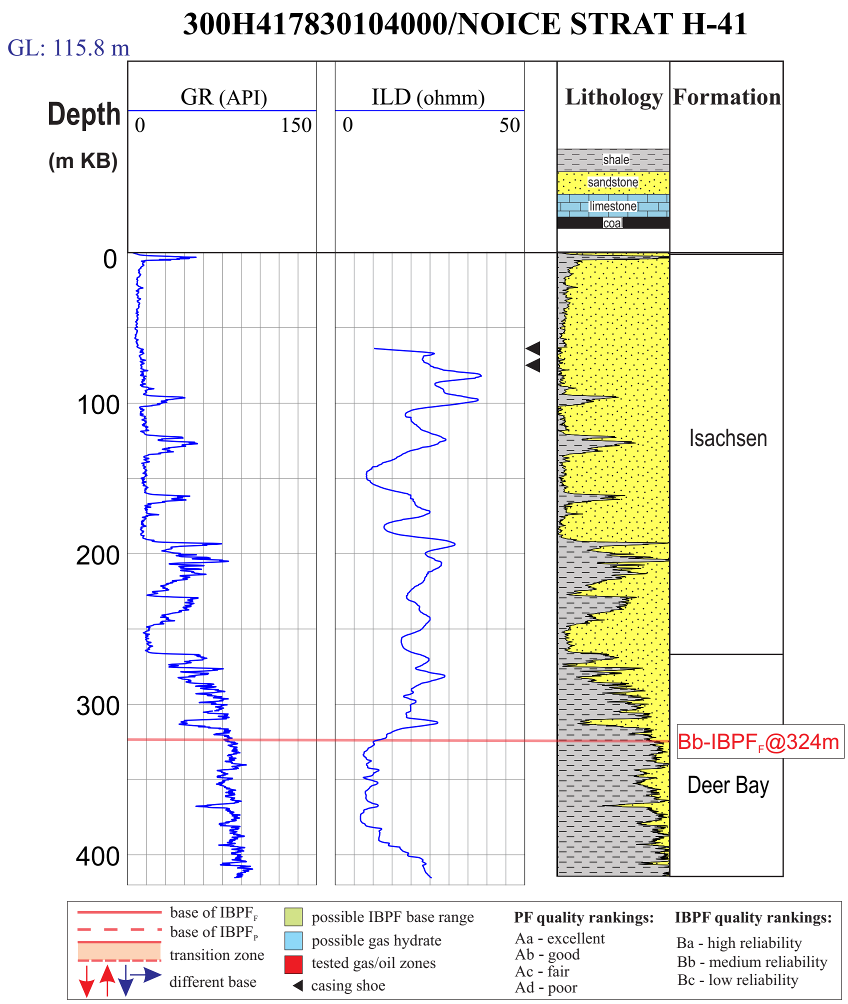

Figure 3-45. Determination of base of $IBPF_F$ with “Bb” quality from well logs for the Noice Strat H-41 well on Ellef Ringnes Island in the Canadian Arctic Islands.

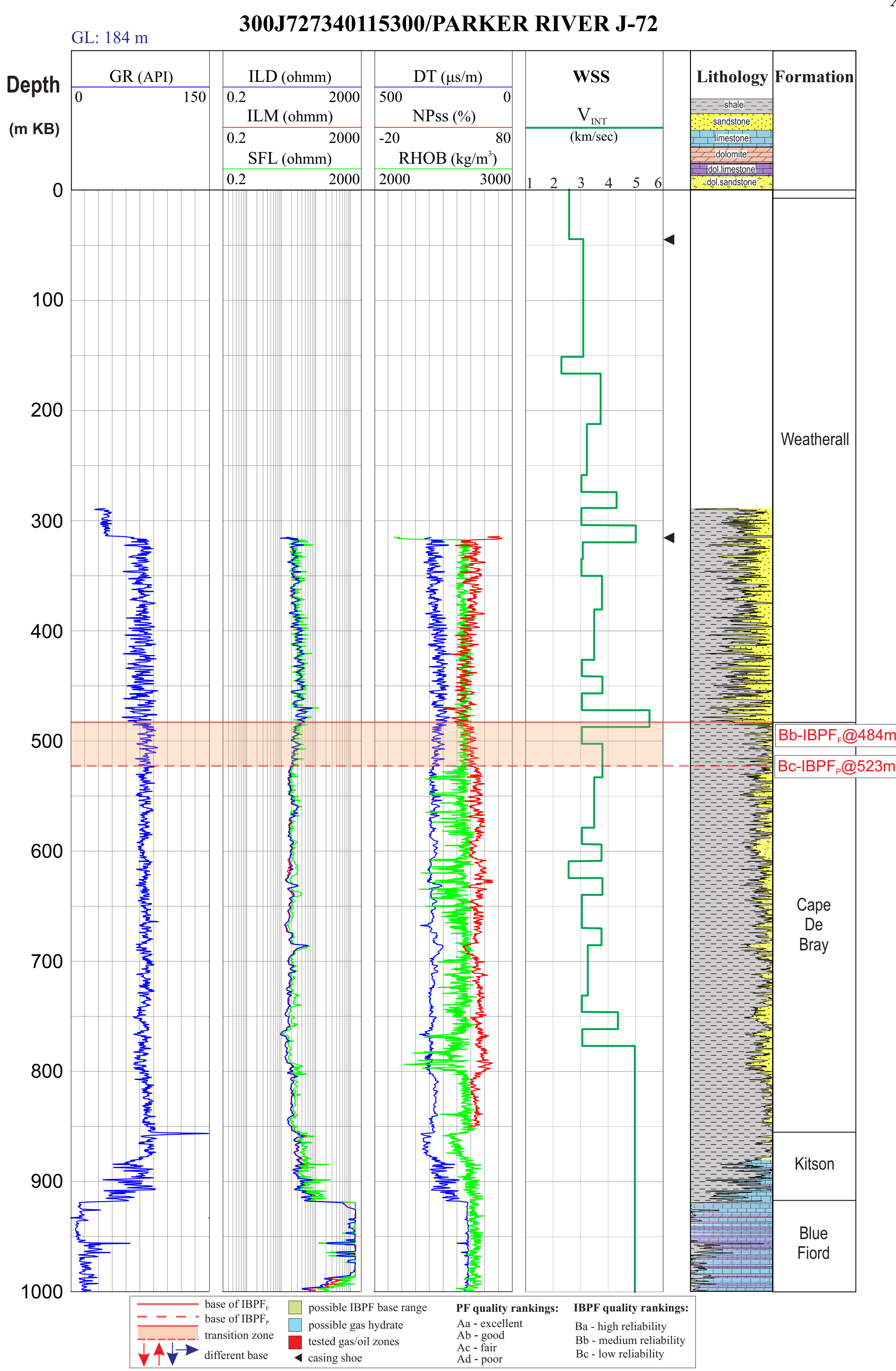

Figure 3-46. Determinations of base of $IBPF_F$ with “Bb” quality and $IBPF_P$ with “Bc” quality using well logs and welll seismic surveys for the Parker River J-72 well on Banks Island in the Canadian Arctic Islands.

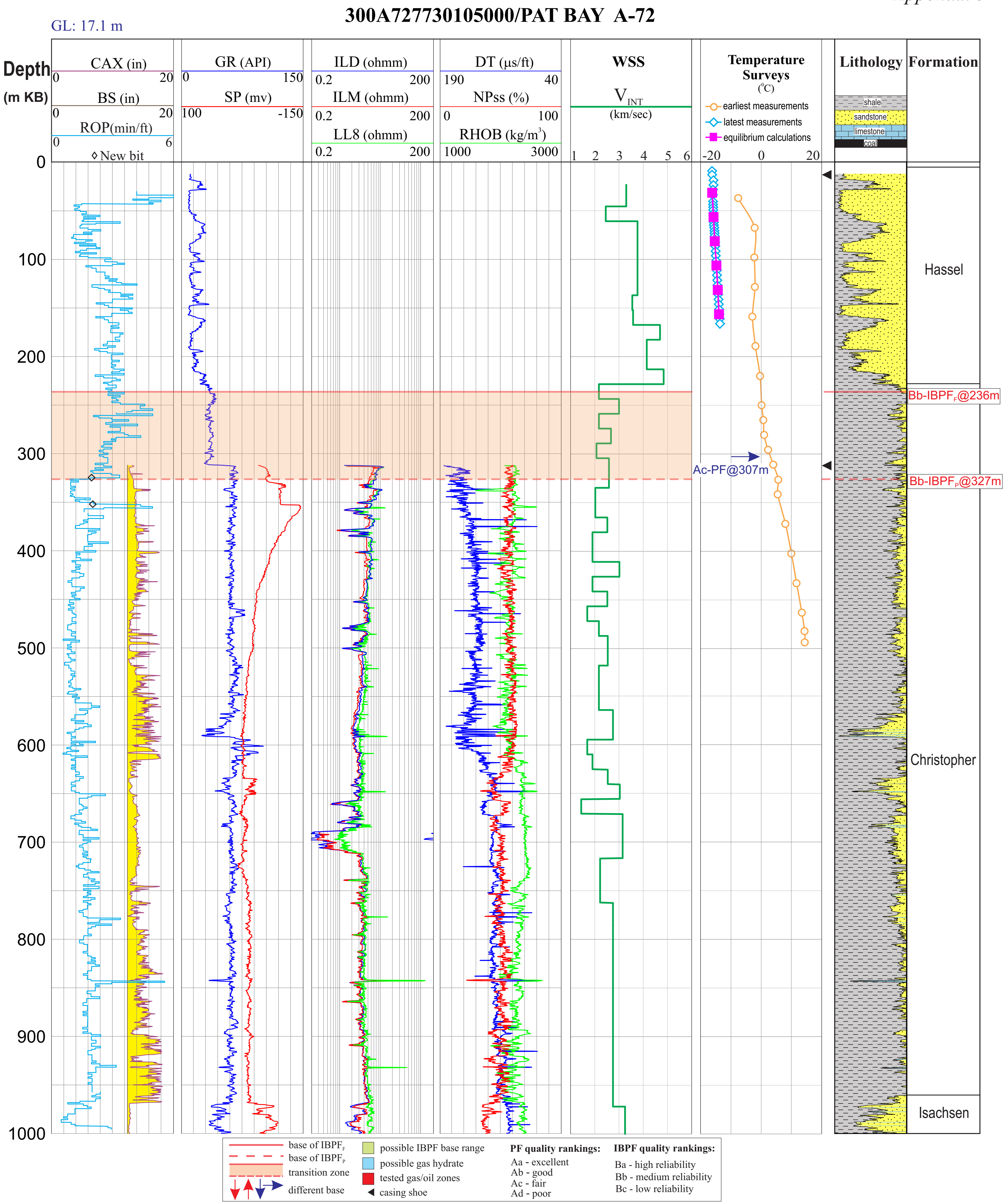

Figure 3-47. Estimations of base of $IBPF_F$ with “Bb” quality and $IBPF_P$ with “Bb” quality mainly from well seismic surveys and drilling rate, and base of PF from temperature surveys with "Ac" quality for the Pat Bay A-72 well on Lougheed Island in the Canadian Arctic Islands.

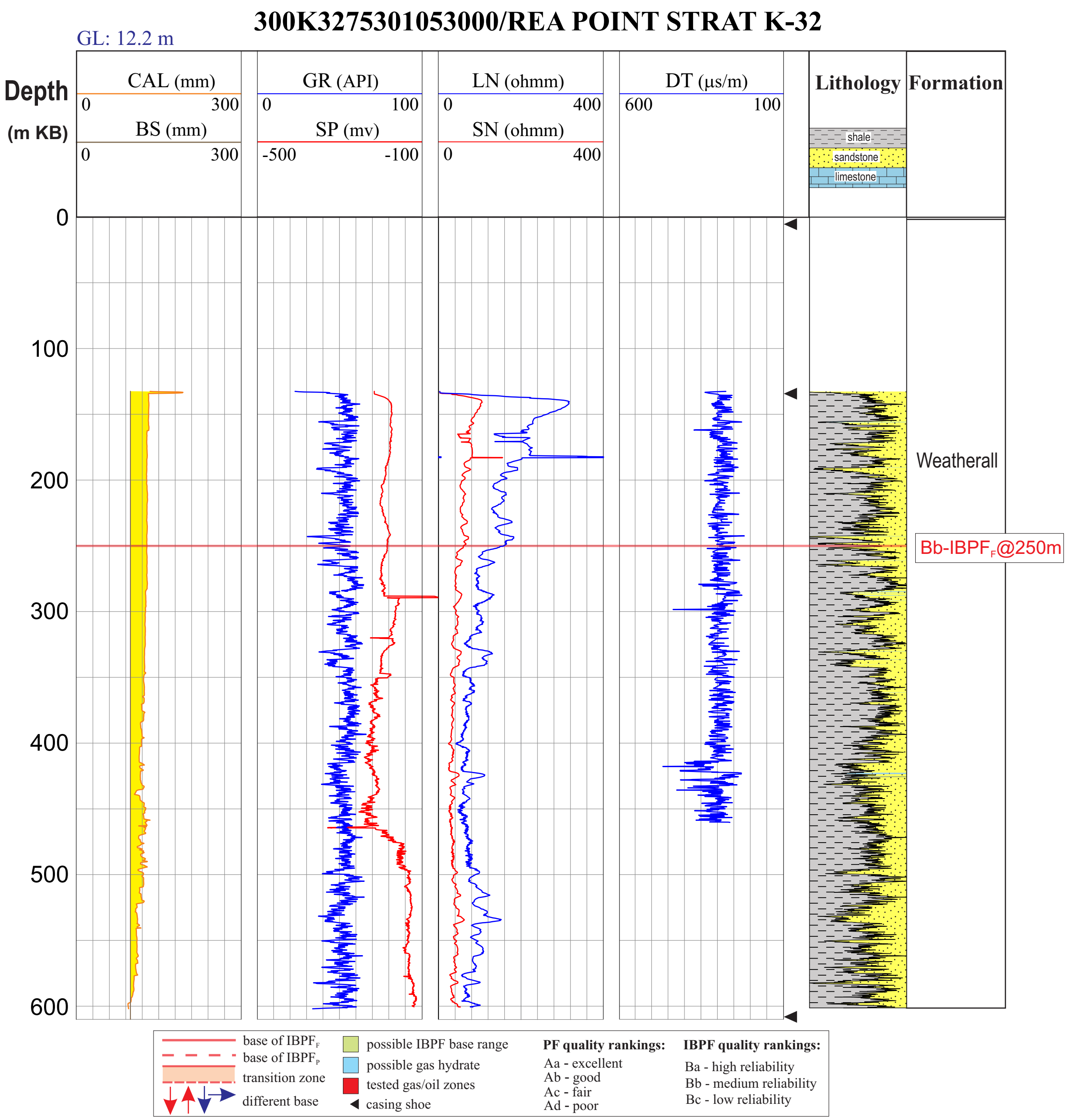

Figure 3-48. Determination of base of $IBPF_F$ with "Bb" quality using well logs for the Rea Point Strat K-32 well on Melville Island in the Canadian Arctic Islands.

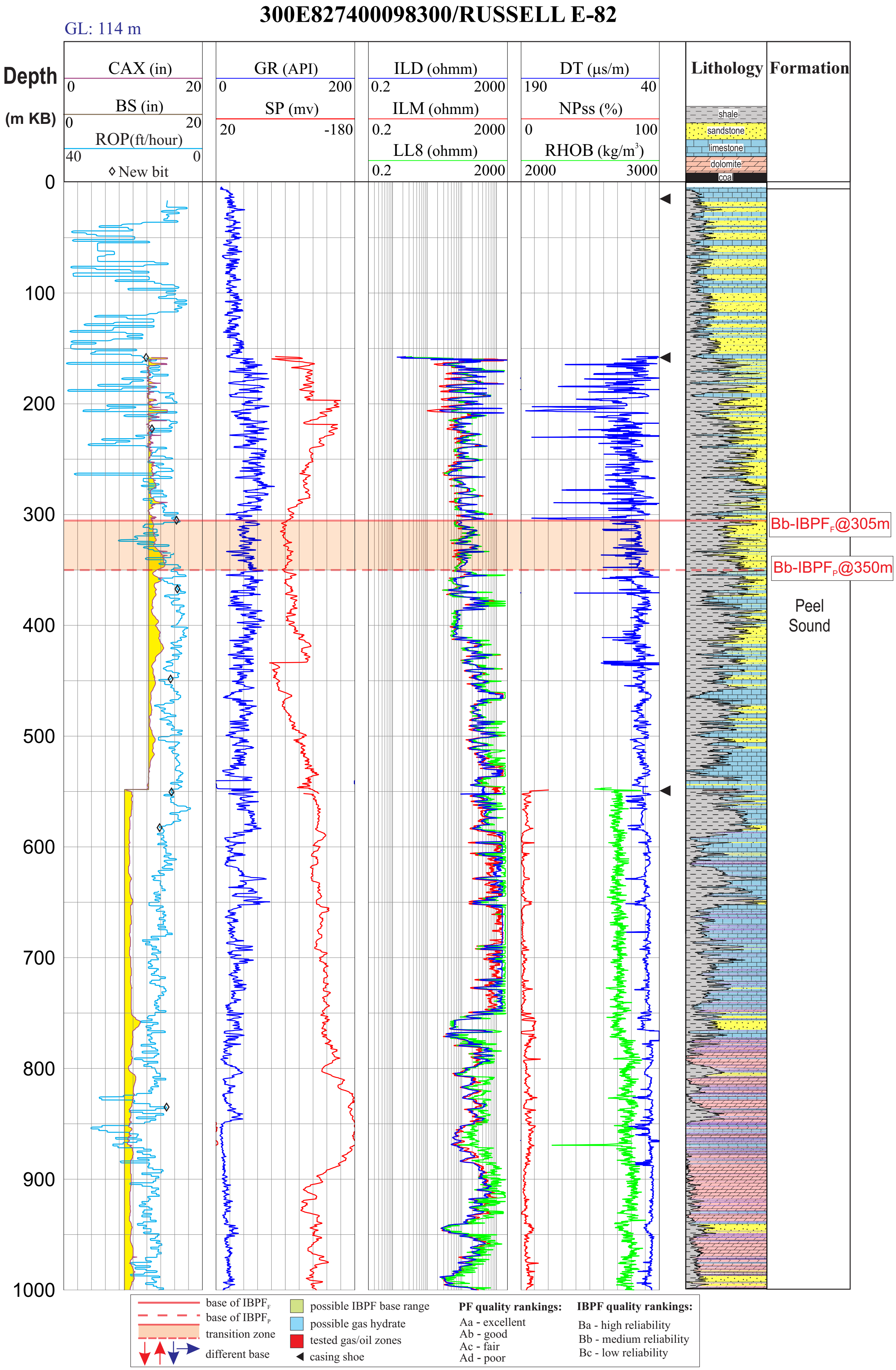

Figure 3-49. Determinations of base of $IBPF_F$ with “Bb” quality and $IBPF_P$ with “Bb” quality from well logs for the Russell E-82 well on Melville Island in the Canadian Arctic Islands.

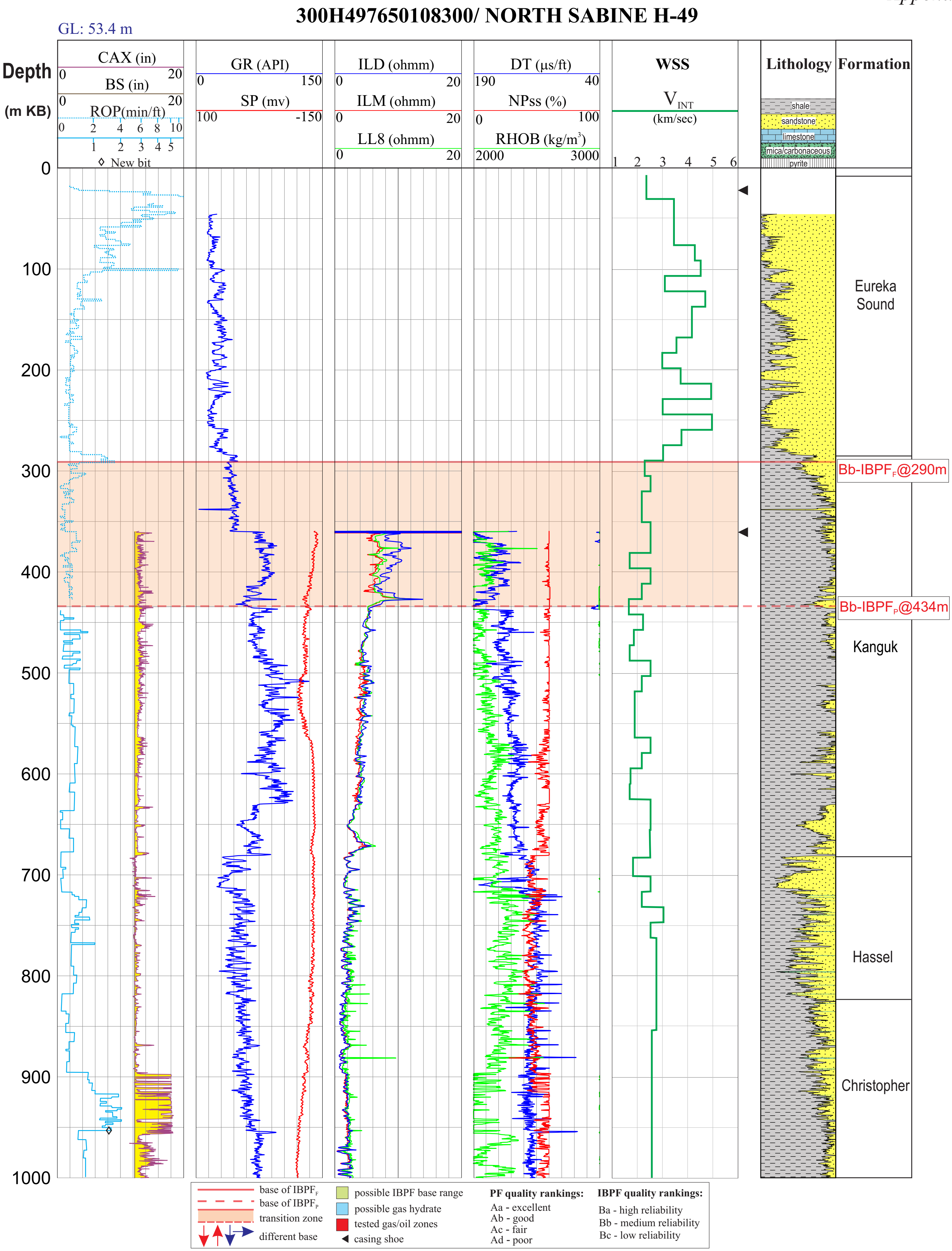

Figure 3-50. Determinations of base of $IBPF_F$ with “Bb” quality and $IBPF_P$ with “Bb” quality using well logs and welll seismic surveys for the North Sabine H-49 well on Melville Island in the Canadian Arctic Islands.

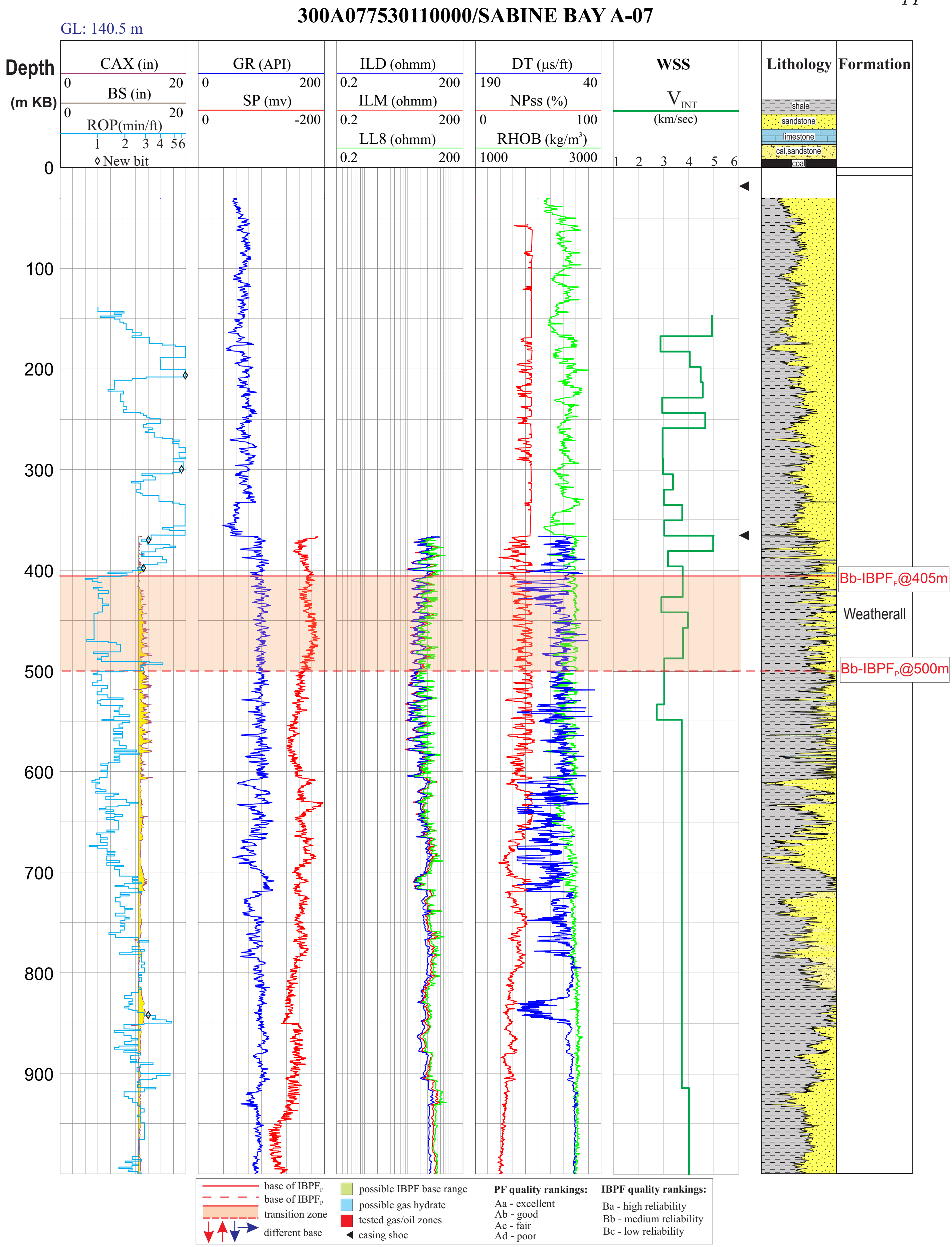

Figure 3-51. Determinations of base of $IBPF_F$ with "Bb" quality and $IBPF_P$ with "Bb" quality using well logs and welll seismic surveys for the Sabine Bay A-07 well on Melville Island in the Canadian Arctic Islands.

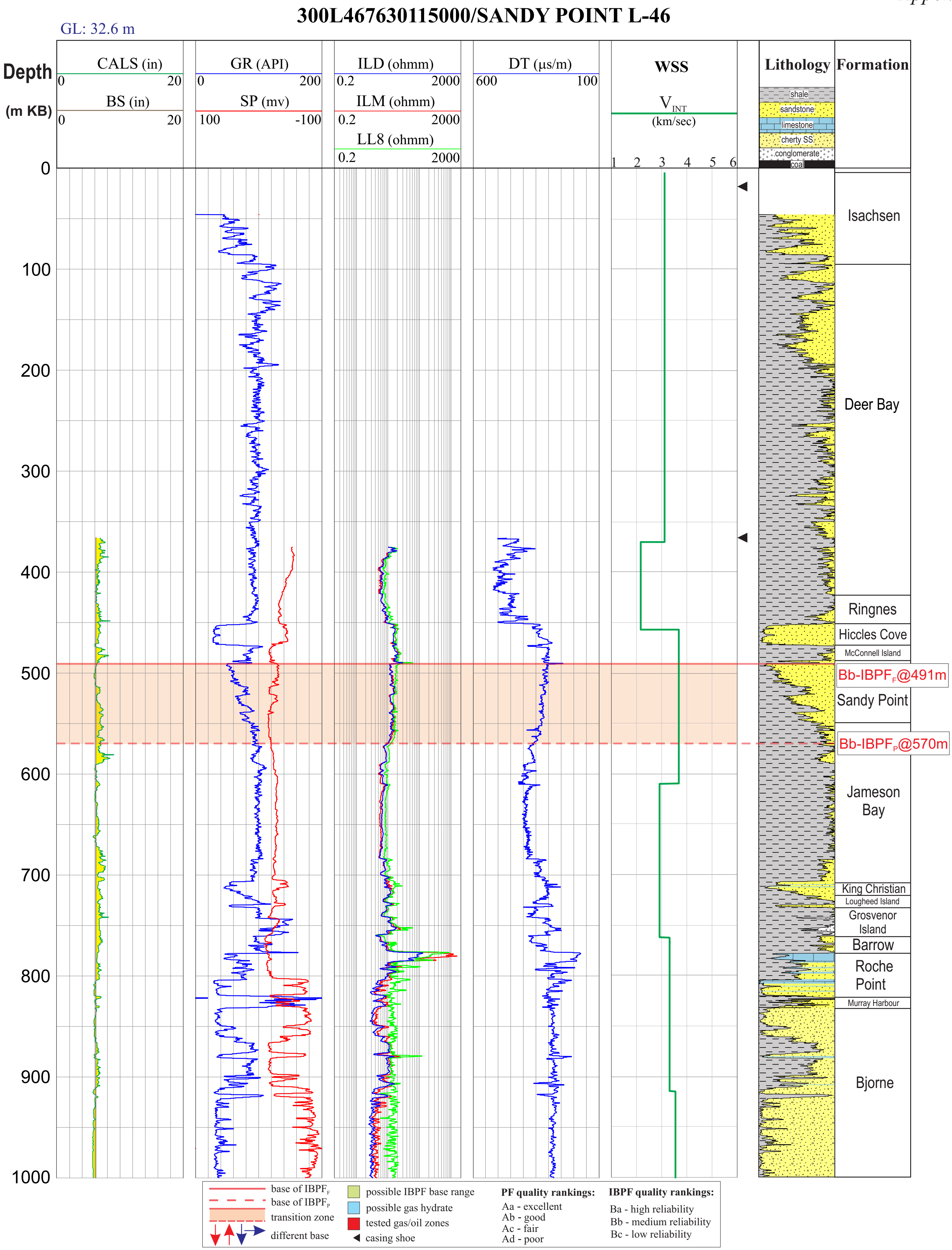

Figure 3-52. Determinations of base of $IBPF_F$ with “Bb” quality and $IBPF_P$ with “Bb” quality using well logs and welll seismic surveys for the Sandy Point L-46 well on Melville Island in the Canadian Arctic Islands.

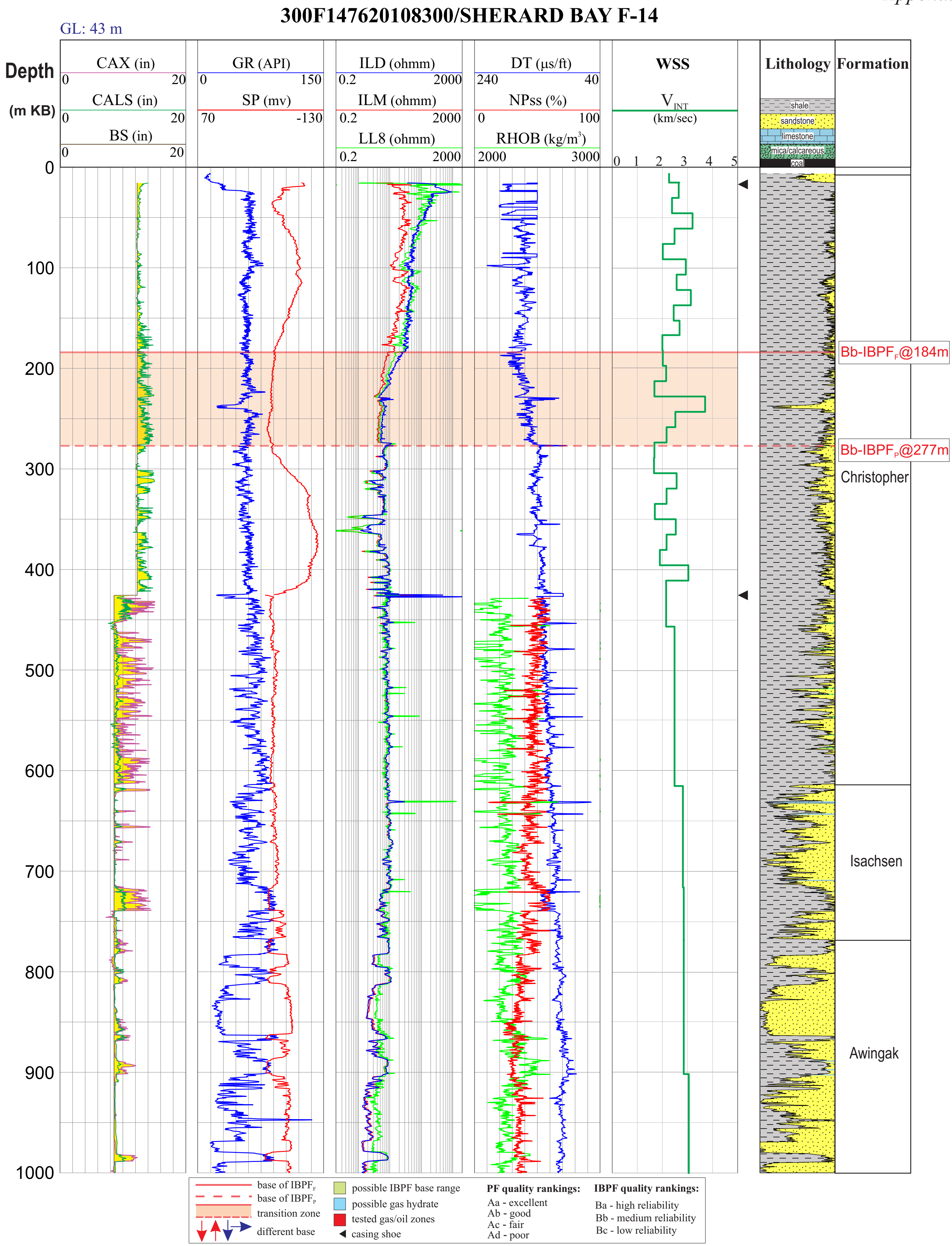

Figure 3-53. Determinations of base of $IBPF_F$ with "Bb" quality and $IBPF_P$ with "Bb" quality using well logs and welll seismic surveys for the Sherard Bay F-14 well on Melville Island in the Canadian Arctic Islands.

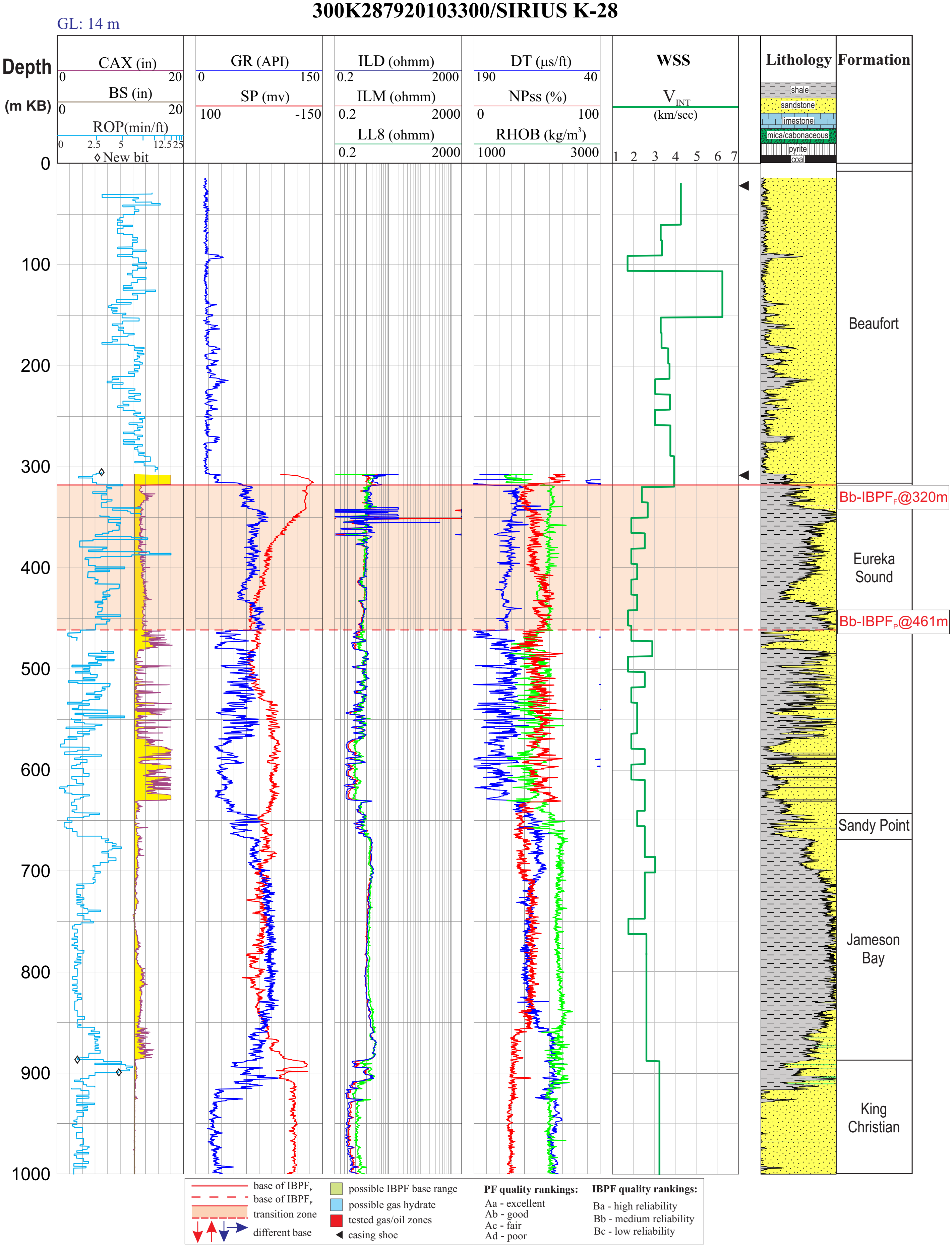

Figure 3-54. Determinations of base of $IBPF_F$ with "Bb" quality and $IBPF_P$ with "Bb" quality using well logs and welll seismic surveys for the Sirius K-28 well on Ellef Ringnes Island in the Canadian Arctic Islands.

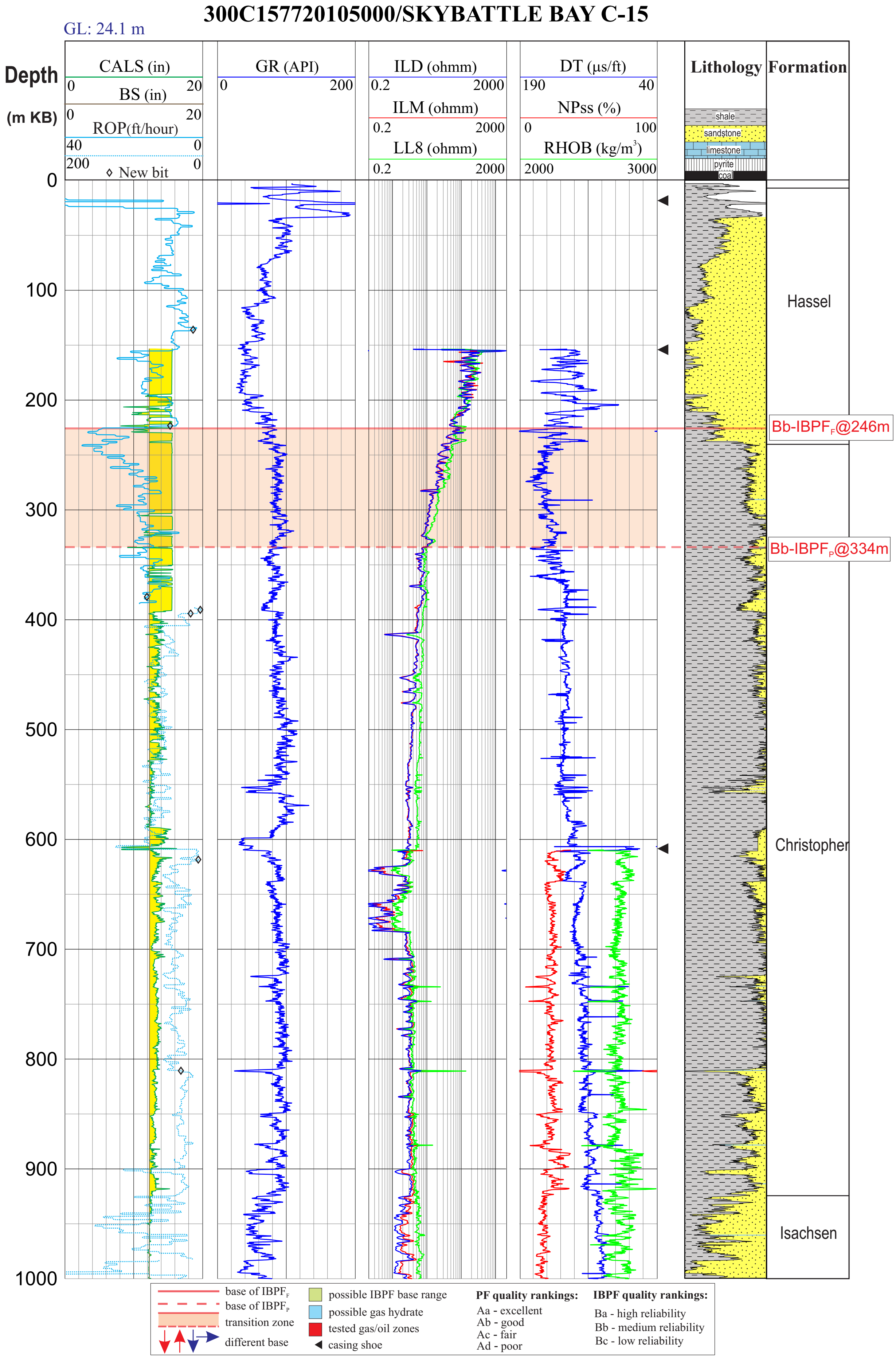

Figure 3-55. Determinations of base of $IBPF_F$ with "Bb" quality and $IBPF_P$ with "Bb" quality from well logs for the Skybattle Bay C-15 well on Lougheed Island in the Canadian Arctic Islands.

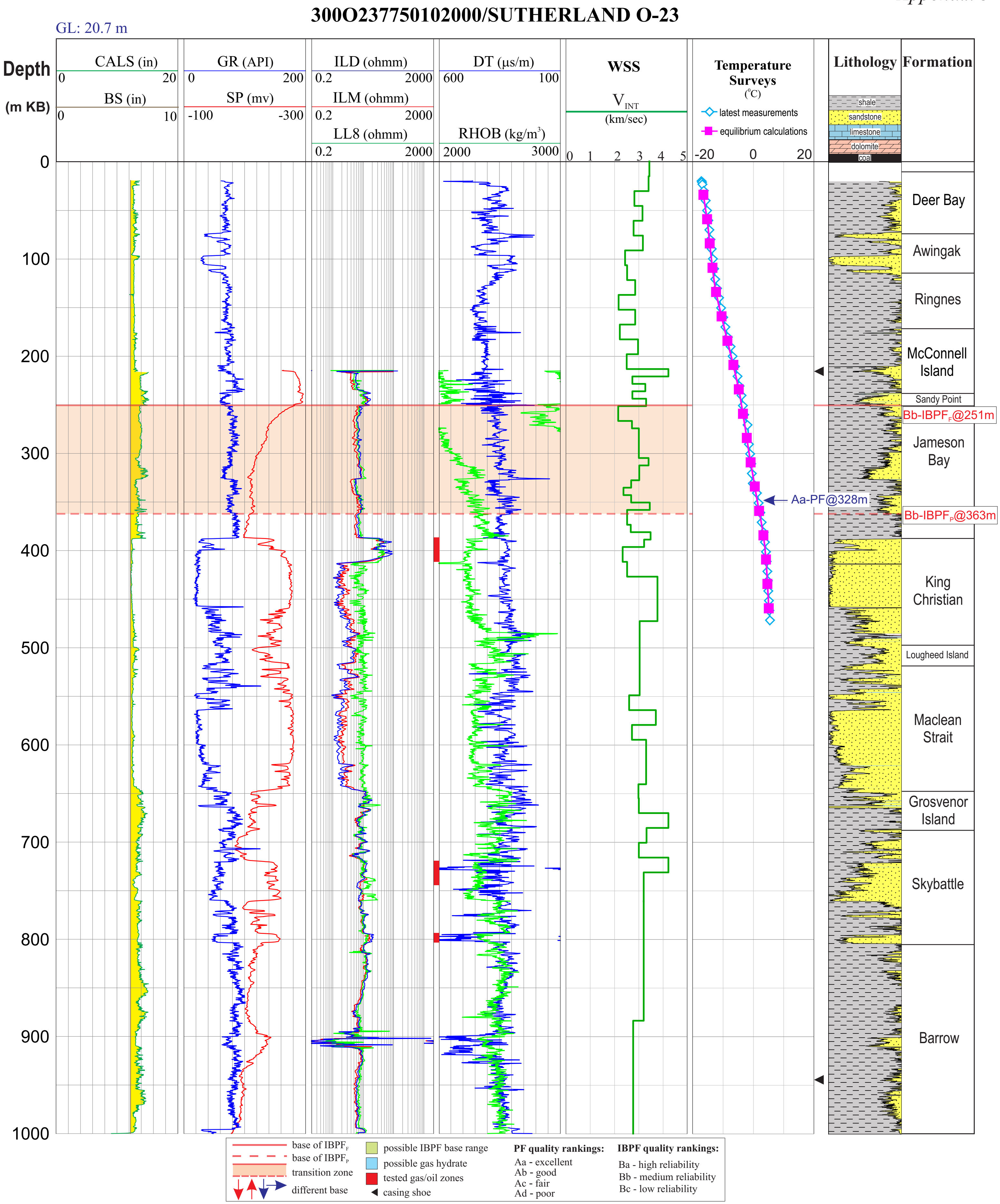

Figure 3-56. Determinations of base of $IBPF_F$ with "Bb" quality and $IBPF_P$ with "Bb" quality using well logs and welll seismic surveys, and base of PF from temperature surveys for the Sutherland O-23 well on King Christian Island in the Canadian Arctic Islands.

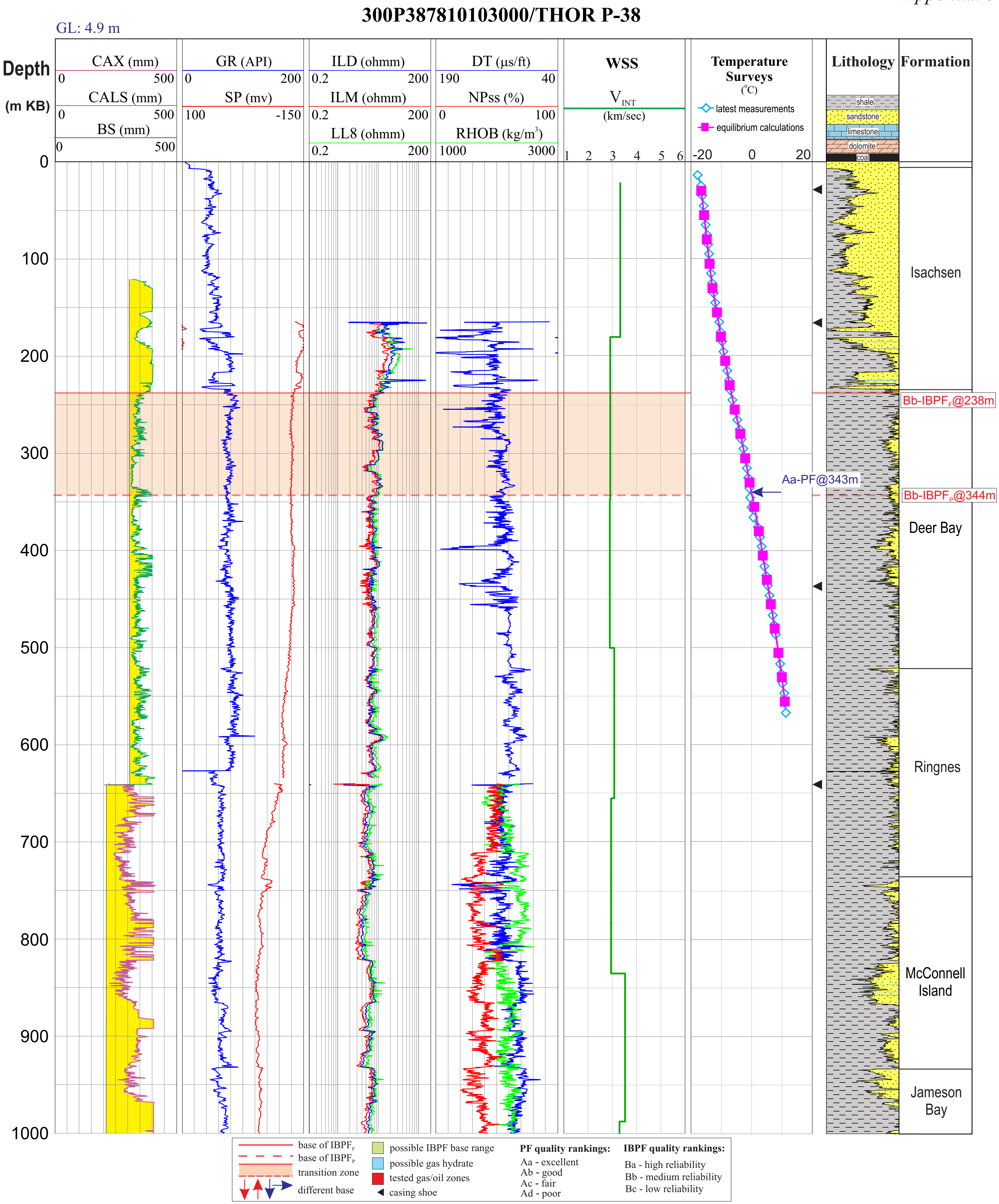

Figure 3-57. Determinations of base of $IBPF_F$ with “Bb” quality and $IBPF_P$ with “Bb” quality using well logs and welll seismic surveys, and base of PF from temperature surveys for the Thor P-38 well on Thor Island in the Canadian Arctic Islands.

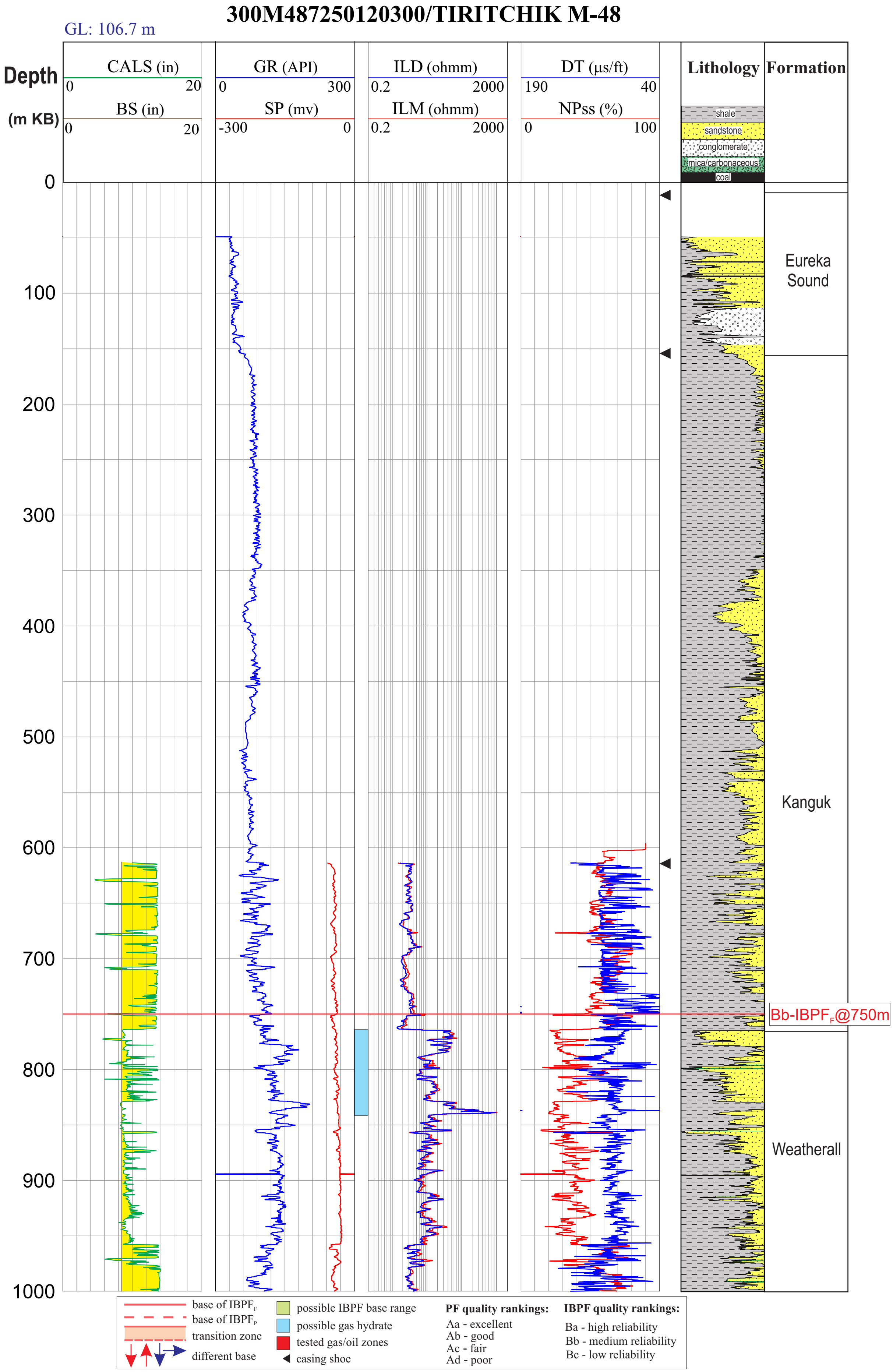

Figure 3-58. Determination of base of $IBPF_F$ with "Bb" quality from well logs for the Tiritchik M-48 well on Banks Island in the Canadian Arctic Islands.

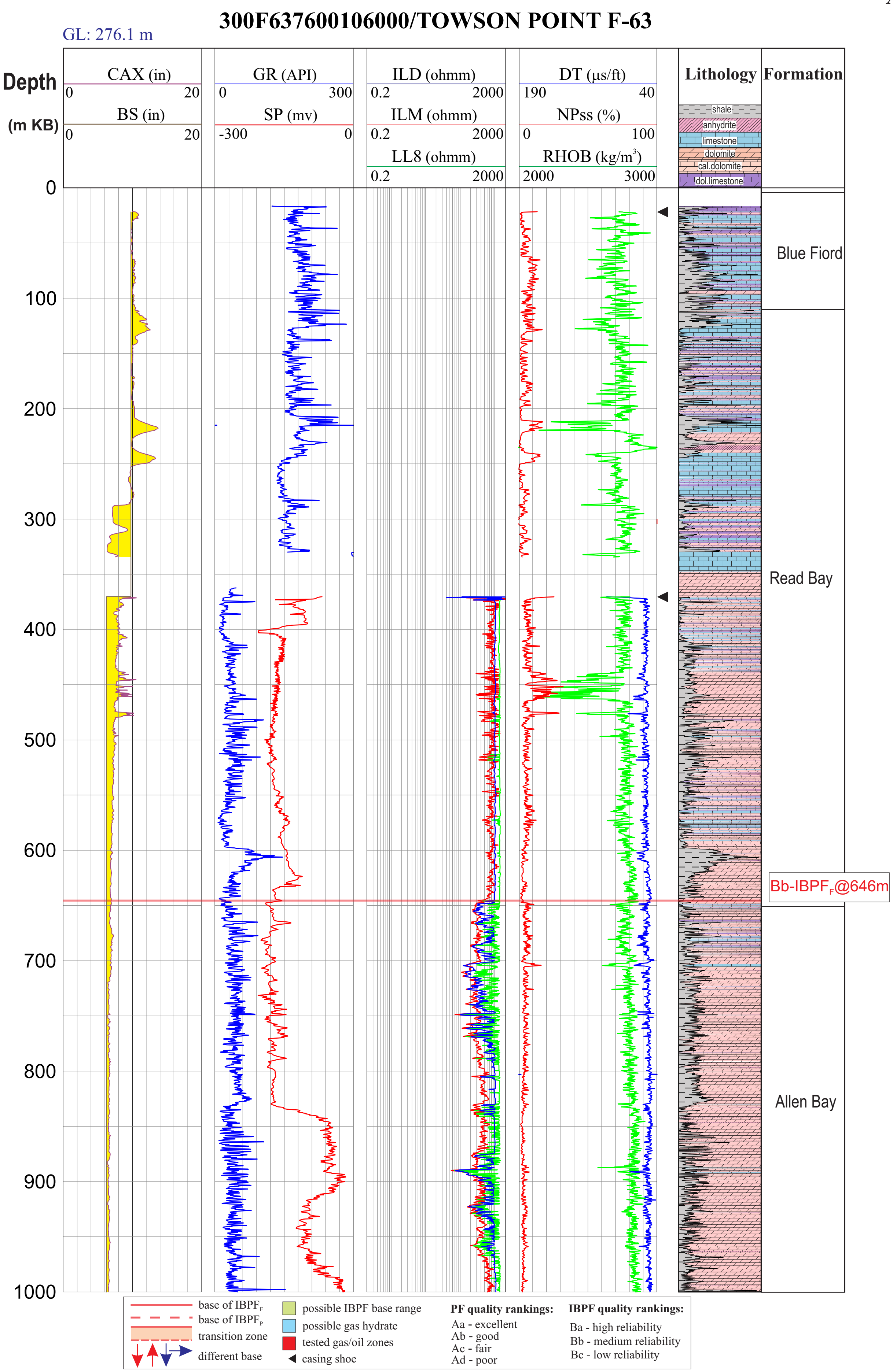

Figure 3-59. Determination of base of $IBPF_F$ with "Bb" quality from well logs for the Towson Point F-63 well on Melville Island in the Canadian Arctic Islands.

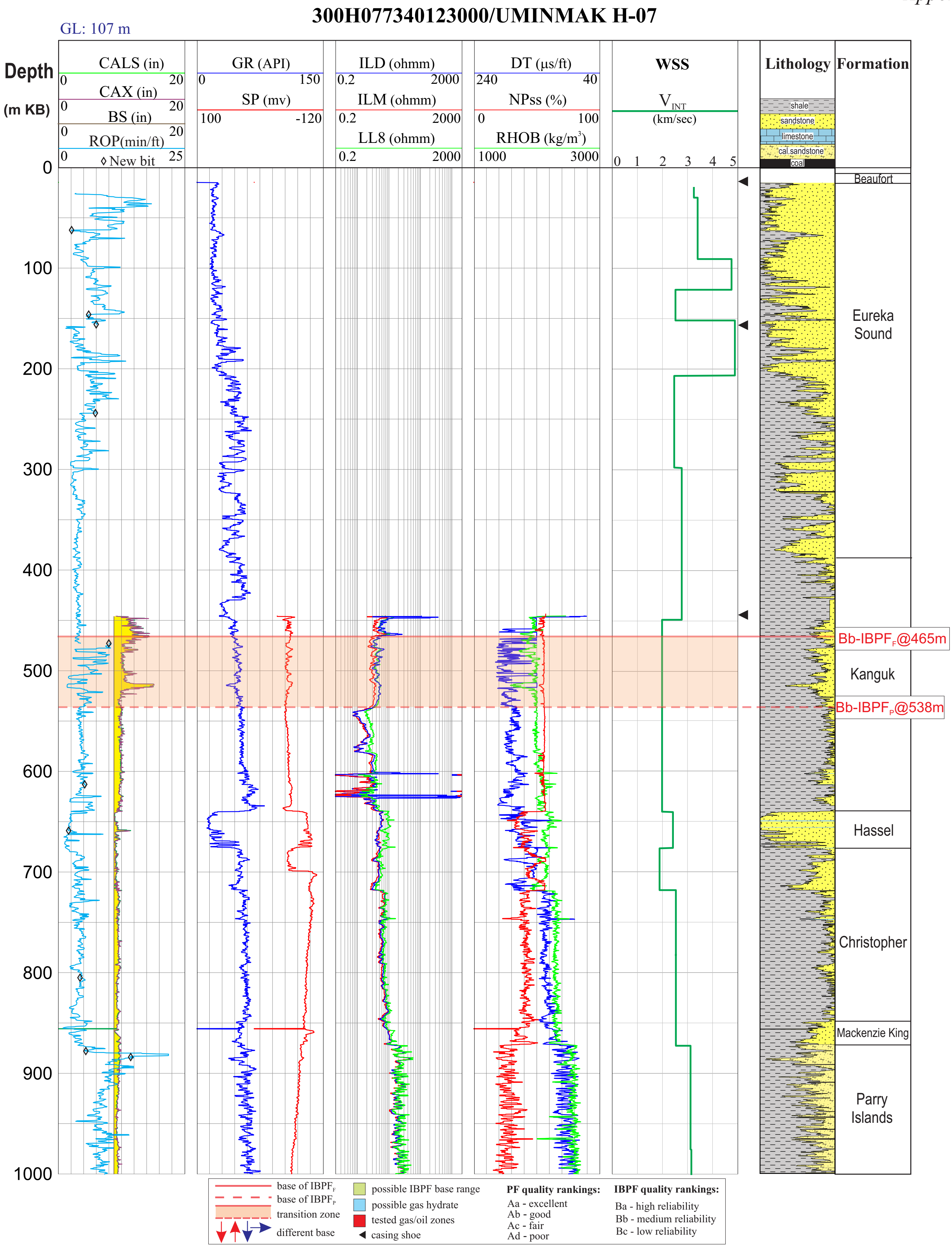

Figure 3-60. Determinations of base of $IBPF_F$ with "Bb" quality and $IBPF_P$ with "Bb" quality using well logs and welll seismic surveys for the Uminmak H-07 well on Banks Island in the Canadian Arctic Islands.

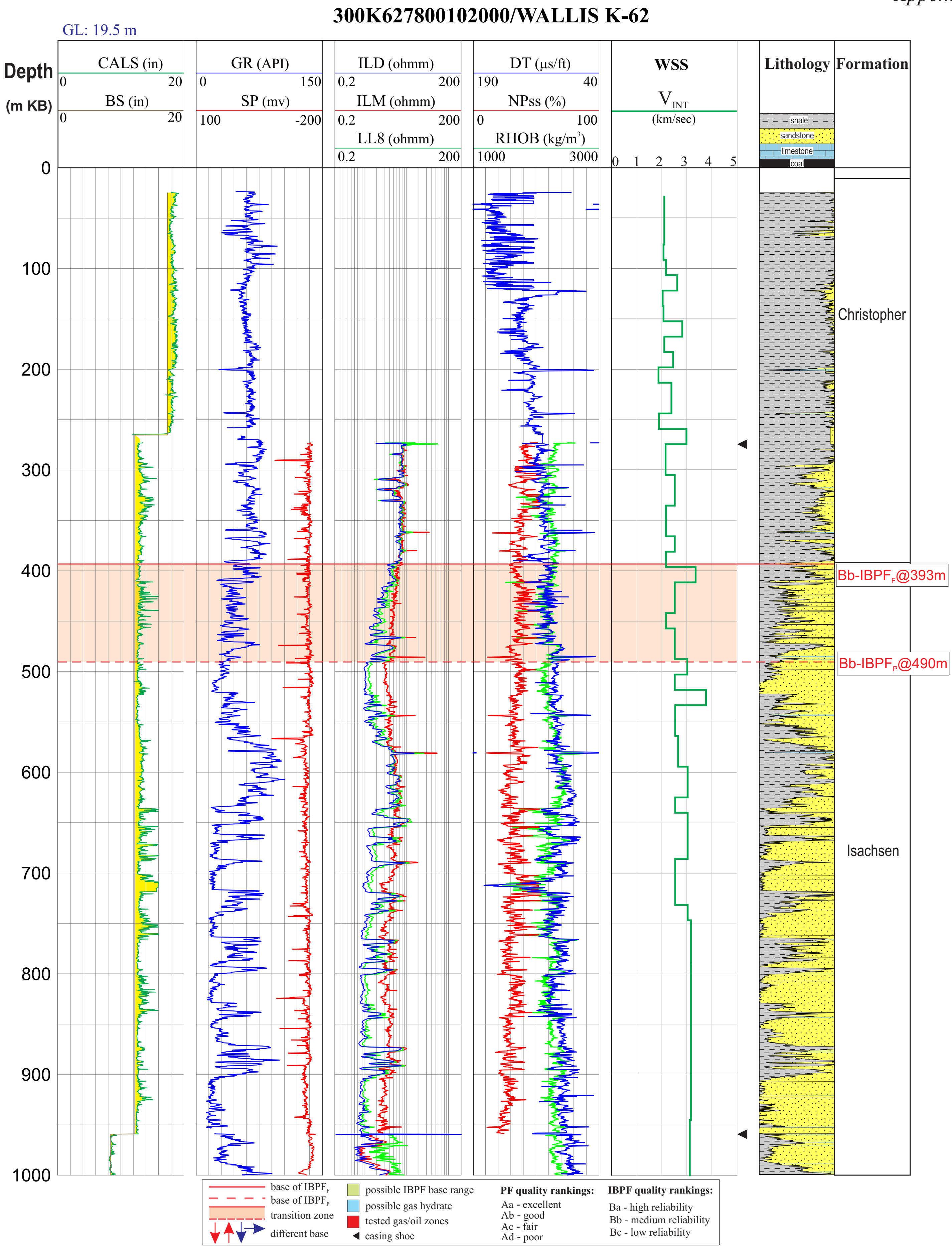

Figure 3-61. Determinations of base of $IBPF_F$ with "Bb" quality and $IBPF_P$ with "Bb" quality using well logs and well seismic surveys for the Wallis K-62 well on King Christian Island in the Canadian Arctic Islands.

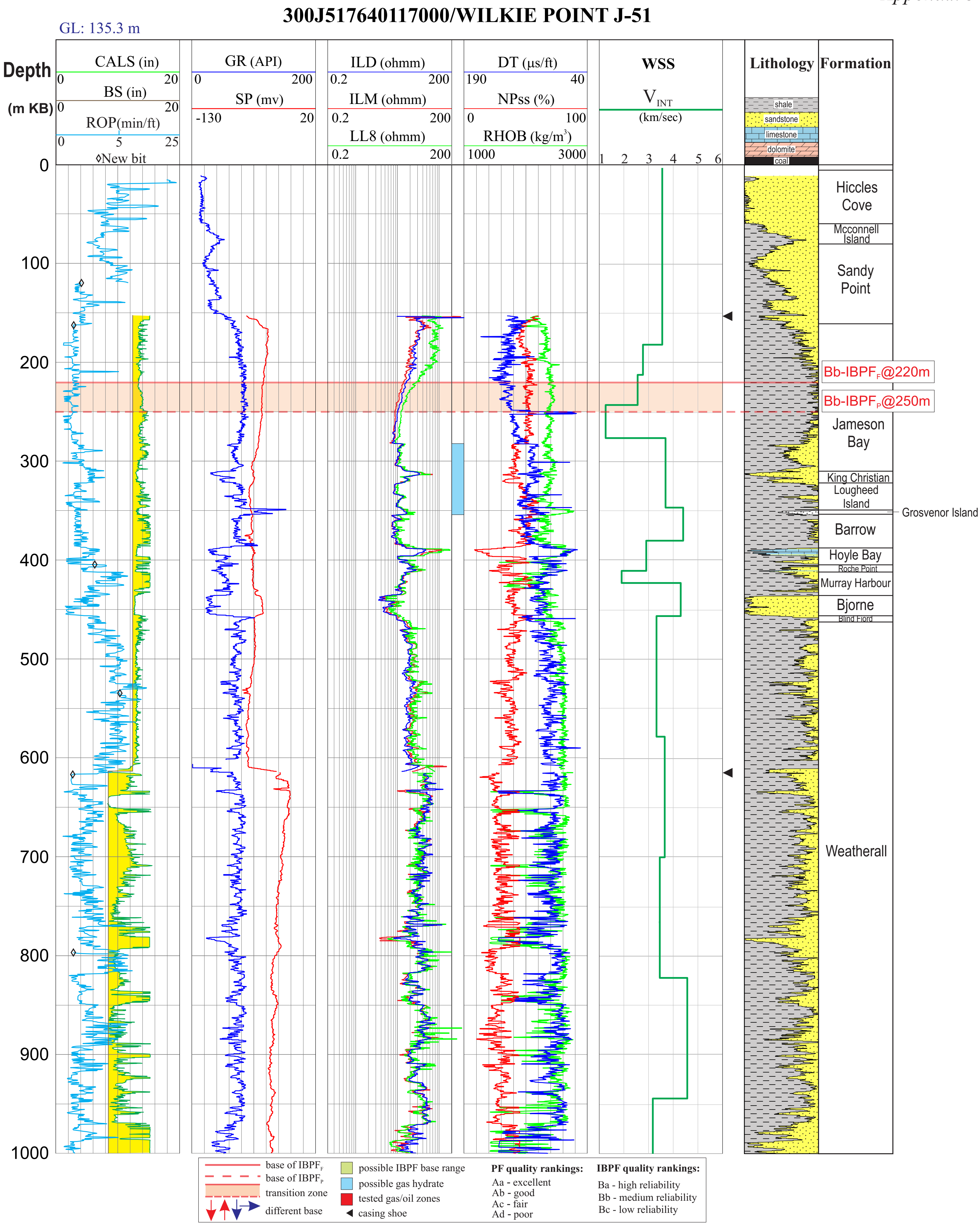

Figure 3-62. Determinations of base of $IBPF_F$ with "Bb" quality and $IBPF_P$ with "Bb" quality using well logs and welll seismic surveys for the Wilkie Point J-51 well on Prince Patrick Island in the Canadian Arctic Islands.

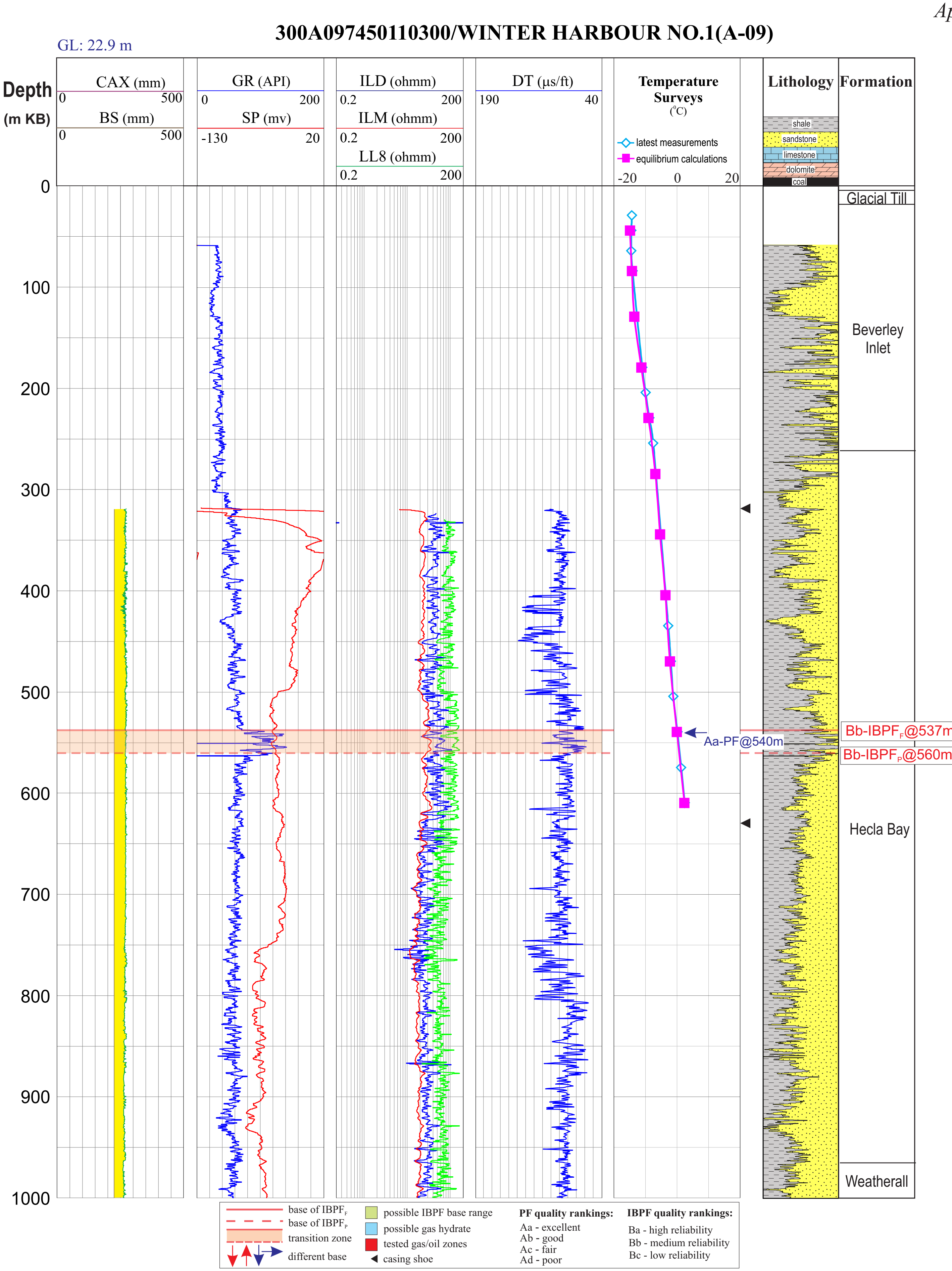

Figure 3-63. Determinations of base of $IBPF_F$ with "Bb" quality and $IBPF_P$ with "Bb" quality from well logs, and base of PF from temperature surveys for the Winter Harbour No.1 (A-09) well on Melville Island in the Canadian Arctic Islands.

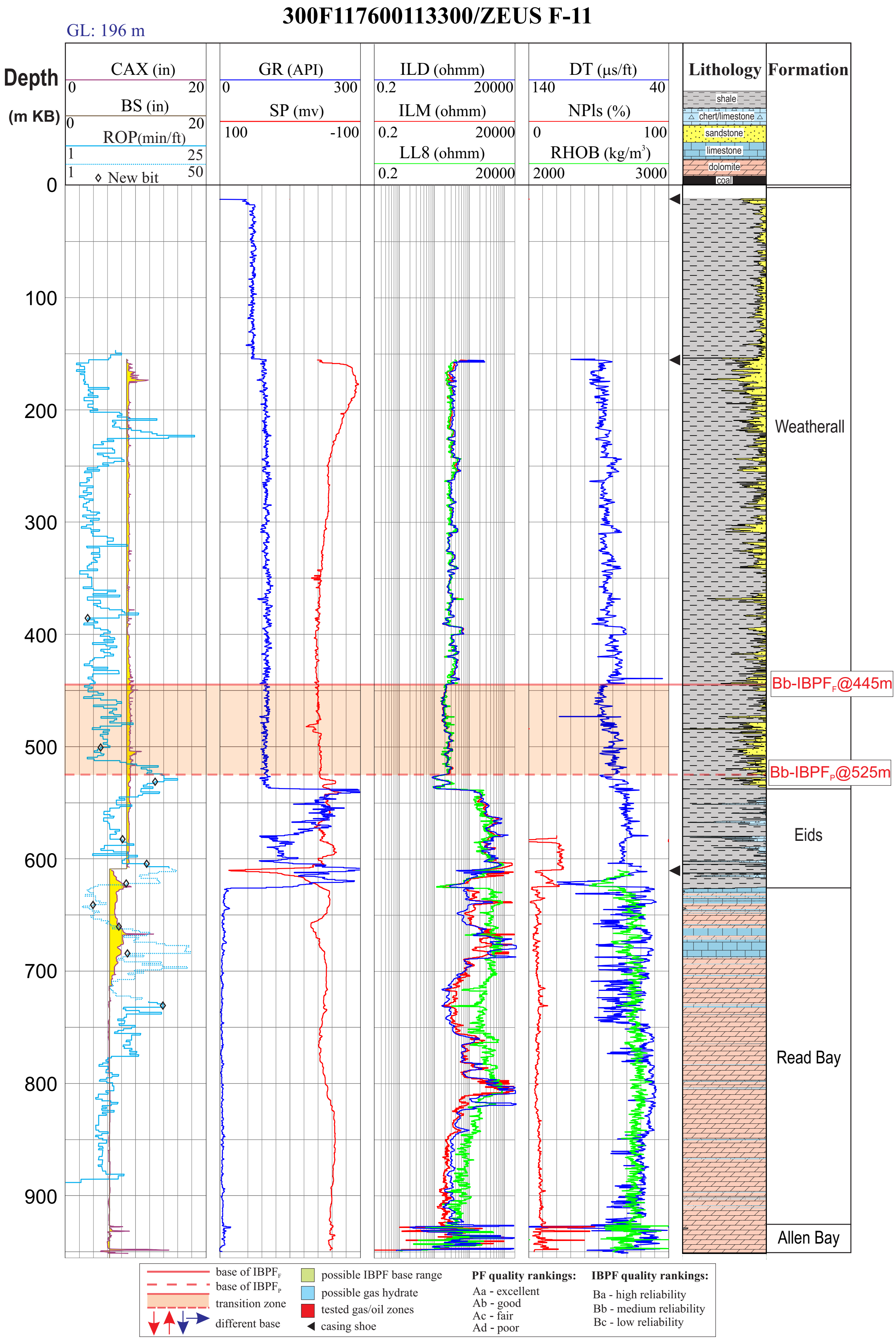

Figure 3-64. Determinations of base of $IBPF_F$ with "Bb" quality and $IBPF_P$ with "Bb" quality using well logs for the Zeus F-11 well on Melville Island in the Canadian Arctic Islands.

300E467720086000/BLUE FIORD E-46

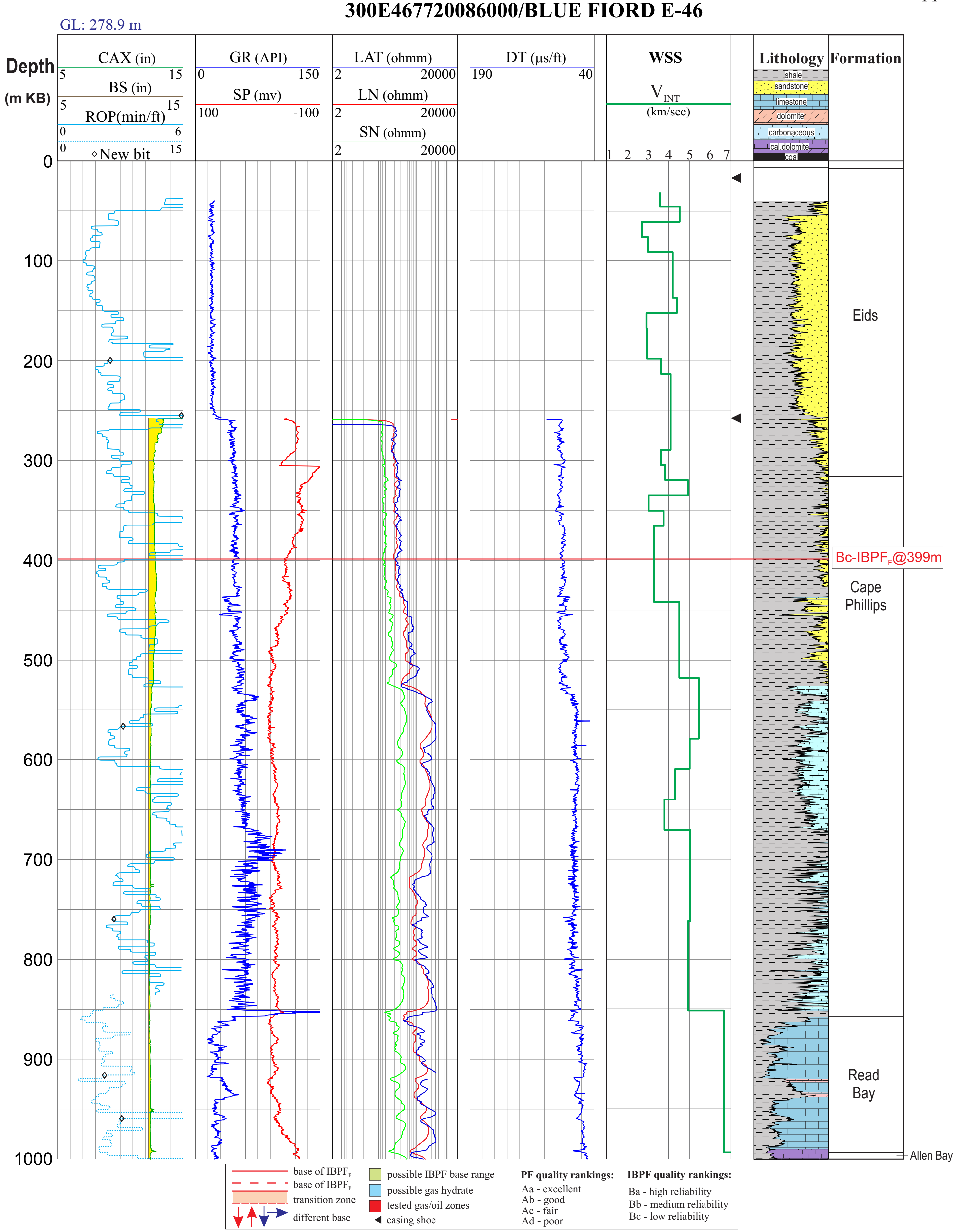

Figure 4-1. Estimation of base of $IBPF_F$ with "Bc" quality using well logs and well seismic surveys for the Blue Fiord E-46 well on Ellesmere Island in the Canadian Arctic Islands.

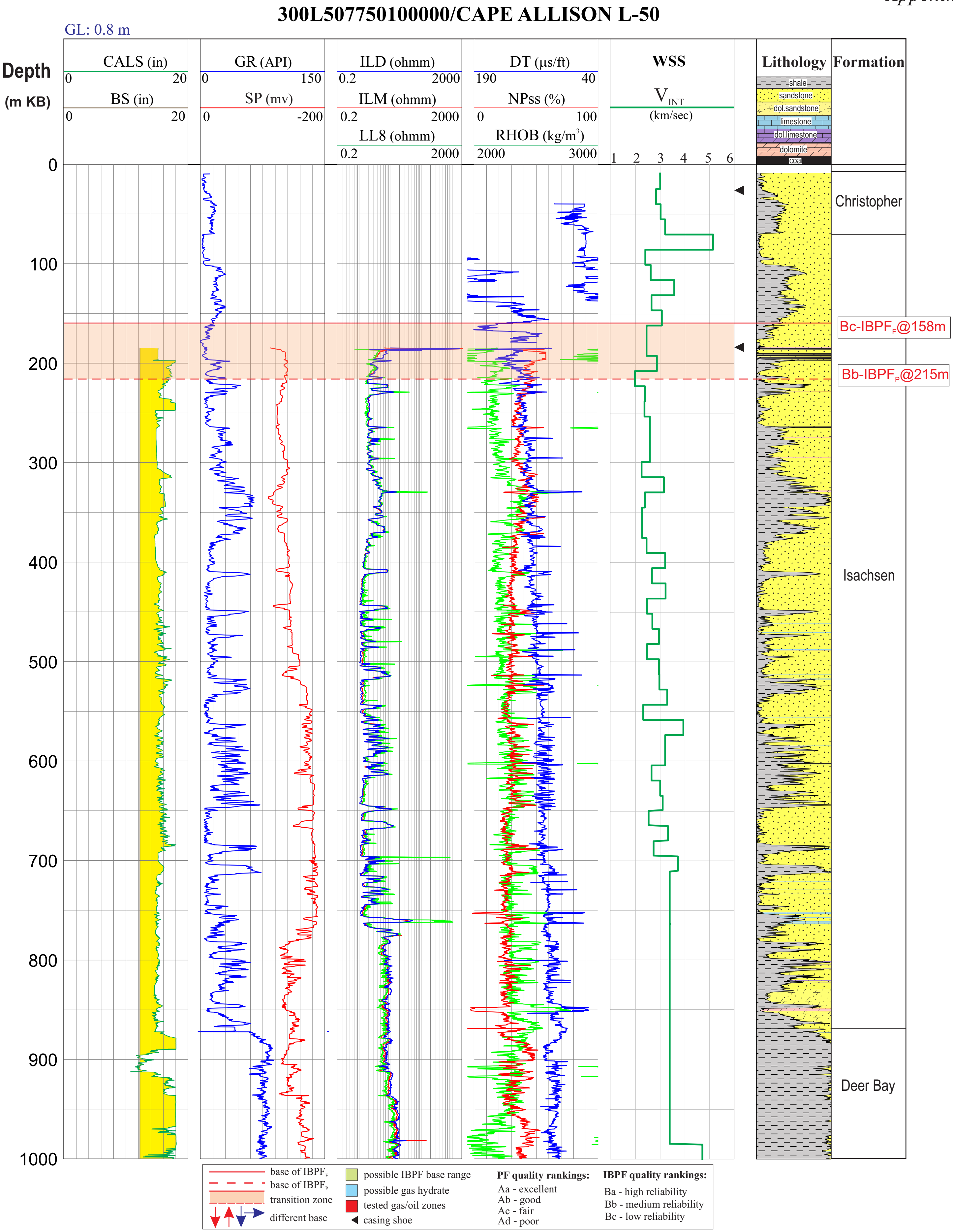

Figure 4-2. Estimations of base of $IBPF_F$ with “Bc” quality and $IBPF_P$ with “Bb” quality using well logs and well seismic surveys for the Cape Allison L-50 well on Ellef Ringnes Island in the Canadian Arctic Islands.

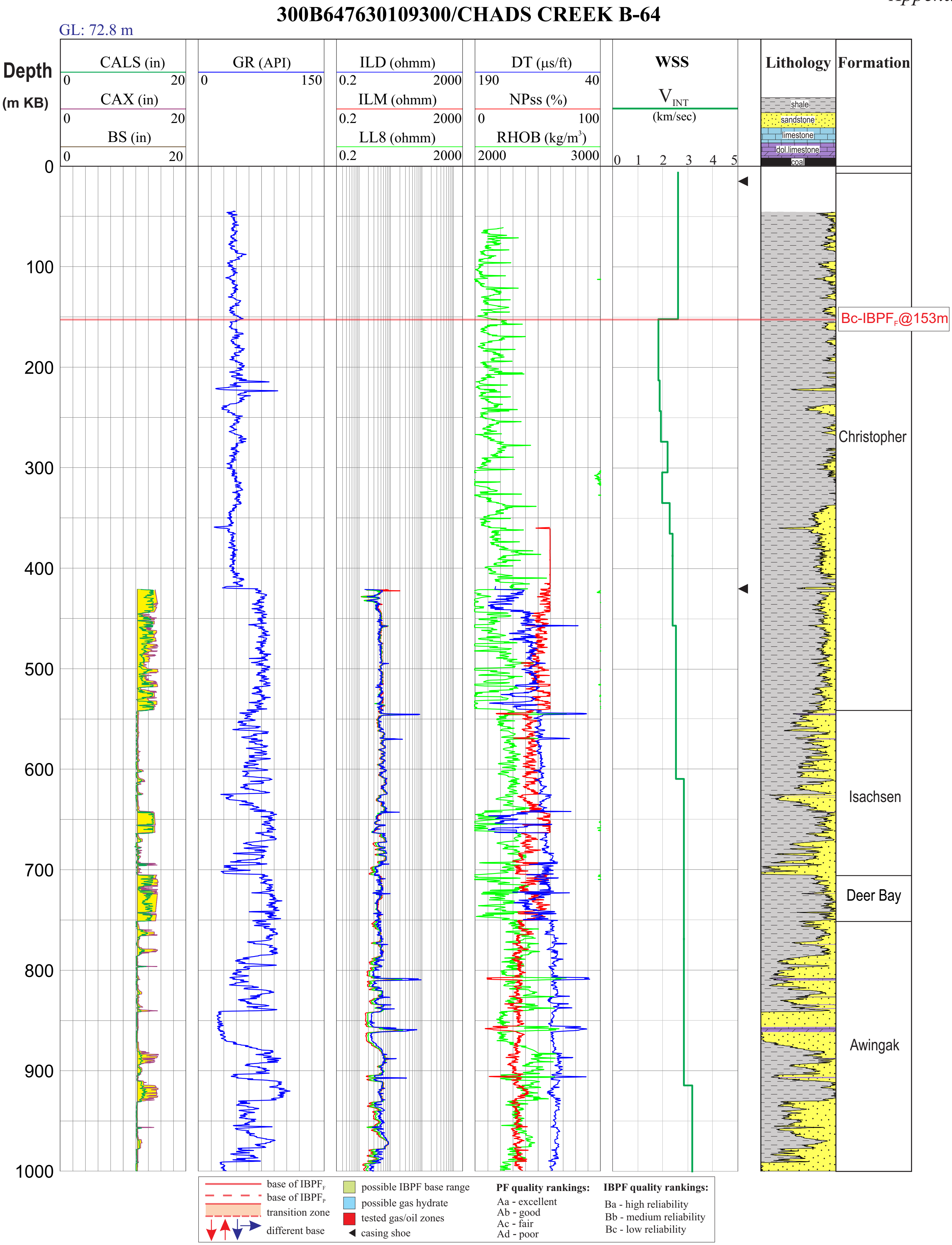

Figure 4-3. Estimation of base of $IBPF_F$ with "Bc" quality mainly from well seismic surveys for the Chads Creek B-64 well on Melville Island in the Canadian Arctic Islands.

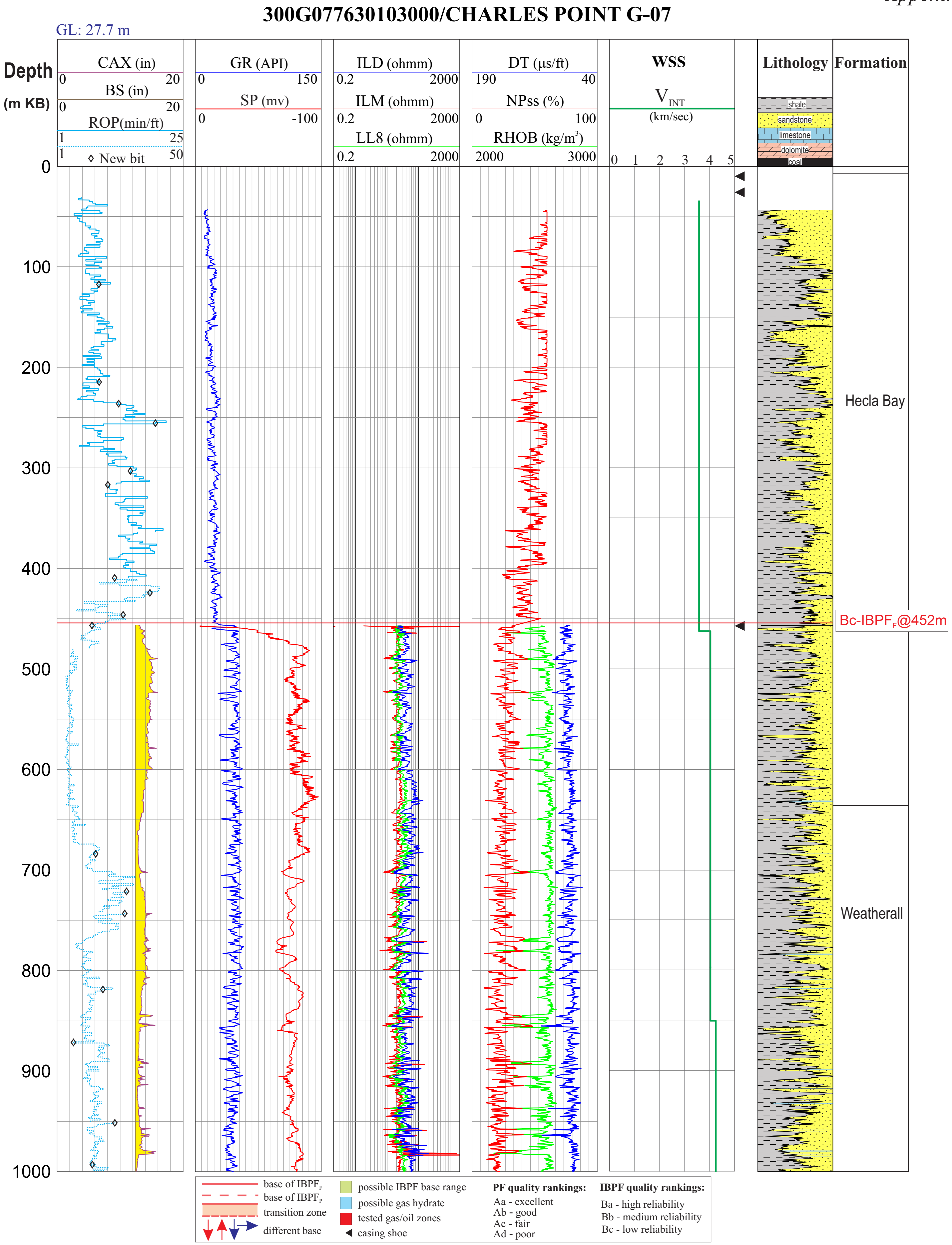

Figure 4-4. Estimation of base of $IBPF_F$ with "Bc" quality mainly from drilling rate and wireline logs for the Charles Point G-07 well on Cameron Island in the Canadian Arctic Islands.

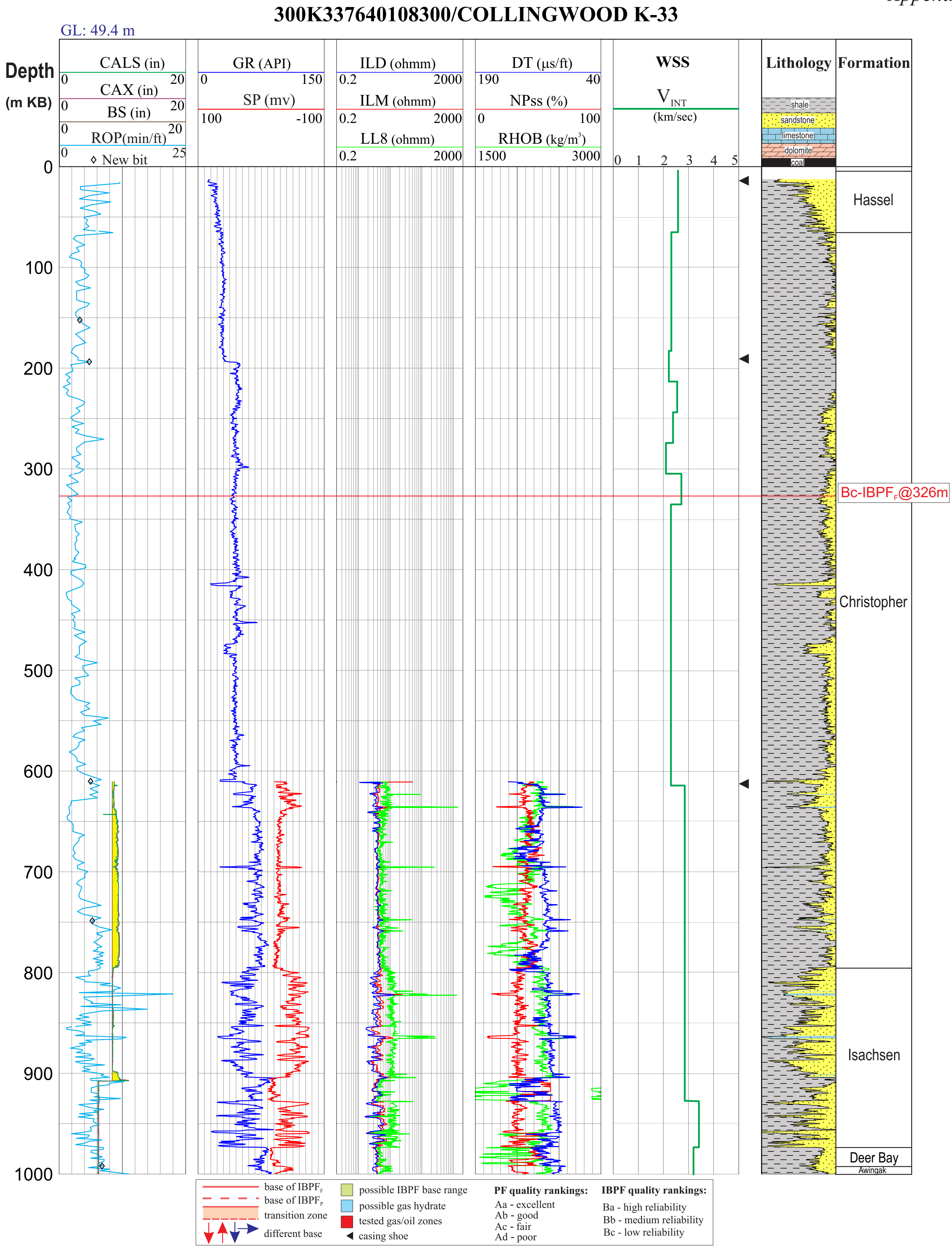

Figure 4-5. Estimation of base of $IBPF_F$ with “Bc” quality from well seismic surveys and drilling rate for the Collingwood K-33 well on Melville Island in the Canadian Arctic Islands.

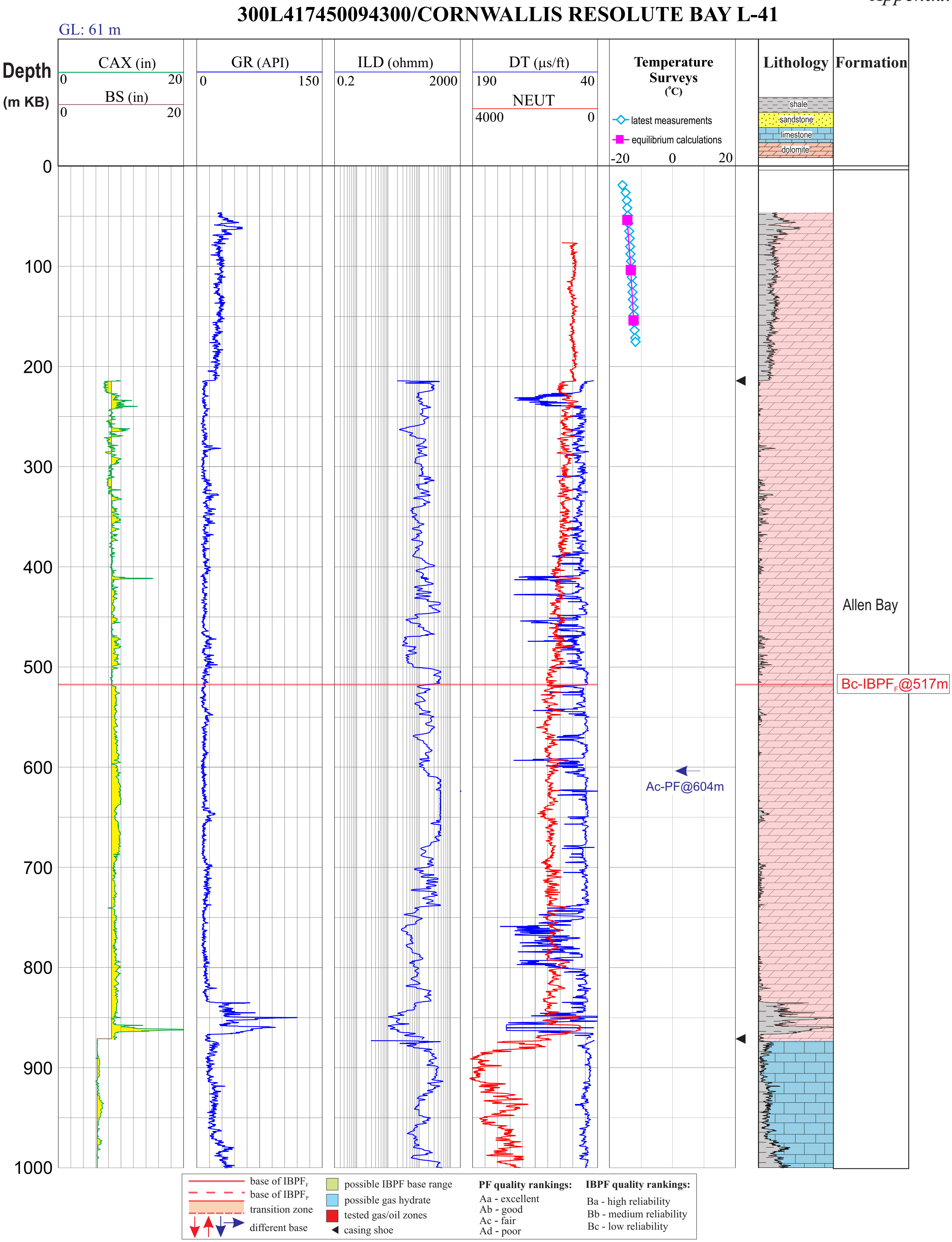

Figure 4-6. Estimations of base of $IBPF_F$ with "Bc" quality from well logs, and base of PF from temperature surveys for the Cornwallis Resolute Bay L-41 well on Cornwallis Island in the Canadian Arctic Islands.

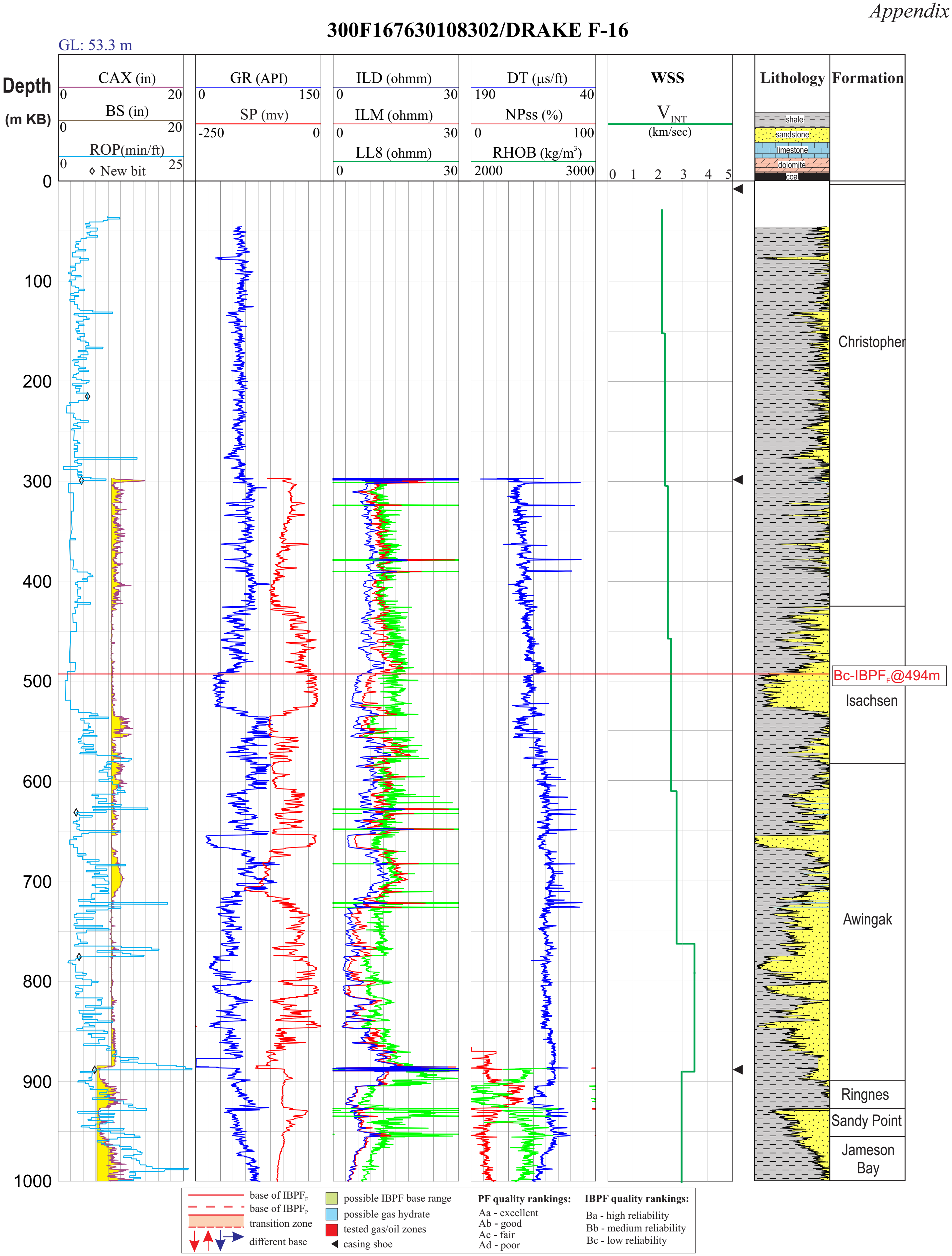

Figure 4-7. Estimation of base of IBPF$_F$ with "Bc" quality from well logs and well seismic surveys for the Drake F-16 well on Melville Island in the Canadian Arctic Islands.

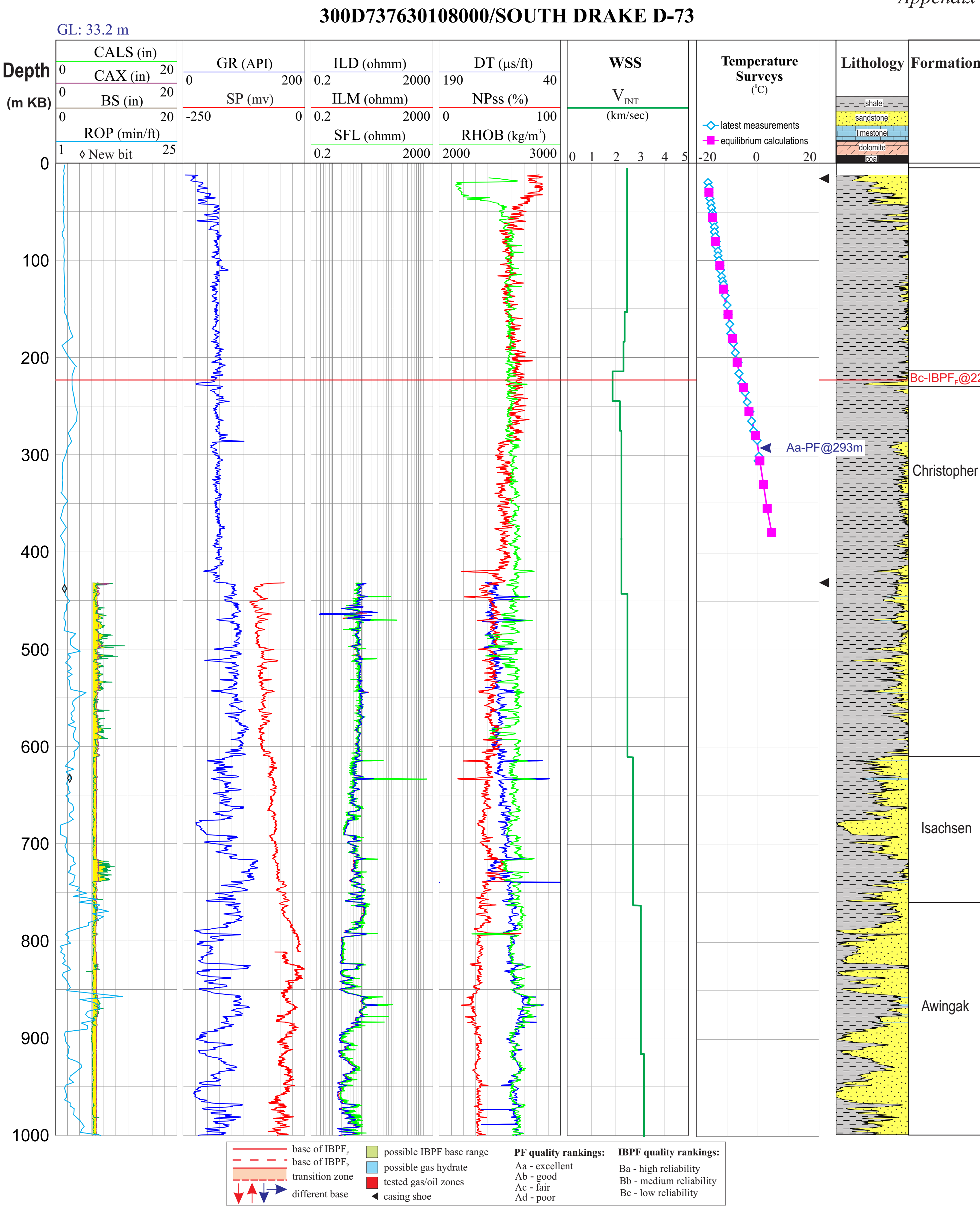

Figure 4-8. Estimation of base of IBPF$_F$ with “Bc” quality mainly using well seismic surveys, and determination of base of PF for the South Drake D-73 well on Melville Island in the Canadian Arctic Islands.

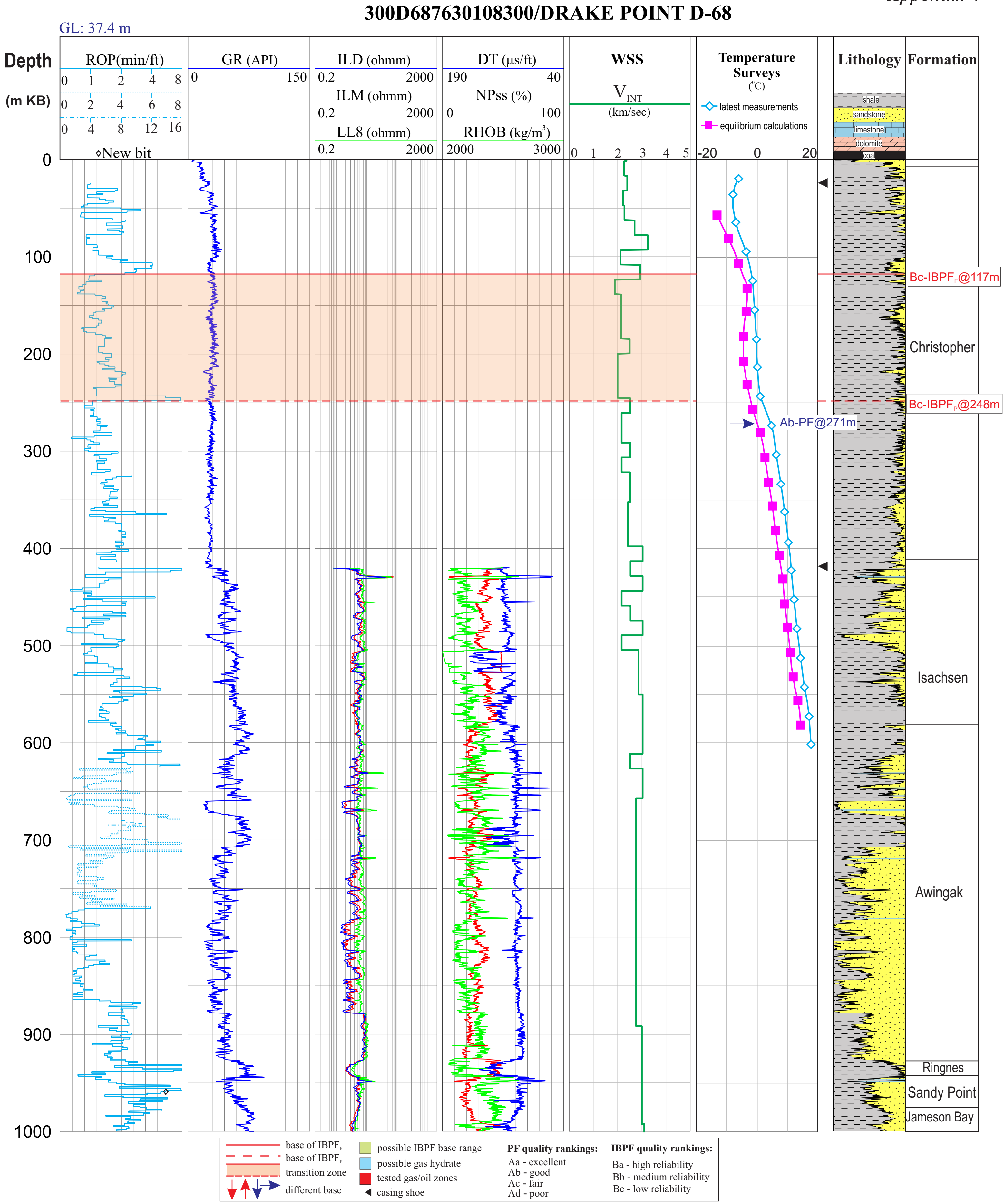

Figure 4-9. Determinations of base of $IBPF_F$ with "Bc" quality and $IBPF_P$ with "Bc" quality using well seismic surveys and drilling rate, and base of PF from temperature surveys for the Drake Point D-68 well on Melville Island in the Canadian Arctic Islands.

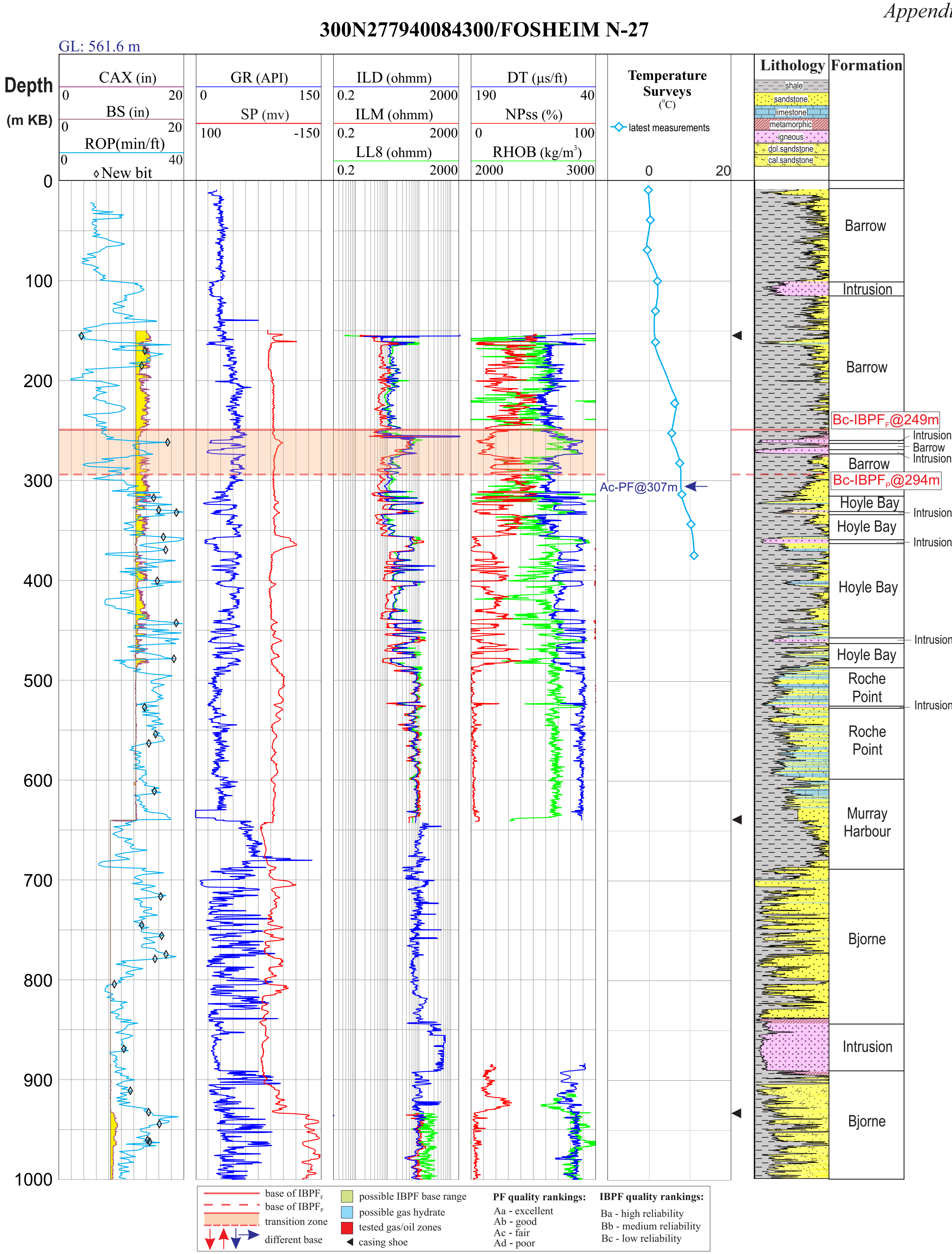

Figure 4-10. Estimations of base of $IBPF_F$ with "Bc" quality and $IBPF_P$ with "Bc" quality using well logs, and base of PF from temperature surveys for the Fosheim N-27 well on Ellesmere Island in the Canadian Arctic Islands.

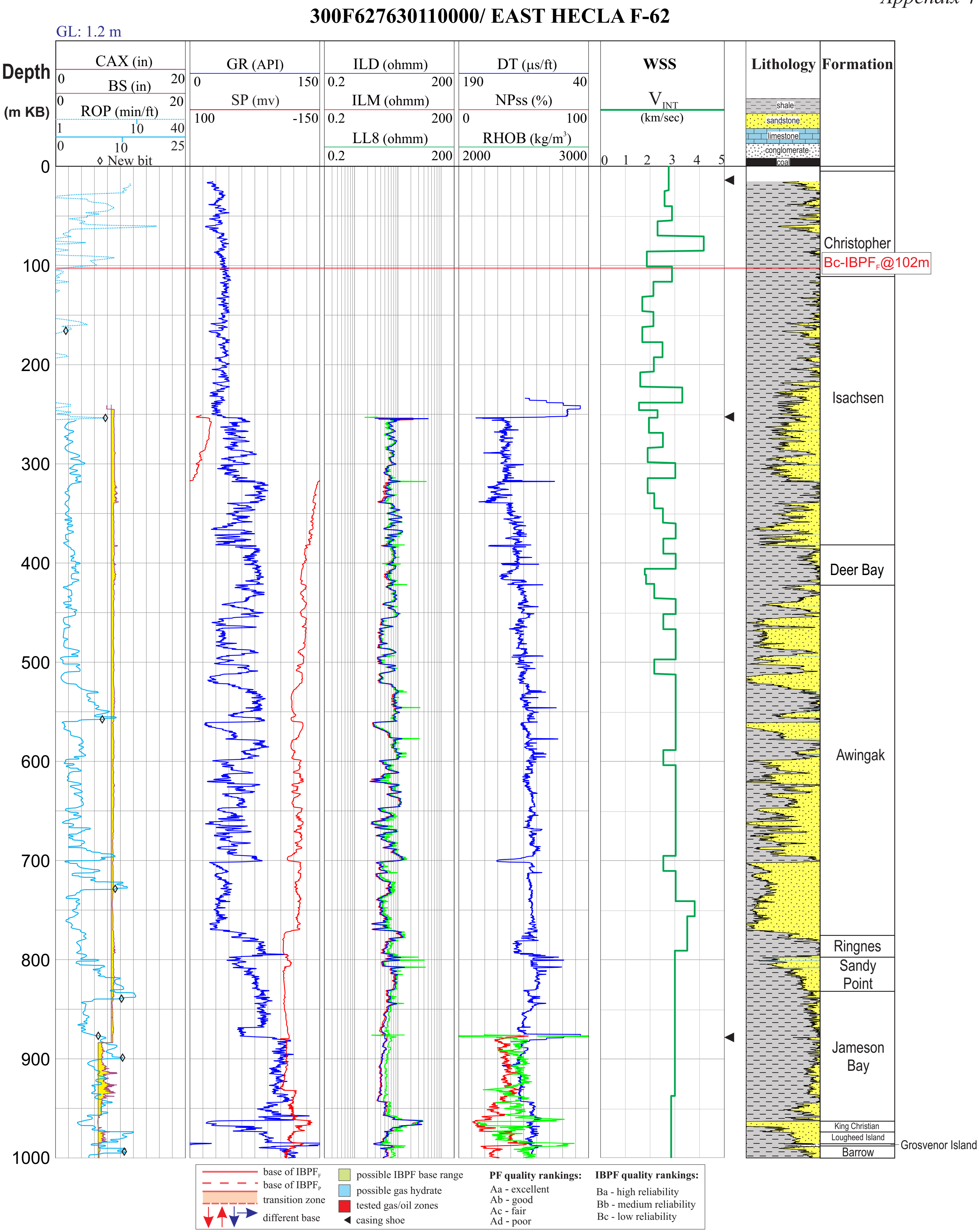

Figure 4-11. Determination of base of IBPF$_F$ with “Bc” quality using well logs and well seismic surveys for the East Hecla F-62 well on Melville Island in the Canadian Arctic Islands.

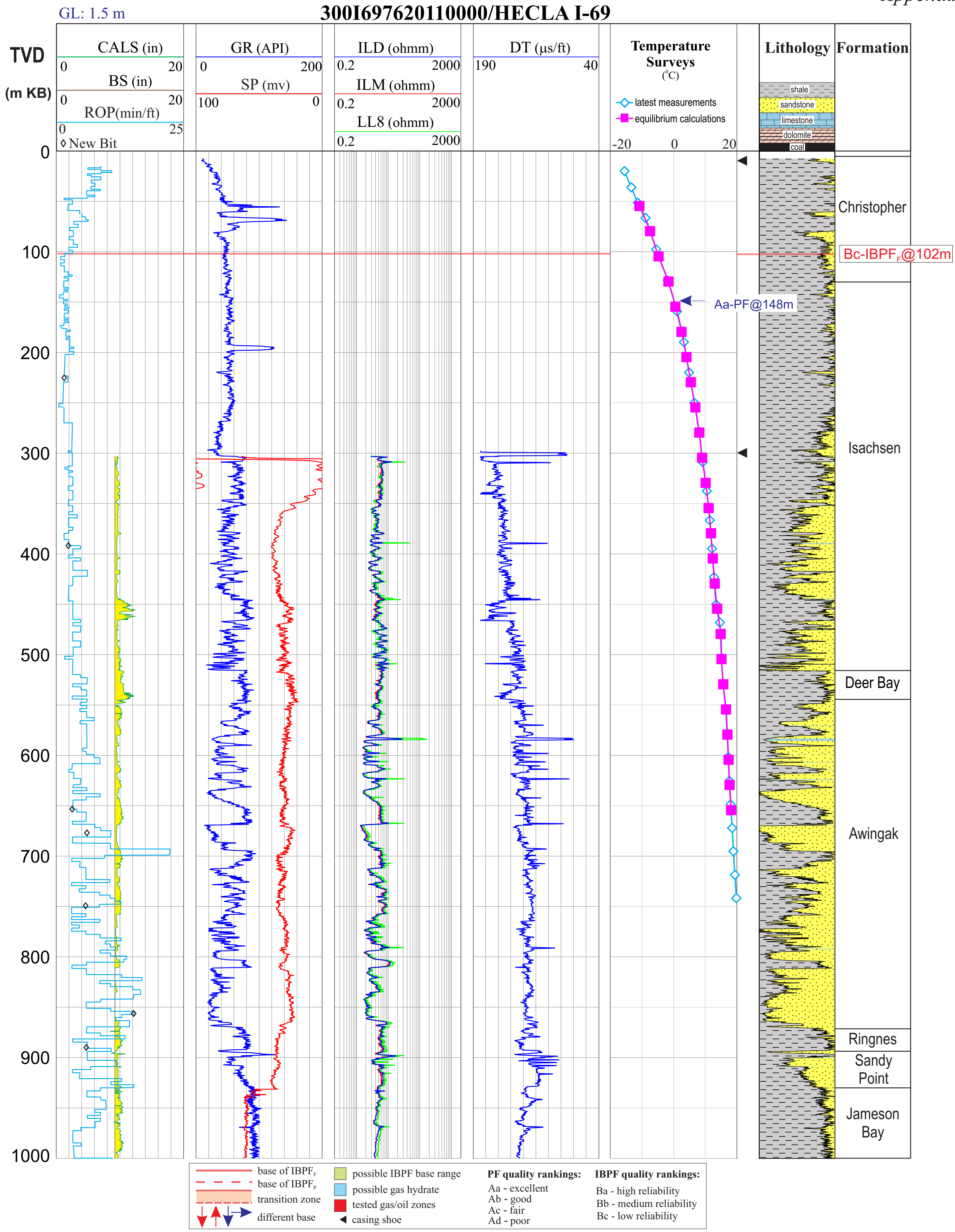

Figure 4-12. Estimation of base of $IBPF_F$ with "Bc" quality from drilling rate, and determination of base of PF from temperature surveys for the Hecla I-69 well on Melville Island in the Canadian Arctic Islands.

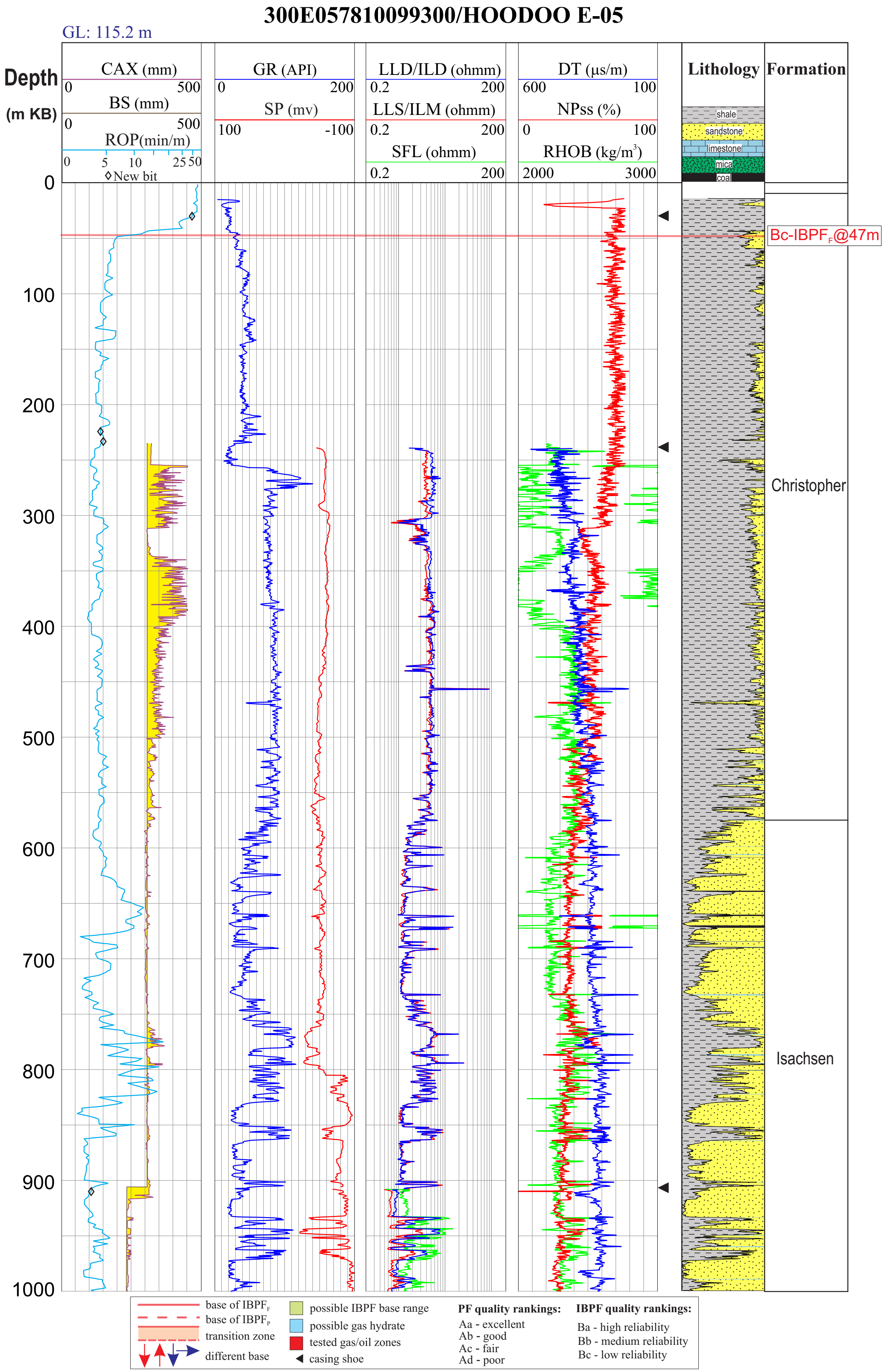

Figure 4-13. Estimation of base of $IBPF_F$ with "Bc" quality from drilling rate for the Hoodoo E-05 well on Ellef Ringnes Island in the Canadian Arctic Islands.

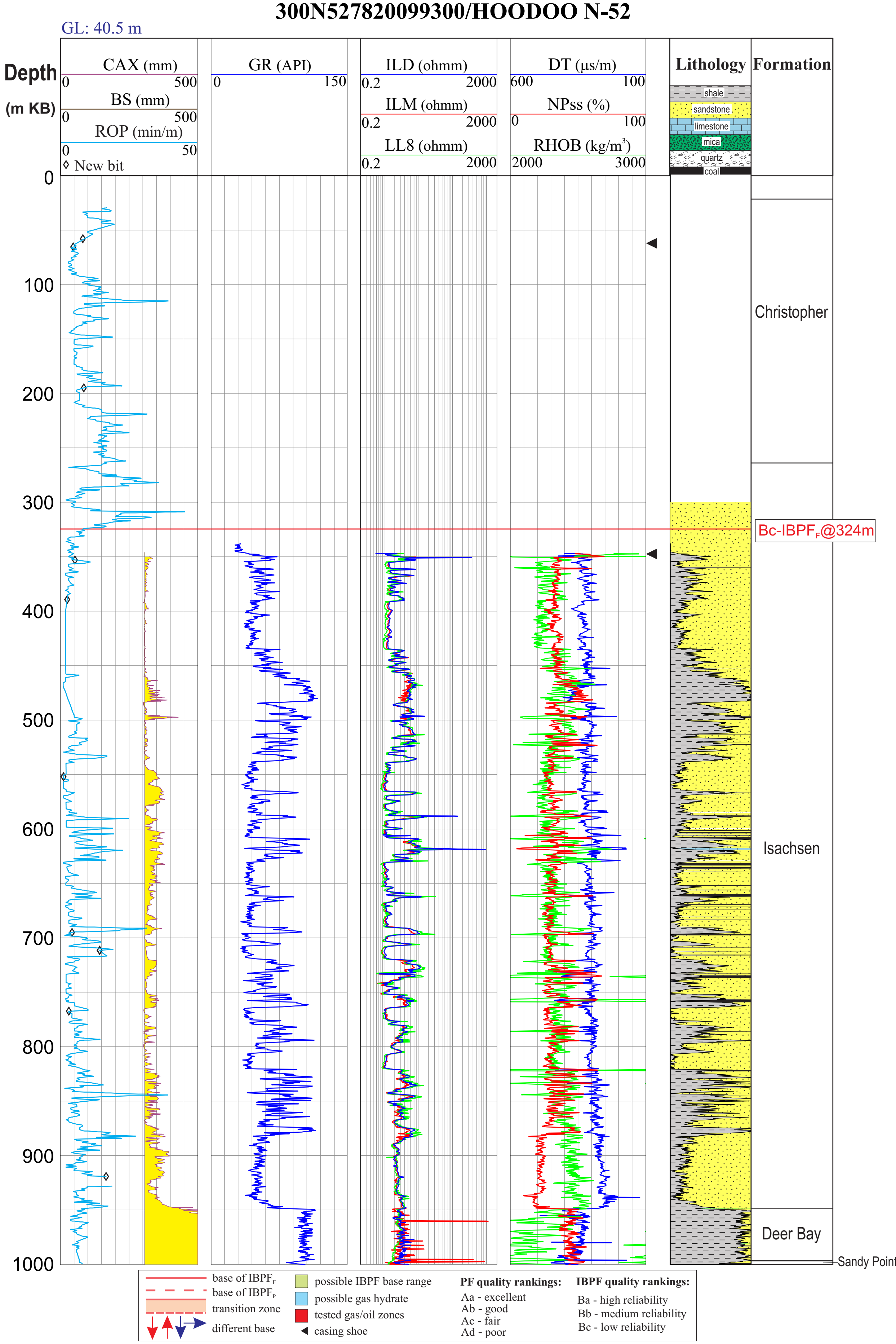

Figure 4-14. Estimation of base of $IBPF_F$ with "Bc" quality from drilling rate for the Hoodoo N-52 well on Ellef Ringnes Island in the Canadian Arctic Islands.

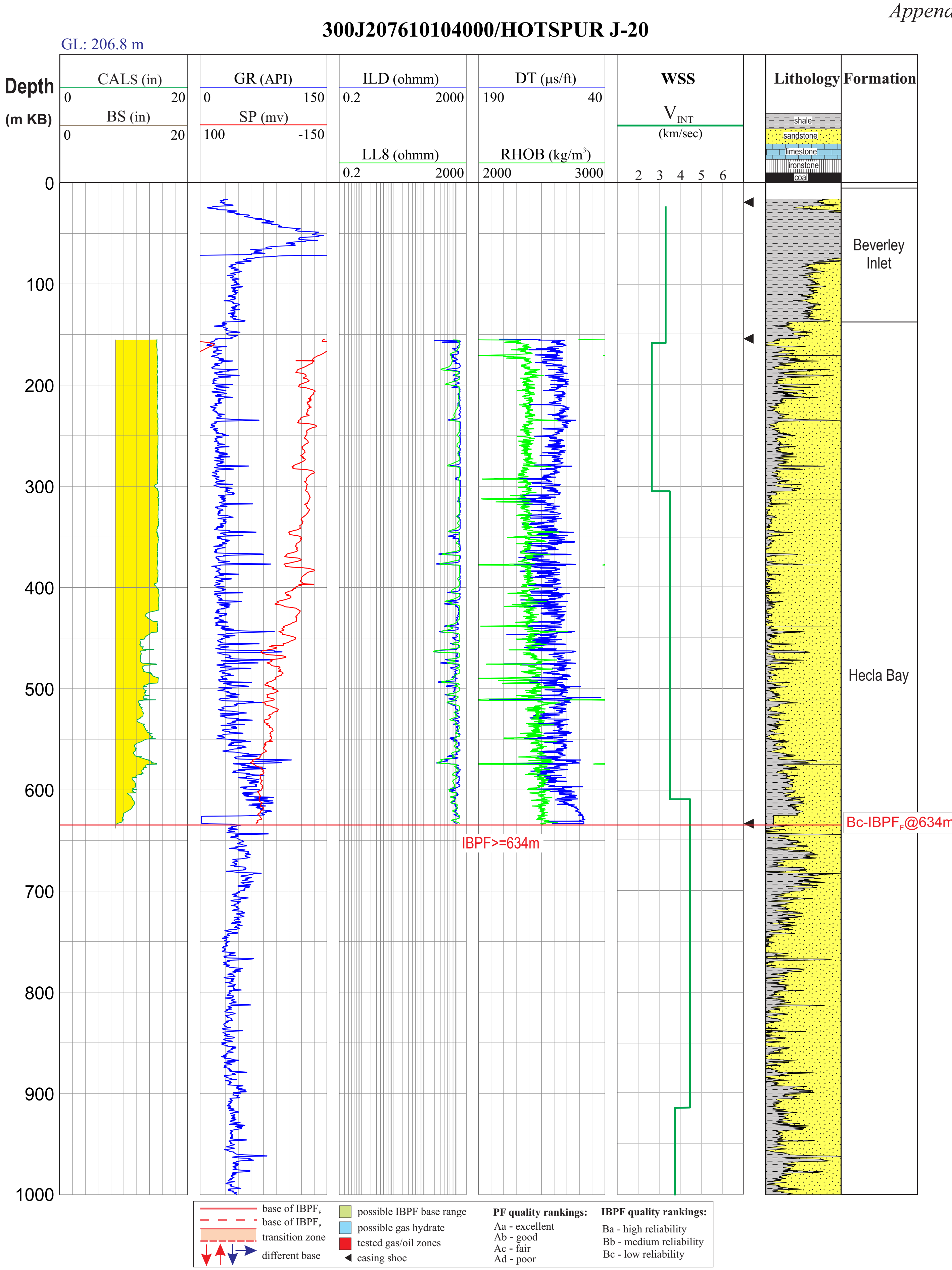

Figure 4-15. Minimum base of $IBPF_F$ with “Bc” quality is estimated using well logs and well seismic surveys for the Hotspur J-20 well on Vanier Island in the Canadian Arctic Islands.

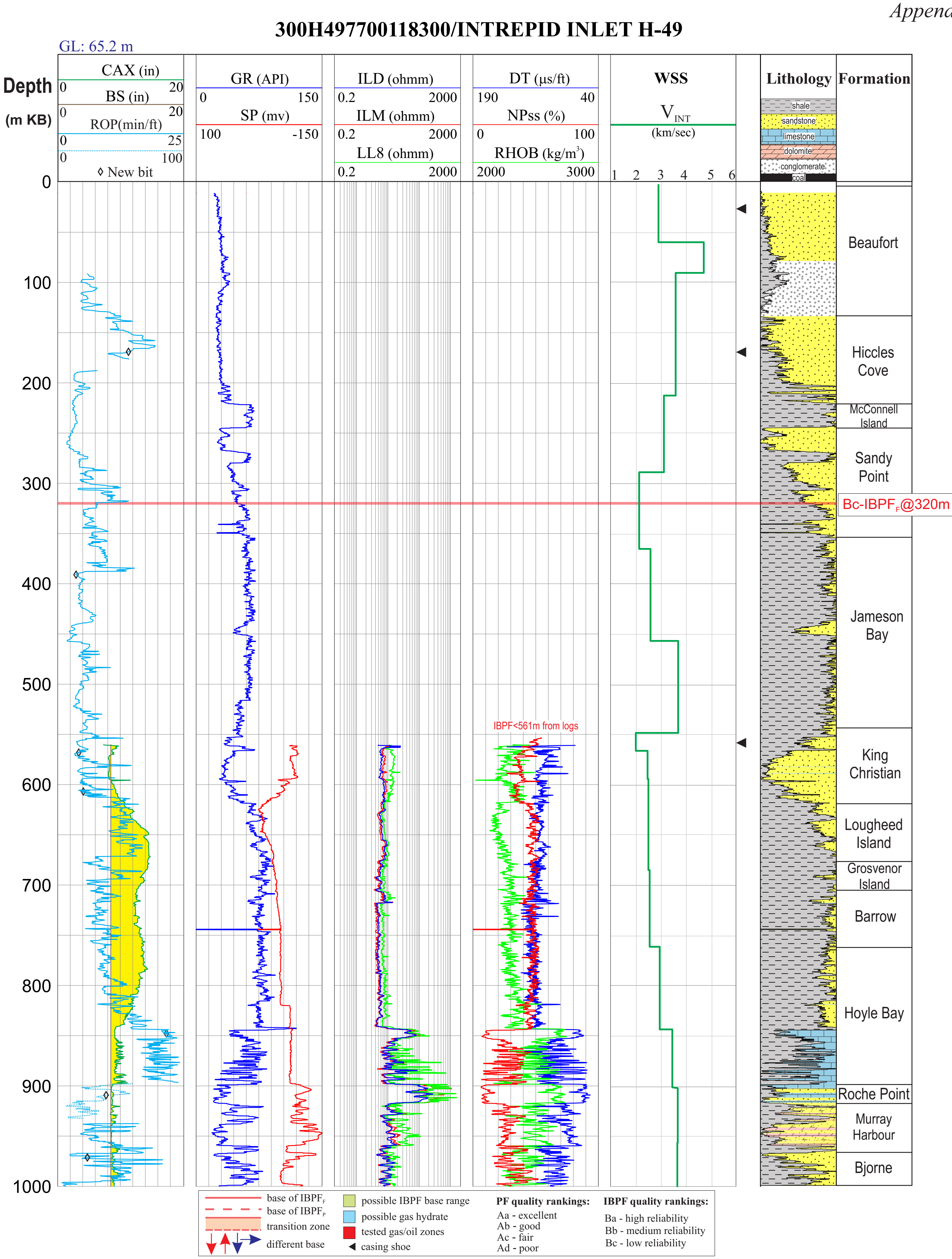

Figure 4-16. Estimation of base of $IBPF_F$ with "Bc" quality from well seismic surveys and drilling rate for the Intrepid Inlet H-49 well on Prince Patrick Island in the Canadian Arctic Islands.

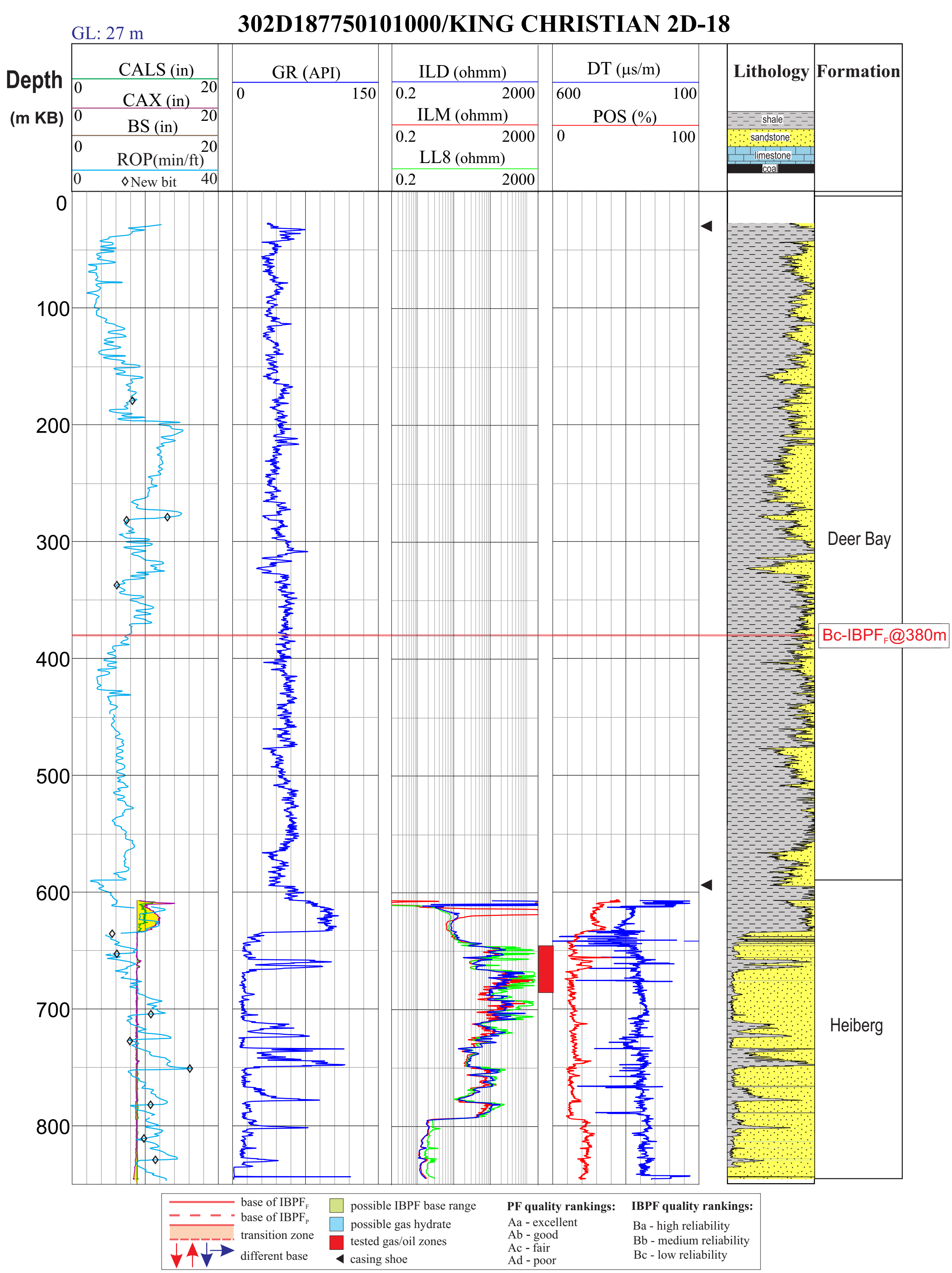

Figure 4-17. Estimation of base of $IBPF_F$ with "Bc" quality from drilling rate and other information (well tests) for the King Christian 2D-18 well on King Christian Island in the Canadian Arctic Islands.

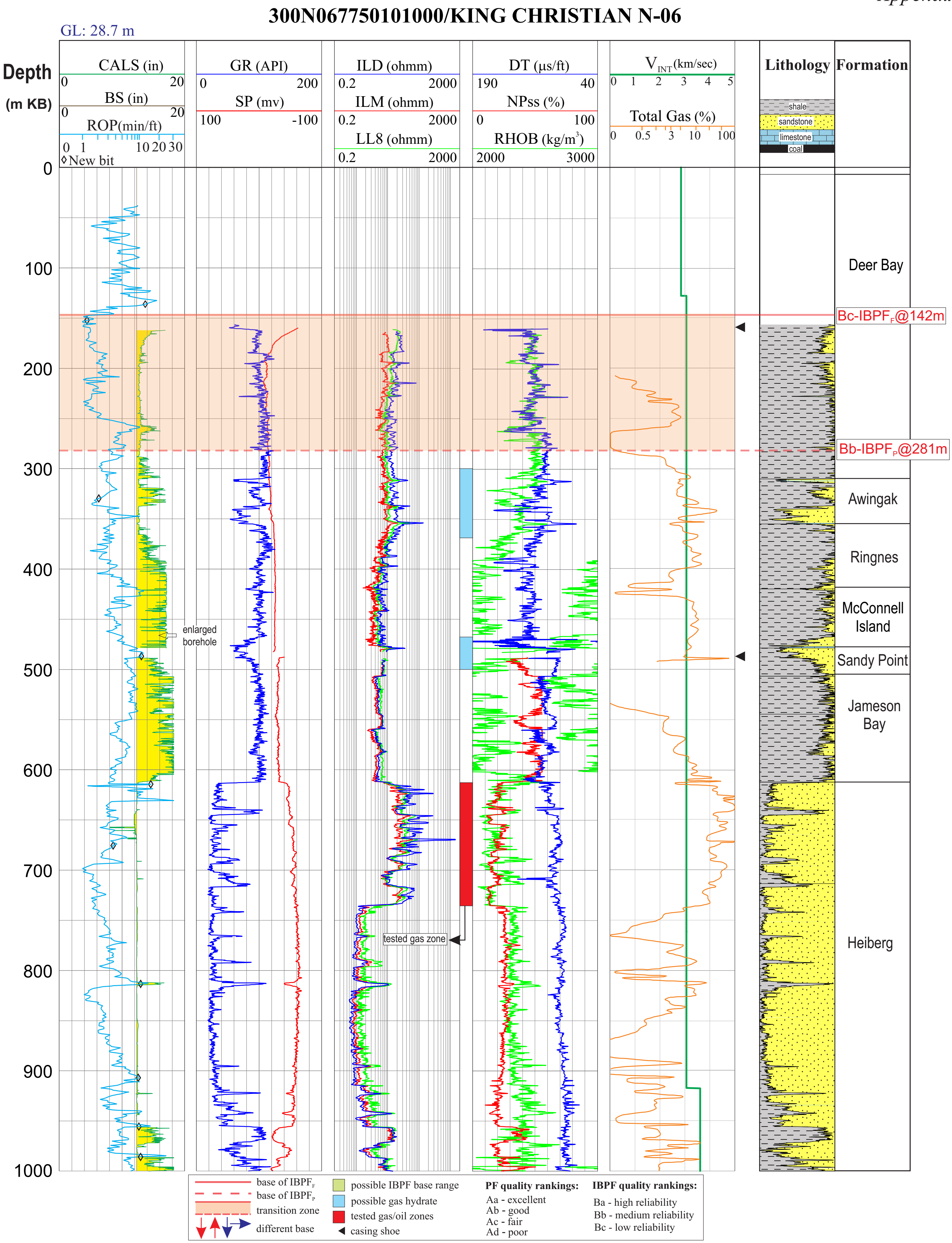

Figure 4-18. Estimations of base of $IBPF_F$ with "Bc" quality and $IBPF_P$ with "Bb" quality mainly from well logs and other information (gas log and possible gas hydrate interpretation) for the King Christian N-06 well on King Christian Island in the Canadian Arctic Islands.

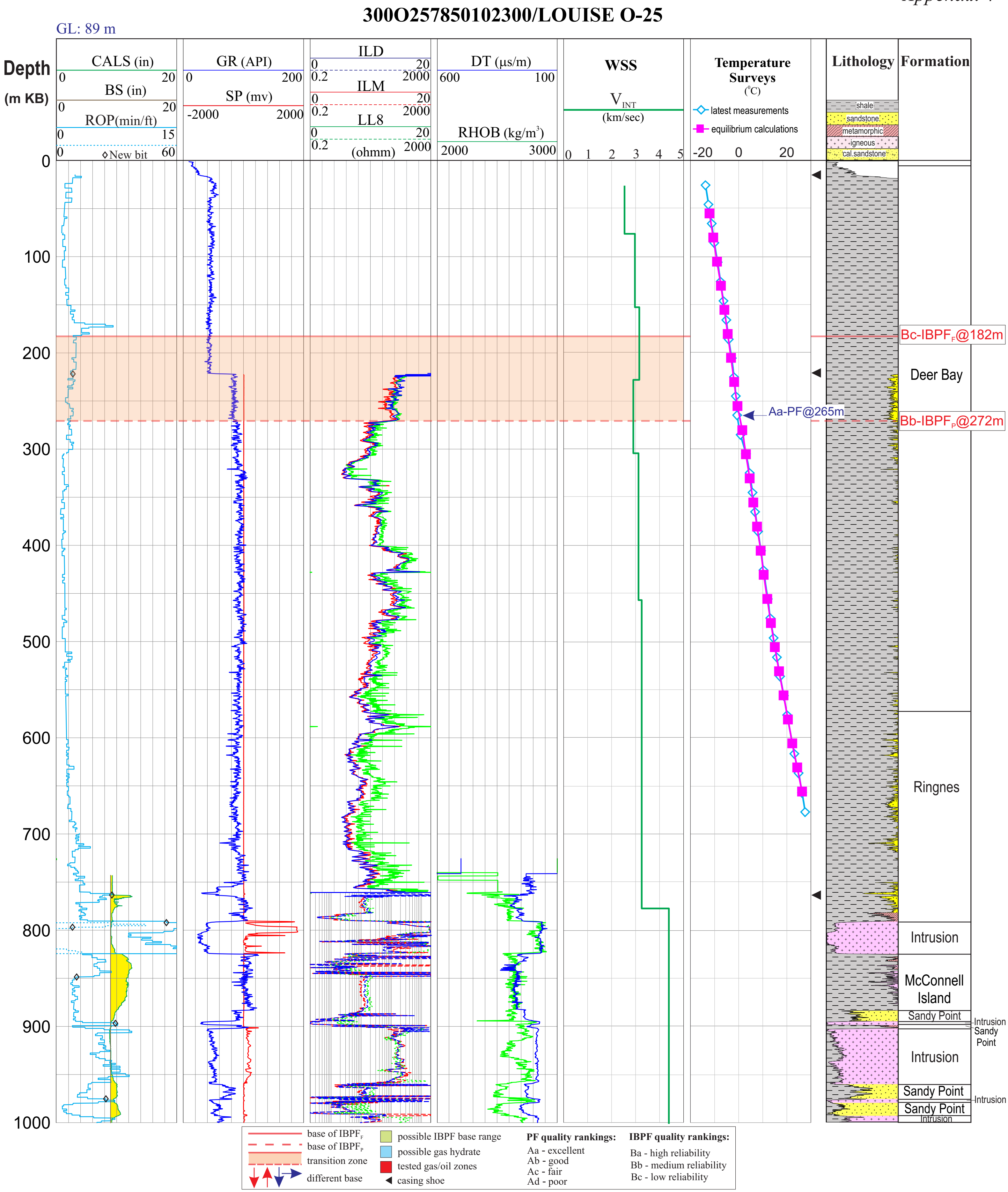

Figure 4-19. Estimations of base of $IBPF_F$ with "Bc" quality and $IBPF_P$ with "Bb" quality using well logs and well seismic survey, and determination of base of PF from temperature surveys for the Louise O-25 well on Ellef Ringnes Island in the Canadian Arctic Islands.

300D767310123000/NANUK D-76

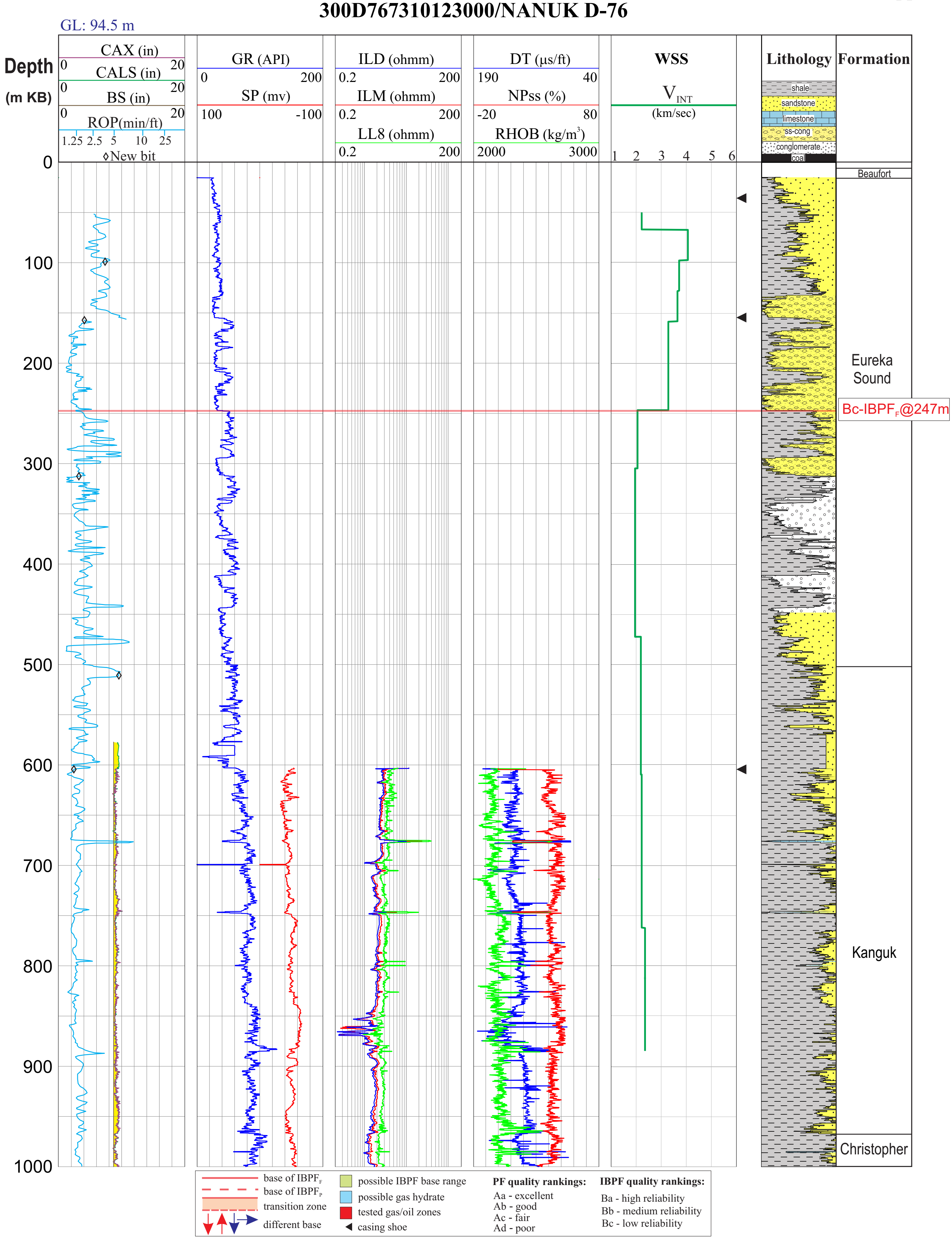

Figure 4-20. Estimation of base of IBPF$_F$ with "Bc" quality from well seismic surveys and drilling rate for the Nanuk D-76 well on Banks Island in the Canadian Arctic Islands.

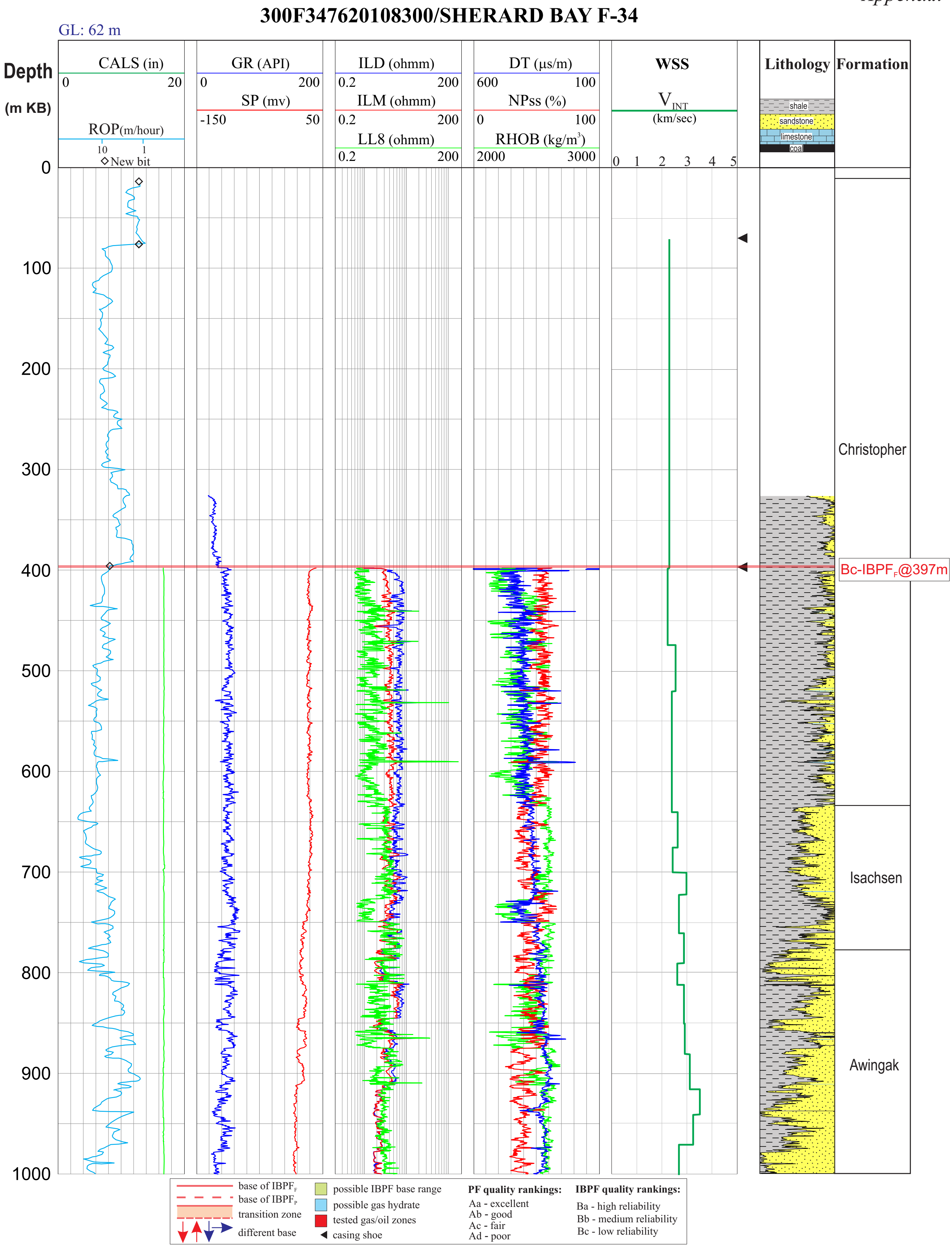

Figure 4-21. Estimation of base of $IBPF_F$ with "Bc" quality from drilling rate and well seismic surveys for the Sherard Bay F-34 well on Melville Island in the Canadian Arctic Islands.

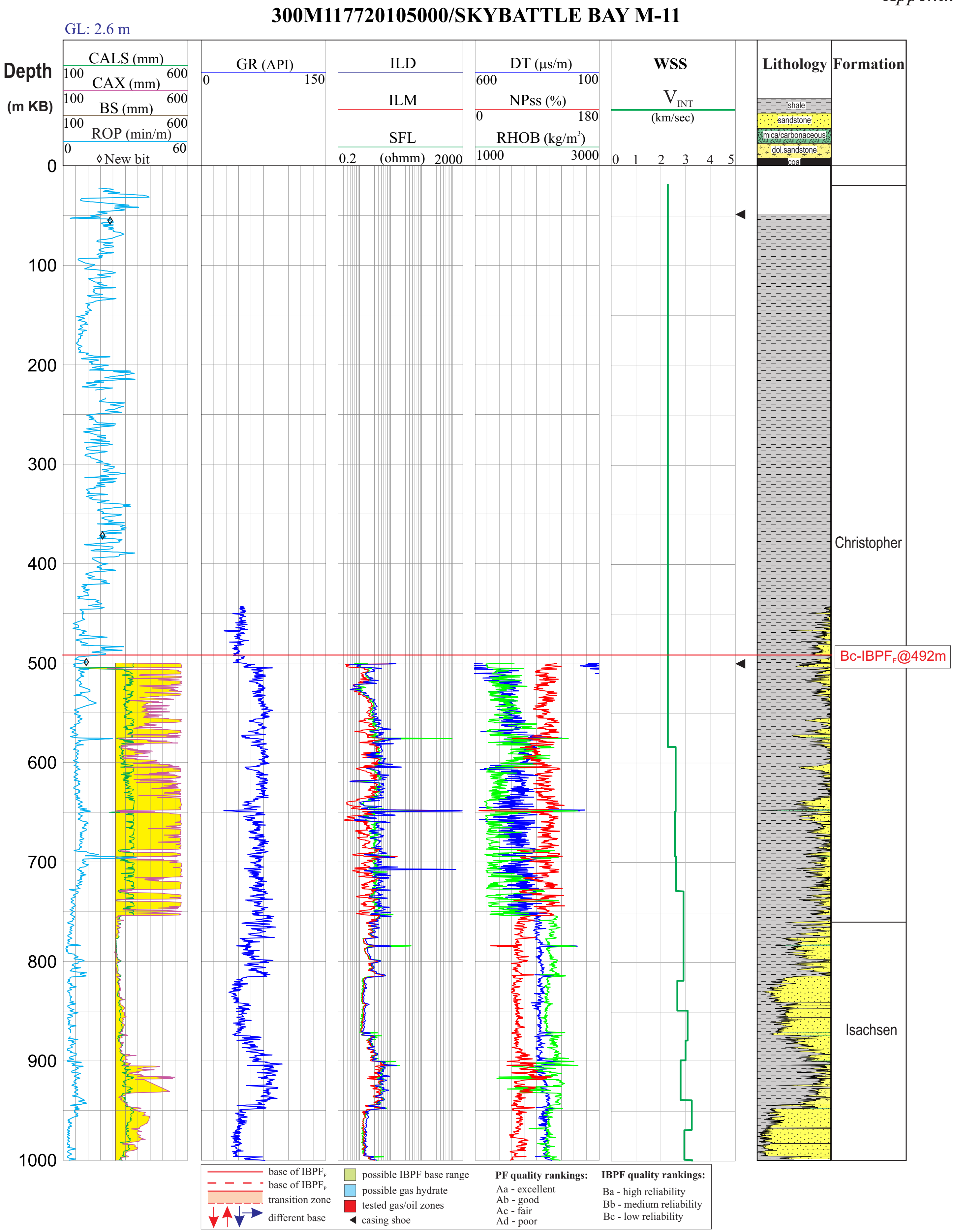

Figure 4-22. Estimation of base of $IBPF_F$ with "Bc" quality mainly from drilling rate for the well Skybattle Bay M-11 on Lougheed Island in the Canadian Arctic Islands.

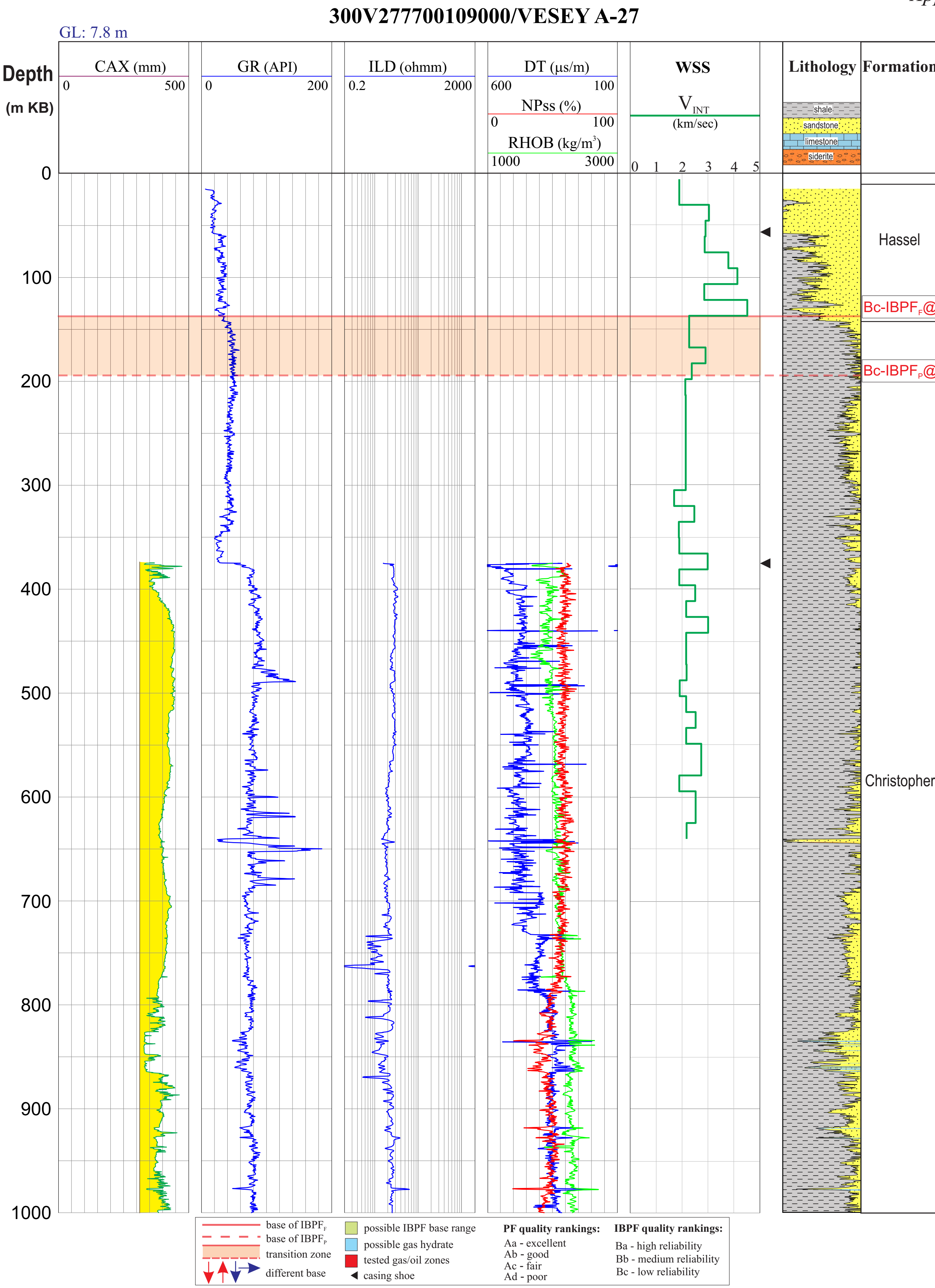

Figure 4-23. Estimations of base of $IBPF_F$ with “Bc” quality and $IBPF_P$ with “Bc” quality from well seismic surveys for the Vesey A-27 well on Hamilton Island in the Canadian Arctic Islands.

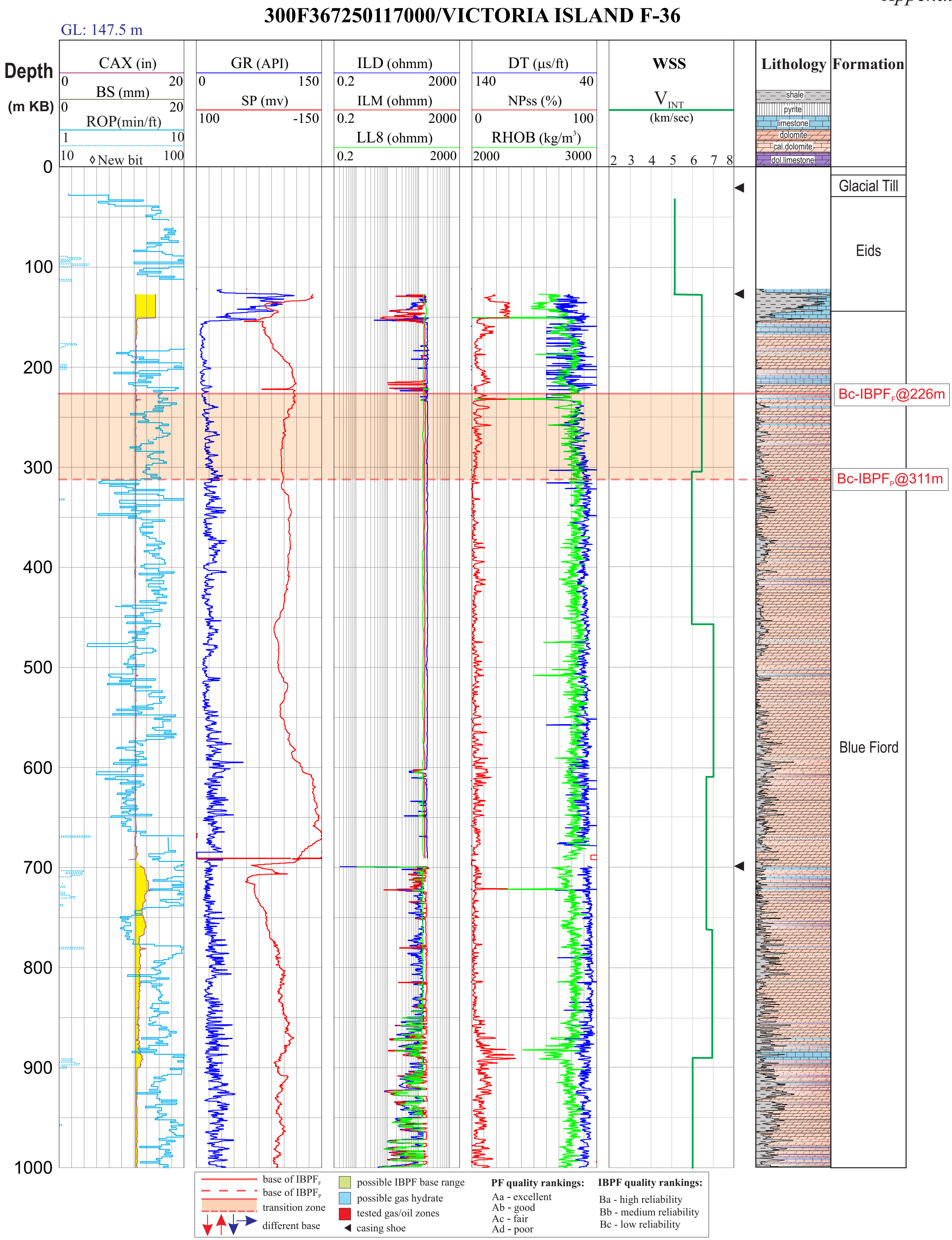

Figure 4-24. Estimations of base of IBPF$_F$ with "Bc" quality and IBPF$_P$ with "Bc" quality using well logs and well seismic surveys for the Victoria Island F-36 well on Victoria Island in the Canadian Arctic Islands.

300E607800111000/WILKINS E-60

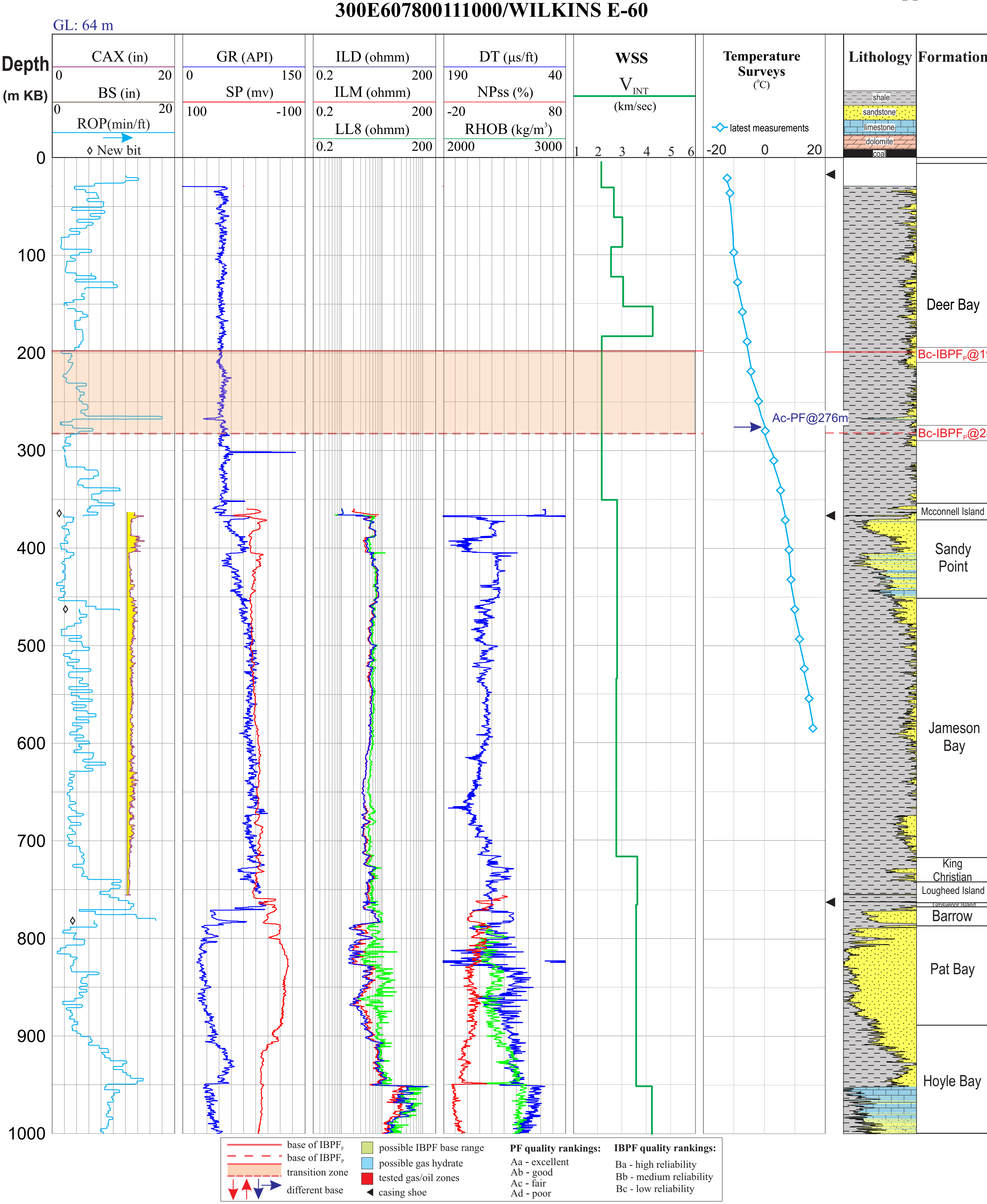

Figure 4-25. Estimations of base of $IBPF_F$ and $IBPF_P$ with “Bc” quality using well seismic surveys and drilling rate, and base of PF from temperature surveys for the Wilkins E-60 well on Mackenzie King Island in the Canadian Arctic Islands.

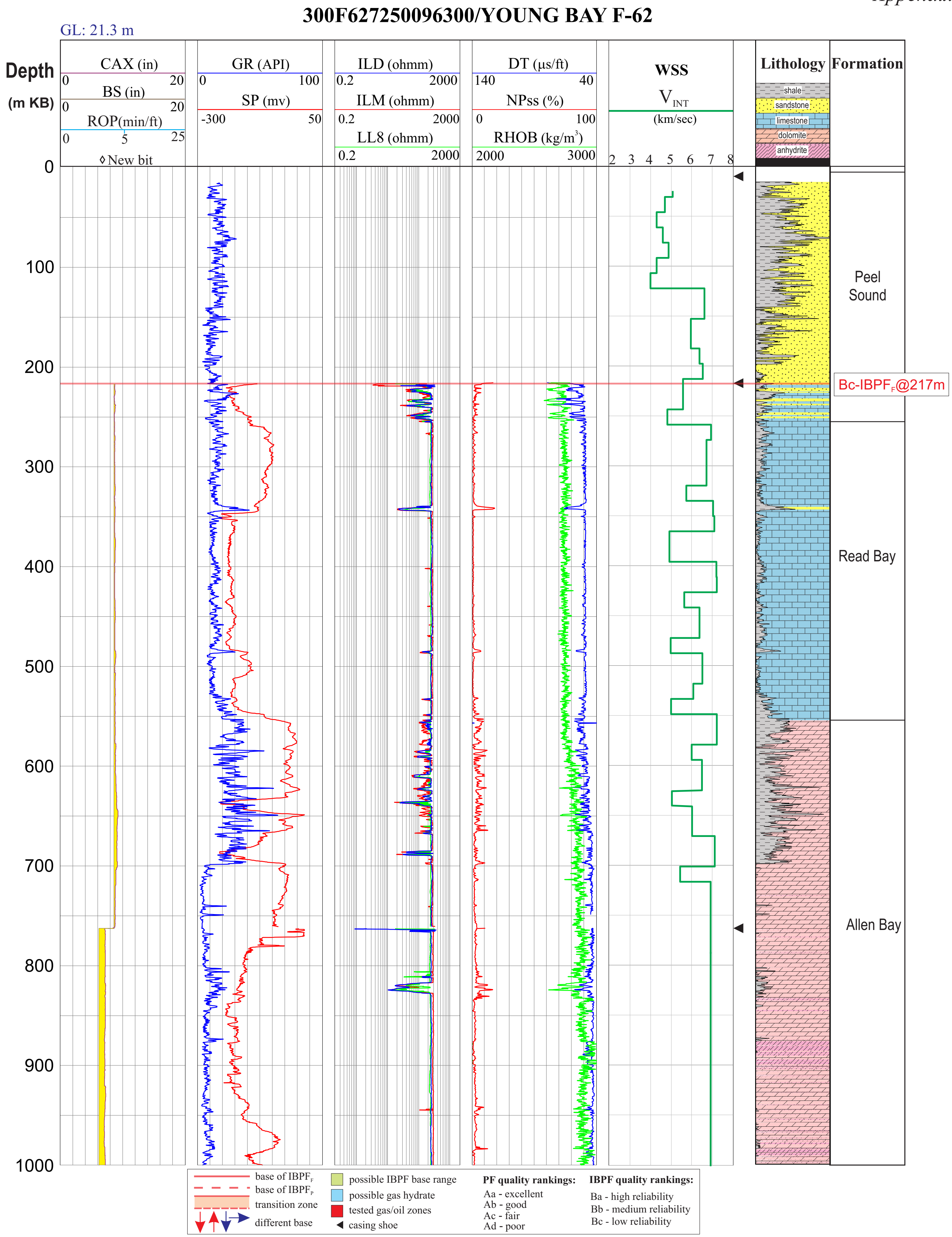

Figure 4-26. Estimation of base of $IBPF_F$ with "Bc" quality using well seismic surveys for the Young Bay F-62 well on Prince of Wales Island in the Canadian Arctic Islands.